Gianni Boris Bradac

Cerebral Angiography

Normal Anatomy and Vascular Pathology

Springer

Cerebral Angiography

Gianni Boris Bradac

Cerebral Angiography

Normal Anatomy and Vascular Pathology

Springer

Author
Gianni Boris Bradac MD
Professor Emeritus of Neuroradiology
Department of Neuroscience
University of Turin Ospedale Molinette
Via Cherasco 15
10126 Turin
Italy
gianniboris.bradac@unito.it

With the collaboration of
Edoardo Boccardi MD
Director of Neuroradiology
Ospedale Niguarda "Ca Granda"
Piazza Ospedale Maggiore 3
20162 Milan
Italy

ISBN 978-3-642-15677-9 e-ISBN 978-3-642-15678-6
DOI 10.1007/978-3-642-15678-6
Springer Heidelberg Dordrecht London New York

Library of Congress Control Number: 2011931164

Cover design: eStudioCalamar, Figueres/Berlin

Printed on acid-free paper

Springer is part of Springer Science+Business Media (www.springer.com)

Preface

In July 1927, E. Moniz presented at the Congress of the Neurological French Society in Paris his first experiences with a new method to study the cerebral vessels that he called "l'encéphalographie artérielle" (Moniz 1927). Cerebral angiography was thus born.

Since then, much technical progress has been made, starting with the introduction of the catheter technique (Seldinger 1953), the subtraction (Ziedses des Plantes 1963), followed by the use of more and more suitable catheters, guide wires, and less toxic contrast media, characterizing the evolution of cerebral angiography, which has progressively developed into an important neuroradiological diagnostic method. Later, in the 1980s, the basis of the endovascular treatment aimed at treating extracranial pathologies first followed by intracranial ones.

Diagnostic and therapeutic angiography has today reached a high technical standard present in all neuroradiological units. Its technical aspects have already been described in detail in previous works. Describing it again would be unnecessary.

The target of this book is to present, on the basis of findings obtained mainly by cerebral angiography, a study of the normal anatomy of cerebral vessels, covering the most and least frequent findings, their functions, and possible implications in pathological situations.

The second part of the book is dedicated to the various vascular pathologies emphasizing, in particular, those changes of the anatomy responsible for the clinical symptoms. Tumor pathology has not been described; however, some lesions involving the skull base and meningiomas have been covered.

Certainly, the evolution of new methods (angio-CT, angio-MR, ultrasound) allows us to effectively study cerebral vessels. In many cases, when the diagnosis is not clear or when specific details are required to understand the clinical symptoms or to plan the therapy, cerebral angiography remains the method of choice.

This is not a book about endovascular treatments. However, different pathologies have been discussed along with examples to provide a better understanding of this type of therapy.

We hope that this book will be of practical use for all physicians involved in the study of cerebral vessels and treatment of vascular pathology.

G.B. Bradac
E. Boccardi

References

Moniz E (1927) Revue neurologique 34:72
Seldinger SI (1953) Catheter replacement of the needle in percutaneous arteriography. Acta Radiol (Stock) 39:368
Ziedses des Plantes BG (1963) Application of the roentgenographic subtraction method in neuroradiology. Acta Radiol Diagn 1:961

Acknowledgments

This book reflects the work done and experiences gained in the Neuroradiological Unit at Molinette Hospital of Turin's University and at Ospedale Niguarda in Milan. It would not have been possible without the involvement, both direct or indirect, of many of our colleagues: M. Bergui (M.D.), G. Stura (M.D.), D. Daniele (M.D.), M. Corsico (M.D.), G. Ventilii (M.D.), M.F. Ferrio (M.D.), G. Gozzoli (M.D.), F. Venturi (M.D.), G.P. Vaudano (M.D.), L. Valvassori (M.D.), G. Pero (M.D.), and L. Quilici (M.D.). We would also like to express our sincere thanks to the radiographers and nursing staff of both units.

We are especially grateful to M. Coriasco, B.Sc. (medical technician), for his help with the technical aspects of the manuscript and in preparing the figures, and together with D. Daniele, M.D., for revising the text and preparing the subject index.

Finally, we would like to express our gratitude to all the members of Springer-Verlag, especially Mrs U. Heilmann, Ph.D., Mrs D. Mennecke-Bühler, Mr C.-D. Bachem, Mr G. Hippman and Mr G. Karthikeyan.

G.B. Bradac
E. Boccardi

Contents

Aortic Arch and Origin of the Cranial Cerebral Arteries

1

The study of the cranial cerebral vessels begins at the aortic arch. Short considerations about their embryogenesis are necessary.

In the embryogenesis, the brachiocephalic vessels develop from several primitive vascular arches. The progressive involution of these vascular structures leads to the formation of the final normal aortic arch, which is characterized by the persistence of the left fourth primitive arch, from which arise (right to left) the brachiocephalic trunk (innominate artery), the left common carotid artery, and the left subclavian artery. From the brachiocephalic trunk arise the right common carotid artery and the subclavian artery, giving off the right vertebral artery. The left vertebral artery arises from the left subclavian artery (Figs. 1.1 and 1.2).

Changes in this embryogenic process (Haughton and Rosenbaum 1974; Beigelman et al. 1995; Morris 1997; Osborn 1999) lead to anomalies of the aortic arch and the origin and course of the brachiocephalic vessels. Among the most frequent and simple anomalies are the common origin of the left common carotid artery (LC) and the brachiocephalic trunk or origin of the LC from the brachiocephalic trunk. The left vertebral artery can arise from the aortic arch. In addition, the right vertebral artery may originate from the aortic arch, but this is a very rare condition. (Figs. 1.3 and 1.4).

Less frequent, complex conditions are those concerning the laterality of the aortic arch and changes in the origin of the brachiocephalic vessels. An exceptional anomaly is a double aortic arch.

In the majority of cases, these anomalies are asymptomatic, being discovered during an angiographic study performed for a cerebral pathology. However,

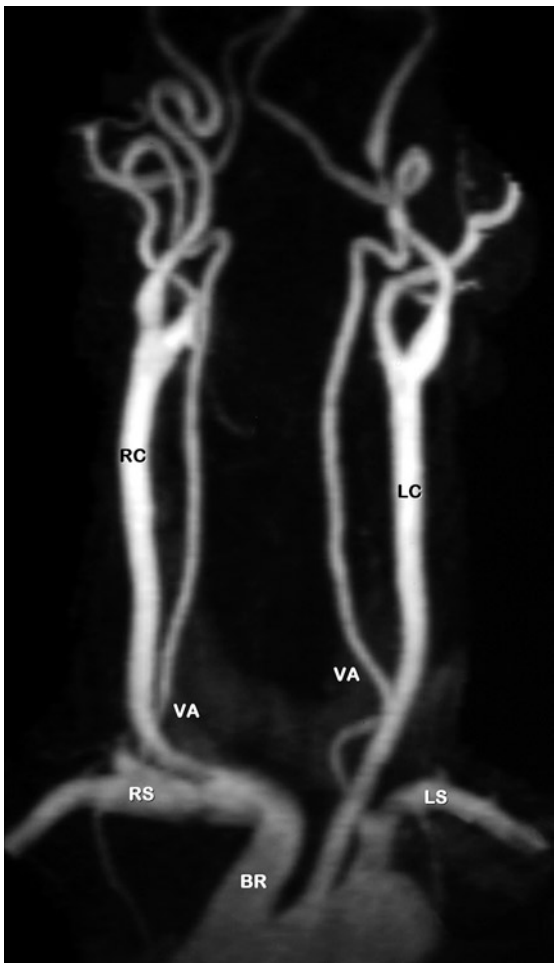

Fig. 1.1 Normal aortic arch, magnetic resonance imaging (MRI) angiography. Brachiocephalic trunk (*BR*), from which arise the right common carotid artery (*RC*) and right subclavian artery (*RS*). Common left carotid artery (*LC*), left subclavian artery (*LS*). Normal origin of both vertebral arteries (*VA*). The bifurcation of the two common carotid arteries is well demonstrated

G.B. Bradac, *Cerebral Angiography*,
DOI: 10.1007/978-3-642-15678-6_1,

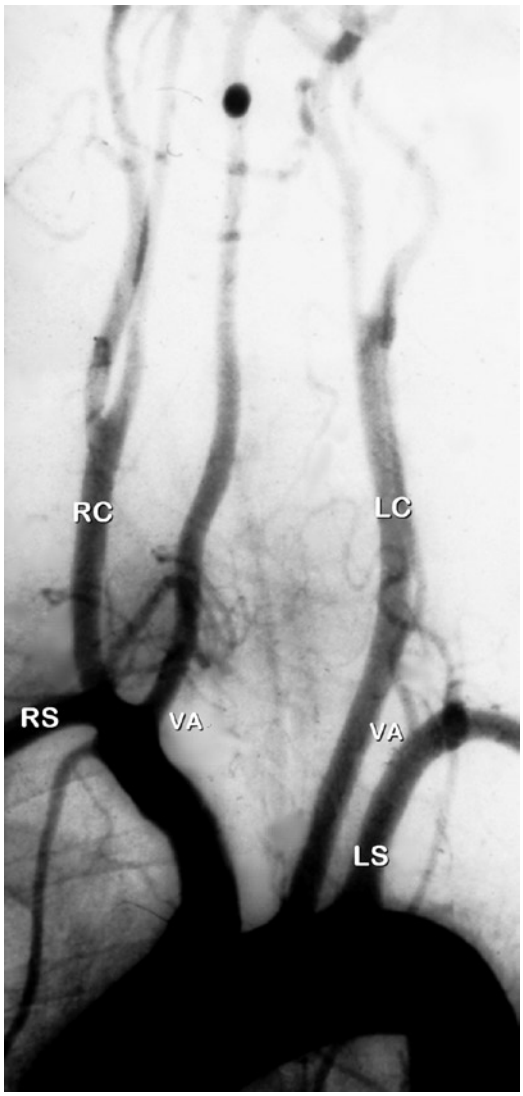

Fig. 1.2 Normal aortic arch angiogram with typical origin of the left and right common carotid arteries (*LC*, *RC*). Subclavian arteries (*RS*, *LS*), asymmetry of the vertebral arteries (*VA*). That of the left is hypoplastic

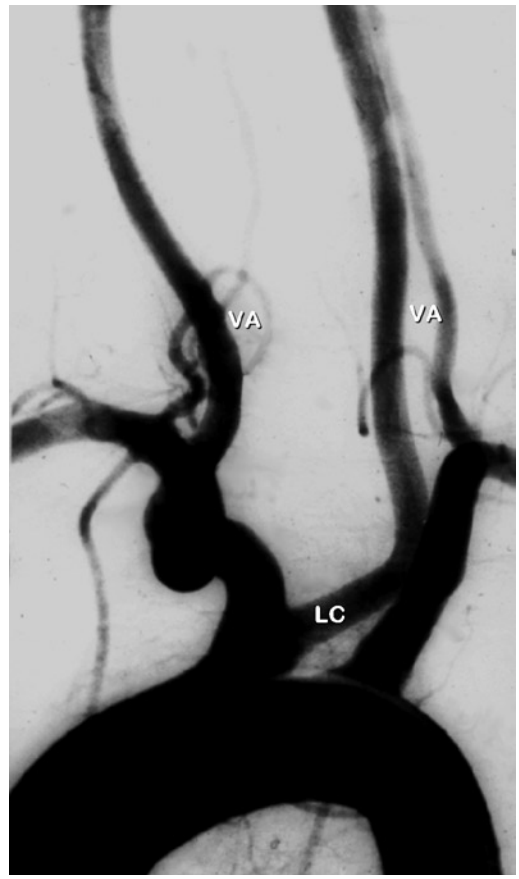

Fig. 1.3 Aortic arch angiogram, showing the origin of the left common carotid artery (*LC*) from the brachiocephalic trunk. The left vertebral artery (*VA*) is well developed, while that of the right is hypoplastic

the possibility of such anomalies should be taken into account by the angiographer. Infrequently, dysphagia and congenital heart disease can be present, especially in an aberrant course of the right subclavian artery and in the right aortic arch (Figs. 1.5–1.7).

From each common carotid artery arises the external carotid artery which supplies mainly the extra cranial territories and the internal carotid artery which intracranially divides in its branches responsible of the vascularization of the corresponding cerebral hemisphere. The vertebral arteries appear first as segmental channels in the cervical area and are connected later proximally with the developed subclavian artery. The vertebral arteries unite intracranially continuing in the median single basilar artery which replaces the primitive double basilar artery. From the vertebral and basilar arteries arise the branches supplying brainstem and cerebellum.

At the 6-7 weeks of the fetal development (DeVriese 1905; Padget 1944–1948) at the base of the cerebrum both carotid and basilar arteries are connected to each other by the way of small channels forming the circle of Willis (1684). Both anterior cerebral arteries are linked by the anterior communicating artery, and each

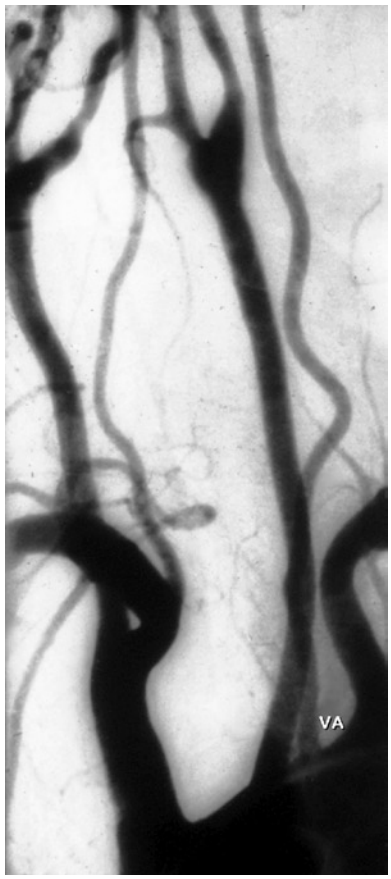

Fig. 1.4 Aortic arch angiogram, showing the origin of the left vertebral artery (*VA*) from the aortic arch. There is a shifting of the origin of the left common carotid artery and brachiocephalic trunk toward the heart owing to atherosclerotic elongation of the aortic arch

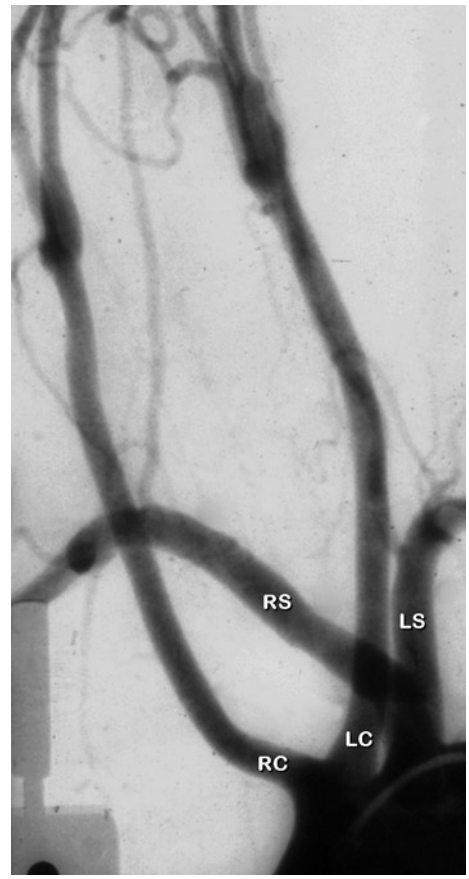

Fig. 1.5 Left aortic arch angiogram anomaly. The left and right common carotid arteries (*LC*, *RC*) arise as a common trunk. The left and right subclavian arteries (*LS*, *RS*) also have a common origin

carotid artery is connected through the posterior communicating artery with the respective posterior cerebral artery, terminal branch of the basilar artery (Fig. 1.8).

This is a natural well-constructed security system. Its functional value, however, is somewhat unpredictable owing to the many variants present. According to several authors (DeVries 1905; Padget 1948; Lazorthes et al. 1976) the variants are due to changes occurring in the circle of Willis in the postnatal period and through the life. All these will be described in the corresponding chapters.

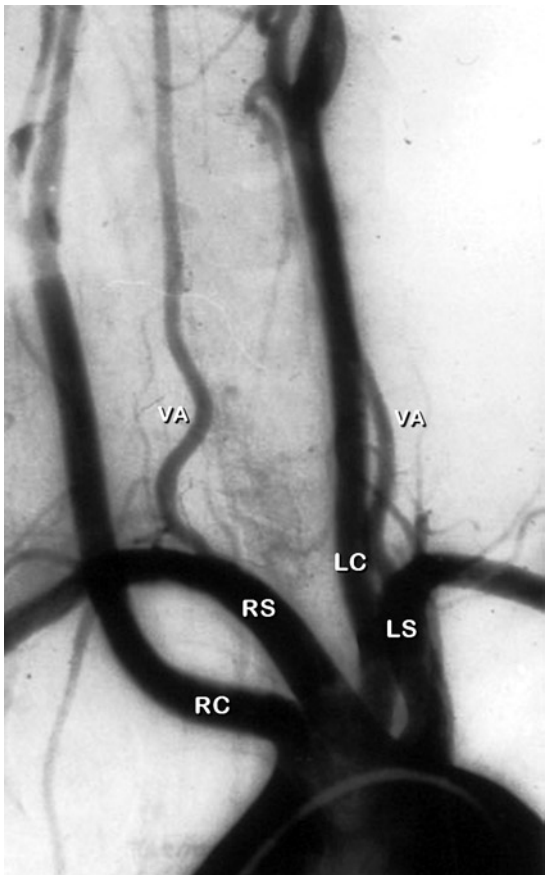

Fig. 1.6 Left aortic arch anomaly (angiogram). All vessels have a separate origin. The first to fill is the right common carotid artery (*RC*), followed by the left common carotid artery (*LC*), right subclavian (*RS*), and left subclavian (*LS*)

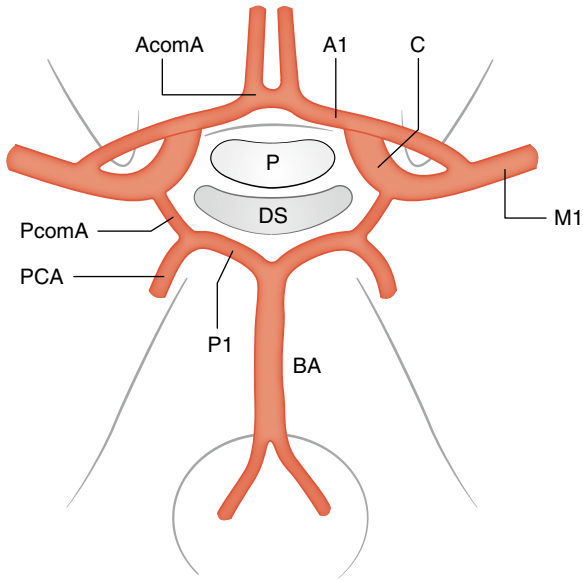

Fig. 1.8 The circle of Willis. Internal carotid artery (*C*), first segment of anterior cerebral artery (*A1*), first segment of middle cerebral artery (*M1*). Basilar artery (*BA*), first segment of posterior cerebral artery (*P1*), posterior cerebral artery (*PCA*), anterior communicating artery (*AcomA*), posterior communicating artery (*PcomA*), pituitary gland (*P*), dorsum sellae (*DS*)

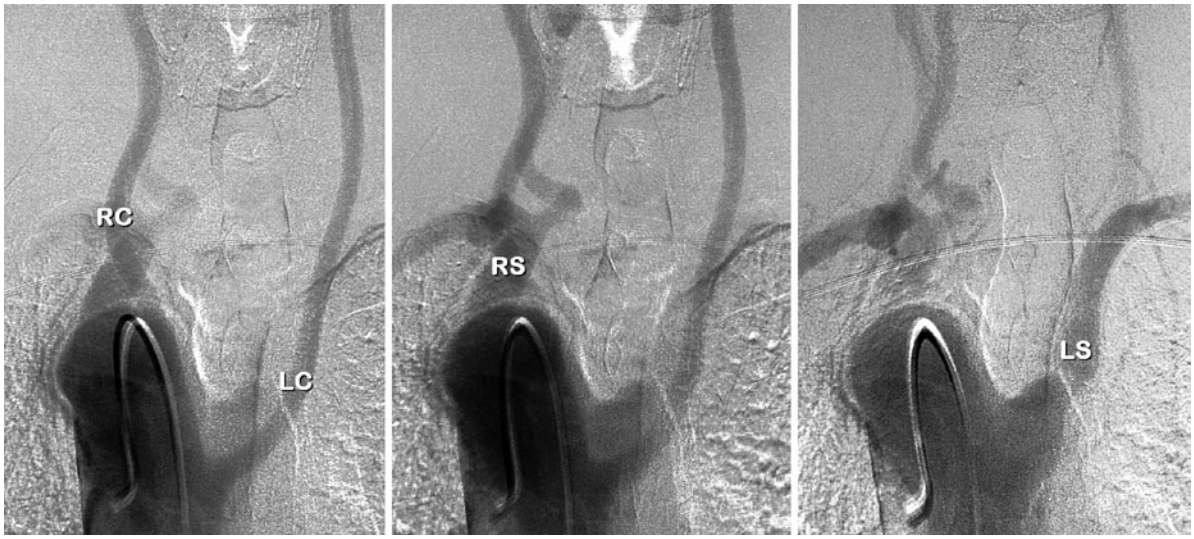

Fig. 1.7 Right aortic arch anomaly (angiogram). The left and right common carotid arteries (*LC*, *RC*) appear first, followed by the injection of the right subclavian and finally of the left aberrant subclavian arteries (*RS*, *LS*)

Carotid Artery (CA)

2

2.1 Cervical Segment

There are two common carotid arteries. The left common (LC) carotid artery arises from the aortic arch and the right common (RC) carotid artery from the brachiocephalic trunk . The common carotid arteries run cranially in the carotid space, surrounded by the three layers of the deep cervical fascia, called the carotid sheet. Approximately at the level of the hyoid bone, usually between the C4 and C6 vertebral bodies, each common carotid artery divides into the internal carotid artery (ICA) and external carotid artery (ECA). Cases of a higher bifurcation, up to the first cervical vertebra (Lie 1968), or lower, in the upper thoracic levels (Vitek and Reaves 1973), have been reported. The carotid sheet is a well-defined structure below the carotid bifurcation, though it is incomplete or absent at the level of the oral-nasal pharynx (Harnsberger 1995). The infrahyoid segment of the carotid space contains the common carotid artery, which is located in the so-called anterior triangle, defined by the sternocleidomastoid muscle, laterally and posteriorly, and by the superior belly of the omohyoid and the posterior belly of the digastric muscle, inferiorly and superiorly. The suprahyoid segment of the carotid space contains the ICA, more laterally and posteriorly the jugular vein, cranial nerves (IX, X, XI, and XII), the sympathetic plexus, and the chain of the lymph nodes (Fig. 2.1). Near the skull base, the borders of the carotid space are as follows: laterally, the parotid space; anteriorly and medially, the parapharyngeal and retropharyngeal spaces, respectively; posteriorly, the perivertebral space (Fig. 2.1c).

The first segment of the ICA (carotid bulb) is slightly enlarged, becoming smaller and narrower 1–2 cm distally. The bulb can be enlarged, particularly in older, atherosclerotic patients, and tortuosity of the distal segment is frequent in very young and older patients. This tortuosity can be congenital or related to dysplastic or atherosclerotic changes. At its origin, the ICA commonly lies posterior and lateral to the ECA. More distally, it is medial to the ECA (Fig. 2.1a, b) (see chapter 3).

2.2 Petrous Segment

The ICA enters the base of the skull at the carotid foramen, anteriorly to the jugular fossa and jugular vein. It runs entirely in the petrous bone, first with a vertical course for about 1 cm, then horizontally medially and slightly upward. Through its course, the ICA lies anteriorly medially and below the tympanic cavity and cochlea. It emerges from the petrous bone, near its apex, running above the cartilage covering the foramen lacerum (Figs. 2.2 and 2.3) and enters the cavernous sinus.

There are two branches: the *caroticotympanic and mandibular arteries*. The caroticotympanic artery is an embryonic remnant that supplies the middle ear cavity. There is possible anastomosis with the tympanic branch of the ascending pharyngeal artery (APhA). The caroticotympanic artery can be involved in tumors of the skull base, particularly in tympanojugular paragangliomas.

The mandibular artery is an embryonic remnant that usually divides into two branches: one runs in the pterygoid canal, anastomosing with the vidian artery; the other is more inferior, anastomosing with the pterygovaginal artery. This artery can be involved in the vascularization of angiofibromas. Apart from the above pathological situations, these branches are not commonly visible on an angiogram.

G.B. Bradac, *Cerebral Angiography*,
DOI: 10.1007/978-3-642-15678-6_2, © Springer-Verlag Berlin Heidelberg 2011

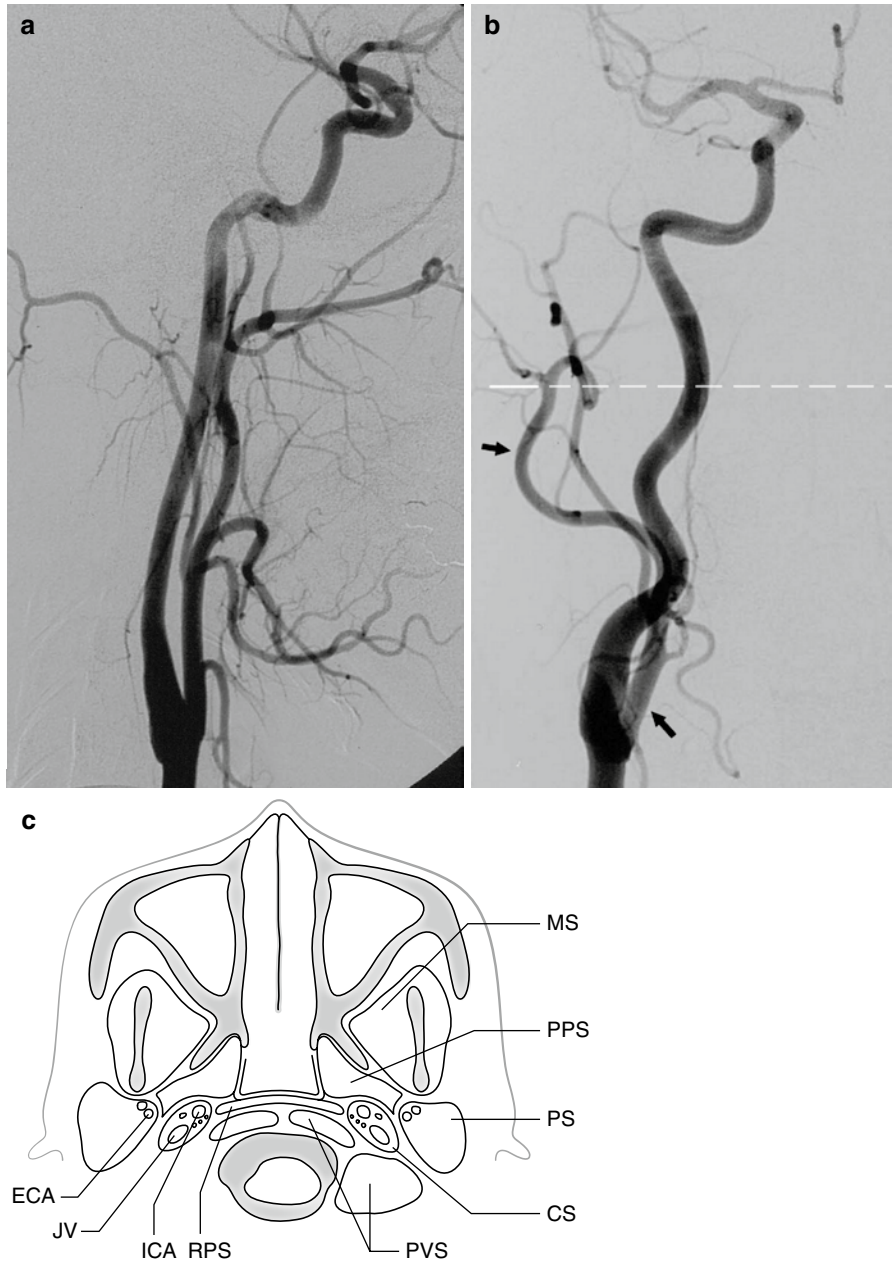

Fig. 2.1 (**a**) Common carotid angiogram, lateral view, showing the course of the external and internal carotid arteries. (**b**) Common carotid angiogram, AP view, showing the course of the external carotid artery (ECA, *arrow*), first medially and more distally lateral to the internal carotid artery (ICA). The dotted line corresponds to the axial plane in c. (**c**) Carotid space (*CS*), surrounded by the parotid space (*PS*), the parapharyngeal space (*PPS*), the retropharyngeal space (*RPS*), and the perivertebral space (*PVS*). Masticator space (*MS*). In the carotid space are indicated the *ICA* (anteriorly) and jugular vein (posteriorly), together with cranial nerves IX, X, X1, and XII. In the parotid space, the *ECA* runs posteriorly and the retromandibular vein anteriorly. The facial nerve runs laterally

2.3 Cavernous Segment

This runs in the space (Taptas 1982; Bradac et al. 1990) formed by a division of the dura into two layers: the lateral one is the medial wall of the middle cranial fossa; the other is medial and in close contact in its inferior part with the periosteum of the sphenoid bone (periosteal layer). In this space, the ICA is directed first forward and upward, then curving posteriorly and slightly medially to the anterior clinoid process. The ICA lies laterally to the sella turcica and pituitary gland, separated by the medial layer of the dura. The ICA is surrounded by a venous plexus, and it has a close relationship with cranial nerves III, IV, and VI and the first and second branch of the trigeminal nerves. The nerves run close to the lateral

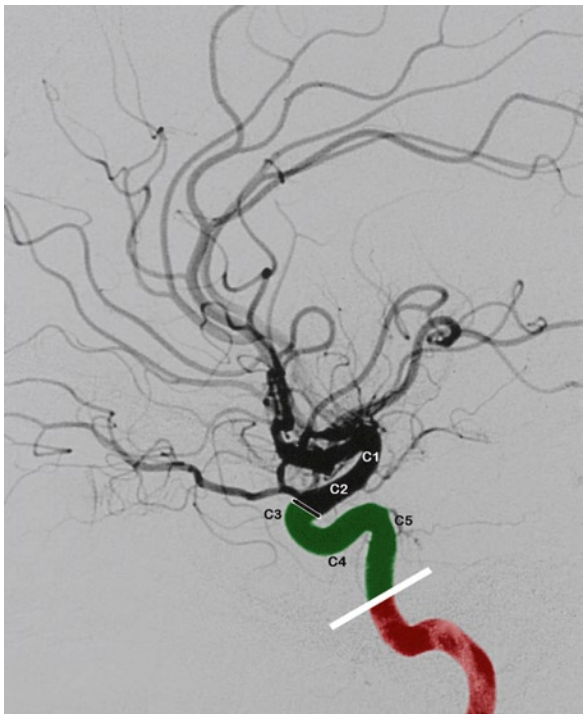

Fig. 2.2 Petrous and cavernous portion of the ICA, lateral carotid angiogram. Petrous portion (in *red*). Cavernous portion (in *green*). Dural ring proximal to the origin of the ophthalmic artery. *C5*, *C4*, and *C3* correspond to the different parts of the cavernous portion of the ICA. *C2* and *C1* define the supraclinoid and subarachnoid ICA

wall of the sinus, attached to it by dural sheaths. The latter can be connected, forming a thin, irregular inner layer adjacent to the external layer of the lateral wall (Umansky and Nathan 1982). Unlike the other nerves, cranial nerve VI runs inside the cavernous sinus.

Due to its S-shaped course, the cavernous segment is also called the siphon, which schematically can be subdivided into three segments. The segment called C5 is directed upward; the C4 is horizontal; and the C3 is a posteriorly directed curve up to the dural ring, through which the ICA passes, entering the subarachnoid space (Figs. 2.2 and 2.3). There are two branches of the cavernous segment: one is the *meningohypophyseal trunk* (MHT); the other is the *inferolateral trunk* (ILT).

- The MHT arises from the medial surface of the C5 segment of the ICA. It gives off a branch supplying the neurohypophysis (inferior hypophyseal artery), which is recognizable on an angiogram as a slight blush. It also gives off dural branches for the clivus and tentorium (clival and tentorial branches). The tentorial branch has been called the artery of Bernasconi and Cassinari (1957), who first reported its angiographic visualization. These dural branches anastomose with meningeal branches of the contralateral ICA and inferiorly with clival branches of the APhA. There are also possible anastomoses with branches of the middle meningeal artery.
- The ILT arise from the lateral surface of the C4 segment; it supplies cranial nerves III, IV, and VI and partially the ganglion Gasseri. It gives off dural branches for the dura of the cavernous sinus and adjacent area. In the supply of this area, there is a balance between the ICA system, represented by the ILT, and branches of the ECA, represented by the middle meningeal artery, accessory meningeal artery, artery of the foramen rotundum, and recurrent meningeal artery of the ophthalmic artery. One system can be dominant over the other. Anastomoses are frequently present.

The ILT and MHT are very fine branches (Fig. 2.4), not always recognizable on a lateral angiogram. They can be dilated and well visible when involved in the supply of pathological processes, especially meningiomas and dural arteriovenous fistulas.

2.4 Supraclinoid Segment

This begins where the artery goes through the dura and enters the subarachnoid space, running posteriorly, superiorly, and slightly laterally between the anterior clinoid process laterally and the optic nerve medially. The dural ring surrounding the ICA, where the artery enters the subarachnoid space, is closely adherent to the artery laterally, but it is frequently less adherent medially, forming a thin cavity (carotid cave). Aneurysms arising below the dural ring (intracavernous aneurysms) can, however, expand the cave and extend superiorly into the subarachnoid space (cave aneurysms) (Kobayashi et al. 1995; Rhoton 2002).

At the level of the anterior perforated space (APS), the artery divides into the anterior and middle cerebral arteries. The supraclinoid segment can subdivided into

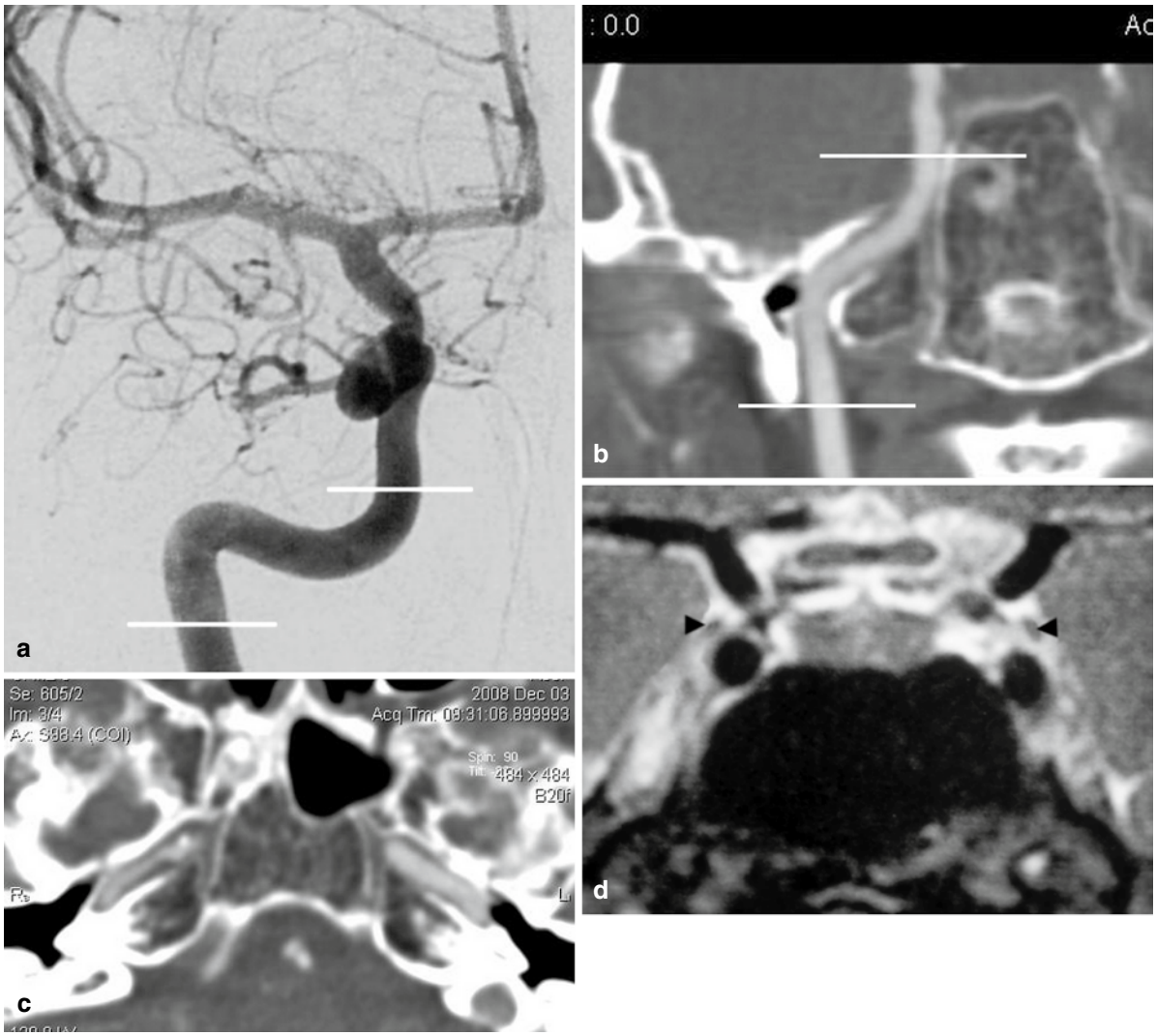

Fig. 2.3 (**a**) Carotid angiogram, AP view. The lines define the course of the petrous segment of the ICA, continuing into the cavernous segment. The end of the latter cannot be precisely defined in the AP view. (**b**) CT angiography, coronal reconstruction, showing the course of the petrous segment. (**c**) CT angiography, showing the horizontal part of the petrous segment of the ICA running above the foramen lacerum. (**d**) MRI, coronal view, sellar and parasellar area, showing the course of the ICA in the cavernous sinus. Cranial nerve III (*arrowheads*)

a proximal and distal part, termed C2 and C1. From the origin of its branches, the supraclinoid segment can be more precisely subdivided as follows (Gibo et al. 1981): the ophthalmic segment, from the origin of the ophthalmic artery to the origin of the posterior communicating artery (PcomA); the communicating segment, from the origin of the PcomA to the origin of the choroidal artery; and the choroidal segment, from origin of the anterior choroidal artery to the terminal bifurcation of the ICA.

2.4.1 *In the Ophthalmic Segment Arise the Ophthalmic Artery and Superior Hypophyseal Arteries*

2.4.1.1 The Ophthalmic Artery

The ophthalmic artery (OA) arises on the superior-medial surface of the ICA. It runs below the optic nerve (Hayreh and Dass 1962a, 1962b; Hayreh 1962) and enters,

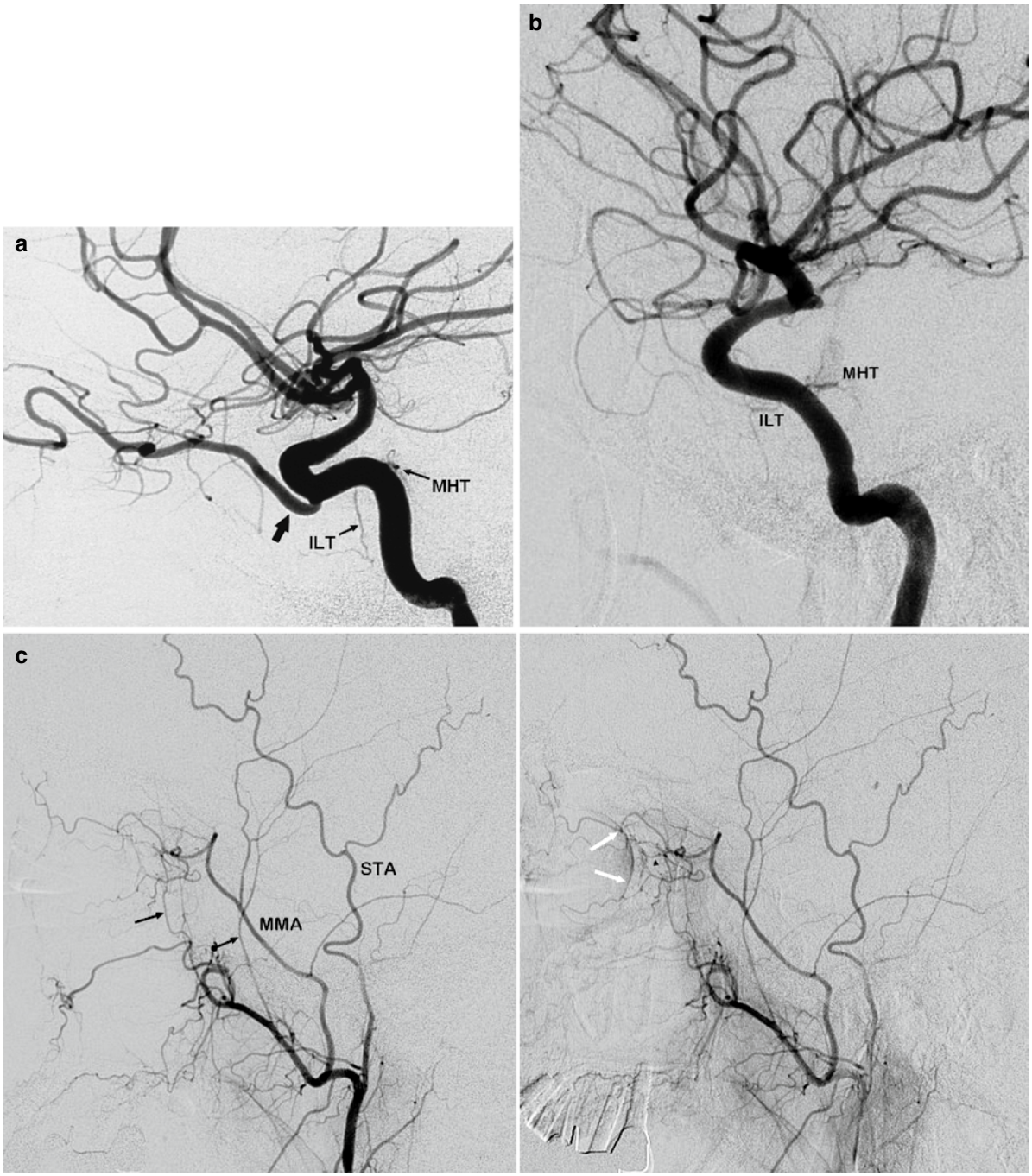

Fig. 2.4 (**a**) Carotid angiogram. Lateral-oblique view. Origin of the ophthalmic artery from the cavernous portion of the ICA (*large arrow*). Meningohypophyseal trunk (*MHT*) and inferolateral trunk (*ILT*). (**b**) ICA angiogram, lateral view. There is no ophthalmic artery. *MHT*, *ILT*. (**c**) ECA angiogram, lateral view of the same patient in B. Origin of the ophthalmic artery from the middle meningeal artery (*MMA*). There is also a possible supply from the anterior deep temporal artery (*arrow*). Middle deep temporal artery (*arrow with dot*). Superficial temporal artery (*STA*). In the later phase, the ocular complex (*arrowhead*) and blush of the choroid plexus (*white arrow*) are recognizable. (**d**) Different patient: origin of the MMA from the ophthalmic artery. Carotid angiogram, lateral view: ophthalmic artery (*O*). Lacrimal artery (*arrowhead*), from which arise the frontoparietal and temporal branches of the MMA (*arrows*). AP view, ophthalmic artery (*O*). Branches of the MMA (*bidirectional arrow*). (Patient with small aneurysm at the level of the posterior communicating artery)

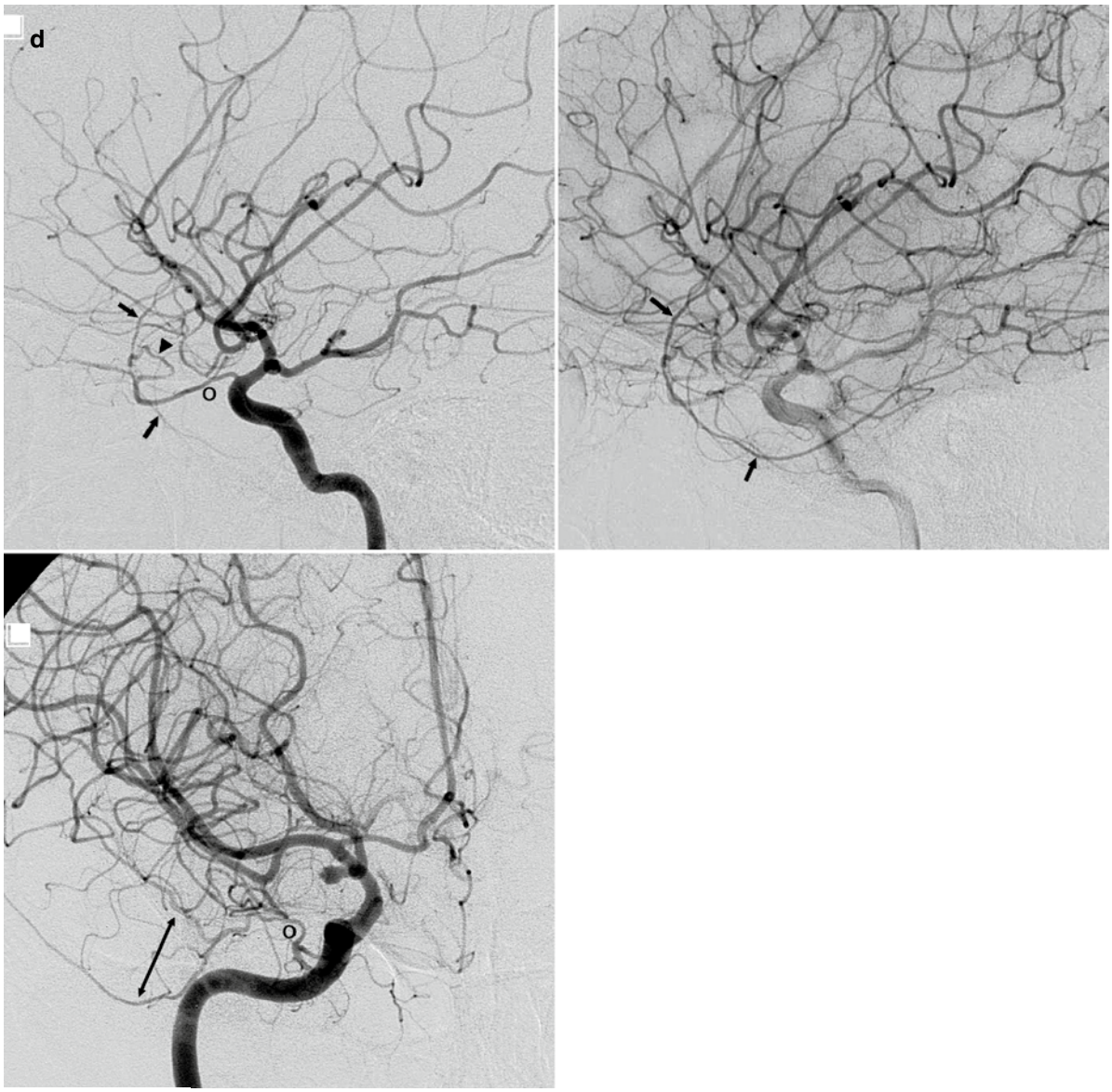

Fig. 2.4 (continued)

together with the nerve, the orbita through the optic canal. Initially, the artery runs inferolaterally to the optic nerve (first segment), then crosses the nerve forming a bend below or above the nerve (second segment), and runs further medially and parallel to it (third segment). It gives off three types of branches: ocular, orbital, and extraorbital.

The ocular branches include the central retinal artery and the ciliary arteries supplying partially the optic nerve and the ocular bulb. These are the first branches arising where the artery crosses the nerve.

The orbital branches include the lacrimal artery, which supplies the lacrimal gland and conjunctiva. An important branch, sometimes present, is the recurrent meningeal artery, which runs backward and passes through the superior orbital fissure, anastomosing with branches of the middle meningeal artery (MMA).

Anastomosis of the lacrimal artery with the anterior deep temporal artery can be an important collateral circulation via the OA in occlusion of the ICA (Fig. 3.12). Other branches are the muscular arteries, which supply the muscle and orbital periosteum.

The extraorbital branches are numerous. They include the posterior and anterior ethmoidal arteries. The posterior arise from the first segment, the anterior from the third. These branches have an ascending course, pass through the lamina cribrosa, supplying the dura of the basal anterior cranial fossa. The anterior falx artery arises from the anterior ethmoidal artery and supplies the falx, anastomosing with the falx branches of the MMA. There are anastomoses between the ethmoidal arteries and the internal maxillary artery (IMA) through its sphenopalatine branches. From the latter arise small vessels with an ascending course; they anastomose with the corresponding descending branches that arise from the ethmoidal arteries. These arteries are typically involved in the vascularization of meningiomas of the basal anterior cranial fossa (Bradac et al. 1990) and in frontobasal dural fistulas (Figs. 3.25, 13.6, and 13.13).

Other arteries of this group are the supraorbital (frequently the most prominent), the dorsonasal, the medial palpebral, and the supratrochlear. These branches anastomose with branches of the ECA, in particular with the facial artery, infraorbital branch of the IMA, and frontal branches of the superficial temporal artery. Such anastomoses may be collateral via the OA toward the ICA when the latter is occluded (Fig. 3.12).

On an angiogram (Vignaud et al. 1972; Huber 1979; Morris 1997; Osborn 1999), the OA is always visible; it is better defined in the lateral view. From its origin, it runs superiorly for 1–2 mm, then anteriorly, forming a slight curve with inferior convexity. About 2 cm from its origin, the OA curves abruptly and crosses the optic nerve. Among its branches, the central retinal and ciliary arteries are sometimes recognizable, arising at the level of the above-described curve (Fig. 2.5). Thus, in embolization procedures involving the OA, the microcatheter should be advanced distally to the above-described curve. The blush corresponding to the plexus of the ocular choroid is always visible as a crescent-shaped structure. The ethmoidal arteries are occasionally evident, especially in the lateral view. The anterior falx artery is also easily identifiable, when present, on a lateral angiogram. These arteries can be well developed if involved in pathological processes (Figs. 3.25, 13.6, and 13.13). The other branches are difficult to recognize under normal conditions.

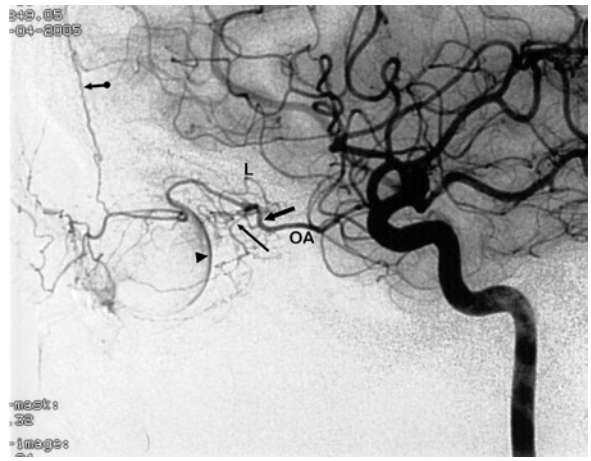

Fig. 2.5 Lateral ICA angiogram. Ophthalmic artery (*OA*). Bend of the artery around the optic nerve (*large arrow*). In this area arises the ocular complex comprising the retina and cilial arteries (*small arrow*). Choroid plexus (*arrowhead*), lachrymal artery (*L*), anterior falx artery (*arrow with dot*)

To explain some variants of the OA, it is useful to recall the most important aspects of its embryogenesis (Hayreh and Dass 1962a, 1962b; Hayreh 1962; Lasjaunias and Berenstein 1987). The definitive OA develops from three sources: the *primitive dorsal* OA, arising in the intracavernous portion of the ICA and entering the orbita through the superior orbital fissure; the *primitive ventral* OA, arising from the anterior cerebral artery and entering the orbita through the optic canal; and the *stapedial artery* (StA), which gives off an orbital branch entering the orbita through the superior orbital fissure. Inside the orbita and around the optic nerve, an arterial anastomotic circle is formed among these three arteries. In the further evolution, the proximal segment of the primitive ventral OA disappears, arising now from the supracavernous portion of the ICA. This artery will become the definitive OA. The primitive dorsal OA regresses, and the intraorbital branches of the StA are annexed by the definitive OA. In this process, important changes can involve the StA, some details of which are presented here.

The StA is the main branch of the hyoid artery (embryonic vessel), arising from the petrous segment of the ICA, which in this phase of embryogenesis is still very small and incompletely developed. The StA enters the middle cranial cavity, passing through the tympanic cavity and dividing into intracranial and extracranial branches (Moret et al. 1977; Lasjaunias and Berenstein 1987). The intracranial branch (supraorbital artery) is anteriorly directed, supplies the dura of the middle cranial fossa, and extends into the orbita, with a medial and lateral (lacrimal) branch. These branches enter the orbita through the superior orbital fissure. In some cases, the lacrimal artery penetrates as an isolated branch through the foramen of Hyrtl, located in the greater wing of the sphenoid bone. The second branch (maxillomandibular artery) is extracranial and passes through the foramen spinosum, anastomosing with the embryonic ECA, from which arise later the IMA and the MMA.

The StA disappears, but in some cases its first segment can persist as a small artery (caroticotympanic branch of the ICA). The extracranial segment becomes the MMA, arising from the developed final IMA; the intracranial segment in the middle cranial fossa partially regresses and is partly annexed by the MMA. The blood flow is now reversed, being intracranial. The intraorbital segment is annexed by the OA.

The embryological evolution can vary and lead to a series of conditions with different angiographic patterns (McLennan et al. 1974; Moret et al. 1977; Lasjaunias and Berenstein 1987; Morris 1997; Perrini et al. 2007). We describe here the most frequent.

- The proximal part of the primitive ventral OA does not regress and so the OA arises from the anterior cerebral artery. This is a very rare condition.
- The primitive ventral OA disappears instead of the primitive dorsal OA, leading to an intracavernous origin of the OA (Figs. 2.4 and 4.8c, d).
- The proximal part of the OA disappears, though the intraorbital section of the StA remains and is connected at the level of the superior orbital fissure with the MMA. In such cases, the OA is only visible on the ECA, not ICA, angiogram (Fig. 2.4b, c).
- The lacrimal branch can persist as an isolated branch of the MMA (meningolacrimal artery), entering the orbita through the foramen of Hirtl and supplying partially the intraorbital structures, while the ocular and neuronal branches arise from the OA. In such cases, the orbital vascularization is partially visible on the ECA and ICA angiogram. There are commonly no anastomoses between these two systems. In other cases, the MMA gives off a branch, which enters the orbita through the superior orbital fissure and anastomoses with the lacrimal branch of the OA.
- Another condition is characterized in addition to the MMA by the presence of the recurrent meningeal artery (Figs. 13.8, 3.20, and 3.25). This is a meningeal branch, arising from the OA in its initial segment or from the lacrimal branch; it runs posteriorly through the superior orbital fissure, supplying the dura in the area of the cavernous sinus and tentorium, where it anastomoses with other branches involved in the supply of this region.
- The MMA arises from the OA, and so it is only recognizable on the ICA angiogram. This occurs when the intracranial part of the MMA does not develop; the proximal part of the intraorbital-transsphenoidal segment of the StA does not regress and anastomoses with the lacrimal branch of the OA (Fig. 2.4d).
- The MMA originates in the petrous segment of the ICA: this occurs when the first and intracranial segments of the STA do not regress and the extracranial portion of the MMA does not develop. In the skull CT, the foramen spinosum is not present, and the MMA is only visible on the ICA angiogram.

2.4.1.2 The Superior Hypophyseal Artery

The superior hypophyseal artery (SHA) is a group of small branches arising commonly from the posteromedial surface of the ophthalmic segment of the ICA. The SHA supplies the infundibulum, anterior lobe of the pituitary gland, and partially the optic nerve, chiasma, and floor of the III ventricle. The SHA is not recognizable on a normal angiogram. The ophthalmic segment is a typical site of aneurysms (carotid-ophthalmic and SHA aneurysms).

2.4.1.3 Supply of the Pituitary Gland

The adenohypophysis is supplied by the superior hypophyseal arteries. These run toward the pituitary stalk, where they connect with a network of capillaries continuing in venules forming the so-called venous portal system, through which flow the releasing and release-inhibiting hormones from the hypothalamus to the adenohypophysis. The neurohypophisis is supplied by the inferior hypophyseal artery. Each half of the pituitary gland drains into the corresponding cavernous sinus, which continues into the inferior petrosal sinus.

2.4.2 In the Communicating Segment Arises the PcomA

The PcomA arises from the posterior surface of the ICA. It runs posteriorly and medially to join the posterior cerebral artery (PCA) in a close relationship with cranial nerve III, which is laterally and sometimes medially located (Gibo et al. 1981). An anomalous origin from the OA has been reported (Bisaria 1984).

Commonly, the PcomA is slightly smaller than the PCA. The PcomA may, however, be very large, continuing directly into the PCA. This variant is termed the "fetal" origin of the PCA. Indeed, in the embryonic phase, the PCA takes its origin from the ICA, while the connection of the PCA with the basilar artery through the P1 segment develops later. In the further evolution, the PcomA (pars carotica of the PCA) becomes hypoplastic or regresses entirely, while the P1 segment (pars basilaris of the PCA) becomes well developed. This evolution occurs in about 70% of cases (Zeal and Rhoton 1978; Huber 1979; Pedroza et al. 1987).

A slight widening of the origin of the PcomA is not rare. It has been described in 6.5% of normal angiograms (Hassler and Saltzmann 1967), and it has been interpreted as an early stage of aneurysm formation. Other studies (Epstein et al. 1970) made on autopsy specimens have demonstrated neither an aneurysmal nor preaneurysmal aspect.

From the PcomA arise many perforating branches. Since the first description by Duret (1874), many anatomical studies have been performed (Foix and Hillemand 1925a, b; Lazorthes and Salamon 1971; Saeki and Rhoton 1977a, b; Zeal and Rhoton 1978; Gibo et al. 1981; Pedroza et al. 1987; Tatu et al. 2001; Ono et al. 1984), and these arteries have been variously termed tuberothalamic, premammillary, and anterior thalamoperforating arteries. The latter definition seems to be the most appropriate and is the one we will adopt. Many branches are present, also in cases of a smaller PcomA. Among them, there is sometimes a large branch arising in front of or beside the mammillary body (Gibo et al. 1981; Pedroza et al. 1987). These perforators supply the posterior part of the chiasma, the optic tract, and the mammillary body; they enter the posterior perforated substance, supplying the hypothalamus, subthalamus, and anterior thalamus. Some authors (Gibo et al. 1981) have found that they supply also the posterior limb of the internal capsule.

A precise angiographic study of the PcomA is possible only by performing carotid and vertebral angiograms. Depending on its caliber and flow effects, the PcomA is visible on both lateral angiograms or on only one (Figs. 2.6, 7.3, 7.9, 6.8, 15.9 and 15.10). The perforators on the lateral vertebral angiogram are evident as small branches, running upward and slightly backward (Fig. 7.6). In the angio-MRI, the PcomA, P1, and PCA complex can be well identified (Figs. 7.2 and 7.9d). Perforators are not commonly visible.

2.4.3 In the Choroidal Segment Arise the Anterior Choroidal Artery and Often Perforators Directly from the ICA

2.4.3.1 The Anterior Choroidal Artery

In all cases studied by Rhoton et al. (1979), the anterior choroidal artery (AChA) arose from the posterior surface of the ICA (2–4 mm distal to the PcomA) and, more laterally, to the site of origin of the PComA. The AChA can be divided into a cisternal segment, from its origin to the choroid fissure, and a distal plexal segment (Goldberg 1974; Rhoton et al. 1979). The cisternal segment, from which arise the main supplying branches for the parenchyma, has an average length of 25 mm (Otomo 1965; Rhoton et al. 1979). The artery runs first posteromedially below the optic tract, then

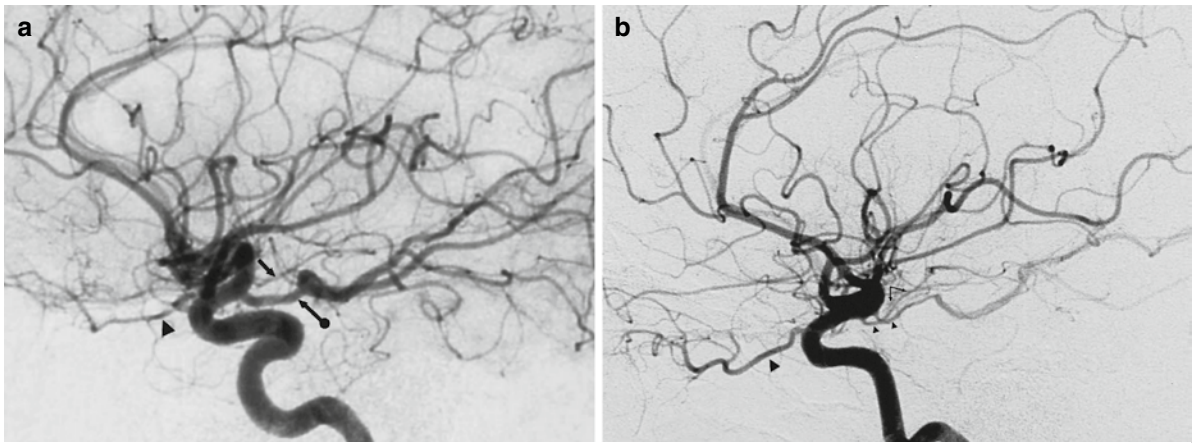

Fig. 2.6 (**a**) Lateral carotid angiogram. Large posterior communicating artery (PComA, *arrow with dot*), anterior choroidal artery (*arrow*), ophthalmic artery (*arrowhead*). (**b**) Small PComA (*arrowhead*) continuing in the posterior cerebral artery. Anterior choroidal artery (*arrow with angle*), ophthalmic artery (*large arrowhead*). Owing to overlap, the anterior choroidal artery erroneously seems to arise proximally to the PComA. This extremely rare condition can occur and should identified by complementary projection

turns laterally into the circumpeduncular cistern around the midbrain; it then runs toward the lateral geniculate body, where it curves sharply, entering the temporal horn through the choroid fissure and joining the choroid plexus. The artery extends posteriorly, reaching the atrium, where it can anastomose with branches of the posterolateral choroidal artery. Rarely, it extends anteriorly toward the foramen of Monro, supplying the plexus and anastomosing with the posterior medial choroidal artery.

The AChA gives off many branches: perforator branches arise from the cisternal segment and penetrate the APS, posteriorly to the perforators of the A1 segment and ICA and medially to those of the MCA. The supplied vascular territories can be divided into superior, lateral, and medial groups (Abbie 1933; Carpenter et al. 1954; Rhoton et al. 1979; Duvernoy 1999; Tatu et al. 2001). The superior group supplies the optic tract, the medial part of the globus pallidus, the tail of the nucleus caudatus, sometimes the genu of the internal capsule (Goldberg 1974), and the inferior part of the posterior limb of the internal capsule, together with its retrolenticular and optic radiations. According to some authors (Hupperts 1994), the AChA also supplies the parietal periventricular area. The lateral group supplies the uncus, amigdala, and hippocampus (Rhoton et al. 1979). The medial group supplies the anterolateral midbrain and lateral geniculate body (Rhoton et al. 1979).

There is a marked interchangeability in the vascular territories described among the AChA, ICA, PCA, PcomA, and MCA (Rhoton et al. 1979). Moreover, there are rich anastomoses between the AChA and PCA via the choroidal arteries and through branches on the surface of the lateral geniculate body and on the temporal lobe near the uncus. All these factors make it difficult to predict the effect of occlusion of the AChA (Rhoton et al. 1979; Friedman et al. 2001).

The artery is commonly well visible on anteriposterior (AP) and LL angiograms. On the lateral angiogram, the artery runs backward, forming an upward convex curve. It runs further downward and enters the choroid fissure (plexal point). The plexal segment extends posteriorly into the temporal horn toward the atrium and lateral ventricle, showing a typical blush in the late arterial-capillary phase. On the AP angiogram, the AChA runs first medially and then laterally, surrounding the cerebral peduncle, mixing with perforators of the middle cerebral artery (Figs. 2.6–2.8).

Many anomalies concerning the origin and development of the AChA have been described. A few cases of origin have been reported from the PcomA or middle cerebral artery (Carpenter et al. 1954; Otomo 1965; Herman et al. 1966; Lasjaunias and Berenstein 1990)

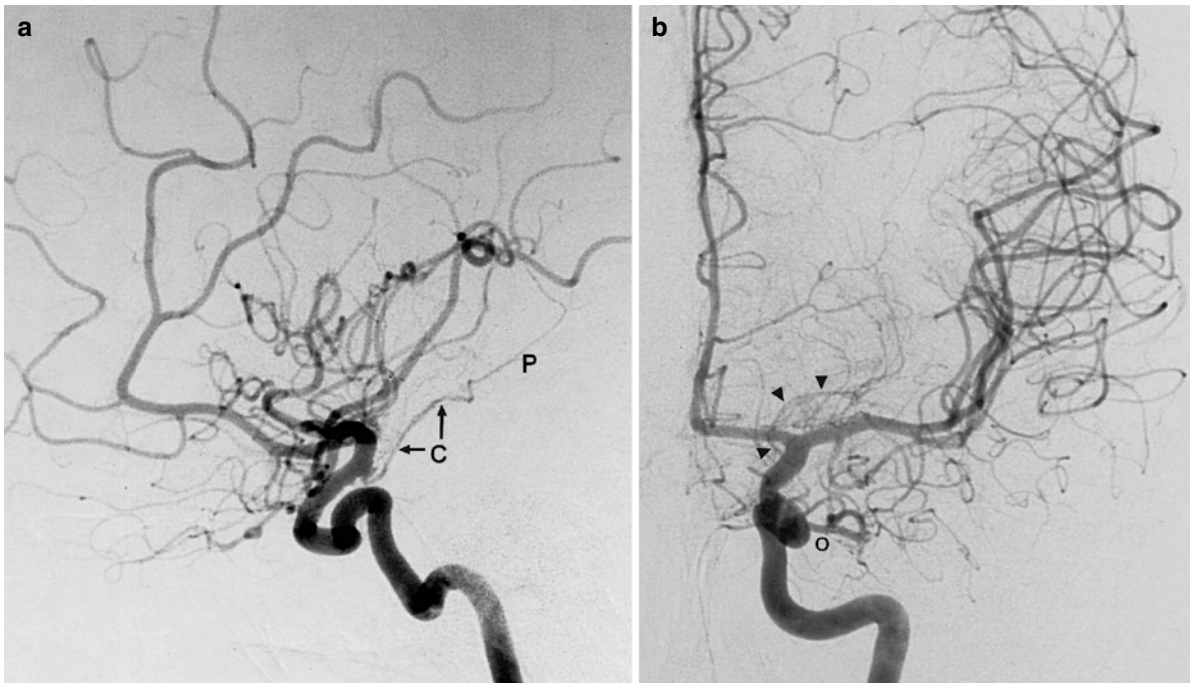

Fig. 2.7 (**a**) Lateral carotid angiogram. Anterior choroidal artery with its cisternal (*C*) and plexal (*P*) segments. (**b**) Carotid angiogram, AP view. Course of the anterior choroidal artery (*arrowhead*)

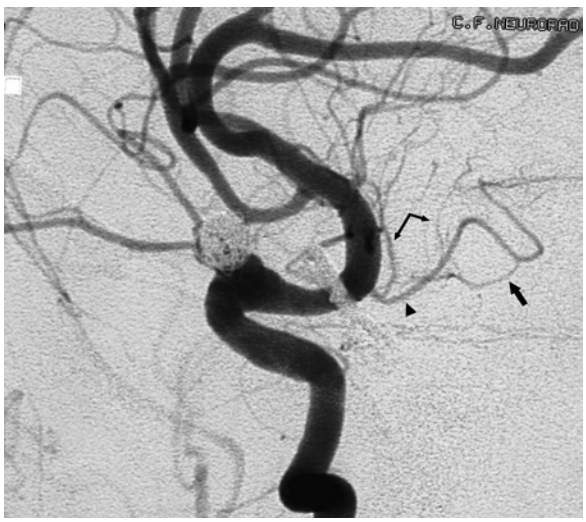

Fig. 2.8 Carotid angiogram (*oblique view*) in a patient with aneurysm treated with coils. Anterior choroidal artery (*arrowhead*). Large perforators directed superiorly are well evident (*arrow with angle*) as well as a large uncal branch (*arrow*). The "clip" projecting on the ICA was used to treat a contralateral aneurysm

and from the ICA proximal to the PcomA (Moyer and Flamm 1992) as well as a case of aplasia (Carpenter et al. 1954). In a more recent extensive study (Takahashi et al. 1990) considering also previous works (Theron and Newton 1976; Saeki and Rhoton 1977; Takahashi et al. 1980), the anomalies concerning the development of the AChA were classified into two groups: hypoplastic and hyperplastic forms. In the first, which is less common, the distal segment (plexal) is hypoplastic and thus not recognizable on an angiogram. In the hyperplastic group, the artery is well developed, taking over partially or completely the vascular territory of the PCA (Fig. 2.8). In some cases, it is difficult to establish whether the situation is one of hypertrophic branches of the AChA or a duplicated PCA (Fig. 7.10).

2.4.3.2 The Perforators of ICA

The perforators of the ICA also arise from the choroidal segment of the ICA, typically from its posterior wall.

They enter the APS and supply the genu of the capsula interna, its posterior limb, and the adjacent part of the pallidum. They can replace perforators of the AChA and parts of perforators of the MCA and vice versa. The perforators are rarely evident on an angiogram.

2.5 Congenital Anomalies of the ICA

These are very uncommon. They are characterized by an anomalous origin from the aortic arch, an aberrant course, and hypo- or aplasia of the artery.

- Cases of hypo- or aplasia can be suspected in CT or MRI, showing, respectively, a small or absent carotid canal and reduction or absence of blood flow. Various type of collateral circulation may be present, involving the circle of Willis. A particular form is characterized by the persistence of the primitive maxillary artery, arising at the cavernous portion of the ICA, leading to an intrasellar anastomosis connecting both ICAs (Lasjaunias and Berenstein 1987; Gozzoli et al. 1998) (Fig. 2.9). This anomaly is very rare; however, it should be taken into consideration in particular in patients in whom a transsphenoidal surgery for intrasellar adenoma is planned. Cases associated with hypopituitarism have been reported (Mellado et al. 2001; Moon et al. 2002).
- Other anomalies are the embryogenic persistence of the connection between the carotid and vertebrobasilar circulation, which normally disappears. Considering these in the craniocaudal direction, the first is represented by the so-called fetal PCA (see Sect. 2.4.2 and Chap. 7). The second most frequent, with an incidence of 0.1–0.2% (Lie 1968; Huber 1979), is the primitive trigeminal artery, which connects the cavernous portion of the ICA with the basilar artery. The primitive trigeminal artery runs in a parasellar or intrasellar fashion and can have contact with the trigeminal nerve. It may be associated with other vascular malformations, particularly aneurysms (Ahmad et al. 1994). The vertebral and proximal basilar arteries are frequently hypoplastic or can be normally developed (Ohshiro et al. 1993). Conversely, this connection may be a collateral circulation from the basilar artery toward the ICA in the case of agenesis of this artery (Lasjaunias and Berenstein 1987) (Fig. 2.10).
- Other less frequent carotid-basilar anastomoses are persistent otic, hypoglossal, and proatlantal arteries. The otic artery connects the petrous ICA with the basilar artery. There are only a few angiographic reports about this anomaly (Reynolds et al. 1980). The persistent hypoglossal artery arises from the cervical ICA at the level of C1–C2 (Kanai et al. 1992), runs dorsally, entering the hypoglossal canal, which is enlarged (visible on the CT skull base), and joins the vertebral artery. The association with aneurysm has been reported (Brismar 1976; Kanai et al. 1992). The vertebral arteries are hypoplastic or absent (Fig. 2.10). The persistent proatlantal artery arises from the cervical ICA or from the ECA, runs dorsally, reaches the atlas and runs horizontally above it, where it connects with the extradural vertebral artery, which is hypoplastic or absent.
- Another rare condition is the origin of the superior cerebellar artery, anterior inferior cerebellar artery, and posterior inferior cerebellar artery from the cavernous portion of the ICA (Scotti 1975; Haughton et al. 1978). This has been interpreted (Lasjaunias and Berenstein 1990) as a partial trigeminal persistence.
- A particular form of aberrant ICA is that in which the artery passes through the temporal bone, more posteriorly than in normal cases, laterally to the jugular bulb and adjacent to the stylomastoid foramen. As it enters the middle ear cavity, the ICA sharply turns medially and anteriorly. This anomaly has been interpreted as an agenesis of the terminal part of the cervical ICA, with the formation of a collateral circulation between the enlarged tympanic branch of the APhA and the caroticotympanic branch remnant of the StA. CT of the skull discloses the presence of a soft tissue mass protruding in the tympanic cavity. Angiographic study clarifies the diagnosis with a small suspected tympanic paraganglioma (Lo et al. 1985; Osborn 1999) (Fig. 2.11).

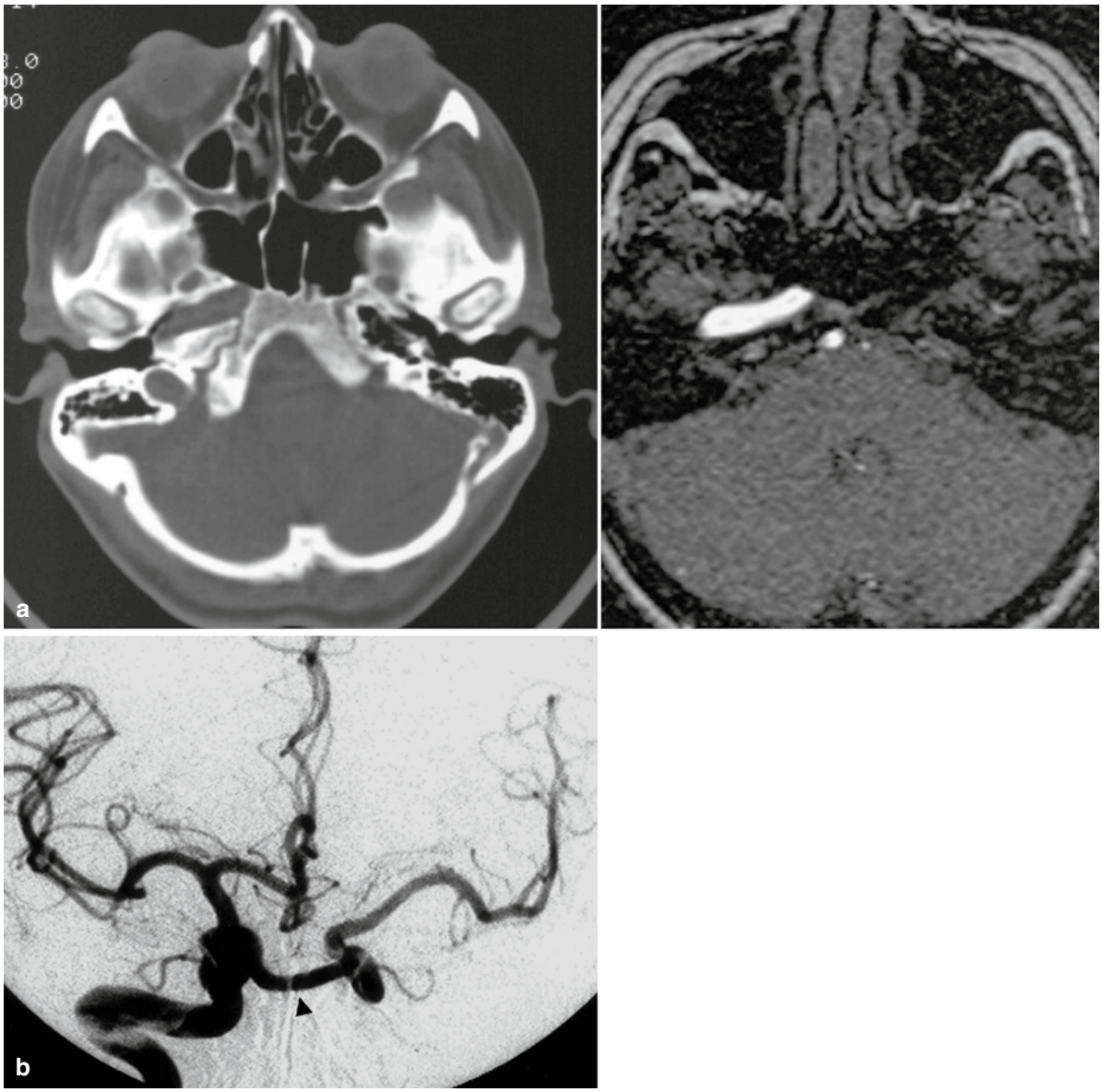

Fig. 2.9 Aplasia of the ICA. (**a**) CT and MRI showing, respectively, that the canal of the horizontal portion of the petrous segment of the ICA on the left is absent and the typical flow signal is only recognizable on the right. (**b**) Right carotid angiogram, AP view. There is filling of the cavernous portion of the left ICA through intrasellar anastomosis (*arrowhead*) corresponding to the primary maxillary artery. There is further filling of the middle cerebral artery. The A1 segment is aplastic

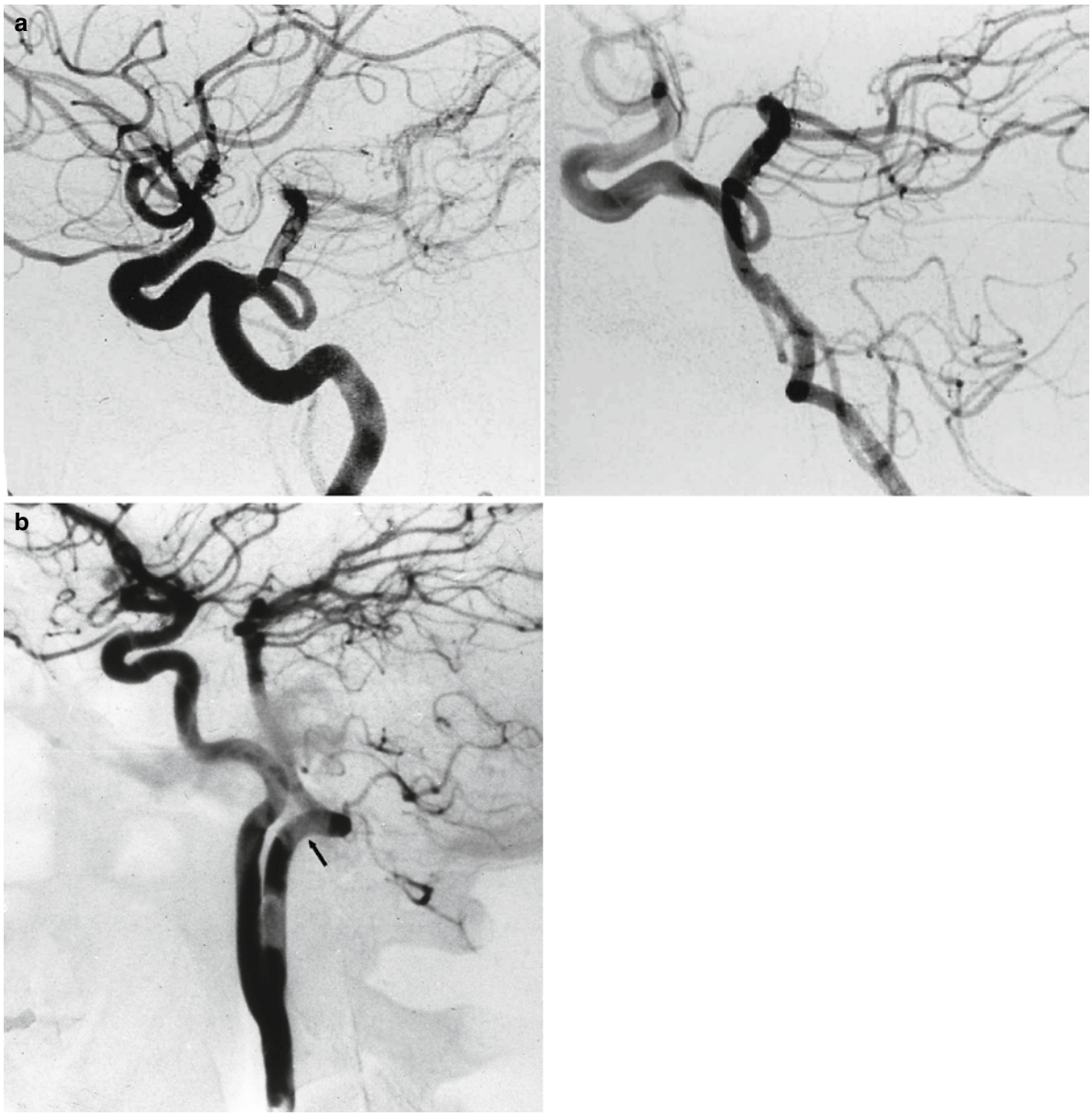

Fig. 2.10 Embryogenic connections between the ICA and vertebrobasilar circulation. (**a**) Persistent primitive trigeminal artery connecting the cavernous portion of the ICA with the basilar artery. The connection is visible on the carotid and vertebral angiograms. (**b**) Persistent hypoglossal artery arising from ICA, entering the hypoglossal canal (*arrow*) and anastomosing with the vertebral artery

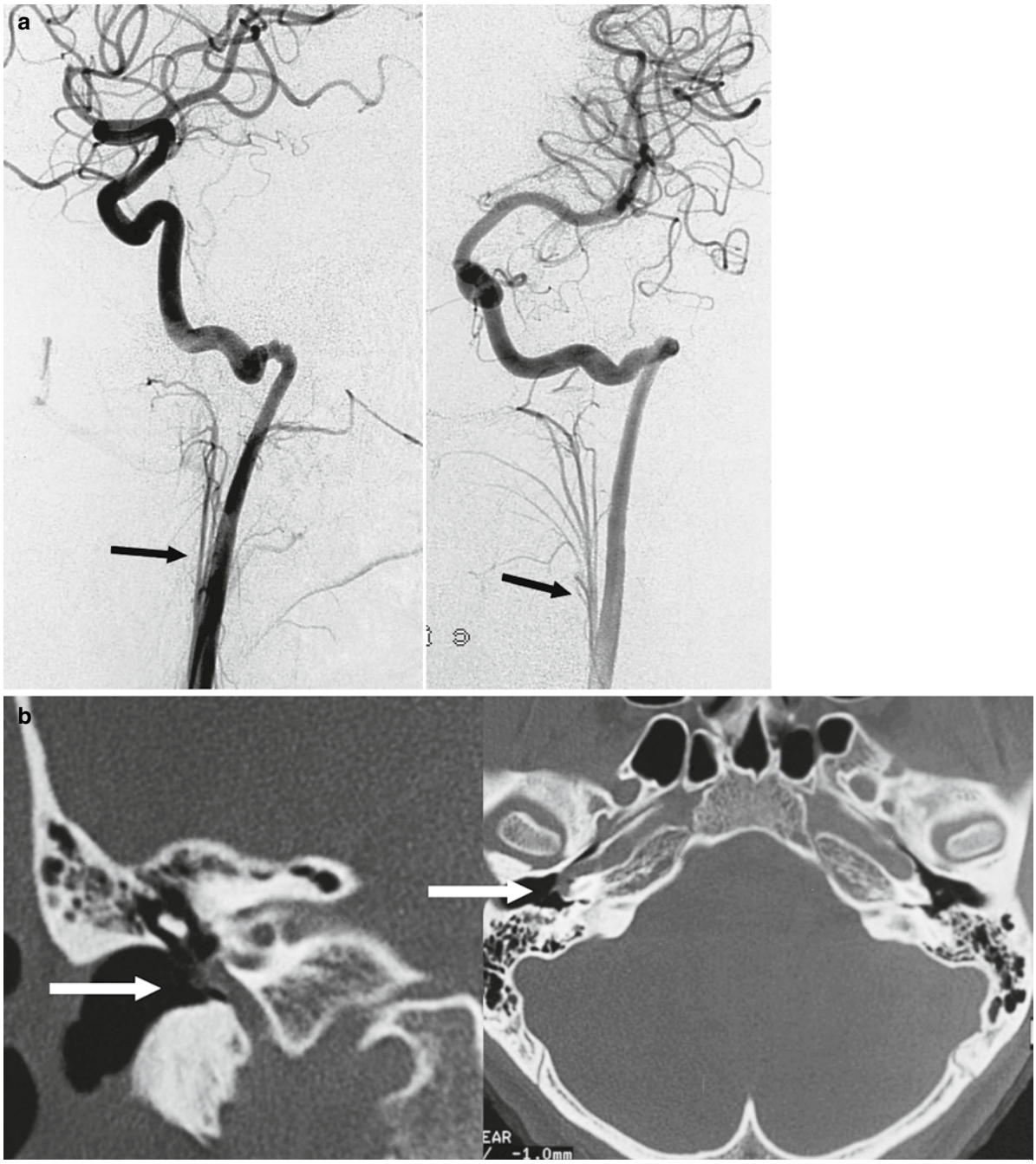

Fig. 2.11 Aberrant course of the ICA. (**a**) Lateral and AP angiogram of internal carotid artery. Origin of the APhA (*arrow*) from the ICA. The ICA runs more posteriorly on the lateral angiogram and more laterally in the AP view. (**b**) CT, coronal and axial view. The ICA enters the middle ear cavity and is visible as a small, rounded, soft-tissue structure (*arrow*)

External Carotid Artery

3

The external carotid artery (ECA) arises from the common carotid bifurcation at the C4 vertebral level. A more proximal or distal origin can occur. Variants of the level of the carotid bifurcation are described in Chap. 2. These variants also involve indirectly the origin of the ECA. The ECA may originate directly from the aortic arch. The ECA lies in the carotid space, initially medial and anterior to the internal carotid artery (ICA), seldom lateral to it. More cranially, the ECA runs anterolateral to the ICA. The jugular vein lies posterolateral to the ICA and ECA. The ECA is covered partially by the sternomastoid muscle and crossed by cranial nerve XII. The vagus nerve lies medially. During its course, the ECA gives off several branches. Near the mandibular condyle within the parotid gland, it divides into its terminal branches (Figs. 3.1 and 2.1).

3.1 Superior Thyroid Artery

The superior thyroid artery arises from the anterior wall of the ECA. It runs inferiorly and somewhat medially toward the thyroid gland. The superior thyroid artery gives off branches for the superior part of

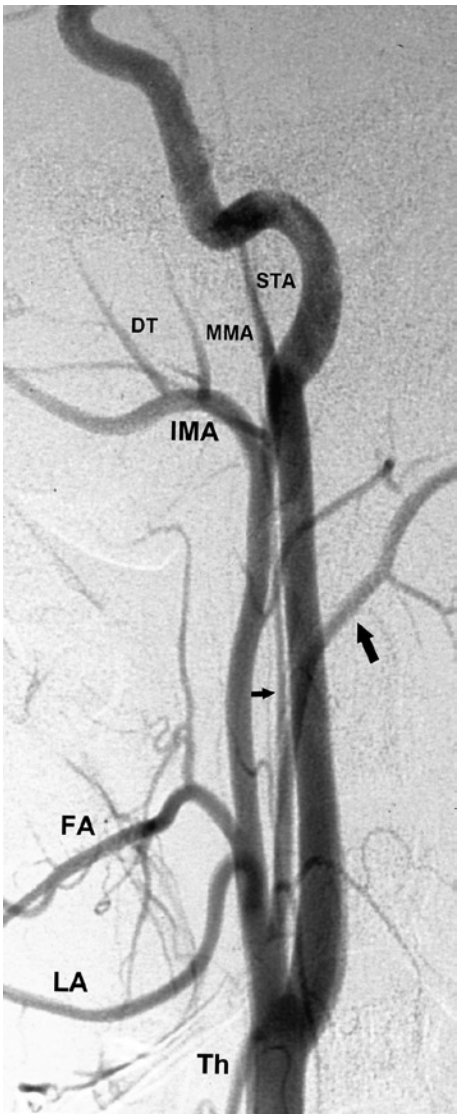

Fig. 3.1 Common carotid angiogram, lateral view, showing the anterior course of the external carotid artery related to the internal carotid artery. Some of the main branches are recognizable. Superior thyroid artery (*Th*), lingual artery (*LA*), facial artery (*FA*), occipital artery (*large arrow*), ascending pharyngeal artery (*small arrow*), internal maxillary artery (*IMA*), middle meningeal artery (*MMA*), middle deep temporal artery (*DT*), superficial temporal artery (*STA*)

G.B. Bradac, *Cerebral Angiography*,
DOI: 10.1007/978-3-642-15678-6_3, © Springer-Verlag Berlin Heidelberg 2011

the thyroid gland and larynx. It anastomoses with the inferior thyroid artery, a branch of the thyrocervical trunk, arising from the subclavian artery (Figs. 3.1 and 2.1).

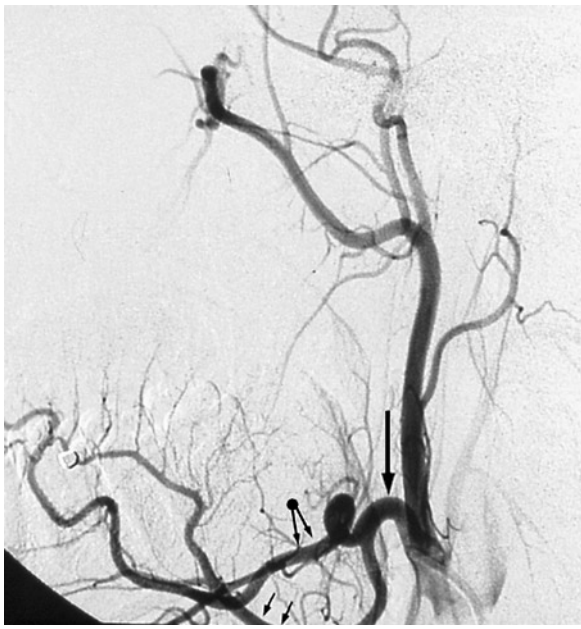

Fig. 3.2 External carotid artery angiogram, lateral view, showing the common trunk of origin (*large arrow*) of the lingual (*small arrows*) and facial arteries (*arrows with dot*)

3.2 Lingual Artery

The lingual artery is the second branch of the ECA and arises from its anterior wall. It is not exceptional for the lingual artery to have a common trunk with the facial artery. It gives off branches for the sublingual and submandibular glands, the pharynx and mandibular mucosa, and the muscle of the floor of the mouth. Its terminal branch is the deep lingual artery, which supplies the muscle and lingual mucosa. On the angiogram, the lingual artery is easy to recognize, especially in the lateral view, because of its course, first upward, then downward, and finally upward again, forming a gentle curve that is superiorly concave. The ascending branches, which supply the tongue, are easily recognizable. Among the lingual artery's branches, the dorsal lingual artery and the sublingual artery, which runs inferiorly to the deep lingual artery, are frequently identifiable. The sublingual artery anastomoses through its submental branch with the corresponding branch of the facial artery (Figs. 3.1–3.3).

3.3 Facial Artery

The facial artery is the third branch arising from the anterior wall of the ECA, sometimes with a unique trunk from that of the lingual artery. It runs forward,

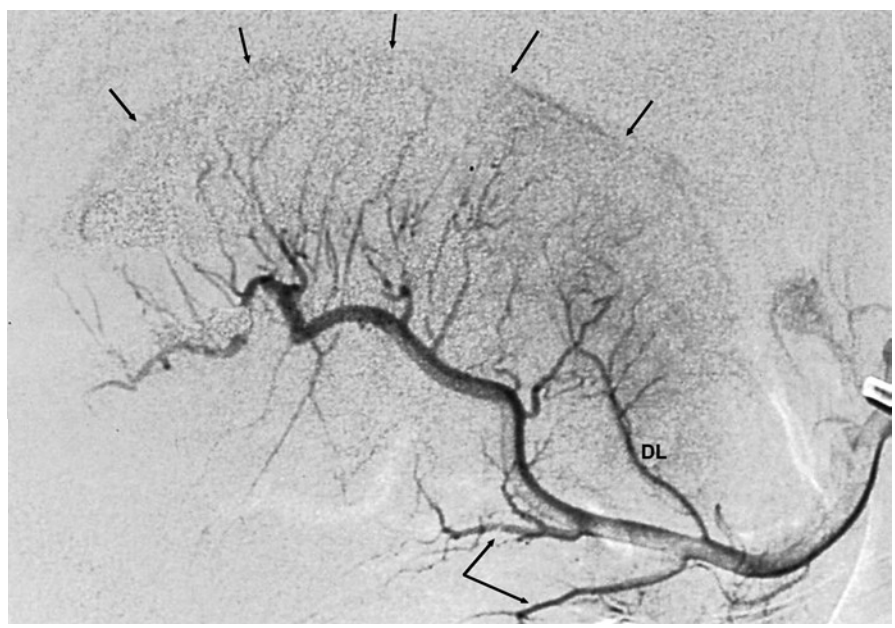

Fig. 3.3 Selective angiographic study of the lingual artery. Branches for the tongue (*arrows*) arising from the main trunk and dorsal lingual artery (*DL*). Sublingual branches (*arrow with angle*)

with an undulating course above the submandibular gland, to which it gives off some branches that are occasionally well developed; the facial artery then curves around the lower edge of the mandible, continuing anteriorly and superiorly and crossing the cheek before ending in the medial angle of the orbita as an "angular artery." The latter anastomoses with branches of the ophthalmic artery, which can establish a collateral circulation when the ICA is occluded (Fig. 3.12). Along its course, the facial artery can anastomose with the transverse facial artery and with branches of the internal maxillary artery (IMA), especially with the infraorbital, buccal, and masseter arteries.

The facial artery gives off branches for the submandibular gland, masseter muscle, mandible, skin and muscle of the submental area, and the cheek, nose, and lip. From its initial segments arises the ascending palatine artery, which anastomoses with the pharyngeal branches of the ascending pharyngeal artery (APhA) and with the descending palatine artery of the IMA. The ascending palatine artery can be hypoplastic and replaced by branches of the APhA. The facial artery may be hypoplastic and represented only by the submental artery. In such cases, part of its vascular territories become replaced by the lingual artery, transverse facial artery, and infraorbital artery (Djindjian and Merland 1978; Lasjaunias and Berenstein 1987).

The initially descending and then the obliquely ascending course of the facial artery is easily discerned on the lateral angiogram. Among its branches, the ascending palatine artery, artery for the submandibular gland, and submental artery are the most frequently identifiable (Figs. 3.1, 3.2, and 3.4).

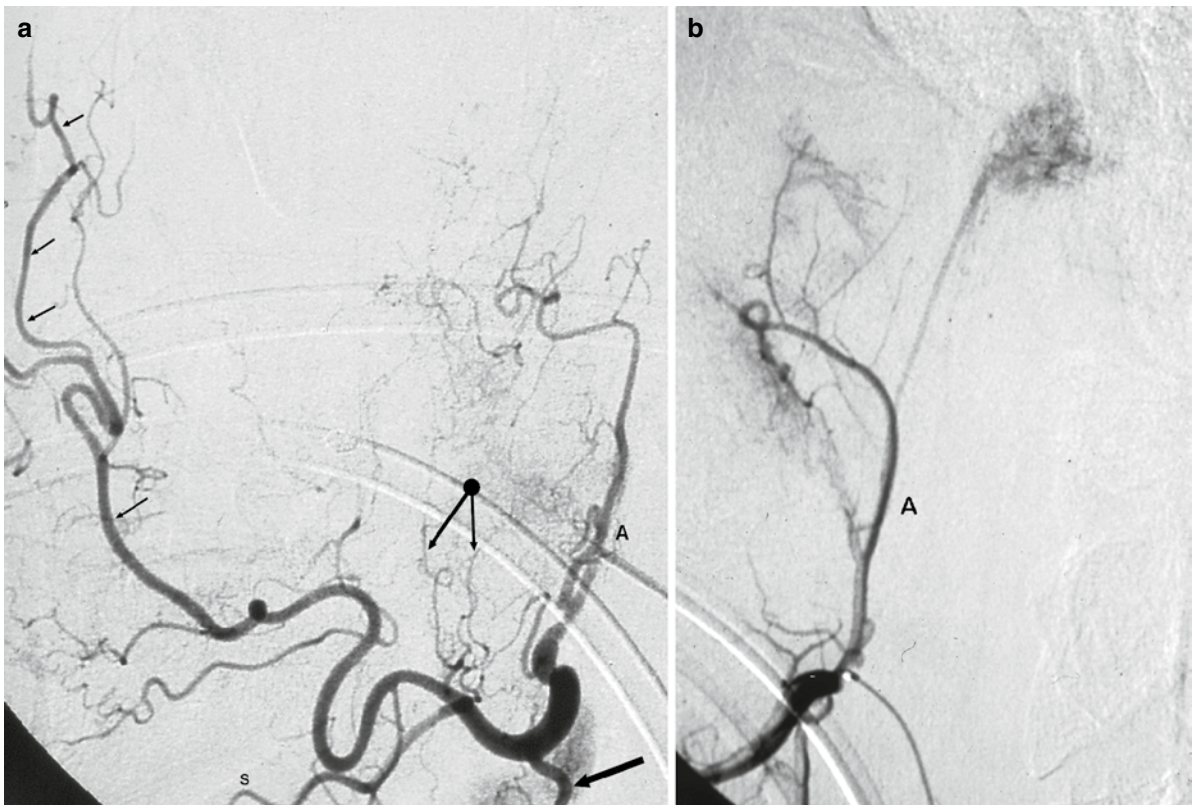

Fig. 3.4 (**a**) Selective angiographic study of the facial artery. Ascending palatine artery (*A*). Branches for the submandibular gland (*arrow*) and masseter muscle (*arrow with dot*). Submental artery (*S*), distal branches (*small arrows*) ending in the angular artery. (**b**) Different patient, selective study of the facial artery. Ascending palatine artery (*A*), from which arises a branch supplying a large vagal paraganglioma

3.4 Ascending Pharyngeal Artery

The APhA is a small vessel that arises from the posterior wall of the ECA, sometimes from the carotid bifurcation or from the proximal segment of the ICA. The APhA can also arise sharing a common trunk with the occipital artery. It runs upward adjacent to the ICA, posteriorly and medially to it (Figs. 3.5 and 3.6).

The APhA gives off pharyngeal branches for the paramedian mucosa of the naso-oro-pharynx, which are divided into superior, middle, and inferior branches. The superior branch can anastomose with pharyngeal branches coming from the accessory meningeal artery and pterygovaginal artery, both branches of the IMA. The middle branches anastomose with the ascending palatine artery of the facial artery, and, when present, with the mandibular artery, an embryological remnant arising from the ICA.

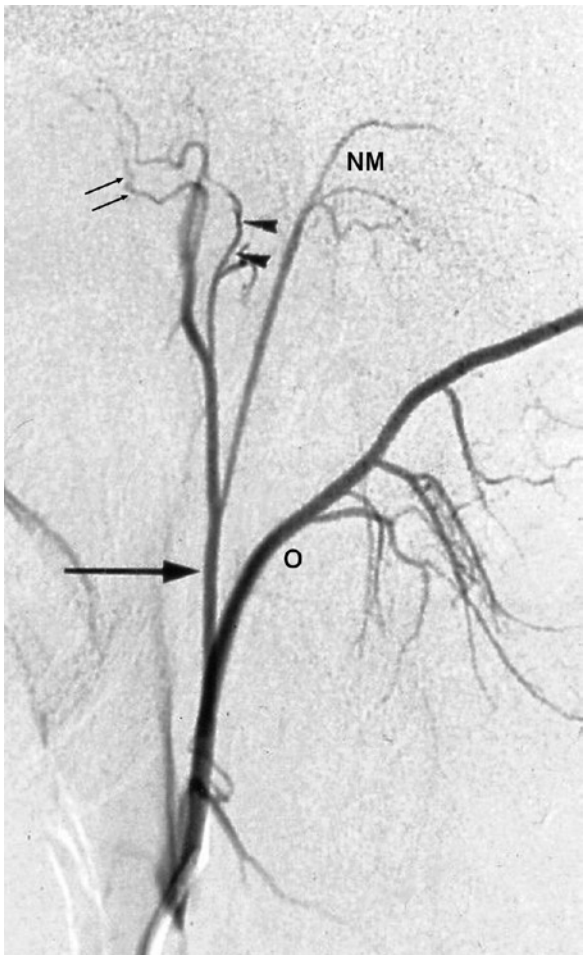

Fig. 3.5 Selective angiographic study, lateral view of the common trunk of the ascending pharyngeal and occipital arteries. Occipital artery (*O*), ascending pharyngeal artery (*arrow*) with its tympanic branches (*arrowhead*), superior pharyngeal branches (*small arrows*) and neuromeningeal trunk (*NM*)

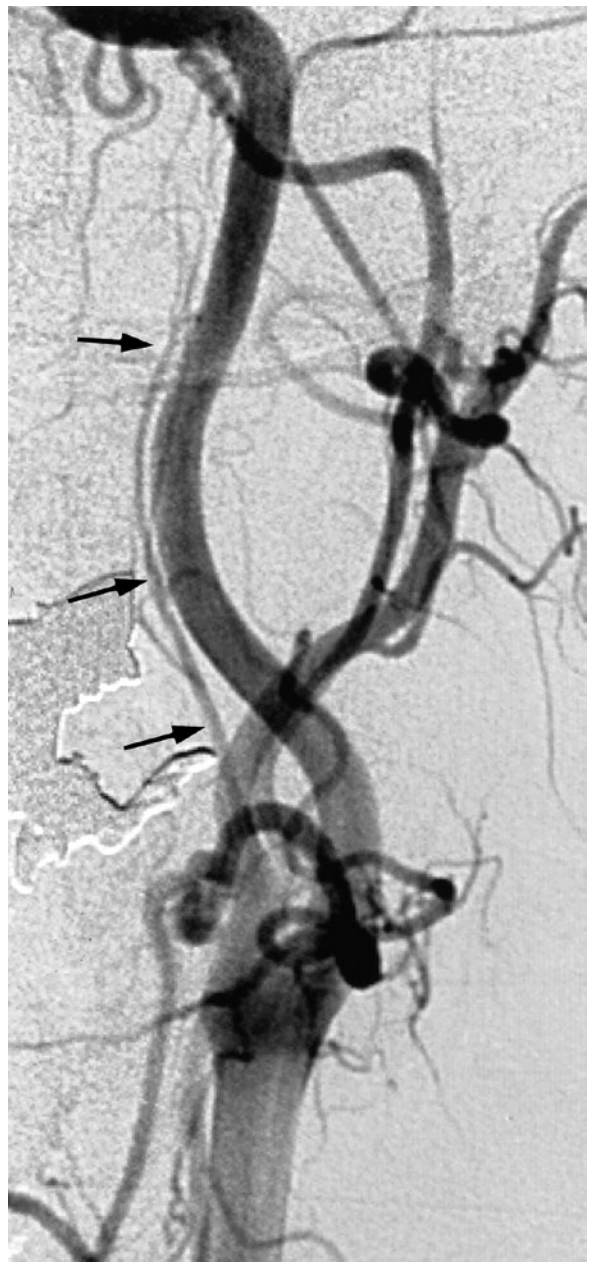

Fig. 3.6 Common carotid angiogram, showing the close relationship of the ascending pharyngeal artery (*arrow*) with the internal carotid artery

Other branches are the musculospinal arteries, which anastomose with branches of the vertebral artery at the C1–C2 level and also with branches of the occipital and ascending cervical arteries. Near the base of the skull, the APhA divides into its terminal branches, described in the following section.

1. Superior pharyngeal branches.
2. The inferior tympanic artery vascularizes the tympanic cavity and can anastomose with the other tympanic branches arising from the stylomastoid artery and IMA. There may also be an anastomosis with the caroticotympanic branch of the ICA, when present (Fig. 3.5).
3. The neuromeningeal trunk can be subdivided into the hypoglossal and jugular branches (Lasjaunias and Berenstein 1987; Djindjian and Merland 1978) (Fig. 3.5).
   - The hypoglossal branch enters the hypoglossal canal, running together with cranial nerve XII and with the anterior condylar vein. It gives off branches for the meninges of the adjacent posterior fossa and a descending branch that anastomoses with the ascending radiculomeningeal branch of the vertebral artery, contributing to form the so-called odontoid arch; see also Chap. 6.1.1. (Figs. 3.8c, 6.2b, c, 6.3, 6.9c, 15.9, and 15.20) and Fig. 3.29. The artery also gives off meningeal branches, which extend upward along the clivus (clival branches), anastomosing with the corresponding medial clival branches of the meningeal hypophyseal trunk (MHT) of the ICA (Figs. 3.28). Because of this anastomosis, the neurohypophisis can sometimes be visible on the lateral angiogram of the APhA (Djindjian and Merland 1978).
   - The jugular branch enters the posterior fossa through the jugular foramen, where it supplies cranial nerves IX, X, and XI (Lasjaunias and Berenstein 1987; Lasjaunias et al. 1978a). It supplies the adjacent dura, anastomosing with the more lateral, descending clival branches of the MHT; it then runs further posteriorly to vascularize the dura of the cerebellar fossa and cerebellopontine angle.
   - The supply of cranial nerves IX, X, Xi, and XII is a very important aspect that should be taken into consideration in the endovascular treatment of lesions involving the APhA. Furthermore, the close relationship of the APhA with the ICA probably explains the palsy of the nerves in many cases of dissection of the ICA (Bradac et al. 1990, 2000) (Fig. 3.6). The branches of the APhA may be involved in different pathological processes (Figs. 3.19, 3.21–3.24, 13.3, 13.9, and 13.14–13.16).

3.5 Occipital Artery

The occipital artery takes its origin from the posterior wall of the ECA, frequently as a common trunk with the APhA (Figs. 3.5 and 3.8). The occipital artery can sometimes arise from the vertebral artery or ICA (Fig. 3.8). It runs posteriorly and slightly superiorly with an undulating course, in which three segments may be identified: the first ascending; the second horizontal; the third ascending again. It gives off several musculocutaneous branches for the neck and posterior part of the head and meningeal branches, among which the following are the most important.

1. The stylomastoid artery arises from the first segment and runs up to the stylomastoid foramen, accompanying the facial nerve supplying it. It anastomoses superiorly with the superior tympanic artery, arising from the petrosquamous artery branch of the middle meningeal artery. The stylomastoid artery also gives off branches for the tympanic cavity and adjacent area (posterior tympanic artery), where they anastomose with the other tympanic branches arising from the APhA and IMA. The stylomastoid artery can arise from the posterior auricular artery or directly from the trunk of the ECA. It is a fine branch, not always evident on the lateral ECA angiogram. It can be dilated and well recognizable when involved in the supply of pathological processes (Figs. 3.22, 3.24c, and 13.1).
2. Of the muscular branches, two arise in the ascending segment. A third branch (the splenial artery) arises from the horizontal segment, has a descending course, and supplies the splenius muscle (Lasjaunias and Berenstein 1987). The muscular branches can anastomose with corresponding branches of the vertebral artery at the C1–C2 level and with branches of the ascending cervical artery (Figs. 3.7, 3.8, and 15.20).
3. The mastoid branch (Fig. 3.7) arises from the second segment, approximately near the origin of the

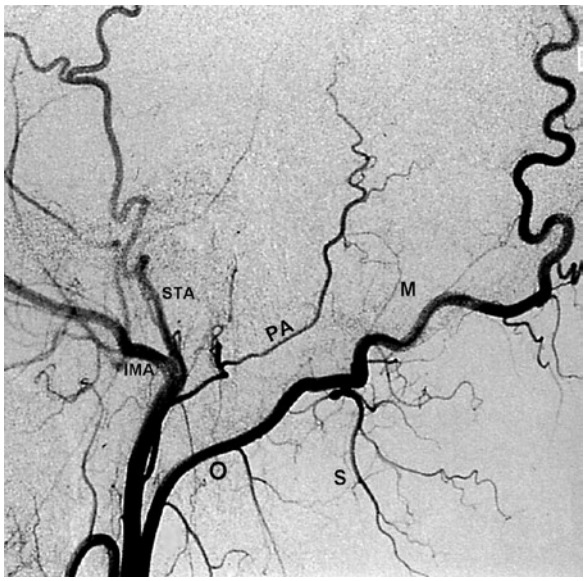

Fig. 3.7 Angiogram of the external carotid artery (*lateral view*). Occipital artery (*O*), with its muscular branches from the ascending segment and horizontal segment splenial artery (*S*). Mastoid branch (*M*), posterior auricular artery (*PA*), superficial temporal artery (*STA*), internal maxillary artery (*IMA*)

splenial artery. It has an ascending course, enters the cranial cavity through the foramen of the emissary vein, and supplies the meninges of the cerebellopontine angle and cerebellar fossa. These branches are in hemodynamic balance with those arising from the neuromeningeal trunk of the APhA, with the petrosquamosal branch of the middle meningeal artery (MMA), and with the meningeal branches of the vertebral artery (Lasjaunias et al. 1978b; Lasjaunias and Berenstein 1987). One of these branches can dominate and completely supply these territories.

The occipital artery is involved in several pathological processes (Figs. 3.21, 3.22, 13.1, 13.6, 13.8–13.11, and 13.15).

3.6 Posterior Auricular Artery

This is a small branch arising near the terminal ECA, sometimes as a common trunk with the occipital artery. It supplies the pinna of the ear, which is frequently evident as a blush in the capillary phase of the ECA angiogram (Fig. 3.7).

3.7 Internal Maxillary Artery

The IMA is the larger of the terminal branches of the ECA. It originates behind the neck of the mandibular, within the parotid gland. It runs obliquely forward and medially in the masticator space, along the border of the lateral pterygoid muscle and ends in the pterygopalatine fossa, where it divides into its terminal branches. It is always distinctive on the lateral and AP angiogram (Figs. 3.9–3.11).

3.7.1 Proximal Branches

Near its origin, the IMA it gives off thin proximal branches for the mandibular joint, external auditory canal, and tympanic cavity (anterior tympanic artery). The latter can be involved in the vascularization of chemodectomas (Fig. 3.22).

3.7.1.1 Middle Meningeal Artery

The MMA is the first largest proximal branch of the IMA. It runs superiorly toward the base of the skull, passes through the foramen spinosum, becoming intracranial, running along the greater sphenoid wing,

Fig. 3.8 (**a**) Internal carotid angiogram, lateral view. Origin of occipital artery (*arrow*) from the internal carotid artery. The ascending pharyngeal artery (*small arrow*) arises as a common trunk from the occipital artery. (**b**) Selective angiogram of the occipital artery (*O*). There is an evident anastomosis (*arrows*) between the muscular branch of the ascendens segment of the occipital with the vertebral artery (*VA*). (**c**) Lateral vertebral angiogram (earlier and later phases) in a patient with proximal surgical ligature of the external carotid artery. Through anastomosis involving muscular branches of the VA and O (*arrow*) complete recanalization of the external carotid artery. Odontoid arch (*arrow with angle*) leading to a retrograde injection of the ascending pharyngeal artery

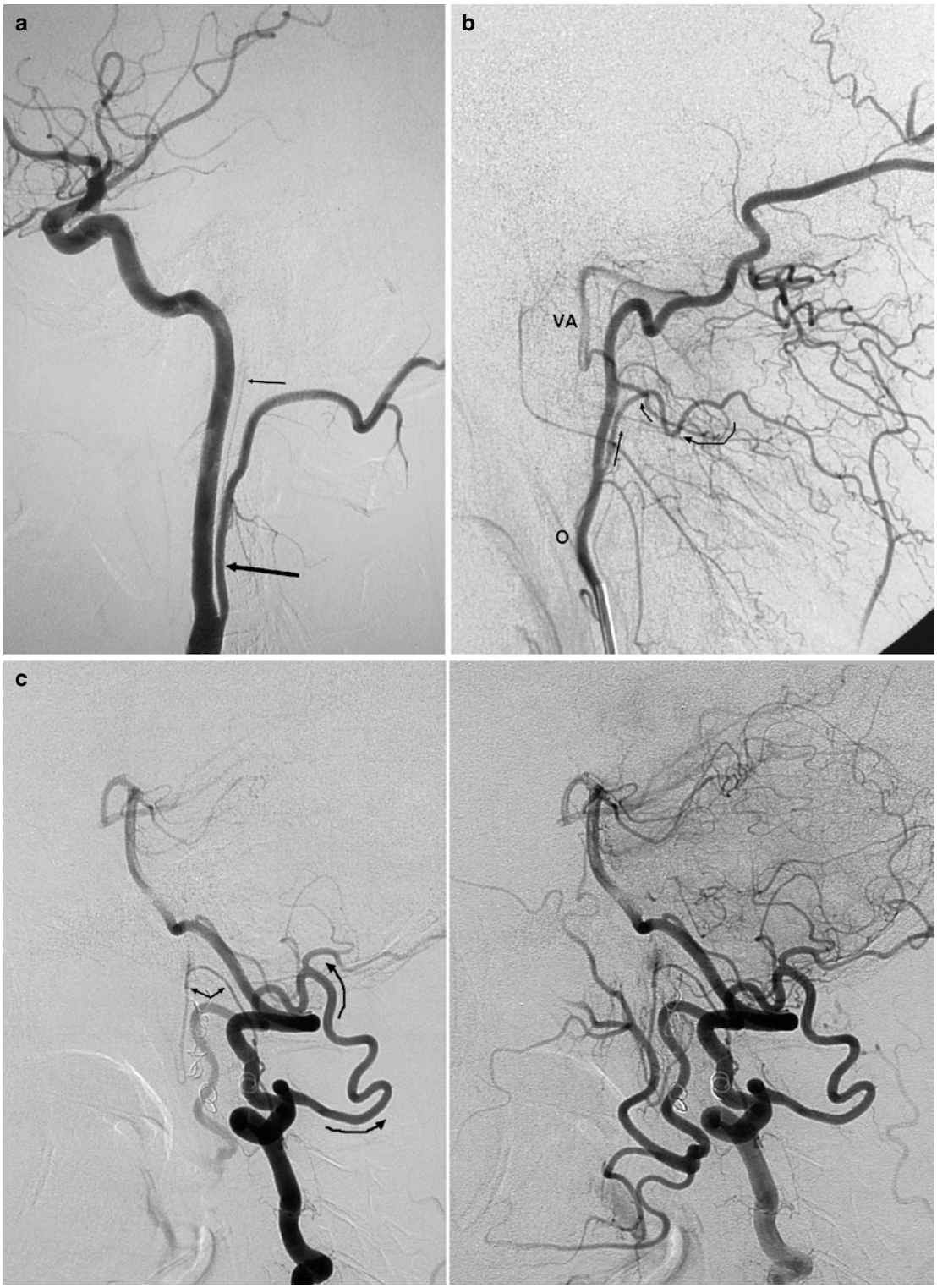
a
b
VA
O
c

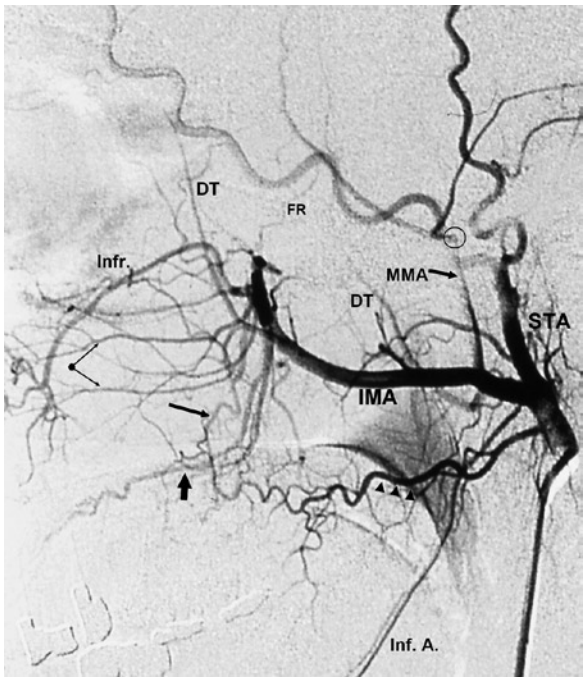

Fig. 3.9 Angiogram of the distal external carotid artery, lateral view. Transverse facial artery (*arrowhead*). Superficial temporal artery (*STA*), internal maxillary artery (*IMA*), middle meningeal artery (*MMA*). The circle shows where the MMA passes through the foramen spinosum. Middle and anterior deep temporal arteries (*DT*), inferior alveolar artery (*Inf. A.*), infraorbital artery (*Infr.*), posterior superior alveolar artery (*arrow*), descending palatine artery (*large arrow*), nasal branches of the sphenopalatine artery (*arrows with dot*), small foramen rotundum artery (*FR*)

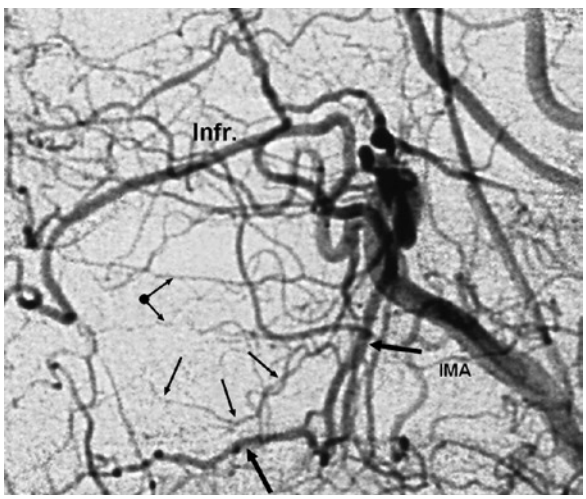

Fig. 3.10 Angiogram of the distal external carotid artery, lateral view, detail. Internal maxillary artery (*IMA*), infraorbital artery (*Infr.*), posterior superior alveolar artery (*small arrows*), descending palatine artery (*large arrow*), nasal branches of the sphenopalatine artery (*arrow with dot*)

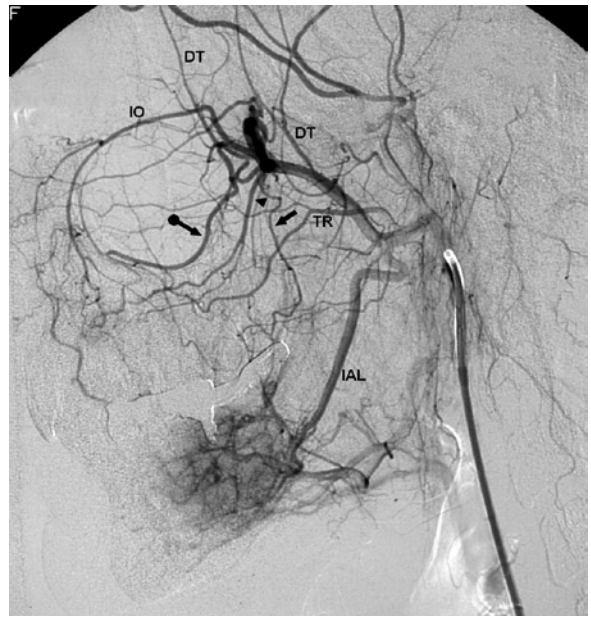

Fig. 3.11 Angiogram of the distal external carotid artery performed to study a capillary-venous vascular malformation of the mandible. Dilated inferior alveolar artery (*IAL*) supplying the malformation. Transverse facial artery (*TR*), buccal artery (*arrow*), deep temporal arteries (*DT*), descending palatine artery (*arrowhead*), posterior superior alveolar artery (*arrow with dot*), infraorbital artery (*IO*). The distal branches of the sphenopalatine artery are evident as fine branches running between the infraorbital and posterior superior alveolar arteries

and it forms a large convex curve anteriorly (lateral angiogram) and laterally (AP angiogram) (Figs. 3.9 and 3.13). It is the most important artery in the vascularization of the dura and gives off the following branches.

- The MMA gives off arteries for the dura of the frontoparietal and temporo-occipital convexity.
- It gives off branches for the frontobasal area, anastomosing with ethmoidal branches, arising from the ophthalmic artery.
- A meningeal branch can enter the orbita through the superior orbital fissure or through the foramen of Hyrtl and anastomose with the lacrimal artery, a branch of the ophthalmic artery, or directly with the latter.
- Branches for the middle cranial fossa, where they anastomose medially near the cavernous sinus with the meningeal branches supplying this area, arise from the inferolateral trunk (ILT), MHT, foramen rotundum artery, and accessory meningeal artery.

- Close to the foramen spinosum arises the petrosquamous branch, which supplies the dura, covering the petrous bone, partially the tentorium, and extends largely in the posterior fossa; there, it anastomoses with the meningeal branches, supplying the dura of the posterior fossa arising from the APhA (clival branches and neuromeningeal trunk), occipital artery, and vertebral artery. The petrosquamous branch gives off a tympanic branch (superior tympanic artery), which runs in the petrous facial canal, where it anastomoses with the stylomastoid artery—a branch of the occipital or posterior auricular artery. These arteries can both supply the nerve, but there is commonly a predominance of the petrosquamous branch (Lasjaunias and Berenstein 1987). Furthermore, the petrosquamous branch gives off branches for the tympanic cavity, where they anastomoses with the anterior, posterior, and inferior tympanic arteries.
- In the paramedian area of the convexity, the branches anastomose with those of the contralateral side. Furthermore, the branches form an arcade from anterior to posterior, situated at the insertion of the lateral wall of the superior sagittal sinus with the meninges of the vault. This arcade anastomoses anteriorly with the artery of the anterior falx, a branch of the anterior ethmoidal artery, and posteriorly with the falx cerebelli artery. The artery of the falx itself arises from the arcade as descending branches.

Branches of the MMA are involved in the supply of extra- and intracranial tumors (Figs. 3.24–3.26) and intracranial vascular malformations (Figs. 13.3, 13.6–13.9, 13.11, 13.13, and 13.17). The MMA can be characterized by numerous variants (Moret et al. 1977; Lasjaunias and Berenstein 1987) mainly because of different embryonic evolution of the stapedial artery and primitive ophthalmic arteries. These are discussed in the Chap. "Ophthalmic artery."

3.7.1.2 Accessory Meningeal Artery

The second branch is the accessory meningeal artery. Frequently small, it may sometimes be well developed and evident on the lateral angiogram as a result of its oblique, anterior, and superior course (Fig. 3.13). The accessory meningeal artery can have a common origin with the MMA and gives off branches for the nasopharynx and palate. A branch enters the cranial cavity through the foramen ovale, supplying the adjacent dura, part of the cavernous sinus, and part of the trigeminal nerve. For the relationship to the ILT see Chap. "Carotid Artery." It can be involved in dural arteriovenous fistulas (DAVFs) (Figs. 13.8 and 13.9).

3.7.1.3 Inferior Alveolar Artery

The third proximal branch is the inferior alveolar artery, which is always visible on the lateral angiogram, despite its small caliber. It runs down toward the mandibular foramen and supplies the teeth and mandibula (Figs. 3.9 and 3.11).

3.7.2 Masticator Space

In the masticator space, the IMA gives off deep temporal branches (middle and anterior branches), which have an ascending course. The anterior of these arteries gives off branches that reach the orbita, perforate the malar bone, or pass through the inferior orbital fissure. The branches anastomose with the lacrimal artery of the ophthalmic artery. This is an important collateral in occlusion of the ICA (Djindjian and Merland 1978) (Fig. 3.12). Other branches in the masticator space are the pterygoid, masseter, and buccal arteries. The latter (Fig. 3.11) supply the buccinator muscle and overlying skin. The buccal artery can be well developed and form anastomoses in the cheek with other arteries of the region (facial, transverse facial, and infraorbital arteries). A frequent large anastomosis also occurs with the ascending palatine artery of the facial artery.

3.7.3 Distal IMA

The distal IMA reaches the pterygopalatine fossa, a space bordered anteriorly by the posterior wall of the maxillary sinus and posteriorly by the pterygoid plate, where it forms a loop, entering finally the sphenopalatine foramen. Before entering, the IMA gives off several branches: the posterior superior alveolar artery, descending palatine artery (great palatine artery), and infraorbital artery.

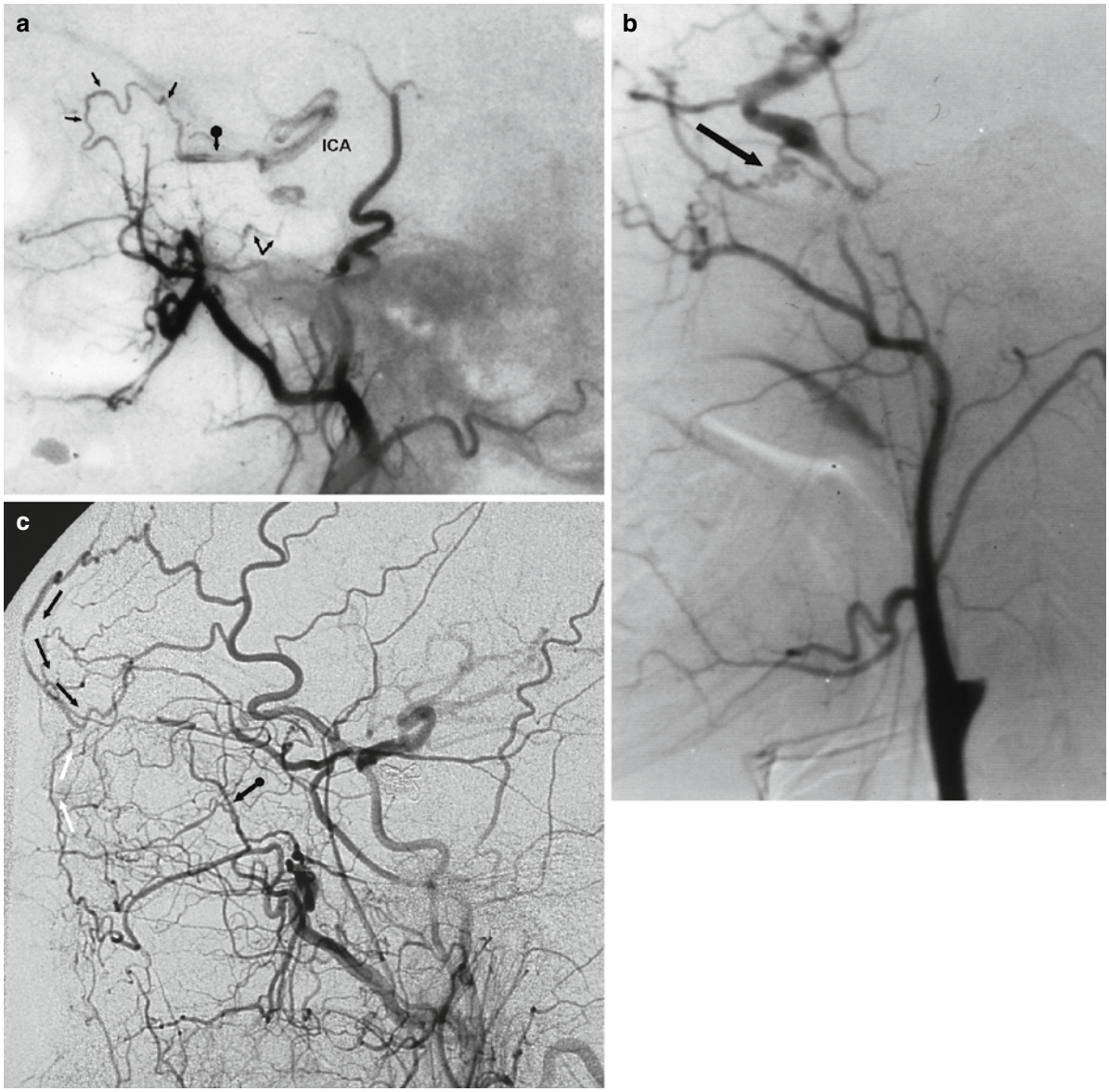

Fig. 3.12 (**a**) Angiogram of the external carotid artery, lateral view, in a patient with occlusion of the internal carotid artery (*ICA*). Injection of distal *ICA* through anastomosis between the deep anterior temporal artery and lacrimal branch (*arrow*) of the ophthalmic artery (*arrow with dot*). There is also a partial injection of the cavernous portion of the *ICA*, through the foramen rotundum artery (*arrow with angle*). (**b**) Angiogram of external carotid artery, lateral view, in another patient with an occluded ICA. In addition to the collateral flow through the deep anterior temporal artery and ophthalmic artery, there is involvement of the foramen rotundum artery (*arrow*). (**c**) Patient with large direct carotid-cavernous fistula treated with occlusion of the fistula and parent artery. On the lateral carotid angiogram, a collateral circulation with retrograde injection of the ophthalmic artery and ICA through several anastomoses, involving the superficial temporal artery (*black arrows*) and deep anterior temporal artery (*arrow with dot*), is visible. The distal branches of the infraorbital artery are anastomosed with the distal branches of the facial artery (*white arrows*), both also involved in the collateral circulation

The posterior superior alveolar artery runs first on the posterior and then on the anterolateral wall of the maxillary sinus. It perforates the maxillary tuberosity running forward and, at the level of the incisive foramen, anastomoses with the descending palatine artery. The posterior superior alveolar artery gives off

branches for the sinus (antral artery) and teeth. It is a small artery, sometimes recognizable on the lateral angiogram with its typical course, first downward, then forming a curve anteriorly and superiorly; it anastomoses distally with branches of the infraorbital artery and descending palatine artery (Figs. 3.9–3.11). The descending palatine artery runs initially downward along the wall of the maxillary sinus, then it forms a typical angle, coursing horizontally and anteriorly through the hard and soft palate supplying it. The descending palatine artery is evident on the lateral angiogram owing to the undulating course in its horizontal segment (Figs. 3.9–3.11). Anteriorly, it ends at the incisive canal, anastomising superiorly with the nasal branches of the sphenopalatine artery. The infraorbital artery enters the orbita at the inferior orbital fissure, runs anteriorly and penetrates the infraorbital canal, where it runs together with the infraorbital nerve. The infraorbital artery is involved in the vascularization of the bone structures of the floor of the orbita and adjacent muscle and fatty tissues. It leaves the canal and gives branches for the cheek, lower lid, upper lip, and nose. The infraorbital artery anastomoses with branches of the ophthalmic, facial, transverse facial, buccal, and posterior superior alveolar arteries (Figs. 3.9–3.11). It can be involved in collateral circulation when the ICA is occluded (Fig. 3.12).

Other branches of the distal IMA are the foramen rotundum artery (FRA), the pterygoid or vidian artery (VA), and the pterygovaginal artery (PVA). The FRA runs with an oblique superoposterior course, passes through the foramen rotundum together with cranial nerve V2, and anastomoses with the ILT. The VA runs posteriorly with a more horizontal course. On the lateral angiogram, it is located below the FRA. It passes through the vidian canal, together with the superficial greater petrosal nerve, and anastomoses with the horizontal branch of the mandibular artery, which is an embryonic remnant arising from the petrous segment of the ICA.

The PVA forms a curve directed posteriorly and inferiorly. On the lateral angiogram, it is commonly located below the VA. It gives off branches for the superior nasopharyngeal mucosa and anastomoses with branches of the accessory meningeal artery and APhA. It passes through the pterygovaginal canal and anastomoses with the inferior branch of the mandibular artery, which arises from the ICA (see Chap. 2).

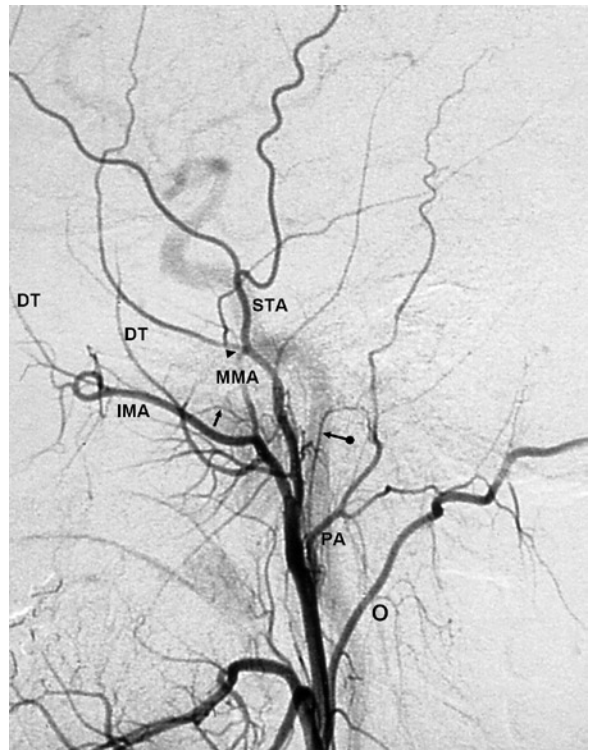

Fig. 3.13 External carotid artery angiogram, lateral view, showing the undulating course of the cutaneous branches of the occipital (*O*), posterior auricular (*PA*), and superficial temporal (*STA*) arteries. The courses of the middle meningeal artery (*MMA*) and middle and anterior deep temporal arteries (*DT*) appear straighter. The arrowhead shows where the *MMA* enters the cranial cavity through the foramen spinosum. Internal maxillary artery (*IMA*), accessory meningeal artery (*arrow*), ascending pharyngeal artery (*arrow with dot*)

The FRA, VA, and PVA can be variously involved in extra- and intracranial tumors and in the supply of DAVFs (Fig. 13.3). Furthermore, the FRA can play a role in the collateral circulation of the ICA when this artery is occluded (Fig. 3.12).

3.7.4 The Terminal Branch

The terminal branch is the sphenopalatine artery. This enters the nasal cavity through the sphenopalatine foramen and gives off branches for the medial and lateral nasal mucosa. The sphenopalatine artery branches appear on the lateral angiogram as a thin vessel, running anteriorly below the infraorbital artery

(Figs. 3.9–3.11). The sphenopalatine artery branches can anastomose with descending branches of the ethmoidal arteries, which arise from the ophthalmic artery, and be indirectly involved in the supply of frontobasal meningiomas (Fig. 3.25) and frontobasal DAVFs (Fig. 13.13). Anteriorly, the sphenopalatine artery branches are connected with branches of the facial, infraorbital, and descending palatine arteries (Djindjian and Merland 1978; Lasjaunias and Berenstein 1987).

3.8 Superficial Temporal Artery

The superficial temporal artery (STA) is the smaller of the terminal branches of the ECA. It runs upward and often forms a sharp curve shortly after its origin as it turns over the zygomatic arch. The STA gives off several branches that run with an undulating course on the scalp, which they supply (Figs. 3.9, 3.13, and 3.26). This feature is characteristic and it allows the differentiation of these cutaneous branches from the more rectilinear course of the MMA. The transverse facial artery arises from the first segment of the STA (Figs. 3.9 and 3.11); the artery courses horizontally along the zygoma and supplies the skin of the cheek. The transverse facial artery can occasionally be well developed, especially when the facial artery is hypoplastic. Through its anastomosis with the supraorbital branch of the ophthalmic artery, the STA can be involved in the collateral circulation toward the ICA when this is occluded (Fig. 3.12c).

3.9 Summary

- The ECA supplies the soft tissues and bone of the craniofacial area.
- This artery represents the main meningeal supply for the intracranial dura. Its branches are in balance with the meningeal branches arising from opthalmic artery, ICA and VA.
- The ECA supplies a few cranial nerves.
- It can be an important collateral path to the intracranial circulation, especially in cases of an occluded ICA.
- The ECA can be involved in the vascularization of pathological processes that affect the extracranial area and base of the skull and those involving the intracranial dura, especially meningiomas and DAVFs.

3.9.1 Vascular Malformations

Vascular malformations represent a congenital pathology that may be present in pediatric patients or clinically appear later owing to the slow growth. They can be classified into high- and slow-flow malformations. The first are arteriovenous (AV) angiomas, with large supplying arteries and early venous drainage because of direct AV shunts. The latter can be very large and form huge fistulas. The slow-flow malformations are capillary-venous angiomas, in which the supplying arteries are commonly normal, without early venous drainage. Both high- and slow-flow malformations can be associated. Intracranial aneurysms and AV malformations may be present.

There is a possible association of extracranial vascular malformations with some neurocutaneous pathologies, such as Sturge-Weber, Louis-Barr, Wyburn-Mason, and Rendu-Osler syndromes (see Chap. 12).

Location. They can involve the skin of the head and facies as well as the oral and nasal cavities. The masticatory muscles and bone structures, are more seldom affected; they may be secondarily affected as extensions of the malformation or primary. The masseter muscle and mandibular bone are particularly involved.

Clinical relevance. This varies from esthetic problems to more important clinical symptoms, involving respiration and deglutition up to severe hemorrhage and cardiac failure.

Diagnosis and treatment. The diagnosis can sometimes be obtained only by clinical observation. Extensive lesions require CT and MRI. Depending on the site and

extension of the malformation, angiography may be necessary to identify the type of lesion and the vessels involved. With regard to location, the supplying arteries can frequently be suspected. However, other vessels may be indirectly involved, and so a complete study of both ECA is frequently necessary. To exclude intracranial malformations, examination of the ICA and VA should also be performed. All this information is necessary to plan the endovascular and/or surgical treatment.

Examples.These appear in Figs. 3.14–3.18.

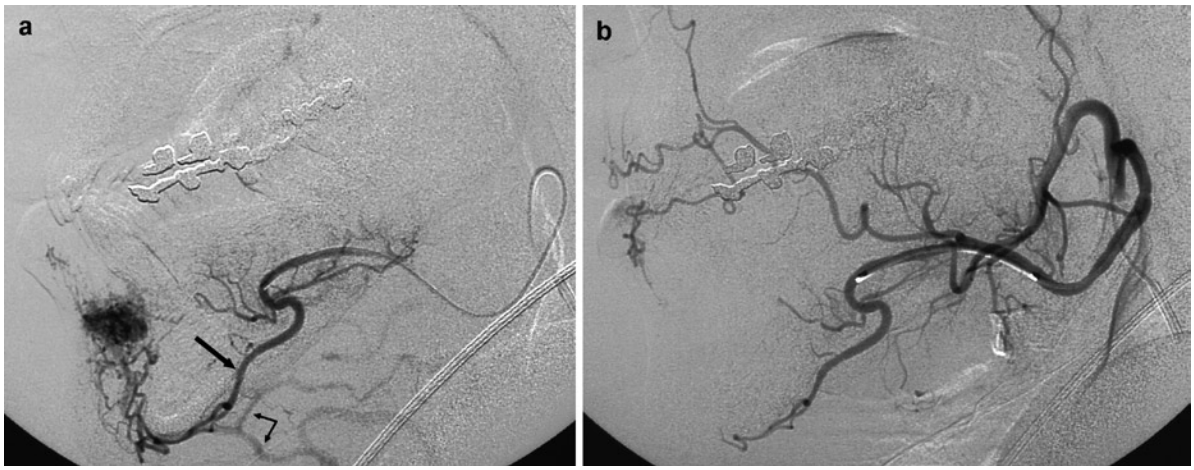

Fig. 3.14 Small arteriovenous angioma of the mental area supplied by the facial artery. (**a**) Lateral angiogram of the selective submental artery (*arrow*) showing the angioma and early drainage in the submental veins (*arrow with angle*). (**b**) Control angiogram after occlusion of the malformation using polyvinyl alcohol (PVA) particles

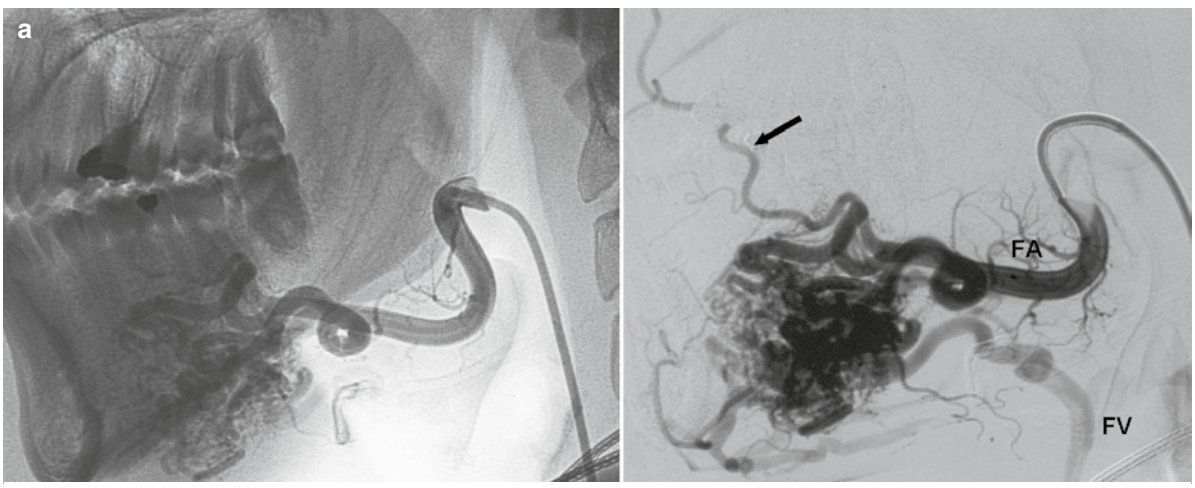

Fig. 3.15 Large arteriovenous angioma of the inferior cheek supplied by the facial artery. (**a**) Lateral angiogram of the facial artery (subtracted and unsubtracted image). Dilated facial artery (*FA*) supplying the malformation. Normal lumen of the artery in its distal segment (*arrow*). Early drainage in the facial vein (*FV*). (**b**) AP angiogram of the *FA*. (**c**) Lateral control angiogram after preoperative devascularization of the lesion

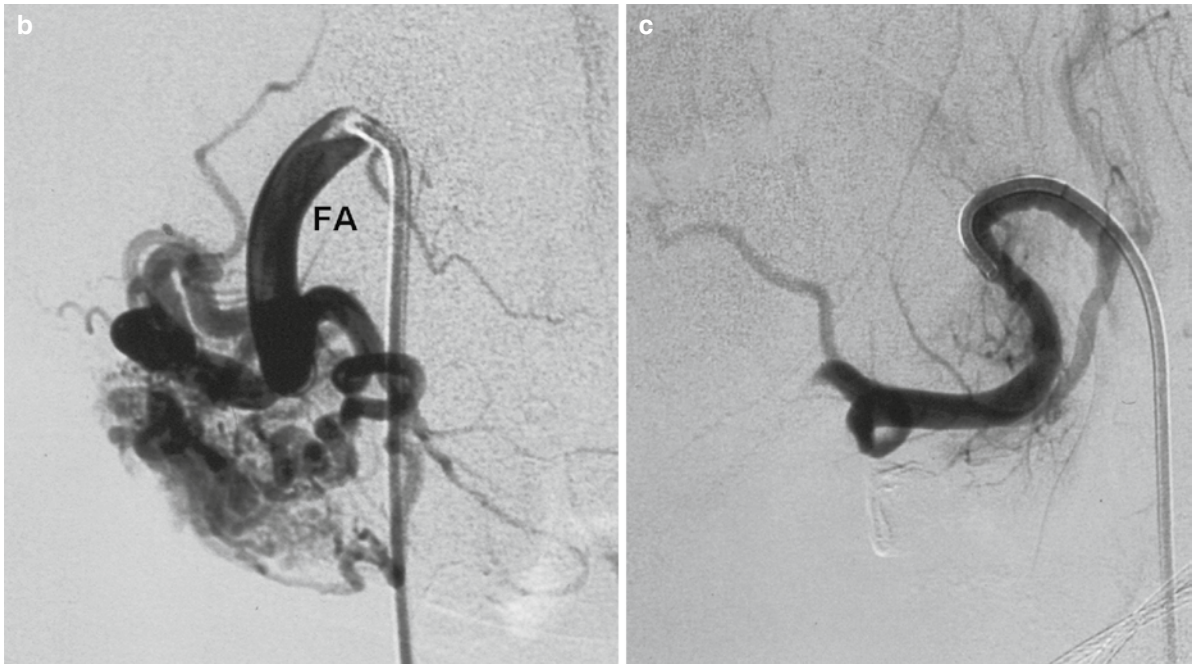

Fig. 3.15 (continued)

3.9.2 Hemangiomas

Hemangiomas are real tumors (Mulliken and Glowacki 1982) and consist prevalently of masses of endothelial cells with or without vascular lumens. They can be present at birth, with a strong prevalence among females, or they can appear in the first months of life. They are characterized by a phase of rapid growth, followed by a period of progressive involution, which can be complete at the age of six to seven years (Pitanguy et al. 1984) in about 95% of the cases.

Depending on the extension and site of the hemangioma, the clinical symptoms can be minimal or severe and include orbital, oral impairment, hemorrhage, and heart failure. Thrombocytopenia (Kasabach-Merritt syndrome) can occur. In selected cases with severe clinical involvement, angiography is necessary to show the rich vascular tumor, which can be devascularized with the PVA (Lasjaunias and Berenstein 1987).

3.9.3 Juvenile Angiofibromas

These are tumors that develop typically in young males before puberty, indicating an influence of male hormones. Rare cases of angiofibromas in older patients and also in females have been described (Osborn 1959).

Juvenile angiofibromas are benign tumors formed by a fibrovascular stroma. The vascular component is very rich and consists of true arterial-capillary vessels and simple endothelialized cavities.

Location. The tumor arises at the level of the sphenopalatine foramen, from which it can extend toward the nasal cavity and involve further the ethmoidal cells, sinus sphenoidalis, and maxillary sinus. The tumor can grow laterally into the pterygopalatine and further into the infratemporal fossa or superiorly, invading the orbita through the inferior orbital fissure. Through the foramina of the base of the skull, it can extend into the middle cranial fossa, with possible involvement of the cavernous sinus. Commonly, juvenile angiofibromas do not primarily destroy the bone structure, which is initially displaced and thinned and only later eroded.

Clinical relevance. The symptoms depend on the growth direction and extension. The most frequent presenting symptoms are epistaxis and nasal obstruction.

Diagnosis and treatment. Initial examinations are CT and MRI, followed by angiography. Pharyngeal branches of the APhA and distal branches of the IMA are commonly involved. Supply from the petrous and

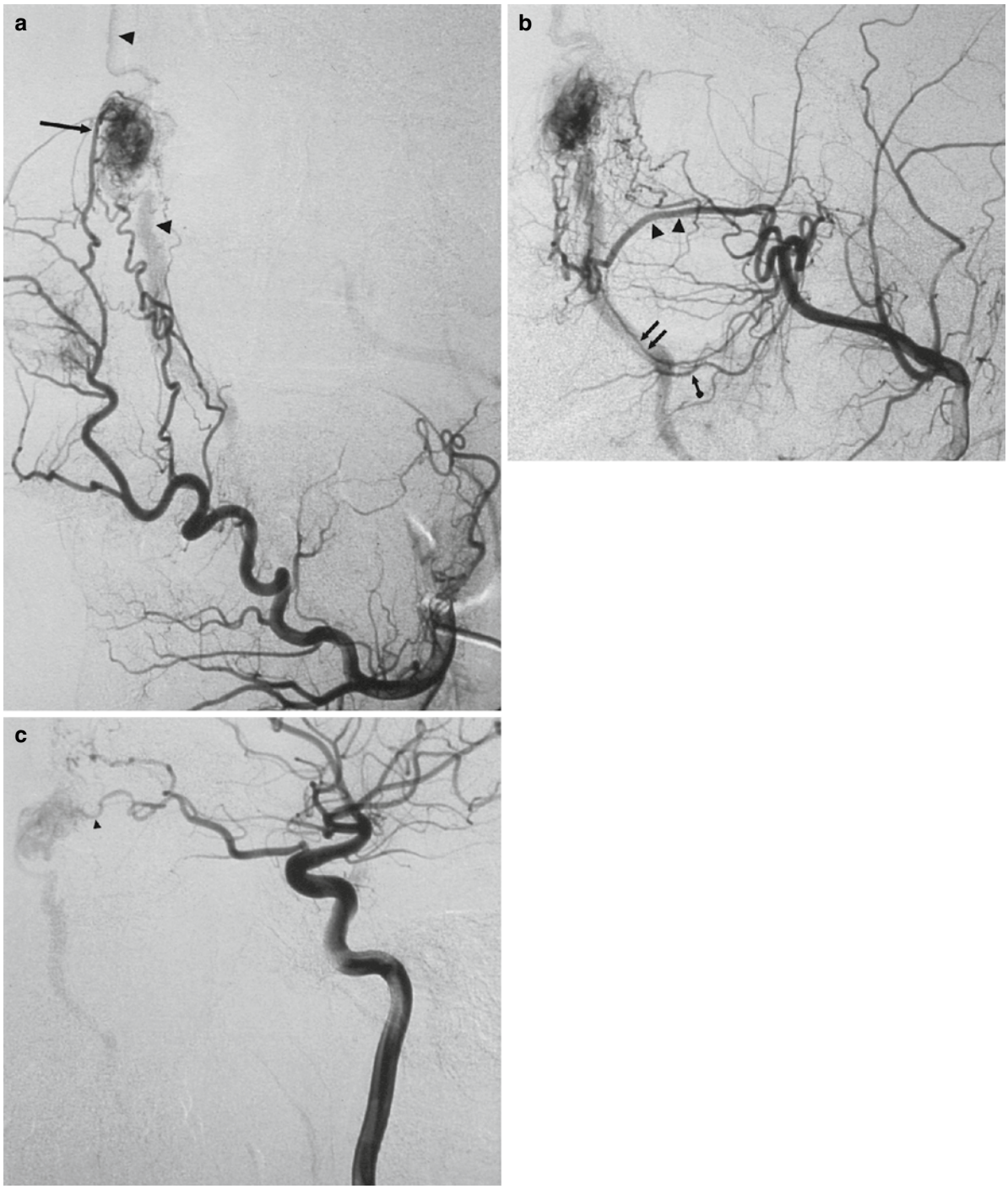

Fig. 3.16 Arteriovenous angioma of the ala of the nose supplied by branches of the facial artery, internal maxillary artery and ophthalmic artery. (**a**) Lateral angiogram of the facial artery. The arteriovenous angioma is supplied by the angular artery (*arrow*) and other small branches of the distal facial artery. Early drainage in the facial and frontal veins (*arrowhead*). (**b**) Lateral angiogram of the internal maxillary artery. Infraorbital artery (*arrowheads*) supplying the angioma. Also partially involved is the posterior superior alveolar artery (*arrows*). Normal descending palatine artery (*arrow with dot*). (**c**) Lateral internal carotid angiogram, showing the partial supplying through the nasal branch of the ophthalmic artery (*arrowhead*). The AVM was devascularized with polyvinyl alcohol (*PVA*), followed by surgical excision

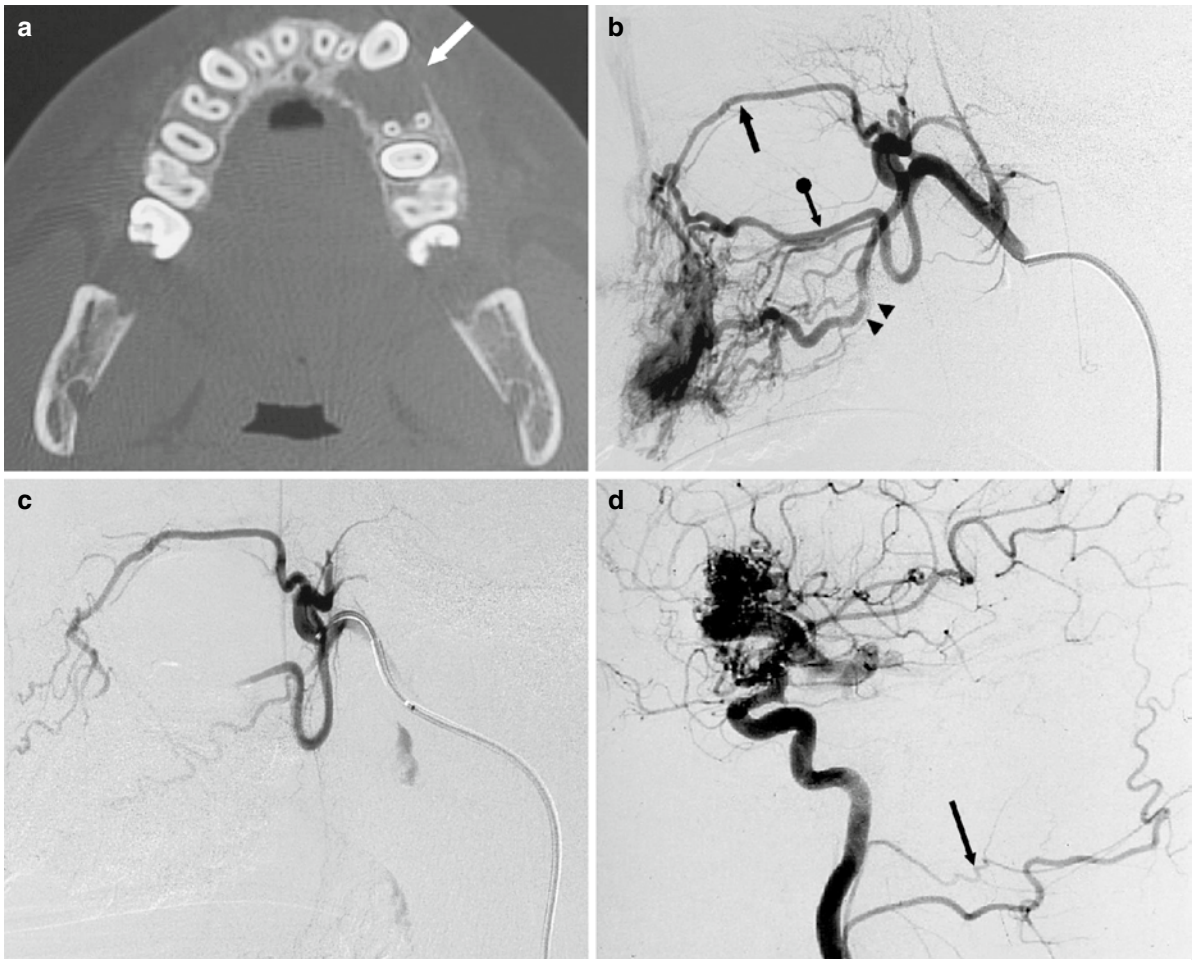

Fig. 3.17 Alveolar maxillary arteriovenous angioma presenting with hemorrhage. (**a**) CT shows the bone changes with displacement of the tooth (*arrow*). (**b**) Lateral angiogram of the internal maxillary artery. The angioma is supplied by branches of the infraorbital artery (*arrow*). Branches of the superior posterior alveolar artery (*arrow with dot*) and descending palatine artery (*arrowhead*) are also involved. (**c**) Acute endovascular treatment with devascularization using polyvinyl alcohol (PVA). (**d**) Internal carotid artery in the same patient showing an asymptomatic arteriovenous malformation. There is a common trunk of the occipital and ascending pharyngeal arteries arising from the internal carotid artery. Well-developed neuromeningeal trunk (*arrow*)

cavernous segments of the ICA through the mandibular artery and ILT, respectively and supply from branches of the opthalmic arteries depending on the extension of the tumor can occur (Figs. 3.19 and 3.20). Preoperative endovascular treatment with devascularization of the tumor is an important part of the therapy.

3.9.4 Paragangliomas (Chemodectomas)

Paragangliomas are tumors arising from ectodermal cells of the neural crest in the head and neck regions. Women in the fourth and fifth decades of life are predominantly affected. In up to 10% of patients, the tumors are multiple. Family factors have been reported. A malignant potential is very rare, but possible, especially in carotid, vagal, and laryngeal locations (Zak and Lawson 1982). In 1% of cases, a secretory activity is present (Zak and Lawson 1982), especially for norepinephrine as in pheochromocytoma (Nelson and Kendall 1987). The tumor appears as an encapsulated mass consisting of epithelial cells with a highly vascular stroma.

Location. Most frequently, paragangliomas are located in the temporal area, which can be subdivided

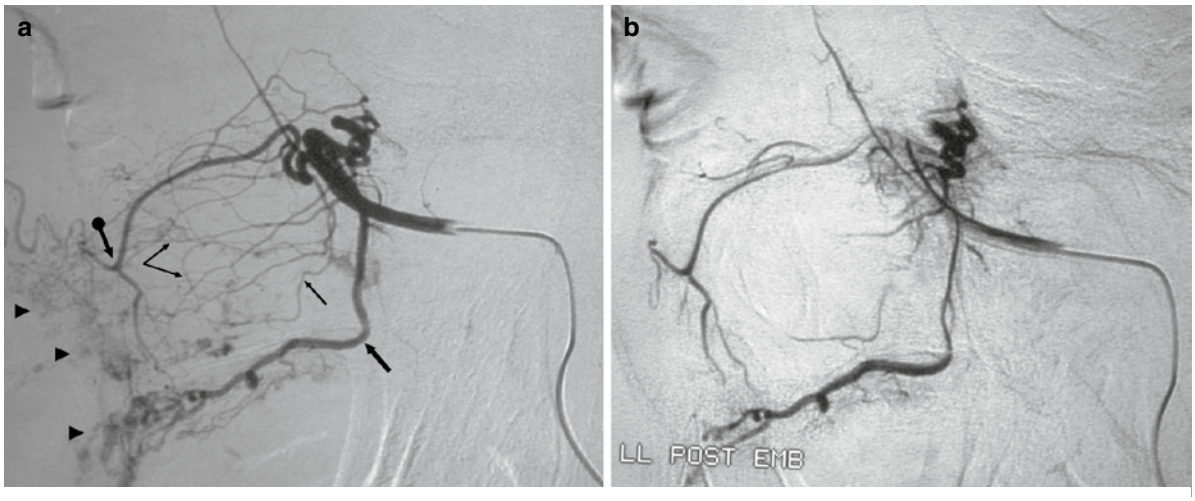

Fig. 3.18 Rendu-Osler syndrome in a middle-aged patient presenting with severe epistaxis. (**a**) Lateral angiogram of the distal internal maxillary artery. There is a diffuse vascular alteration owing to multiple capillary angiomas involving the skin (*arrowhead*) and nasal mucosa. There is also microaneurysmal dilatation along the descending palatine artery. Several arteries are probably involved. Infraorbital artery (*arrow with dot*), nasal branches of the sphenopalatine artery (*arrow with angle*), superior posterior alveolar artery (*small arrow*), descending palatine artery (*large arrow*). (**b**) Lateral angiogram post-treatment with devascularization using polyvinyl alcohol (PVA)

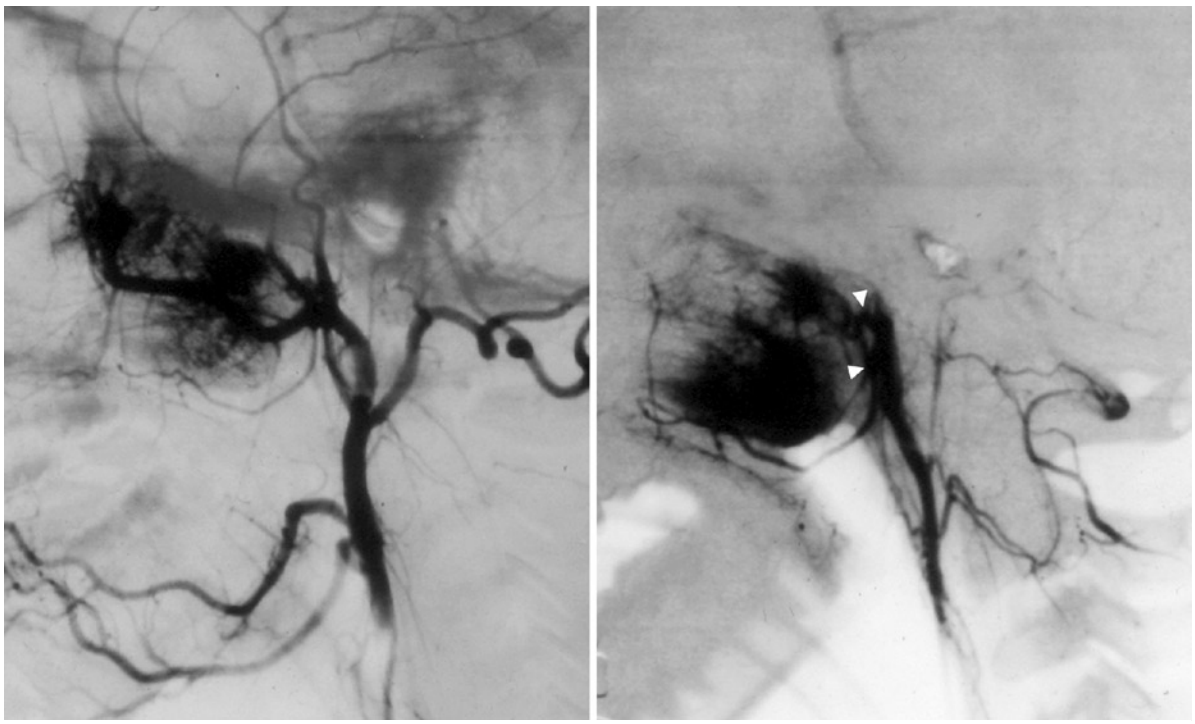

Fig. 3.19 Large juvenile nasopharyngeal angiofibroma, lateral angiogram of the distal external carotid artery (*left*) and of the ascending pharyngeal artery (*right*), showing the richly vascularized tumor supplied by distal branches of the internal maxillary artery and superior and middle pharyngeal branches of the ascending pharyngeal artery (*white arrowheads*). On both angiograms, there is a partial injection of the vertebral artery through muscular anastomosis involving the occipital (*left*) and ascending pharyngeal arteries (*right*). The lesion was preoperatively devascularized with polyvinyl alcohol particles after advancing the catheter distally to the anastomoses

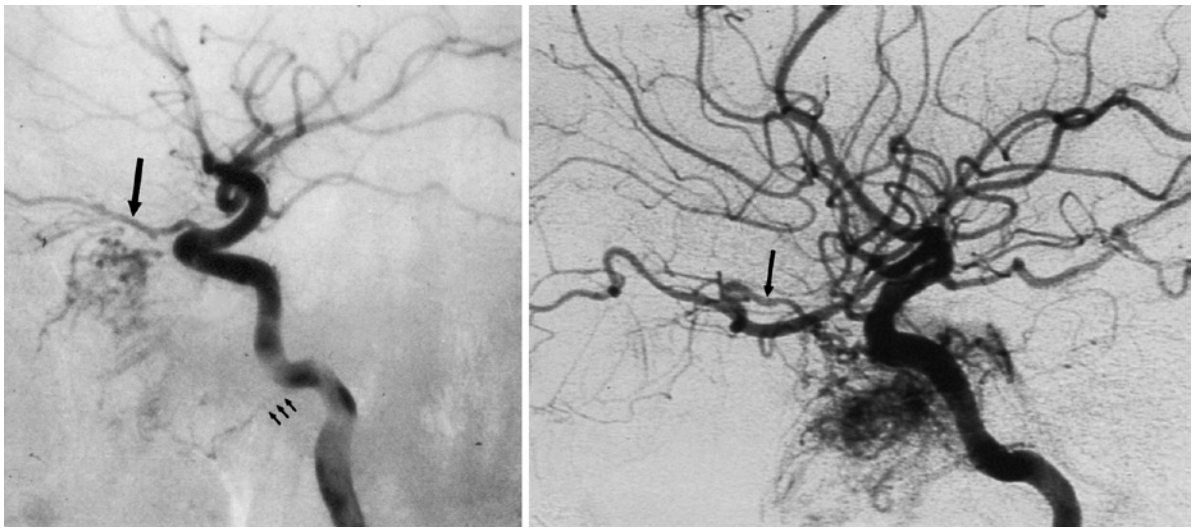

Fig. 3.20 Left internal carotid artery in a large juvenile angiofibroma with an intraorbital extension. On this angiogram, the partial involvement of the mandibular artery (*arrows*) and branches of the ophthalmic artery (*arrow*) are visible. On the right, an example of a juvenile angiofibroma extending intracranially in the parasellar region. This portion of the tumor is richly vascularized by branches of the cavernous portion of the internal carotid artery and by the recurrent meningeal artery of the ophthalmic artery (*arrow*)

into tympanic and jugular types. These are followed in frequency by carotid body and vagal paragangliomas. Less common are locations in the larynx, orbit, nose, and pharynx.

Clinical relevance. The mass effect is a dominant feature in carotid body paragangliomas. Various degrees of involvement of the last four cranial nerves are present in vagal and tympano-jugular lesions. In the latter case, otological symptoms, characterized by hearing loss, tinnitus, and palsy of cranial nerve VII, can occur.

Diagnosis and treatment. Initial examination is by CT and MRI, showing the location and extension of the tumor. Angiography is essential with study of the ICA, ECA, and vertebral artery. The supplying vessels can vary, depending on the location and extension of the tumor. Some basic features can be summarized as follows.

In paragangliomas of the ICA, bifurcation, and vagal paragangliomas, the pharyngeal branches of the APhA and branches of the occipital artery, mainly its musculospinal arteries, are involved. In tympano-jugular paragangliomas, the tympanic branches (anterior from the IMA, posterior from the stylomastoid, superior from the petrosquamous artery, and inferior from the APhA) can be involved in various combinations, depending on the extension of the tumor. The ascending palatine branch of the facial artery can also occasionally be involved (Fig. 3.4). The vertebral artery may be involved through its extracranial branches and also through its intracranial branches in the rare cases of extension of the tumor into the posterior fossa. The ICA can be indirectly involved through its caroticotympanic branch or directly through extension of the tumor into the carotid canal, with also possible encasement of this segment of the ICA. In paragangliomas of the ICA bifurcation, the tumor may infiltrate the adventitia. Venous drainage almost always occurs in the jugular vein, which may also be directly infiltrated and occluded by the tumor. A retrograde injection of the sigmoid sinus and IPS can occur.

Devascularization of the tumor prior to selective catheterization of the supplying arteries is mandatory. Here, it should be noted that chemodectomas can consist of a single or multiple compartments, each supplied by a specific artery. Connections between the compartments may be present (Moret et al. 1980) (Figs. 3.21–3.24). In selective cases, endovascular occlusion with balloon or coils of the ICA and vertebral artery can also be considered.

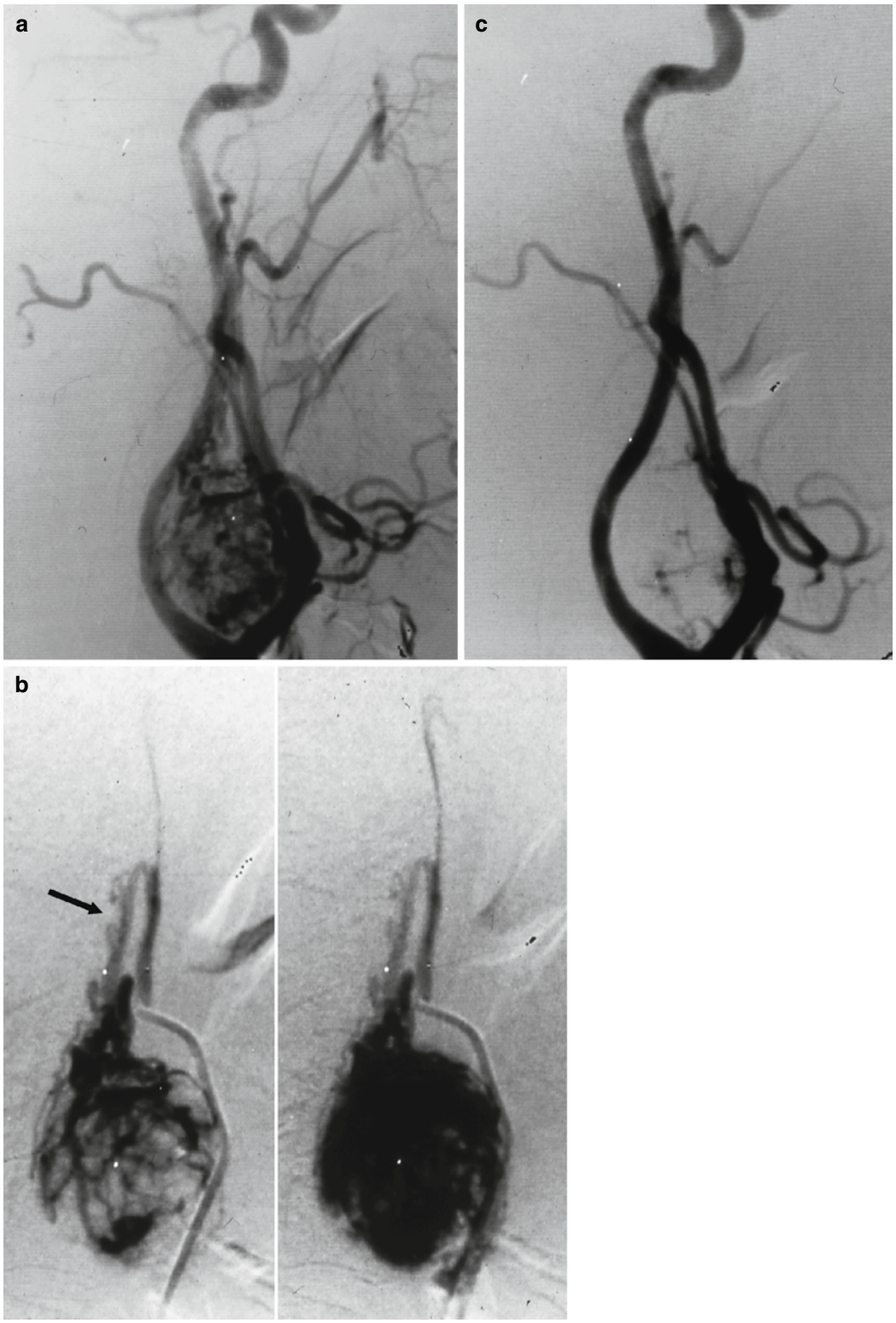

Fig. 3.21 Paraganglioma of the carotid bifurcation. (**a**) Common carotid angiogram, lateral view, showing the typical location of the richly vascularized tumor. (**b**) Selective study of the ascending pharyngeal artery, which is the main supply artery through its inferior pharyngeal branches (*arrow*). (**c**) Control angiogram after devascularization of the tumor with polyvinyl alcohol

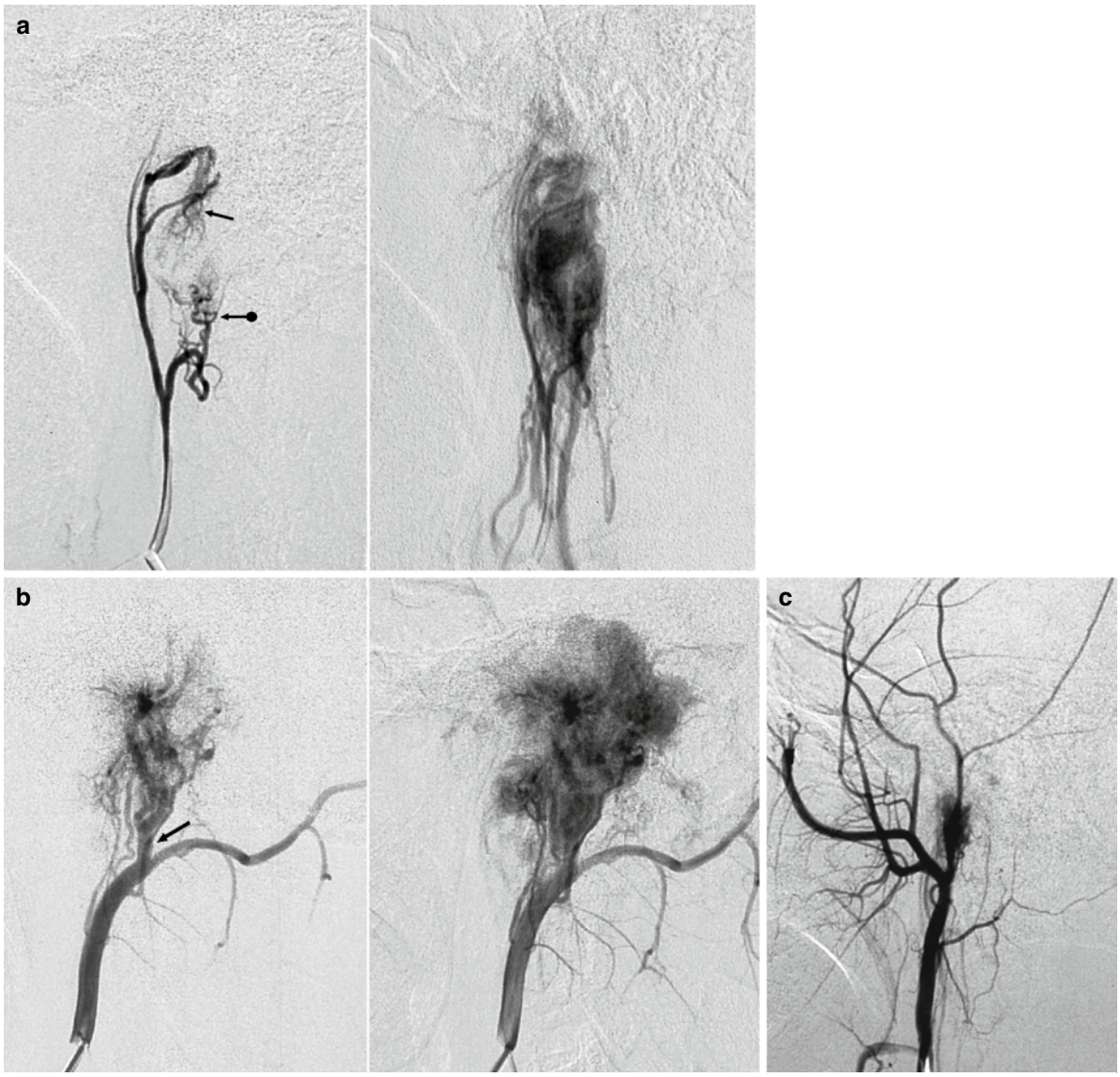

Fig. 3.22 Tympano-jugular paraganglioma supplied by branches of the occipital and ascending pharyngeal arteries. A small component also came from the anterior tympanic artery branch of the internal maxillary artery. (**a**) Lateral angiogram of the ascending pharyngeal artery. The pharyngeal (*arrow with dot*) and tympanic branches (*arrow*) supply the tumor. In the later phase, the anterior compartment of the tumor is well defined. (**b**) Lateral angiogram of the occipital artery. A large stylomastoid artery (*arrow*) is involved in the vascularization of the tumor. In the later phase, the posterior compartment of the tumor is evident. (**c**) A small supply from the anterior tympanic branch is present

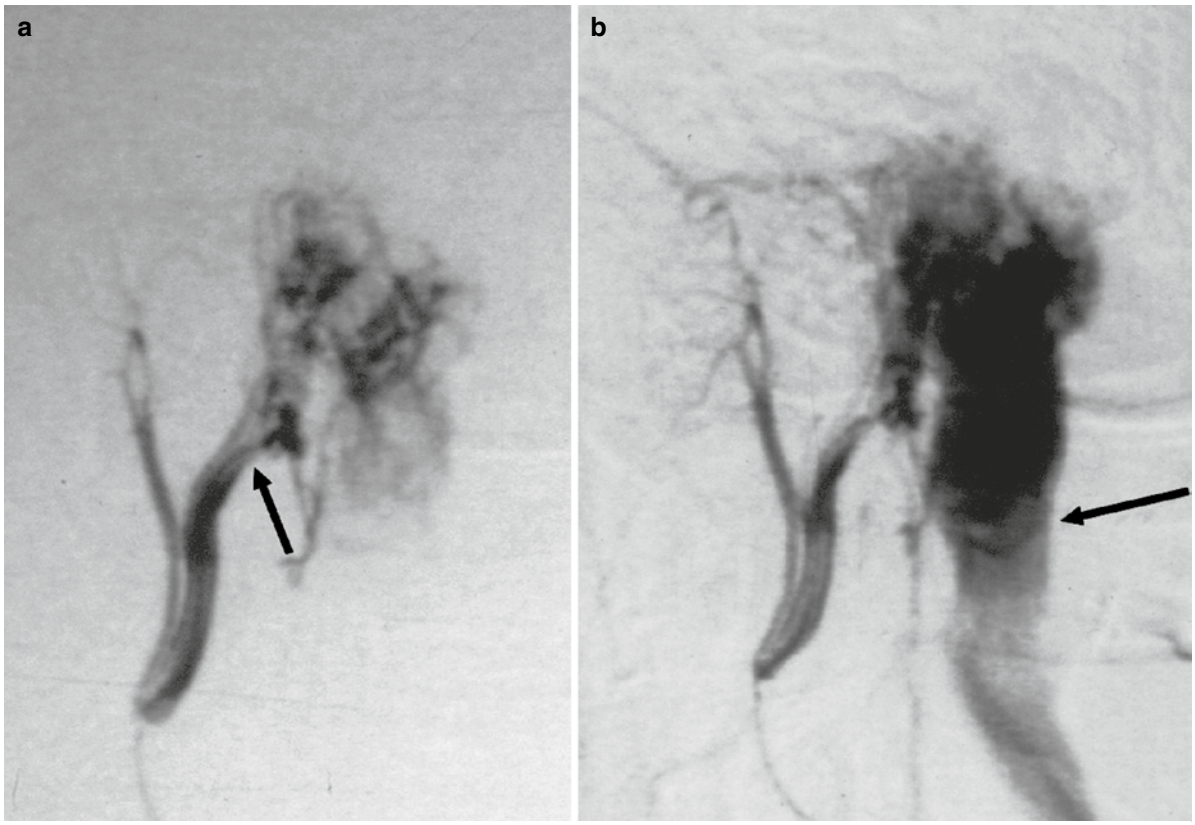

Fig. 3.23 Large tympano-jugular paraganglioma supplied mainly by tympanic branches of the ascending pharyngeal artery. (**a**) Angiogram (*oblique view*) of the selective catheterization of an enormous dilated ascending pharyngeal artery. Tympanic branches (*arrow*) supplying the tumor. (**b**) Drainage in the jugular vein infiltrated by the paraganglioma

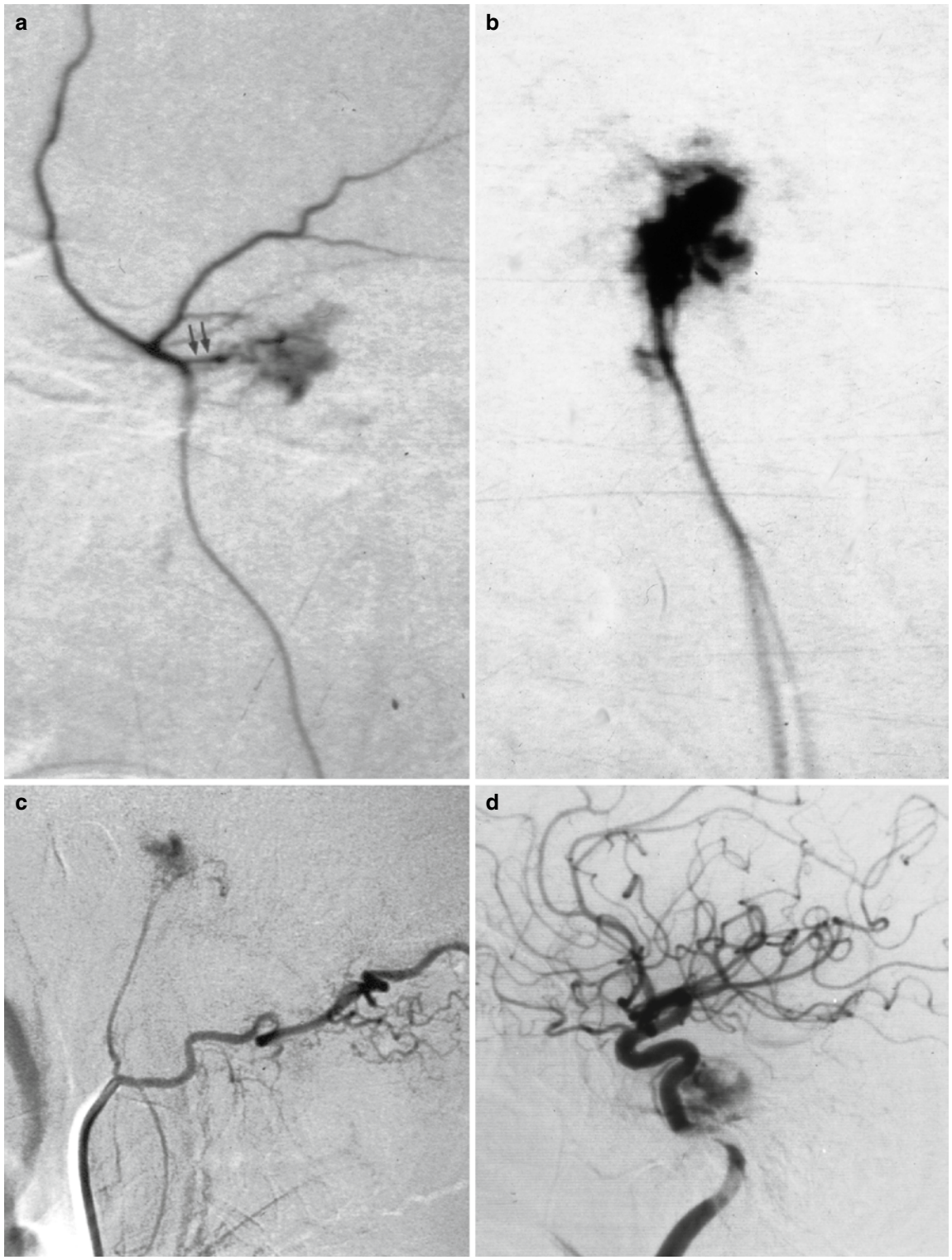

Fig. 3.24 Selective studies of a tympanic paraganglioma supplied by superior tympanic branches (**a**) of the petrosquamous branch (*arrows*) of the middle meningeal artery (*arrows*). There is a second supply arising from the inferior tympanic branch of the ascending pharyngeal artery. (**b**) Small paraganglioma (**c**) in another patient supplied only by the tympanic branch of the stylomastoid artery. Another example (**d**) of a large tympano-jugular paraganglioma with involvement of cavernous and petrous branches of the internal carotid artery

3.9.5 Meningiomas

Meningiomas are a relatively common pathology, having a frequency of about 18% of all intracranial tumors. They typically predominate in women of middle to old age (Bradac et al. 1990). Meningiomas originate in meningothelial cells of the meninges. The richness of vascularization depends on the meningioma subtype. Essentially, there are two groups of supplying arteries. The first consists of meningeal branches entering the tumor at the site of dural attachment and supplying the central part of it; the second consists of pial branches of the ICA and/or vertebral artery, which vascularize the more peripheral part of the tumor. One vascular sector can exert evident predominance over the other. The origin of the meningeal vascularization depends largely on the site of the primary dural attachment of the meningioma. In addition, the tumor can extend and secondarily involve further dural areas, leading to recruitment of other meningeal feeders (Figs. 3.25 and 3.26). Preoperative devascularization may be performed in selective cases.

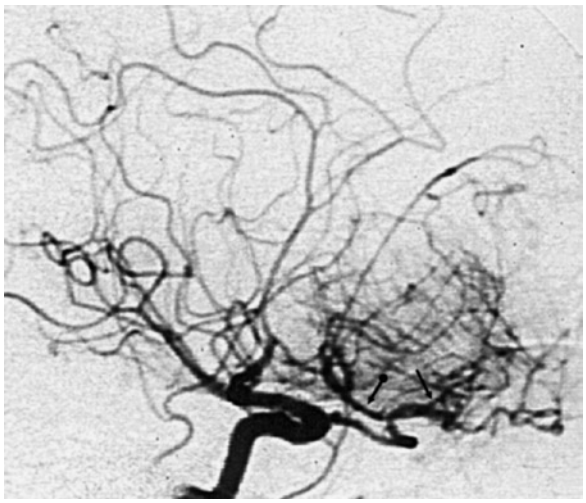

Fig. 3.25 Frontobasal meningioma, carotid angiogram, lateral view. The tumor is richly vascularized by branches of the ophthalmic artery represented by the recurrent meningeal artery (*arrow with dot*) and posterior ethmoidal arteries (*arrow*)

3.9.6 General Considerations in Endovascular Treatment in the ECA Area

- Abundant anastomoses are present among all the branches of the ECA. In the endovascular treatment of the different pathologies of this sector, especially in cases of vascular malformation, proximal occlusion

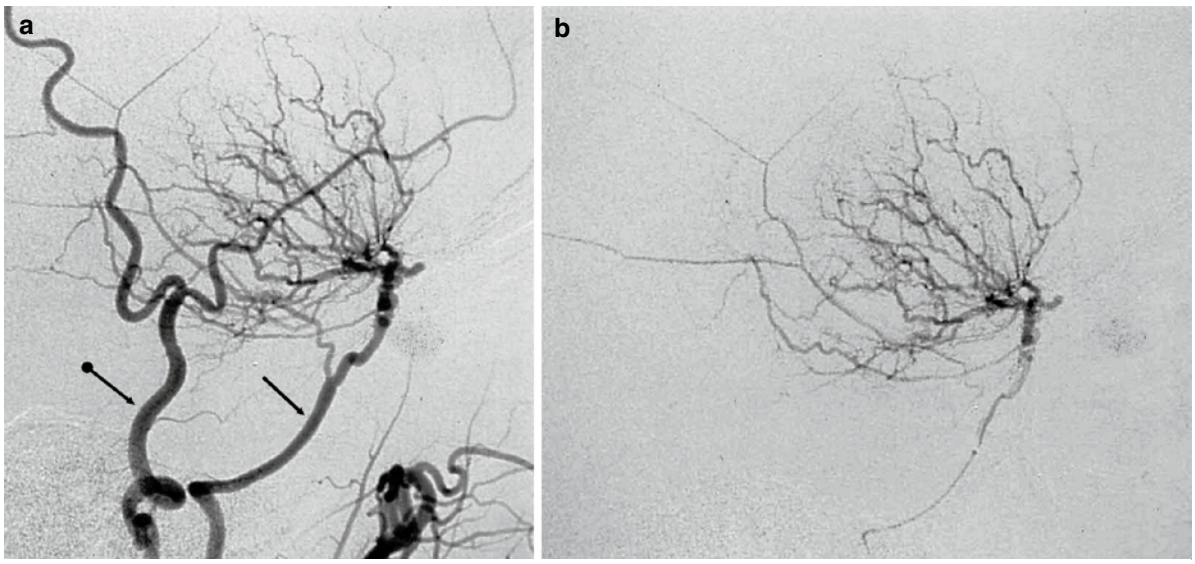

Fig. 3.26 Temporo-basal meningioma, richly vascularized by distal branches of the middle meningeal artery. (**a**) External carotid artery angiogram, lateral view. Middle meningeal artery (*arrow*) supplying the tumor. Superficial temporal artery (*arrow with dot*). (**b**) Selective study of the middle meningeal artery followed by devascularization of the lesion with polyvinyl alcohol. (**c**) Control angiogram post-treatment

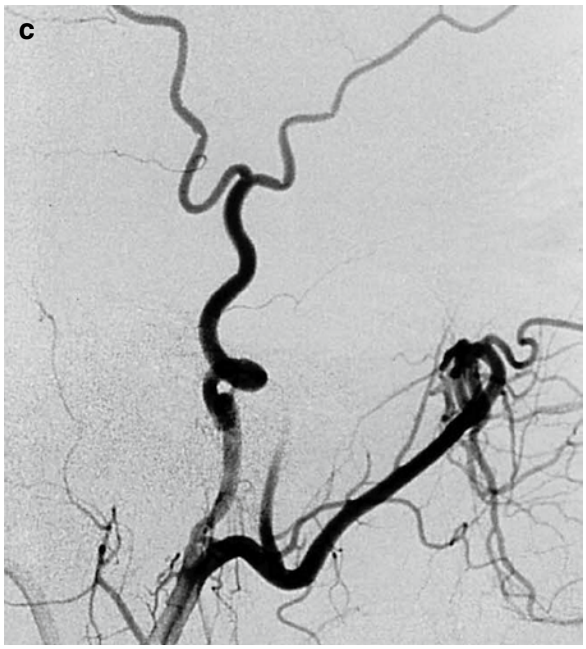

Fig. 3.26 (continued)

of the supplying arteries should be avoided since this would rapidly lead to the formation of a collateral circulation, reinjecting the lesion. The embolic material should be directly injected into the nidus or close to it.

- Many anastomoses (dangerous connections) (Table 3.1) (Figs. 3.27–3.29) can link the ECA with the ICA and vertebral artery. These are listed in Table 3.1 and should be considered when endovascular treatment is planned. These anastomoses can be minimal or large (Lasjaunias and Berenstein 1987; Morris 1997; Geibprasert et al. 2009). They can already be recognizable at the beginning of endovascular treatment or may enlarge and appear during it, following super-selective injection or opening of collateral paths as a consequence of occlusion of other arteries. Frequent angiographic control is mandatory.
- Another important aspect is the supply of a few cranial nerves from branches of the ECA (Table 3.2). This should be considered whenever a vascular treatment involves these branches. It is essential to take particular caution in the choice of embolic material in these cases.

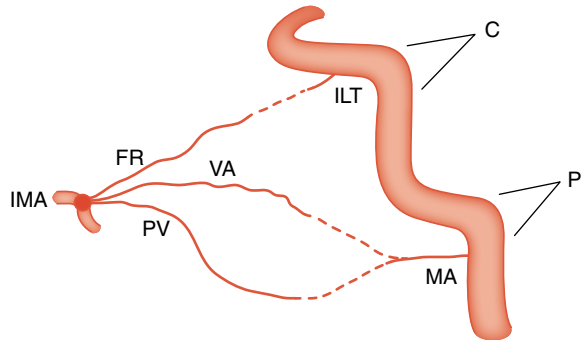

Fig. 3.27 Anastomosis between branches of the distal internal maxillary artery (*IMA*), foramen rotundum artery (*FR*), vidian artery (*VA*), pterygovaginal artery (*PV*) with the inferior lateral trunk (*ILT*), cavernous portion of ICA (*C*) and with the mandibular artery (*MA*), petrous portion of the internal carotid artery (P)

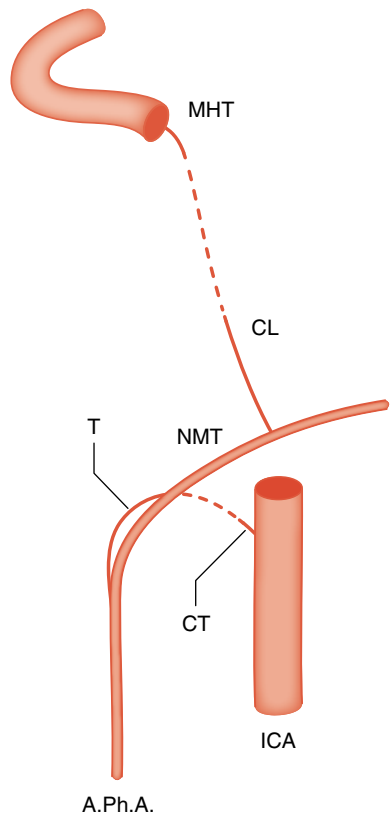

Fig. 3.28 Anastomosis between tympanic branch (*T*) of the ascending pharyngeal artery (*A.Ph:A.*) and caroticotympanic branch (*CT*) of the petrous segment of the internal carotid artery. Anastomosis between clival ascending branches (*CL*) of the neuromeningeal trunk of the APhA with the descending branches of the meningeal hypophyseal trunk (*MHT*) of the cavernous segment of the internal carotid artery

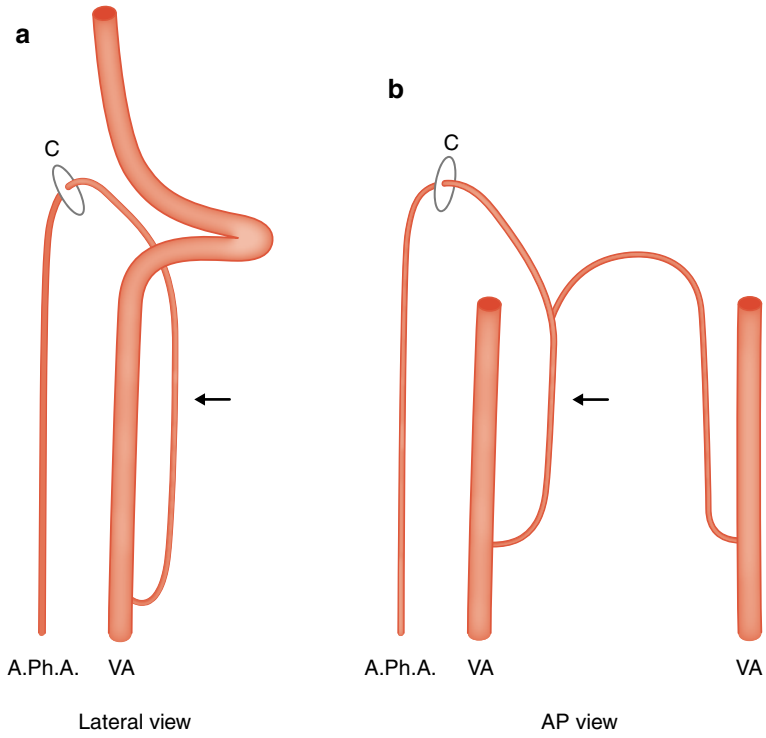

Fig. 3.29 (**a, b**), Lateral and AP view of the connection between the ascending pharyngeal artery and vertebral artery (*VA*). This is formed by the hypoglossal branch, which passes through the hypoglossal canal (*C*), gives off a descending branch anastomosing with the ascending C3 radiculomeningeal branch (*arrow*) of the *VA*. The *AP view* demonstrates also the connection on the dorsal surface of the odontoid process of the radiculomeningeal branch of the *VA* with that of the contralateral vertebral artery. These anastomoses form the so-called arch of the odontoid process

Table 3.1

Anastomosis between the external and internal carotid arteries				
Foramen rotundum a.	(IMA)	–	ILT	(ICA)
Vidian a.	(IMA)	–	Mandibular a.	(ICA)
Pterygovaginal a.	(IMA)	–	Mandibular a.	(ICA)
Middle meningeal a.	(IMA)	–	MHT and ILT	(ICA)
Accessory meningeal a.	(IMA)	–	ILT	(ICA)
Clival branches	(APhA)	–	MHT	(ICA)
Tympanic branches	(A.Ph.A)	–	Carotico-tympanic a.	(ICA)
Anastomosis between the external carotid and vertebral arteries				
Hypoglossal a.	(A.Ph.A)	–	Radiculo-meningeal branch (Odontoid arch)	(VA)
C1–C2 musc. branches	(A.Ph.A)	–	C1–C2 musc. branches	(VA)
C1–C2 musc. branches	(Occ.A.)	–	C1–C2 musc. branches	(VA)
C3–C4–C5 musc. branches	(A.cerv.A.)	–	C3–C4–C5 musc. branches	(VA)
Anastomosis between the external carotid and ophthalmic arteries				
Middle meningeal a.	–		Lachrymal branch	(Oph.A.)
Deep ant. temp. a.	–		Lachrymal branch	(Oph.A.)
Sphenopalatine a.	–		Ethmoidal branches	(Oph.A.)
Superficial temporal a.	–		Supraorbital branch	(Oph.A.)
Facial-infraorbital a.	–		Nasal branches	(Oph.A.)
Ophthalmic artery arising from middle meningeal artery				

Table 3.2 Branches of the external carotid artery supplying cranial nerves

Cranial nerve VII	Tympanic branch of the petrosquamous artery (middle meningeal artery) and stylomastoid artery (occipital or posterior auricular artery)
Cranial nerves IX, X, XI	Jugular branch of the neuromeningeal trunk of the ascending pharyngeal artery.
Cranial nerve XII	Hypoglossal branch of the neuromeningeal trunk of the ascending pharyngeal artery.

Anterior Cerebral Artery

4

The anterior cerebral artery (ACA) is the smaller of the two terminal branches of the internal carotid artery (ICA). It is considered the direct embryonic continuation of the ICA, whereas the middle cerebral artery (MCA) is only a secondary branch of this vessel (De Vriese 1905; Abbie 1934). The ACA can be divided into several segments (Huber 1979) (Fig. 4.1).

- A1 (precommunicating segment): from its origin to the anterior communicating artery (AcomA)
- Distally to the AComA, the ACA continues as the pericallosal artery:
- A2 (infracallosal segment)
- A3 (precallosal segment)
- A4 (supracallosal segment)

4.1 Precommunicating Segment

The first part of the artery is called the A1 or precommunicating segment. It arises at the carotid bifurcation, and it runs medially above the chiasma and optic nerve with a horizontal, sometimes descending, ascending, or tortuous course, joining the contralateral A1 by way of the AcomA. Its length is on average 12.7 mm (Perlmutter and Rhoton 1976) (Fig. 4.2).

Branches. Perforators are found along the length of the A1, but they are more numerous in its proximal section, arising from the superior surface (Dunker and Harris 1976; Perlmutter and Rhoton 1976; Rosner et al. 1984). A few perforators also arise from the AcomA (Dunker and Harris 1976; Perlmutter and Rhoton 1976; Rosner et al. 1984; Krayenbühl et al. 1972; Marinković et al. 1990). The perforators enter the anterior medial part of the anterior perforated substance (APS), supplying the suprachiasmatic anterior portion of the hypothalamus. Other perforators supply the optic nerve and chiasma.

The recurrent artery of Heubner, first described by Heubner (1872), is the largest and longest perforating artery. It commonly takes its origin from the distal A1 or proximal A2 segment, rarely from the

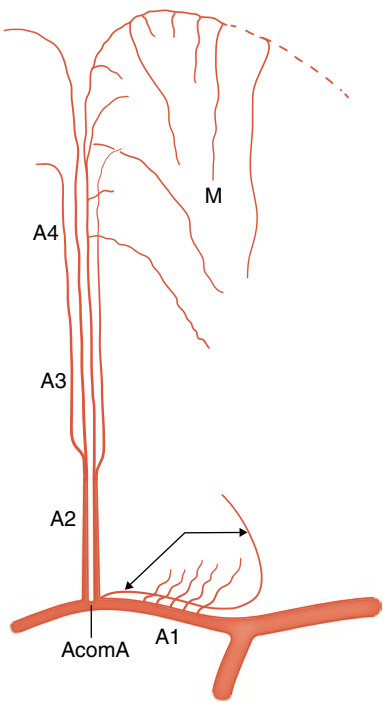

Fig. 4.1 Segments of the anterior cerebral artery: *A1*, *A2*, *A3*, and *A4*. Deep perforators arising from the *A1*. Artery of Heubner (*double arrow*) arising from *A1–A2*. Medullary arteries (*M*, *short and long branches*) arising from cortical branches. Leptomeningeal anastomosis with the MCA (--------)

G.B. Bradac, *Cerebral Angiography*,
DOI: 10.1007/978-3-642-15678-6_4, © Springer-Verlag Berlin Heidelberg 2011

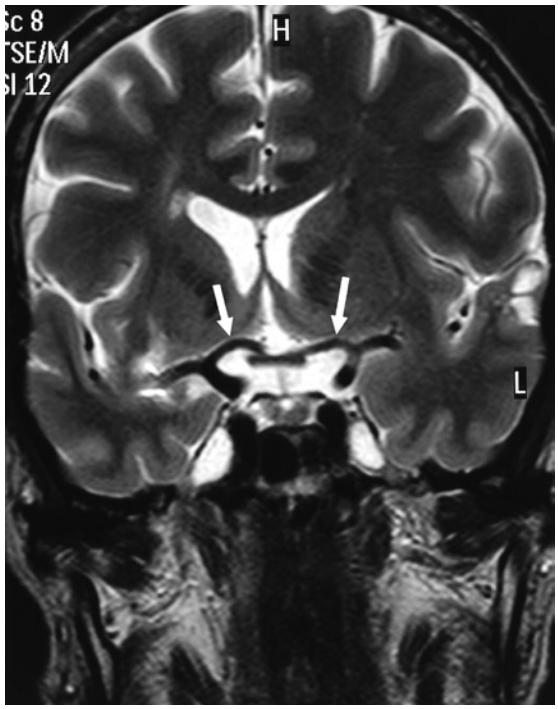

Fig. 4.2 Coronal MRI, T2-weighted image showing the relationship of the A1 to the chiasma (*arrows*)

AcomA. It can have a common origin with the frontopolar artery (Perlmutter and Rhoton 1976; Rosner et al. 1984).

In its course, the artery of Heubner runs back parallel to the A1 and M1 segments to enter the APS anterior to the other perforators of the A1. It can occur as a single or sometimes multiple branches, supplying the inferior part of the head of the nucleus caudatus, the inferior part of the anterior limb of the internal capsule, and adjacent part of the globus pallidus and putamen (Perlmutter and Rhoton 1976; Rosner et al. 1984) (Figs. 4.3, 4.4, 4.8c, and 4.10).

The AComA and the A1-A2 junction are typical sites of aneurysm, which can have a close relationship with the artery of Heubner. When surgical or endovascular treatment is planned, it is very useful to attempt to identify this artery on the angiogram.

4.2 Distal Segments

Distal to the junction with the AComA begins the segment called the pericallosal artery, which can be divided, according to its relationship with the corpus

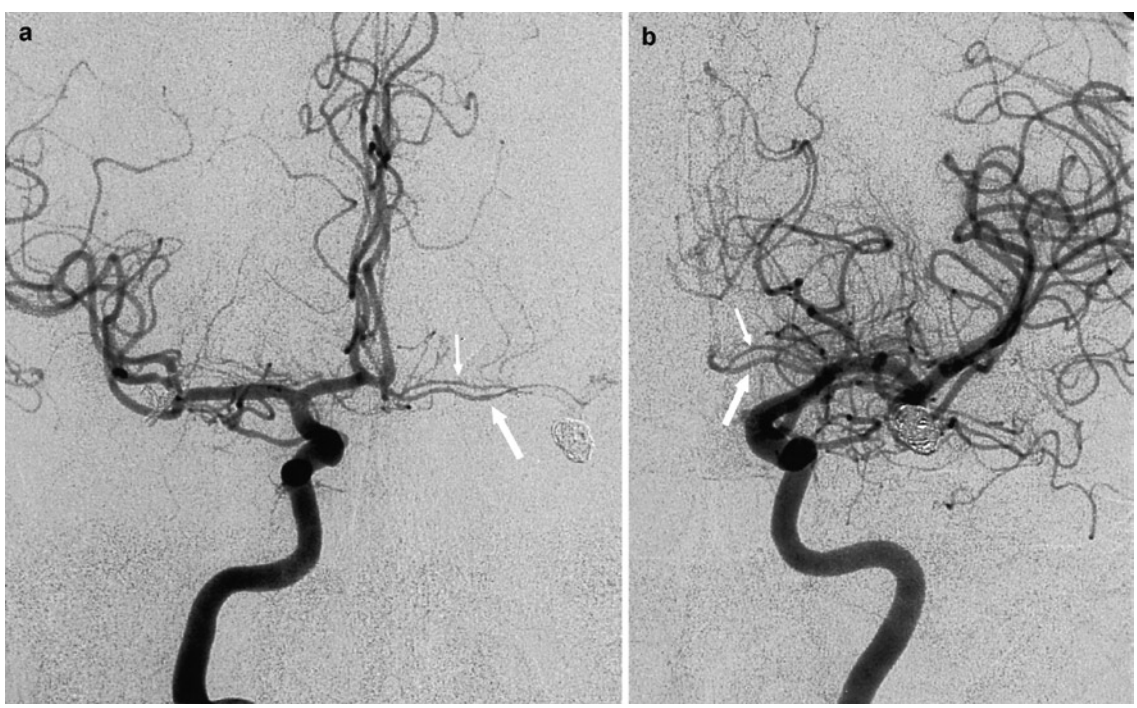

Fig. 4.3 *Right* (**a**) – *left* (**b**) AP carotid angiogram in a patient treated with coils for a ruptured left middle cerebral artery aneurysm. Well-developed A1 on the *right*. Hypoplastic *left* A1 segment (*large white arrow*). Artery of Heubner (*small white arrow*) running parallel to the A1 segment

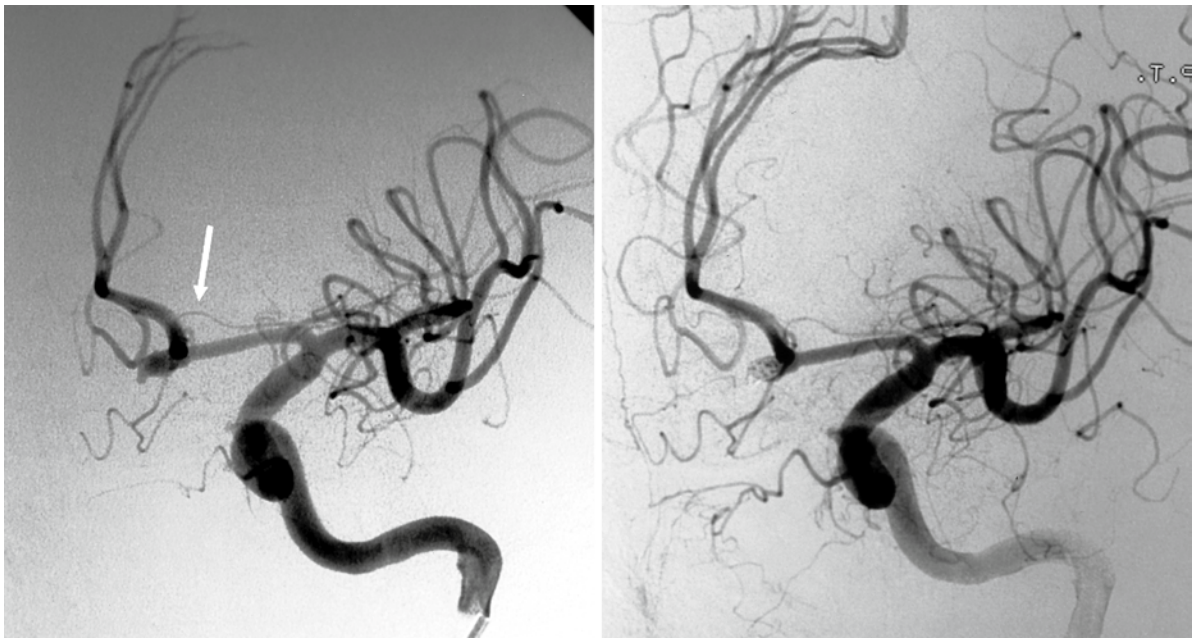

Fig. 4.4 Carotid angiogram, oblique view in a patient examined for ruptured aneurysm of the anterior communicating artery treated in the same section with coils. *Left*, artery of Heubner (*white arrow*) arising close to the aneurysm

callosum, into three further segments (Liu and Kricheff 1974; Huber 1979).

4.2.1 Infracallosal Segment

This is also called the A2, and it runs into the interhemispheric fissure upward in front of the lamina terminalis to the genu of the corpus callosum. It gives off infraorbital and frontopolar branches, supplying, respectively, the frontobasal region (gyrus rectus, orbital gyri, olfactory bulb and tract) and the anterior medial part of the superior frontal gyrus (Figs. 4.5 and 4.6).

4.2.2 Precallosal Segment

This is also called the A3. It is a short segment and curves around the genu of the corpus callosum, to which it gives off small branches (Figs. 4.5 and 4.6). It gives off the callosomarginal artery, which, when well formed,

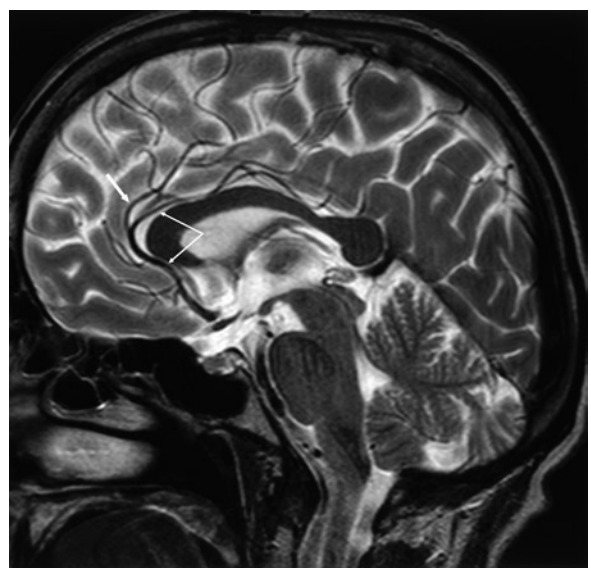

Fig. 4.5 T2-weighted sagittal MRI image. Infra-, pre-, and supracallosal segments of the pericallosal artery (*arrow with angle*). The supracallosal segment runs with an undulating course above the corpus callosum, partially in the pericallosal cistern and partially superior to it. From its precallosal segment arises the callosomarginal artery (*arrow*)

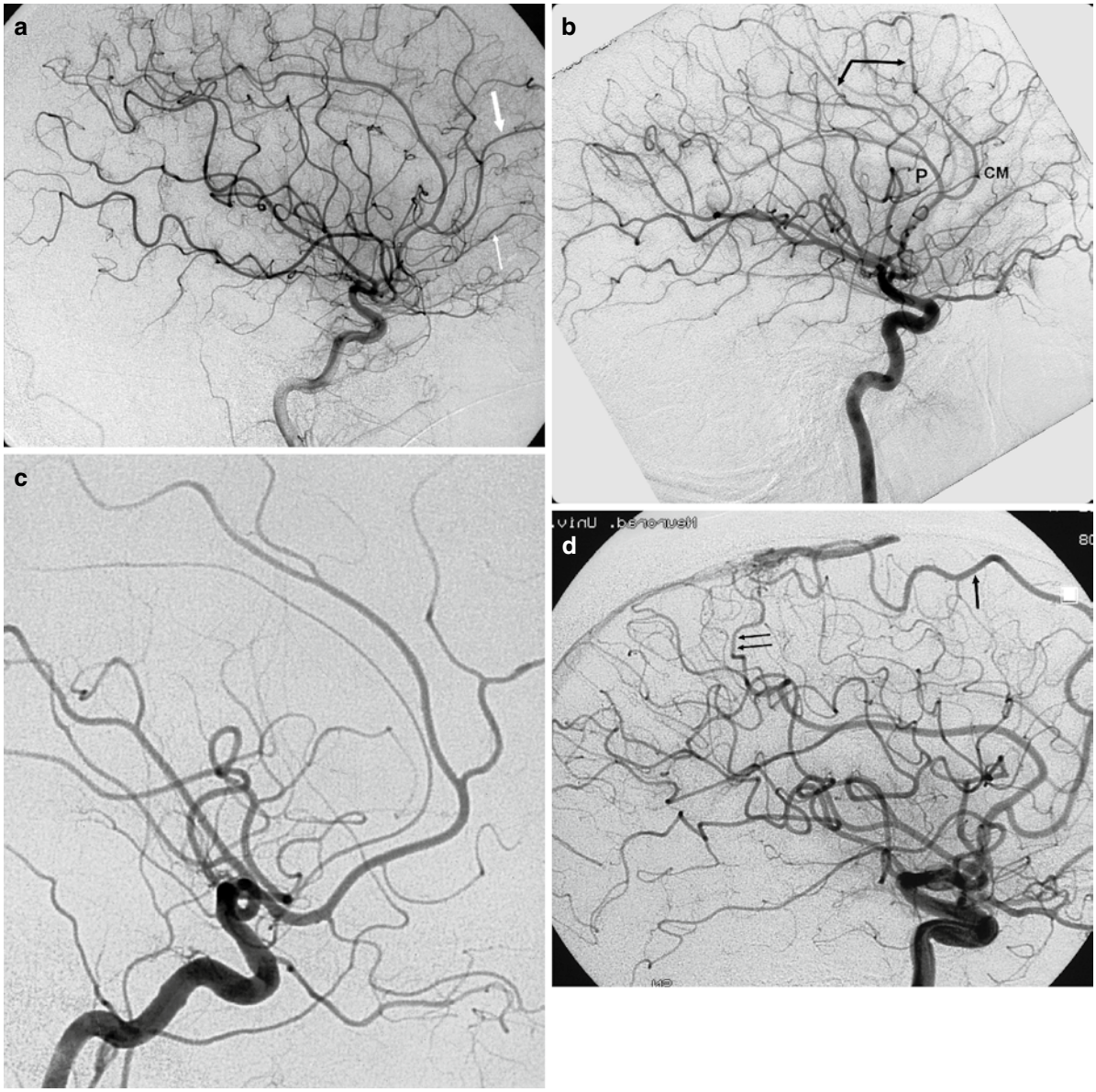

Fig. 4.6 Lateral angiograms. (**a**) Well-developed callosomarginal artery, though the pericallosal artery is hypoplastic. Frontoorbital artery (*small white arrow*), frontopolar artery (*large white arrow*). (**b**) Pericallosal artery (*P*) in its course along the corpus callosum. Callosomarginal artery (*CM*), frontal and parietal branches (*arrow with angle*). (**c**) Hypoplastic pericallosal artery and well-developed callosomarginal arteries arising as a separate trunk. (**d**) Well-developed callosomarginal artery (*large arrow*) supplying small-convexity angiomas. Another branch (*double arrow*), probably a dilated paracentral artery, arises from the dilated pericallosal artery

runs posteriorly in the cingulate sulcus above the gyrus cinguli and appears on the lateral angiogram superior and on the anterioposterior (AP) view slightly medial to the pericallosal artery. The more distal branches extend to the paracentral and precuneus lobes.

The callosomarginal artery can be absent or developed only in its frontal portion. In such cases, its branches are replaced by arteries arising from the presupracallosal segment of the pericallosal artery.

4.2.3 Supracallosal Segment

This segment is also called the A4 (Figs. 4.5 and 4.6). It is the more distal segment of the pericallosal artery. It runs posteriorly in the pericallosal cistern, above the surface of the corpus callosum, toward the splenium. Its posterior extent depends on the size of the posterior pericallosal branch (artery of the splenium) of the posterior cerebral artery. Occasionally, it can extend below the corpus callosum toward the foramen of Monro (Perlmutter and Rhoton 1978), as in embryological life. The supracallosal artery may have an undulating course and sometimes show an upward distension in its midportion. The artery can be well formed, hypoplastic, or uni- or bilaterally absent.

A meningeal branch can arise from the presupracallosal segment, and this branch supplies the inferior portion of the falx (Lasjaunias and Berenstein 1990). It anastomoses with the branches of the middle meningeal artery, which descend along the falx. The meningeal branch can also be connected with the meningeal branch that arises from the posterior cerebral artery (see Sect. 7.1).

4.2.4 Cortical Branches

Several arteries arise from the supracallosal segment of the pericallosal artery and/or callosomarginal artery and run on the medial surface of the hemisphere. There is a close relationship between the pericallosal and callosomarginal arteries; when one of these is hypoplastic or absent, the other can replace its vascular territory.

From anterior to posterior, the cortical branches are represented first by the frontal branches. The second artery is the small paracentral branch, which runs toward the paracentral lobule and extends to the central sulcus, supplying the paracentral lobule and superior part of the precentral and postcentral gyri. The more distal arteries are the inferior and superior parietal branches. The superior parietal artery is usually a large branch that runs in the marginal segment of the cingulate sulcus and marks the boundary between the paracentral lobule and precuneus, with branches supplying both arteries (Figs. 4.5 and 4.6).

4.3 Anatomical Variations

One A1 segment is hypoplastic (diameter of 1.5 mm or less) in 10% of cases and severely hypoplastic (diameter of less than 1 mm) or absent in 1% (Perlmutter and Rhoton 1976; Huber 1979; Yaşargyl 1984a, 1984b) (Figs. 4.3, 4.7 and 7.2). This variation is frequently associated with aneurysm of the AComA (Perlmutter and Rhoton 1976; Huber 1979; Yaşargyl 1984a, 1984b).Two or three AComAs may be present in up to 40% of cases (Perlmutter and Rhoton 1976; Marinković et al. 1990) (Fig. 4.8). The same artery can be hypoplastic, being as small as 0.2 mm (Perlmutter and Rhoton 1976.

Another, more infrequent, variation is a duplicated A1. In such cases, the inferior branch, which arises from the ICA, close to the origin of the ophthalmic artery, has an ascending course and passes inferiorly to the optic nerve; the superior branch has a normal origin from the distal ICA and runs superiorly to the nerve. The superior branch can be hypoplastic or absent (Turnbull 1962; Nutik and Dilenge 1976; Milenkovic 1985; Friedlander and Ogilvy 1996; Morris 1997). The A1 segment may have a normal origin, but along its course it features duplication or fenestration (Fig. 4.9).

The pericallosal artery can be unique (azygos pericallosal artery); in other cases, there may be a third branch, which can predominate over the others (Perlmutter and Rhoton 1976; Dunker and Harris 1976; Marinković et al. 1990) (Figs. 4.10–4.12). In these cases, aneurysms are also frequently present and involve the AComA or pericallosal artery. The artery of Heubner is rarely absent on one side. One should bear in mind that if the A1 is hypoplastic, the artery of Heubner may be very large and can be confused with the A1. Variations concerning the pericallosal and callosomarginal arteries have already been described.

4.4 Vascular Territories

The vascular territories supplied by the perforating branches arising from the A1 and by the recurrent artery of Heubner have already been described. These branches are end arteries, without anastomoses to each other or with the branches descending through the white matter (medullary arteries). The distal segments of the ACA supply the frontobasal region and medial surface of the hemisphere in the frontoparietal region.

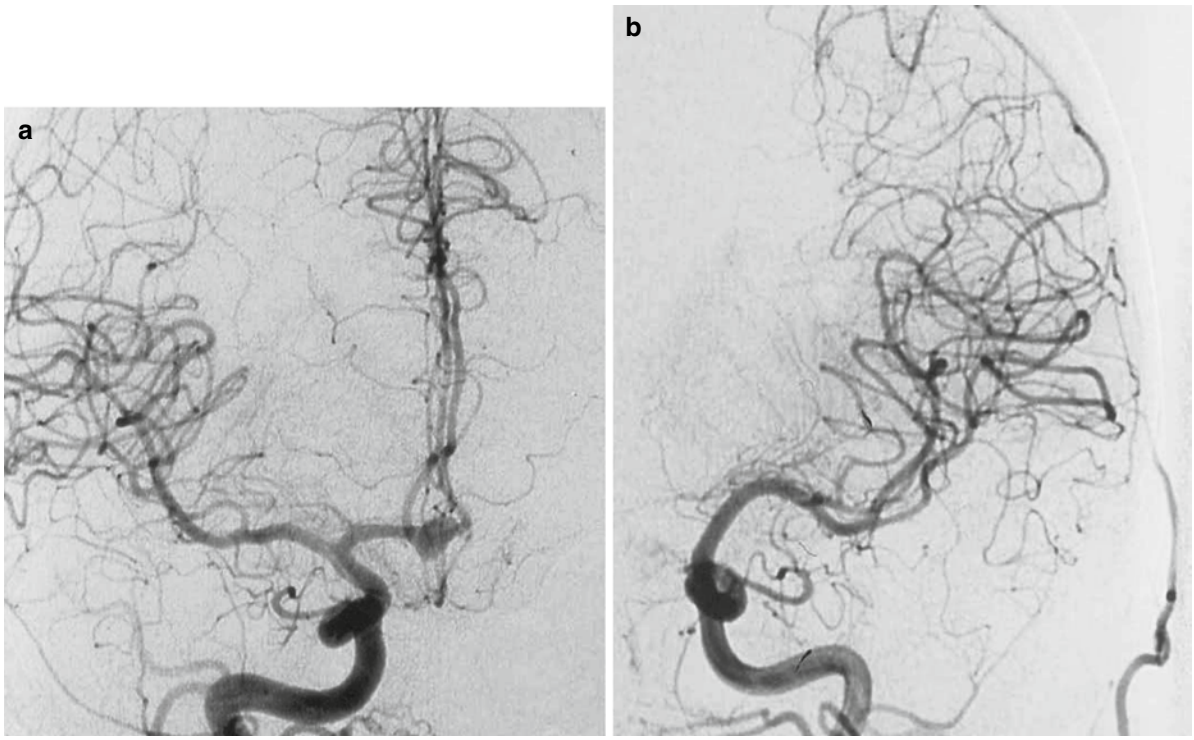

Fig. 4.7 Hypo/aplastic left A1 segment in a patient with aneurysm of the anterior communicating artery well developed right A1

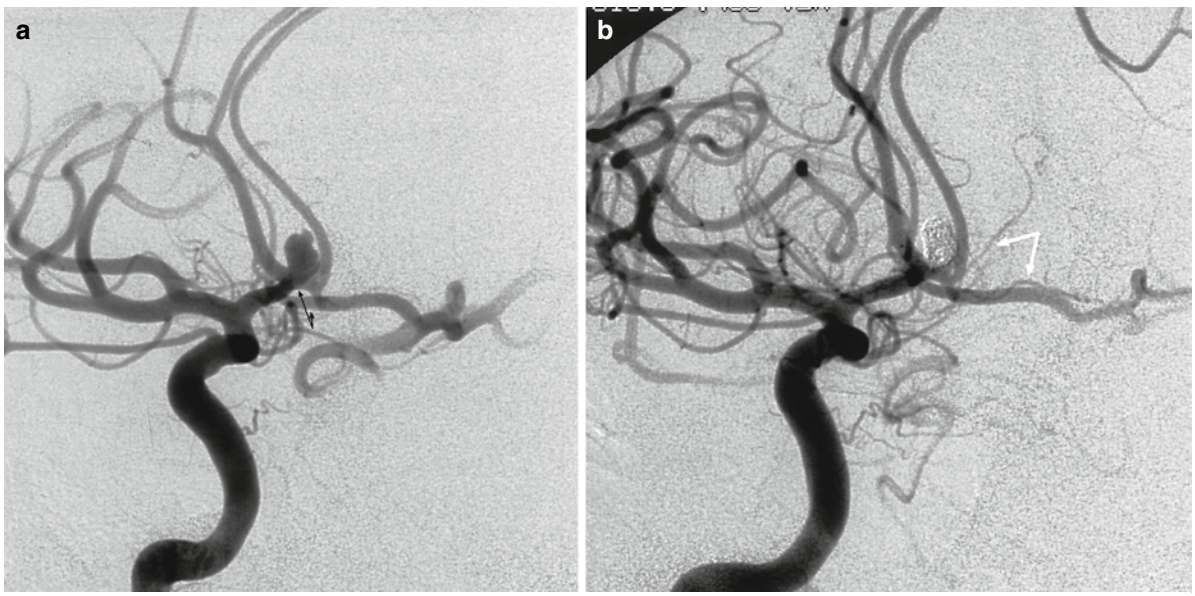

Fig. 4.8 (**a**) Internal carotid angiogram (*oblique view*) in a patient with ruptured aneurysm with the neck in the angle of the A1–A2 segments of the right anterior cerebral artery. Duplication of anterior communicating artery (*arrows with angle*). In cases with such anomalies, many projections are frequently necessary in an attempt to identify the aneurysm neck. (**b**) Angiogram post-coiling. The artery of Heubner, arising as a common trunk with the frontopolar artery (*white arrows with angle*) is visible. (**c**) Another patient with an anomaly involving the anterior communicating artery, carotid angiogram, oblique view. There is triplication of the anterior communicating artery (*arrows*). The artery of Heubner is well visualized (*arrowheads*). There is an origin of the ophthalmic artery from the cavernous portion of the internal carotid artery. (**d**) Carotid angiogram of the same patient, better indicating the anomalous origin of the ophthalmic artery

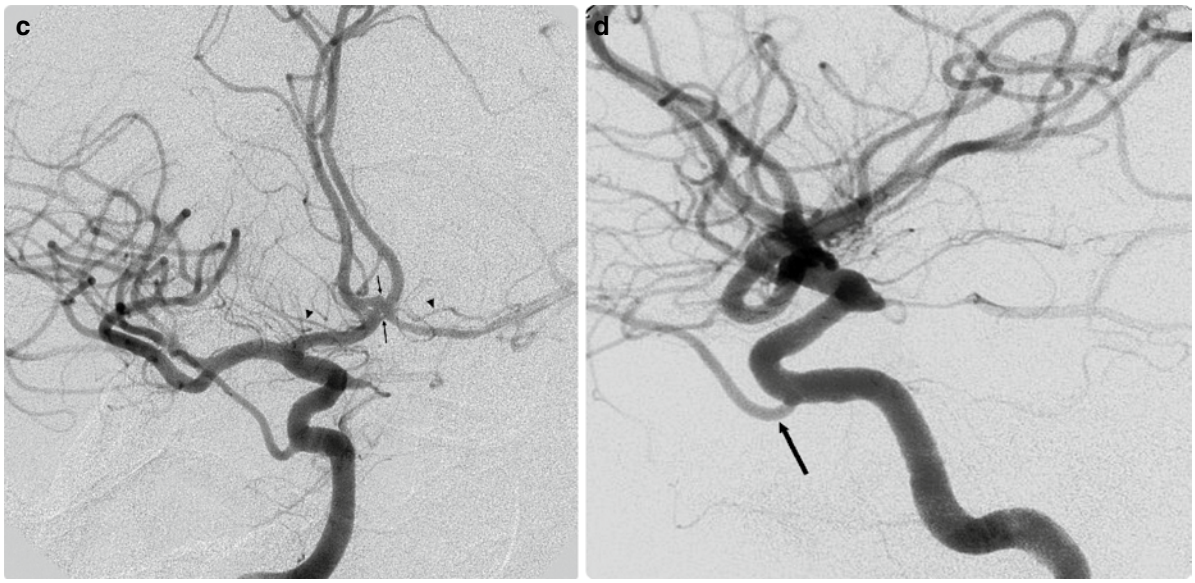

Fig. 4.8 (continued)

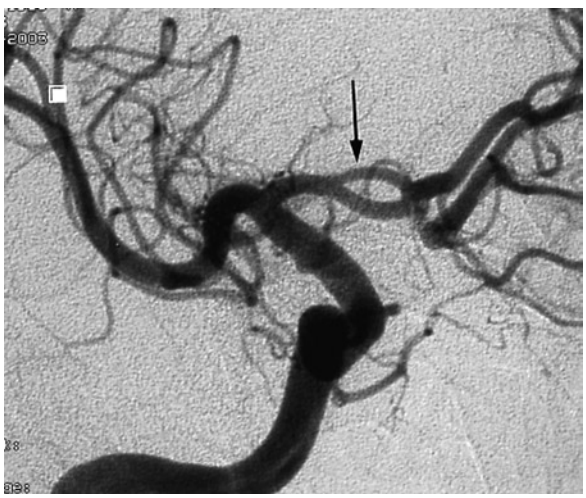

Fig. 4.9 Duplication of the A1

The involved branches extend also to the cortex of the convexity for about 1–3 cm. Among these branches, the paracentral and, partially, the superior parietal arteries are involved in the supply of the medial and superior section of the primary motor cortex.

Along its course, the pericallosal artery gives off perforators for the corpus callosum, septum pellucidum, fornix, and anterior commissure. From the distal branches, running on the surface of the cortex, arise small arteries that supply the brain parenchyma. These arteries enter the parenchyma with a perpendicular course and can be subdivided into cortical, medullary, and corticomedullary arteries. The first of these supply the cortex and end with horizontal branches in the various cellular layers. The medullary arteries supply the superficial (short medullary branches) and deep white matter (long medullary branches). The latter run toward the ventricular wall. The corticomedullary arteries have aspects of both. These arteries are end arteries (De Reuck 1972). In their course, the medullary arteries are surrounded by a thin space (perimedullary spaces, Virchow-Robin spaces). It had been supposed that the perivascular space was continuous with the subarachnoid space. This, however, was not confirmed by electron microscopy (Hutchings - Weller 1986), which showed that the pia mater represents a clear barrier, separating the subarachnoid space from the subpial space and perivascular space. But neither the subarachnoid space nor the pia matter extends into the brain, accompanying the blood vessels as they run into the perivascular space.

Conversely, potential leptomeningeal (pial) anastomoses are present at the surface of the hemisphere in the border zone of the vascular territories between superficial branches of the ACA, MCA, and the posterior cerebral artery (PCA). Anastomoses are also present between both posterior pericallosal arteries arising from the ACA and PCA (see Fig. 4.1).

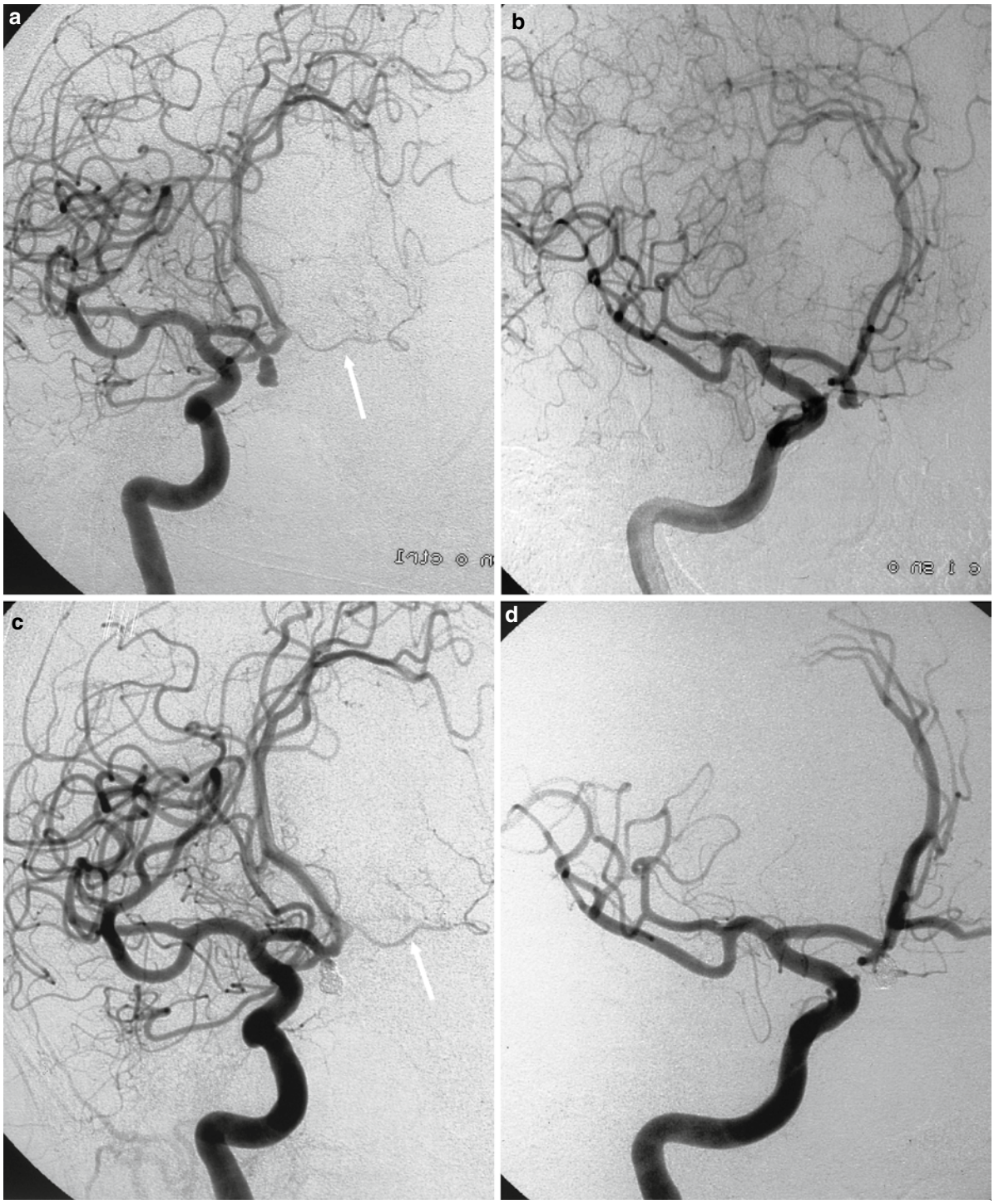

Fig. 4.10 Angiograms with two oblique views (**a** and **b**) in a patient with ruptured aneurysm in the angle of the A1–A2 of the right anterior cerebral artery. There is a unique pericallosal artery (azygos pericallosal artery). Notable is the artery of Heubner (*white arrow*), running parallel to the left A1. Control angiogram (**c** and **d**) after occlusion of the aneurysm with coils

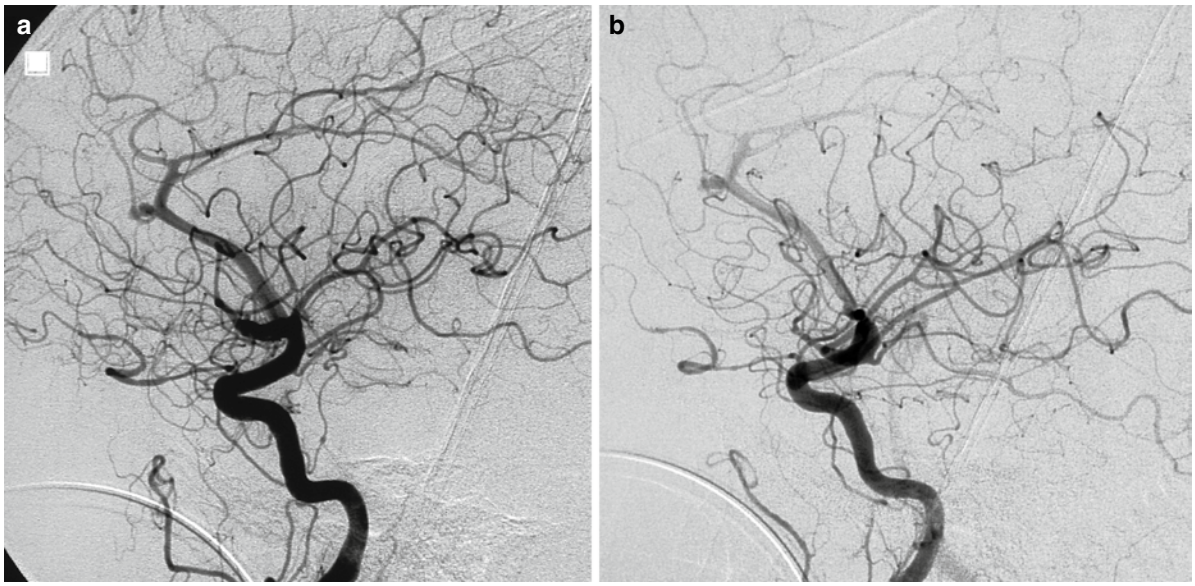

Fig. 4.11 Azygos pericallosal artery associated with a pericallosal aneurysm with subarachnoid hemorrhage. A large pericallosal artery (**a**) is evident on the left carotid angiogram. The same pericallosal artery (**b**) is visible on the right carotid angiogram, less injected owing to a hypoplastic A1 segment

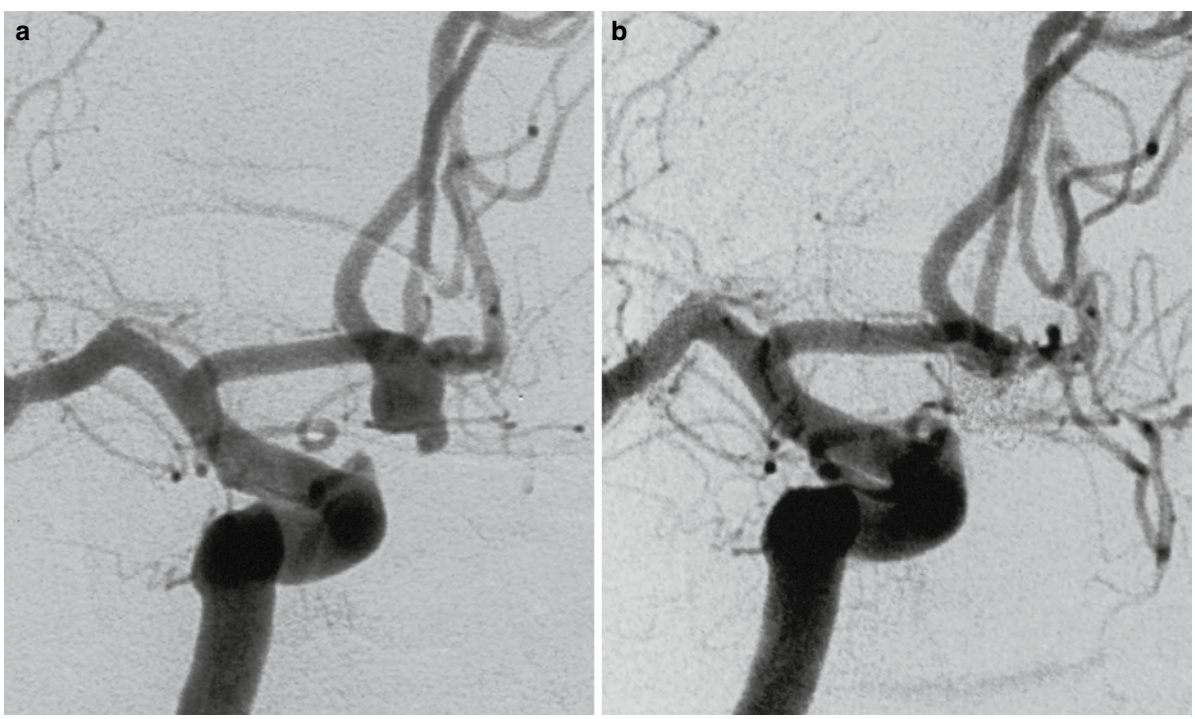

Fig. 4.12 Angiogram showing three pericallosal arteries (A. pericallosal triplex – arteria mediana corporis callosi) in a patient with ruptured aneurysm (**a**) treated with coils (**b**)

4.5 Angiogram

On the angiogram, the A1 segment is well recognizable in the AP oblique view (Figs. 4.3, 4.4, 4.7–4.10, and 4.12). It can be more difficult to make a precise identification of the AComA when bifurcation or trifurcation is present (Fig. 4.8). Among the perforators, the artery of Heubner can frequently be identified as a small branch, running back parallel to the A1 with a straight or undulating course (Figs. 4.3, 4.4, 4.8, and 4.10). See also Fig. 11.11 in Chap. 11.

The pericallosal and the callosomarginal arteries can be well discerned in the AP view. The course of these arteries as well as of their cortical branches, especially in the frontal area, may be more precisely demonstrated on the lateral angiogram. The posterior cortical branches (paracentral and parietal arteries) frequently cannot be identified because of overlapping with branches of the MCA. They can be identified when they are dilated and supply a vascular malformation (Fig. 4.6). Angio-MRI and Angio-CT are other diagnostic possibilities, though the angiogram offers better specific information. Some relationship to the cerebral parenchyma (chiasma, diencephalon, and corpus callosum) can be readily identified with MRI (Figs. 4.2 and 4.5).

Middle Cerebral Artery

5

The middle cerebral artery (MCA) is the larger of the two terminal branches of the internal carotid artery (ICA), supplying a big part of the cerebral hemispheres and basal ganglia. It can be divided into four segments (Figs. 5.1 and 5.2):

- M1 segment, running horizontally in the sylvian fissure
- M2 segment, running vertically on the surface of the insula
- M3 segment, running laterally and exiting the insular cistern
- M4 segment, which comprises the distal cortical branches

5.1 M1 Segment

The first segment (M1) arises at the ICA bifurcation and runs horizontally and laterally in the sylvian fissure below the anterior perforated substance (APS) toward the insula. Also called the sphenoidal segment because it runs parallel 1 cm posterior to the sphenoid ridge, the M1 ends at the limen insulae, where it sharply turns superiorly and posteriorly to form the M2 segment. The M1 divides distally into two or three branches (bi-trifurcation). Its length varies; it is, on average, 16 mm in length (Umansky et al. 1985). It can be very short, and so the bi-trifurcation may be located near the bifurcation of the ICA. It gives off two types of important branches.

Perforators. Since the first anatomical description of perforating branches by Duret (1874), many detailed studies have been performed. Also called the lenticulostriate arteries, these branches arise along the length of the M1 from its superior surface. They arise prevalently from the prebifurcation segment, more rarely from the postbifurcation or M2 segment (Westberg (1966); Rosner et al. 1984). The branches can be subdivided into medial, intermediate, and lateral groups. The medial are the least constant and can be replaced by the artery of

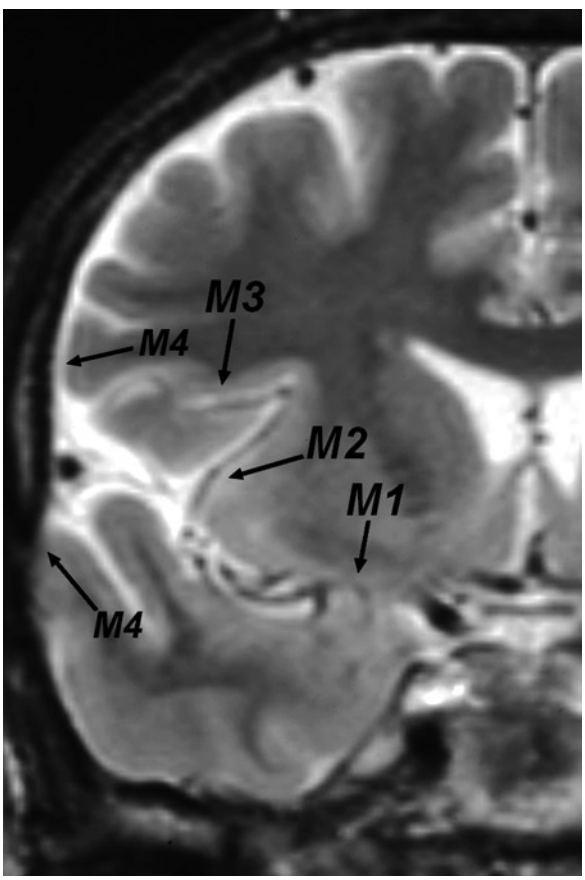

Fig. 5.1 RM Coronal: the MCA runs first horizontally in the sylvian cistern (*M1*), then on the surface of the insula (*M2*), further laterally (*M3*) exiting the insular cistern, and reaching the convexity (*M4*)

G.B. Bradac, *Cerebral Angiography*,
DOI: 10.1007/978-3-642-15678-6_5, © Springer-Verlag Berlin Heidelberg 2011

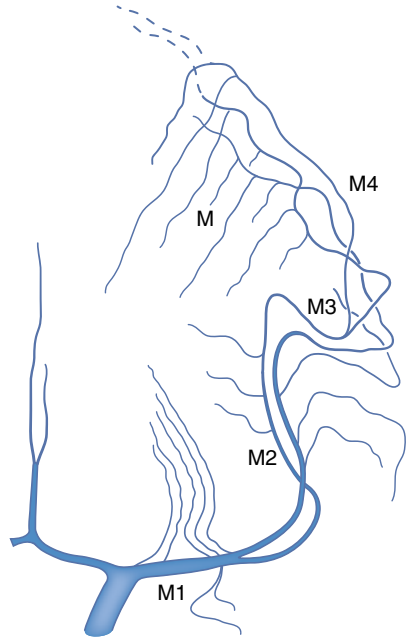

Fig. 5.2 Segments of the MCA: *M1*, *M2*, *M3*, and *M4*. Deep perforators arising from the *M1*. Medullary arteries (*short and long branches*) arising from the cortical branches (*M*). Anastomoses with the anterior cerebral artery (----------)

Heubner (Rosner et al. 1984). In the microanatomical study of Umansky et al. (1985), the perforators of the MCA were partially replaced by perforators of the anterior cerebral artery (ACA), especially by the artery of Heubner, in 26% of cases. The medial branches have a straight course, the intermediate a slightly tortuous course, and the lateral display the typical S-shaped aspect (Fig. 5.3).

The shorter the M1 segment with an early bifurcation, the greater is the number of perforators arising near the bifurcation, immediately proximal or distal to it from one of the postbifurcation branches (Kaplan 1965; Lazorthes et al. 1976; Rosner et al. 1984; Umansky et al. 1985) (Figs. 5.4 and 5.5). Perforators can originate as a common trunk (Umansky et al. 1985), and we have observed cases in which perforators and distal cortical branches arose from a common trunk (Fig. 5.5).

These different aspects concerning the deep perforators should be carefully considered in the surgical endovascular treatment of aneurysms of the M1 segment. In addition, they explain the different patterns of ischemic lesions in the case of occlusion of the M1.

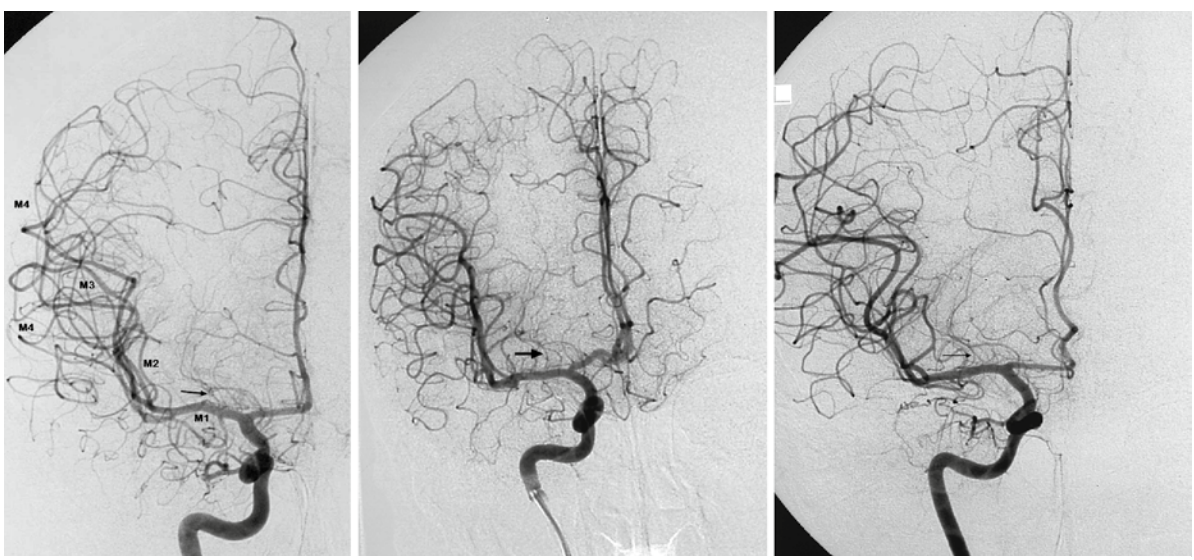

Fig. 5.3 AP angiograms: example of a long *M1* segment, from which arise the perforators prevalently grouped in the intermediate segment of the *M1*. The more distal perforators show the typical S shape (*arrow*). A temporal branch arising from the *M1* is also present, running anteriorly and inferiorly to the temporal pole. Distally to the bifurcation, the branches of the middle cerebral artery run on the surface of the insula (*M2*), turn further laterally (*M3*), exiting finally from the insular cistern and reaching the convexity (*M4*). In (B), there is minimal fenestration of the A1

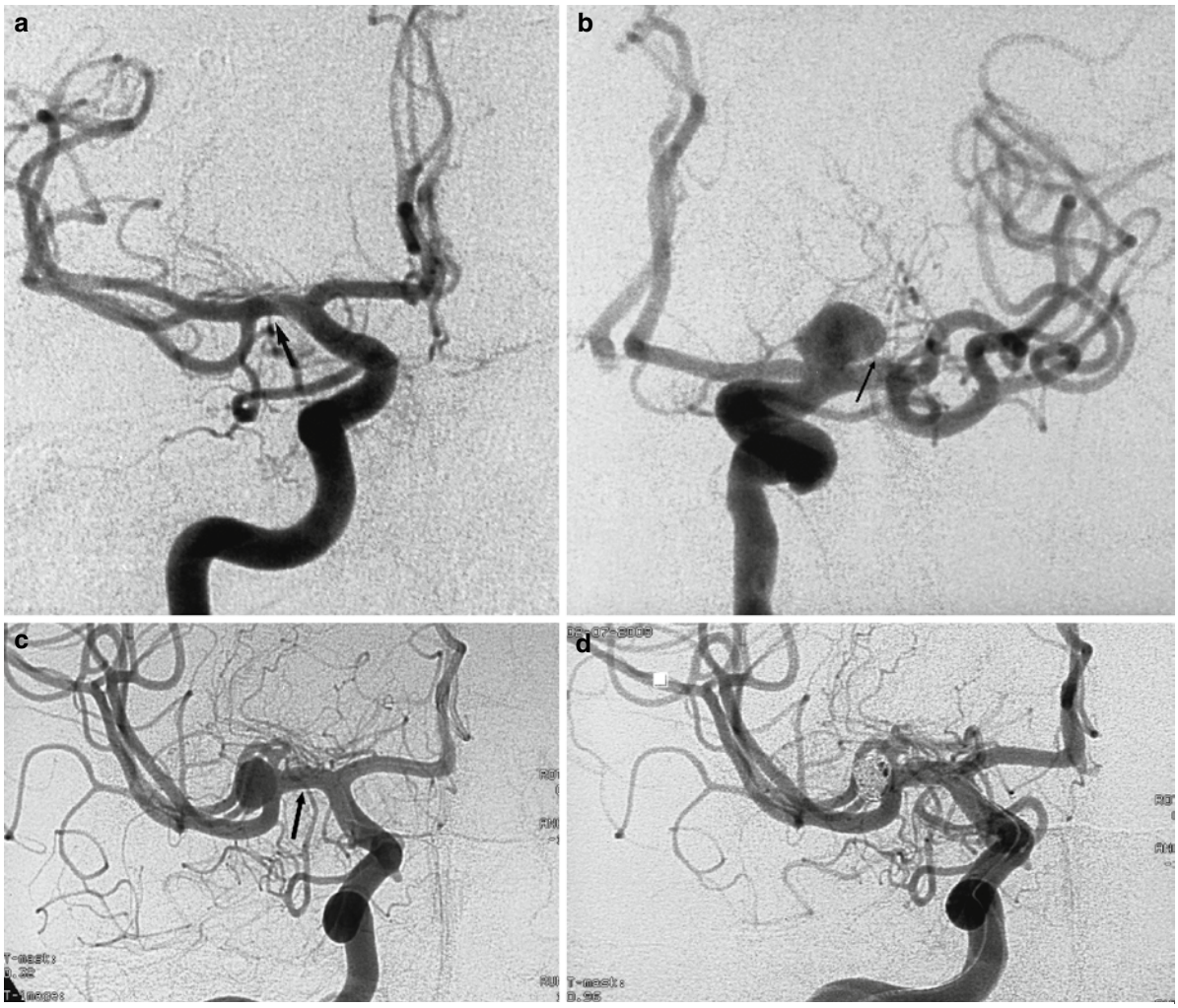

Fig. 5.4 (**a**) An apparently very short M1 (*arrow*) owing to the early arising of a large temporal branch. The main trunk from which arise the perforators bifurcates more distally. (**b**) Large aneurysm with a neck at the carotid bifurcation, showing partial involvement also of the proximal middle cerebral artery. Because of the short M1, the origin (*arrow*) of the perforators is close to the aneurysm (**c** and **d**). A very short M1 (*arrow*) gives off perforators that are close to the trifurcation, from which arises an aneurysm, treated with coils

Perforators commonly enter the lateral part of the APS (Rosner et al. 1984; Rhoton 2002) and supply the superior part of the head of the nucleus caudatus and its body. They entirely supply the superior part of the internal capsules as well as the globus pallidus and putamen.

Cortical branches. From the M1 segment, a branch for the pole of the temporal lobe can frequently arise early, and sometimes also an orbitofrontal branch for the pars orbitalis of the inferior frontal gyrus can arise. In exceptional cases, a temporal branch arises from the ICA.

5.2 M2, M3, and M4 Segments

The M2 segment, also called the insular segment, begins at the limen insulae and runs on the surface of the insula in the sylvian insular cistern with a superior-posterior direction. The M2 segment consists of two or three branches that arise from the bi-trifurcation of the M1. After reaching the top of the insula, these branches turn inferolaterally and exit from the sylvian insular cistern, forming the M3 segment. The last segment, the M4, comprises the distal cortical arteries. These arteries, which arise from the M2 and M3 segments,

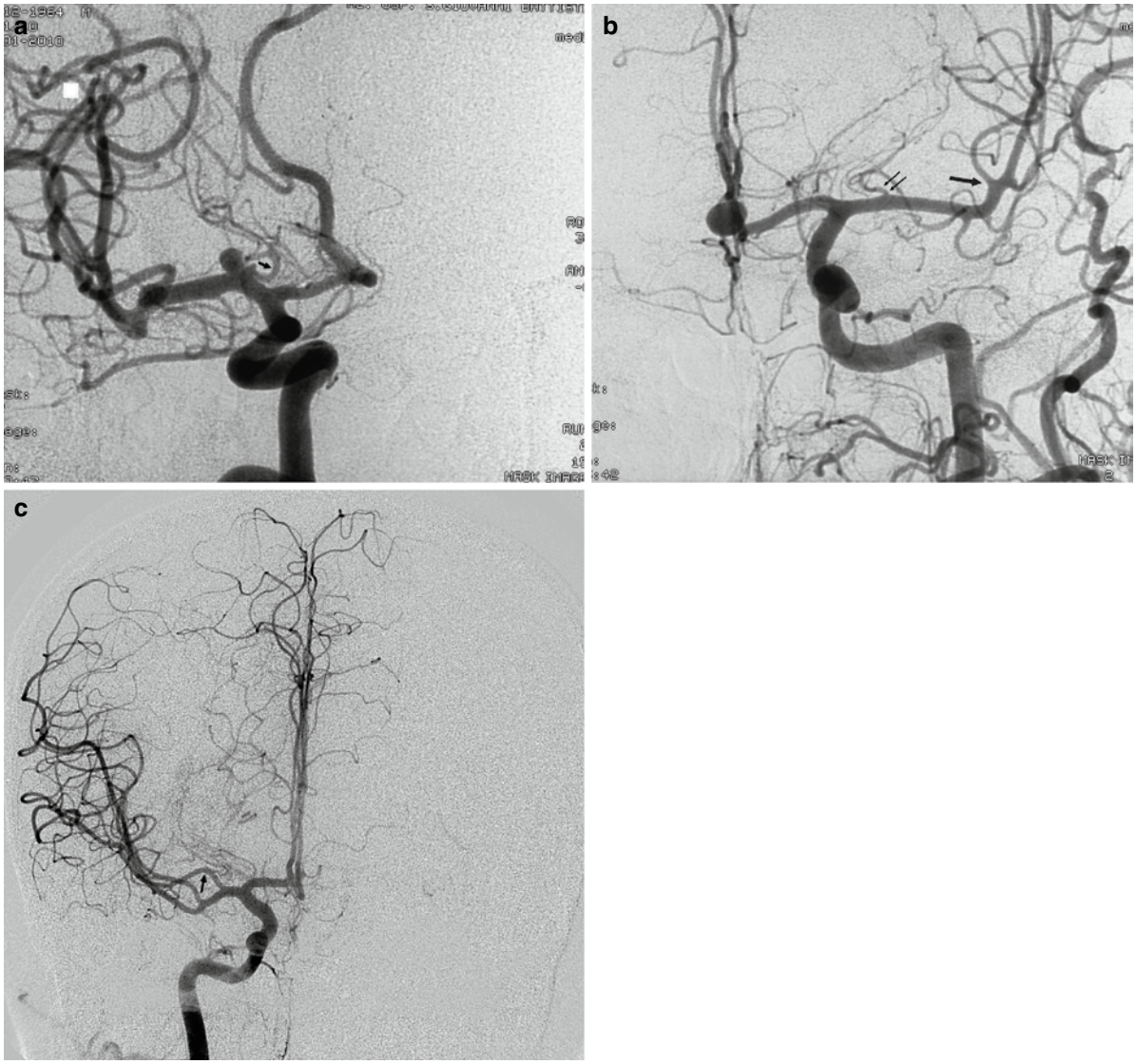

Fig. 5.5 (**a**) Oblique view in a patient examined for an unruptured aneurysm with a neck located on the M1 segment at the junction of a large perforator. This seems to be almost the only trunk (*arrow*) from which all distal perforators arise. (**b**) AP view in a patient examined for ruptured aneurysm of the anterior communicating artery. There is a long M1 with a trifurcation, from which the M2 branches arise located distally (*large arrow*). From the M1 arises a common trunk (*arrows*), giving off perforators and distal insular and temporal branches. A few other perforators seem to originate from the A1. (**c**) Another example of anomalous bifurcation, AP view. The M1 segment is very short. It divides into a smaller superior branch (*arrow*), from which the perforators arise, and into a large inferior branch, which divides further distally

can be divided into frontal, parietal, temporal, and terminal branches. From their course and the area they supply, the cortical branches can be divided into the orbitofrontal artery, the ascending frontal arteries (operculofrontal artery, central arteries), ascending parietal arteries (anterior and posterior), descending arteries (temporal branches), and the terminal group (gyrus angularis artery) (Ring and Waddington 1967; Ring 1974; Huber 1979). Overlaps in the course of the cortical branches and variations in their size and origin make it difficult in a given case to identify precisely the different arteries on an angiogram. Thus, on the basis of anatomical and angiographic studies, Michotey et al. (1974) and Salamon and Huang (1976) described two basic patterns that can help in identifying these arteries (Fig. 5.6a, b).

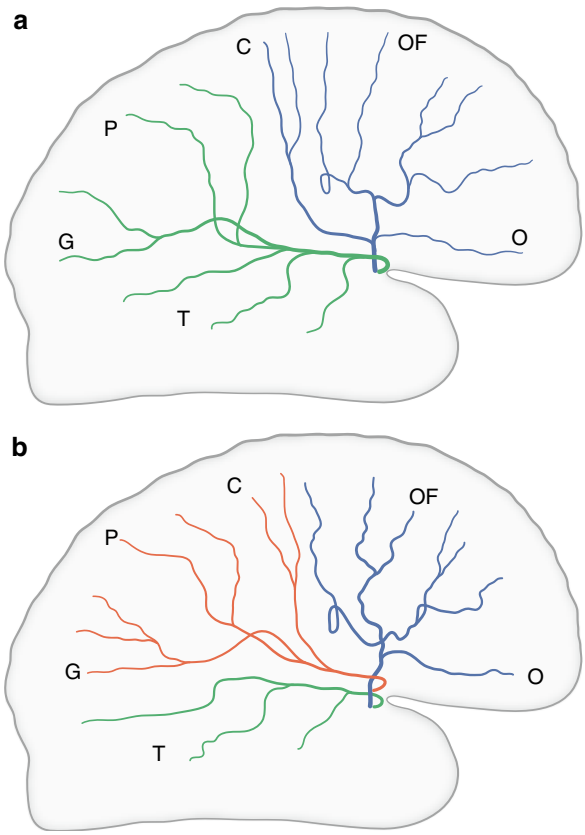

Fig. 5.6 (**a**) In the bifurcation pattern, the orbitofrontal (*O*), operculofrontal (*OF*), and central arteries (*C*) arise from the anterior trunk. All other branches—anterior and posterior parietal (*P*), gyrus angularis (*G*), and temporal (*T*) arteries—arise from the posterior trunk. (**b**) In the trifurcation pattern, the orbitofrontal (*O*) and operculofrontal (*OF*) arteries arise from the anterior trunk. The central (*C*), anterior and posterior parietal (*P*), and gyrus angularis (*G*) arteries arise from the middle trunk, the temporal (*T*) branches from the posterior branch

In cases of bifurcation of the M1, two trunks are present: one anterior, the other posterior. The orbitofrontal, operculofrontal, and central arteries arise from the anterior trunk. The remaining branches take their origin from the posterior trunk. In cases of trifurcation, the orbitofrontal and operculofrontal arise from the anterior trunk; the central, parietal, and gyrus angular arteries arise from the middle trunk; the temporal branches arise from the posterior trunk.

The orbitofrontal artery is the first branch to leave the sylvian insular cistern. It is not constant and sometimes can originate directly from the M1 segment. It is directed anteriorly, with a slightly horizontal course, toward the pars orbitalis of the inferior frontal gyrus. It is in balance with the fronto-orbital branch of the ACA.

The operculofrontal branch leaves the insular cistern and is directed first to the pars triangularis of the inferior frontal gyrus; in its ascending course, it divides further into three or more branches, which resemble a candelabrum. It supplies Broca's and the other frontal areas.

The central arteries. These are the most posterior ascending frontal branches. They are formed by one or two arteries, which divide distally into smaller branches that supply the primary motor and primary sensory cortex. The branches are very fine and cannot be identified with certainty on the lateral angiogram. The parietal group consists of two arteries: the anterior parietal and posterior parietal arteries, which can arise from the sylvian fissure at its posterior extremity; they do so as separate branches or as a common trunk that divides later. The anterior branch runs first in the postcentral sulcus, sometimes giving off branches to the postcentral gyrus. It extends further to the parietal lobe. The anterior branch is commonly very small and difficult to identify on the lateral angiogram. Unlike the other ascending branches that run in the sulci, the posterior branch has a superficial course toward the parietal lobe, which marks the anterior margin of the supramarginal gyrus (Salamon and Huang 1976). On the lateral angiogram, the posterior branch can be more easily recognized since it is frequently larger than the anterior parietal branch and has a less upward, more posteriorly directed course than the other ascending arteries. Its identification on the angiogram can be useful since the central arteries course in an area approximately 2–2.5 cm to its anterior.

The temporal group consists of several branches that emerge from the sylvian fissure and take a descending course directed inferoposteriorly in supplying the temporal lobe. From their origin and extension, they are termed anterior, middle, and posterior. The latter also extends to the lateral surface of the occipital lobe (temporo-occipital artery).

The angular artery is considered the terminal branch of the M4 group. It emerges from the distal part of the sylvian fissure and runs posteriorly. The angular artery supplies the angular and supramarginal gyri. It is frequently identified on the lateral angiogram and forms an upward convex curve as it turns around Heschl's gyrus (Ring 1974; Huber 1979). It is not uncommon for the artery to extend with some branches to the parietal and temporo-occipital areas, thereby replacing the corresponding arteries (Figs. 5.6–5.8).

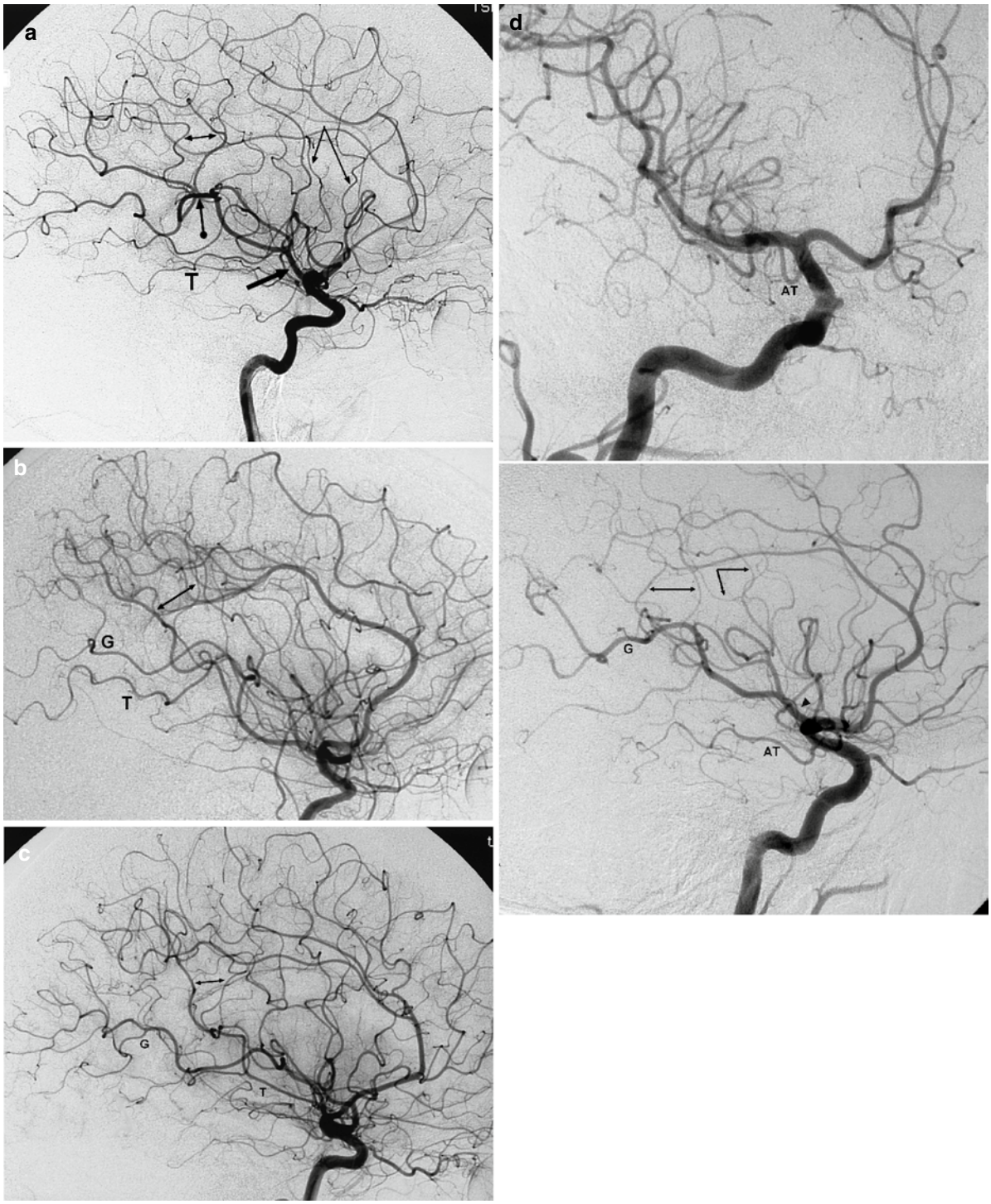
a
T
b
G
T
c
G
T
d
AT
G
AT

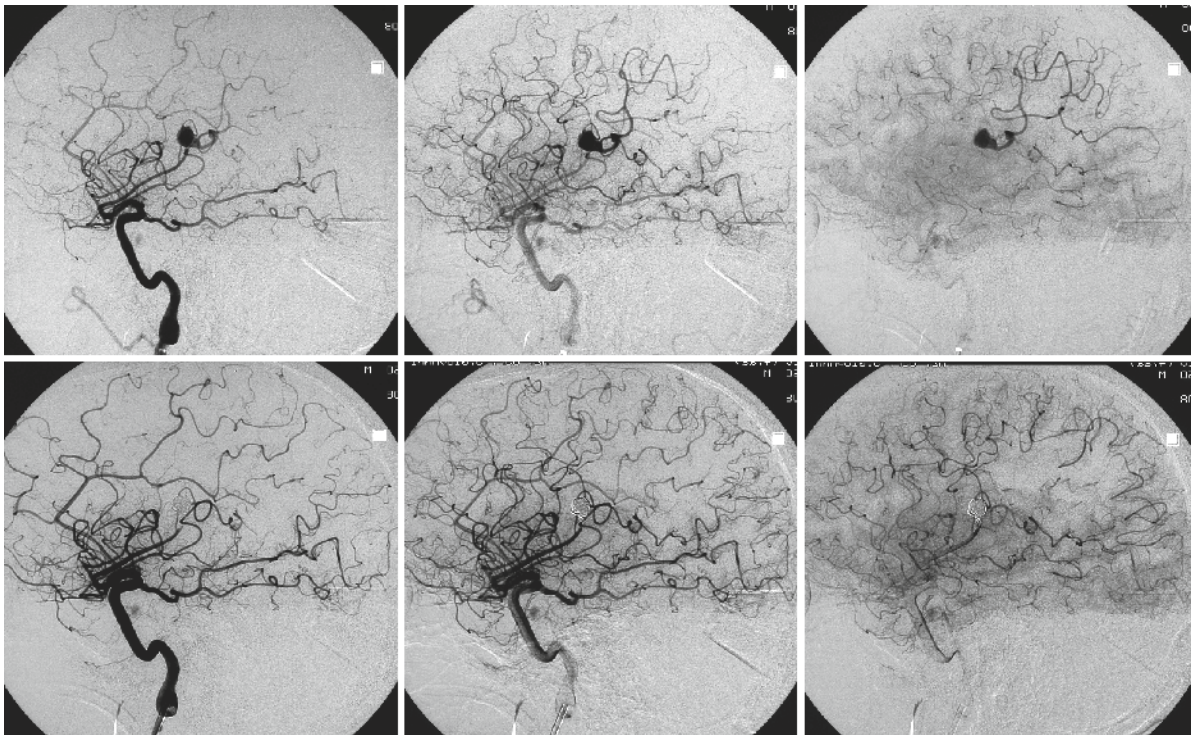

Fig. 5.8 Dissecting aneurysm of a peripheral branch of the middle cerebral artery, which from its course could belong to the parietal group. The treatment with coils, leading to occlusion of the aneurysm and parent artery, proceeded uneventfully

5.3 Anatomical Variations

Some variant conditions concerning the M1 segment and perforators have already been described. Fenestration of the M1 segment rarely occurs (Fig. 5.9). Duplication of the MCA and the presence of an accessory MCA have also been noted. The term accessory middle cerebral artery (AMCA) was coined by Crompton (1962), who described a supplementary branch arising from the ICA or, less frequently, from the ACA. Today, the term AMCA is reserved for cases in which the vessel arises from the ACA, and the term MCA duplication is used for when the vessel arises from the ICA. Some authors (Handa et al. 1970a, 1970b) proposed that the AMCA represents a large recurrent artery of Heubner. But this is no longer accepted by the majority of authors (Huber 1979; Umansky et al. 1988; Takahashi et al. 1989; Müller et al. 1991; Tacconi et al. 1995) since in all the cases studied the AMCA gave off perforators and cortical branches, while the recurrent artery of Heubner, which was always present, ended as a perforator (Figs. 5.10–5.12).

Fig. 5.7 (**a**) Lateral angiogram. Operculofrontal arteries (*arrows with angle*). Common trunk (*large black arrow*) for gyrus angularis, parietal, and temporal arteries. Anterior and posterior parietal arteries (*bidirectional arrow*). Typical curve of gyrus angularis artery (*arrow with black dot*), which continues in its main trunk and gives off a temporo-occipital branch. Small temporal branches (*T*). (**b**) Lateral angiogram. Common trunk for parietal (*bidirectional arrow*), gyrus angularis (*G*), and temporo-occipital arteries (*T*). (**c**) Parietal (*bidirectional arrow*) and temporal (*T*) branches seem to arise from a common trunk. There is a large gyrus angularis artery (*G*), supplying partially also the parietal area. (**d**) AP, lateral view. The anterior temporal artery (*AT*) arises from the distal internal carotid artery. There is a common trunk (*arrowhead*), from which the posterior temporal, gyrus angularis (*G*), and anterior and posterior parietal arteries (*bidirectional arrow*) arise. Anterior to the parietal arteries run small branches arising from the same common trunk, corresponding probably to the central arteries (*arrow with angle*). Precise identification of the central arteries is commonly not possible. They can be assumed to course in an area anterior to the parietal arteries

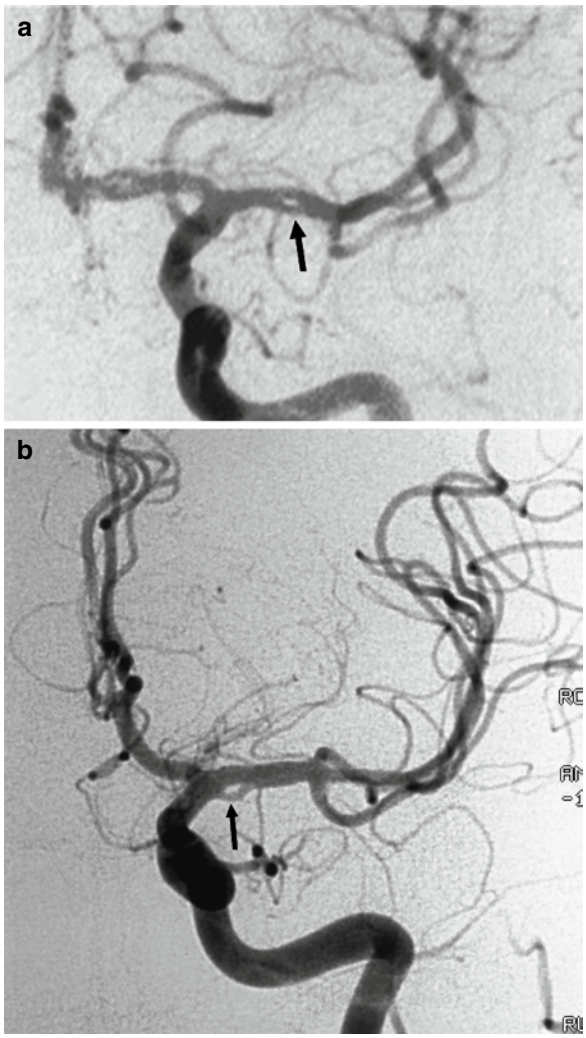

Fig. 5.9 (**a**) Fenestration of the M1 (*arrow*). Note also a small fenestration of the A1. (**b**) Another example of fenestration involving the M1 and its origin (*arrow*)

5.4 Vascular Territories

The MCA entirely supplies the lateral portion of the frontal and parietal lobes, the paramedian area being supplied by the ACA and posterior cerebral artery. Further, the MCA supplies the laterotemporal and, to a variable extent, the lateral part of the occipital lobe. Finally, the MCA supplies the laterobasal part of the frontal area, the laterobasal temporal area, and the temporal pole.

The vascular territories of the deep perforators have already been described. These arteries are end arteries, i.e., there is no anastomosis between the single branches

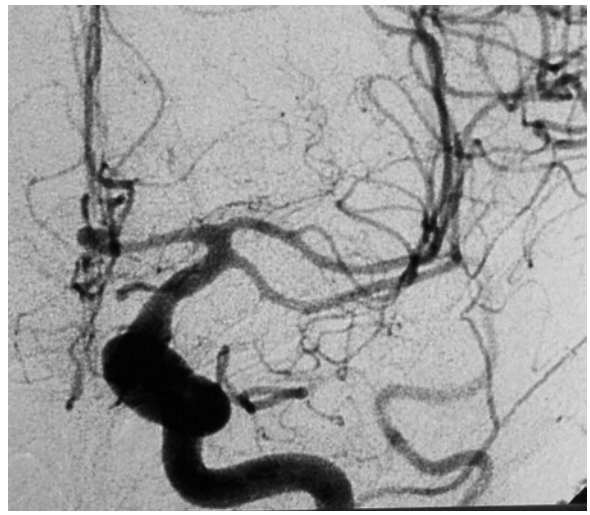

Fig. 5.10 There are two equally well-developed branches arising from the internal carotid artery. Perforators arise from the superior branch. There is a small aneurysm of the anterior communicating artery

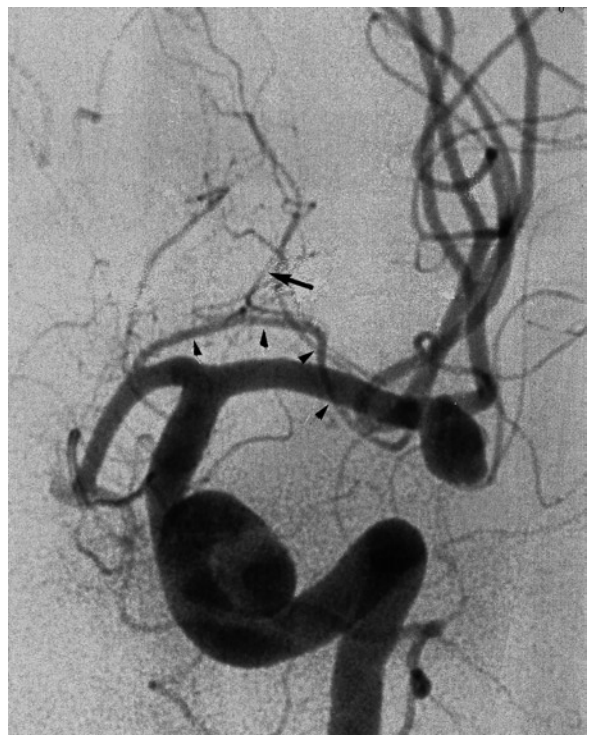

Fig. 5.11 Patient examined for a middle cerebral artery aneurysm. Example of an accessory middle cerebral artery. Parallel to the large M1 trunk, there is another smaller branch (*small black arrowheads*) arising from the anterior cerebral artery. Perforators mostly arise distally, close to the trifurcation. At least one perforator seems to originate from the accessory middle cerebral artery (*arrow*)

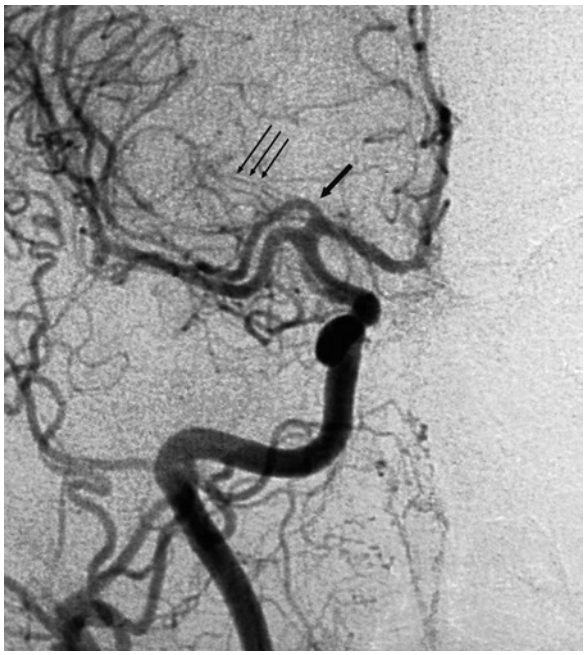

Fig. 5.12 Another example of an accessory middle cerebral artery. The inferior trunk arising from the internal carotid artery probably corresponds to the real M1 of the middle cerebral artery. The superior trunk (*arrow*) arising from the A1 is the accessory middle cerebral artery, from which the perforators arise (*small arrows*)

and no connection with the medullary arteries. This is probably true in the majority of the cases. In some cases, however, anastomotic connections between perforators of the MCA and the artery of Heubner have been demonstrated (Umansky et al. 1985). Other authors (Kodama and Suzuki 1974) have shown in microangiographic studies the existence of some anastomosis between deep perforators and the medullary artery.

From the branches running on the surface of the cortex arise cortical branches, which supply the cortex, and the medullary arteries; the medullary arteries enter the white matter, supplying its superficial (short branches) and deep part (long branches). The latter branches converge toward the periventricular region and basal ganglia. From the insular branches also arise the medullary arteries, which supply the subinsular area, without reaching, however, the deep perforators of the basal ganglia. The medullary arteries are end arteries, with no possibility of collateral circulation. Conversely, there is a potential collateral circulation via anastomoses among the superficial leptomeningeal (pial) branches of the middle, anterior and posterior cerebral arteries (Fig. 5.2).

5.5 Angiogram

The M1 segment and the perforators are always well recognizable on the AP view. The length of the segment can vary, as already described, and this influences the origin of the perforators (Figs. 5.3–5.5). The M1 segment can have a horizontal course; in children, the course is more frequently upward; in older patients, it is more commonly downward (Huber 1979).

Some typical features can be cited with regard to the M2 and M3 segments. On the AP angiogram, where the arteries of the M2 segment from the top of the insula turn laterally to reach the convexity of the hemisphere, they typically form a loop. The highest and most medial segments commonly correspond to the most distal (parietal and angular arteries) artery. This is also called the sylvian point (Chase and Taveras 1963; Huber 1979; Osborn 1999). On the lateral angiogram, all these loops, from anterior to posterior, can be located on an ideal horizontal line. The last loop corresponds to the sylvian point.

The arteries of the M4 segment are better evident on the lateral angiogram, with the features already described (Figs. 5.6 and 5.7). The difficulty in discerning the single branches has been emphasized. In this instance, 3D angiography can help.

Extra- and Intracranial Vertebrobasilar Sector

6

6.1 Extracranial Sector

The vertebral artery (VA) originates from the subclavian artery. It runs posterosuperiorly behind the anterior scalene muscle, commonly reaching the foramen of the transverse process of the sixth cervical vertebra. This first segment of the VA has been called V1 (Huber 1979; Osborn 1999). The artery can enter the foramen at the inferior or superior level (Huber 1979). Furthermore, the artery runs vertically through the foramina of the transverse processes from C6 to C2 (the V2 segment), surrounded by the venous plexus. The spinal nerves lie behind. Between the foramina of C2 and C1, the artery curves laterally and somewhat anteriorly. Exiting from C1 begins the V3 segment, which curves backward, running in the sulcus of the posterior arch of C1; it then forms a second upward and forward curve and reaches the foramen magnum, where the artery penetrates the dura and forms its last segment (V4). It is conceivable that these curves protect the VA, allowing it to accommodate more easily movement in the atlanto-occipital region (Fig. 6.1).

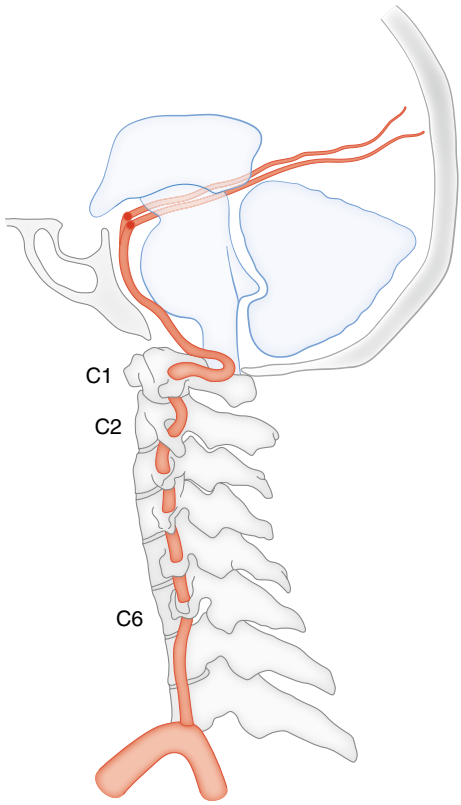

Fig. 6.1 Extracranial course of the vertebral artery arising from the subclavian artery and entering the intracranial cavity at the foramen magnum

6.1.1 Branches

- Muscular spinal branches have possible anastomoses with branches of the external carotid artery (Figs. 6.2 and 6.7a) and with the cervical ascending artery (Fig. 15.18).
- Spinal branches include branches for the dura and bone structures, and radicular branches supply the nerves. After supplying the nerves, other radicular branches (radiculomedullary arteries) reach the spinal cord, continuing in the anterior spinal artery (ASA) and posterior spinal artery (PSA). An anterior radiculomedullary artery, supplying the ASA is frequently visible on the VA angiogram at the C4–C6 level. The ascending and descending segments are easily recognizable, anastomosing cranially with the descending ASA, arising from the intracranial VA, and caudally with the segment arising from the radiculomedullary artery of the intercostal arteries (Fig. 6.2). Alternatively, the radiculomedullary artery

G.B. Bradac, *Cerebral Angiography*,
DOI: 10.1007/978-3-642-15678-6_6, © Springer-Verlag Berlin Heidelberg 2011

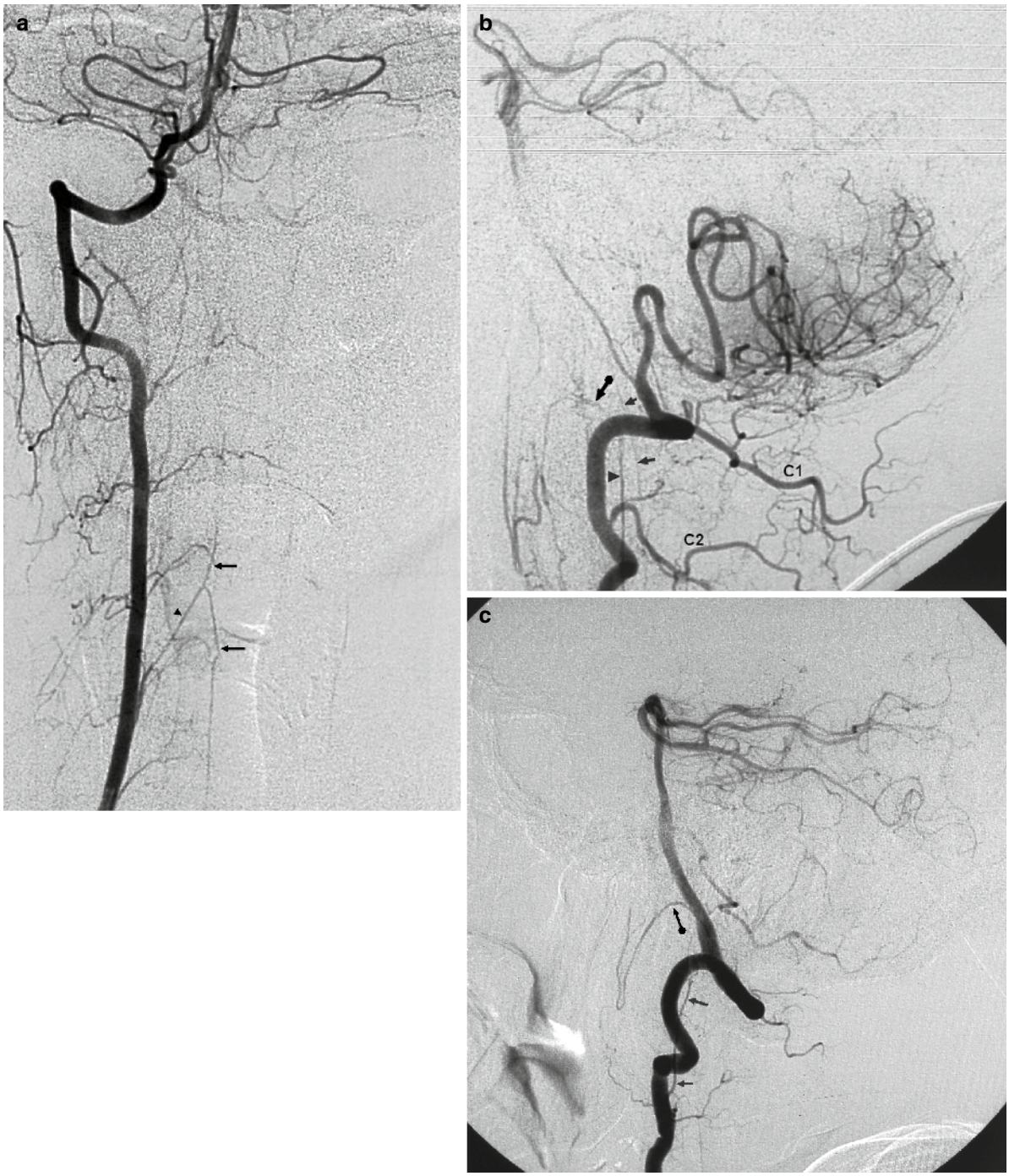

Fig. 6.2 (**a**) AP angiogram of the right vertebral artery, showing its extracranial course. Radiculomedullary artery (*arrowhead*) continuing in the ascending and descending segments (*arrow*) of the anterior spinal artery. (**b**) Vertebral angiogram, lateral view: hypoplastic vertebral artery (VA) ending in the posterior inferior cerebellar artery. Hypoglossal branch of the ascending pharyngeal artery (*arrow with dot*) anastomising with the ascending radiculomeningeal branch of the VA (*arrowhead*), contributing to form the so-called odontoid arch. Posteriorly runs the anterior spinal artery (ASA; *double arrow*). Muscular branch at the *C1–C2* level, which presents possible anastomosis with the corresponding branches of the occipital and ascending pharyngeal arteries. (**c**) Another example of a connection between the hypoglossal branch of the ascending pharyngeal artery (*arrow with dot*) and ascending radiculomeningeal branch of the VA (*arrows*)

can sometimes arise from the ascending cervical artery. The PSAs are seldom identifiable on the normal vertebral angiogram.

- Meningeal branches of the distal extracranial VA are as follows.
  - On the vertebral angiogram, a small branch is frequently visible anterior and lateral to the ASA on the lateral and AP views, respectively. This artery, first described by Greitz and Lauren (1968), has been called the anterior meningeal artery. Further studies (Lasjaunias et al. 1978a) have demonstrated that this artery is a radiculomeningeal branch and arises from the VA at the level of the third vertebral body. The anterior meningeal artery runs cranially in the spinal canal and anastomoses with the contralateral branch at the level of the dorsal surface of the odontoid process. The anterior meningeal artery is connected further with the hypoglossal artery, which is a branch of the ascending pharyngeal artery; this passes the hypoglossal foramen and enters the spinal canal. This connection is also called the odontoid arch (Figs. 6.2, 6.3, 6.9, 3.8, 3.29, 15.19, and 15.20). See also Sect. 3.4.
  - The falx cerebelli and posterior meningeal arteries originate from the extracranial, sometimes from the intracranial, VA. They may also originate from the posterior inferior cerebellar, occipital, or ascending pharyngeal arteries. There is a balance between these arteries, and so one can predominate in supplying the dura of the posterior fossa. The falx cerebelli artery (FCA) runs close to the falx cerebelli and continues in the meningeal branch along the straight sinus; it anastomoses superiorly with the FCA of the middle meningeal artery. On the lateral angiogram, the FCA runs slightly away from the inner table of the skull, and it is near the midline in the AP view (Figs. 6.3, 13.7 and 13.11). The posterior meningeal artery runs on the dura covering the cerebellar hemispheres, and so it has a more lateral course in the AP view; it runs close to the inner table of the skull on the lateral angiogram (Fig. 13.1 and 15.22).

6.2 Intracranial Sector

At the level of the foramen magnum, the VA penetrates the dura, where it is sometimes identifiable owing to a small change in the caliber. The artery runs in the subarachnoid space ventrolateral to the medulla oblongata and joins the contralateral artery at the bulbopontine

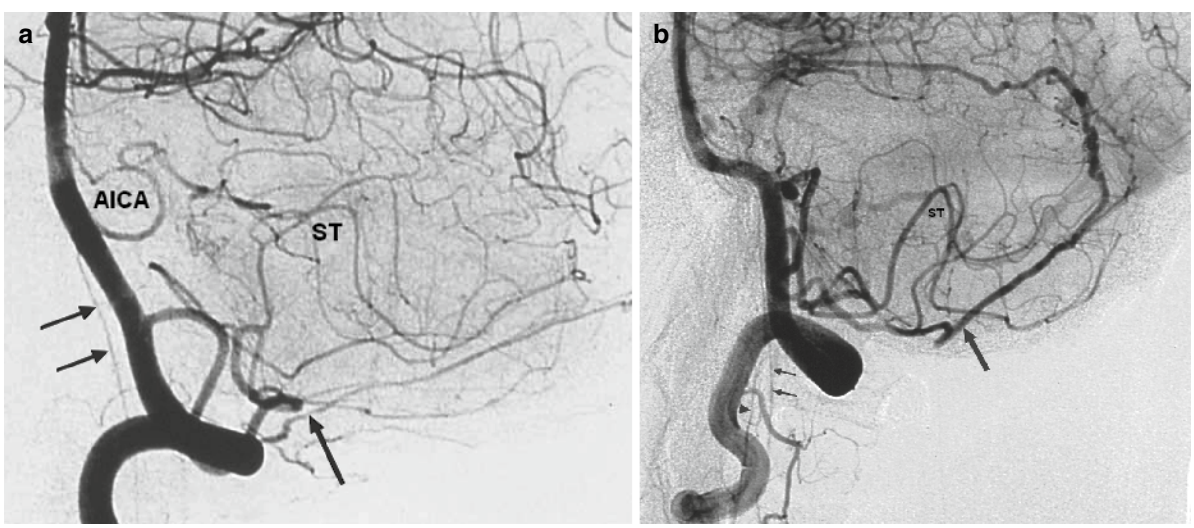

Fig. 6.3 Vertebral angiogram, lateral view. (**a**) Falx cerebelli artery (FCA; *arrow*); ASA (*double arrow*). Tortuous first segments of the PICA, typical pattern of the supratonsillar segment (*ST*), *AICA*. (**b**) FCA (*arrow*) is dilated, supplying a dural arteriovenous fistula. The FICA continues in the meningeal branch along the straight sinus. ASA (*double arrow*). Ascending meningeal branch of the VA (*arrowhead*)

junction to form the basilar artery. The basilar artery runs on the ventral surface of the pons in the median–paramedian position; it sometimes adopts a tortuous course and displays a lateral extension toward the cerebellopontine angle (Fig. 6.12). In the interpeduncular fossa under the floor of the third ventricle the basilar artery divides into the two posterior cerebral arteries (PCAs) (Fig. 6.8, 6.10, 6.11 and 7.5). The point of the division can be more caudally located with a cranial course of the PCAs (Fig. 7.5c). The basilar artery may be elongated, especially in hypertensive and atherosclerotic patients, and it bulges to the floor of the III ventricle. In such cases, the PCAs have first a caudally directed course before they encircle the midbrain. Many arteries arise from the intracranial sector of the vertebrobasilar system. They can be schematically divided into branches for the medulla and pons, branches for the midbrain (Chap. 7) and branches for the cerebellum.

6.2.1 Branches of the VA

6.2.1.1 Perforators of the VA

Small arteries arising from the posterior surface of the VA sometimes form a dense network on the anterior surface of the medulla, where anastomoses may be present. Perforators supplying the anterior part of the medulla arise from this network. Some arteries first run shortly on the anterolateral surface of the medulla before penetrating it. Other branches have a longer course and extend on the lateral surface before giving off perforators.

These branches are not recognizable on the angiogram. Perforating branches are basically end arteries, which means that there are no anastomoses among them. This is a common feature for all perforators of the brainstem (Duvernoy 1999).

6.2.1.2 Posterior Inferior Cerebellar Artery

The posterior inferior cerebellar artery (PICA) arises bilaterally from the first intradural segment of the VA; the PICA sometimes arises from the VA's extradural segments or from the basilar artery. The PICA runs anterolaterally to the medulla, reaching its posterior border after a variable course. During its course, the PICA has a close relationship with cranial nerves IX, X, XI, and XII. Further, it takes an upward course along the anterior surface of the tonsilla, which it surrounds superiorly and forms a typical loop on the angiogram that is commonly recognizable. The PICA further divides into the vermian and hemispheric branches.

Vascular territories. The PICA gives off perforators for the lateral medulla in balance with the perforators coming from the VA (Duvernoy 1999). Furthermore, the PICA supplies the posterior medulla, together with the PSA. The distal branches supply the tonsilla, the inferior vermis, and inferior surface of the cerebellar hemisphere.

Variants. The PICA can be very large and also partially supply the contralateral hemisphere. Sometimes, the PICA is hypoplastic or absent and is replaced by a large anterior inferior cerebellar artery (AICA).

On the angiogram, the PICA and its segments can be better studied in the lateral view (Fig. 6.4). The first segments (anterior medullary and lateral medullary) can be characterized by a tortuous course. It is always easy to identify the retromedullary and supratonsillar segments, which surround the tonsilla and the inferior vermian and hemispheric branches. In the AP view, the different segments cannot easily be separately distinguished (Figs. 6.2, 6.3 and 6.6–6.11).

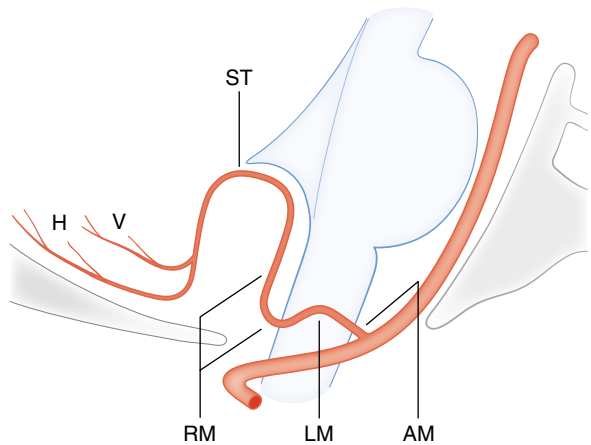

Fig. 6.4 Course of the PICA as seen on the lateral angiogram. Anterior medullary segment (*AM*), lateral medullary segment (*LM*), retromedullary segment (*RM*), supratonsillar segment (*ST*), vermian (*V*), hemispheric branches (*H*)

6.2.1.3 Anterior Spinal Artery

The ASA is formed by two small branches that arise from each VA distal to the PICA. In 10% of cases, the ASA's origin is unilateral. The ASA gives off perforators for the anterior median and paramedian parts of the inferior medulla, while the anterior median and paramedian parts of the superior medulla are supplied by the VA (Duvernoy 1999). The ASA is frequently, but not always, recognizable on the angiogram (Figs. 6.2, 6.3, 6.7–6.10, 16.6, 16.8, and 15.20).

6.2.1.4 Posterior Spinal Artery

The PSA arises from the PICA or distal VA. The PSA is a very small vessel and is not recognizable on normal vertebral angiograms; it supplies the posterior medulla. The PSA can be involved in the supply in pathological processes (Fig. 6.7b).

6.2.2 Branches of the Basilar Artery

6.2.2.1 Median–Paramedian Perforators

The median-paramedian perforators are small branches and are not recognizable on the angiogram; they arise on the posterior surface of the basilar artery. The majority enter the pons at the level of the basilar sulcus. Others adopt first a transverse path before entering the pons. Some of these arteries are long and reach the floor of the IV ventricle; others are more lateral and shorter. They supply the median–paramedian and, partially, the lateral part of the pons (Kaplan and Ford 1966; Tatu et al. 2001; Duvernoy 1999).

6.2.2.2 Lateral Pontine Branches

These are frequently visible on the AP angiogram as small vessels running from the basilar artery laterally toward the middle cerebellar peduncle (MCP). The lateral pontine branches give off perforating branches that supply the lateral pons and middle cerebral peduncle (Figs. 6.8, 6.10, 12.13, and 12.14).

6.2.2.3 Anterior Inferior Cerebellar Artery

The AICA arises from the basilar artery, commonly from its first or second third (Scialfa et al. 1976; Naidich et al. 1976). It runs laterally with a straight course toward the lateral inferior part of the pons and MCP. In its course, the artery crosses cranial nerve VI; shortly after, it divides into two major branches: the rostro-lateral (RL) and the caudomedial (CM) branches (Naidich et al. 1976). Anterior to the flocculus, the lateral branch reaches cranial nerves VII–VIII. Here, it describes a rather complex loop, which can partially extend into the meatus acusticus. In this part of its course, the lateral branch gives off the labyrinthine artery. The latter rarely arises directly from the basilar artery (Naidich et al. 1976; Brunsteins and Ferreri 1990). The lateral branch runs further in the horizontal fissure of the cerebellum, where it can replace the marginal artery of the superior cerebellar artery (SCA). The CM branch is frequently smaller; it is directed to the anterior medial surface of the cerebellum. Sometimes, it can arise as a separate trunk from the basilar artery and be well developed, supplying the vascular territory of the PICA.

Vascular territories. The arteries give off perforators that supply the lateral portion of the pons and MCP in balance with the lateral pontine arteries of the basilar artery. The distal branches supply the anterior part of the cerebellum. The labyrinthine artery supplies cranial nerves VII–VIII.

Variants. The sizes of the AICA and PICA are closely correlated: when one is well developed, the other is commonly small or absent. In an angiographic study (Takahashi et al. 1968), in 48% of cases both the AICA and PICA were well developed. In 40% of cases, one or both AICA were dominant, replacing the PICA. In 10% of cases, the AICA was hypoplastic or absent, and its vascular territories were replaced by a well-developed PICA. In addition to the main trunk of the AICA, an accessory AICA with a separate origin may sometimes be present (Naidich et al. 1976).

Angiogram. The AICA is easily recognizable on the lateral and particularly on the AP vertebral angiogram. In this latter view, the lateral branch runs toward the internal meatus acusticus, where it forms a loop from which the LA arises. LA, however cannot be identified with certainty. More distal branches extend to the anterior surface of the hemisphere and vermis (Figs. 6.3,

6.6, 6.8, 6.10, 6.11, 12.14, 12.15, and 7.5). The medial branch can be particularly well distinguished when the PICA is absent (Figs. 6.8, 6.11, and 6.14).

6.2.2.4 Superior Cerebellar Artery

The SCA is the most constant among the cerebellar arteries and is almost always present. It arises as a unique trunk, which divides into superior and inferior branches. The SCA can sometimes be double or, rarely, triple (Mani et al. 1968; Hardy and Rhoton 1978). An origin from the P1 may also occur infrequently. From its origin, the SCA runs laterally on the surface of the superior part of the pons (pontine segment) and lies inferiorly to cranial nerve III. The SCA then turns posteriorly and courses around the midbrain inferiorly to the posterior cerebral artery (midbrain segment). The trunk or one of its branches can make a loop caudally and come in contact with the trigeminal nerve (Hardy and Rhoton 1978). The SCA reaches the quadrigeminal plate (quadrigeminal segment), where both the right and left SCA approach each other.

Branches. In the course around the midbrain, the SCA gives off small branches for the superior posterior part of the pons and midbrain in addition to the hemispheric cerebellar branches. The first of the latter is the marginal artery, which runs laterally toward the horizontal fissure and supplies the corresponding cerebellar area, together with a lateral branch of the AICA. One of these arteries can predominate.

There are two or three other cortical branches, which arise more distally. In its course around the midbrain, the SCA lies inferiorly to the superior surface of the cerebellum; so to reach this, the cortical hemispheric branches run first upward, then downward. The superior vermian artery is the terminal branch, and it commonly arises from the quadrigeminal segment. The vermis branches from both SCAs approach each other and run almost parallel. From its midbrain segment, a meningeal artery, sending small branches to the posterior part of the tentorium, has been described (Wolschlaeger and Wolschlaeger 1974).

Vascular territories. Each artery supplies the upper posterior part of the pons and midbrain. In supplying the postero-lateral midbrain, there is a balance between the SCA and its branches and the small perforators of the posterior cerebral artery, the collicular artery, and the posterior medial choroidal artery (Duvernoy 1999). The distal branches supply the superior vermis and superior cerebellar hemisphere.

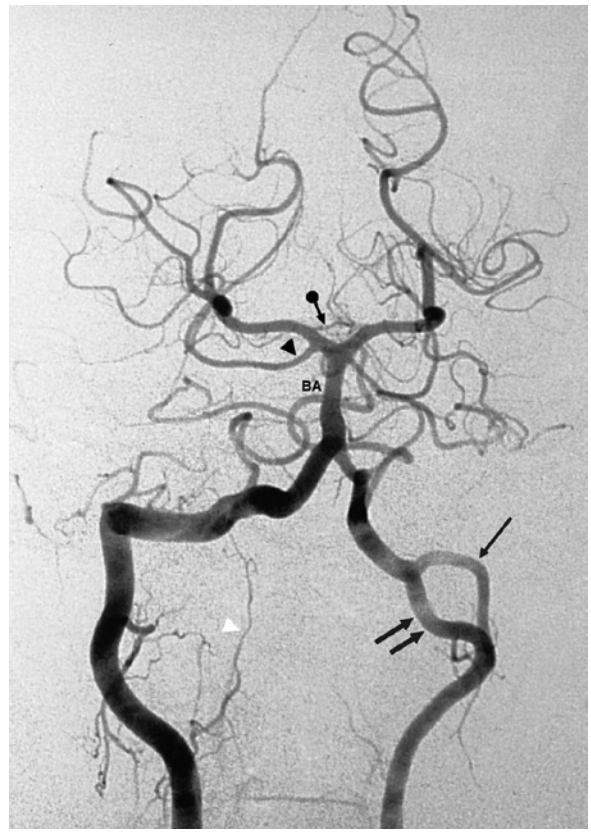

Fig. 6.5 Vertebral angiogram, AP view. Asymmetric lumen of the vertebral arteries. There is duplication of the left vertebral artery. The anomalous vessel (*double arrow*) is larger than the true artery (*arrow*). Normal basilar artery (*BA*), continuing in both PCAs. From the right P1 arises a large posterior thalamoperforating branch, dividing distally into small branches (*arrow with dot*). The right superior cerebellar artery (SCA) arises from the right P1 (*arrowhead*). Presence on the right of a radiculomeningeal branch (*white arrowhead*)

Variants. The SCA can arise uni- or bilaterally from the P1 segment of the PCA (Fig. 6.5). When the SCA is duplicated, one branch can arise from the basilar artery and the other from the P1.

On the angiogram the pontine, midbrain, and quadrigeminal segments are well evident in the AP view (Figs. 6.8a and 7.5b). The midbrain segment is identified in the lateral view and runs inferiorly to the PCA (Fig. 6.6). Because of overlapping, it is frequently difficult to distinguish the cerebellar branches from branches of the PCA. In the lateral view, the cerebellar arteries can be identified; they form a superior convex

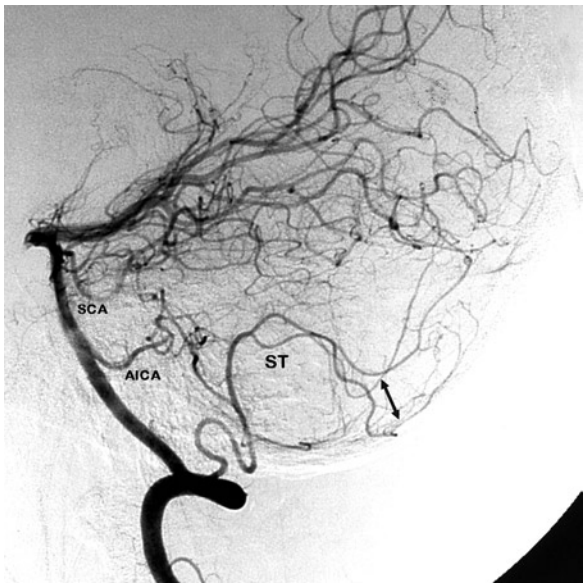

Fig. 6.6 Lateral vertebral angiogram. Tortuous first segments of the PICA. Typical supratonsillar loop (*ST*). Vermian and hemispheric branches (*bidirectional arrow*). *AICA*, *SCA*

curve and run below the tentorium with a stepladder appearance. The vermis branches are the superior ones. In the AP view, their course projects below the tentorium. Among these branches, the marginal artery is the most easily recognizable (Figs. 6.5, 6.8, 6.10, 6.11, 6.14, 7.5, 7.6, 7.9, 12.11, 12.13, and 12.14).

6.2.3 Cortical-Subcortical Branches of the Cerebellar Arteries

Branches supplying the cortex and branches extending to the white matter and deep nuclei (medullary arteries) arise from the cortical branches and run on the

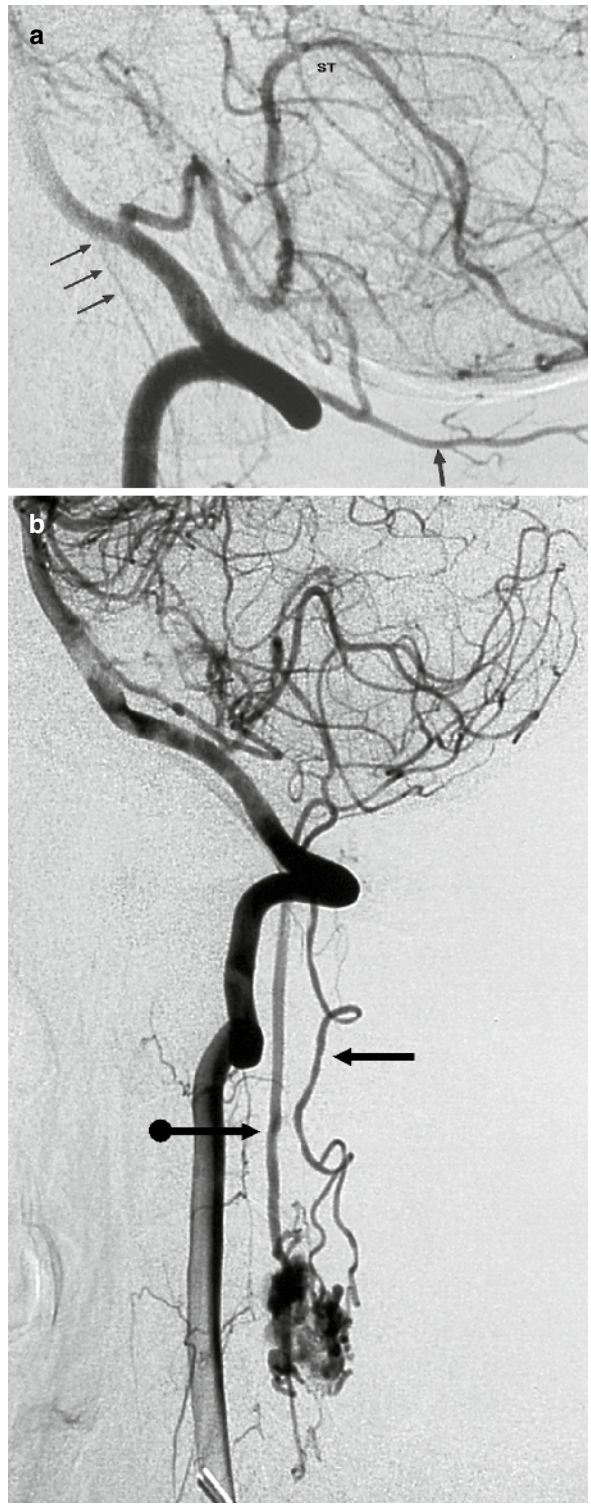

Fig. 6.7 (**a**) Lateral vertebral angiogram (detail). PICA with its typical supratonsillar loop (*ST*). ASA (*arrows*). Muscular branch at the level of C1, which can potentially anastomose with the corresponding branch of the occipital artery (*arrow*). (**b**) Patient with arteriovenous malformation involving the cervical spinal cord. Lateral vertebral angiogram showing the supply by a very dilated ASA (*arrow with dot*) and PSA (*arrow*)

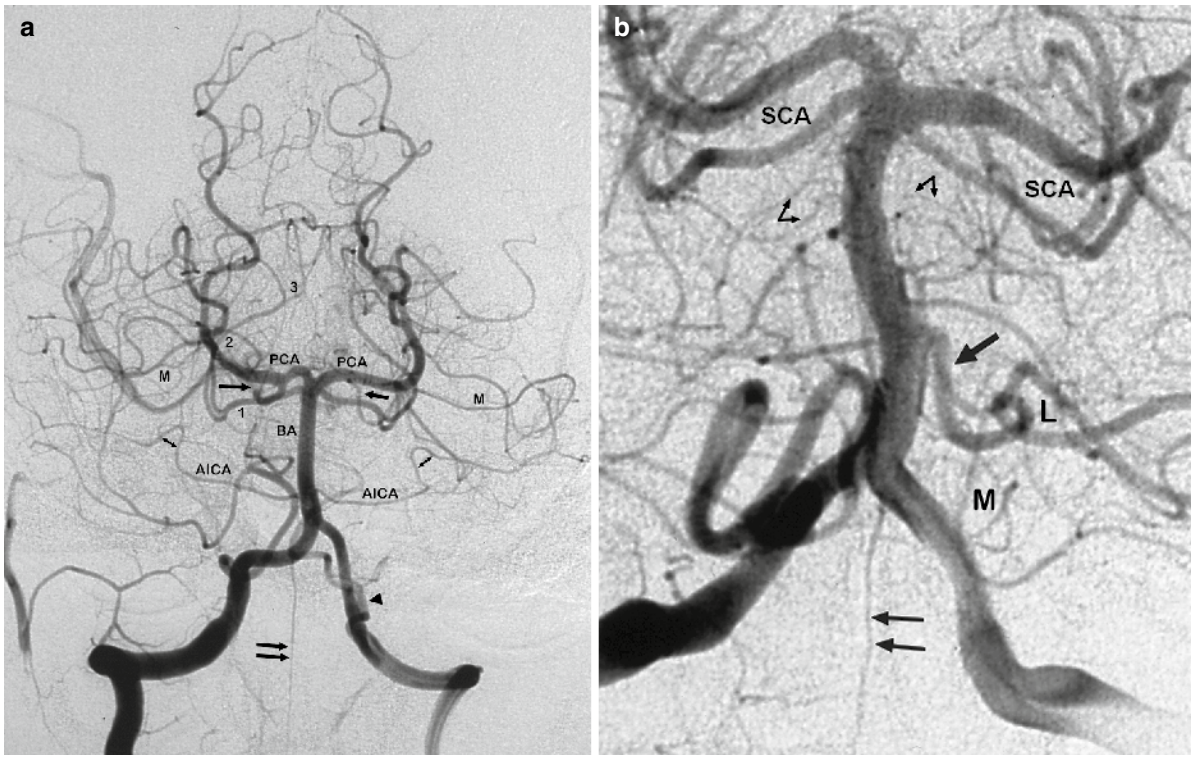

Fig. 6.8 Vertebral angiogram, AP view. (**a**) Asymmetric vertebral artery. Basilar artery (*BA*). Both PICAs are well developed. That on the left probably has an extracranial origin (*arrowhead*). Unilateral origin of ASA (*double arrow*). Bilateral *AICA*. Note the loop in front of the internal meatus acusticus (*bidirectional arrows*). The numbers *1*, *2*, and *3* indicate, respectively, the pontine, midbrain, and quadrigeminal segments of the SCA. The latter continues in its terminal vermian branches. Marginal branch (*M*) of the SCA. From both *PCA*, retrograde injection of the posterior communicatinig artery (*arrow*) is particularly well developed on the right. This allows identification of the P1 segment of the posterior cerebral artery (*PCA*). On the right, there is an anastomosis between a branch of the vertebral artery and the occipital artery. (**b**) Bilateral voluminous vertebral artery. On the right, a well-developed PICA arises from the VA. On the left, a voluminous AICA replaces the absent PICA (*arrow*). Lateral branch (*L*), medial branch (*M*), superior cerebellar artery (*SCA*). Lateral pontine arteries (*arrow with angle*) take their origin from the basilar artery (*arrow*). Unilateral ASA (*double arrow*)

surface of the cerebellar cortex. The medullary arteries are end arteries, with no possibility of collateral circulation. Instead, there are abundant anastomoses among the superficial cortical branches on the border zones of the vascular territories of the PICA, AICA, and SCA (De Reuck 1972).

6.2.4 Variants of Vertebral and Basilar Arteries

There is frequent asymmetry of the lumen of the VA. The left VA is dominant in the majority of cases; less frequently the right VA is larger.

It can be indirectly involved in aortic arch anomalies. Duplication of the VA, where two branches arise separately from the subclavian artery and join them in the midcervical region, has been reported (Goddard et al. 2001). The left VA can take its origin from the aortic arch in 7–10% of cases (Figs. 1.4 and 15.17); in very rare cases, it take its origin from the internal or external carotid artery. One VA may be hypoplastic and end intracranially in the PICA. In cases of unilateral ASA, the presence of a hypoplastic VA does not exclude the possibility that this artery takes its origin from the hypoplastic VA (Fig. 6.9). Other rare conditions are fenestration and duplication of the VA and basilar artery. According to the literature, the definition of these variants in a given case is not

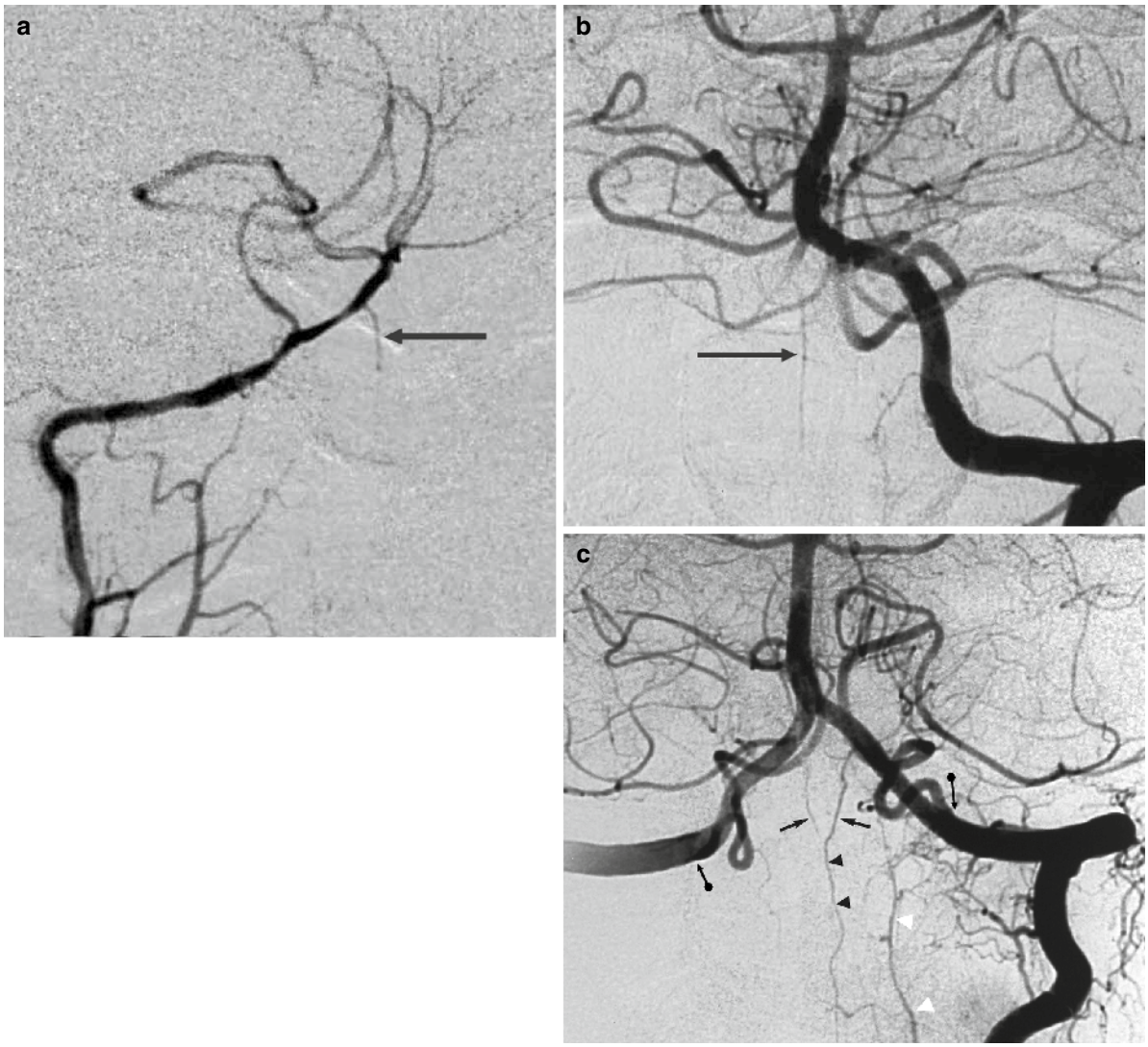

Fig. 6.9 *Left* and *right* vertebral angiogram in the same patient. On the angiogram of the well-developed left vertebral artery (**b**) there is a partial injection of the hypoplastic right vertebral artery injected also selectively (**a**). Unilateral origin of the ASA (*arrow*) from the hypoplastic right vertebral artery. Study in a different patient (**c**). *Left* vertebral angiogram with retrograde injection of the contralateral vertebral artery. ASA (*arrowhead*) with its bilateral contribution (*arrow*) deriving from the vertebral arteries. Radiculomeningeal artery (*white arrowhead*) arising at the C3 level of VA. Probable bilateral extradural origin of the PICA (*arrow with dot*)

homogeneous (Takahashi et al. 1973; Wolschlaeger and Wolschlaeger 1974; Lasjaunias and Berenstein 1987; Osborn 1999). Indeed, it may often be difficult to undertake a differential diagnoses between these two conditions, which are probably different aspects of the same anomalous development. To simplify matters from a practical point of view, we define duplication and triplication (Wolschlaeger and Wolschlaeger 1974) as occurring when two or three clearly separated vessels are present (Figs. 6.5 and 6.14). In the case of fenestration, the vessel is unique, but on part of its course there is a double lumen (Fig. 6.13).

Duplication and fenestration can be associated with aneurysms (Picard et al. 1993; Tanaka et al. 2006) (Fig. 6.14). For the connection between the carotid and vertebrobasilar circulation, see Sect. 2.5.

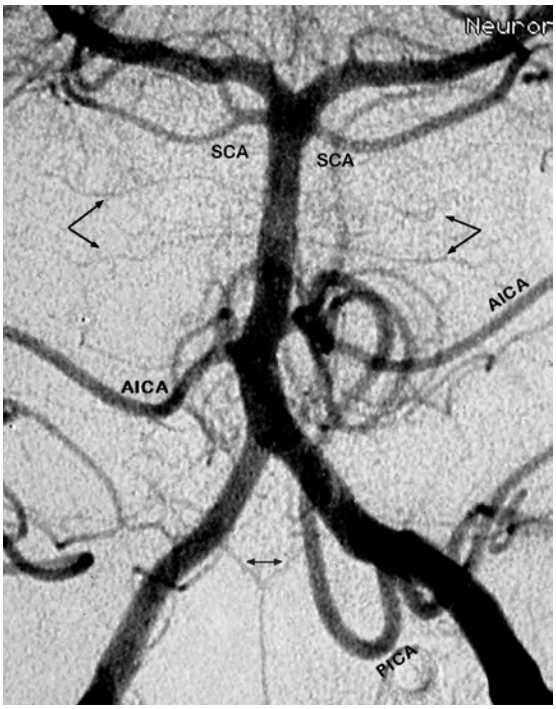

Fig. 6.10 Vertebral angiogram, AP view. Dominant left VA, which gives off a large *PICA*. There are two well-developed *AICA*s, that on the right replaces the vascular territory of the *PICA*. Bilateral origin of ASA (*bidirectional arrow*). Lateral pontine arteries arising from the basilar artery are well visible (*arrows with angle*). Note on the right the early division of the *SCA*

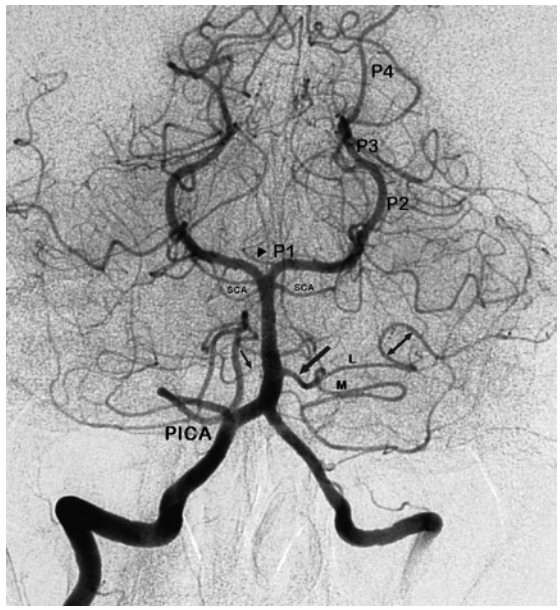

Fig. 6.11 Vertebral angiogram, AP view. Asymmetric vertebral artery. On the right, a well-developed *PICA* replaces mainly the vascular territory of the small AICA (*small arrow*). On the left, there is a well-developed AICA (*large arrow*), supplying mainly the vascular territory of the PICA. On the *left*, the lateral and medial branches of the AICA (*L* and *M*) are well developed. Note the typical loop of the lateral branch in front of the meatus acusticus (*bidirectional arrow*), particularly evident on the *left*. The lateral branch runs further toward the horizontal fissure. The *SCA* is double on the *right*. The four segments of the PCA (*P1–P4*) show their typical course. A large posterior thalamoperforating branch arising from the *left P1* is recognizable

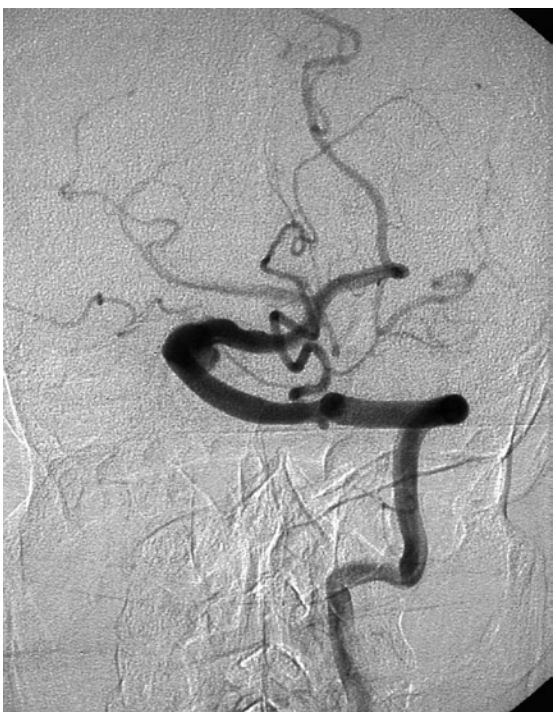

Fig. 6.12 Tortuous basilar artery, probably due to atherosclerosis extending into the cerebellopontine angle, causing facial spasm

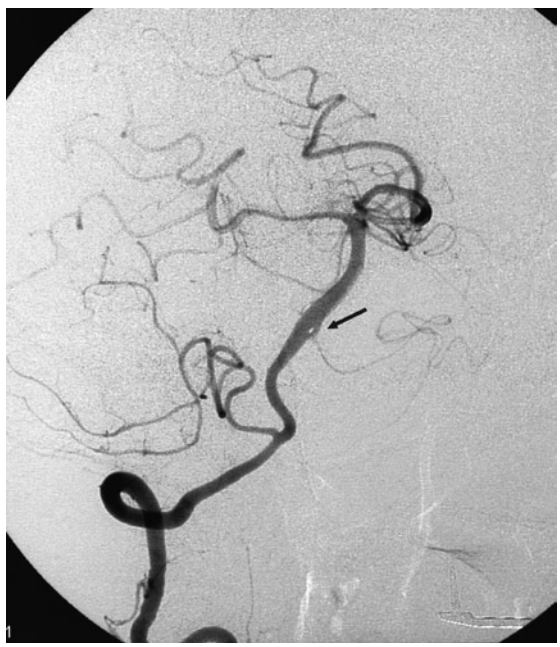

Fig. 6.13 Fenestration (*arrow*) of the basilar artery near the origin of the AICA

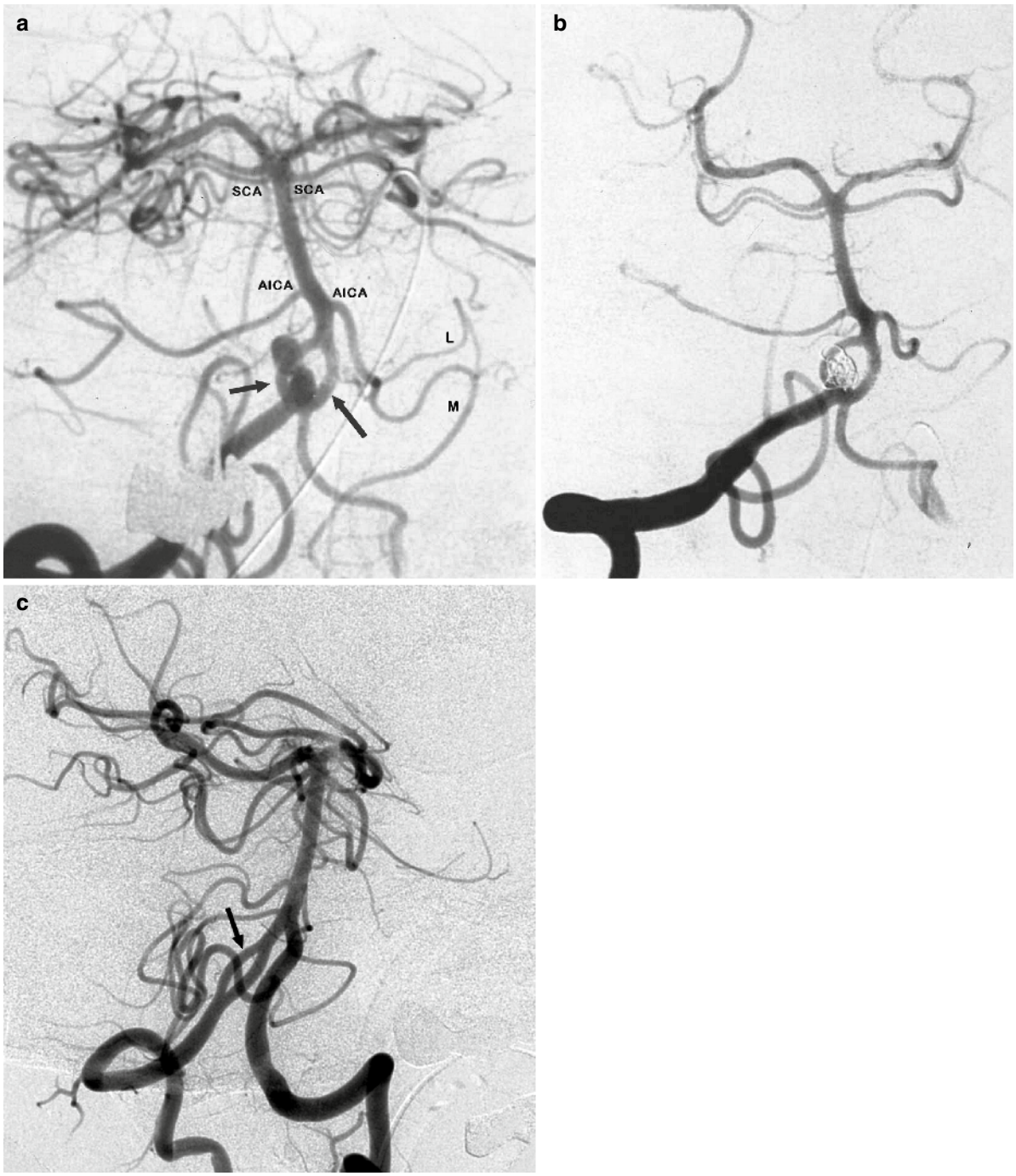

Fig. 6.14 (**a**) Angiogram in a duplicated proximal basilar artery (*arrows*) associated with ruptured aneurysm treated acutely with coils (**b**). There is asymmetry of the vertebral arteries: that of the left is hypoplastic. Bilateral well-developed AICA. That on the left replaces the absent PICA. Lateral branch (L), medial branch (M), superior cerebellar arteries (SCA) duplicated on the right. Duplication (**c**) of the vertebral artery (*arrow*) in another patient. *Left* vertebral angiogram with reflux in the *right* duplicated vertebral artery

Posterior Cerebral Artery

7

Embryologically, the posterior cerebral artery (PCA) is a branch of the internal carotid artery (ICA); the connection with the basilar artery (pars basilaris) develops later. The connection with the ICA (pars carotica) can completely regress or persist as a large or small vessel, becoming the posterior communicating artery (PComA). Variants in this evolution will be described later.

As it arises from the basilar artery, the PCA can be divided into four segments (Huber 1979) (Fig. 7.1).

- P1 (precommunicating segment): from its origin from the basilar artery to the junction with the PComA.
- P2 (ambient segment): around the midbrain toward the quadrigeminal plate.
- P3 (quadrigeminal segment): on the surface of the quadrigeminal plate.
- P4 (distal segments).

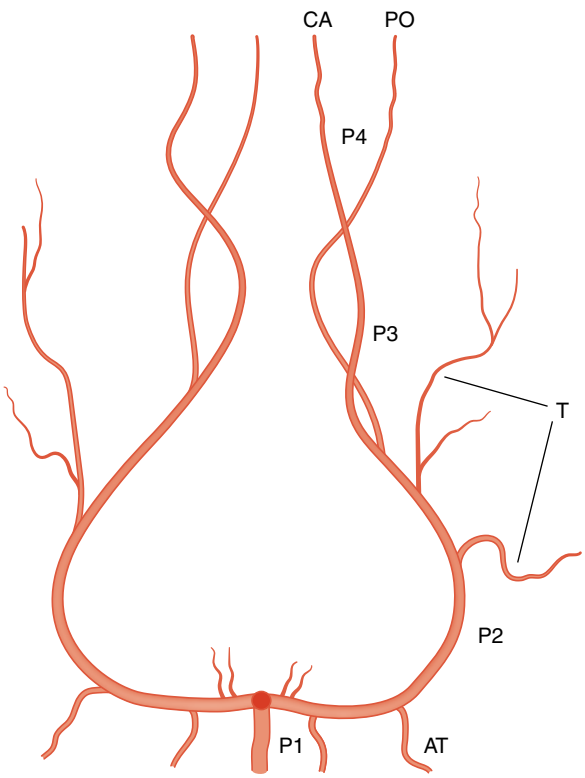

Fig. 7.1 Course of the *P1*, *P2*, *P3*, and *P4* segments of the posterior cerebral artery (PCA) in the AP view. Anterior temporal artery (*AT*), middle temporal and temporo-occipital branches (*T*), calcarine artery (*CA*), parieto-occipital artery (*PA*)

7.1 P1 Segment

This is the first segment, extending from its origin in the basilar artery to its junction with the PComA (Figs. 7.1 and 7.2). The P1 segment is the pars basilaris of the PCA that embryologically appears later. It is a short segment, running in the interpeduncular fossa, where it has a close relationship with cranial nerve III, located inferiorly. The P1 segment can have a horizontal course or form a slightly ascending or descending course. Its length varies, with an average of 7.1 mm (Zeal and Rhoton 1978).

The P1 segment gives off perforating branches called the thalamoperforating pedicles (Foix and Hillemand 1925a, 1925b) or paramedian thalamic arteries (Percheron 1976a, 1976b). It would be simpler to call these arteries the posterior thalamoperforating branches. They enter the posterior perforated substance (PPS), supplying the medial part of the mesencephalon, the medial part of the thalamus, and the posterior part of the hypothalamus (Lazorthes and Salamon 1971; Saeki and Rhoton 1977; Zeal and Rhoton 1978; Duvernoy 1999; Tatu et al. 2001).

G.B. Bradac, *Cerebral Angiography*,
DOI: 10.1007/978-3-642-15678-6_7, © Springer-Verlag Berlin Heidelberg 2011

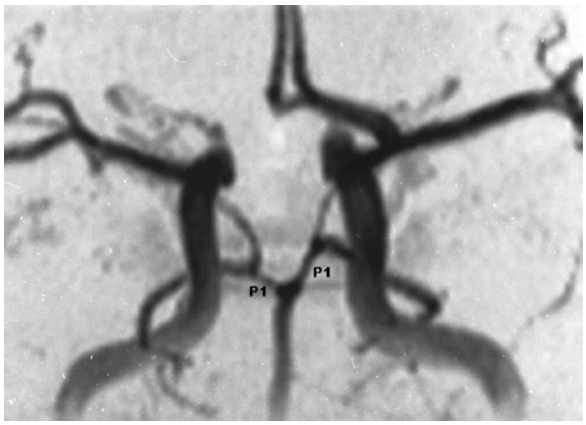

Fig. 7.2 Angio-MRI. the *P1* segments are well defined owing to the presence of the posterior communicating artery (PComA) bilaterally

The posterior thalamoperforating branches commonly consist of several small branches, although frequently a larger branch, further dividing into small branches, may predominate. They can arise entirely only from one P1, as previously described (Percheron 1976a, 1976b; Saeki and Rhoton 1977; Zeal and Rhoton 1978; Castaigne et al. 1981); this has also been documented more recently (Brassier et al. 1998; Lazzaro et al. 2010). Finally, even with hypoplasia of the P1, perforators may arise from it (Zeal and Rhoton 1978). All these variants probably explain the different pattern of midbrain and thalamic infarction in cases of proximal occlusion of the P1 (Figs. 7.5, 7.6, 6.5, and 6.11).

The collicular (quadrigeminal) artery, which arises from the P1 and sometimes from the P2 and runs around the midbrain, supplies the lateral and posterior portions of the midbrain. There is frequently a second small artery, running close and parallel to the collicular artery, called the accessory collicular artery (Zeal and Rhoton 1978; Duvernoy 1999; Tatu et al. 2001).

From the P1 and sometimes from the P2 or the parieto-occipital branch arises the posterior medial choroidal artery, which, after reaching the quadrigeminal plate and giving off branches for the posterior thalamus, courses forward in the roof of the third ventricle together with the internal cerebral vein toward the foramen of Monro. It supplies the choroid plexus of the third ventricle (Galloway and Greitz 1960; Wackenheim and Braun 1970; Margolis et al. 1974; Fujii et al. 1980).

Near the origin of the P1 arises a meningeal branch. This runs around the midbrain close to and inferiorly to the PCA. The meningeal branch extends to the junction of the tentorium with the falx, vascularizing these dural structures. The meningeal branch is not rare, but it is very fine and so not recognizable on the normal angiogram (Wollschlaeger and Wollschlaeger 1965). It can be involved in pathological processes, especially in the dural arteriovenous fistula of the tentorium (Weinstein et al. 1974) (Fig. 13.12).

7.2 P2 Segment

Also called the circumpeduncular segment, the P2 segment runs around the midbrain (Figs. 7.1, 7.3, and 7.4), commonly separated from it by several millimeters, and the P2 segment terminates on the surface of the quadrigeminal plate. The P2 segment lies inferior to the optic tract and basal vein, and it is superior to the superior cerebellar artery. The parahippocampal gyrus lies laterally, with the free margin of the tentorium above. The P2 segment gives off the thalamogeniculate artery, which can be a single branch. Sometimes, there are two or three branches, which supply the lateral thalamus (Duvernoy 1999; Tatu et al. 2001). The

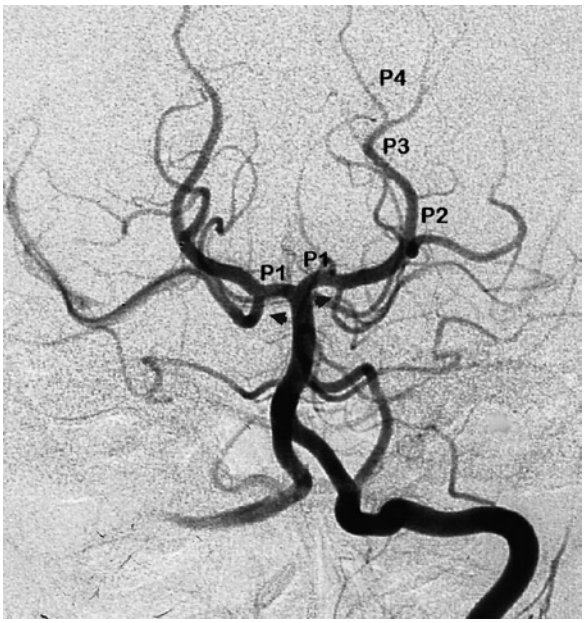

Fig. 7.3 Vertebral angiogram, AP view. The retrograde injection of the PComA bilaterally (*arrow*) allows the precise definition of the *P1* segment of the posterior cerebral artery (PCA). The *P2*, *P3*, and *P4* are also shown

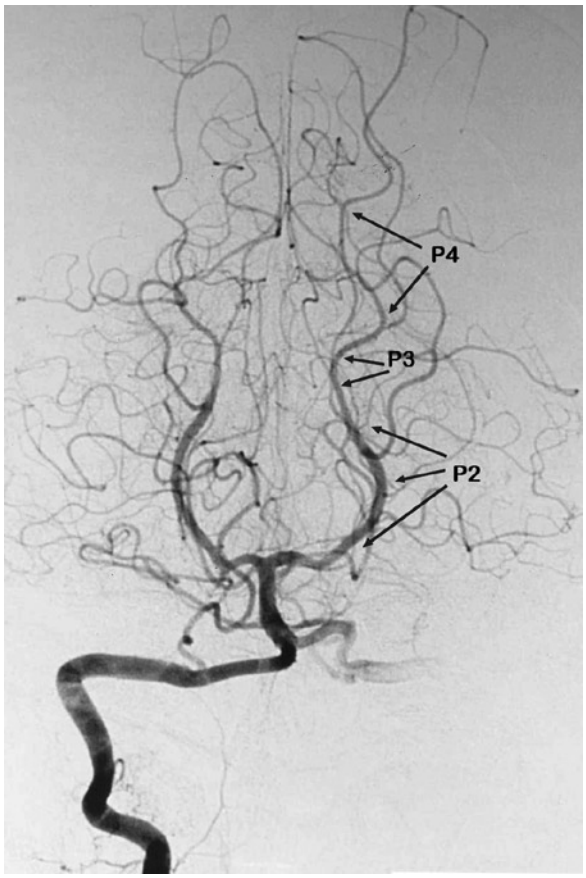

Fig. 7.4 Vertebral angiogram, AP view, showing the typical course of the PCA with its typical *P2*, *P3*, and *P4* segments

artery can arise in the proximal or more distal P2 segment (Zeal and Rhoton 1978).

Other branches are the peduncular perforators for the lateral midbrain and the posterior lateral choroidal artery. The latter, which can sometimes arise from the parieto-occipital artery, consists of a single or several branches (Zeal and Rhoton 1978). Basically, there is an anterior branch, which runs in the circumpeduncular cistern, enters the choroid fissure, extends forward to supply the plexus of the temporal horn, and anastomoses with the anterior choroidal artery (AchA). A posterior branch reaches the pulvinar, gives branches to it, and terminates in the choroid plexus of the lateral ventricle at the level of the atrium, anastomosing with branches of the AchA (Galloway and Greitz 1960; Wackenheim and Braun 1970; Margolis et al. 1974; Fujii et al. 1980; Duvernoy 1999).

From the P2 arise cortical branches for the temporal lobe. They are also called the inferior temporal arteries and supply entirely the inferior surface of the temporal lobe, including the hippocampus and partially the inferior surface of the occipital lobe. The cortical branches for the temporal lobe are classified in relation to the site of origin and vascular territories involved: anterior, middle, and posterior (Zeal and Rhoton 1978).

7.3 P3 Segment

The P3 segment is short and runs in the quadrigeminal cistern on the surface of the quadrigeminal plate, approaching that of the other side at a variable distance, averaging 16 mm (Margolis et al. 1974) (Figs. 7.1, 7.3, and 7.4).

7.4 P4 Segment

The main trunk divides into terminal branches: the parieto-occipital, calcarine, and splenial arteries. The parieto-occipital artery arises either together with the calcarine artery, at the level of the calcarine fissure, or sometimes as a single trunk, more proximally from the P2 segment. The parieto-occipital artery runs posterosuperiorly on the medial surface of the hemisphere and gives off branches for the precuneus, cuneus, and, as reported (Margolis et al. 1974) in 35% of cases, for the primary visual cortex.

The calcarine artery arises at the calcarine fissure, usually in its first segment lateral to the parieto-occipital artery. Further, it runs medially and inferiorly along the calcarine fissure, supplying the primary visual cortex (Figs. 7.1, 7.4, 7.6, and 7.7).

The splenial artery, also called the posterior pericallosal artery, has a variable origin, frequently from the P3 segment or from the parieto-occipital artery. It runs around the splenium and anastomoses anteriorly with the branch of the pericallosal artery (Figs. 7.6 and 7.7).

7.5 Anatomical Variations

The P1 segment can be hypoplastic or absent. When the P1 is absent, the PCA takes its origin directly from the ICA via a large PComA. This aspect, corresponding to

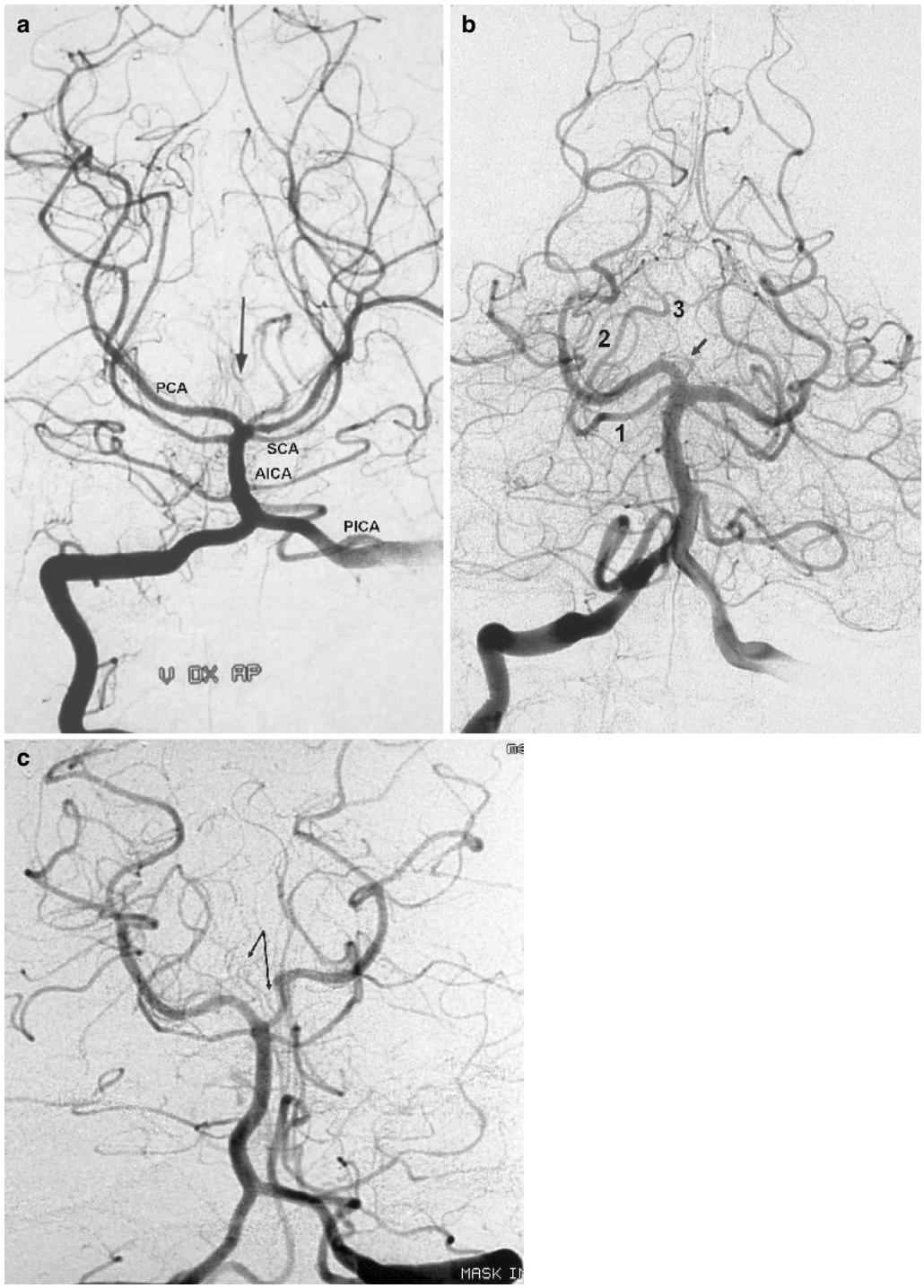

Fig. 7.5 (**a**) Vertebral angiogram, AP view. The posterior thalamo-perforating branches (*arrow*) are well visible. They arise prevalently from the right P1. There is a partial overlap with distal branches of the left posterior inferior cerebellar artery (*PICA*). Anterior inferior cerebellar artery (*AICA*), superior cerebellar artery (*SCA*), posterior cerebral artery (*PCA*). The *PCA* and *SCA* both run around the midbrain. In the AP view, the *SCA* is medially located. (**b**) Vertebral angiogram, AP view. A faint network of vessels corresponding to the posterior thalamo-perforating artery is recognizable, in which a larger branch arising from the right P1 (*arrow*) predominates. The numbers *1*, *2*, and *3* correspond, respectively, to the pontine, midbrain, and quadrigeminal segments of the SCA. (**c**) Vertebral angiogram, AP view. Ascending course of the P1 owing to a short basilar artery. At least three well-developed posterior thalamo-perforating arteries are recognizable: two on the *left*, one on the *right* (*double arrow*)

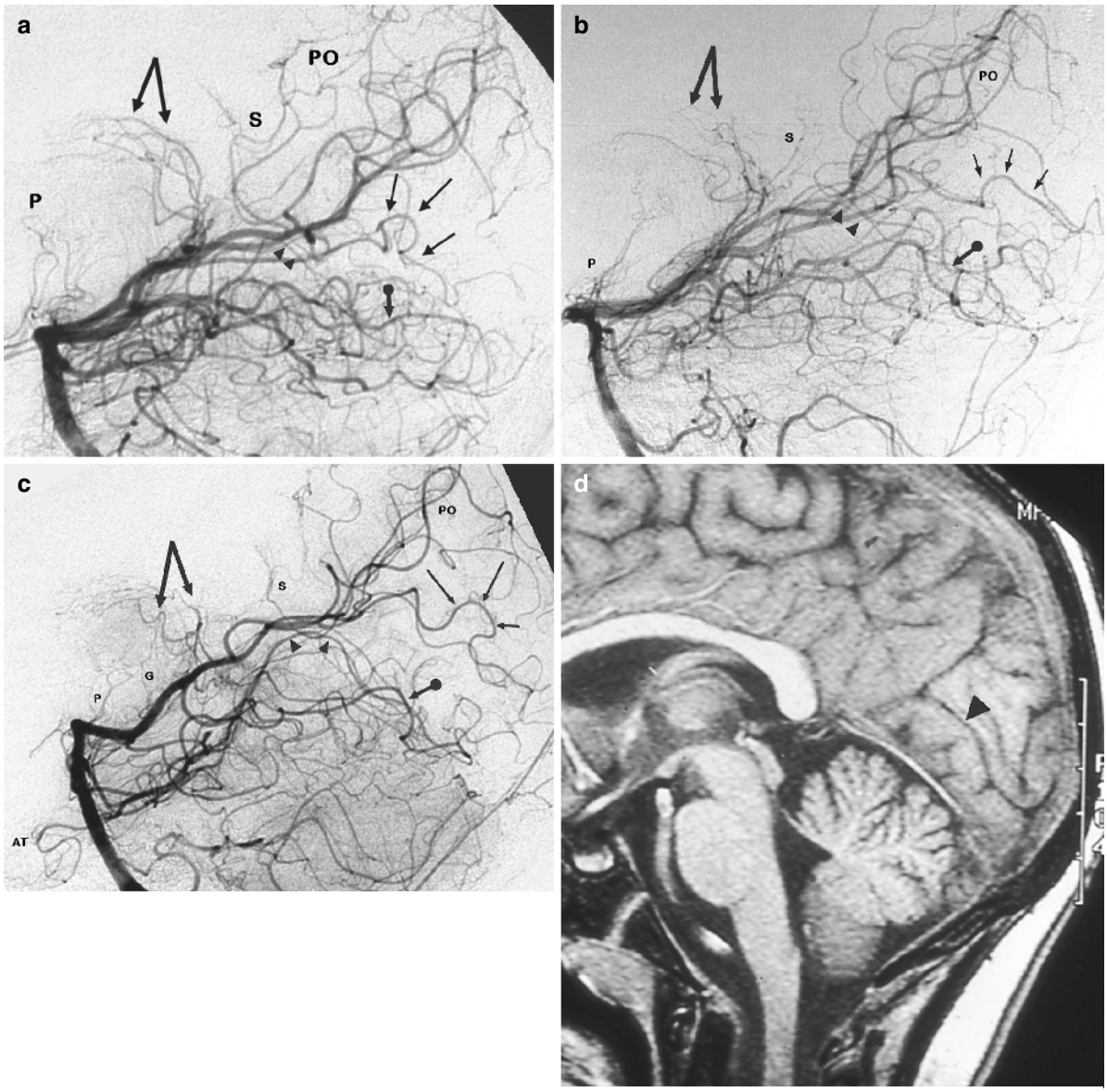

Fig. 7.6 (**a**), (**b**), and (**c**) vertebral angiogram, lateral view. Posterior thalamo-perforating branches (*P*) arising from the P1. In (**a**) there are also anterior thalamo-perforating branches arising from the PComA. In (**c**) a predominant large perforator is recognizable. Thalamogeniculate artery (*G*), posterior medial and lateral choroidal arteries (*double arrow*). Note the typical S-shaped medial arteries located anteriorly to the lateral branches. Splenial artery (*S*), calcarine artery (*three arrows*), parieto-occipital artery (*PO*), anterior temporal artery (*AT*), tempo-ro-occipital artery (*arrow with dot*). There is overlap of the temporal branches of the PCA and cerebellar branches. The latter can be identified owing to their typical superiorly convex curve (*arrowheads*). (**d**) T1-weighted MRI showing the typical calcarine fissure (*arrow*)

the initial embryological pattern, is called the fetal origin of the PCA (Figs. 7.9a–c). It can occur uni- or bilaterally; its frequency is reported as being between 30% and 40% of cases (Zeal and Rhoton 1978; Pedroza et al. 1987). Conversely, when the P1 is well developed, the PComA is commonly small or can be completely absent (Fig. 7.9d). Among the variants concerning the proximal segment of the PCA, duplication, with two separated branches arising from the ICA or one from the ICA and the other from the basilar artery, has been reported (Hoyt et al. 1974). A recent study has shown that in the majority of cases this duplication is a variant of the AchA, which can be hypertrophic and take over partially or completely the vascular territory of the PCA

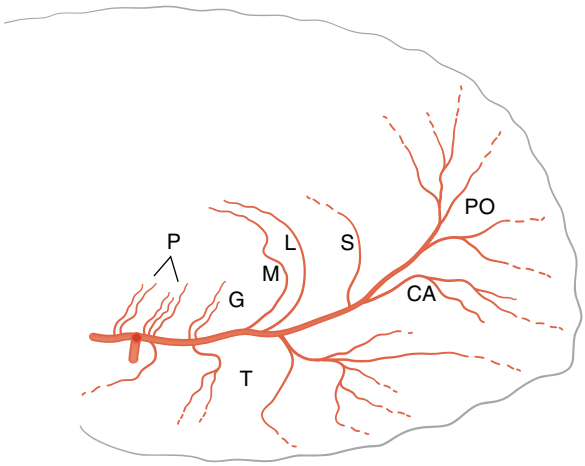

Fig. 7.7 Course of the PCA and its branches in the lateral view. Anterior from PComA and posterior from P1 thalamo-perforating arteries (*p*), thalamogeniculate artery (*G*), posterior choroidal arteries, medial (*M*), lateral (*L*), splenial artery (*S*), parieto-occipital arteries (*PO*), calcarine artery (*CA*), temporal arteries (*T*), anastomoses with the anterior cerebral artery (ACA) and middle cerebral artery (MCA) (……)

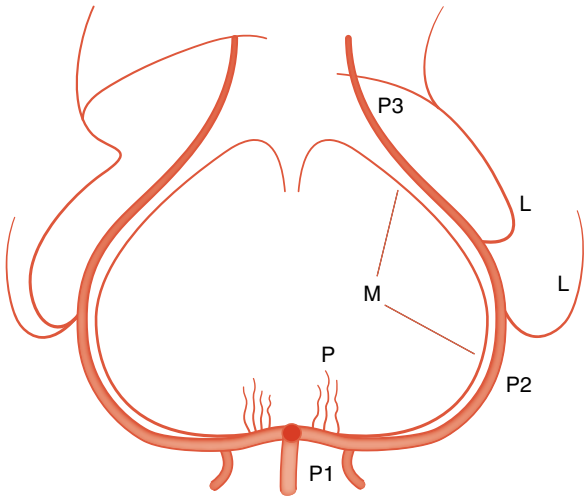

Fig. 7.8 Course of the *P1*, *P2*, and *P3* segments of the PCA in the AP view. Posterior thalamo-perforating branches (*P*), medial (*M*) and lateral (*L*) posterior choroidal arteries

(see Sect. 2.4.3.1). It is important to recognize this condition even though it is not always easy or possible to establish with certainty on the angiogram which is the dominant vessel (Fig. 7.10). Variants involving the posterior thalamo-perforating arteries have already been described.

7.6 Vascular Territories

- The posterior thalamo-perforating arteries (P1) supply the medial anterior part of the midbrain and medial thalamus. Frequently, a common large trunk supplies the midbrain and thalamus. In addition, other smaller branches are present, supplying selectively the midbrain or thalamus.
- The collicular artery (P1) supplies the lateral and posterior part of the midbrain, together with the middle posterior choroidal artery and small perforators arising directly from the P1-P2 segments of the PCA.
- The thalamogeniculate artery (P2) supplies the lateral part of thalamus, optic tract, and posterior limb of the internal capsule.
- The posterior choroidal arteries (P1 and P2) supply the posterior part of the thalamus.
- There are many variants concerning the origin and extension of the vascular territories of all these arteries. Furthermore, they form a rich anastomotic network on the surface of the midbrain and posterior thalamus that involves also the superior cerebellar artery and, partially, the AchA. This probably explains the presence or absence and different extensions of ischemic lesions in occlusion of the PCA distal to the P1.
- The cortical branches comprise the temporal arteries (P2) supplying the inferior surface of the temporal and occipital lobes, the parieto-occipital artery (P3) supplying the medial surface of the hemisphere in the parieto-occipital area, and the calcarine artery (P3) supplying the primary visual cortex and adjacent areas. Contributors in the supply of the primary visual cortex also come from the parieto-occipital and temporo-posterior arteries.
- The splenial artery (P3) supplies the splenium.

Between the branches of the PCA surrounding the midbrain and running toward the thalamic area, there are many superficial anastomoses. The perforating branches, however, which arise from them and penetrate the parenchyma, are basically end arteries (Duvernoy 1999).

From superficial branches running on the surface of the cortex arise arteries that supply the cortex and white matter (medullary arteries). The medullary arteries are similar to the branches of the anterior and

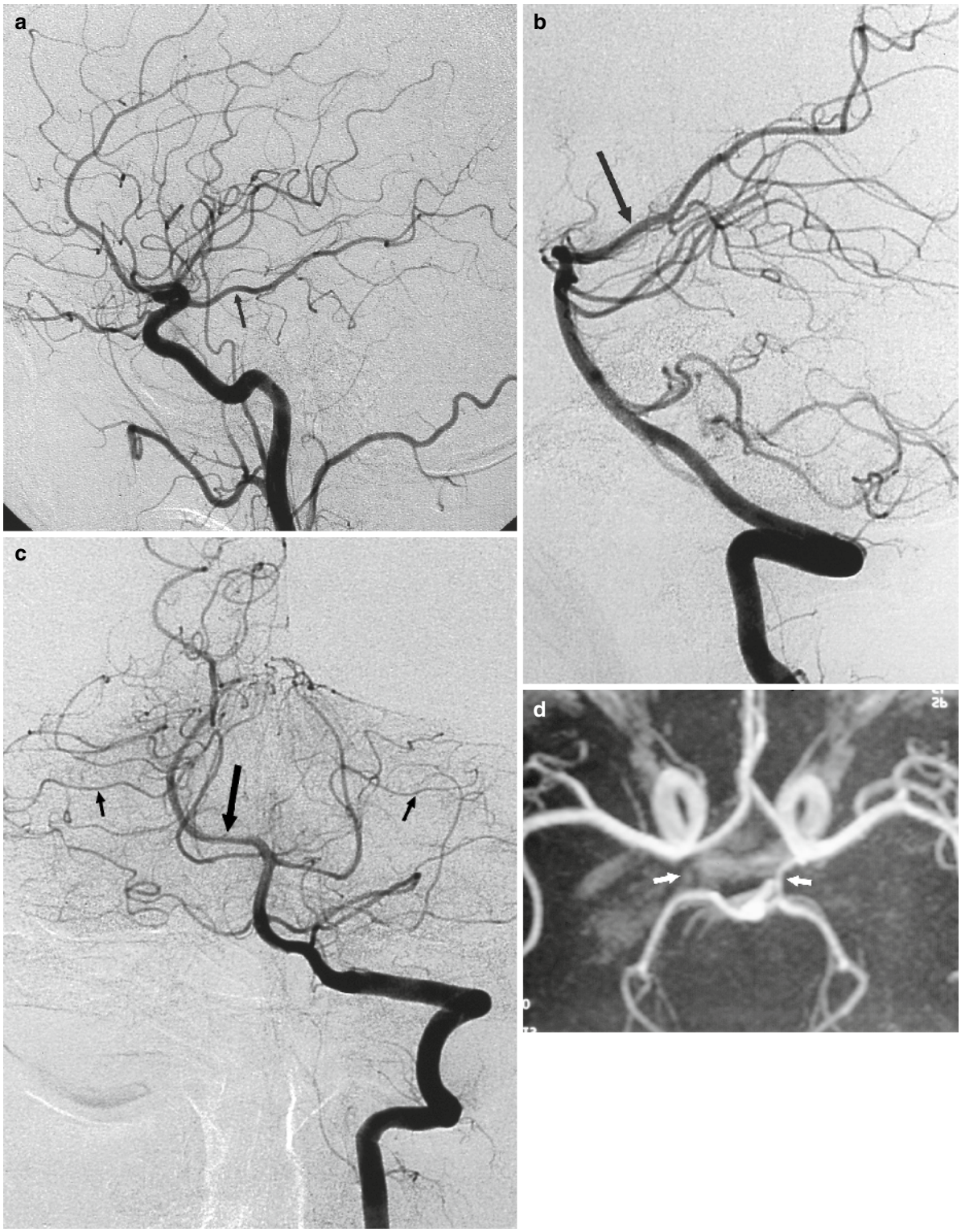

Fig. 7.9 (**a**) *Left* PCA arising directly from the ICA (fetal pattern; *arrow*), (**b**) lateral vertebral angiogram showing the right PCA (*arrow*), (**c**) vertebral angiogram, AP view. Right PCA (*arrow*) arising from the basilar artery. Hypo/aplastic left P1. The marginal artery of the left superior cerebellar artery (*small arrow*) is easily identifiable. Owing to the minimal overlap, the right marginal artery is also well recognizable (*small arrow*). There are two well-developed AICA. (**d**) Angio-MRI in another patient. *Left* PComA (*arrow*). On the *right*, absence of the PComA (*arrow*)

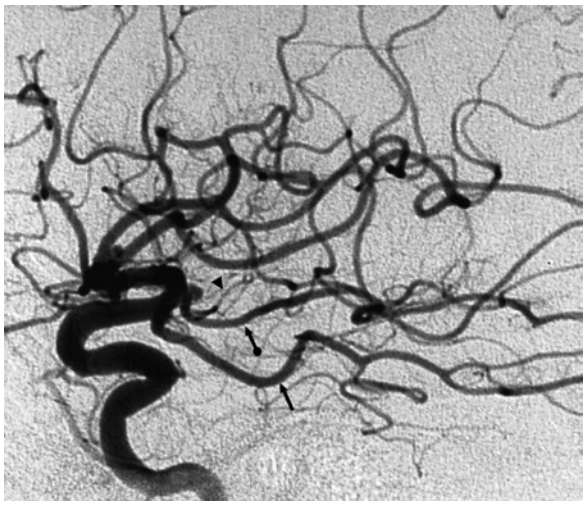

Fig. 7.10 Lateral carotid angiogram. Three branches are recognizable, arising from supraclinoid ICA: a small one (*arrowhead*), which could be the cisternal segment of the AchA, and two other large branches, one superior (*arrow with dot*), directed to the occipito-parietal, and the other inferior (*arrow*), directed to the temporo-occipital region. There is a false image of an aneurysm, excluded by other projections. It is difficult to say whether this is a normal AchA and a duplicated PCA or a hypertrophic AchA, taking over completely the vascular territory of the PCA

middle cerebral arteries and are end arteries. Potential leptomeningeal anastomoses are present in the terminal cortical territories among the PCA, anterior cerebral artery, and middle cerebral artery. The splenial artery can anastomose with the pericallosal artery (Fig. 7.7).

7.7 Angiogram

The P1 segment is well demonstrated in the AP view (Figs. 7.3 and 7.4). Its perforators branch directed upward and somewhat posteriorly; they are frequently well recognizable on AP and always on lateral angiograms (Figs. 7.5, 7.6, 6.5, and 6.11). The P2 segment is better visualized in the AP view surrounding the midbrain. In the lateral view, the segments of both sides are superimposed. Among the branches arising from the P2, the thalamogeniculate and both medial and lateral choroidal arteries (Figs. 7.6 and 7.7) are distinct on the lateral angiogram. The thalamogeniculate arteries are one or more small branches running upward and slightly posteriorly between the posterior thalamo-perforator branches and choroidal arteries. The medial choroidal arteries commonly have an S-shaped pattern, and the lateral choroidal arteries form an anteriorly directed concave curve posterior to the medial choroidal arteries (Wackenheim and Braun 1970). Commonly, the choroidal arteries cannot be identified in the AP view. Their course is schematically demonstrated in Fig. 7.8. The choroidal arteries can be recognized when they are dilated, particularly when supplying arteriovenous malformations. The lateral branch of the posterior choroidal artery can lead to a blush in the capillary-venous phase, which is visible in the AP and lateral views and corresponds to the plexus of the lateral ventricle.

Concerning the branches supplying the hemisphere, the anterior temporal branches, which arise from the P2, are well recognized in the AP view. On the lateral angiogram, these branches have a course that is anterior to the basilar artery (Fig. 7.6). The more distal hemispheric branches arising from the P2 and P3 can be visible on the AP and lateral angiogram (Figs. 7.4–7.7). However, a more precise identification is possible with the lateral angiogram, where, in particular, the calcarine artery can be easily identified because of its typical course (Fig. 7.6). The parieto-occipital branches are superiorly located to the calcarine artery and the temporo-occipital inferiorly. In the AP view, superimposition of these branches, can make precise identification difficult. Basically, the calcarine artery runs in the paramedian region, medially to the parieto-occipital. The splenial artery is easily identified on the lateral angiogram posteriorly to the choroidal artery (Fig. 7.6).

Vascular Territories

8

In this chapter, the vascular territories of the brain as viewed in the axial planes on CT or MRI are presented.

The cerebral hemispheres are vascularized by the anterior cerebral (ACA), middle cerebral (MCA), posterior cerebral (PCA), and anterior choroidal (AchA) arteries. From the proximal segments of these arteries (A1, M1, P1) and cisternal segment of the choroidal artery, small branches (deep perforators) arise that enter the brain parenchyma at the level of the anterior and posterior perforated substance supplying basal ganglia, thalamus, and internal capsule. Other perforators arise from the anterior communicating (AComA) and posterior communicating (PComA) arteries, which belong to the circle of Willis, and from the distal segment of the internal carotid artery. The perforators are end arteries with no possible collateral circulation. From the more distal branches of ACA, MCA, PCA, and AchA cortical arteries that supply the cortex and arteries that enter the white matter (medullary arteries) arise. The deep perforators of the medullary arteries are also end-arteries. On the contrary, there are potential pial (leptomeningeal) anastomoses among the cortical branches of all the main trunks (Fig. 8.1).

In the posterior fossa, medulla and pons are vascularized by perforators arising from the vertebral basilar, and anterior and posterior spinal arteries. The midbrain is vascularized by perforators of PCA and AchA. Furthermore, perforating branches for medulla, pons, and midbrain arise from the first segments of the three cerebellar arteries (PICA, AICA, and SCA). All these perforators are end-arteries. Cerebellum is supplied by the three cerebellar arteries: the cortical branches supply the cortex and the medullary arteries supply the white cerebellar matter and deep nuclei. Medullary arteries are end-arteries, while potential pial anastomoses are present among the cortical branches (Fig. 8.2).

More details about the vascularization are presented in Chaps. 2 and 4–7.

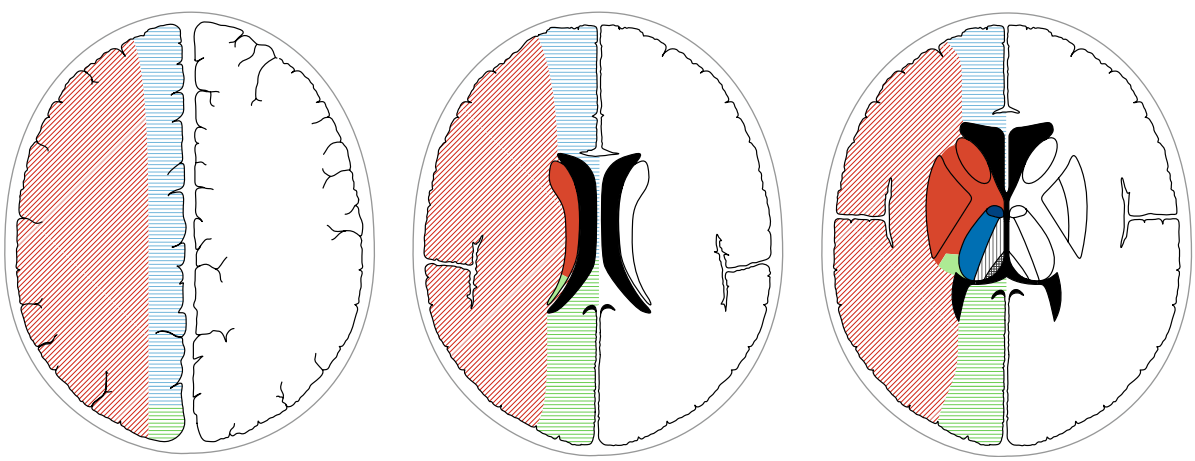

Fig. 8.1 Vascular territories of the cerebral hemispheres

G.B. Bradac, *Cerebral Angiography*,
DOI: 10.1007/978-3-642-15678-6_8, © Springer-Verlag Berlin Heidelberg 2011

Fig. 8.1 (continued)

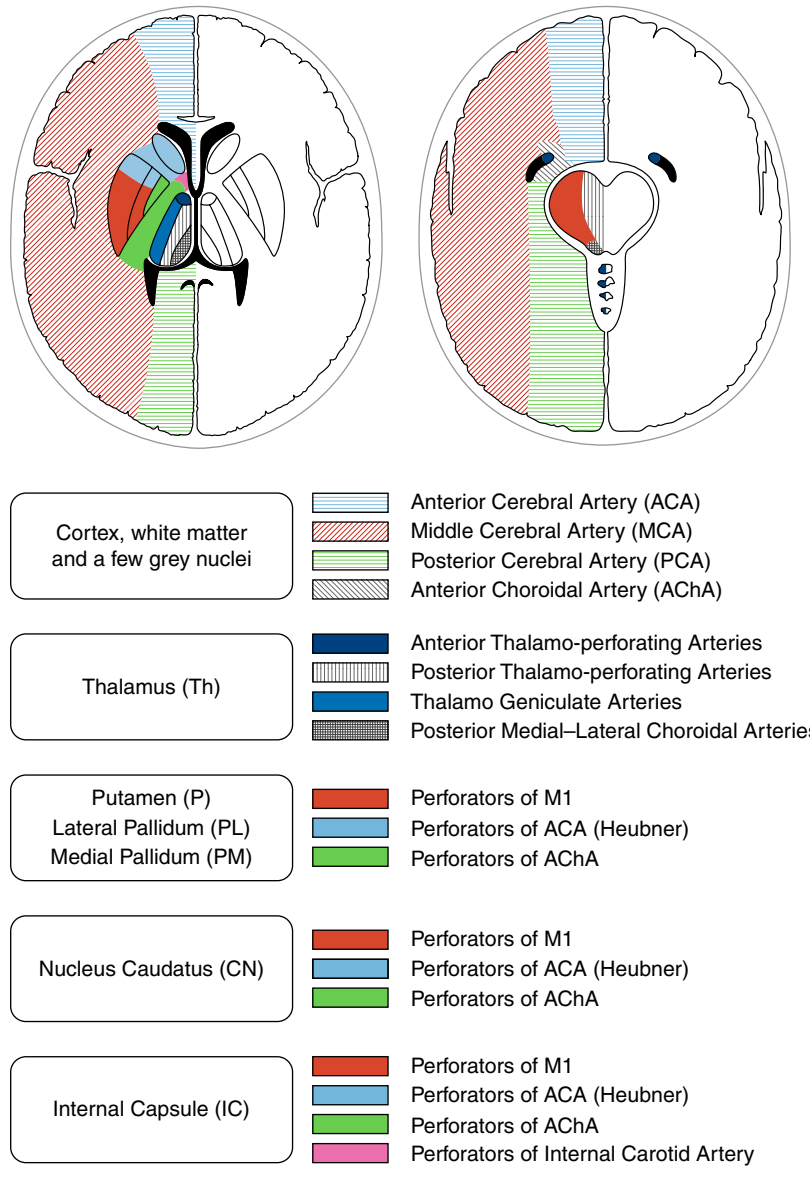

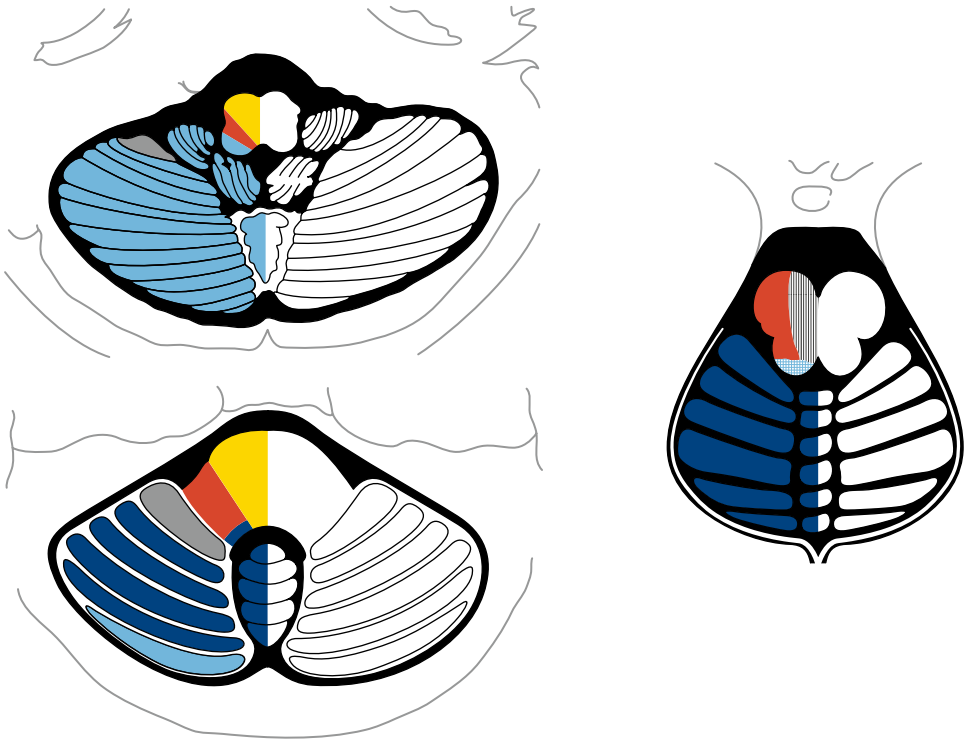

Medulla
- Perforators of VA and ASA
- Perforators of VA and PICA
- Perforators of PICA and PSA

Pons
- Perforators of BA
- Perforators of BA (latero-pontine arteries) and perforators of AICA
- Perforators of SCA (only in the superior part of the pons)

Midbrain
- Posterior thalamo perforating arteries
- Small perforators of PCA, collicular, postero-medial choroidal and anterior choroidal arteries
- Collicular, postero-medial choroidal, superior cerebellar arteries

Cerebellum
- PICA
- AICA
- SCA

ASA anterior spinal artery
PSA posterior spinal artery
BA basilar artery
VA vertebral artery
PICA postero-inferior cerebella artery
AICA antero-inferior cerebella artery
SCA superior cerebellar artery

Fig. 8.2 Vascular territories of the brainstem and cerebellum, with the section at the level of the medulla, pons, and midbrain

Cerebral Veins

9

The variations in the course, development, and presence of cerebral veins are greater than those of the cerebral arteries. Nevertheless, some typical venous patterns can be recognized on an angiogram. Considering these patterns and the area of venous drainage, the cerebral veins can be classified into supratentorial and infratentorial groups.

9.1 Supratentorial Cerebral Veins

The supratentorial cerebral veins can be subdivided into the superficial and deep systems (Kaplan and Ford 1966; Salamon and Huang 1976).

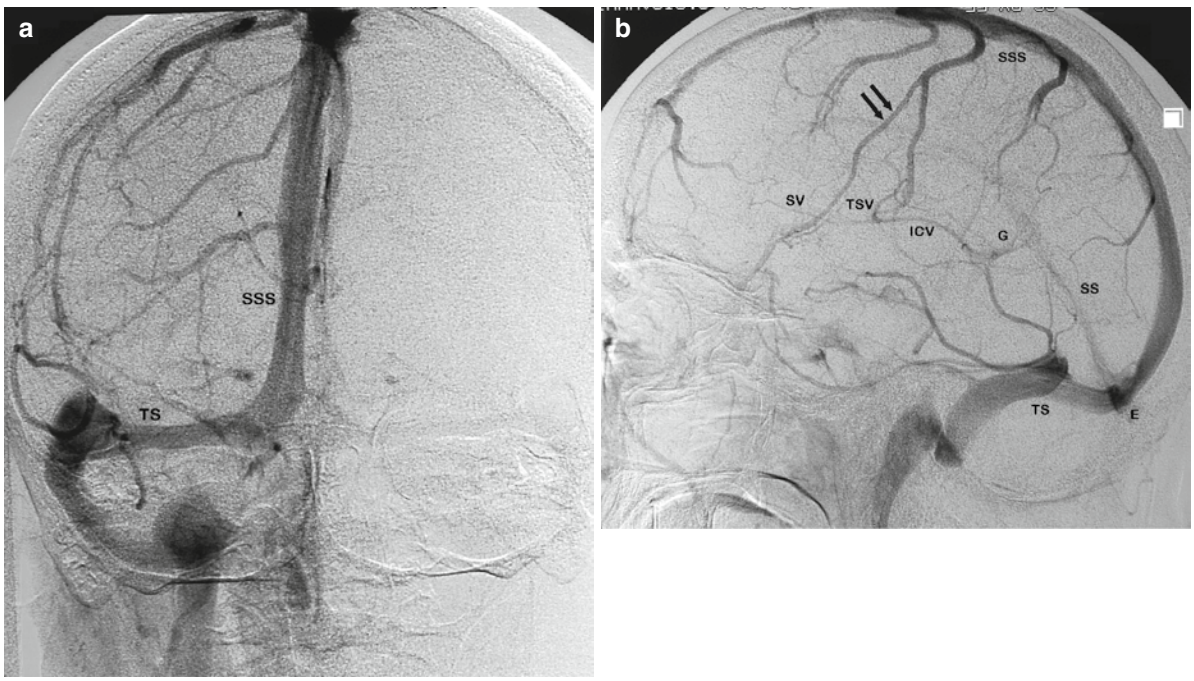

Fig. 9.1 Carotid angiogram, anteroposterior (*AP*) and lateral view. Venous phase (**a** and **b**). The *SSS* drains predominantly into the *right TS*. Among the cortical veins entering the *SSS*, there is a large Trolard vein (*double arrow*). Thalamostriate vein (*TSV*), septal vein (*SV*), internal cerebral vein (*ICV*) with its typical S-shaped course, vein of Galen (*G*), straight sinus (*SS*), torcular herophili (*E*). Vertebral angiogram (**c**) in the same patient. On this angiogram is documented the presence of the *left TS*, in which drains predominantly the SS. There is a complementary dural channel connecting the right and left *TS* at the torcular herophili (*arrow*) (Patient treated for distal PICA aneurysm, with occlusion also of the distal PICA with coils)

G.B. Bradac, *Cerebral Angiography*,
DOI: 10.1007/978-3-642-15678-6_9, © Springer-Verlag Berlin Heidelberg 2011

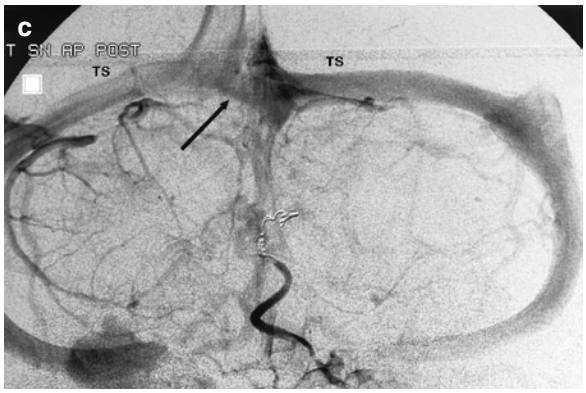

Fig. 9.1 (continued)

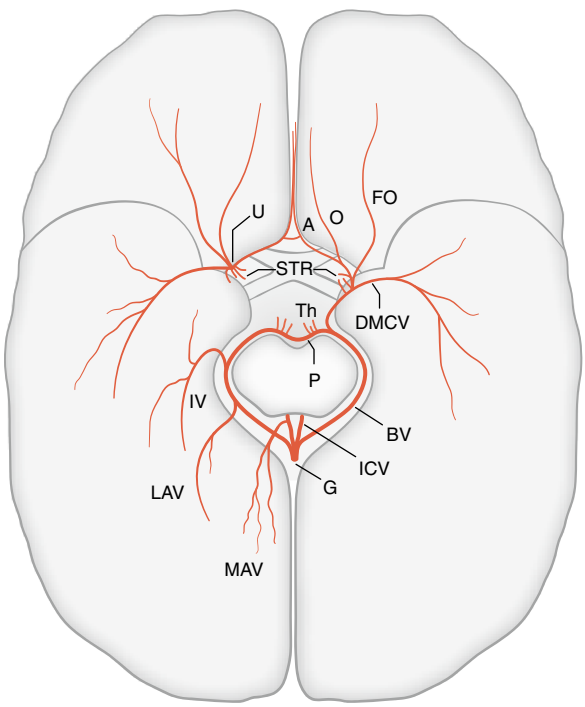

BV	Basal vein
ICV	Internal cerebral vein
G	Galen vein
MAV	Medial atrial vein
LAV	Lateral atrial vein
IV	Inferior ventricular vein
P	Peduncolar vein (both peduncolar vein can be connected by small posterior communicating vein)
Th	Thalamo striate veins (draining in the peduncular veins)
DMCV	Deep middle cerebral vein (draining in the BV on the right and in the uncal vein on the left)
U	Uncal vein
STR	Striate vein (draining in the DMCV)
O	Olfactory vein
Fo	Fronto orbital vein
A	Anterior cerebral vein (both anterior cerebral vein can be connected by a small anterior communicating vein)

Fig. 9.2 The basal vein and its tributaries seen from below

9.1.1 The Superficial System

This comprises the cortical veins draining the cortex and superficial medullary veins, which drain the more superficial white matter. The medullary veins run in a centrifugal direction toward the cortex, where they join the cortical veins. The latter run within the subarachnoid space along the superficial sulci, frequently crossing the gyri. Close to the sinuses, they perforate the arachnoid and dura, where they run through their internal layers before entering the sinuses (Figs. 9.1, 9.4, 9.5, 9.7, 9.8, and 9.10).

9.1.1.1 Superior Group

The veins of this group run up toward the superior sagittal sinus (SSS), draining the superolateral and superomedial surface of the hemispheres. Sometimes, a large vein called the vein of Trolard, which connects the SSS with the superficial middle cerebral vein, can predominate. The veins on the medial surface commonly originate near the corpus callosum and run up toward the convexity, where they turn laterally to join the vein of the lateral surface and together these veins enter the SSS.

Some of the veins draining the cingulate gyrus and corpus callosum enter the inferior sagittal sinus. Parts of the corpus callosum and adjacent structures drain into the posterior pericallosal vein (splenial vein) (Fig. 9.6), which runs in the pericallosal cistern around the

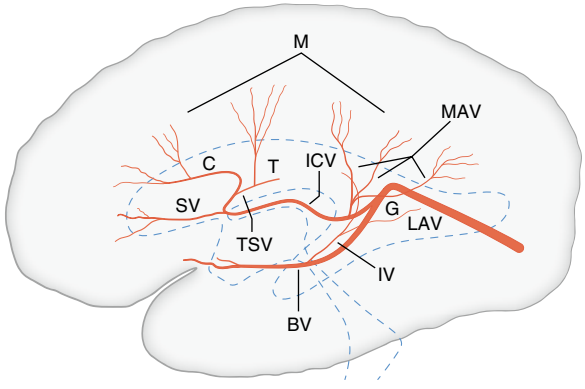

ICV	Internal cerebral vein	IV	Inferior ventricular vein
TSV	Thalamo-striate vein	M	Deep medullary veins
C	Caudate vein	BV	Basal vein
SV	Septal vein	G	Galen vein
MAV	Medial atrial vein	T	Terminal vein
LAV	Lateral atrial vein		

Fig. 9.3 Lateral view of the deep cerebral veins

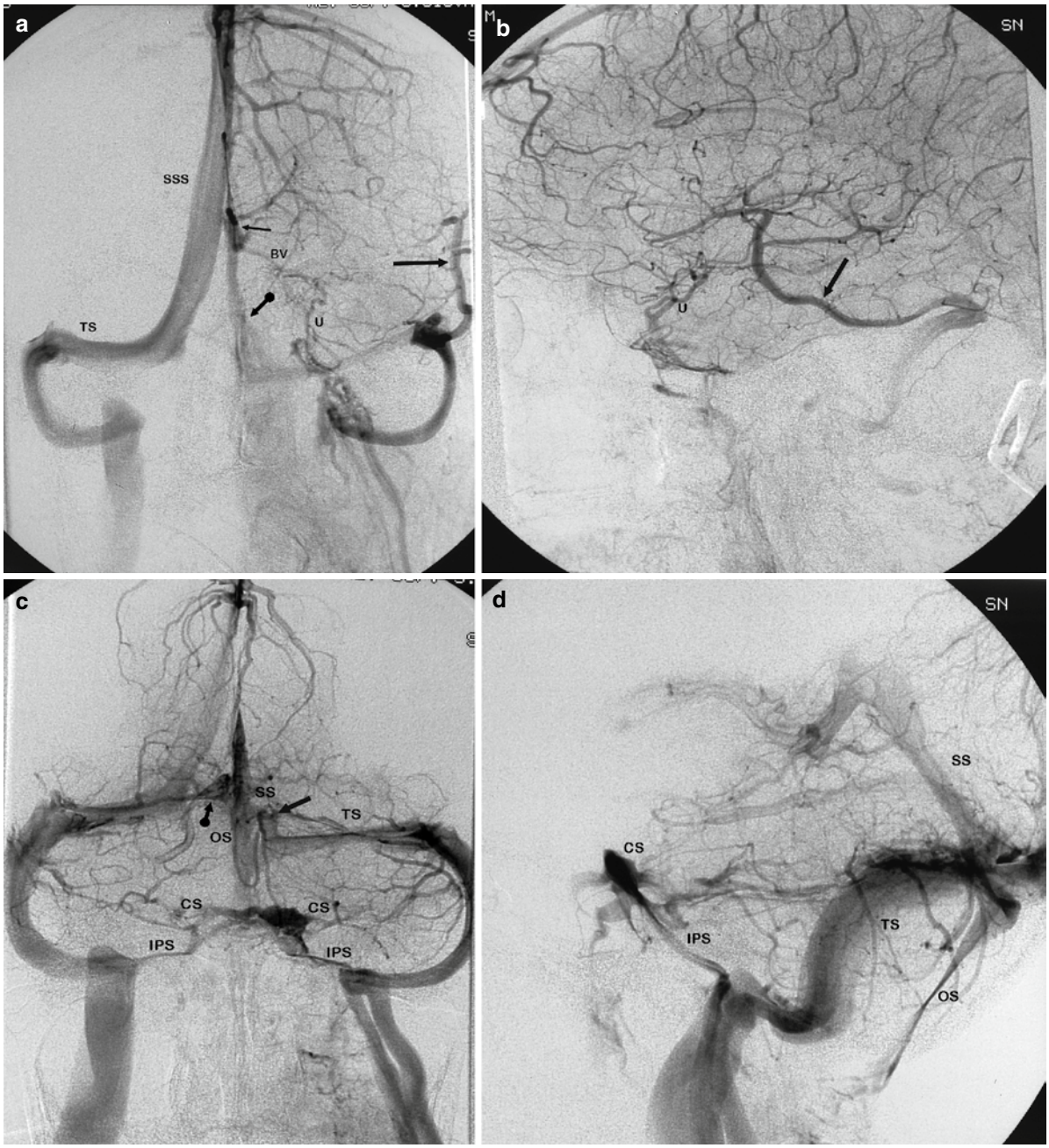

Fig. 9.4 Carotid angiogram, AP and lateral view, venous phase (**a** and **b**). The *SSS* drains into the *right TS*. The *left TS* is partially injected through the straight sinus (*arrow with dot*). There is a large vein of Labbé (*arrow*) draining into the distal part of the *left TS*. Large uncal vein (*U*) receiving blood from the anterior tributaries of the basal vein (*BV*). Typical paramedian course of internal cerebral vein (*arrow*) receiving its tributaries. Vertebral angiogram in the same patient, AP and lateral view, venous phase (**c** and **d**). Better filling of the straight sinus (*SS*) and of the *left TS*. There is a complementary venous channel to the TS (*arrow*). There is also a connection (*arrow with dot*) with the *right TS*. There is a large occipital sinus (*OS*) connected posteriorly with the *SS* and *TS*. Inferior petrosal sinus (*IPS*), cavernous sinus (*CS*)

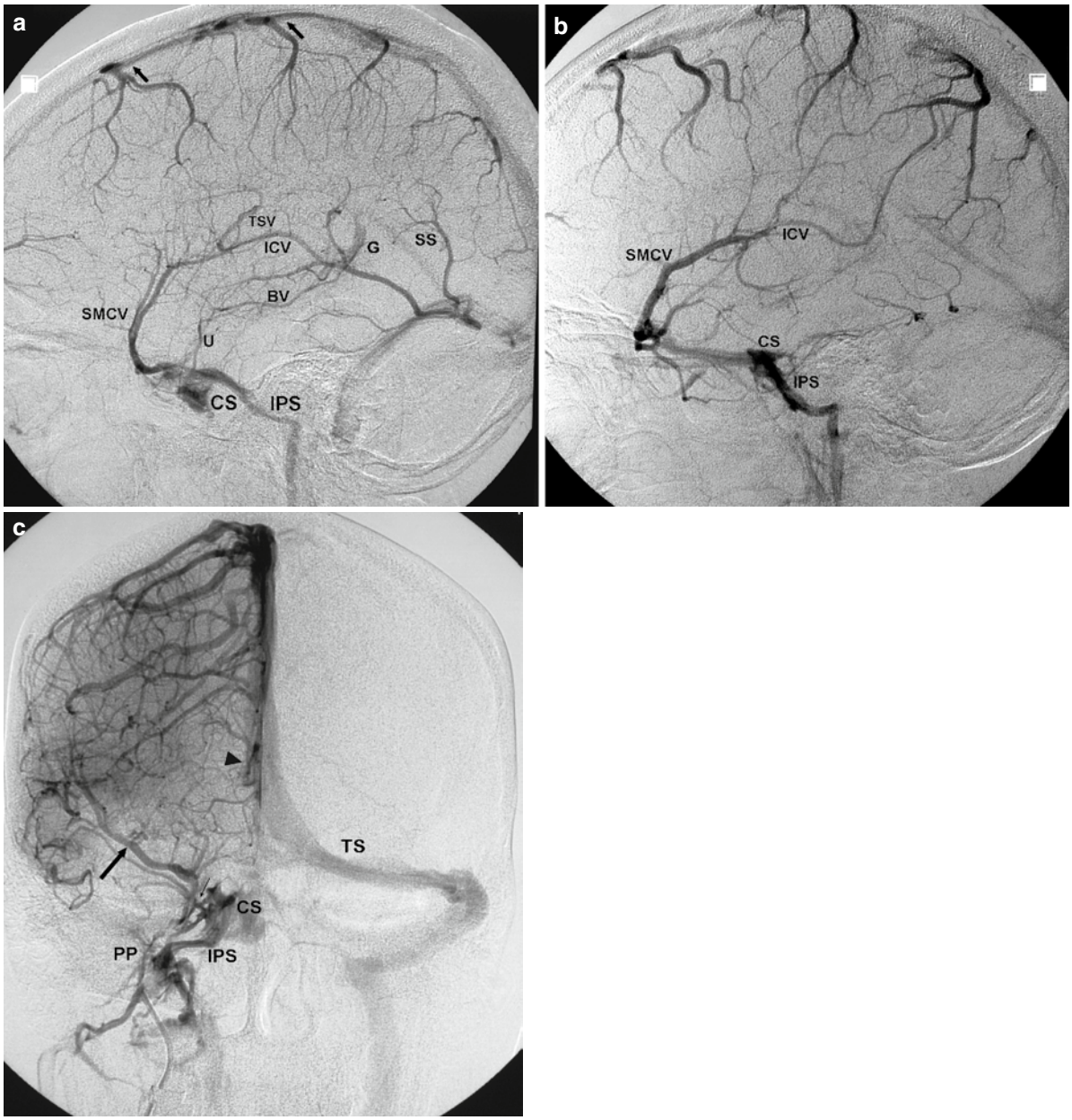

Fig. 9.5 Carotid angiograms. Venous phases in three different cases. (**a**) Large superficial middle cerebral vein (*SMCV*) draining into the cavernous sinus and farther into the *IPS*. There is a small uncal vein (*U*) draining partially the anterior tributaries of the basal vein (*BV*). Internal cerebral vein (*ICV*), thalamostriate vein (*TSV*). The septal vein is not recognizable; it appears frequently in later venous phases. Vein of Galen (*G*), straight sinus (*SS*). Cortical veins draining into the SSS with a typical anterior course with a progressively reverse direction to the flow of the sinus from frontal to occipital. (**b**) Large *SMCV* draining into the cavernous sinus and farther into the *IPS*. Basal vein is not recognizable. Internal cerebral vein (*ICV*). (**c**) AP view. ICV (*arrowhead*). The duplicated *SMCV* (*large arrow*) drains into venous channels located lateral to the cavernous sinus (*CS*). The lateral venous channels correspond partially to the "paracavernous sinus" and to the "lateral cavernous sinus," both draining into the pterygoid plexus (*PP*). Rich anastomoses (*small arrow*) connect the paracavernous sinus and lateral cavernous sinus with the *CS*. The *CS* drains further into the *IPS*. There is no injection of the *TS* on the *right*. The drainage of SSS occurs in the *TS* of the *left*. This is a frequent normal angiographic condition. A complementary contralateral carotid angiography and vertebral angiography should be performed whenever a complete study of the dural sinuses is required

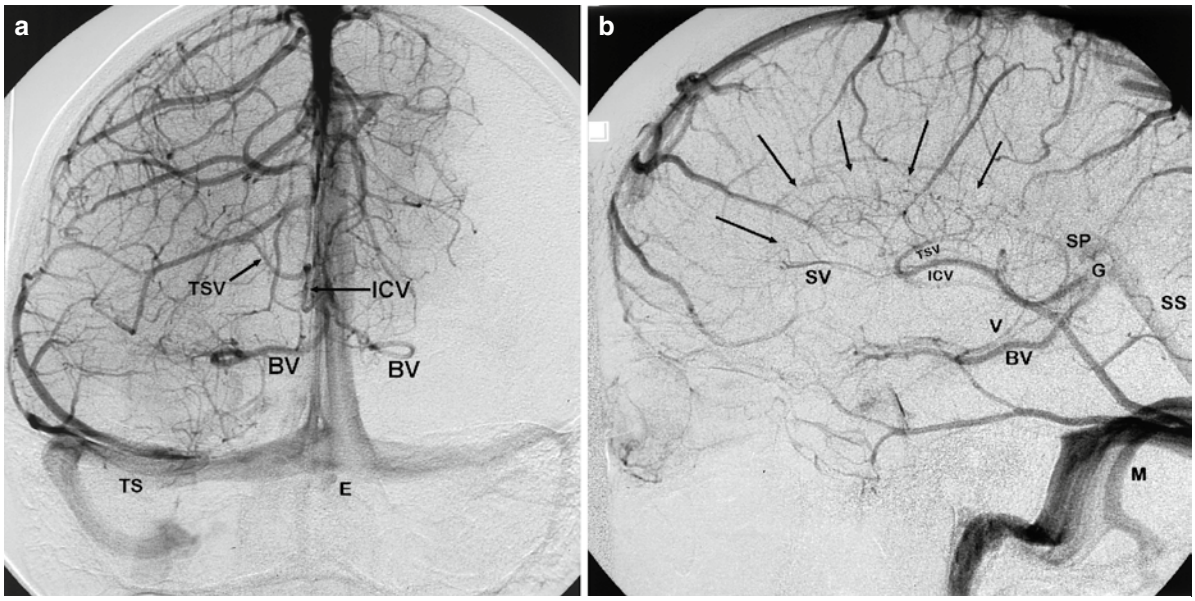

Fig. 9.6 AP (**a**) and lateral (**b**) angiograms. Venous phase. There is a bilateral injection of the cortical frontal vein and basal vein (*BV*). In the late venous phase visible on the lateral angiogram, there is a faint network (*arrows*) corresponding to the medullary veins draining into the subependymal veins (*ICV*, *TSV*, *SV*). There is also an injection of the inferior ventricular vein (*V*) with its typical anterior concave curve, to which converge fine branches of the lateral atrial vein. Splenial vein (*SP*), vein of Galen (*G*), straight sinus (*SS*). There is no superficial middle cerebral vein. The drainage is directed posteriorly by the way of two large temporal veins draining into the TS. Mastoid emissary vein (*M*). There is duplication of SSS in two channels, well recognizable in the AP view; the smaller one is divided further. All these channels enter the torcular herophili (*E*)

splenium, entering the vein of Galen. The most anterior veins of the medial surface drain into the anterior pericallosal vein, which courses around the genu further into the cistern of the lamina terminalis (vena lamina terminalis); this continues to the anterior cerebral vein, which is a tributary of the basal vein (Duvernoy 1975; Salamon and Huang 1976) (Fig. 9.2).

Medial and lateral veins are superimposed on a lateral angiogram. The veins in the frontal area enter the sinus and form a right angle with it; the more posterior veins enter the sinus, forming a progressively more oblique angle in the direction against the current of blood into the SSS.

9.1.1.2 Anterior–Inferior Group

The main vein in this group is the superficial middle cerebral vein (SMCV), which collects several branches of the lateral inferior surface of the frontal and parietal area and from the lateral superior surface of the temporal lobe. It can be single or represented by a group of veins.

The SMCV runs along the surface of the sylvian fissure and continues into the sphenoparietal sinus, entering the cavernous sinus. It can also run directly toward the base of the skull, where it divides into small channels that pass through the foramina of the base of the skull, reaching the pterygoid plexus. This variant is called paracavernous drainage (see also chap. 9.3.10). In another type of drainage, the SMCV runs around the deep portions of the temporal lobe, then along the floor of the middle temporal fossa, entering the transverse sinus. When the SMCV is absent, drainage mostly occurs via a large channel called the vein of Labbé, which is directed posteriorly toward the transverse sinus (Hacker 1968, 1974). The veins of the insula (Wolf and Huang 1963) drain into the deep middle cerebral vein (see Sect. 9.1.2.7) (Fig. 9.2).

9.1.1.3 Posteroinferior Group

The veins of this group drain the lower lateral surface and under surface of the temporo–occipital lobes. The majority of these veins enter the transverse sinus,

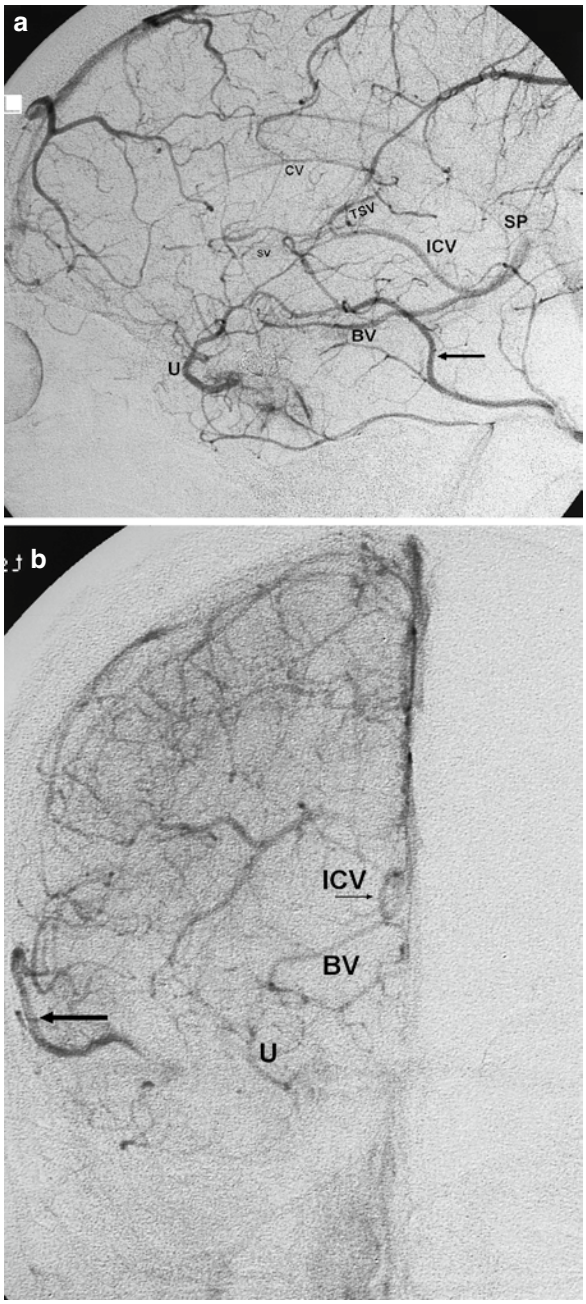

Fig. 9.7 AP and lateral angiogram, venous phase. Part of the anterior tributary of the basal vein (*BV*) drains anteriorly into the uncal vein (*U*), which ends in the cavernous sinus. Internal cerebral vein (*ICV*). There is a very long caudate vein (*CV*). Thalamostriate vein (*TSV*), small septal vein (*SV*), splenial vein (*SP*), basal vein (*BV*). There is no SMCV. The drainage of the temporal region is directed prevalently into the vein of Labbé (*arrow*) and into the large frontal and parietal veins

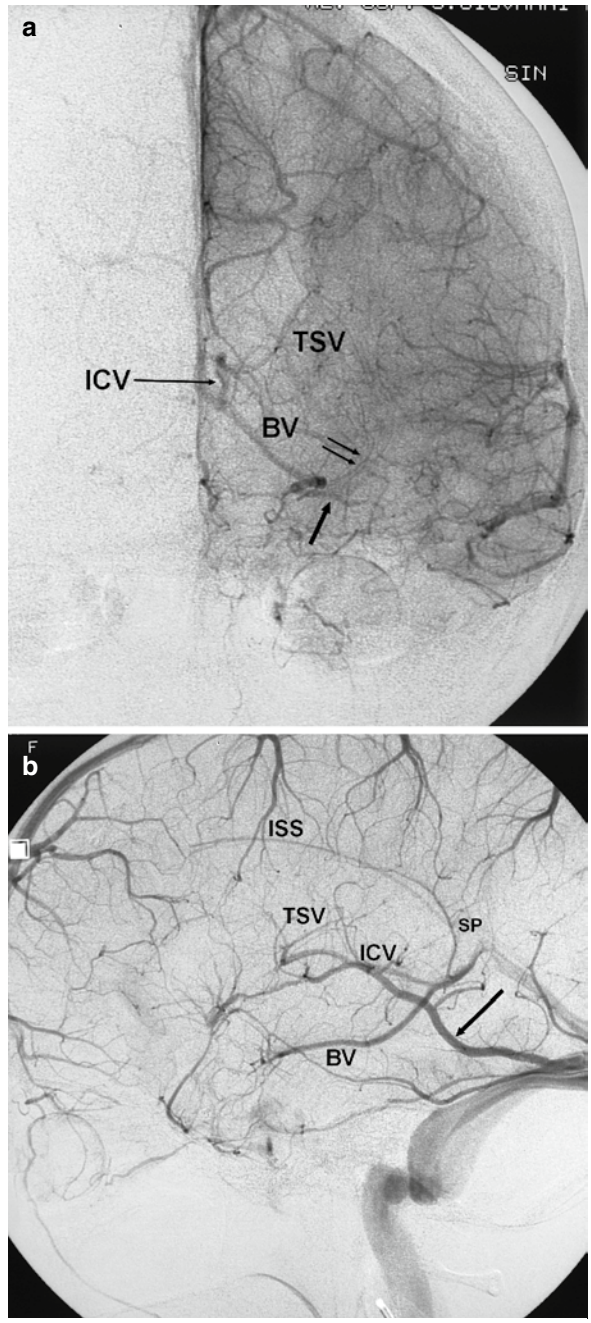

Fig. 9.8 Lateral (**b**) and AP (**a**) view of the carotid angiogram, venous phase. Basal vein (*BV*). In the AP view, its tributaries, represented by the deep middle cerebral vein (*arrow*) collecting the inferior striate veins (*double arrow*), are visible. There is a small superficial middle cerebral vein, while drainage of the temporal region occurs prevalently into the large temporal vein (*Labbé*) toward the TS (*large arrow* on lateral angiogram). Internal cerebral vein (*ICV*) collecting thalamostriate vein (*TSV*). Splenial vein (*SP*). Presence of the inferior sagittal sinus (*ISS*). The septal vein is not visible in this venous phase; it appears later. This angiographic finding is not rare. Indeed, the septal vein drains mainly the white matter and not the gray matter, and so its circulation time is prolonged

whereas those of the more medial part can drain into the basal vein. The main drainage is often represented by a large vein of Labbé. When a large vein of Labbé is present, the SCMV and the vein of Trolard can be absent or small or vice versa.

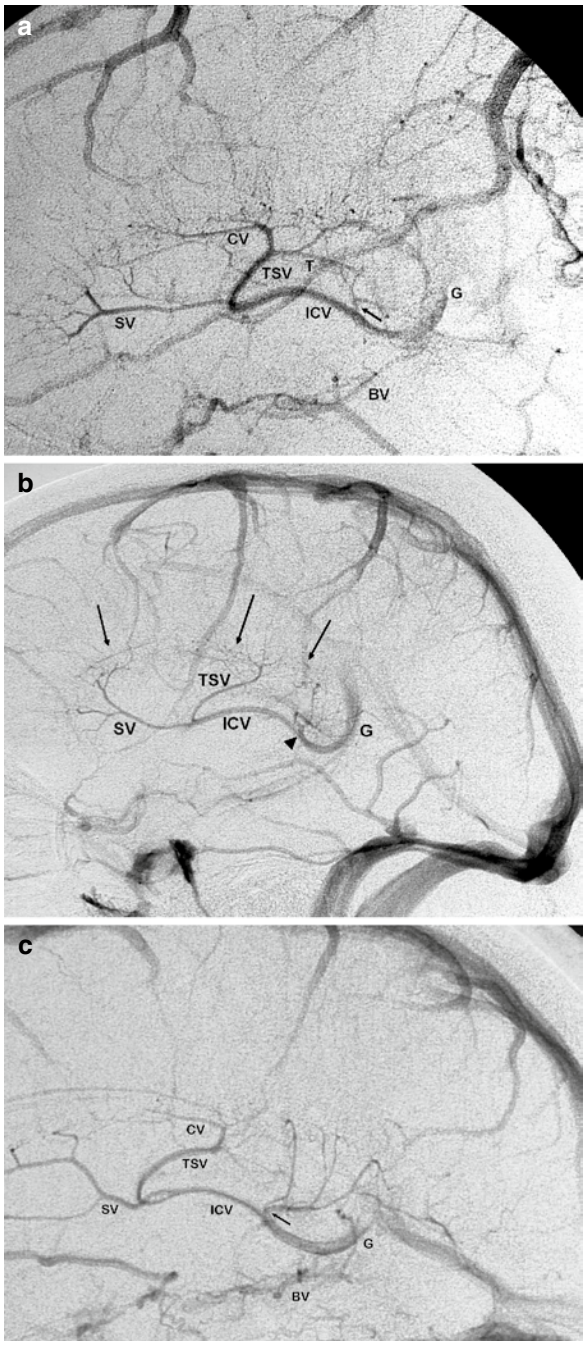

9.1.2 The Deep System

The deep system drains the blood centripetally from the deeper white matter, including that of the corpus callosum and internal capsule, and from the deep structures of the gray substance (basal ganglia, thalamus, septum pellucidum, fornix, and claustrum) into two main collectors: the internal cerebral vein and basal vein. To this system belong the medullary veins, the subependymal veins, the veins of the basal ganglia, the internal capsule, the claustrum, the thalamic veins, and the choroidal vein (Figs. 9.2, 9.3, and 9.5–9.9).

9.1.2.1 Medullary Veins

These veins originate in the deep white matter and run toward the lateral ventricle, where they enter the subependymal veins (Huang and Wolf 1964; Wolf and Huang 1964). The deep and superficial medullary vein can anastomose, forming a continuous venous channel that extends from the cortex to the subependymal veins (Schlesinger 1939; Kaplan 1959). On a lateral carotid angiogram, the medullary veins are frequently well visible as very fine vessels, which are directed centrally with an oblique or perpendicular course, before joining the subependymal veins (Figs. 9.3, 9.6, and 9.9).

9.1.2.2 Subependymal Veins

The subependymal veins derive their blood from the medullary veins and from the basal ganglia, septum pellucidum, fornix, and corpus callosum of each

Fig. 9.9 (**a**) Lateral angiogram, venous phase, magnification. The network corresponding to the deep medullary veins, draining in the subependymal veins, is well recognizable. Septal vein (*SV*). Thalamostriate veins (*TSV*) formed by the junction of the terminal vein (*T*) and caudate vein (*CV*). Medial atrial vein (*arrow*), to which converge many tributaries. Internal cerebral vein (*ICV*) continuing to the vein of Galen (*G*). Basal vein (*BV*). (**b**) Later angiogram, venous phase. Deep medullary veins (*arrows*) draining into the subependymal veins [SV, TSV, stem (*arrowhead*), to which converge the tributaries of the medial atrial vein]. Internal cerebral vein (*ICV*). (**c**) Lateral angiogram, late phase, showing better the deep venous system. Internal cerebral vein (*ICV*), to which converge the thalamostriate veins (*TSV*), caudate veins (*CV*), and medial atrial veins (*arrow*) with their tributaries. vein of Galen (*G*). Anomalous septal vein formed by two tributaries entering the *ICV* behind the foramen of Monro

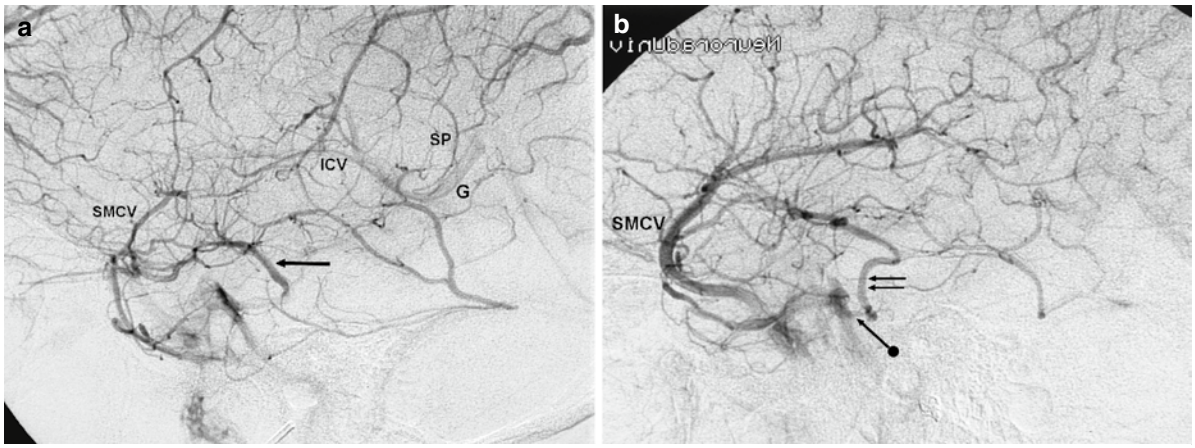

Fig. 9.10 Lateral carotid angiogram, venous phase (**a** and **b**). Two examples in which the anterior tributaries of the basal vein drain infratentorially into a lateral pontine vein (**a**, *arrow*) and into the anterior ponto-mesencephalic vein (**b**, *double arrow*). In both cases, the drainage is directed also partially anteriorly owing to a connection with *SMCV*, which drain typically into the CS (**b**) and paracavernous sinus (**a**). The basal vein is not really recognizable. Bridging vein (**b**, *arrow with dot*) between ponto-mesencephalic vein and cavernous sinus. Splenial vein (*SP*), internal cerebral vein (*ICV*), vein of Galen (*G*)

hemisphere (Wolf and Huang 1964; Salamon and Huang 1976). Some of these veins are relatively constant; the presence of others can be very variable. We describe the most typical.

The septal vein (SV, vein of the septum pellucidum) arises from several tributaries running to the anterior medial corner of the frontal horn; it then turns backward, continuing to the two sleeves of the septum pellucidum, joining the internal cerebral vein at the foramen of Monro. It can have an anomalous course (anomalous SV), running in the superior part of the septum pellucidum, turning then downward and reaching the internal cerebral vein behind the foramen of Monro.

The thalamostriate vein (TSV) is usually prominent among the subependymal veins. It is formed by the junction of the terminal vein, which runs beneath the stria terminalis between the thalamus and the body of the nucleus caudatus, and the caudate veins draining the nucleus caudatus. Among the caudate veins, the anterior caudate vein is frequently the larger. Sometimes, the caudate veins drain more posteriorly, reaching the internal cerebral vein directly through a vein called the direct lateral vein, which courses horizontally across the floor of the lateral ventricle. The TSV joints the internal cerebral vein together with the SV at the foramen of Monro or near to it (Salamon and Huang 1976). Despite its name, the TSV does not drain the thalamus (Giudicelli et al. 1970; Salamon and Huang 1976).

Among other subependymal veins, we briefly describe the atrial veins and inferior ventricular vein. The medial atrial veins (MAV) and lateral atrial veins (LAV) receive tributaries from the medial and lateral walls of the atrium and occipital horn. The tributaries of the MAV run anteriorly, converging to a stem, which enters the internal cerebral vein near the vein of Galen. The LAV is rarer. Its tributaries run more inferiorly, reaching the distal segment of the basal vein or inferior ventricular vein (IVV).

The IVV begins in the body of the lateral ventricle, accompanies the body and tail of the nucleus caudatus, and runs anteriorly in the roof of the temporal horn, forming an anterior concave curve. It exits to the choroid fissure, entering the basal vein. Several tributaries reach the vein, in particular those from the hippocampus and adjacent temporal areas.

9.1.2.3 Veins of the Basal Ganglia, Internal Capsule, and Claustrum

The superior part of these structures drains by the way of the superior striate veins into the subependymal veins (see Sect. 9.1.2). The inferior part drains into the

inferior striate veins, which run downward, pass through the anterior perforate space, reaching the deep portions of the sylvian fissure and the stem of the deep middle cerebral vein, which is a tributary of the basal vein (Wolf and Huang 1963; Salamon and Huang 1976). They are rarely recognizable on an angiogram (Fig. 9.8).

9.1.2.4 Thalamic Veins

These veins are divided into the superior, inferior, anterior, and posterior groups. The superior group has the largest draining vein, which runs first parallel to the internal cerebral vein, entering then its posterior part. The inferior group emerges at the posterior perforated substance, reaching the peduncular vein (tributary of the basal vein). The anterior group drains into the internal cerebral vein (ICV) near the foramen of Monro, the posterior group into the basal vein (Giudicelli et al. 1970; Salamon and Huang 1976) (Figs. 9.12 and 9.13). They are visible in the venous phase of the vertebral angiogram.

9.1.2.5 Choroidal Veins

The choroidal plexus is drained by the superior and inferior choroidal veins; their tributaries are, respectively, the ICV and the basal vein (BV) (Ben Amor et al. 1971; Salamon and Huang 1976). The superior and inferior choroidal veins belong to the subependymal veins, but they receive blood only from the choroidal plexus and are recognizable on an angiogram as a faint blush in the capillary phase.

9.1.2.6 Internal Cerebral Vein

The ICV is a paired venous channel, arising at the level of the foramen of Monro or near to it. It is located near the midline, where it runs in the tela choroidea on the roof of the third ventricle.

Each vein arises as a junction of the SV with the TSV and receives during its course several subependymal veins. Each ICV ends in the cistern of the quadrigeminal plate, below the splenium, where both veins unite and, together with both BV, enter the vein of Galen. The ICV is always recognizable on the lateral carotid angiogram owing to its typical S-shaped form and in the anteroposterior (AP) view owing to its paramedian position.

The ICV and some of its tributaries (SV, TSV) are a constant venous finding on a lateral angiogram. The other veins can only occasionally be identified with certainty. In the AP view, only the ICV is frequently recognizable (Figs. 9.5–9.8). Due to overlapping of several venous structures, certain identification of the other subependymal veins is very difficult and only occasionally possible. The situation is different when these veins are dilated, like in the drainage of vascular malformation (Figs. 12.8, 12.9, and 12.12).

9.1.2.7 Basal Vein (BV)

First described by Rosenthal (1824), the BV is an important, frequently large vein, collecting blood from the supratentorial and infratentorial veins. It is formed on the undersurface of the anterior perforated substance (APS) by the union of several veins. In most cases, the deep middle cerebral vein (DMCV) is the most important tributary, and so the BV appears as its direct continuation (Duvernoy 1975). The DMCV is formed by several veins running on the surface of the insula, directed inferiorly and anteriorly toward the pole of the insula. The stem of the DMCV runs further medially in the deep portions of the sylvian fissure, where it is joined by the inferior striate veins. At the level of the APS, the DMCV is connected with the other tributaries of the BV, which are the veins of the frontobasal region (olfactory and fronto-orbital veins) and the anterior cerebral vein. This latter receives blood from the rostrum and the genu of the corpus callosum by way of the anterior pericallosal vein, continuing to the vein of the lamina terminalis, which enters the anterior cerebral vein. Both the anterior cerebral veins are linked by the anterior communicating vein, running above the optic chiasma (Duvernoy 1975; Ono et al. 1984).

From its point of origin, the BV runs along the base of the brain, around the cerebral peduncle medially and the uncus laterally, forming an S-shaped curve.

The posterior cerebral artery lies inferiorly while the anterior choroidal artery crosses the BV superiorly from medial to lateral. In its more distal segment, the BV runs slightly upward along the posterior side of the thalamus to join the vein of Galen or the ICV.

The BV receives many tributaries; the most prominent from the proximal to the distal segment are the peduncular vein, the IVV, and the veins of the inferomedial temporal and medial occipital lobes. In addition, the lateral atrial vein drains in the BV directly or indirectly to the IVV. The peduncular veins run in the interpeduncular fossa, draining the inferior thalamic tributaries and joining the BV. Both peduncular veins can be connected to each other by a small posterior communicating vein (Duvernoy 1975; Salamon and Huang 1976). The IVV has already been described. Another vein that can be connected with the BV is the lateral mesencephalic vein, which runs in the lateral mesencephalic sulcus and can be also connected with the petrosal vein, in which case it forms an anastomosis between the supratentorial and infratentorial venous sectors (Wolf et al. 1963; Bradac 1970; Wackenheim and Braun 1970; Salamon and Huang 1976).

Many variants have been described (Padget 1957; Bekov 1965; Babin 1971; Duvernoy 1975; Salamon and Huang 1976): one is represented by the posterior mesencephalic vein, which arises from the mesencephalon and runs to the vein of Galen. It can replace the BV or may be present in addition to it. In the latter case, Duvernoy (1975) proposed that it be called the accessory basilar vein. The distal segments of the BV can be absent, and so the proximal segments drain infratentorially through the lateral mesencephalic vein into the petrosal vein. The first segment does not anastomose with the more distal segment. In this case, the first tributaries, mainly the DMCV and frontal veins, join to form a common trunk (uncal vein), which usually drains into the cavernous or paracavernous sinus. A complementary connection with the SMCV can coexist with a drainage directed into the cavernous or paracavernous sinus, which is associated with a drainage into the vein of Galen. Rarely, the BV can drain posteriorly into the transverse or straight sinus (SS) after a short course within the tentorium (Johanson 1954; Padget 1956; Wolf et al. 1963; Duvernoy 1975).

On an angiogram, the BV is well recognizable in the lateral view as a venous channel, forming a slight upwardly concave curve in its course to the vein of Galen. In the AP view, the main trunk forms a small curve corresponding to the peduncular vein before showing a straight, medially directed course toward the vein of Galen. The presence and recognition of its tributaries are irregular.

In contrast to some subependymal veins (ICV, SV, and TSV), which are always recognizable with a typical pattern, the BV, in its normal course is not always present owing to the above-described variants. The BV and the posterior mesencephalic vein can have the same pattern on an angiogram. Furthermore, the same vessel may be differently filled depending on the injection of its tributaries, which can differ on carotid and vertebral angiograms. Despite this, we believe that in routine daily work, it is acceptable to define the vein visible on the carotid angiogram as the BV, since it drains blood from the supratentorial area, while the vessel visible on the vertebral angiogram is the posterior mesencephalic vein, draining blood from the infratentorial area (Figs. 9.2–9.4, 9.6–9.10).

9.1.2.8 Vein of Galen

The vein of Galen is a unique trunk running in the cistern, which takes its name, around the splenium, from the curve it adopts, which has a downward convexity. The vein of Galen ends in the SS.

9.2 Infratentorial Cerebral Veins (Veins of the Posterior Fossa)

Owing to the irregularity in the development and course of the veins of the posterior fossa and the frequent overlapping, it is difficult or impossible to identify all these venous channels in a given case. Some patterns, however, permit recognition on a venous angiogram of many of these veins. Three major venous drainage groups can be considered: the superior or Galen group, draining into the vein of Galen; the anterior or petrosal group, draining into the petrosal vein; and the posterior group – tentorial, draining into the transverse, and SS directly or indirectly through the tentorial sinus (Huang and Wolf 1965; Huang et al.

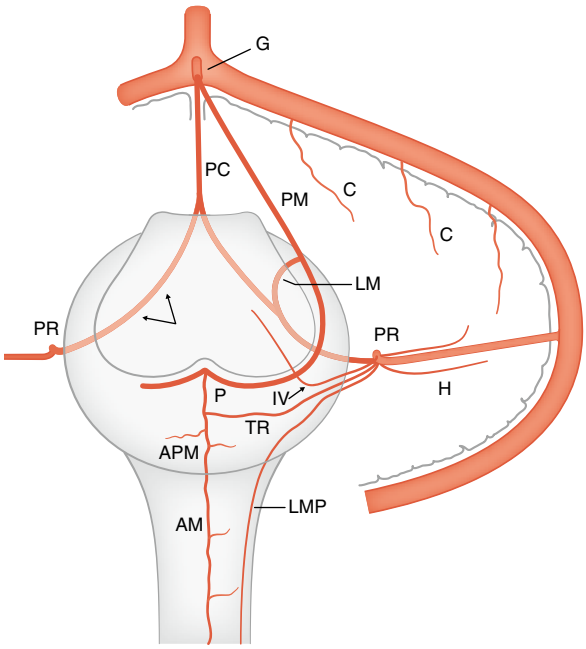

APM	Antero-ponto-mesencephalic vein
LM	Latero-mesencephalic vein
PM	Posterior mesencephalic vein
AM	Anterior medullary vein
LMP	Latero medullo-pontine vein
P	Peduncular vein
TR	Transverse pontine vein
PC	Precentral vein
⩘	Brachial vein
IV →	Vein of lateral recess of the IV ventricle
G	Galen vein
PR	Petrosal vein draining in the superior petrosal sinus
C	Hemispheric cerebellar veins
H	Vein of the horizontal cerebellar fissure

Fig. 9.11 Posterior fossa veins seen in the AP view

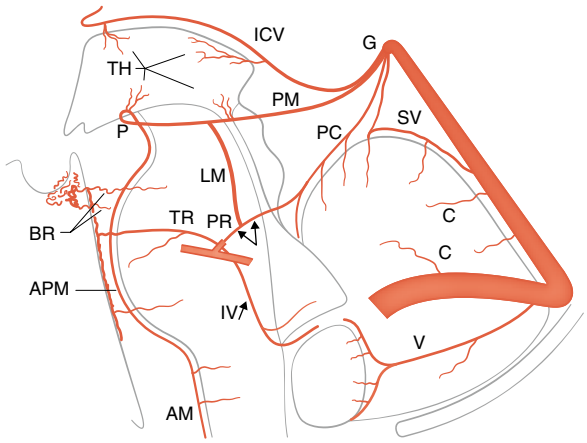

APM	Antero-ponto-mesencephalic vein
LM	Latero-mesencephalic vein
PM	Posterior mesencephalic vein
AM	Anterior medullary vein
P	Peduncular vein
TR	Transverse pontine vein
PC	Precentral vein
⩘	Brachial vein
TH	Thalamic veins
ICV	Internal cerebral vein
G	Galen vein
PR	Petrosal vein (→) draining in the superior petrosal sinus
BR	Bridging veins
SV	Superior vermian vein
IV	Vein of lateral recess of the IV ventricle
C	Hemispheric cerebellar veins
V	Inferior vermian vein

Fig. 9.12 Lateral view of the posterior fossa veins

1968, 1969; Bradac et al. 1967; Rosa and Viale 1970; Salamon and Huang 1976; Wackenheim and Braun 1978; Matsushima et al. 1983) (Figs. 9.11–9.15).

9.2.1 Superior Group

This group includes many venous channels partially draining superiorly into the vein of Galen and partially into the petrosal vein, which belongs to the anterior group. The veins of this group are the ponto-mesencephalic, medullary, precentral, and superior vermian veins (Bradac 1970; Bradac et al. 1971; Huang and Wolf 1965; Tournade 1972; Duvernoy 1975; Salamon and Huang 1976).

The anterior ponto-mesencephalic vein (APM) is a longitudinal venous channel, running on the anterior surface of the pons in or adjacent to the midline. Superiorly, it is often connected through the peduncular vein with the BV or posterior mesencephalic vein. For the relationship of these venous channels, see Sect. 9.1.2.7. On a lateral angiogram, the anterior profile of the pons and medulla is well defined. Sometimes, the APM is more laterally located, and so a precise morphological definition of these structures cannot be achieved. The APM is connected caudally with the anterior medullary (AM) vein, which runs on the anterior surface of the medulla, continuing caudally into the anterior spinal vein. As described in Sect. 9.3.10, bridging veins frequently connect the cavernous sinus with the APM.

In addition to the anteromedial channel, there is another longitudinally running vein or group of small

veins more laterally located, forming the so-called lateral medullo-pontine vein (Tournade 1972; Duvernoy 1975). This venous channel runs posteriorly to the inferior olive, reaching the lateral surface of the pons, joining cranially the anterior cerebellar vein (vein of the horizontal cerebellar fissure) tributary of the petrosal vein.

The APM is connected at the level of the pons through transversely running veins (transverse pontine veins) with the petrosal vein. At the level of the medulla, the AM is connected through transverse veins (transverse medullary veins) with the lateral medullary vein, which is the inferior segment of the lateral medullo-pontine vein. This latter drainage is especially developed when the junction between the APM and AM at the level of the foramen cecum is absent (Duvernoy 1975). Finally, connections through the lateral medullary vein and sigmoid sinus can occur.

The lateral medullary vein also collects blood from the posterior median vein of the medulla. This is a venous channel running on the posterior surface of the medulla, continuing to the posterior spinal vein. Cranially, it leaves the median position and takes a lateral course, lining the fourth ventricle and finally joining the lateral medullary vein.

The lateral mesencephalic vein runs in the lateral mesencephalic sulcus, draining superiorly into the BV or into the posterior mesencephalic vein (PM), or draining inferiorly into the petrosal vein through the brachial veins. Both connections can be present, and so the vein becomes an anastomotic channel, connecting supra- and infratentorial venous sectors. It is well recognizable

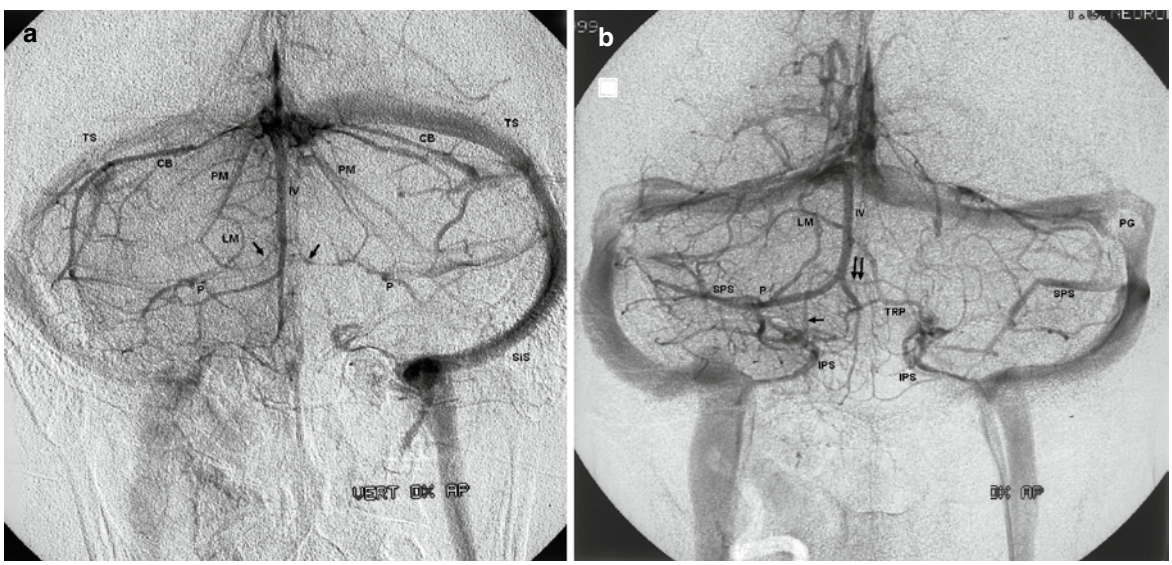

Fig. 9.13 Vertebral angiograms, venous phase. (**a**) AP view: peduncular veins (*arrow*) continuing to the posterior mesencephalic vein (*PM*). On the right, there is a lateral mesencephalic vein (*LM*), connected superiorly with the *PM* and inferiorly with the petrosal vein (*P*) through the brachial vein. Inferior vermian vein (*IV*) with its tonsillar tributaries. Hemispheric cerebellar vein (*CB*) draining into the *TS*, some after a short transtentorial course. Signoid sinus (*SiS*) continuing to the jugular vein. (**b**) AP view: on the right, *LM* connecting PM with the petrosal vein (*P*). Inferior vermian vein (*IV*). Hemispheric cerebellar veins draining into the TS. Vein of the lateral recess of *IV* ventricle (*arrow*) connected through a transverse vein (*double arrow*) to that of the other side. Larger transverse pontine vein (*TRP*) entering the petrosal vein. Superior petrosal sinus (*SpS*), inferior petrosal sinus (*IpS*), TS with pacchionian granulation (*PG*). (**c**) Lateral view corresponding to the AP view in (**b**). Anterior ponto-mesencephalic vein (*APM*) draining predominantly inferiorly into the petrosal vein (P) via the transverse pontine vein. Bridging veins toward the CS and IPS (*arrow with dot*). Posterior mesencephalic vein (*PM*), lateral mesencephalic vein (*LM*), vein of Galen (*G*), straight sinus (*SS*). Inferior vermian vein (*IV*), joined also by a hemispheric branch. Retrotonsillar tributaries (*bidirectional arrow*), vein of the lateral recess of IV ventricle (*arrow*), occipital veins (*bidirectional arrow with dot*), precentral vein (*PR*). (**d**) AP view. *Right LM* connecting *PM* with petrosal vein (*P*) through brachial vein (*BR*). Inferior vermian vein. Hemispheric cerebellar vein. (**e**) Lateral angiogram corresponding to the AP view in D. *LM* connecting *PM* with the petrosal vein (*P*) through the brachial vein (*BR*). Precentral vein (*arrow*). Inferior vermian vein with its retrotonsillar tributaries (*bidirectional arrow*). Faint injection of APM. Vein recessi *IV* ventricle (*Double arrow*). (**f**) Magnified detail of C, showing the superior choroidal vein (*CH*) and thalamic veins (*arrows*) draining into the peduncular, posterior mesencephalic vein and into the internal cerebral vein (*ICV*)

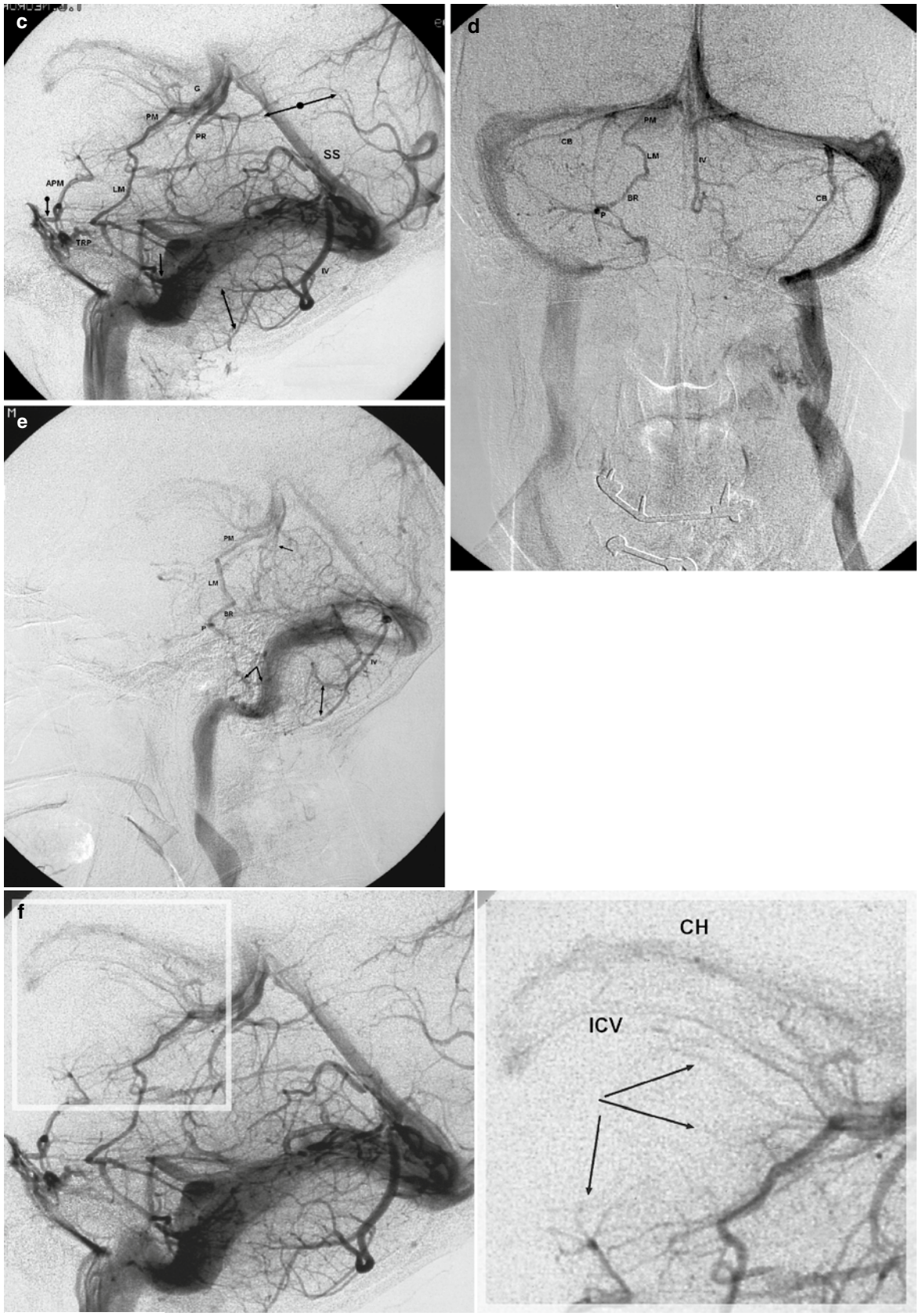

Fig. 9.13 (continued)

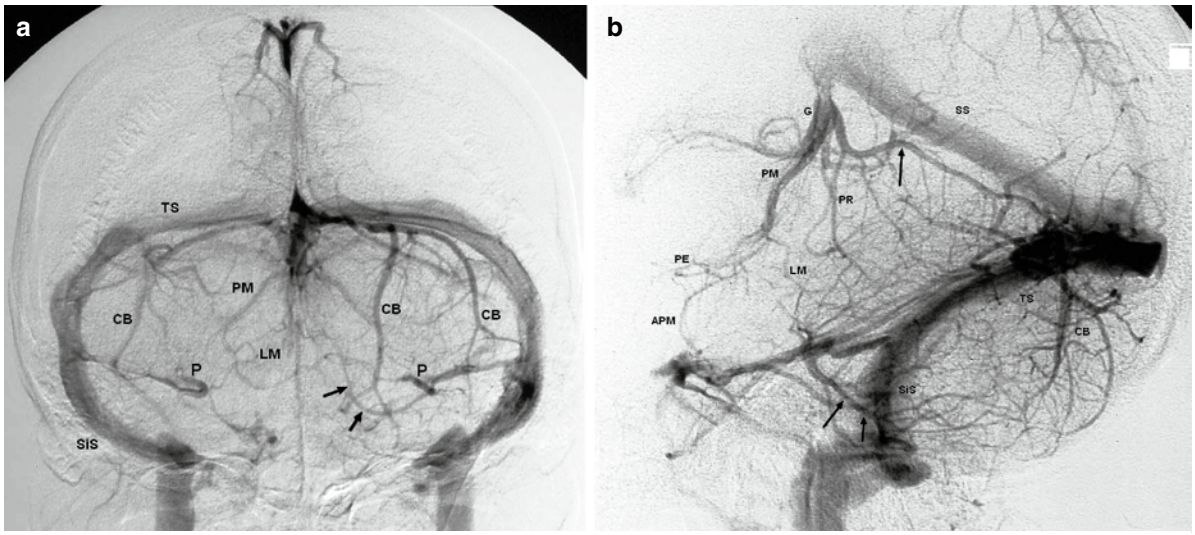

Fig. 9.14 (**a**) AP view. Small lateral mesencephalic vein (*LM*) on the *right*, connecting the posterior mesencephalic vein (*PM*) with the petrosal vein (*P*) draining into the superior petrosal sinus. Hemispheric cerebellar veins (*CB*) draining into the *TS*. Sigmoid sinus continuing to the jugular vein. Vein of the lateral recess of IV ventricle (*double arrow*). The typical inferior vermis vein is not recognizable. Its drainage is probably replaced partially by the hemispheric cerebellar vein and partially by the vein of the lateral recess. (**b**) Lateral angiogram corresponding to the AP view in (**a**). Small LM. Anterior ponto-mesencephalic vein (*APM*) connected through the peduncular vein (*PE*) with the PM. Precentral vein (*PR*), superior vermian vein (*arrow*), hemispheric cerebellar vein (*CB*), vein of the lateral recess of IV ventricle (*double arrow*), vein of Galen (*G*), straight sinus (*SS*), transverse sinus (*TS*), sigmoid sinus (*SiS*)

on a lateral angiogram, in particular the segment running in the sulcus mesencephalic. In the AP view, it forms a convex curve medially to the BA or PM, running downward and lateral to the petrosal vein.

The precentral vein (PC) is a single midline vessel, originating in the precentral cerebellar fissure between the lingula and central lobule by the junction of two to three branches called the brachial veins since they cross the brachium pontis and brachium conjunctivum. The brachial veins are connected downward with the petrosal vein. The PC runs upward, entering the vein of Galen.

The superior vermian vein (SV) can be a single large trunk or be represented by several smaller branches, which run median or paramedian over the culmen with a superior anterior course. Further, they form a curve directed upward to join the precentral or vein of Galen. The PC and SV are well defined on a lateral angiogram, the superior border of the superior vermis.

9.2.2 Anterior Petrosal Group

This group consists of several tributaries converging on a single trunk represented by the petrosal vein, which enters the superior petrosal sinus above the internal auditory meatus (Huang et al. 1968; Bull and Kozlowski 1970; Duvernoy 1975; Naidich et al. 1976; Salamon and Huang 1976). The petrosal vein is a large, but very short (a few millimeters), venous channel, located in the cerebellopontine angle, running in close relationship with the trigeminal nerve. Tributaries of the petrosal vein are the APM via the transverse pontine veins and the lateral mesencephalic and precentral veins. The latter are connected with the petrosal vein by way of the brachial veins. These can be identified in the AP view as an inverted V when they are bilaterally injected. On a lateral angiogram, the brachial tributaries can be recognized as a channel directed downward and forward, joining the petrosal vein.

Other veins of this group are the anterior cerebellar hemispheric veins and the veins of the lateral recess of the IV ventricle, both draining into the petrosal vein. The vein of the lateral recess receives several tributaries, in particular from the flocculus and tonsilla. It runs first inferiorly and anteriorly, then turns superiorly to reach the petrosal vein. Sometimes, it is well recognizable in an AP lateral angiogram owing to its typical course. The anterior cerebellar hemispheric veins comprise the superior and inferior hemispheric veins,

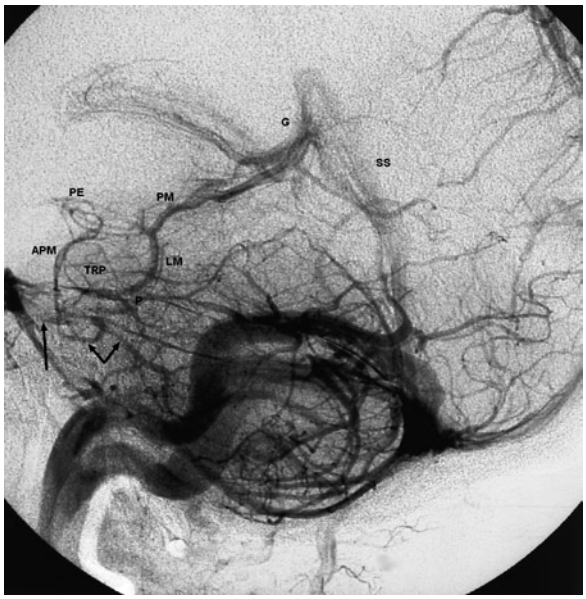

Fig. 9.15 Lateral angiogram. Anterior ponto-mesencephalic vein (*APM*) connected with the posterior mesencephalic vein (*PM*) through the peduncular veins (*PE*) and inferiorly with the petrosal vein (*P*) through transverse pontine veins (*TRP*). Bridging veins with CS and IPS (*arrow*). *LM* connecting *PM* with petrosal vein (*P*). Lateral anterior ponto-medullary vein, connected through the transverse vein with the anterior ponto-mesencephalic vein (*arrow with angle*). Vein of Galen (*G*), straight sinus (*SS*) with slightly undulating course. The inferior vermian vein is not identifiable owing to overlap with the cerebellar hemispheric vein

draining mainly into the vein of the great horizontal fissure (anterior cerebellar vein), which joins the petrosal vein.

9.2.3 Posterior Tentorial Group

The most important vein is the inferior vermian vein. It is formed by the union of the superior and inferior retrotonsillar tributaries, localized behind the cerebellar tonsil. The inferior vermian vein is a paired vein, running posterosuperiorly in the inferior paramedian vermis sulcus, entering the straight or transverse sinus, sometimes after a short course within the tentorium. On a lateral angiogram, the vein is recognizable by its typical course at a variable distance from the occipital bone. In the AP view, it has a median-paramedian localization. The vein of the posterior part of the cerebellar hemisphere runs back to the transverse sinus, directly or indirectly, through the tentorium (Huang et al. 1969; Salamon and Huang 1976).

9.3 Dural Sinuses

The cranial sinuses are venous channels lying in the dura, enclosed between its external (periosteal) and internal (meningeal) layers. The wall has endothelial lining and no musculature. There is no valve inside, but frequently there are fibrous trabiculae crossing the sinus. Arachnoid villi (pacchionian granulations), sometimes very large, project into the sinus, especially in the parietal part of the SSS, but also in the SS and transverse sinus (TS). The dural sinuses collect blood from superficial and deep cerebral veins and from the meninges through the meningeal veins, which accompany the respective meningeal arteries. The dural sinuses are also connected with the diploic veins and through emissary veins communicate with the extracranial venous system (see Sects. 10.7 and 10.8). The main drainage occurs bilaterally in the jugular vein.

9.3.1 Superior Sagittal Sinus (SSS)

The SSS arises anteriorly at the junction of the falx cerebri, with the dura lining the inner table of the calvarium. At this level, the SSS communicates with veins of the nasal cavity and with the facial vein. It extends on the midline posteriorly, following the calvarium, forming a typical upward convex curve, and ends in the torcular herophili. The SSS is very small, sometimes absent anteriorly, while it increases progressively in caliber in this medial posterior portion. Several variants are possible (Hacker 1974). It can occasionally drain predominantly or only more laterally into one of the TS. In such cases, one of the TS can be hypo/aplastic. The SSS can divide into separate segments proximal to the torcular herophili, draining each segment into the corresponding TS. A small horizontal venous channel can be present and unite more distally the two segments. Otherwise, the distal SSS and torcular herophili form a complex network of small channels continuing in the TS. This is always well recognizable in AP and lateral angiograms. The flow in the SSS is laminar, and so on a carotid angiogram it can sometimes appear smaller, since the other part depends on the other carotid sector (Figs. 9.1, 9.4–9.6 and 9.16).

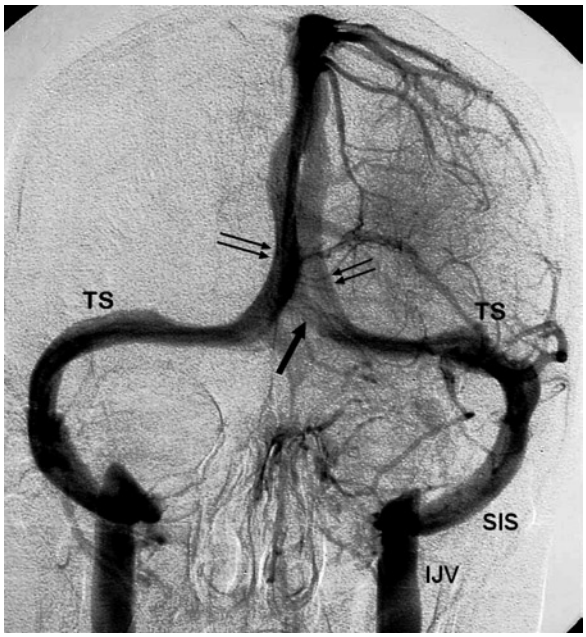

Fig. 9.16 Carotid angiogram, AP view, late venous phase. The SSS (*double arrow*) divides at the torcular herophili in two channels, each draining into the *right* and *left TS*. A complementary dural channel (*arrow*) links both sinuses

9.3.2 Inferior Sagittal Sinus (ISS)

The inferior sagittal sinus (ISS) is a relatively small channel, running within the inferior free margin of the falx cerebri. It begins in the anterior middle part of the falx above the anterior part of the body of the corpus callosum. The ISS becomes larger in its course posteriorly. It ends in the falcotentorial apex, joining the vein of Galen, which enters the SS. The ISS is not always visible on an angiogram (Fig. 9.8).

9.3.3 Straight Sinus (SS)

The SS is formed by the confluence of the vein of Galen and the ISS. Occasionally, the BV drains directly into it. The SS lies on the midline, at the junction of the falx cerebri with the tentorium cerebelli; it runs downward and backward, entering the torcular herophili. It occasionally receives venous channels running in the tentorium. It can be a double or tripled structure and enters laterally into one TS. Since it drains blood from the cerebral hemispheres and also from the posterior fossa, it can be only partially filled and may give a false image of a small sinus when only a carotid or vertebral angiogram is performed (Figs. 9.1, 9.3, 9.4, 9.6, 9.11–9.13 and 9.15).

9.3.4 Occipital Sinus (OS), Marginal Sinus (MS)

This is a small channel, exceptionally sometimes very large, running on the midline from the torcular herophili, with which it is connected at its posterosuperior end. It extends anteriorly to the posterior margin of the foramen magnum, ending in the jugular vein. Medially, it communicates with the marginal sinus, which is a small venous channel that bilaterally surrounds the foramen magnum. The marginal sinus is connected anteriorly with the clival plexus and the jugular bulb, and anteroinferiorly it is connected with the anterior internal vertebral plexus (McDougall et al. 1997) (Figs. 9.4 and 9.17).

9.3.5 Transverse Sinus (TS)

Also called the lateral sinus, the TS is contained within two layers of the tentorium when it is connected with the dura of the calvarium. The TS begins at the internal occipital protuberance at the torcular herophili, and it runs laterally and slightly anteriorly along the groove of the squamous portion of the occipital bone. It then turns downward and medially, leaving the tentorium and becoming the sigmoid sinus. The two TS are frequently asymmetric, that of the right being larger. The proximal part of the TS can be hypo/aplastic (Kaplan et al. 1973; Hacker 1974), its distal part being frequently injected by the large vein of Labbé. As with the SS, a precise morphological image of the sinus can be obtained in many cases only when both carotid and vertebral angiograms are performed (Figs. 9.1, 9.4–9.6, 9.13, 9.14, and 9.16).

9.3.6 Sigmoid Sinus (SiSs)

This is the direct continuation of the TS. The sigmoid sinus curves inferiorly and medially behind the inferior part of the petrous temporal bone, reaching the

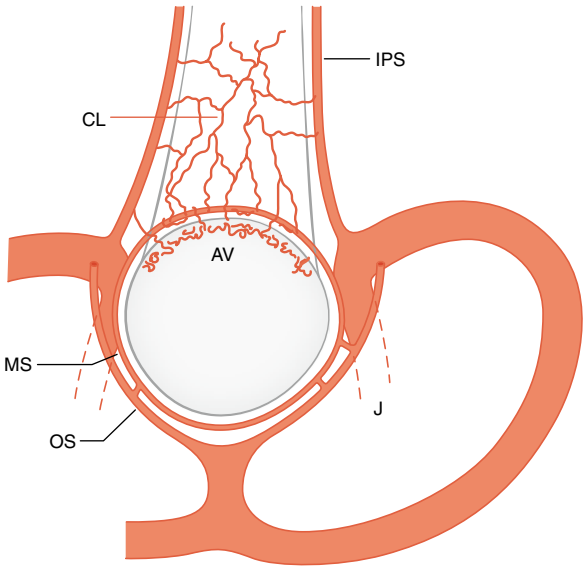

MS	Marginal sinus, with its connections with CL, AV and OS
OS	Occipital sinus, draining in the jugular bulb
IPS	Inferior petrosal sinus
J	Internal jugular vein
CL	Venous plexus of the clivus
AV	Anterior epidural vertebral venous plexus

Fig. 9.17 The marginal and occipital sinuses and tributaries. The marginal sinus (*MS*) circling the foramen magnum connected anterosuperiorly with the venous plexus of the clivus (*CL*), anteroinferiorly with the anterior epidural vertebral venous plexus (*AV*), and posteriorly with the occipital sinus (*OS*). The latter drains anteriorly into the jugular bulb or sigmoid sinus. The inferior petrosal sinus (*IPS*) is connected with the clival venous plexus and through the anterior condylar vein (*ACV*) with the anterior epidural vertebral plexus (*AV*) and jugular vein (*J*)

jugular foramen, where it ends in the jugular vein. The first segment of the jugular vein (jugular bulb) bulges upward in a rounded fossa of the temporal bone, below the internal auditory canal. The bulb is usually larger on the right, since the transverse sigmoid sinus is larger on this side (Hacker 1974; Katsuta et al. 1997) (Figs. 9.13, 9.14, and 9.16).

9.3.7 Superior Petrosal Sinus (SPS)

The superior petrosal sinus (SPS) is a small channel lying within the attachment of the tentorium to the superior border of the petrous bone. It extends laterally, connecting with the TS, where this continues in the sigmoid sinus, to medially, where it enters the posterior part of the cavernous sinus. The most important tributary of the SPS is the petrosal vein (Figs. 9.11–9.14 and 9.19–9.21).

9.3.8 Inferior Petrosal Sinus (IPS)

The inferior petrosal sinus (IPS) lies in the groove between the petrous temporal bone and the clivus. It begins in the posterior part of the cavernous sinus, runs inferiorly and slightly laterally to join the jugular vein. Many reports have been devoted to the

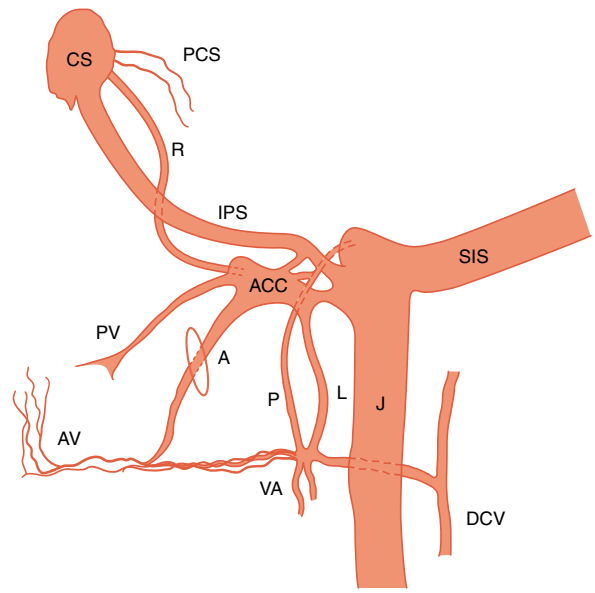

ACC	Anterior condylar confluence
A	Anterior condylar vein running through the hypoglossal canal reaching the AV
L	Lateral condylar vein connecting ACC with the VA
P	Posterior condylar vein connecting jugular bulb with the VA and the DCV
IPS	Inferior petrosal sinus
CS	Cavernous sinus
PCS	Paracavernous sinus
R	Rektorzik plexus
J	Jugular vein
SIS	Sigmoid sinus
AV	Anterior epidural vertebral plexus with some connection with the clival venous plexus
VA	Vertebral artery venous plexus
PV	Prevertebral venous plexus
DCV	Deep cervical vein

Fig. 9.18 Venous drainage in the craniocervical region considering especially the anterior condylar confluence and its connections, AP view. Anterior condylar confluence (*ACC*), anterior condylar vein running through the hypoglossal canal, reaching the *AV* (*A*), lateral condylar vein connecting the *ACC* with the *VA* (*L*), posterior condylar vein connecting jugular bulb with the *VA* and the *DCV* (*P*), inferior petrosal sinus (*IPS*), cavernous sinus (*CS*), paracavernous sinus (*PCS*), Rektorzik plexus (*R*), jugular vein (*J*), sigmoid sinus (*SIS*), anterior epidural vertebral plexus with some connection with the clival venous plexus (*AV*), vertebral artery venous plexus (*VA*), prevertebral venous plexus (*PV*), deep cervical vein (*DCV*) (Modified from San Millar Ruiz)

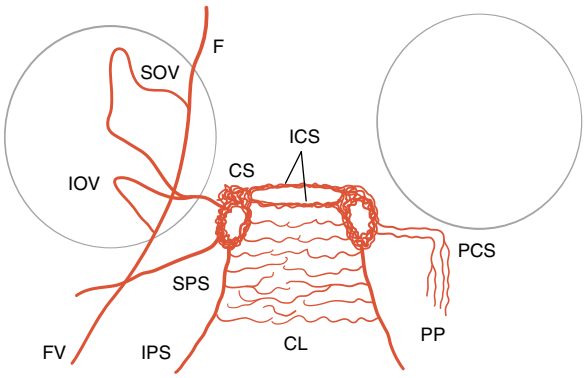

ICS	Intercavernous anastomosis	CL	Clival venous plexus
CS	Cavernous sinus	SOV	Superior ophthalmic vein
PCS	Paracavernous sinus	IOV	Inferior ophthalmic vein
PP	Pterigoid plexus	FV	Facial vein
SPS	Superior petrosal sinus	F	Frontal vein
IPS	Inferior petrosal sinus		

Fig. 9.19 Cavernous sinus and its tributaries, region seen in AP view

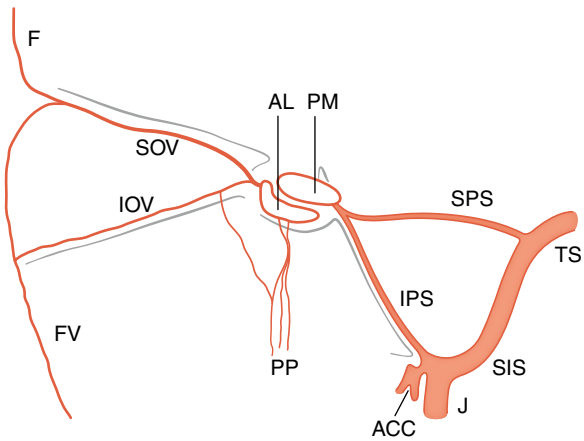

PP	Pterigoid plexus
AL-PM	Anterolateral-posteromedial segment of CS
SPS	Superior petrosal sinus
IPS	Inferior petrosal sinus
SOV	Superior ophthalmic vein
IOV	Inferior ophthalmic vein
FV	Facial vein
F	Frontal vein
ACC	Anterior condylar confluence
J	Internal jugular vein
TS	Transvers sinus
SIS	Sygmoid sinus

Fig. 9.20 Lateral view of cavernous sinus and its tributaries

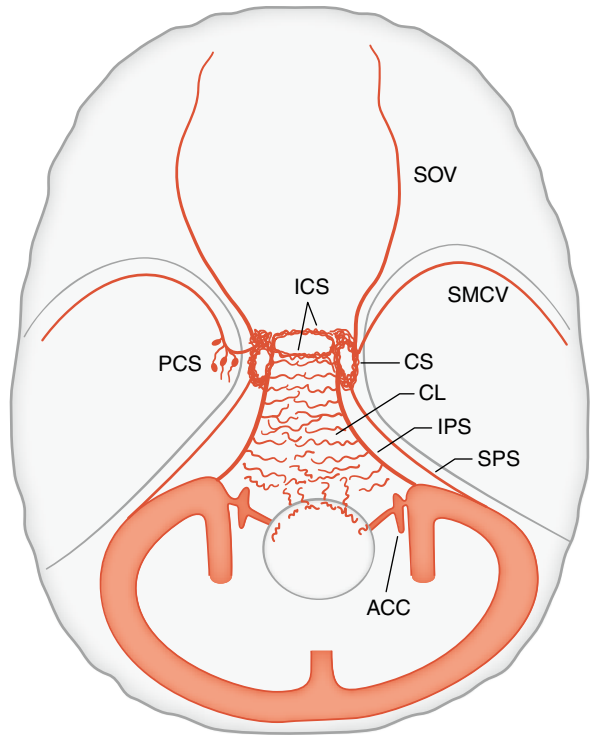

ICS	Intercavernous anastomosis
CS	Cavernous sinus
PCS	Paracavernous sinus
SPS	Superior petrosal sinus
IPS	Inferior petrosal sinus
CL	Clival venous plexus
SMCV	Superficial middle cerebral vein draining in the CS on the right and in the PCS on the left
SOV	Superior ophthalmic vein
ACC	Anterior condylar confluence

Fig. 9.21 Cavernous sinus and its tributaries seen from above

anatomy around the jugular foramen, considering especially the relationship of the drainage of the IPS into the jugular vein (Shiu et al. 1968; Miller et al. 1993; Gailloud et al. 1997; Benndorf and Campi 2002; Calzolari 2002; Mitsuhashi et al. 2007). These studies have shown that the IPS is commonly represented by a unique channel, but occasionally it consists of a plexus of veins. It usually enters the jugular bulb, but it can also extend extracranially, joining the jugular vein 3–4 cm below the base of the skull. It can occasionally drain into the anterior condylar confluence and further into the anterior condylar vein, thereby having no connection with the jugular vein. Finally, in extremely rare cases, the IPS can be absent. The IPS can be identified on carotid or vertebral angiograms or by selective catheterization (Figs. 9.4, 9.5 and 9.17–9.22).

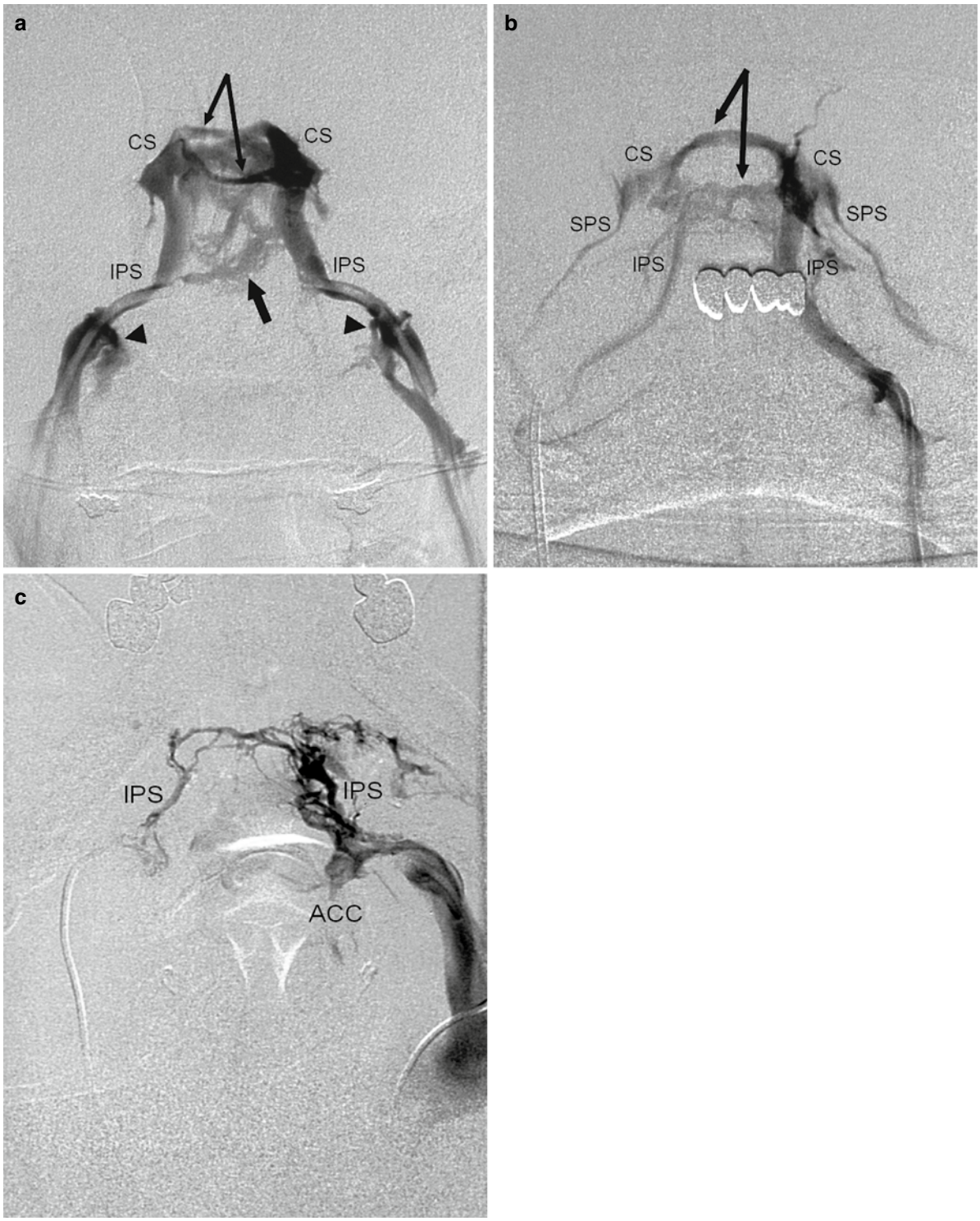

Fig. 9.22 Selective catheterization of the inferior petrosal sinus. (**a**) Catheter in both IPS. Cavernous sinus (*CS*). Connection between both cavernous sinuses (coronary sinus, *arrow with angle*). Clival venous plexus (*arrow*). Anterior condylar confluence (*arrowhead*). Filling also of the lateral condylar vein, better visible on the *left*. (**b**) Injection in the *left IPS* with retrograde injection also of the right *IPS*. Cavernous sinus (*CS*), superior petrosal sinus (*SPS*). Connections between the cavernous sinuses (*arrow with angle*). (**c**) The injection in the *IPS* shows that it consists of a network of veins. Partial retrograde injection in the contralateral *IPS*. Anterior condylar confluence (*ACC*)

All these studies are very useful; however, they do not give a full description of several venous channels present in this area that were precisely identified in the reports of Katsuta et al. (1997) and San Millan Ruiz et al. (2002) on the basis of anatomical and magnetic resonance imaging (MRI) examinations. These authors describe the almost constant presence of a venous pouch called the anterior condylar confluence (ACC), which was described by Trolard in 1868. It is located extracranially, medially to the jugular vein, in front of the hypoglossal canal, slightly caudal to the junction of the IPS with the jugular bulb. The ACC is formed by the confluence of several venous channels: the anterior, lateral, and posterior condylar veins; small anastomoses with the IPS and jugular bulb; connection of the prevertebral venous plexus and of the internal carotid artery venous plexus, also called the plexus of Rektorzik or petro-occipital venous plexus (Figs. 9.18–9.21).

The anterior condylar veins pass through the hypoglossal canal, reaching the anterior internal vertebral plexus (AV). This is an epidural venous network, connected cranially with the clival plexus and marginal sinus, and laterally with the venous plexus surrounding the vertebral artery (VA). The lateral condylar vein connects the ACC with the VA and further with the AV. The posterior condylar vein passes through the posterior condylar foramen, located behind the occipital condyle. It connects the jugular bulb with the VA medially and the deep cervical vein posteriorly. The posterior condylar vein is also connected with the ACC. The petro-occipital venous plexus runs extracranially along the petro-occipital suture, connecting the ACC with the ICA venous plexus and cavernous sinus.

All these venous channels should be taken into consideration since the IPS is an important way in the cavernous sinus sampling for the diagnosis of pituitary adenoma. In this context, it should be mentioned that in the catheterization of the IPS, a frequent occurrence is that the catheter erroneously enters the ACC. The IPS is also often used in the endovascular treatment of cavernous sinus fistulae. Further, knowledge of the various venous channels present in this area is useful in the endovascular treatment of dural fistulae, involving the venous drainage of the cervicocranial region (Ernst et al. 1999; Miyachi et al. 2008; Abiko et al. 2008), and of direct fistulae involving the VA (see Chap. 14). Finally, as already reported by some authors (Valdueza et al. 2000; San Millan Ruiz et al. 2002), it should be mentioned that through these connections, venous drainage of the brain can change with a flow directed prevalently in the jugular vein, in the supine position of the body, or in the AV and VA in the upright position.

9.3.9 Sphenoparietal Sinus (SpS)

The sphenoparietal sinus (SpS) courses medially along the surface of the lesser wing of the sphenoid, being formed by the junction of the anterior meningeal vein with the SMCV. It can drain into the cavernous sinus or into the pterygoid plexus via the emissary veins passing through the foramina of the base of the skull, especially through the foramen ovale (paracavernous drainage). The SpS can also run along the middle cranial fossa, draining posteriorly into the TS.

9.3.10 Cavernous Sinus (CS)

The cavernous sinus (CS) is a paired structure lying adjacent to either side of the body of the sphenoid bone (Figs. 9.18–9.21). It originates in a division of the dura in two layers: one medial (periosteal), adherent to the periosteum of the sphenoid; and one lateral, forming the medial wall of the middle cranial fossa. The lateral layer also forms the roof of the sinus, continuing medially into the diaphragma sellae. The resulting space has been called the space of the CS (Taptas 1982; Bradac et al. 1990). It extends from the superior orbital fissure anteriorly to the petrous apex posteriorly. In the CS runs the intracavernous portion of the ICA and cranial nerve VI. Cranial nerves III and IV and the ophthalmic and the second division of cranial nerve V lie in the lateral wall of the sinus. The CS contains, further, a plexus of several small veins, separated by trabiculae. The presence of the ICA leads to the formation of two venous compartments, one anterolateral and the other posteromedial, with varying connections to each other.

The venous plexuses of the CS communicate to each other via the anterior and posterior small channels running in the dura of the diaphragma sellae, forming the so-called coronary sinus. The coronary sinus, combined with both CS, completely surrounds the pituitary gland.

Anteriorly, each sinus receives the superior and inferior ophthalmic veins passing in the sinus through the superior orbital fissure. Laterally, the sinus is joined by the SMCV. The latter can instead drain into the paracavernous sinus (PCS), which is characterized by a plexus of small veins, passing through the foramina of the base of the skull and entering the pterygoid plexus. Many connections link the PCS and CS. In some cases, the SMCV can enter the so-called lateral CS. This is a small venous space, described by San Millan Ruiz et al. (1999) and Gailloud et al. (2000), located within the lateral wall of the CS. The lateral CS can be connected with the CS or drain either directly into the pterygoid plexus or, posteriorly, into the TS, via the SPS. On an AP angiogram, it can sometimes be recognized as a thin venous structure lateral to the CS (Fig. 9.5). Another lateral tributary is the DMCV, which drains normally into the BV, but it can occasionally enter the CS or PCS through the uncal vein.

Posteriorly, the CS is connected with the SPS and IPS and with a network of dural veins, which extend on the clivus down to the foramen magnum. The latter unites the two CS (Hanafee et al. 1965; Doyon et al. 1974). The clival plexus is connected caudally with the anterior vertebral venous plexus and lateroposteriorly with the marginal sinus. Bridging veins can connect the CS and clivus venous network with the pontine and peduncular veins (Matsushima et al. 1993; Kiyosue et al. 2008) (Figs. 9.10 and 9.13–9.15).

The CS can be recognized on carotid and vertebral angiograms or by selective catheterization through the IPS or facial and ophthalmic veins (Figs. 9.4, 9.5, 9.7, 9.10, and 9.22). These latter ways can be used in the treatment of dural arteriovenous fistula of the area (Figs. 13.4 and 13.5).

9.3.11 Superior Ophthalmic Vein (SOV)

The superior ophthalmic vein (SOV) arises near the roof of the nose in the superomedial angle of the orbita by the junction of the superior tributary, continuation of the frontal vein, and inferior tributary continuation of the angular vein (facial vein) (Figs. 9.19–9.21). It runs backward and laterally, first outside the muscle cone; then it enters the cone, running further laterally along the under surface of the superior rectus muscle.

In its course, the vein crosses superiorly the ophthalmic artery and optic nerve. The vein runs finally medially and downward, leaving again the muscle cone, passing the superior orbital fissure, and entering the anterior part of the CS (Hanafee et al. 1965, 1968; Lombardi and Passerini 1967; Doyon et al. 1974).

9.3.12 Inferior Ophthalmic Vein (IOV)

The inferior ophthalmic vein (IOV) is a small vein, sometimes replaced by a network of fine venous channels. It runs backward within the muscle cone above the inferior rectus muscle. The IOV drains into the CV directly or after entering the SOV. Anteriorly, it communicates with the facial vein; posteriorly, it communicates with the pterygoid plexus through fine anastomosis passing via the inferior orbital fissure.

The SOV and IOV enter the CS, draining blood from the intraorbital (globe, muscles, fat, lachrymal gland) and craniofacial structures through the connection with the facial, frontal veins, and pterygoid plexus. This explains also the fact that the ophthalmic veins, especially the SOV, are frequently recognizable in the venous phase of external carotid angiograms (Tornow and Piscol 1971; Hacker and Porrero 1969; Bradac et al. 1974).

The SOV is an important route in the treatment of fistulae involving the cavernous sinus. This is particularly true when the IPS (thrombotic occlusion, anomalous drainage) cannot be catheterized or in cases where the venous drainage is directed predominantly in the SOV, which can be reached through the facial or frontal and superficial temporal veins (Agid et al. 2004; Kirsch et al. 2006; Kato et al. 2007).

Extracranial Venous Drainage

10

10.1 Orbital Veins

These are represented by the superior and inferior ophthalmic veins, which drain posteriorly in the cavernous sinus. They communicate anteriorly with the facial and frontal veins. There are connections with the pterygoid plexus (see also "Superior – inferior ophthalmic vein" in Chap. 9) (Fig. 10.1).

10.2 Facial Veins

The anterior facial vein begins in the naso-orbital angle, with the angular vein, which has an anastomosis with the ophthalmic veins. The anterior facial vein runs inferiorly and posteriorly in an oblique course along the face; it crosses over the mandible, and shortly after it is joined by the retromandibular vein; together they form the common facial vein, which enters the internal jugular vein at the level of the hyoid bone (Osborn 1999).

The anterior facial vein receives tributaries from the orbit, lips, and facial skin and muscles and from the menton-submental region. Occasionally, the lingual and superior thyroid veins also join the anterior facial vein, instead to drain separately into the internal jugular vein. The anterior facial vein is connected posteriorly with the pterygoid venous plexus through the deep facial vein.

10.3 Retromandibular Vein

Also known as the posterior facial vein, the retromandibular vein arises at the junction of the maxillary vein and superficial temporal vein, below the neck of the

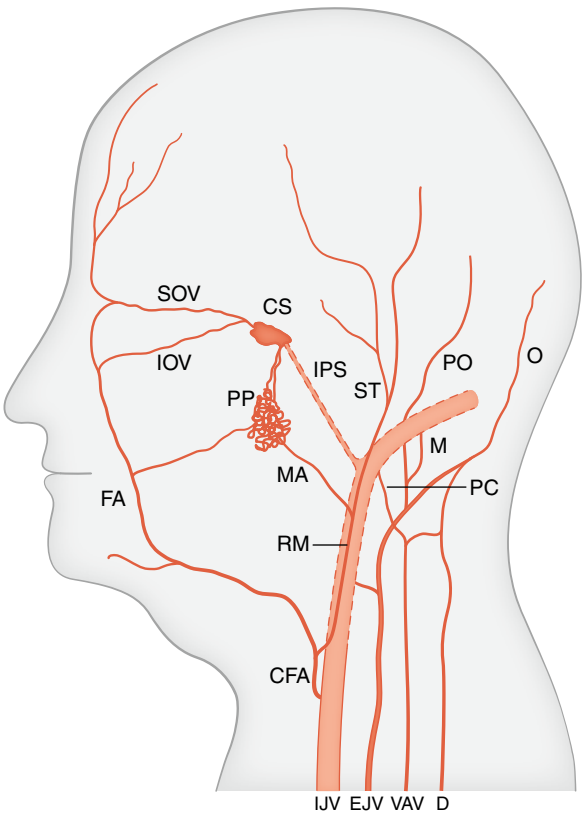

Fig. 10.1 Internal jugular vein (*IJV*), retromandibular vein (*RM*), to which converge the superficial temporal vein (*ST*) and the maxillary vein (*MA*). Pterygoid plexus (*PP*), facial vein (*FA*), common facial vein (*CFA*), formed by the confluence of the *RM* and *FA* entering the *IJV*. Posterior auricular vein (*PO*), superficial temporal vein (*ST*), occipital vein (*O*), external jugular vein (*EJV*), to which converge *PO* and *O*. Mastoid vein (*M*), posterior condylar vein (*PC*), deep cervical vein (*D*), to which drain partially the occipital vein and venous plexus of the vertebral artery (*VAV*), with some of its connections. Superior-inferior ophthalmic veins (*SOV-IOV*), connected anteriorly with the facial and frontal veins and posteriorly with the cavernous sinus (*CS*). Inferior petrosal sinus (*IPS*)

G.B. Bradac, *Cerebral Angiography*,
DOI: 10.1007/978-3-642-15678-6_10, © Springer-Verlag Berlin Heidelberg 2011

mandible. The maxillary vein drains the pterygoid venous plexus, which is a venous network, lying between the pterygoid muscle, which receives numerous tributaries from the naso-oral and masticator areas. The pterygoid venous plexus is connected with the anterior facial vein through the deep facial vein and intracranially with the paracavernous-cavernous sinus. The superficial temporal vein drains the temporal region.

The retromandibular vein runs through the parotid gland together with the external carotid artery, which is posteromedially located, and the facial nerve, which is laterally located (Fig. 2.1). The retromandibular vein joins the anterior facial vein, and together the form the common facial vein, which enters the internal jugular vein.

10.4 Posterior Auricular and Occipital Veins

The posterior auricular vein runs posterior to the pinna; it connects with the occipital vein and together they join the external jugular vein (EJV) below the mandible angle. The two veins drain the pinna and the scalp and muscle of the occipital region. The EJV, which also receives an anastomotic branch from the retromandibular vein, runs superficially between the platysma and superficial fascia, ending in the brachiocephalic vein, near and lateral to the internal jugular vein (IJV).

10.5 Deep Cervical Vein

This drains the deep muscles of the neck, between which it runs. The deep cervical vein drains the occipital vein, and it is connected with the posterior condylar vein and venous plexus of the vertebral artery (Fig. 9.18). Distally, it enters the brachiocephalic vein, either as an isolated structure or after joining the venous plexus of the vertebral artery.

10.6 Venous Plexus of the Vertebral Artery

This is formed by a venous network surrounding the vertebral artery within its course through the transverse foramina. Through anastomoses with the lateral and posterior condylar veins, the venous plexus of the vertebral artery can connect with the epidural anterior vertebral plexus, the anterior condylar confluence (ACC), the deep cervical vein, and also with the sigmoid sinus. Distally, it ends together with the deep cervical vein in the brachiocephalic vein (Fig. 9.18).

10.7 Emissary Veins

These veins pass through the cranial vault and link the intracranial dural venous sinuses with the extracranial veins. Their presence is not constant. They can be classified with regard to the dural sinus involved.

1. Those related to the superior sagittal sinus (SSS): an emissary vein can connect the SSS with the vein of the nasal cavity passing through the foramen cecum. Another emissary vein can connect the SSS with the scalp vein in the parietal region.
2. Those related to the torcular herophili and/or transverse sinus (TS) and sigmoid sinus (SiS): the most frequent are the mastoid vein, which connects the TS with the posterior auricular or occipital veins and passes through the mastoid foramen, and the posterior condylar vein, which arises from the SiS or jugular bulb and is connected with the venous plexus surrounding the vertebral artery. In this group, we would include also the anterior condylar vein, which passes through the condylar foramen and connects the ACC with the epidural anterior vertebral plexus (Fig. 9.18). A rare connection can be present between the TS-torcular herophili and occipital vein.
3. Those related with the cavernous sinus (CS): a small anastomosis connects the CS and pterygoid plexus via the paracavernous sinus. An infrequent connection is presented by the petro-occipital sinus, linking the CS with the ACC.

10.8 Diploic Veins

These veins run within the diploe and are connected with the scalp veins, dural sinuses, and meningeal veins. They are not recognizable on the normal angiogram but are visible in pathological processes involving the scalp,

bone, sinus thrombosis, and occasionally brain arteriovenous malformations and tumors.

10.9 Internal Jugular Vein

The IJV is the inferior continuation of the SiS, and it begins in the posterior segment of the jugular foramen, forming at its origin a small dilatation called the jugular bulb. Extracranially, the IJV runs in the carotid space (Fig. 2.1), lateral to the internal carotid artery, and terminates in the brachiocephalic vein. The latter is very short on the left side. The IJVs are frequently asymmetric, one being larger than the other.

The IJV is the main venous extracranial drainage of the brain parenchyma. Among the extracranial tributaries, the most important is the common facial vein. For the connections of the IJV with the inferior petrosal sinus and condylar veins, see Sect. 9.3.8.

Aneurysms

11

11.1 Incidence

The precise incidence of cerebral aneurysms is unknown. From autopsy studies, the incidence is estimated at 5% (Stehbens 1972, 1990).

11.2 Type and Location

Cerebral aneurysms are commonly of a saccular type (berry aneurysm) located at the bifurcation of the arteries of the circle of Willis. The most frequent sites are the internal carotid artery (ICA; 30–35%). Among them, those in the area of the junction of the posterior communicating artery (PcomA) account for more than the half. Also occurring very frequently are aneurysms involving the sector of the anterior cerebral artery (ACA; 33–34%) and those of the middle cerebral artery (20%).

Aneurysms in the posterior circulation are less common (10%). Of these, half are basilar artery aneurysms (Locksley 1966a and b; Weir 1987; Nakstad et al. 1988).

Multiple cerebral aneurysms frequently occur together, with an incidence that varies from 20% to 40% (Locksley 1966a and b; Nakstad et al. 1988; Osborn 1999; Rinne et al. 1994). Multiple aneurysms occur more frequently among women than men.

11.3 Macroscopic Appearance

Saccular aneurysms vary in size. In in vivo studies, the majority have a diameter of 5–7 mm, though smaller and larger aneurysms also occur; those larger than 25 mm are termed giant aneurysms. Saccular aneurysms can be round or more elongated. The surface may be regular or irregular with estroflexion (blebs), which in the case of a subarchnoid hemorrhage (SAH) can indicate the point of rupture. Pathological studies show that the neck and sac have no internal elastic lamina and no tunica media.

11.4 Pathogenesis

Intracranial cerebral vessels and intracranial aneurysms have some unique features. The arteries are composed of four layers, represented by the adventitia, media, internal elastic lamina, and intima. There is no external elastic lamina. The arteries have thin walls and are located in the subarachnoid space, where they have relatively little external support. Typical aneurysms of the intracranial cerebral vessels are saccular and thus different from aneurysms affecting the aorta or other extracranial arteries, which are commonly fusiform (Stehbens 1990; Powell 1991). In the early 1930s, some authors (Forbus 1930) showed in histological studies a congenital gap defect of the media in the wall of the cerebral artery, which was interpreted as a locus minoris resistentiae, where aneurysms could develop. Later, however, it was demonstrated that these gaps are very frequent in normal individuals without aneurysms. Today, it is commonly accepted that aneurysms are acquired lesions linked to a degenerative process involving the connective tissue of the media and internal elastic lamina, in which atherosclerosis probably plays an important role (Glynn 1940; Carmichel 1950; Crompton 1966a, 1966b; Stehbens 1959, 1972, 1989, 1990). Others (Pope et al. 1981; Pope 1989; Ostergaard and Oxlund 1987; Chyatte et al. 1990) have demonstrated a reduction in reticular fibers owing to a decrease in type-III collagen in the tunica media of cerebral arteries of patients with aneurysms; this is perhaps due to an undetected metabolic

G.B. Bradac, *Cerebral Angiography*,
DOI: 10.1007/978-3-642-15678-6_11, © Springer-Verlag Berlin Heidelberg 2011

disorder of connective tissue proteins. In a few of these patients, genetic disorders could be demonstrated (Chyatte and Mjerzejewski 1991).

These degenerative changes lead to mural fragility, upon which hemodynamic factors, such as hypertension, variations in the circle of Willis, and arteriovenous malformation (AVM), could act further toward the formation of aneurysms. For aneurysms linked to AVM, see Chap. 12.

There are other more uncommon pathological conditions in which cerebral aneurysm can occur. Among them are a few systemic diseases of the connective tissue, such as fibromuscular dysplasia, Ehlers-Danlos syndrome, Marfan syndrome, neurofibromatosis, polycystic kidney, and aortic coarctation. In some of these patients, hypertension is also present as an adjuvant factor (Schwartz and Baronofsky 1960; Handa et al. 1970a; Stehbens 1989; Osborn 1999).

Aneurysms can occur in infectious diseases, arteritis, cases of cardiac myxoma, and following craniocervical traumas. Other factors reported to promote aneurysm formation are smoking, consumption of alcohol, and oral contraceptives (Hillbom and Kaste 1982; Lindergärd et al. 1987; Juvela et al. 1993). The incidence of aneurysms is reported to be high in some families (Edelsohn et al. 1972; Hashimoto 1977; Crompton 1979; Norrgard et al. 1987). Spontaneous dissections can lead to the formation of aneurysms of the cervicocerebral vessels (see Chap. 16).

11.5 Clinical Presentation

Aneurysms are typical in patients of adult age, and there is a predominance among women. Aneurysms in pediatric patients are rare, but they are more frequent in boys. In 90% of cases, the aneurysm presents with SAH (10 cases of SAH/year/100,000 people). In other cases, the patient presents with neuropathy, particularly oculomotor palsy, in PComA and basilar artery aneurysms. Trigeminal neuralgia can also occur in large aneurysms in this location. Visual symptoms, due to compression of the chiasma and/or optic nerve, and sometimes hydrocephalus, due to compression of the third ventricle, can be present in large aneurysms involving the anterior communicating artery (AComA) and in carotid ophthalmic lesions. Symptoms as a result of brain compression can occur in large basilar artery and middle cerebral artery (MCA) aneurysms.

The typical cavernous sinus syndrome is present in intracavernous aneurysms. In exceptional cases, aneurysms are present with ischemia. This occurs especially in nonruptured, partially thrombosed aneurysms (Antunes and Correll 1976; Stewart et al. 1980). Ischemia can be due to the distal embolization or involvement of perforators adjacent to the aneurysm.

In addition to aneurysms in patients presenting with related symptoms, an increasing number of asymptomatic aneurysms today are diagnosed with CT and MRI in patients who underwent the examination for other reasons. The clinical problems and therapeutic considerations with such aneurysms are discussed in Chap. “Unruptured aneurysms.”

11.6 Aneurysm Location

11.6.1 Extracranial ICA Aneurysms

Aneurysms in this location are uncommon. Trauma is a possible etiology. Atherosclerosis can be another cause in older patients. In younger patients, aneurysms may be associated with FMD or collagenopathies, such as Ehlers-Danlos syndrome. In the latter syndromes, dissecting aneurysms are frequent (Fig. 16.3).

11.6.2 Petrous Segment ICA Aneurysms

These are very rare. Atherosclerosis and dysplasia can be assumed to be the etiological mechanism (Fig. 11.1).

11.6.3 ICA Paraclinoid Aneurysms

These are aneurysms arising adjacent to the anterior clinoid process. They can be divided into three groups: cavernous, ophthalmic, and superior hypophyseal.

Cavernous aneurysms are located in the cavernous sinus and are thus extradural. They can be asymptomatic or, when large, present with the typical cavernous sinus syndrome, first described by Jefferson, characterized by involvement of cranial nerves III, IV, VI and, partially, V (Fig. 11.2). There is no risk of SAH, and in general the clinical prognosis is good, and so the

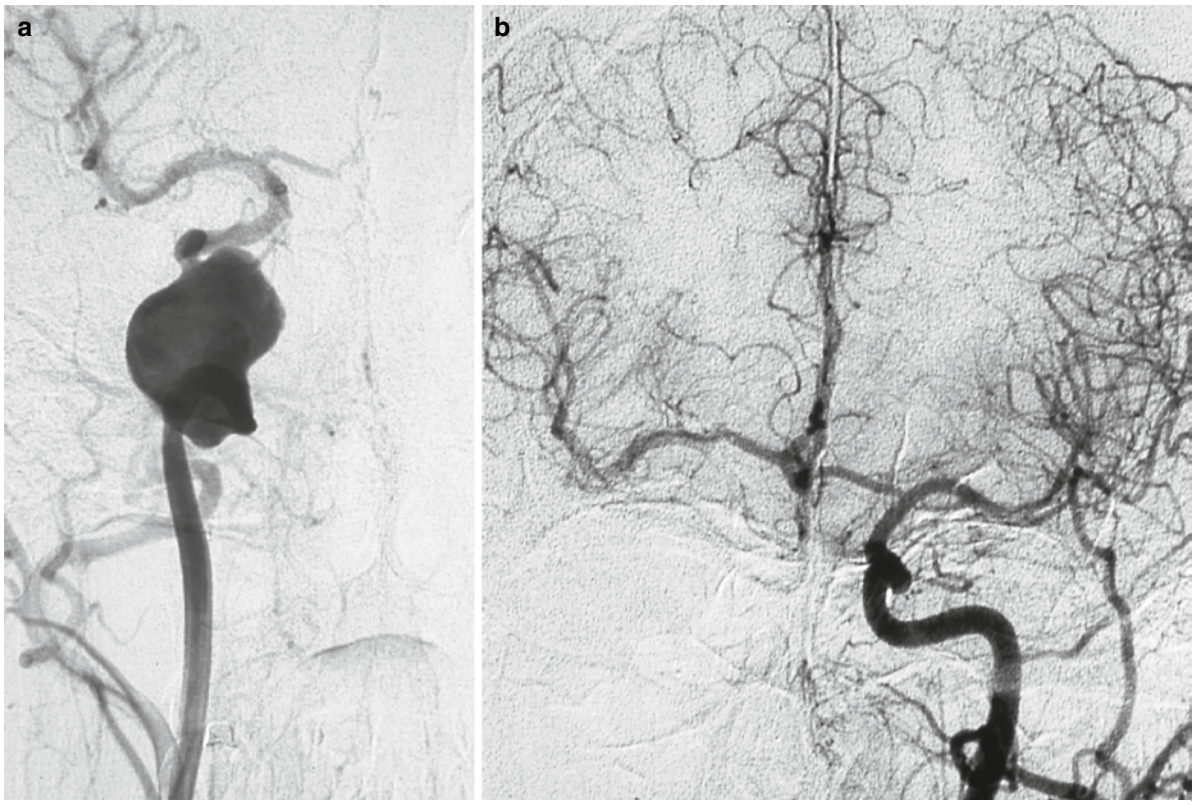

Fig. 11.1 Giant aneurysm of the petrous segment of the right internal carotid artery (ICA) presenting with palsy of cranial nerve VI. (**a**) Carotid angiogram showing the aneurysm, which was treated with occlusion of the ICA. (**b**) Left control angiogram, showing a good collateral circulation and exclusion of the aneurysm. The occlusion was preceded by ICA balloon test occlusion, during which an injection of the contralateral ICA was performed to examine the effectiveness of the circle of Willis and the appearance of the contralateral venous phase. In the tested territory, the venous phase should not have a delay greater than 1–2 s

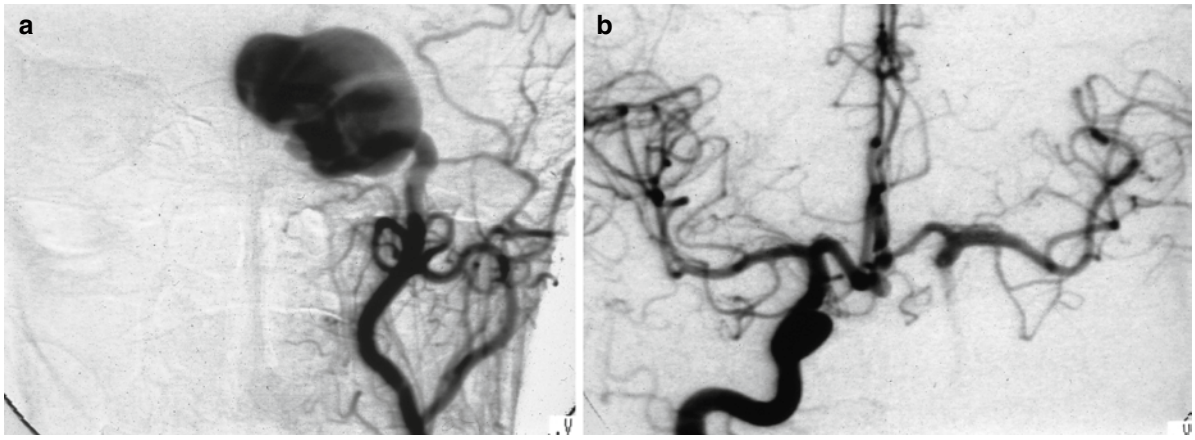

Fig. 11.2 Giant aneurysm of the cavernous segment of the ICA presenting acutely with a typical cavernous sinus syndrome. Left carotid angiogram (**a**) showing the aneurysm. There is no injection of the intracranial branches. The right angiogram (**b**) showed a good collateral circulation through the circle of Willis. After a balloon test occlusion, as described in Fig. 11.1, the left ICA was occluded with a balloon

treatment (endovascular occlusion of the ICA, or selective occlusion of the aneurysm with stent plus coils and flow-diverter stents) is not always indicated. The aneurysms can rupture in the sphenoid sinus and nasal cavity, leading to a dramatic epistaxis. This is, however, an extremely rare possibility (Linskey et al. 1990). In some cases, intracavernous aneurysms, even small, can extend upward, reach the subarachnoid space, and rupture, causing SAH. This can occur since the dural ring surrounding the ICA, through which the ICA passes and becomes intradural, is not medially adherent to the artery; a small cavity (or cave) is thereby formed, through which the intracavernous aneurysm or those arising at the level of the medial ring can extend intradurally. This kind of aneurysm is called a cave aneurysm (Fig. 11.3).

Carotid-ophthalmic aneurysms arise in the ophthalmic segment of the ICA (see anatomy).They originate

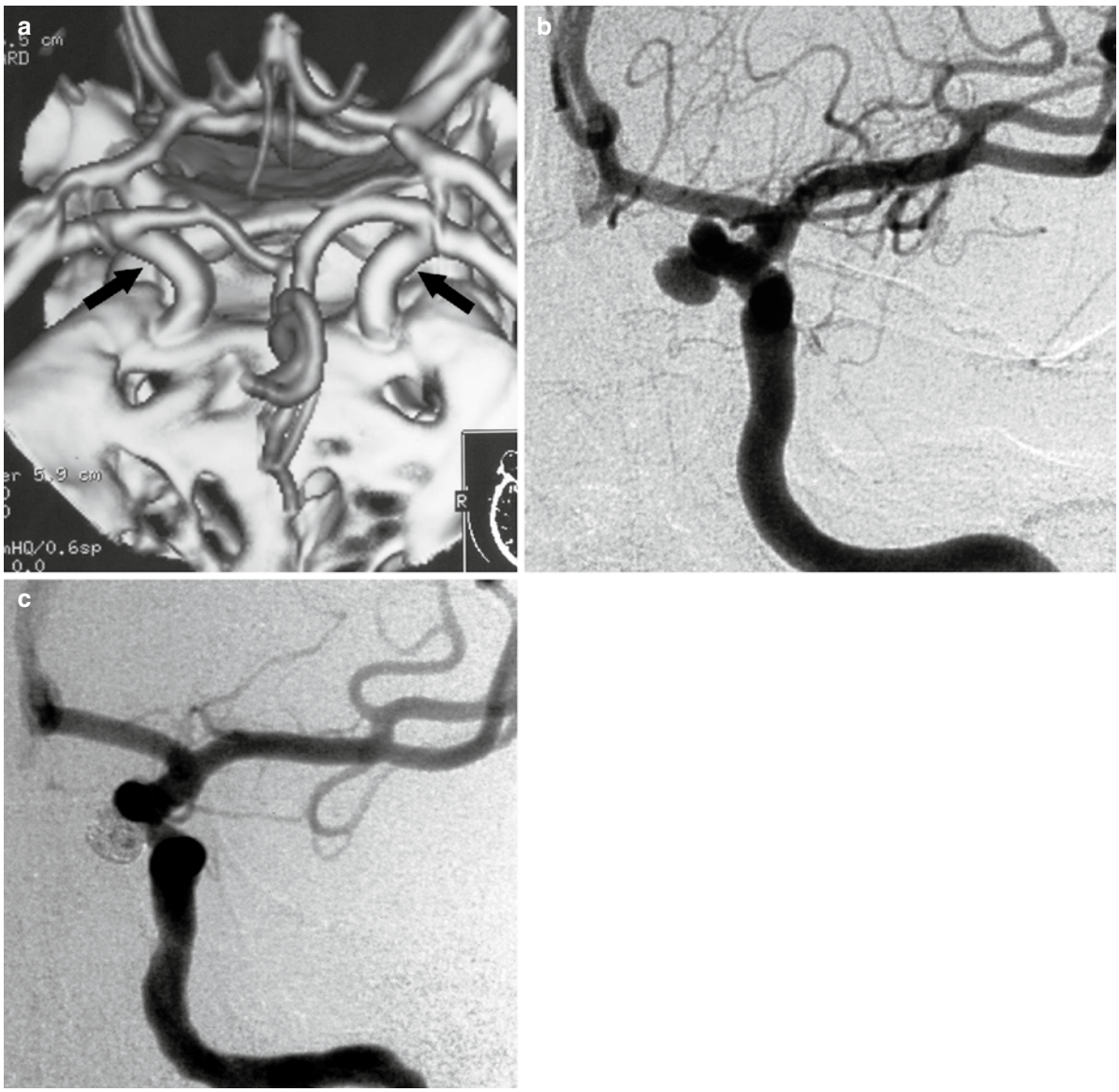

Fig. 11.3 Small cave left aneurysm presenting with hemorrhage. CT angiography (**a**) did not show the aneurysm. Both distal ICA (*arrows*). The left carotid angiogram (**b**) showed the small aneurysm, which probably had a small intradural estroflession. Control angiogram (**c**) post-treatment with coils

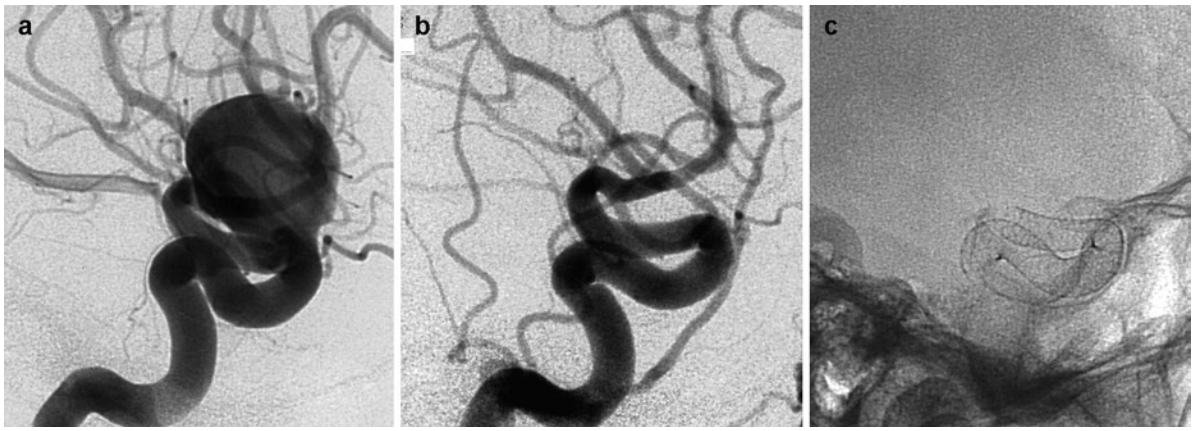

Fig. 11.4 Large carotid ophthalmic aneurysm presenting with progressively worsening visual acuity. A complete angiographic control to study the aneurysm and the circle of Willis was performed. The aneurysm was occluded with a flow-diverter stent. The patient improved slowly. Lateral carotid angiogram pretreatment (**a**), posttreatment (**b**). RX image showing the stent (**c**) (pipeline)

in association with the ophthalmic artery or its adjacent structures. They are directed upward, sometimes medially, and are frequently large (Figs. 11.4–11.6).

Superior hypophyseal aneurysms are very rare. They arise in conjunction with the superior hypophyseal artery. They are directed downward and medially toward the chiasma and sella turcica, becoming intrasellar when large (Fig. 11.7).

11.6.4 Aneurysms of the Communicating and Choroidal Segments

These consist of aneurysms of the PComA and anterior choroidal artery (AChA). PComA aneurysms arise at the origin of the PComA; they are posteriorly directed and can compress cranial nerve III. They are frequently large, elongated, and with an irregular wall (Fig. 11.8). AChA aneurysms arise at the origin or just distal to the AChA (Fig. 11.9). They are directed posteriorly and laterally and are frequently smaller than PComA aneurysms. A variable number of perforators arise from the choroidal segment of the ICA and can be found stretched around the neck of the aneurysm. In endovascular treatment, it is sometimes difficult to separate the neck of the aneurysm from the parent artery despite the use of several projections. Furthermore, the aneurysm can arise directly from the first segment of the PComA and AChA.

11.6.5 Aneurysms of the Carotid Bifurcation

These are typical T-bifurcation aneurysms similar to basilar-tip aneurysms (Ingebrigtsen et al. 2004). They are relatively rare and easily recognizable on the angiogram. They can sometimes be very large and have a sizeable neck. Perforating branches arising from the choroidal segment and from A1 and M1 may be stretched around the neck and posterior wall of the aneurysm (Figs. 11.10 and 5.4b).

11.6.6 Anterior Cerebral Artery Aneurysms

These are very frequent aneurysms and arise mainly in the A1-A2 angle of the ACA. The neck of the aneurysm can be large and partially involve the adjacent A1-A2 segments or AcomA. As has been described in the anatomy, these aneurysms are frequently associated with anomalies of the anterior part of the circle of Willis (Figs. 4.3, 4.7, 4.8, 4.10, and 4.12).

Many perforators arise from the A1 and AcomA. This should be taken into account in the surgical-endovascular treatment of these lesions (Figs. 11.11, 4.3, 4.4, 4.8, and 4.10). Infrequently, the aneurysm can be found along the A1 segment. In such cases, it can be

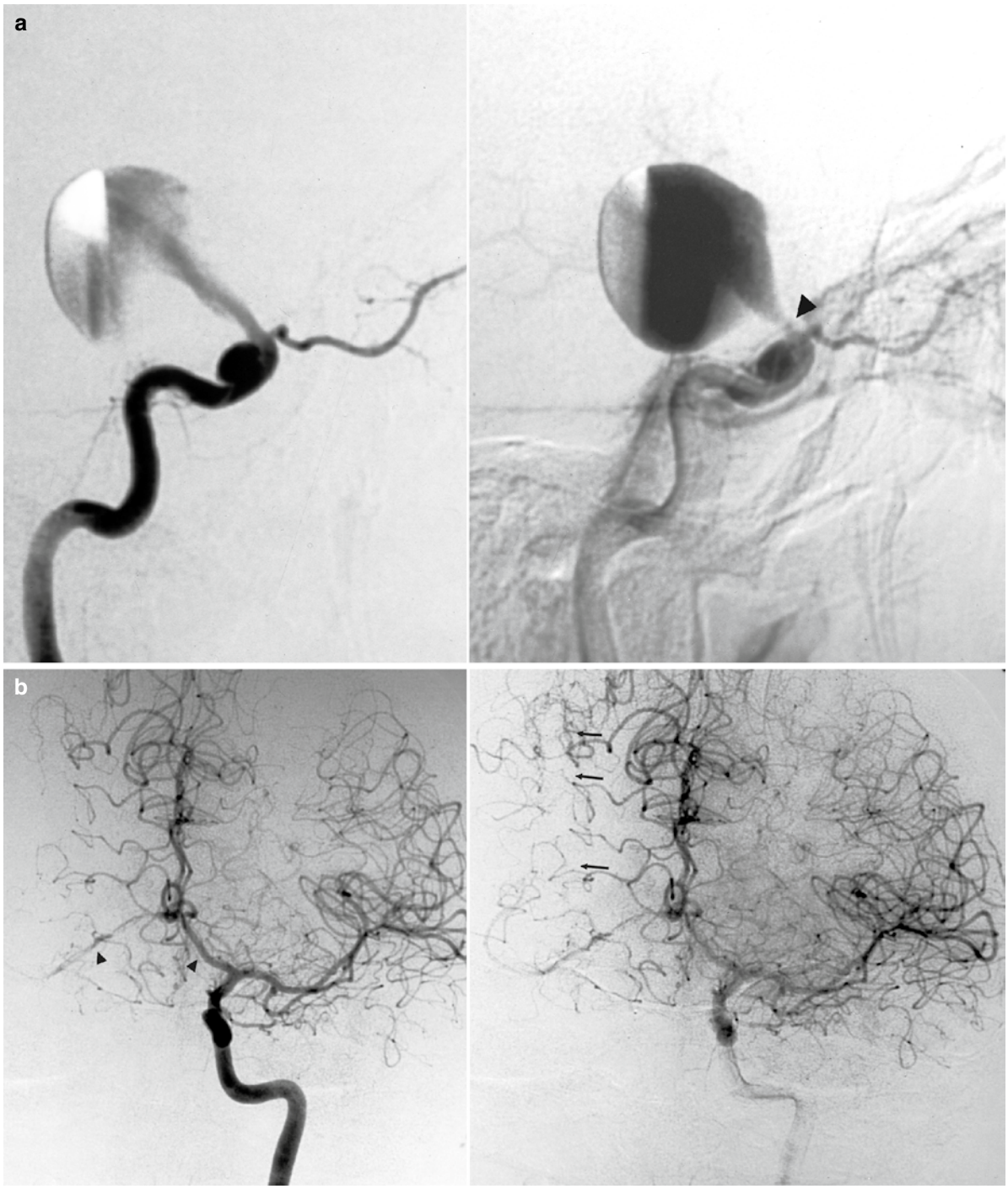

Fig. 11.5 Giant carotid ophthalmic aneurysm presenting acutely with severe disturbances of visual acuity. (**a**) Right lateral carotid angiogram, early and late phases, showing the progressive injection of the aneurysm through a relatively small neck, close to the origin of the ophthalmic artery (*arrowhead*). A second small intracavernous aneurysm is present. (**b**) Left carotid angiogram, upward displacement (*arrowheads*) of both A1 segments and partial filling of the right middle cerebral artery (MCA) through leptomeningeal anastomoses (*arrows*) with the right anterior cerebral artery (ACA). (**c**) Right vertebral angiogram, showing the leptomeningeal collateral circulation toward the right MCA from the posterior cerebral artery (PCA; *arrows*). (**d**) The ICA was occluded with a balloon positioned in the intracavernous segment. The patient recovered completely and a left control angiogram, 2 months later showed the normal course of both the A1 and filling of the right MCA. (**e**) Right common carotid angiogram showing the retrograde injection of the distal ICA and MCA through the ophthalmic artery via a collateral circulation involving an anastomosis between the anterior deep temporal artery and the lacrimal branch of the ophthalmic artery (*angled arrow*). The aneurysm is completely excluded

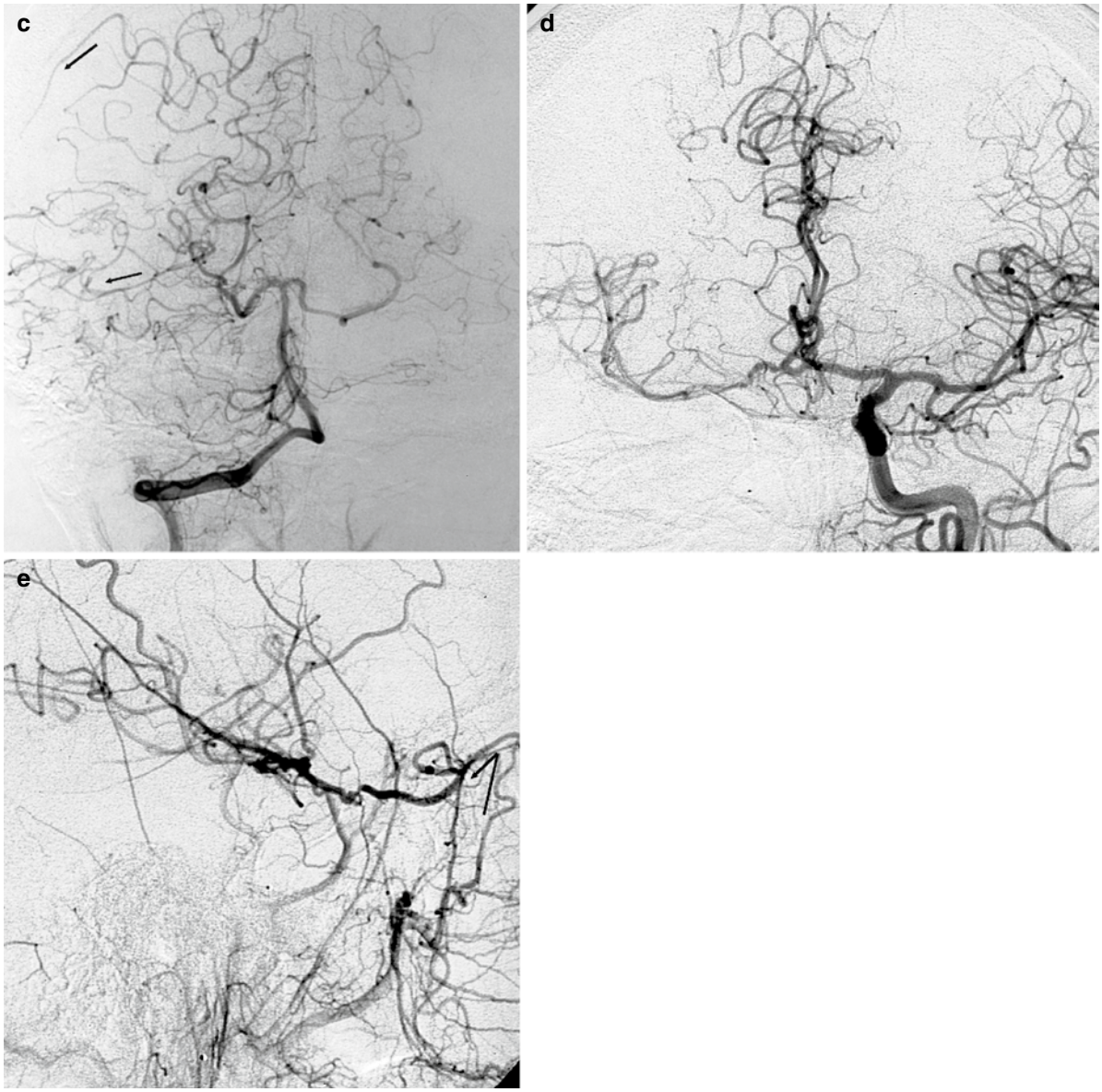

Fig. 11.5 (continued)

assumed that the aneurysm takes its origin at the junction with a perforating branch.

Another typical location, though more uncommon, is at the pericallosal-callosomarginal junction. Depending on the site of the junction, the aneurysms can be located anterior to the genu of the corpus callosum, distal to it, or, more rarely, proximal beneath the genu (Figs. 11.12 and 4.11). Dissecting, mycotic, "flow-dependent" aneurysms are very infrequent. They can occur in every segment of the ACA, usually in its distal segments (Figs. 11.13 and 16.10).

11.6.7 MCA Aneurysms

Most of these aneurysms arise at the bi-trifurcation of the M1 (Fig. 11.14). It is not always easy to separate the bifurcation branches from the neck of the aneurysm. Furthermore, in cases of early division of the M1 (short M1), perforators can be very close to the aneurysm (Figs. 5.4, 5.5, and 5.11). Despite improvements in endovascular techniques, surgery remains the method of choice in many cases. Peripheral aneurysms (dissecting, mycotic, flow-dependent, resulting from

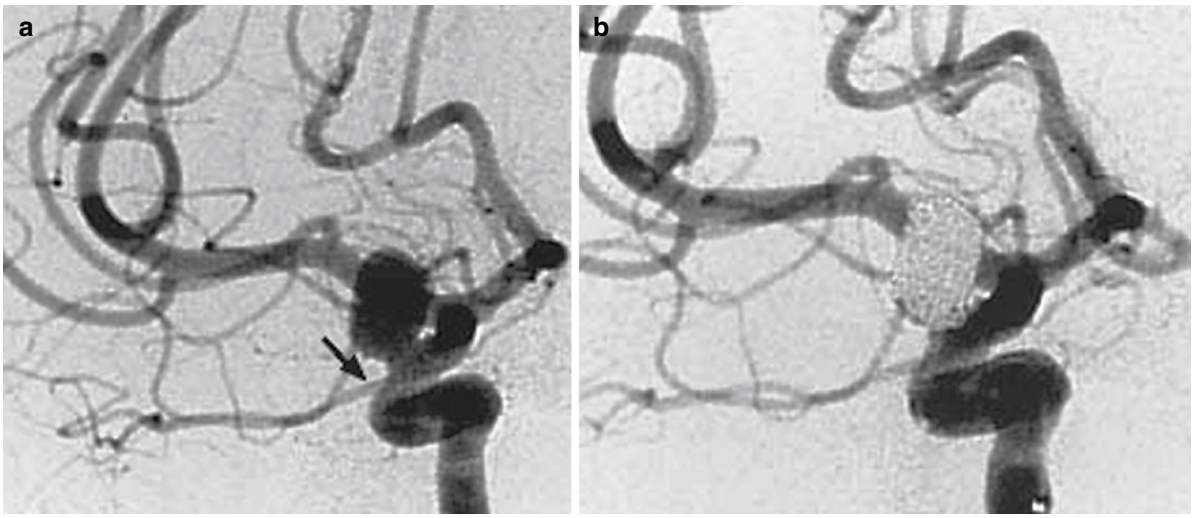

Fig. 11.6 Carotid ophthalmic aneurysm presenting with hemorrhage. (**a**) Carotid angiogram, oblique view showing the aneurysm. Origin of the ophthalmic artery (*arrow*). (**b**) Carotid angiogram showing the occluded aneurysm with coils

nonatherosclerotic vascular or cardiac diseases) can occur but are very infrequent (Figs. 5.8, 18.1, 18.4, 17.1, and 17.5).

11.6.8 Aneurysms of the Posterior Circulation

Basilar aneurysms are the most frequent in the vertebrobasilar sector. They are typically located at the top of the artery. The perforators can shift and be stretched along the sac, but they are not directly involved since they arise from the P1; this can, however, occur when the neck enlarges and also involves the proximal part of the P1 (Figs. 11.15–11.17). Other locations are the distal lateral basilar artery between the origin of the posterior cerebral artery (PCA) and the SCA (Fig. 11.18). Also typical are aneurysms of the trunk of the basilar artery, more frequently distal to or at the level of the anterior inferior cerebellar artery (AICA). Frequently, the latter aneurysms are relatively large, with a fusiform aspect, often due to dissection (Fig. 11.25).

Vertebral–posterior inferior cerebellar artery (PICA) aneurysms. The vertebral–PICA junction is another typical site of aneurysms. These aneurysms are sometimes located not exactly at the junction, but close to it, in the proximal part of the PICA (Mukonoweshuro et al. 2003; Bradac and Bergui 2004; Cellerini et al. 2008) (Figs. 11.19 and 11.20).

Distal aneurysms of the cerebellar arteries. These are very rare, occurring in fewer than 1% of all aneurysms (Lubicz et al. 2003; Mitsos et al. 2008). The great majority are located in the PICA (Figs. 11.21 and 11.22) (Bradac and Bergui 2004; Mitsos et al. 2008), followed by the SCA and AICA (Kurosu et al. 2000; Mitsos et al. 2008). (Gacs et al. 1983; Chaloupka et al. 1986; Leonardi et al. 2001; Zager et al. 2002). Unlike the majority of intracranial aneurysms, which arise at an arterial branching point, distal cerebellar aneurysm frequently arise directly from the artery where it forms a curve. The course of the cerebellar arteries, especially the PICA, is sometimes characterized by a sharp curve, which could be the cause of the hemodynamic stress on the wall and contribute to the formation of the aneurysm (Lewis et al. 2002; Horiuchi et al. 2003; Mitsos et al. 2008). In other cases, the pathogenesis is probably a dissection (see Chap. 16) (Bradac and Bergui 2004; Mitsos et al. 2008). Flow-dependent aneurysms of the cerebellar arteries related to a more distal AVM and occasionally to DAVF are relatively frequent in our experience (Figs. 12.13–12.16). In aneurysms involving the distal segment of the cerebellar arteries, the occlusion, also of the parent artery, is commonly performed without clinical problems since the perforators for the medulla arise in the proximal segment (see anatomy). Furthermore, the distal cortical branches are

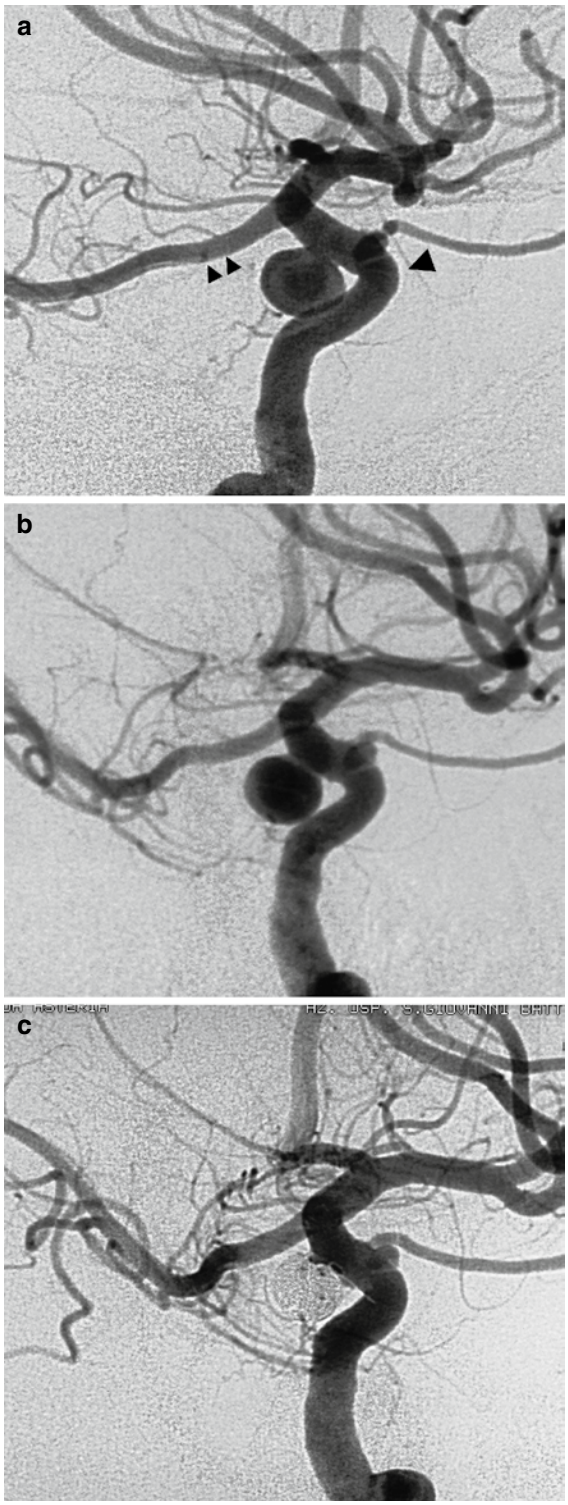

Fig. 11.7 Superior hypophyseal aneurysm presenting with hemorrhage. Two different oblique (**a** and **b**) views of the carotid angiogram to better identify the aneurysm and its neck. PCA (*arrowheads*), ophthalmic artery (*arrowhead*). Control angiogram (**c**) after occlusion of the aneurysm with coils

revascularized through a frequently rich collateral circulation via anastomoses involving leptomeningeal branches of the cerebellar arteries.

Aneurysms of the posterior cerebral arteries. These rare aneurysms present with a relatively typical location, which is at the P1-P2 passage. More uncommon are aneurysms located along the course of the P2 and at the P2-P3 passage. Such aneurysms are frequently large, sometimes with a fusiform aspect (Li et al. 2007). The etiology is frequently thought to be a dissection (Figs. 11.23 and 11.24). This is especially true for such aneurysms in pediatric patients (Laughlin et al. 1997; Lasjaunias et al. 2005; Vilela and Goulão 2006; Bradac et al. 2008a).

Occlusion of the aneurysm and parent artery frequently cannot be avoided in the treatment (endovascular, surgical); in dissecting cases, a dangerous recanalization should be avoided. The risk of an occipito-temporal infarction is relatively low, owing to the rich collateral circulation. Greater risk can occur in more proximal occlusions as a result of involvement of perforators supplying the midbrain and thalamus, arising from P1-P2 (Pia and Fontana 1977; Sakata et al. 1993; Ciceri et al. 2001; Arat et al. 2002; Hallacq et al. 2002; Roh et al. 2008). Owing to anatomical variations in the perforating branches, the ischemic lesion is unpredictable (see also anatomy). Fortunately, when ischemia occurs, the clinical impairment is commonly mild and resolves over ensuing weeks.

11.7 Dissecting Aneurysms

These are discussed more extensively in Chap. 16. They are most frequent in the posterior circulation, where they typically affect the basilar and vertebral arteries. Aneurysms of distal branches of the cerebellar and posterior cerebral arteries can also be due to dissection. Dissecting aneurysms are less common in the anterior circulation. The distal ICA, proximal MCA, and ACA are the most usual locations. Distal branches can occasionally be involved.

11.8 Fusiform and Giant Aneurysms

Fusiform aneurysms are a relatively uncommon form found in the anterior circulation (supraclinoid ICA and MCA), though more frequently in the posterior

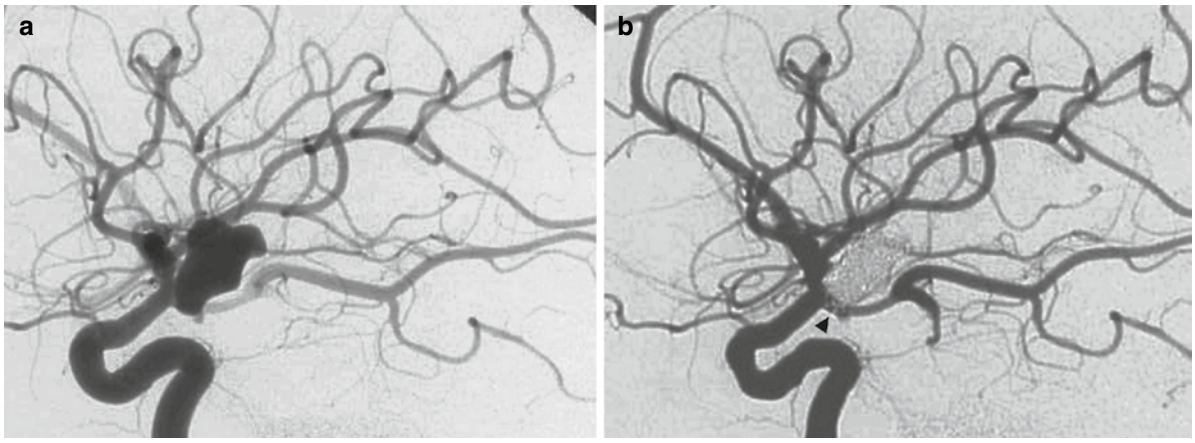

Fig. 11.8 Large irregular aneurysm with a neck close to the origin of a fetal PCA in a patient with subarchnoid hemorrhage (SAH). (**a**) Lateral carotid angiogram showing the irregularly shaped aneurysm. The inferior part of the aneurysm is superimposed on the origin of the fetal PCA. (**b**) Lateral carotid angiogram. Occlusion of the aneurysm with coils. The origin of the PCA is now better recognizable (*arrowhead*)

circulation (vertebral and basilar arteries) (Fig. 11.26). Unlike saccular aneurysms, in which a neck is recognizable, in fusiform aneurysms the entire vessel expands. The pathogenesis is a particular form of arteriosclerosis, in which the initial event is lipid deposition in the intima, with disruption of the internal elastic lamina and infiltration and fibrosis of the media, leading to progressive dilatation and tortuosity of the artery, which is promoted also by the frequent presence of hypertension. The increased luminal diameter leads to a slowing down of the circulation and to thrombosis on the wall, which causes further changes, characterized by fibrosis and rigidity, which promote further dilatation (Hegedus 1985; Echiverri et al. 1989).

Fusiform aneurysms can also occur in children and young nonatheromatous patients as a result of collagen-displastic diseases, in which spontaneous dissection may also be a cause. The prognosis of these patients is frequently very poor. The progressive dilatation leads to compression of the brain parenchyma. Ischemia, especially involving the perforating branches, can occur. Hemorrhage is uncommon (Little et al. 1981; Echiverri et al. 1989; Pessin et al. 1989), even though in some studies it has been reported as being not so rare (Flemming et al. 2004).

Giant aneurysms (Figs. 11.2, 11.4, 11.5, and 11.25) are very infrequent and can be found in the anterior circulation (cavernous, supraclinoid portion of the ICA, anterior and middle cerebral arteries) and posterior circulation (basilar artery and PCA aneurysm). They can grow in similar fashion to smaller lesions owing to the weakness of the wall and the effect of the blood flow. Sometimes, however, the growth is a result of intramural hemorrhage from rupture of the vasa vasorum. The hemorrhage and resultant thrombus can lead to a dissection of the wall, which acts as a triggering factor and stimulates additional proliferation of the vessel in the wall with further hemorrhage (Schubiger et al. 1987; Nagahiro et al. 1993; Katayama et al. 1991; Kaneko et al. 2001; Krings et al. 2007). This process also explains why the aneurysm continues to expand despite the fact that no patent lumen is present. Taking this into consideration, the ideal treatment should be complete surgical excision. This is, however, not always possible and is linked with high risks.

11.9 Diagnosis and Treatment

In patients with SAH, CT angiography can be a very useful diagnostic method instead of angiography. However, negative results, especially with small aneurysms near the base of the skull, do not exclude with certainty the presence of an aneurysm. MRI angiography can be employed as a screening method to detect aneurysms in particular groups of patients, such as those with polycystic kidney or with a family incidence of aneurysms. MRI angiography is not commonly used in the acute phase of SAH. Vessel angiography remains

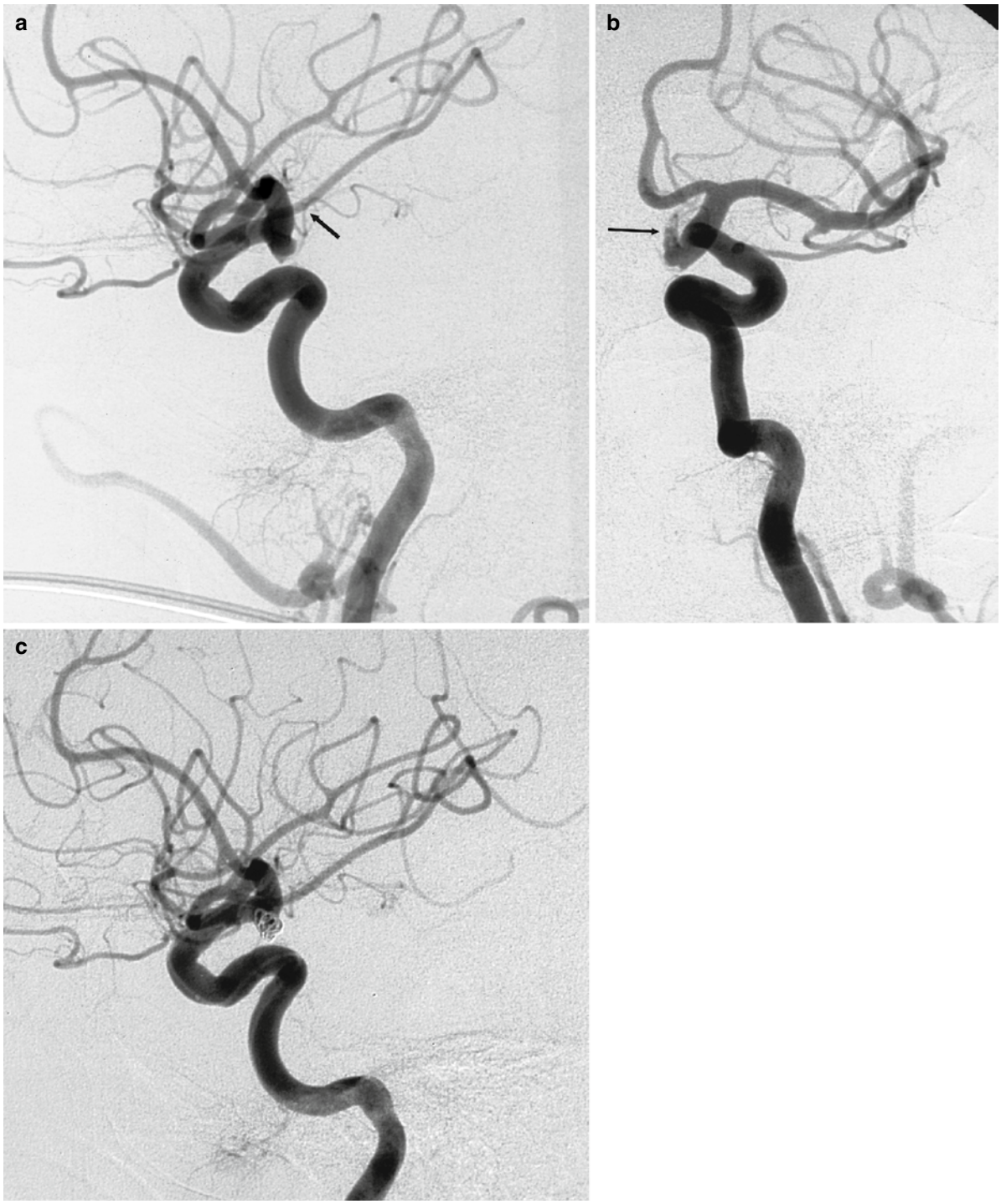

Fig. 11.9 Irregular ruptured aneurysm with neck close to the origin of the anterior choroidal artery (AChA). (**a**) Lateral carotid angiogram, showing the small aneurysm. AChA (*arrow*). (**b**) Oblique view better showing the irregular and elongated part (*arrow*) of the aneurysm. (**c**) Lateral carotid angiogram, post-treatment showing the occluded aneurysm with coils

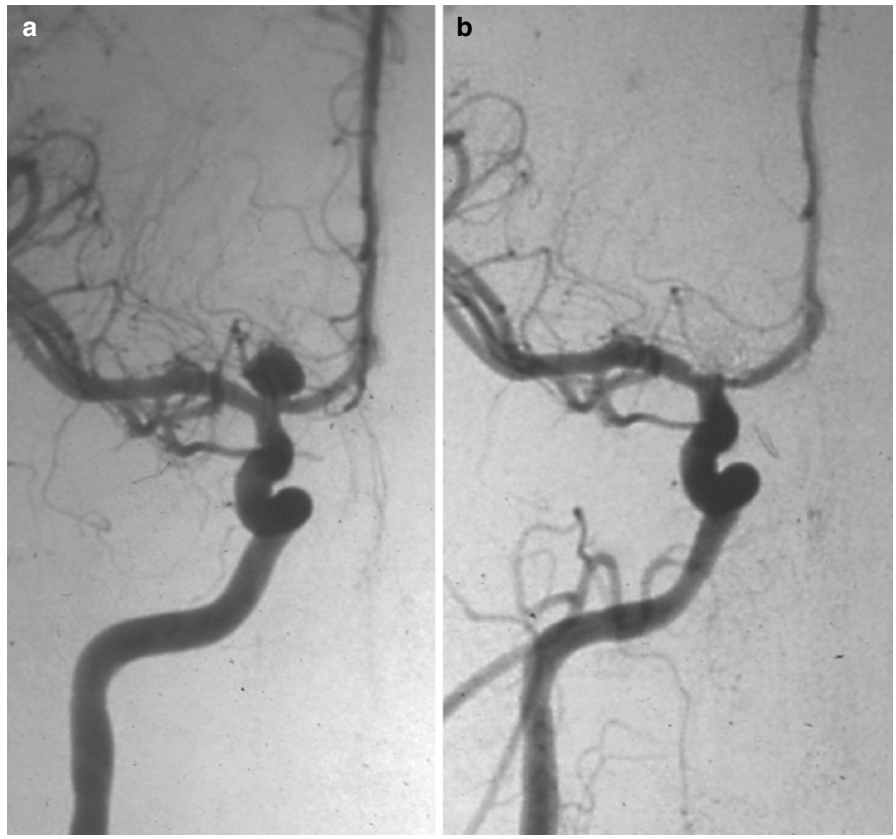

Fig. 11.10 Aneurysm of the distal carotid bifurcation, presenting with hemorrhage. (**a**) Carotid angiogram, AP view, showing the aneurysm. (**b**) Control angiogram showing the occluded aneurysm with coils

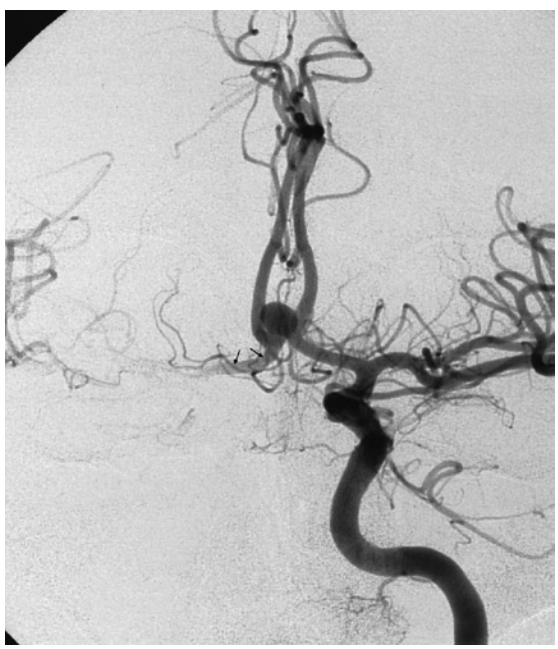

Fig. 11.11 Anterior communicating artery (AComA) aneurysm. Carotid angiogram, AP view. The right artery of Heubner (*arrows*) is evident. On the left, it cannot be identified with certainty owing to the presence of other branches

the gold standard that is to be performed every time there is an unclear diagnosis or if an endovascular treatment is being considered.

The introduction of the Guglielmi detachable coil in 1991 opened a new era in the treatment of cerebral aneurysms. Since then, the increasing quality of coils and microcatheters, the application in selected cases of new techniques (remodeling technique, Moret et al. 1997), and the more recent introduction of stents associated with coils and flow-diverter stents have progressively expanded the indications for endovascular treatment and brought about an improvement in the results (Moret et al. 1997; Boccardi et al. 1998; Molineux et al. 2002; Murayama et al. 2003a; Henkes et al. 2004; Gallas et al. 2005; Bradac et al. 2007; Kurre and Berkefeld 2008).

More problematic remains the treatment of giant and fusiform aneurysms. For these, different endovascular strategies can be applied: occlusion of the parent vessel with coils and balloon technology. This has been frequently used in paraclinoid ICA aneurysms with excellent results, provided that there is good collateral circulation at the circle of Willis. The technique

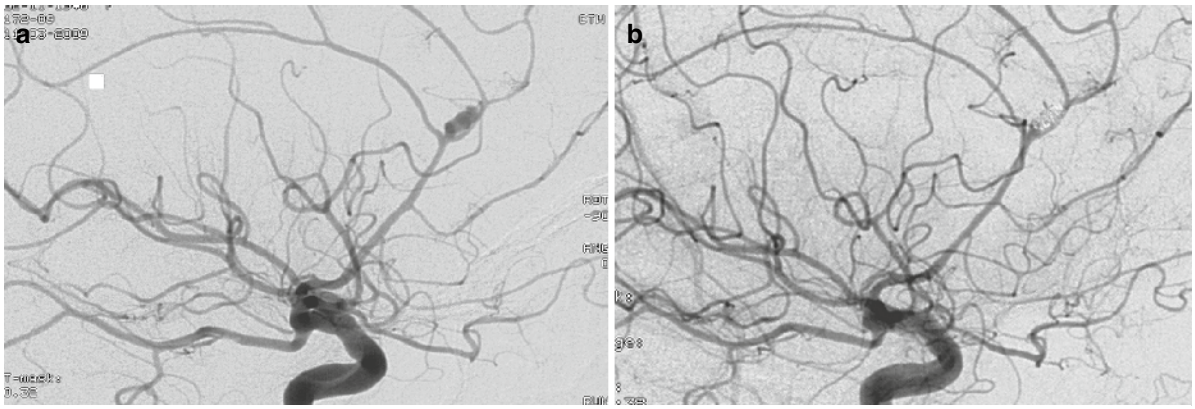

Fig. 11.12 (**a**) Lateral angiogram showing the typical site of a peripheral aneurysm of the ACA at the pericallosal-callosomarginal junction. (**b**) Control angiogram post-treatment with coils

is also useful in the occlusion of one VA, where the posterior circulation is guaranteed by the contralateral VA. In addition, more distal aneurysms can be treated with this method when a good leptomeningeal collateral circulation is present. If this is insufficient, the parent vessel occlusion can be preceded by bypass surgery (Van Roij and Sluzewski 2009). More recently, the introduction of stents, associated with coils and flow-diverter stents, has opened new way in the treatment of these lesions (Yang et al. 2007; Lubicz et al. 2008; Liebig and Henkes 2008; Gall and Nepper Rasmussen 2009; Chapot et al. 2009).

11.10 Unruptured Aneurysms

Modern diagnostic methods have revealed an increasing number of unruptured aneurysms, raising the question of whether they should be treated or not. The rupture of an aneurysm can have catastrophic clinical consequences for the patient. Technical improvements in surgery and endovascular treatment today mean that unruptured aneurysms can be treated and good results obtained, with a low rate of complications, though they are not completely excluded (Roy et al. 2001; Henkes et al. 2004; Bradac et al. 2007).

Some factors that can influence the decision have been reported in an international study (Wiebers et al. 2003) of unruptured aneurysms that appeared in *Lancet* (2003). According to this study, the risk of hemorrhage is low in aneurysms with a diameter of less than 7 mm, but it increases progressively with greater diameters. Independent of the diameter, the risk of rupture is greater in aneurysms of the posterior circulation and in patients who have already undergone treatment for another ruptured aneurysm.

In an attempt to clarify this matter, further studies have been performed related to the morphology of the aneurysm (irregular shape, multilobar, presence of blebs) as well as to the perianeurysmal environment. The latter involves constraints on the shape of the aneurysm that could favor its rupture (Rüfenacht 2005). Another factor could be the transmission of pressure and flow rates within the aneurysm, which are reported to be higher in bifurcation aneurysms than in the sidewall (Sorteberg and Farhoudi 2006). Postprocessing analysis of 3D visualization of the angiogram has shown the possible influence of the flow within the aneurysm being dependent on its location (Cebral et al. 2005) and also on its geometry, particularly when the aneurysm has a main axis parallel to the parent artery (Szikora et al. 2008).

In spite of such interesting findings, there is today no consensus for or against the preventive treatment of an unruptured aneurysm (Raymond et al. 2008). The decision still depends on the experience and attitude of the medical team involved and also on the emotional reaction of the patient who is aware of the pathology.

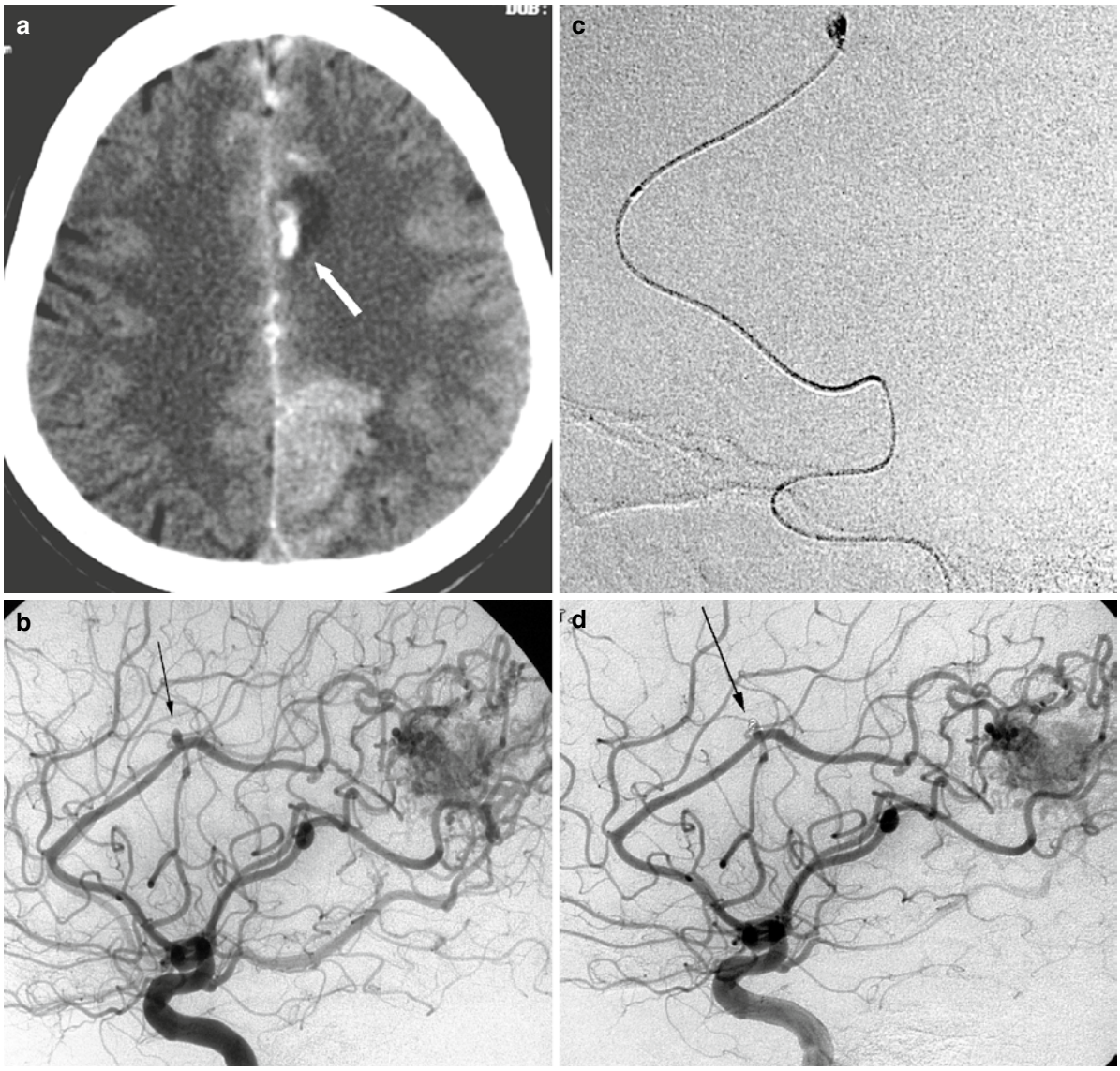

Fig. 11.13 Patient with known parietal arteriovenous malformation (AVM) presenting with minimal inter-hemispheric SAH and small hemorrhage involving the parenchyma not related to the AVM. (**a**) CT demonstrating the small hemorrhage with surrounding edema (*arrow*) (**b**). The angiography showed a small pericallosal, probably flow-dependent aneurysm (*arrow*). (**c**) Selective catheterization of the aneurysm occluded with coils. (**d**) Final control angiogram showing the occluded aneurysm (*arrow*)

11.11 Negative Angiograms in Patients with SAH

In about 15–20% of patients with SAH, the aneurysm is not detected on the angiogram. In some patients, particular in cases with a perimesencephalic pattern of bleeding, the SAH is frequently not due to the aneurysm (Rinkel et al. 1991). In other cases, the aneurysm can be definitely thrombosed at the time of the bleeding and thus no longer recognizable, even in later controls.

Vasospasm and large hematoma can temporarily hide the presence of an aneurysm that is demonstrated later. In rare cases, however, where no spasm or hematoma are present, the aneurysm is not visualized on the

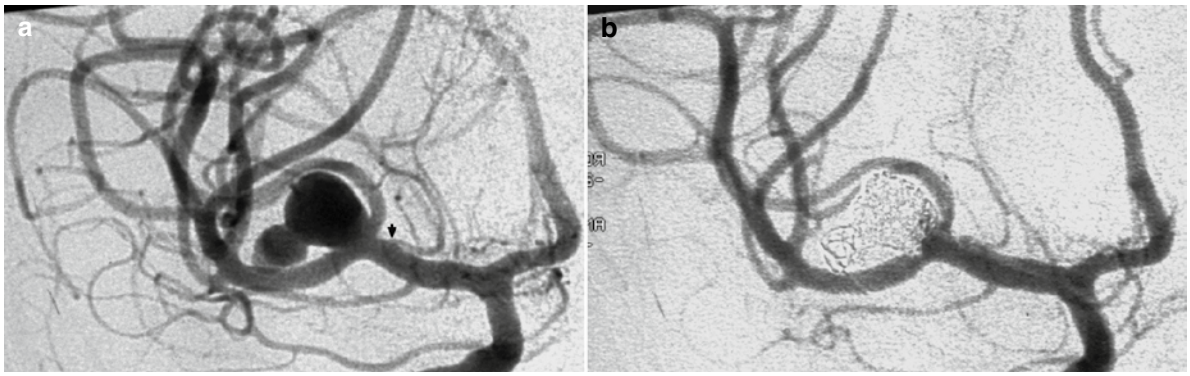

Fig. 11.14 Bilobated large saccular aneurysm at the MCA bifurcation, presenting with hemorrhage. Origin of the distal perforator close to the aneurysm (*arrow*). Pretreatment angiogram (**a**), post-treatment with coils (**b**)

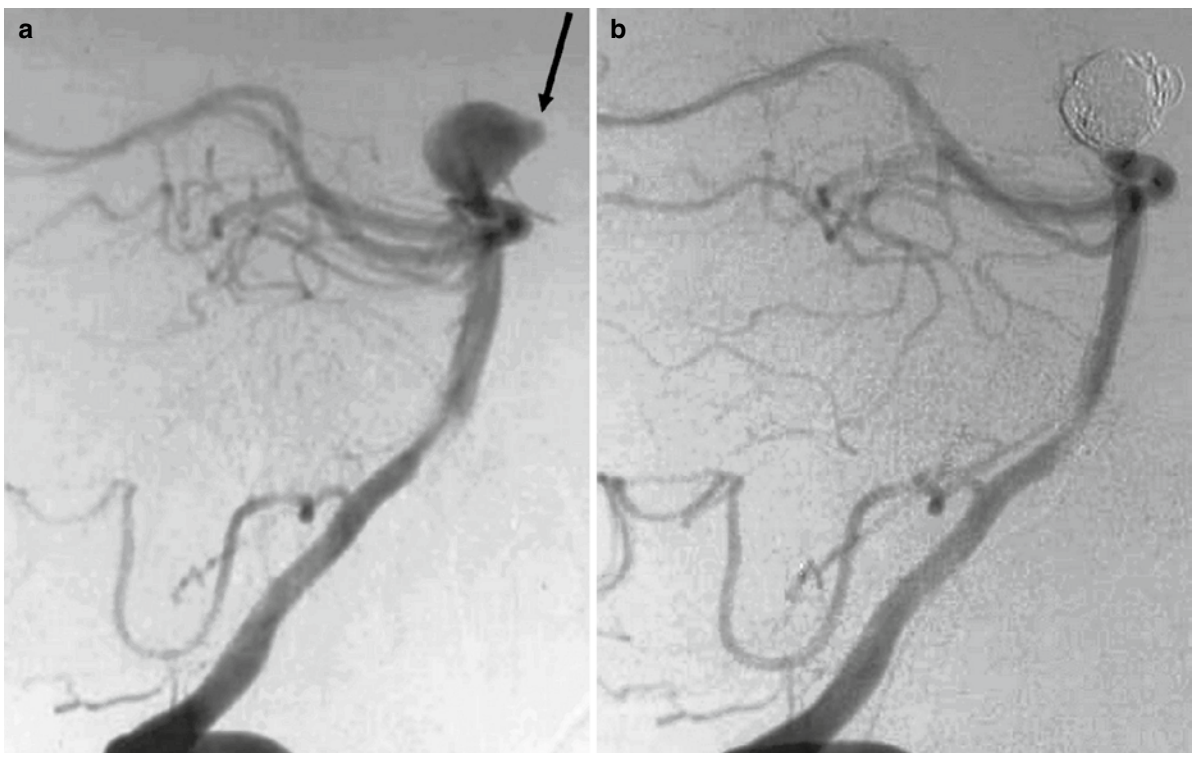

Fig. 11.15 Patient presenting with SAH. Vertebral angiogram (**a**) showing basilar tip aneurysm with a bleb (*arrow*) probably indicating the site of rupture. Control angiogram (**b**) post-treatment with coils

angiogram performed in the acute phase, but it can be detected one or two weeks later. This has been reported in about 10–19% of the cases in which the first angiogram was negative (Bradac et al. 1997; Urbach et al. 1998; Alves et al. 2005) (Fig. 11.27).

The cause of this phenomenon is not completely known. A temporary thrombosis of the aneurysm could occur. Other cases could be due to a dissection involving the wall of the artery responsible for the bleeding, but not recognizable on the angiogram. Later, this leads to the

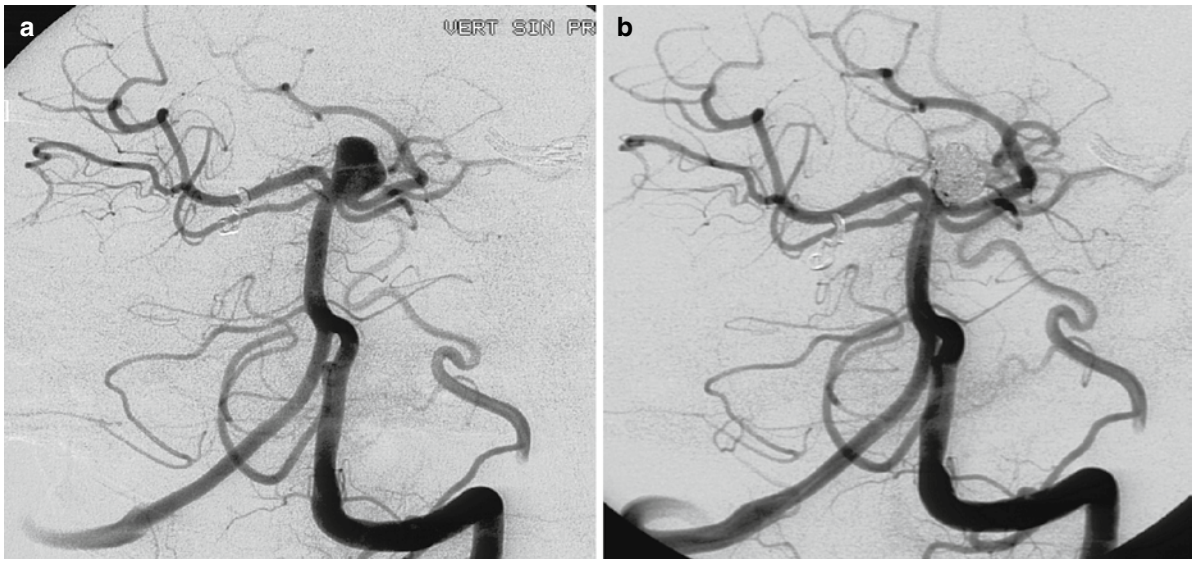

Fig. 11.16 Nonruptured basilar tip aneurysm with a neck involving partially also the left P1 segment. The patient had already been treated for a ruptured aneurysm of the AComA. (**a**) Angiographic study pretreatment. (**b**) Control angiogram post-treatment. Occlusion with coils and stent

formation of an aneurysm. This probably occurs in the so-called blister aneurysms of the dorsal wall of the ICA.

11.12 Vasospasm

This is a frequent complication of SAH, with an incidence as high as 70% of cases. Among them, symptomatic ischemia occurs in about 35% (Wintermark et al. 2006; Komotar et al. 2007; Hänggi et al. 2008). Symptomatic ischemia can occur in every SAH, but younger patients and those with a severe hemorrhage, visible on CT, are more at risk of developing vasospasm.

Diagnosis. All patients with SAH should be closely monitored for vasospasm in the days after SAH. This can be done using daily transcranial Doppler (TCD), followed on the third or fourth day by CT and perfusion CT whenever the TCD shows an increased velocity (more than 120–130 cm/s), especially when this occurs over a short period of time. Independently of and/or in association with these technical controls, every clinical worsening of the patient that is not due to rebleeding or hydrocephalus, excluded by CT examination, can be an indirect sign of spasm. In all these cases, angiography should be performed, followed by confirmation of vasospasm by endovascular therapy.

Therapy. Medical therapy consists of prophylactic nimodipine, oral or intravenous, depending on the grade of risk for a given patient. Nimodipine is a calcium antagonist that acts by reducing the constriction of smooth muscle and by decreasing the release of vasoactive factors from the endothelium and platelets (Pickard et al. 1987). In many centers, this is associated with monitored hypertensive, hypervolemic, and hemodilution ("triple-H") therapy. With confirmed spasm on angiography, the most used therapy today is the injection of nimodipine into the ICA uni- or bilaterally at a dose of 1–2 mg per vascular territory (Fig. 11.28). Selective injection in the A1-M1 segments can be useful in certain cases as well as injection into the vertebrobasilar sector. A partial or complete resolution is obtained in 60–70% of cases (Boker et al. 1985; Bracard et al. 1999; Biondi et al.

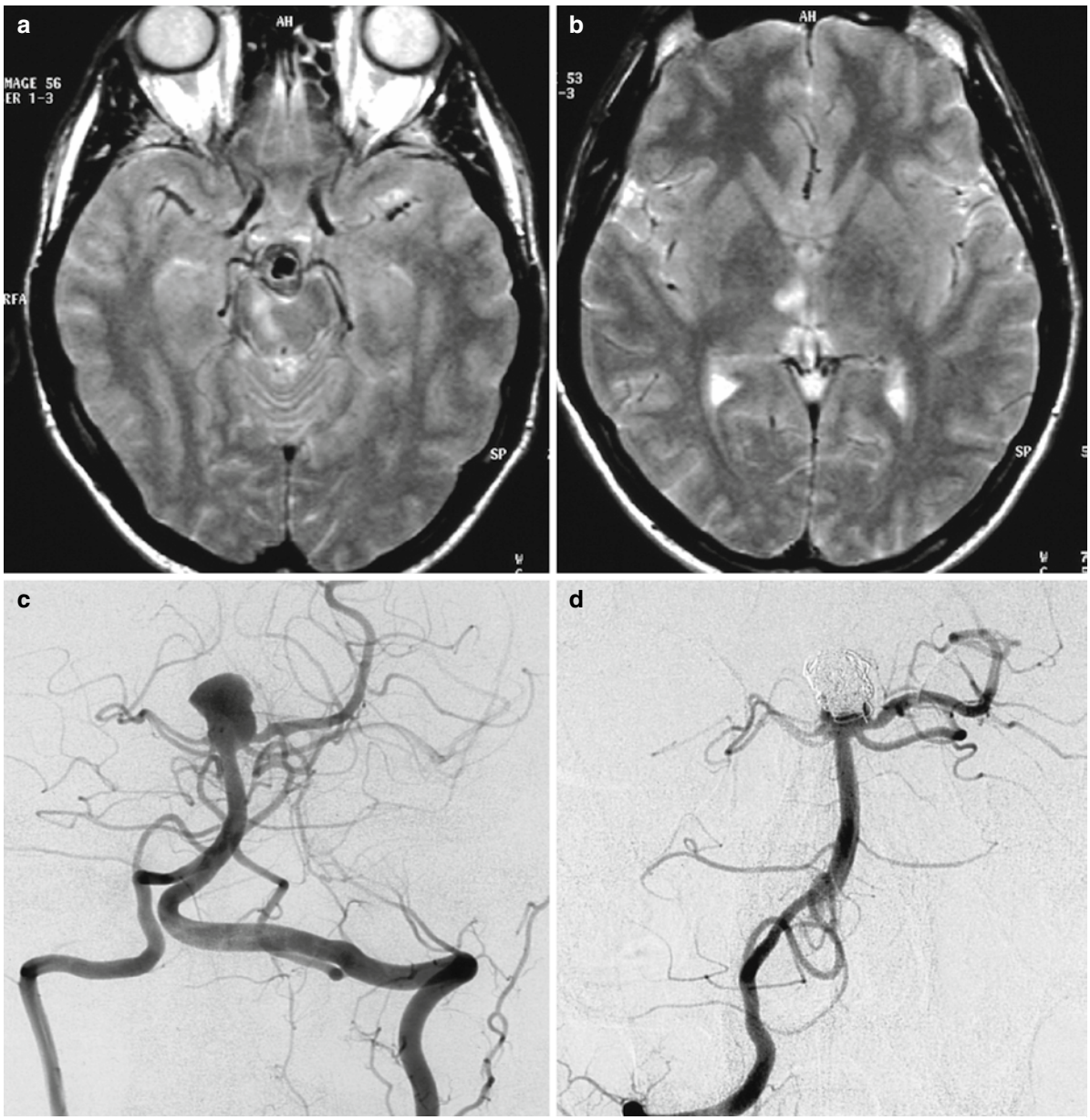

Fig. 11.17 A 40-year-old man with acute midbrain-thalamic syndrome. On MRI (**a**, **b**) small ischemic lesions were recognizable in the medial midbrain and medial thalamus on the right, corresponding to the vascular territory of perforators arising from the P1. A large basilar tip aneurysm, probably responsible for the thromboembolic occlusion of the homolateral P1 was diagnosed (**c**). The patient recovered and was treated endovascularly a week later (**d**)

2004; Bandeira et al. 2007; Hänggi et al. 2008). The resolution of the spasm may be only temporary, and so a second or additional administrations can be necessary over the following days (Biondi et al. 2004). In selected cases of severe spasm not responsive to nimodipine, balloon angioplasty of the distal segment of the ICA (A1-M1 segment) can be performed. Improvements in the endovascular material make it possible today to perform this treatment with a low risk (Murayama et al. 2003b).

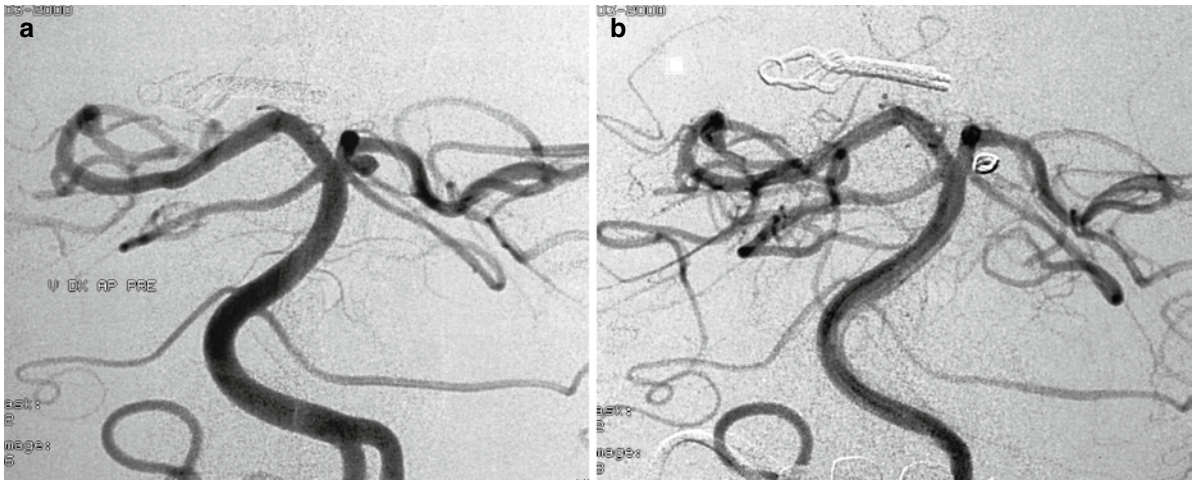

Fig. 11.18 A patient already operated on for an AComA aneurysm. A second aneurysm was present at the junction of the left PCA and SCA. Vertebral angiogram (**a**). Control angiogram (**b**), post-coiling

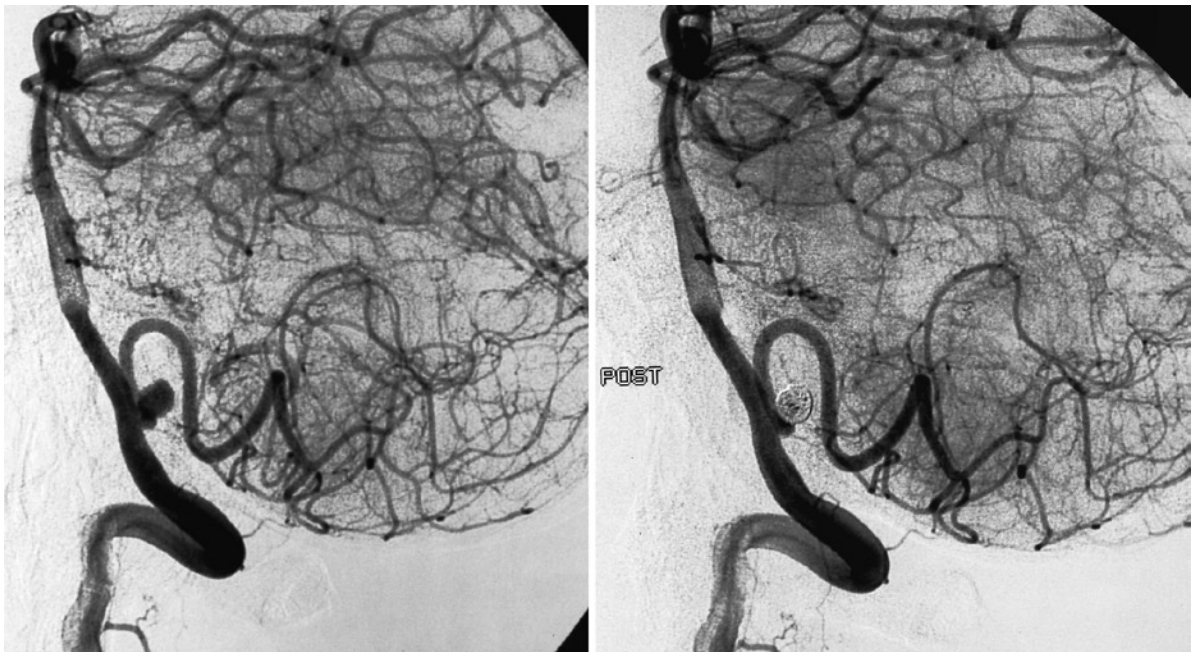

Fig. 11.19 Typical vertebral-posterior inferior cerebellar artery (PICA) junction aneurysm in a patient with SAH, pre- and post-treatment with coils

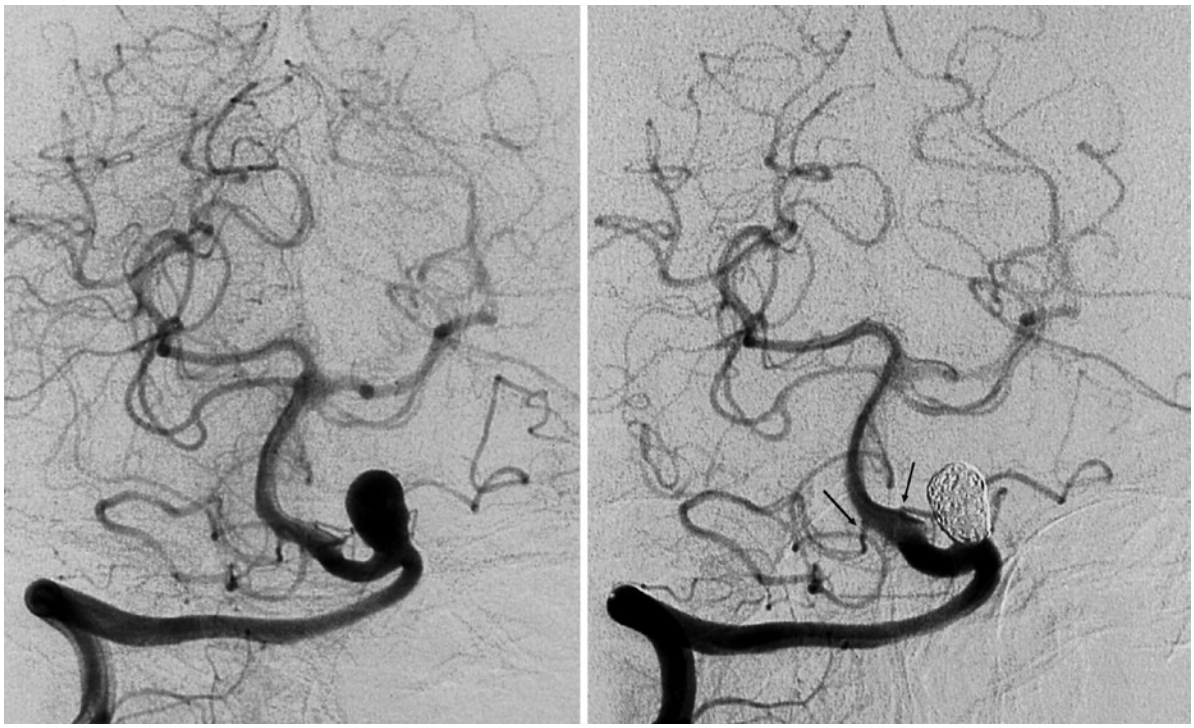

Fig. 11.20 Large unruptured aneurysm in a young patient. There was a well-developed right vertebral artery and a hypoplastic left vertebral artery. The aneurysm was located at the junction of the vertebral artery with a hypoplastic left PICA. There was a bilateral well-developed anterior inferior cerebellar artery (AICA; *arrows*), supplying the vascular territory of both PICAs. Right vertebral angiogram pre- and post-treatment with coils

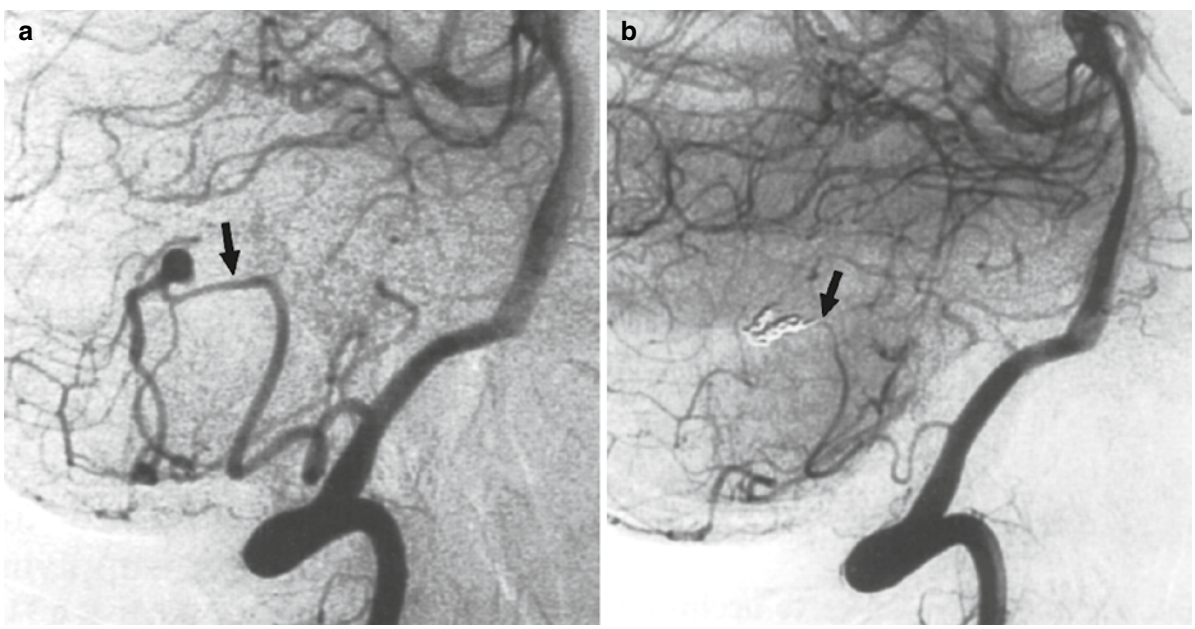

Fig. 11.21 Aneurysm of the supratonsillar segment of the PICA presenting with hemorrhage. (**a**) Vertebral angiogram showing the aneurysm. Supratonsillar segment (*arrow*). There is also a dilatation of the retrotonsillar segment of the PICA distal to the aneurysm, suggesting dissection. (**b**) Post-treatment angiogram with occlusion of the aneurysm with coils and of the PICA in the supratonsillar segment (*arrow*). The patient recovered completely

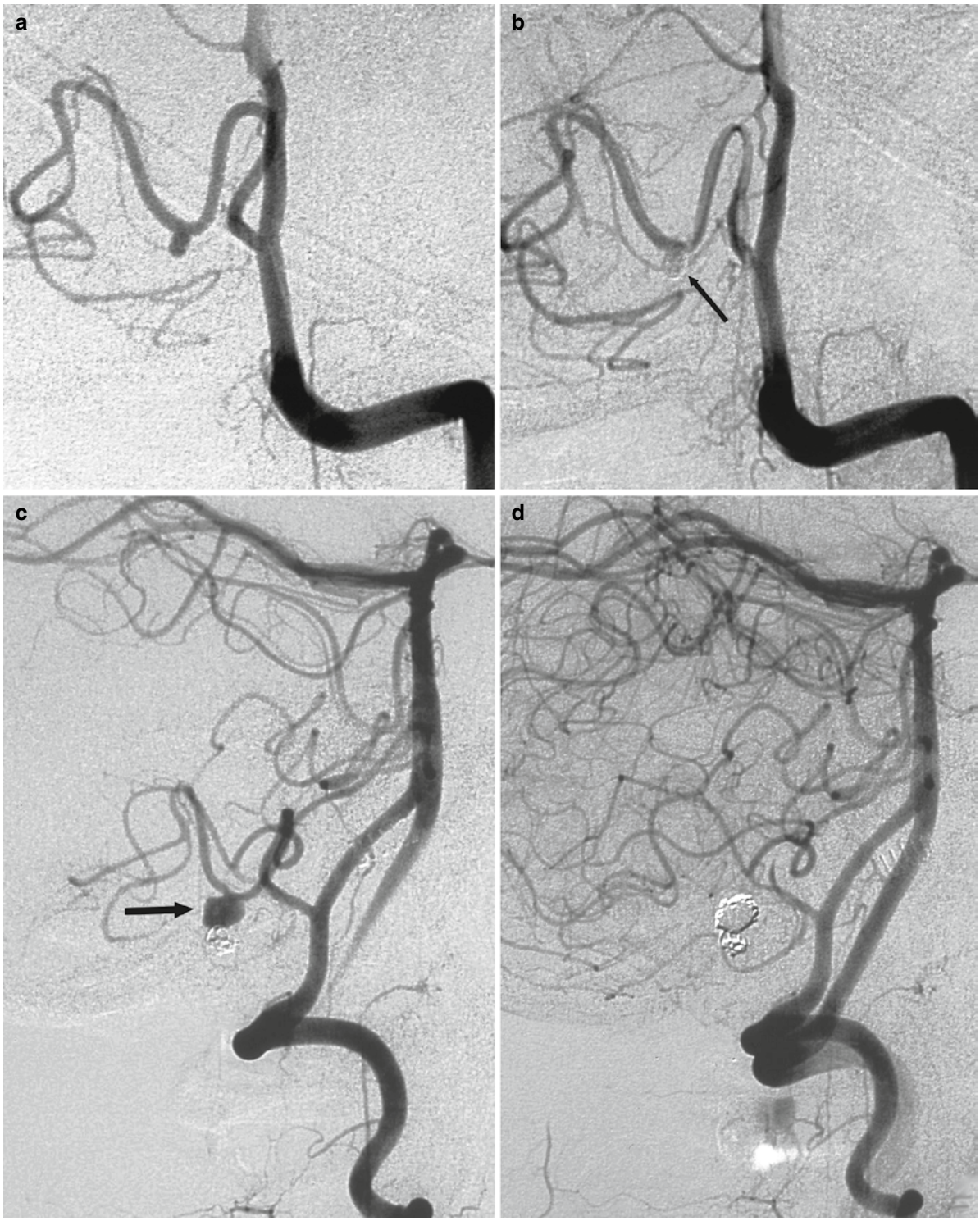

Fig. 11.22 Aneurysm of the pretonsillar segment of the PICA presenting with hemorrhage. Pretreatment vertebral angiogram (**a**) presenting the aneurysm and post-treatment angiogram (**b**) showing its occlusion with coils (*arrow*). Two months later, the patient was admitted again owing to a new hemorrhage. The angiogram (**c**) showed regrowth of the aneurysm (*arrow*), which probably was originally a dissecting aneurysm. Occlusion of the aneurysm and of the parent artery was performed (**d**). The patient recovered completely

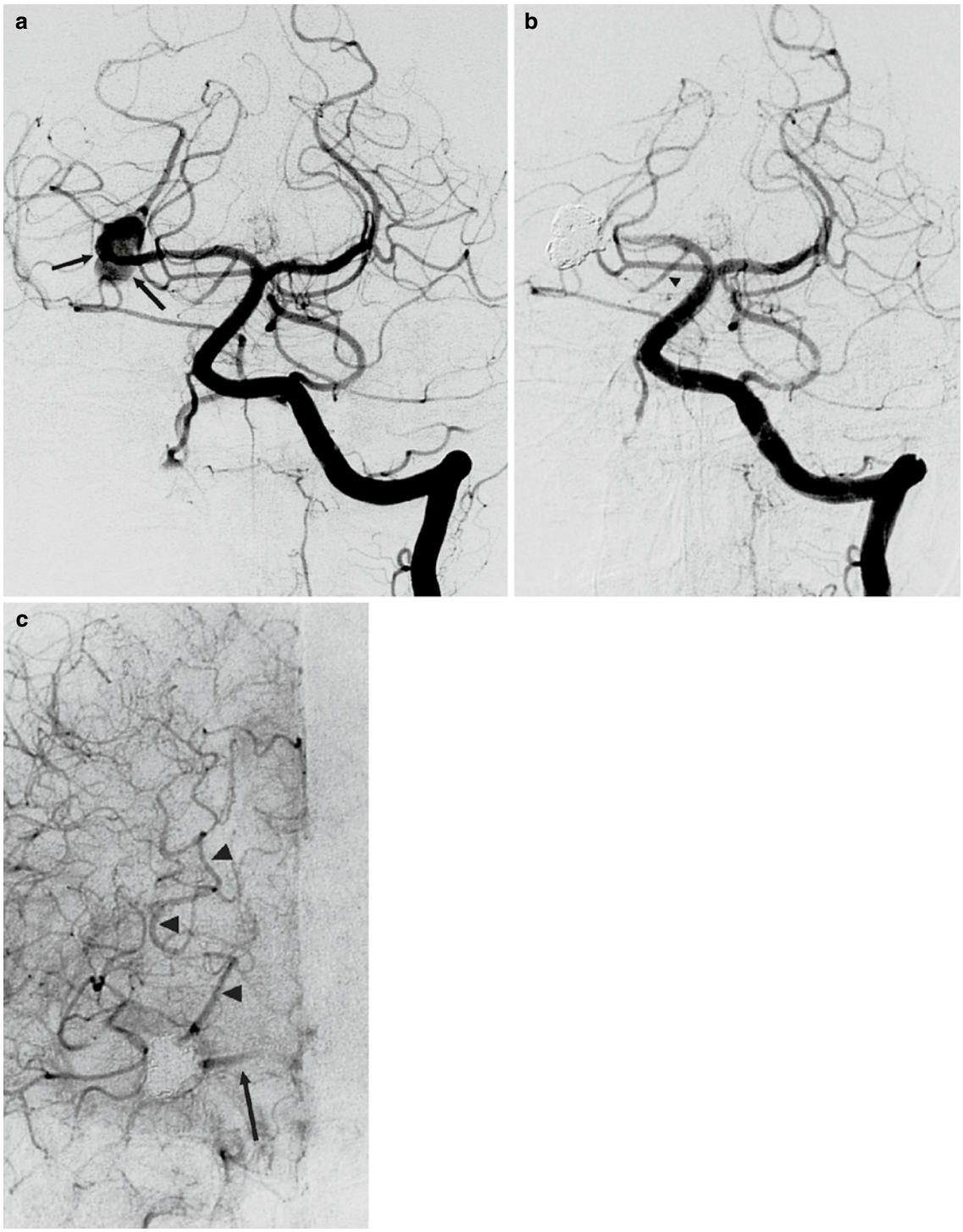

Fig. 11.23 Unruptured irregular, probably dissecting aneurysm involving the P2 segment of the right PCA in a patient presenting with a transient episode of hemianesthesia. Left vertebral angiogram (**a**) showing the aneurysm (*arrows*). Post-treatment angiogram (**b**) with occlusion of the aneurysm and the P2 segment of the PCA. Note the posterior communicating artery (*arrowhead*). Carotid angiogram (**c**) with retrograde injection of the posterior cerebral artery up to the aneurysm (*arrowheads*). Through leptomeningeal anastomosis between the MCA and PCA. There is also injection of the proximal P2 (*arrow*) through the posterior communicating artery. The patient tolerated the treatment well despite a small ischemic lesion in the lateral thalamus owing to involvement of the thalamogeniculate artery, as demonstrated by MRI

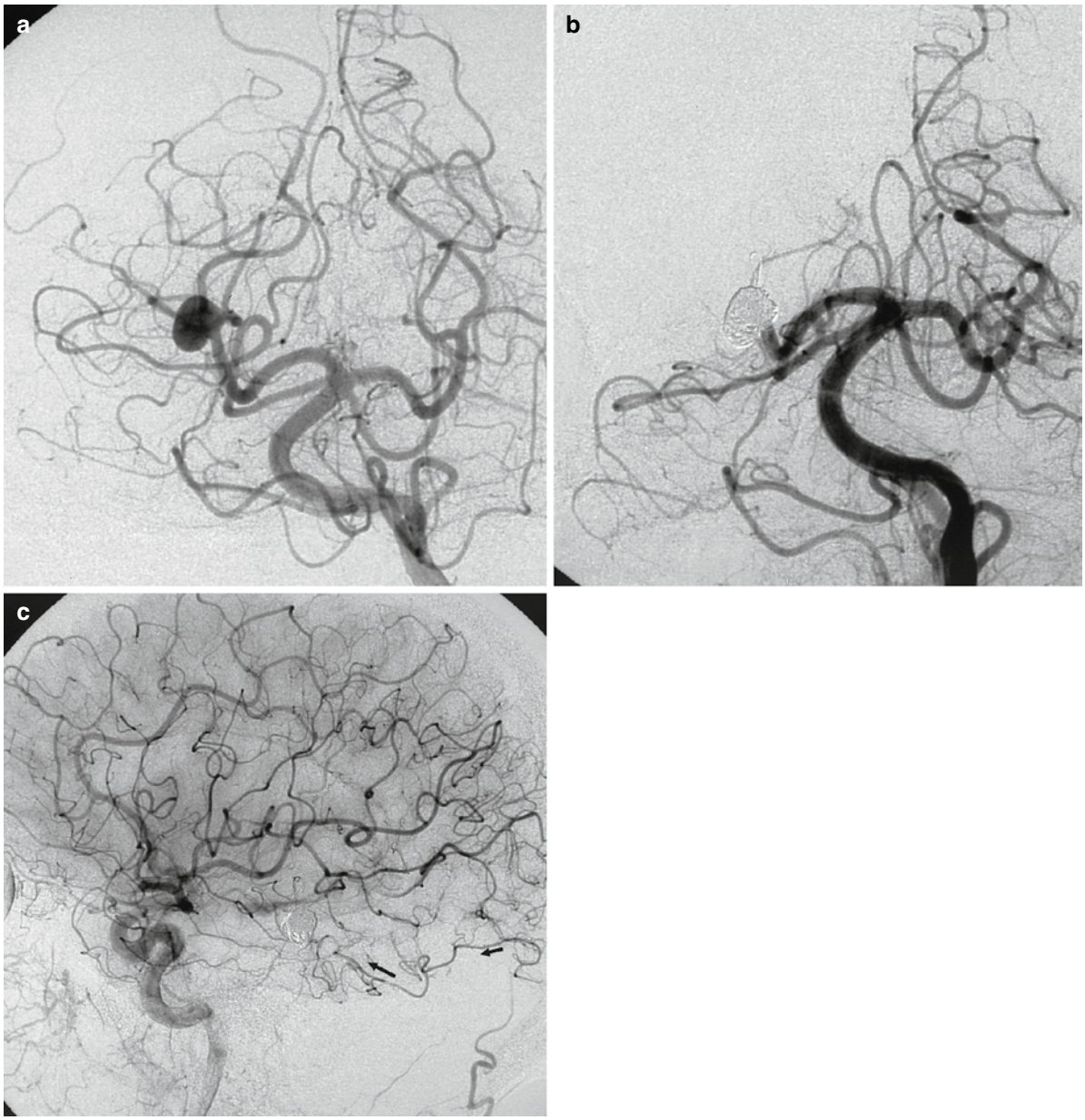

Fig. 11.24 Unruptured aneurysm without a defined neck in a young patient. (**a**) Left vertebral angiogram, showing the aneurysm at the P2 segment of the right PCA. (**b**) Control angiogram after occlusion of the aneurysm and the parent artery. (**c**) Carotid angiogram. Retrograde injection of distal branches of the PCA (*arrows*) through opening of a leptomeningeal anastomosis with branches of the MCA

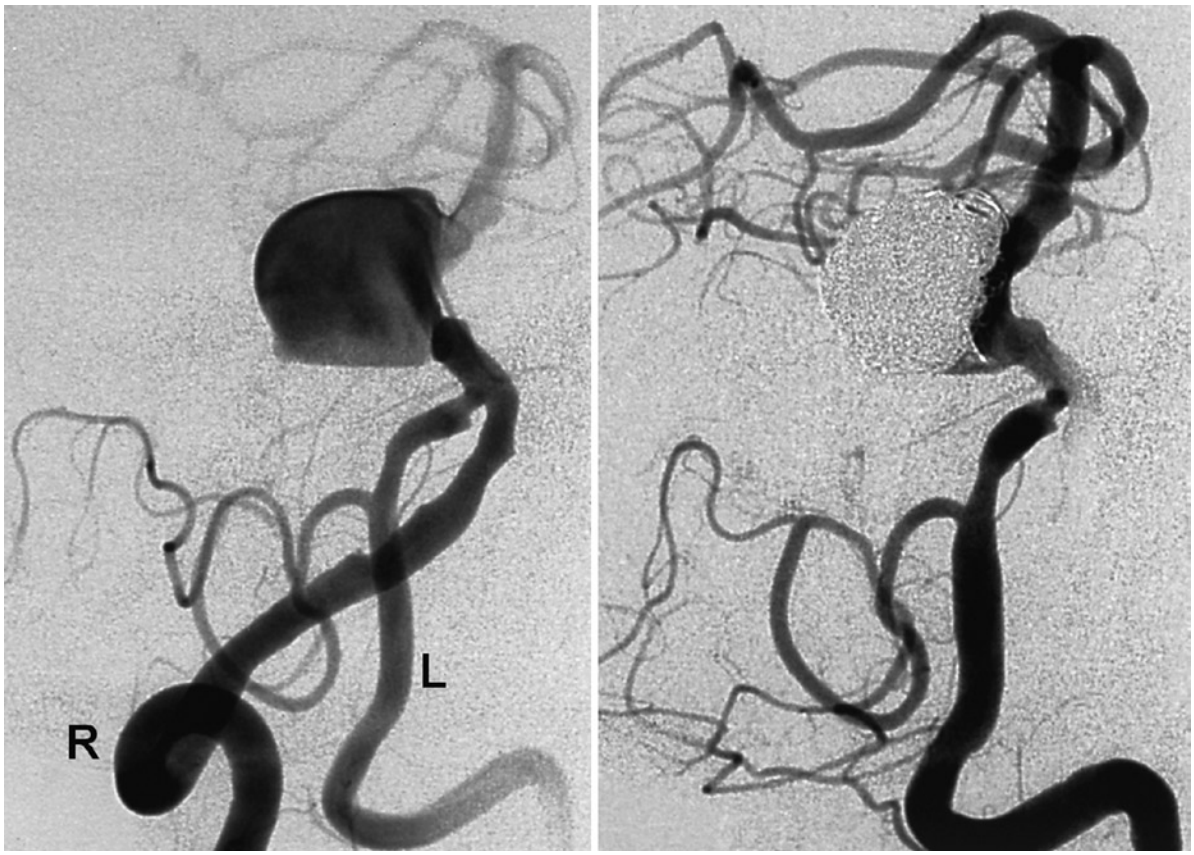

Fig. 11.25 Giant aneurysm of the middle basilar artery presenting with brainstem syndrome in an older patient. The aneurysm was probably dissecting. The angiogram showed in addition several irregularities of the wall of the vertebral and basilar arteries owing to atheromasia. Left and right vertebral artery (L and R) pre- and post-treatment with occlusion using coils supported by balloon (remodeling technique). The clinical symptoms improved

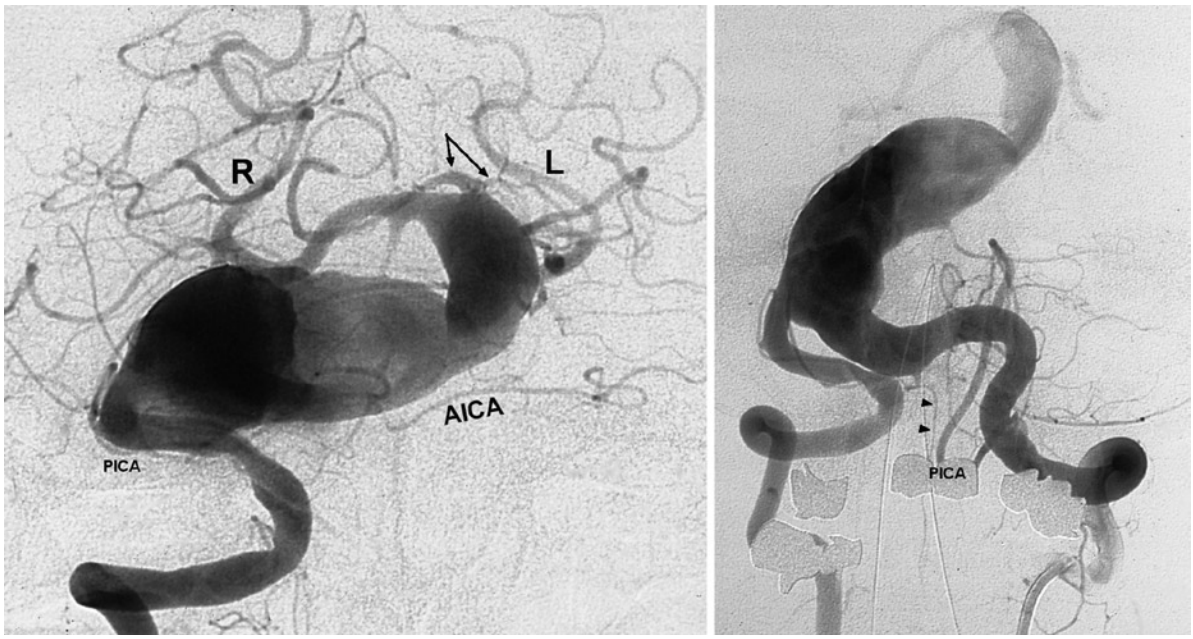

Fig. 11.26 Patient presenting with progressive tetraplegia due to giant fusiform aneurysm of the basilar artery compressing the brainstem. Left and right vertebral angiogram. The left and right PCA are well recognizable (L and R) as is the right superior cerebellar artery (*arrow with angle*). That on the left is very small. AICA on the left. Well-developed PICA on the left and small PICA on the right. Anterior spinal artery (*arrowheads*). Occlusion of the left vertebral artery with a balloon, proximal to the PICA, was performed to reduce the flow in the aneurysm. There was a partial clinical improvement, followed by a severe fatal subarachnoid hemorrhage 1 month later

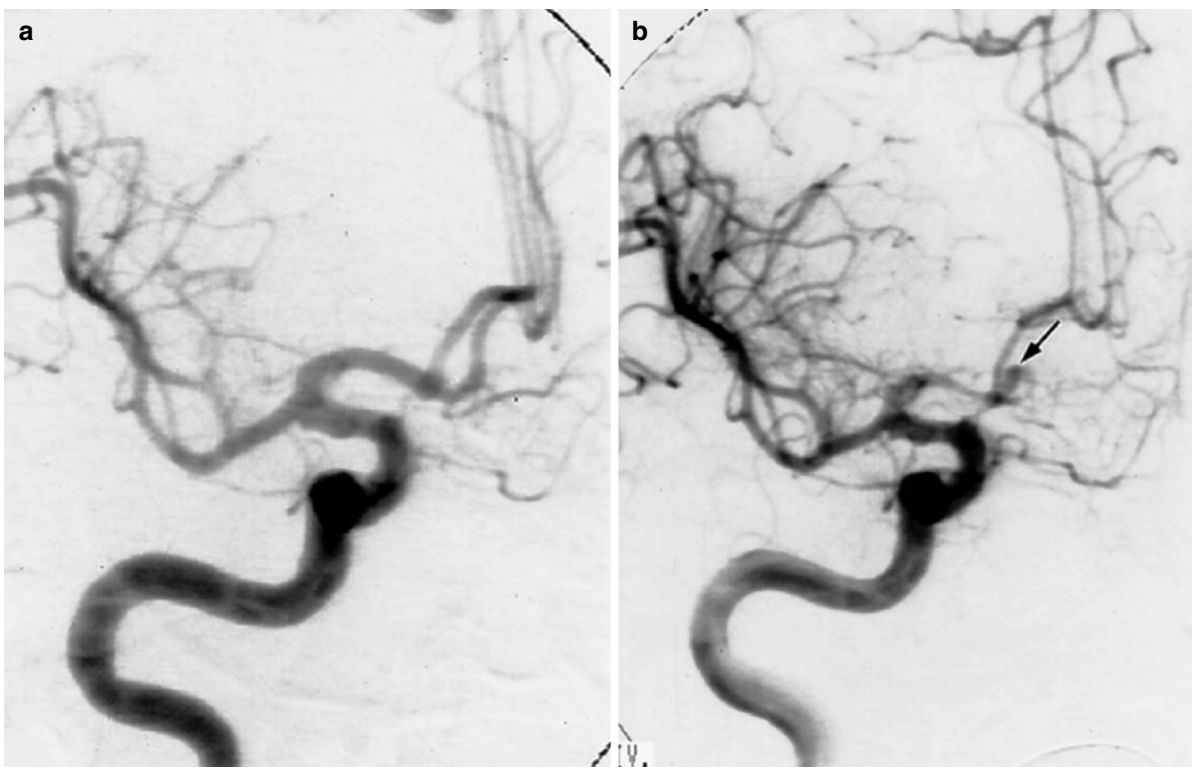

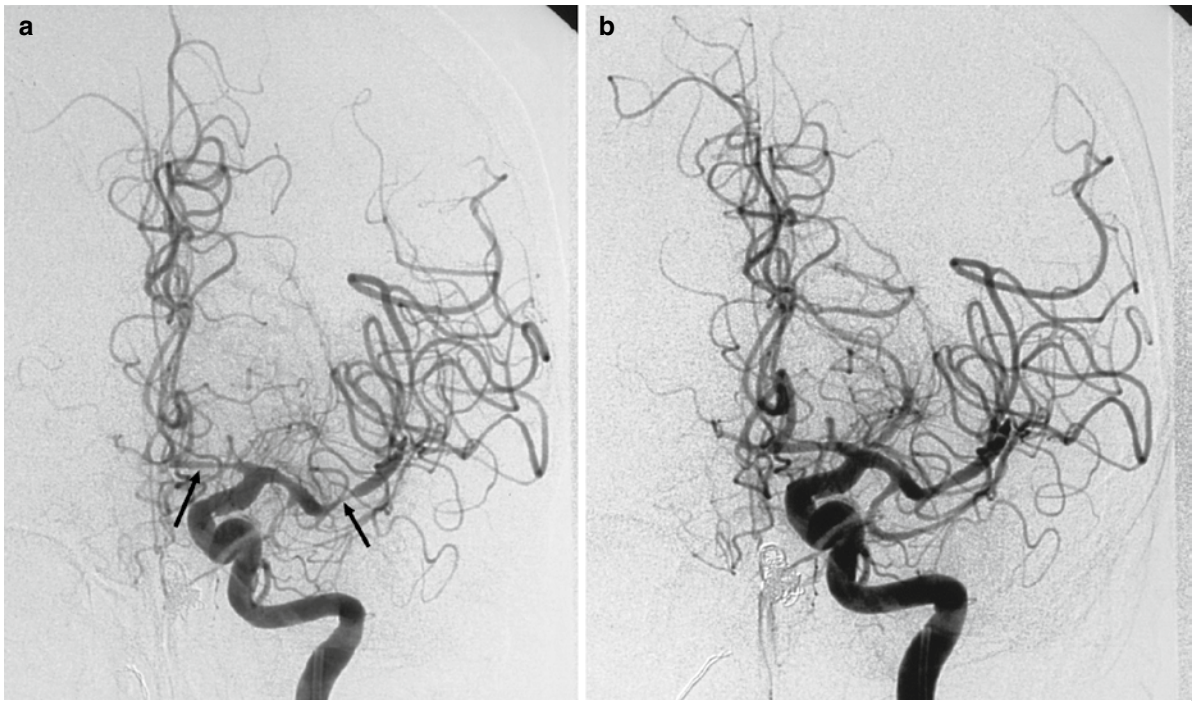

Fig. 11.28 Middle-aged patient with severe SAH due to rupture of a PICA aneurysm that was occluded with coils. The asymptomatic patient deteriorated a few days later owing to severe spasm involving, in particular, the anterior circulation. Left carotid angiogram (**a**) showing the severe spasm involving the A1 and M2 segments (*arrows*). Also, minimal spasm of the M1 segment. A similar pattern was seen on the right. The patient was treated with an injection of nymodipine in the ICA, with excellent angiographic results, demonstrated on the left angiogram (**b**). Similar result on the right

11.13 Aneurysms in Children

Intracranial aneurysms in children are rare. They differ from those in adults in the localization, etiology, and clinical presentation. They are more frequent in boys, whereas among adults there is a predominance among women. This seems to indicate a gender influence (Ostergaard and Voldby 1983; Laughlin et al. 1997; Proust et al. 2001; Lasjaunias et al. 2005; Huang et al. 2005). The commonest site is reported to be the ICA (cavernous portion, carotid bifurcation) (Heiskanen 1989; Laughlin et al. 1997; Proust et al. 2001; Huang et al. 2005). A relatively high frequency also of aneurysms of the basilar and PCA has been reported (Meyer et al. 1989; Huang et al. 2005). At the time of diagnosis, the aneurysm is frequently large, with clinical symptoms frequently not due to hemorrhage but to the mass effect (Lasjaunias et al. 2005).

Unlike in adults, a frequent cause of aneurysms in children is trauma, even minor (Yazbak et al. 1995; Ventureyra and Higgins 1994). Other causes are infectious, collagen diseases, hemoglobinopathies as well as a family history of aneurysm (Ostergaard and Voldby 1983; Roche 1988; Meyer et al. 1989; Pasqualin et al. 1986). More recently, spontaneous dissection has been increasingly recognized as a cause of cerebral aneurysm in children (Laughlin et al. 1997; Massimi et al. 2003; Lasjaunias et al. 2005; Vilela and Goulão 2006; Bradac et al. 2008a) (Fig. 16.12).

Fig. 11.27 Middle-aged woman with SAH, in which a complete angiographic study did not reveal a vascular malformation. A second SAH occurred 2 weeks later. The angiographic study then revealed the aneurysm. (**a**) First right carotid angiogram. (**b**) Repeated angiogram showing the AcomA aneurysm (*arrow*). There was also a minimal spasm involving the A1 and A2 segment of the right anterior cerebral artery

Vascular Malformations of the Central Nervous System

12

12.1 Introduction

It was Virchow (1862–1863) who first differentiated tumors from brain angiomas, which were identified as vascular malformations of congenital derivation. The concept that brain arteriovenous malformation (BAVM) is an anomaly caused by errors during vascular development in the embryo was suggested by Cushing and Bailey (1928) and Dandy (1928). However, some difficulties in the differential diagnosis between BAVMs and tumors remained, as noted by Zülch (1957) and Russell et al. (1959). An accurate description of this pathology as a definite congenital malformation was proposed by McCormick (1966). The same author made a classification, which, with some modification (Challa et al. 1995; Yaşargyl 1987, 1999; Chaloupka and Huddle 1998; Valavanis et al. 2004), is still valid today.

12.2 Classification

- Arteriovenous malformation (AVM)
- Vein of Galen AVM
- Cavernous malformations (cavernomas)
- Capillary malformations (telangiectasias)
- Developmental venous anomaly (DVA), venous angiomas
- Transition forms
- Vascular malformations part of well-defined congenital-hereditary syndromes
- Rendu–Osler Syndrome
- Sturge–Weber Syndrome
- Wyburn–Mason Syndrome
- Klippel–Trenaunay–Weber Syndrome

12.3 Arteriovenous Malformations

12.3.1 Pathogenesis and Pathology

The certain pathogenesis of AVMs is not clear. They are considered to be congenital malformations. When considering the embryological development of the cerebral arteries and veins, some authors (Mullan et al. 1996a, 1996b) have suggested that AVMs could already be present before the third month of gestation. In some cases, an AVM may be relatively small at birth and grow later. There are, however, reports describing the appearance of cerebral AVMs later in life among patients in whom previously performed magnetic resonance imaging (MRI) showed no malformations. In some of these patients, cerebral AVMs occurred in the pathologically altered brain as a result of different causes, such as vascular pathology (Schmit et al. 1996; Song et al. 2007), heterotopia (Stevens et al. 2009), and changes after radiosurgery (Rodriguez-Arias et al. 2000); in others, the brain parenchyma was completely normal (Gonzalez et al. 2005; Bulsara et al. 2002). These observations raise doubts about the congenital nature of cerebral AVMs, which—at least in some cases—seem to be acquired lesions caused by different nonspecific insults on the brain.

The main angioarchitectural characteristic of an AVM is an area called the nidus, in which a direct shunting between arteries and veins occurs without interposed capillaries. The elevated intravascular flow leads to changes of the vessels. Histology shows the nidus to be composed basically of dilated arteries and veins. In some vessels, the wall structure is still recognizable, characterized by the presence of a media with smooth muscle cells and an elastic lamina in the arteries and an absence of muscle cells in the veins. In other

G.B. Bradac, *Cerebral Angiography*,
DOI: 10.1007/978-3-642-15678-6_12, © Springer-Verlag Berlin Heidelberg 2011

arteries, prominent changes, characterized by areas of wall thickening caused by proliferation of fibroblasts, muscle cells, and an increase in connective tissue, are present. Segments with a thinning of the wall also occur, which potentially can lead to aneurysm formation. Severe changes take place in the venous sector, forming so-called arterialized veins, characterized by wall thickening, which is particularly due to fibroblast proliferation, not smooth muscle cells. The interposed parenchyma shows gliosis, hemosiderin pigmentation, and calcifications, resulting from ischemia or previous hemorrhages. The surrounding parenchyma may appear normal or show similar changes (Challa et al. 1995; Kalimo et al. 1997; Brocheriou and Capron 2004).

12.3.2 Incidence

The incidence of AVMs is not completely known. In general autopsy, they are discovered with a frequency of 0.15–0.8% (McCormick 1984; Jellinger 1986). Multifocal lesions can occur with a frequency of 1–10% (Perret and Nischioka 1966; Rodesch et al. 1988; Willinsky et al. 1990). The latter are more frequent in pediatric patients, where they are reported to be twice as common as in adults (Rodesch et al. 1988; Lasjaunias 1997).

12.3.3 Clinical Relevance

Of AVMs, 5–10% remain asymptomatic and are diagnosed incidentally by computed tomography (CT) or MRI investigations performed for other reasons. Some 40–50% present with intracranial hemorrhage, 30% with seizures, 10–15% with headaches, and 5–10% with neurological deficits (Perini et al. 1995; Stapf et al. 2002; Hofmeister et al. 2000; Valavanis et al. 2004). The incidence of symptomatic cerebral malformation in the adult population is reported to be one-tenth the frequency of intracranial aneurysm (Berenstein and Lasjaunias 1992; Valavanis et al. 2004). The most important risk in AVM is hemorrhage, which is calculated to be 2–4% per year, with an annual rate of mortality of 1% and severe morbidity of 1.7% (Graf et al. 1983; Crawford et al. 1986; Ondra et al. 1990; Mast et al. 1997). The risk of a repeated hemorrhage after an initial episode is reported to increase in the first year, later decreasing until it reaches the level of the initial risk (Graf et al. 1983; Mast et al. 1997). It is the most frequent initial symptom in children (Berenstein and Lasjaunias 1992; Rodesch et al. 1995; Lasjaunias 1997).

12.3.4 Location

The majority of AVMs (85%) are located in the supratentorial area, and only 15% are infratentorial (Perret and Nischioka 1966; Yaşargyl 1999). Supratentorial AVMs can be further divided (Valavanis et al. 2004): neopallial, including AVMs in the frontal, parietal, temporal, and occipital lobes and corpus callosum; and archi- and paleopallial, including those in the limbic and paralimbic system (amigdala, hippocampal, parahippocampal, septal, gyrus cinguli, and insular AVMs). AVMs can be located in a sulcus (sulcal), gyrus (gyral), or both (sulco-gyral). They can remain superficial or extend deeply toward the ventricle, basal ganglia, and thalamus. AVMs involving primary deep structures or ventricles are rarer. They are more frequent in pediatric patients (Berenstein and Lasjaunias 1992).

Infratentorial AVMs can be divided into those involving the cerebellum (hemisphere, vermis), located on the super–inferior convexity, or on its anterior surface. Deep structures can be primarily involved or be an extension of a superficial lesion. Primary AVMs in the brainstem are very rare, as are those of the fourth ventricle (Garcia Monaco et al. 1990; Liu et al. 2003).

12.3.5 Diagnosis

MRI, including functional studies, has provided information about the site and extension of AVMs. Furthermore, shows which functional changes have occurred in the affected and unaffected hemisphere (Alkadhi et al. 2000). Angiography is essential in defining the angioarchitecture of the AVM. Both investigations are today essential to obtain the necessary information in planning therapy (surgery, endovascular treatment, radiosurgery) (Spetzler and Martin 1986; Berenstein

and Lasjaunias 1992; Valavanis 1996). Angiographic study comprises selective angiography of the internal and external carotid arteries and the vertebral artery, followed, when necessary, by super-selective examinations aimed to characterize the supplying arteries, venous drainage, and aspects of the nidus.

12.3.5.1 Supplying Arteries (Feeders)

These can be fairly dilated and tortuous, unique or multiple, and arise from one or more vascular territories. Cortical branches are involved in superficial AVMs. Perforators (deep–medullary arteries) and choroidal arteries can be recruited every time deep structures and ventricles are affected (Figs. 12.3, 12.7, and 12.9).

Each feeder can end in the nidus, connected through one or more small branches with one or more venous channels, in various combinations (Houdart et al. 1993), forming what is termed the plexiform aspect of the nidus (Figs. 12.1 and 12.2). Otherwise, after giving branches to the AVM, the feeders continue distally to supply the normal parenchyma. On an angiogram, they appear to end in the nidus, though they do in fact run further distally. The distal part, however, is not always recognizable, owing to the steal phenomenon present in the nidus. In other cases, a large artery running adjacent to the nidus can give some small branches to the nidus en passage feeders, coursing further to the normal parenchyma (Figs. 12.5 and 12.6). All these aspects should be carefully studied with selective injections since embolization of these feeders carries the risk of ischemia of the normal parenchyma (Berenstein and Lasjaunias 1992; Valavanis 1996; Chaloupka and Huddle 1998; Pierot et al. 2004; Valavanis et al. 2004).

Sometimes, indirect feeders can reach the nidus through the opening of leptomeningeal (pial) anastomoses. This occurs when an important branch supplying the AVM ends completely in the nidus and no branches reach the distal normal parenchyma, which is supplied indirectly by the collateral circulation. The latter can extend to the AVM and supply its distal part (Berenstein and Lasjaunias 1992; Chaloupka and Huddle 1998; Valavanis et al. 2004).

Dural feeders are reported in about 30% of cases (Newton and Cronquist 1969). In this context, it should

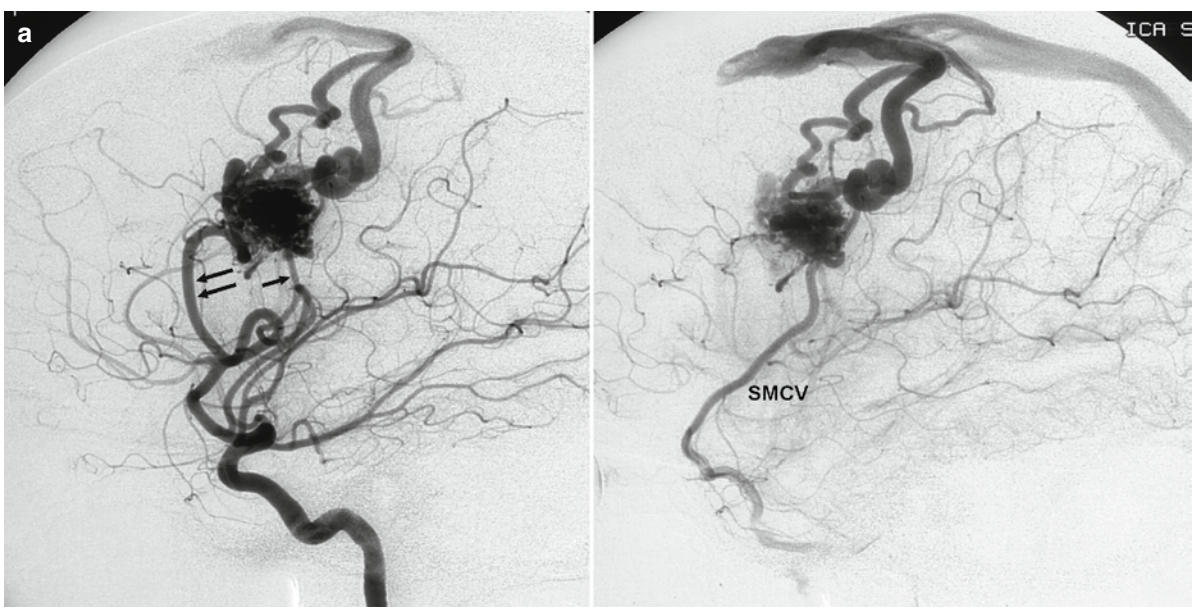

Fig. 12.1 Well-defined nidus of lateral frontal AVM presenting with epilepsy. Lateral angiogram, early and late phases (**a**) The AVM is supplied by a dilated insular branch (*double arrow*). A second, smaller feeder appears posteriorly (*arrow*). Cortical drainage in the superior sagittal sinus, with partial retrograding injection of the anterior segment, and inferiorly into the superficial middle cerebral vein (SMCV). (**b**) Super-selective catheterization preceding embolization with Onyx. (**c**) Lateral angiogram, arteriovenous phase performed 2 months after complete occlusion of the AVM, showing normalization of the arteries and draining veins

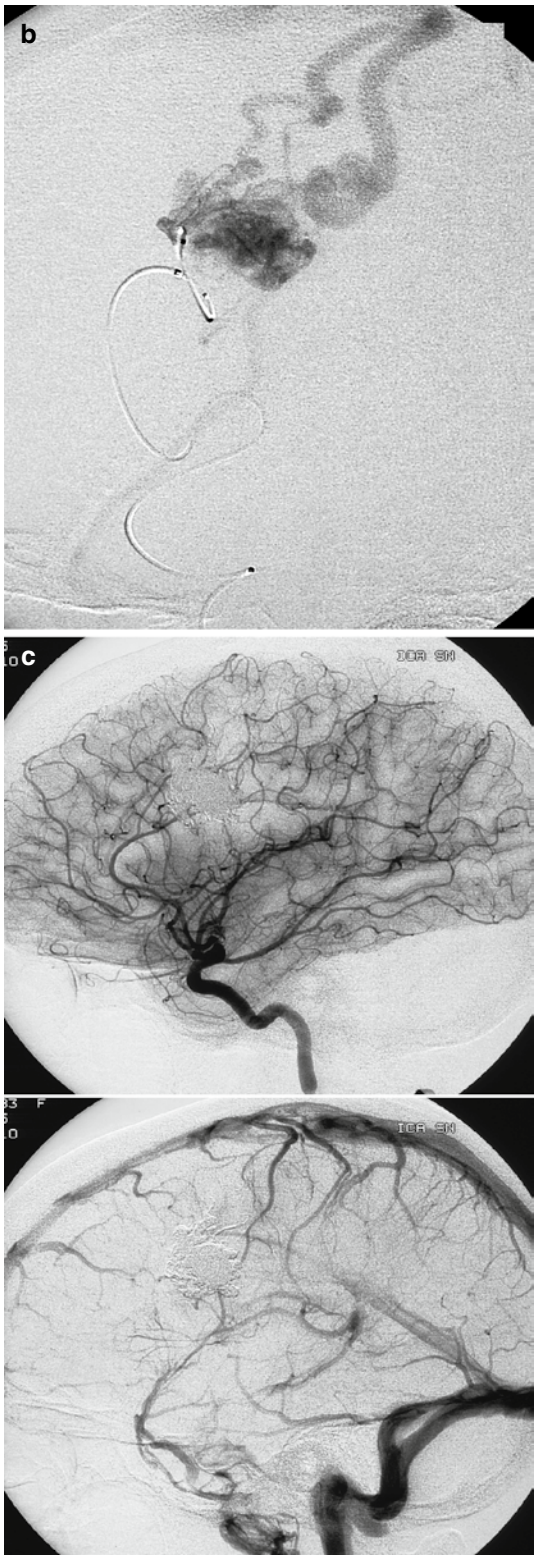

Fig. 12.1 (continued)

be remembered that dilated dural branches can be a cause of headache. Furthermore, in selected cases, the dural branches can be catheterized and used to reach the nidus of the malformation and inject embolic material.

12.3.5.2 Aneurysms

These can be located far from the nidus on one or more supplying arteries. They are thought to be due to the increased flow (flow-related or stress aneurysm) and frequently, though not always, disappear when the AVM is excluded (Berenstein and Lasjaunias 1992; Valavanis and Yaşargil 1998). They can be the cause of subarachnoid hemorrhage (SAH) in patients with AVM. The frequency of aneurysms is reported to increase with the age of the AVM (Berenstein and Lasjaunias 1992). This probably means that the development of these aneurysms is due to the high flow associated with the AVM, but it is also the result of the chronicity of the shunt (Valavanis 1996). In our experience, the majority of these aneurysms occur in old patients, especially in the vertebrobasilar sector (Figs. 12.13, 12.14, 12.16, and 11.13). Rarely, aneurysms can be found on an arterial branch independent of the AVM; these are probably dysplastic in origin.

Other small aneurysms are located near or within the nidus (intranidal aneurysms). These can be better identified by selective studies. They are very frequent and are thought to be responsible for hemorrhage in many cases (Willinsky et al. 1988; Marks et al. 1992; Turjman et al. 1994; Pollock et al. 1996; Redekop et al. 1998; Bradac et al. 2001; Pierot et al. 2004; Valavanis et al. 2004) (Figs. 12.4, 12.6, 12.7, and 12.11).

One notable type is the pseudoaneurysm, which develops at the site of rupture of the AVM; these are detected in patients presenting clinically with recent AVM rupture (Valavanis et al. 2004). Pseudoaneurysms lack a true vessel wall and consist of a pouch arising from a partially reabsorbed hematoma. They can be angiographically identified by their irregular shape and location at the margin of a recent hematoma (Berenstein and Lasjaunias 1992; Garcia Monaco et al. 1993; Valavanis 1996; Valavanis et al. 2004) (Fig. 12.9).

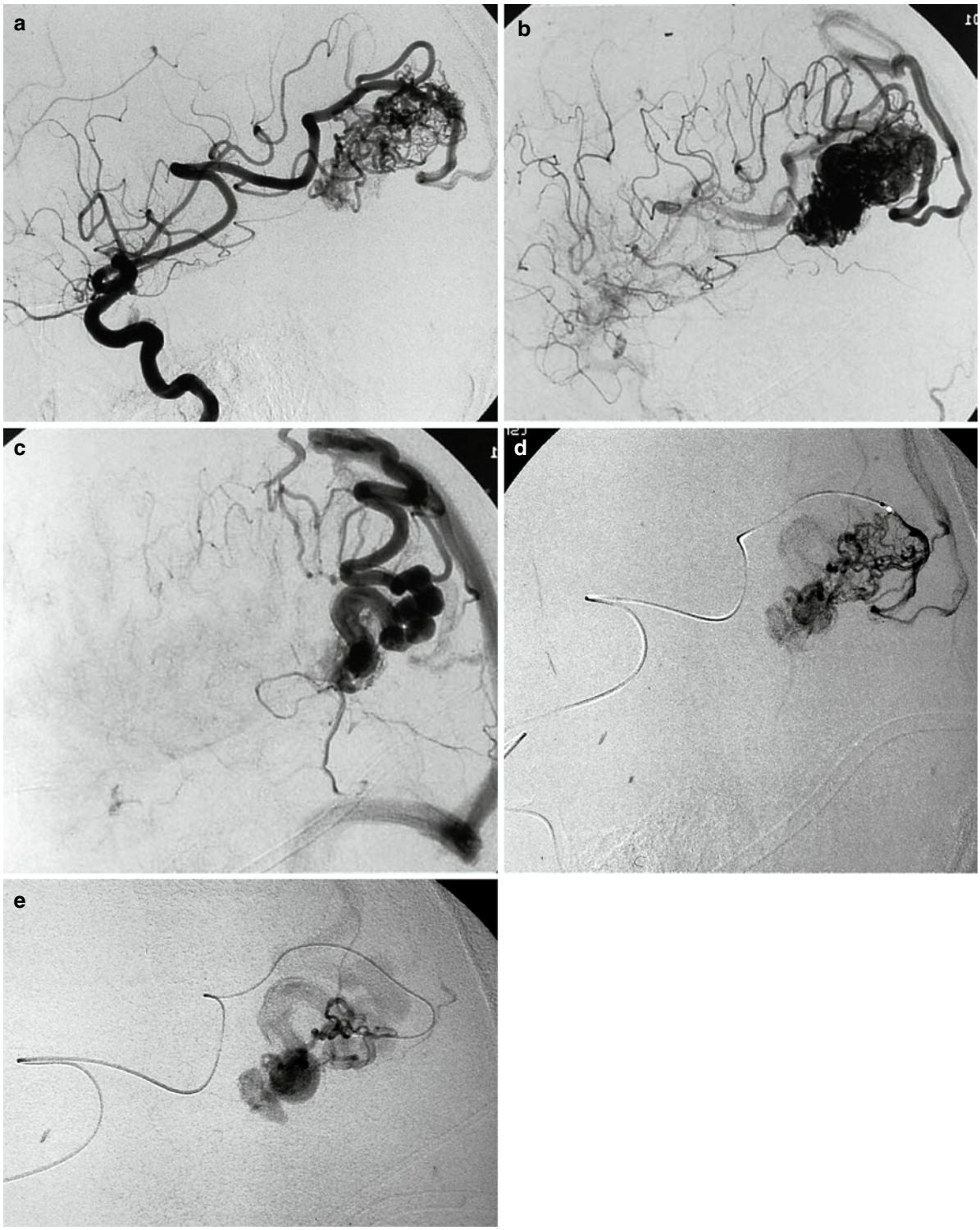

Fig. 12.2 Laterotemporal occipital AVM, presenting with hemorrhage, supplied by distal branches of the gyrus angularis artery. Carotid angiogram, lateral view, arterial (**a**) and venous phases (**b**, **c**). There is a different venous drainage related to the corresponding compartments. These are well demonstrated on super-selective studies (**d**, **e**). At the periphery of the nidus, an isolated arteriovenous shunt is recognizable (**d**)

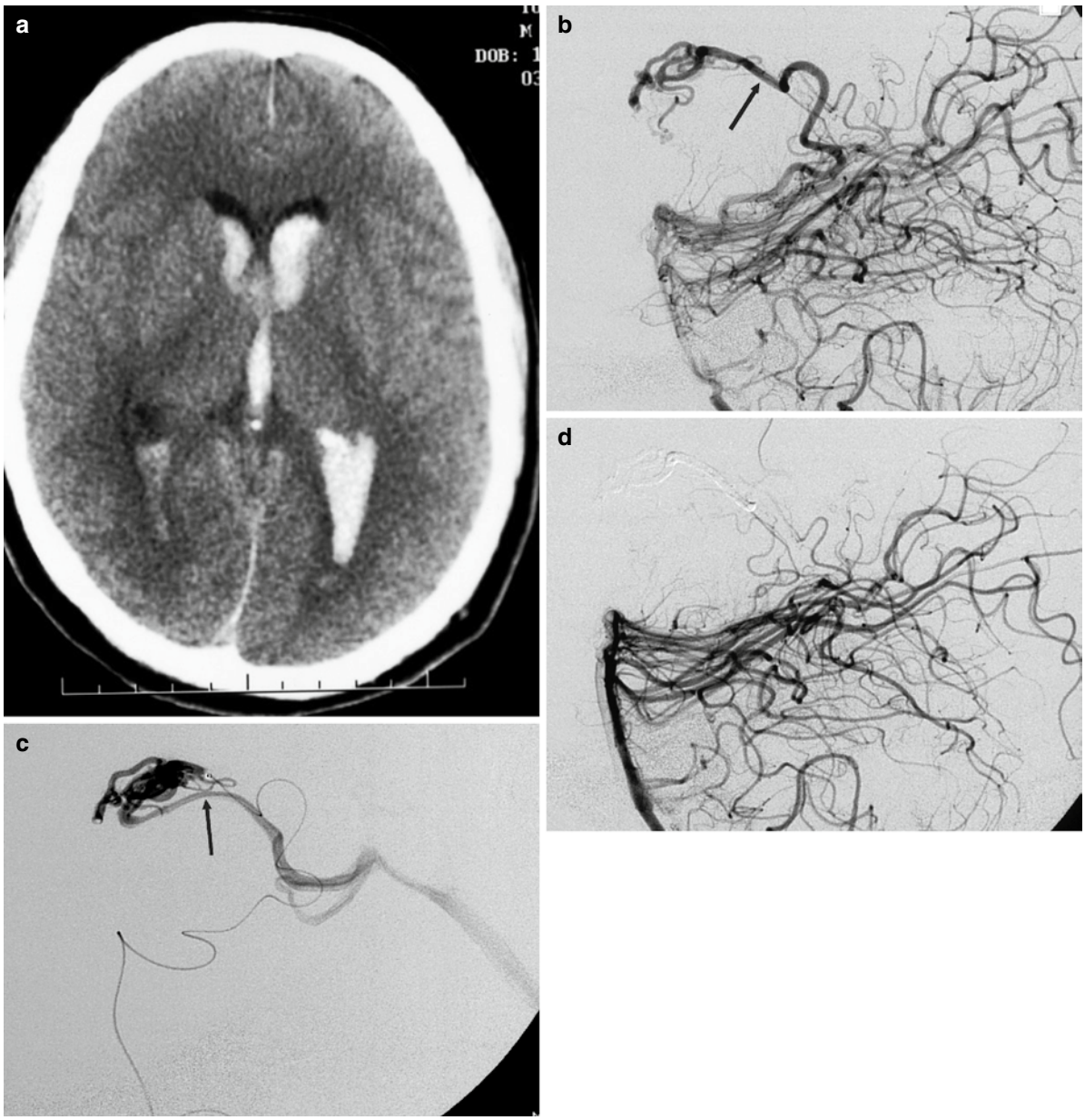

Fig. 12.3 AVM in young patient presenting with hemorrhage involving the third and lateral ventricles. (**a**) CT showing the hemorrhage. (**b**) Lateral vertebral angiogram. There is a dilated posterior medial choroidal artery (*arrow*) supplying the AVM in the roof of the third ventricle. (**c**) Selective study showing nidus of the AVM and drainage in the internal cerebral vein (*arrow*), continuing into the Galen vein and straight sinus. (**d**) Control angiogram after endovascular treatment with occlusion of the AVM with acrylic glue

12.3.5.3 Other Changes

Among other changes of the supplying arteries, there is stenosis, which is commonly due to intrinsic changes in the wall and is characterized by intimal hyperplasia, mesenchymal proliferation, and capillary proliferation through the adventitia (Willinsky et al. 1988) (Fig. 12.11). Moyamoya pattern at the base of the brain has also been reported, probably being the result of hemodynamic stress (Mawad et al. 1984; Berenstein and Lasjaunias 1992).

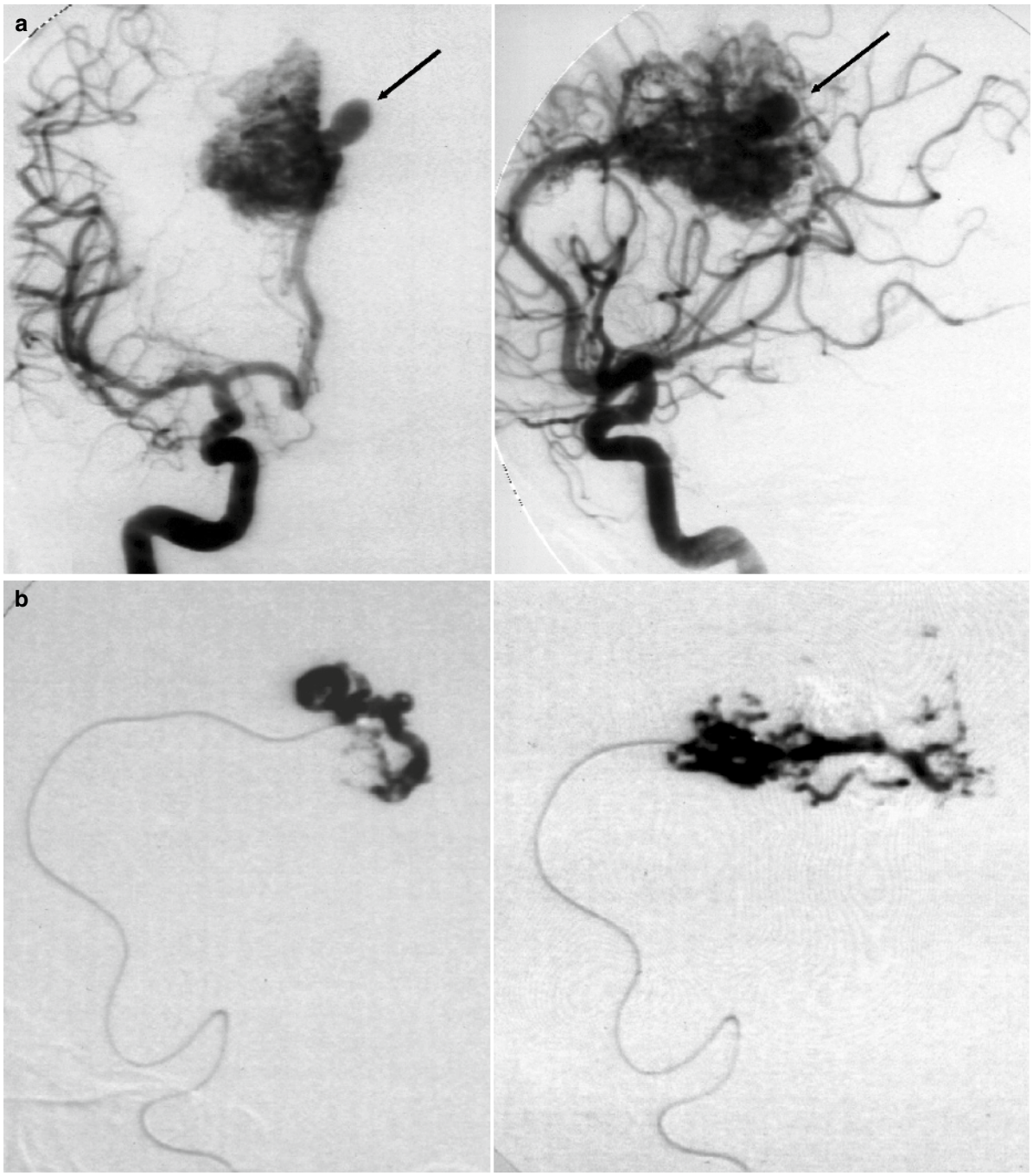

Fig. 12.4 AVM involving the corpus callosum and adjacent gyrus cinguli presenting with hemorrhage. (**a**) Internal carotid angiogram (AP, lateral view) showing the compact nidus supplied by the pericallosal artery. In the posterior medial part of the nidus, a dilated vascular structure is recognizable (*arrow*). It is not possible to determine whether this corresponds to a nidal aneurysm or a pseudovenous aneurysm. (**b**) Two selective studies of branches of the pericallosal artery preceding injection of acrylic glue aimed to occlude partially the nidus and especially the aneurysm. (**c**) Control angiogram post-treatment, well tolerated by the patient, who was operated on 1 month later with finally clinical good results

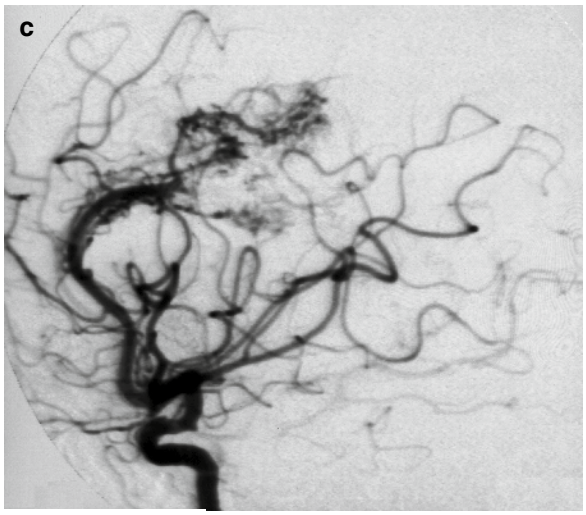

Fig. 12.4 (continued)

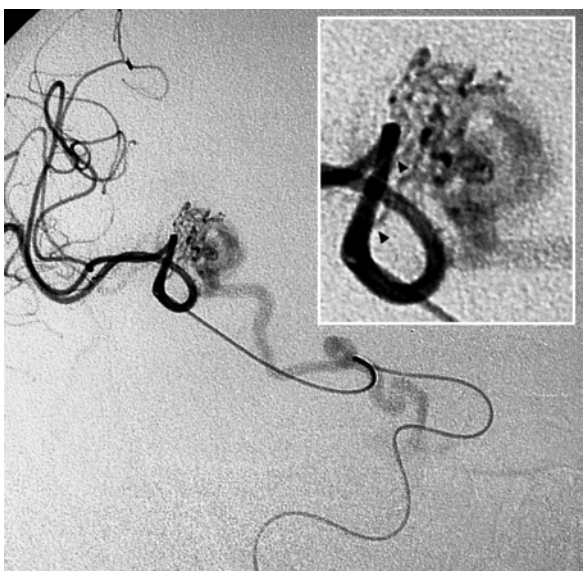

Fig. 12.5 Example of en passage feeders arising from the M2 segment of the middle cerebral artery (MCA) in a patient with temporo-insular AVM

12.3.5.4 Venous Drainage

The type of drainage commonly depends on the location of the AVM and is thus predictable. It can, however, be aberrant due to preexistent variants or the formation of a collateral circulation following occlusion or stenosis in the venous sector; it may be a venous adaptation in an attempt to reduce the high intranidal pressure. Venous drainage can be superficial, deep, or both, and it consists of a single draining vein or several venous channels (Figs. 12.1, 12.2, 12.8, 12.9, and 12.12). In the latter case, a specific venous drainage can be seen after injection of each correspondent supplying artery. In other cases, the same venous drainage is recognizable after injecting different feeders. When several venous channels are involved, it is a multiple-compartment AVM; where there is just a single draining vein, it is a unique-compartment AVM (Yaşargil 1987; Berenstein and Lasjaunias 1992; Valavanis et al. 2004). In this context, it should be considered that multiple venous drainage can be only apparent owing to the fact that the unique draining vein divides early into more veins.

The veins draining the AVM are always dilated. The dilatation is sometimes enormous, forming large pouches, which can be the result of distal stenosis or thrombotic occlusion. The cause of the stenosis may differ. It can be due to hyperplasia of the wall components as a reaction to the increased flow and pressure. Otherwise, the stenosis occurs when the vein enters the dura; it may be the result of a kinking of an ectatic vein or bone compression. Sometimes, these pouches result from pseudoaneurysms, similar to those in the arterial sector (Fig. 12.9). Some aspects of the venous drainage (unique veins, deep venous drainage, stenosis, and large pouches) are considered potential risks or may already be risks because of hemorrhage (Vinuela et al. 1985, 1987; Berenstein and Lasjaunias 1992; Turjman et al. 1995; Muller-Forell and Valavanis 1996; Pierot et al. 2004; Valavanis et al. 2004).

12.3.5.5 Nidus

The extension of the nidus varies from very large to very small. Small AVMs have a greater tendency to rupture (Fig. 12.10) (Graf et al. 1983; Pierot et al. 2004). The same is true for deeply located and posterior fossa AVMs (Figs. 12.3, 12.6, 12.7, and 12.9). Some authors (Garcia Monaco et al. 1990; Berenstein and Lasjaunias 1992) reported a higher tendency for hemorrhage also in temporo-insular and callosal AVMs (Fig. 12.4). The nidus can be mono- or multicompartimental (Fig. 12.2). It is interesting to note that with increasing experience in vascular treatment, small connections through the different compartments may become recognizable, and so the slow injection of embolic material can penetrate

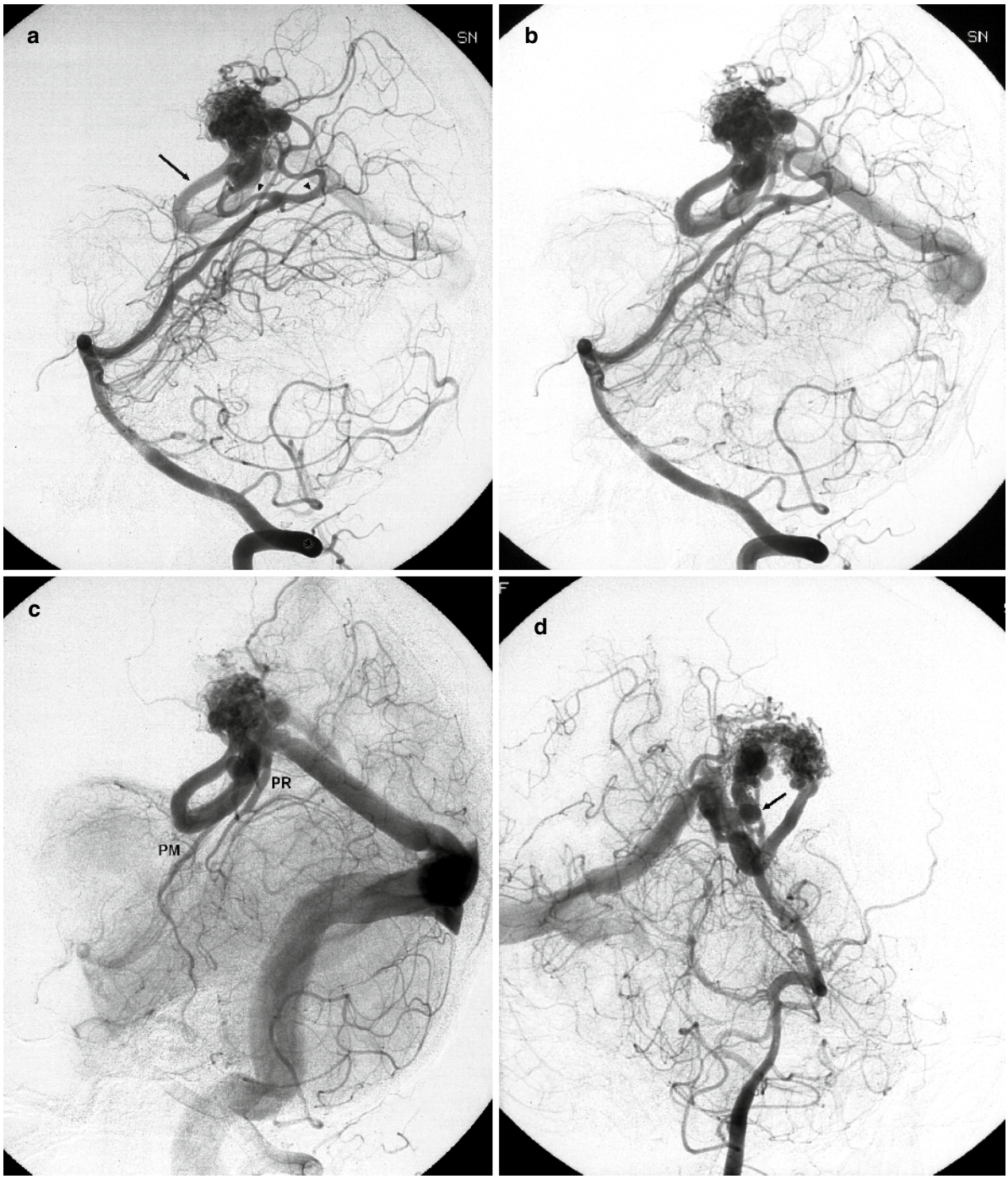

Fig. 12.6 Patient with large hematoma located in the left deep medial occipital retrosplenial area, removed in the acute phase. After clinical improvement, vertebral angiography (**a**) showed the AVM supplied by two feeders (*arrowhead*) arising from the P4 segment of the left PCA. Drainage (**b**) into a large medial atrial vein (*arrow*), continuing into the Galen vein and straight sinus. Owing to hypertension (**c**) in the Galen vein, there is a retrograde injection of the precentral vein (PR) and posterior mesencephalic vein (PM). There is a proximal duplication of the straight sinus. In the oblique view (**d**), a second smaller drainage (*arrow*) is visible, also entering the Galen vein. Catheterization of the branch (**e**) supplying the compartment with intranidal aneurysm (*arrow*). Catheterization of the second branch (**f**) with a progressive advance of the microcatheter distal to a normal parenchymal branch (*arrow*). Post-treatment angiogram (**g**). The remaining minimal component of the AVM supplied by the pericallosal artery was treated by radiosurgery

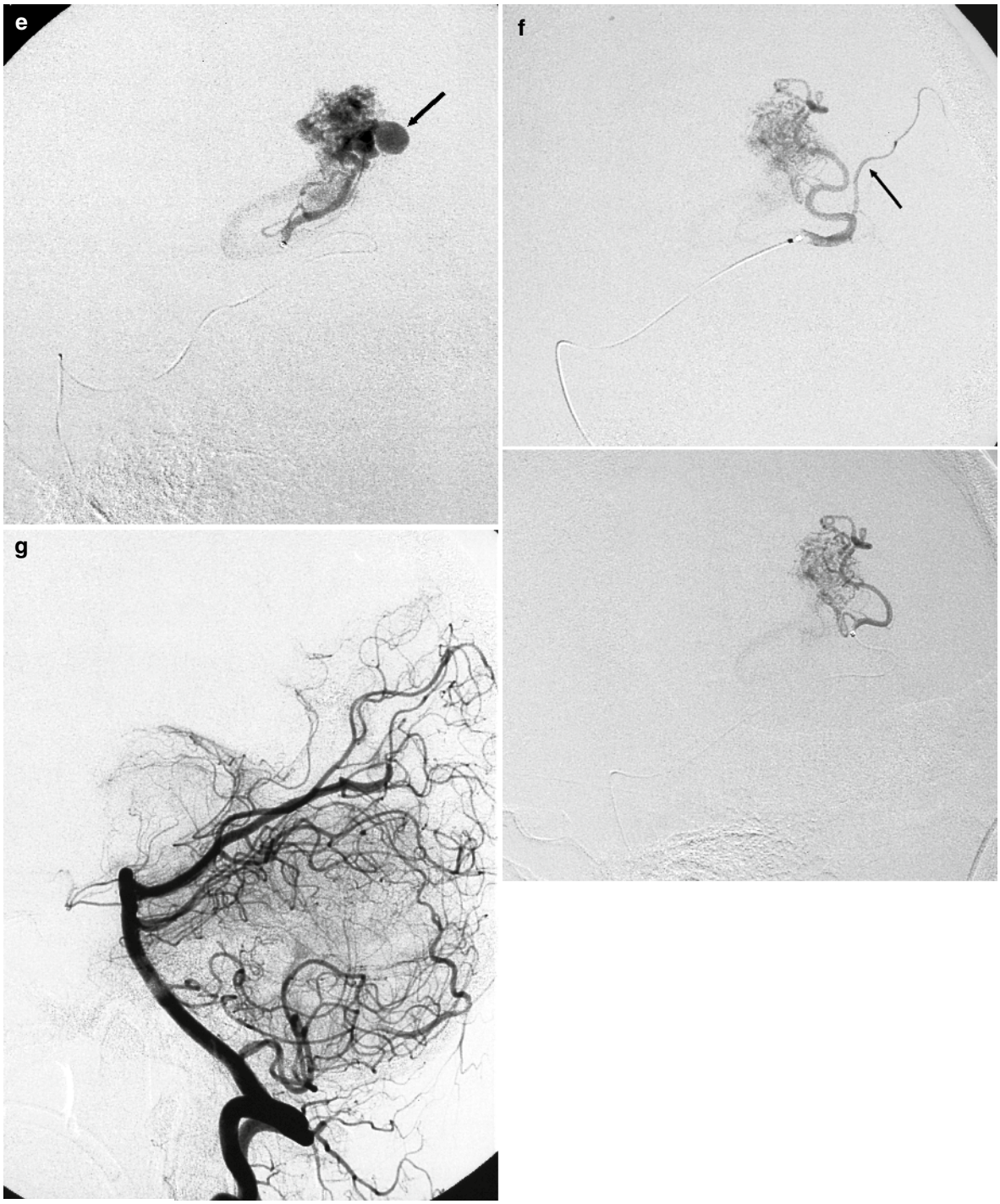

Fig. 12.6 (continued)

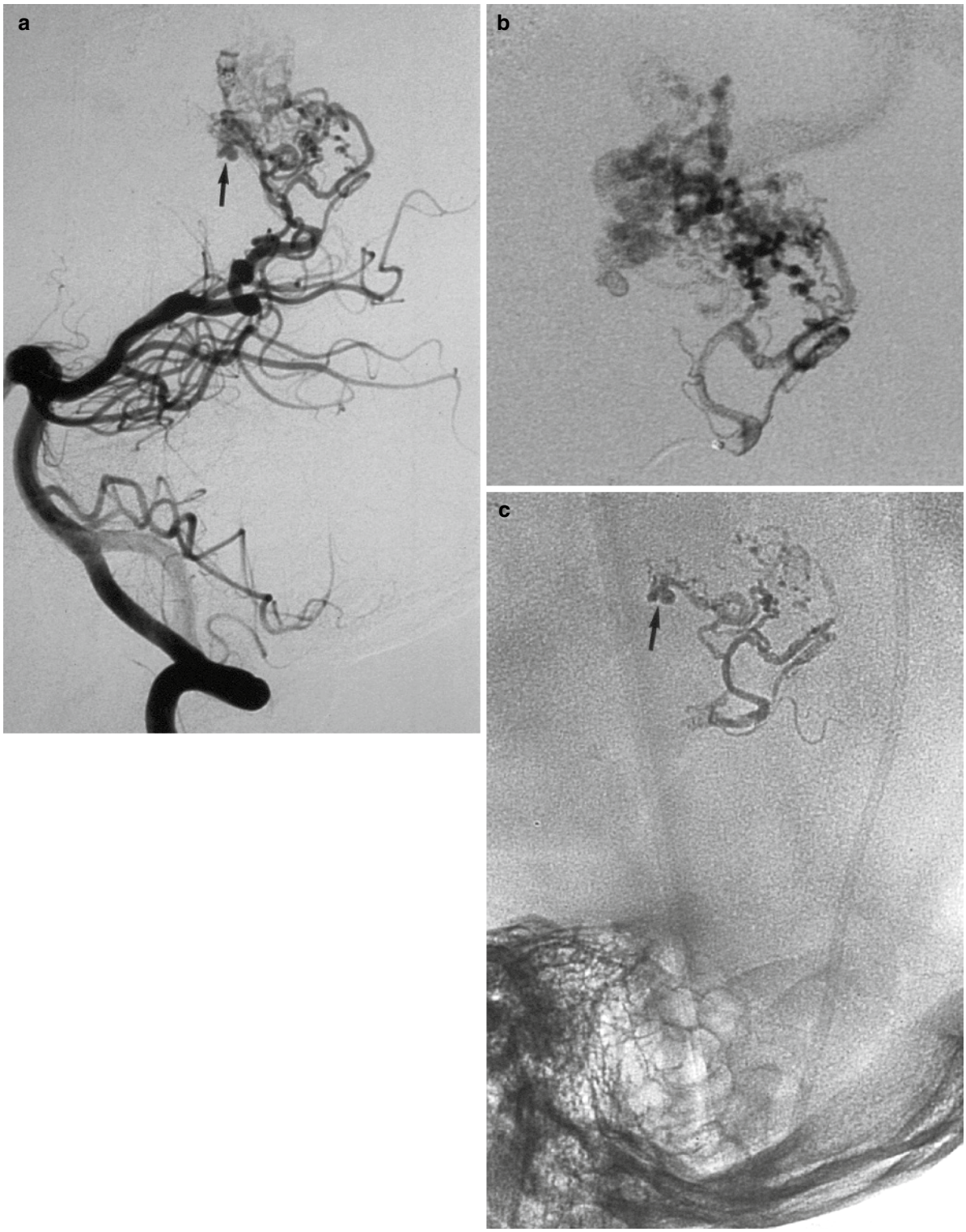

Fig. 12.7 Example of an intranidal aneurysm, probably responsible for repetitive small intraventricular hemorrhage in a patient with a very large right parietal AVM extending deeply toward the lateral ventricle. Lateral vertebral angiogram (**a**) showing part of the AVM with an intranidal aneurysm (*arrow*) in the vascular territory of the medial posterior choroidal artery. Selective study (**b**) preceding injection of acrylic glue. Cast of the glue (**c**) involving part of the nidus and also the aneurysm (*arrow*). Despite only partial treatment, the hemorrhagic episodes arrested completely over a period of many years

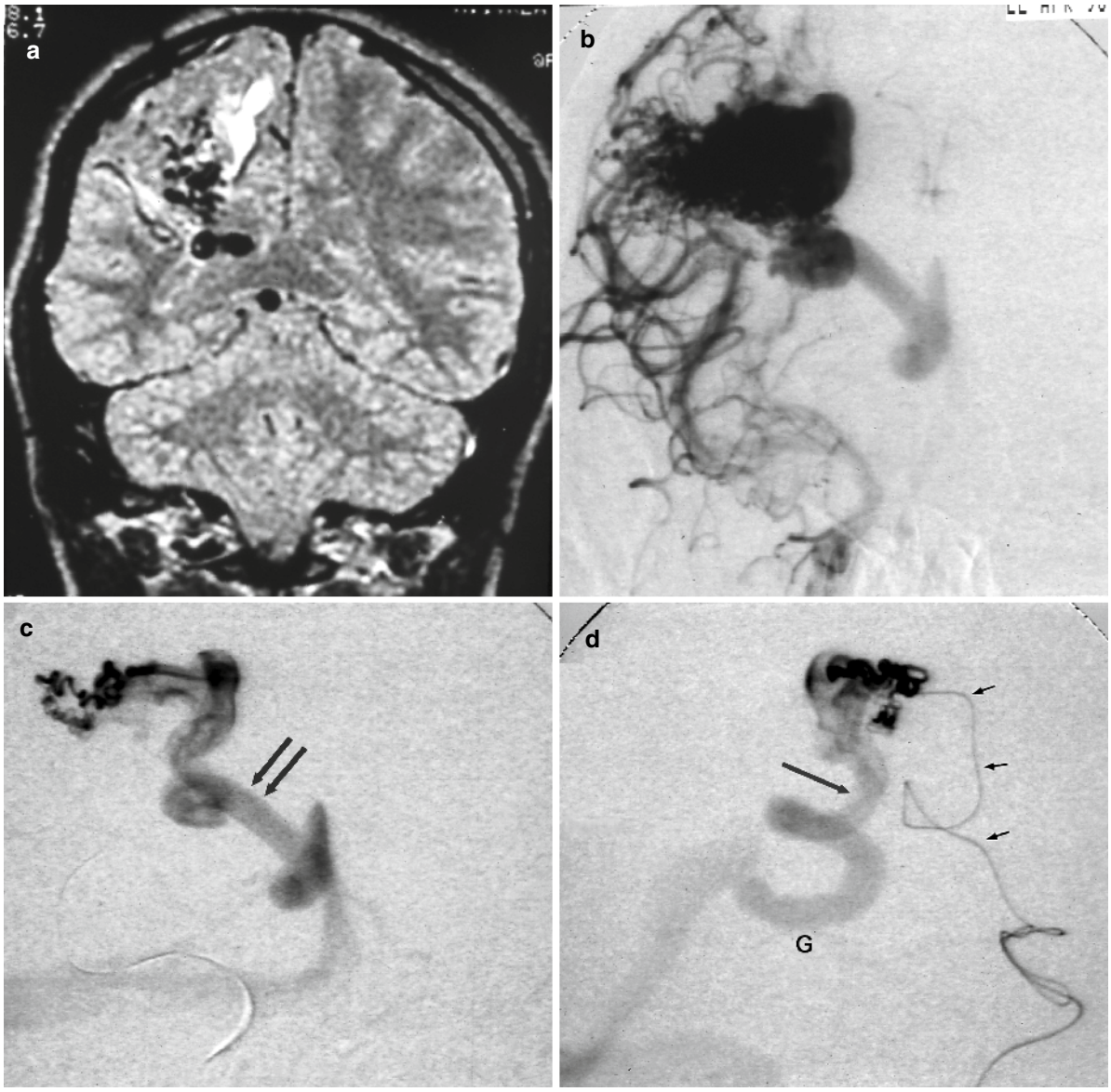

Fig. 12.8 Parietal AVM. (**a**) Coronal MRI T2-weighted image showing the extension of the lesion toward the ventricle. There is gliosis due to a previous hemorrhage. (**b**) Carotid angiogram, AP view, showing the compact nidus and deep venous drainage. (**c**) AP view, during selective study. The drainage occurs through a very dilated medullary vein, continuing into the medial atrial vein (*arrows*) entering the Galen vein. (**d**) Lateral view, corresponding to the image in (**c**). Microcatheter (*small arrows*). Dilated medial atrial vein (*arrow*) draining into the Galen vein (*G*)

completely the nidus. In this context, it is possible for numerous small supplying branches to arise from a large main feeding artery. During the injection of embolic material into the nidus through one of the small branches chosen, a retrograde injection of another arterial feeder can occur. This should be immediately recognized to avoid retrograde injection also of the main feeder.

The presence of an intranidal aneurysm has already been described. Arteriovenous shunts can be very large, leading to the formation of large fistulas, characterized on an angiogram by an immediate injection of the venous sector. The fistula can be the unique feature of the AVM or only part of the plexiform nidus (Fig. 12.12) (Aletich et al. 1997; Berenstein and Lasjaunias 1992; Chaloupka and

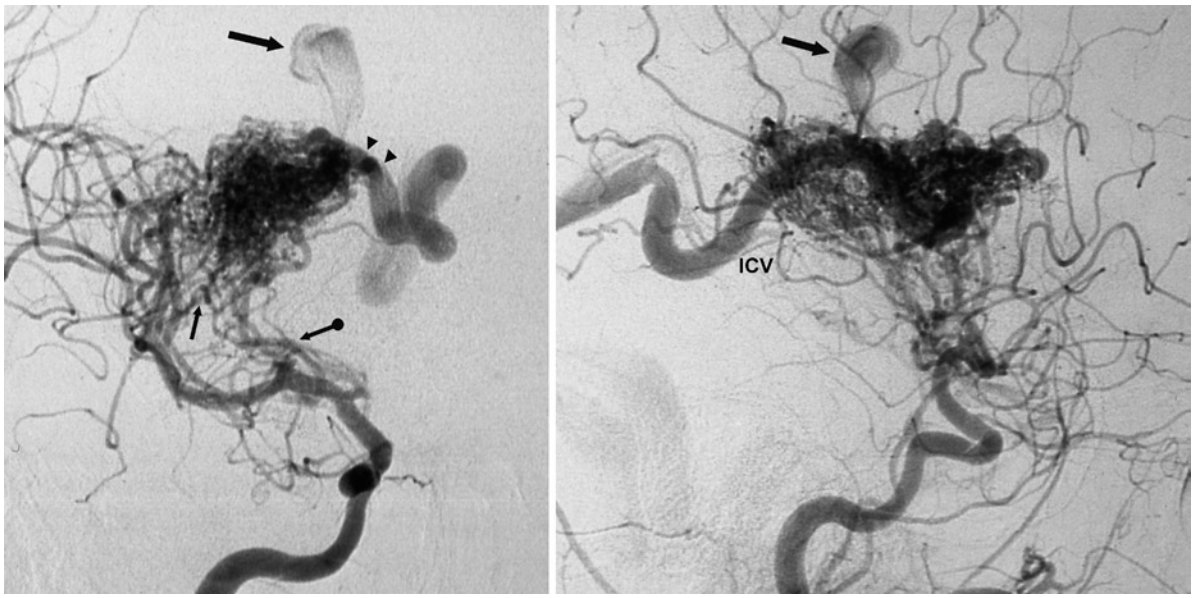

Fig. 12.9 AVM in a young patient presenting with hemorrhage involving the basal ganglia and white matter. Carotid angiogram, AP and lateral views. The AVM is supplied by dilated perforators (*arrow with dot*) and by several branches arising from the M2 segment of the MCA (*arrow*). The drainage occurs in the thalamostriate vein (*arrowhead*), continuing into the internal cerebral vein (*ICV*). There is another partially injected venous pouch (*large arrow*), which probably corresponds to a pseudoaneurysm. The patient underwent operation

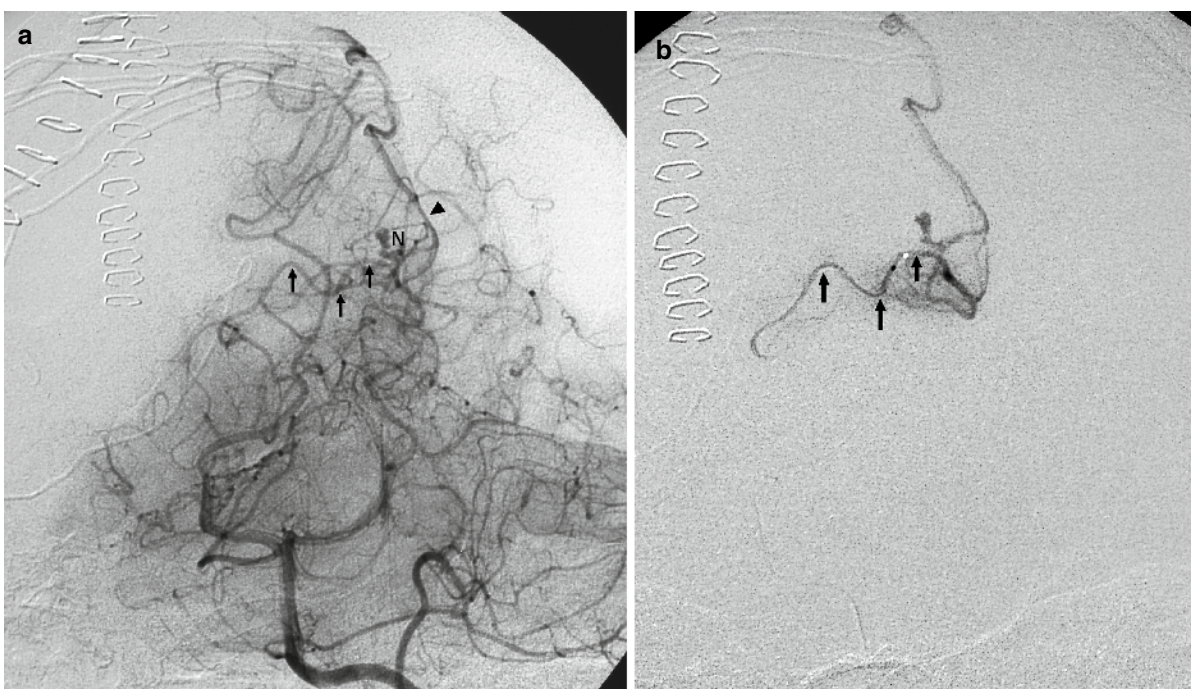

Fig. 12.10 Example of a very small medial occipital AVM presenting with hemorrhage. Vertebral angiogram, oblique view (**a**) Feeding artery (*arrows*) arising from the P4 segment of the PCA. Small nidus (*N*). Unique draining vein (*arrowhead*). Superselective study (**b**) preceding occlusion with acrylic glue. Control angiogram (**c**) post-treatment

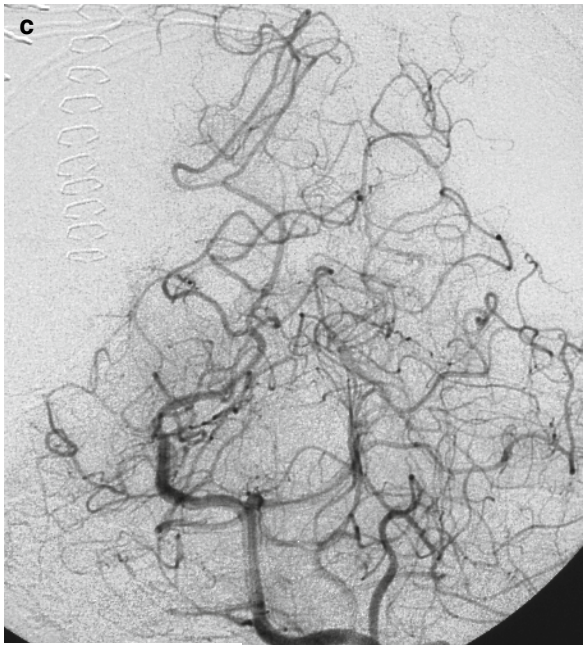

Fig. 12.10 (continued)

Huddle 1998; Valavanis et al. 2004). The fistulas are more frequent in children (Rodesch et al. 1995; Lasjaunias 1997).

Finally, the nidus can be well defined (compact nidus) (Figs. 12.1, 12.2, and 12.4) or without precisely identified borders (diffuse nidus) (Fig. 12.11). In the latter condition, the feeders are numerous, not particularly dilated, and without a specific dominant sector. Endovascular as well as surgical treatment is particularly difficult or impossible (Yaşargyl 1987; Berenstein and Lasjaunias 1992). Location of the AVM in the so-called eloquent areas has been regarded as signifying an increased risk of complications. Though this is true, we agree with other authors (Valavanis et al. 2004) who consider all areas of the brain highly functionally eloquent. That means that when endovascular treatment is performed, the deposition of the embolic material should be strictly confined to the nidus of the AVM. This can avoid damage of the normal parenchyma reducing the risk of complications.

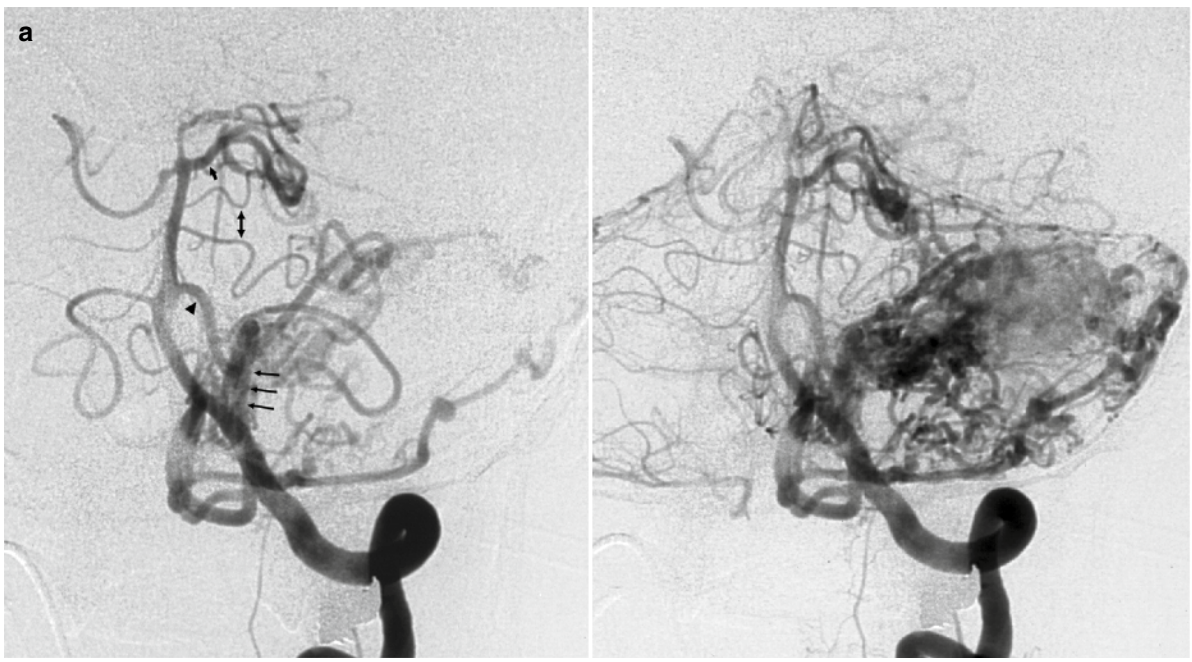

Fig. 12.11 AVM with a diffuse character, involving largely the left cerebellar hemisphere, presenting with subarachnoid hemorrhage (SAH). (**a**) Left AP vertebral angiogram (early and late phases), showing the AVM supplied by branches of the posterior inferior (*three arrows*), anterior inferior (*arrow head*), and superior cerebellar (*small arrow*) arteries. The lateral pontine arteries (*bidirectional arrow*) are very dilated and probably also involved. Several aneurysms, intranidal and also on the feeding branches, are recognizable. (**b**) Selective study of the posterior inferior cerebellar artery (PICA) preceding embolization showing better the multiple aneurysms

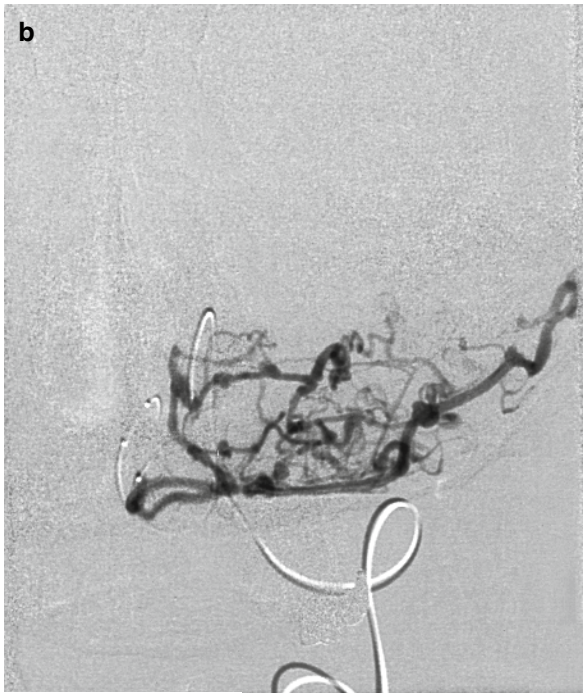

Fig. 12.11 (continued)

12.3.5.6 Perinidal Changes

In a number of cases around the nidus, one can observe the presence of a rich vascular network, consisting of tiny vessels; this is usually due to the dilatation of collaterals following the demand of blood flow from the AVM. Some authors have described the development of new vessels, called angiogenesis, in response to chronic ischemia of the perinidal parenchyma (Berenstein and Lasjaunias 1992; Valavanis et al. 2004).

12.3.6 Treatment

Progressive technical improvements in surgical and endovascular treatment as well as radiotherapy, applied in varied combinations, combined with better knowledge of the pathophysiology of AVMs, today offer many possibilities to achieve a complete cure in many patients, with relatively low rates of morbidity and mortality (Berenstein and Lasjaunias 1992; Colombo et al. 1994; Valavanis 1996; Debrun et al. 1997;

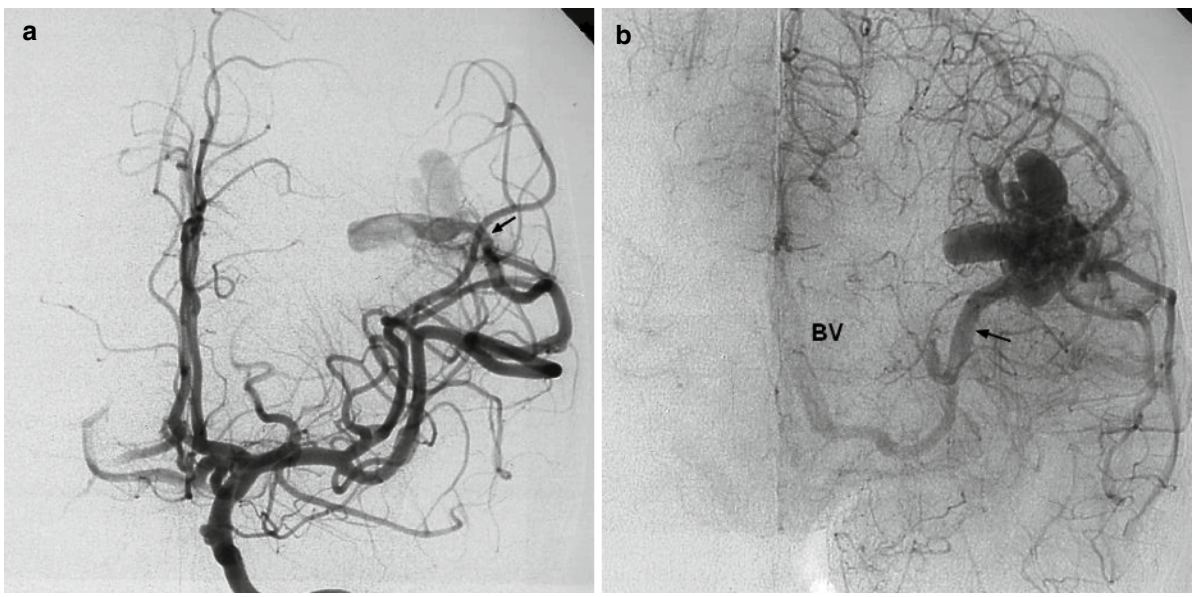

Fig. 12.12 Laterotemporal occipital AVM presenting with epileptic seizures. (**a**) Carotid angiogram, AP view. The AVM consists mainly of a direct fistula (*arrow*) between the gyrus angularis artery and the venous sector, characterized by a venous pouch directly communicating with the adjacent dilated vein. A typical plexiform nidus is not definitively recognizable. (**b**) Late phase, showing the cortical and deep drainage. The latter occurs through a dilated lateral atrial vein (*arrow*) continuing into the distal basal vein (BV). (**c**) Super-selective study showing more clearly the fistulous shunt and deep venous drainage. (**d**) Carotid angiogram, lateral view, early and late phase, showing the feeding arteries and drainage involving the lateral atrial vein (*arrow*). (**e**) Carotid angiogram, lateral view, after occlusion of the fistula with acrylic glue, a minimal network corresponding to the persistent nidus is still recognizable. This was treated later with radiotherapy

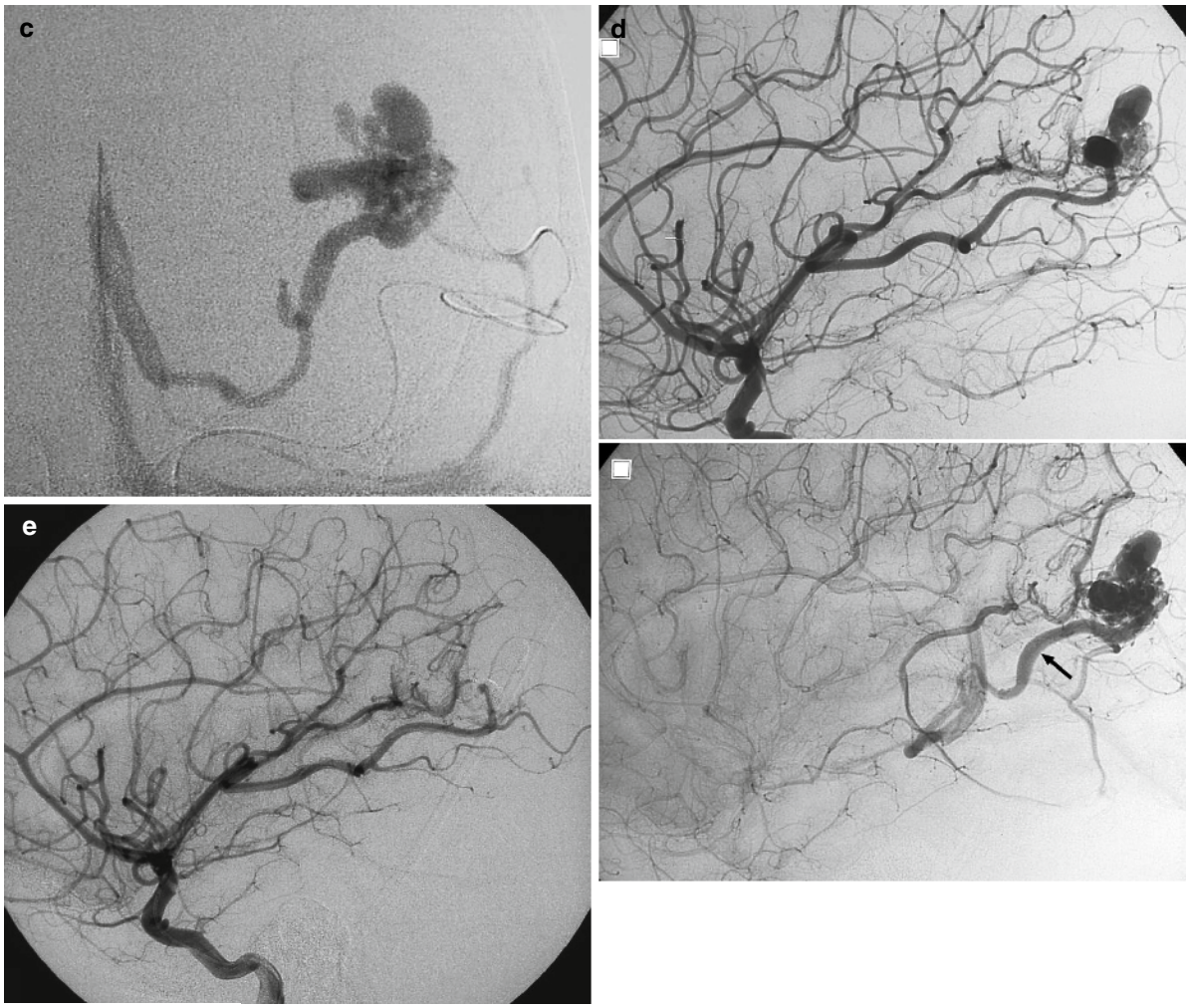

Fig. 12.12 (continued)

Valavanis and Yaşargil 1998; Valavanis et al. 2004; Beltramello et al. 2005; Picard et al. 2005; Vinuela et al. 2005; Raymond et al. 2005; Nagaraja et al. 2006; Panagiotopoulos et al. 2009; Grzyska and Fieler 2009). It is still open to question whether an invasive therapy or noninvasive management should be performed in cases of asymptomatic AVM or those with minimal symptoms. The age of the patient, location and extension of the AVM, and anticipated difficulty of treatment will play a role in the decision. Also, aspects of the angioarchitecture thought to increase the risk of hemorrhage should be considered, even if some of these aspects have recently been questioned (Stapf et al. 2006). Furthermore, other authors have suggested (Achrol et al. 2006) that inflammatory cytokines play a role in the pathogenesis of hemorrhage of AVM.

More information is certainly needed about the evolution of this very complicated pathology. Such data may emerge from a multicenter, randomized trial (Fiehler and Stapf: Aruba 2008), assessing possible invasive treatment and noninvasive management of patients with AVM.

12.4 Cavernous Malformations (Cavernomas)

12.4.1 Pathology

These appear as well-circumscribed masses, formed by dilated vascular channels without intervening brain parenchyma. The wall of the channels is lined by a

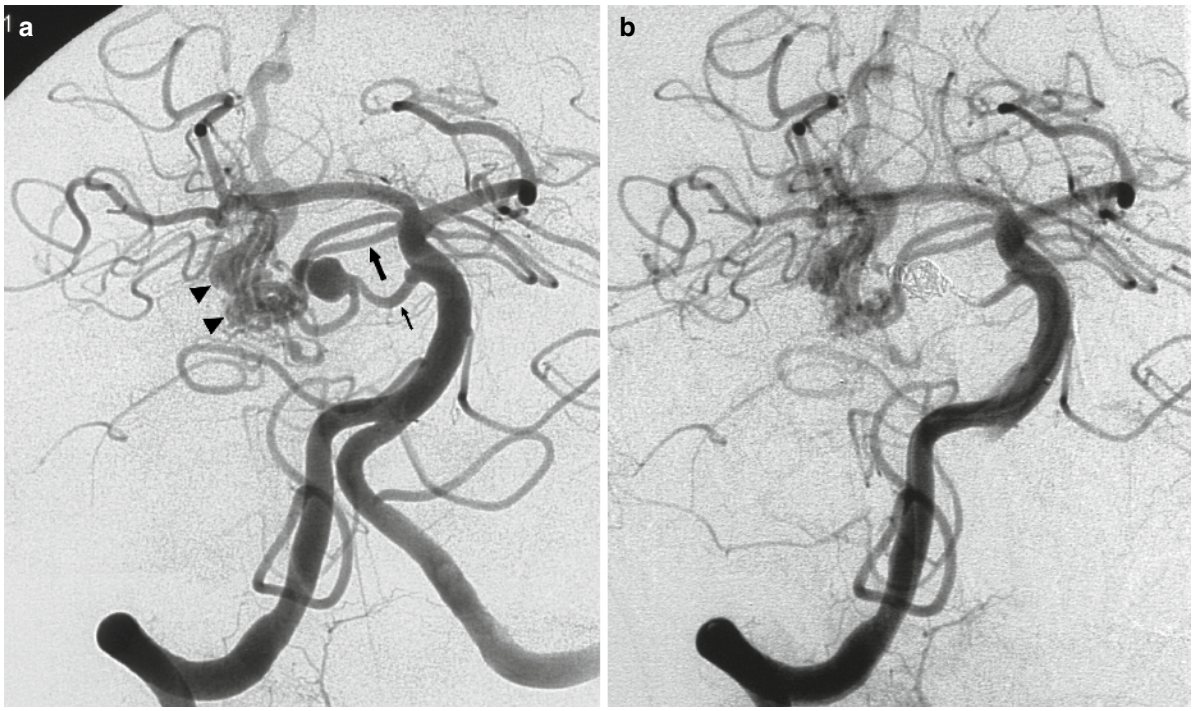

Fig. 12.13 Older patient presenting with severe SAH involving predominantly the right cerebellopontine angle. Vertebral angiogram (**a**) showing a small AVM in the cerebellopontine angle (*arrowheads*) supplied by a double superior cerebellar artery (*large arrow*) and dilated lateral pontine artery (*small arrow*). With the latter, an aneurysm, probably flow dependent, is recognizable. This was thought to be responsible for the SAH and was acutely occluded with coils (**b**), together with the parent artery. The comatose patient recovered well

single layer of vascular endothelium, surrounded by fibrous tissue. Some of the channels show thrombosis. Evidence of hemosiderin due to previous hemorrhage is present within and around the malformation. There may be calcification. Cavernous malformations can grow following hemorrhage or because of their intrinsic activity.

12.4.2 Incidence

Based on MRI and autoptic studies, the incidence is reported to be 0.4–0.9% of the general population (McCormick 1984; Otten et al. 1989; Robinson et al. 1991; Maraire and Awad 1995). Cavernous malformations can be single or, frequently, multiple. Familial cases have been recognized, increasingly, especially, in patients of Hispanic origin (Rigamonti and Brown 1994; Zambranski et al. 1994; Gunnel et al. 1996). In this latter group, an autosomal pattern of inheritance has been identified (Gunnel et al. 1996). Cavernous angiomas have been considered congenital; however, de novo lesions can appear, particularly in familial cases (Pozzati et al. 1996; Tekkök and Ventureyra 1996).

12.4.3 Location

Cavernomas can be found throughout the brain and spinal cord. They are more frequent in the subcortical white matter and pons. Extraparenchymal lesions can occur (Meyer et al. 1990; Sepehrnia et al. 1990). They originate in the dural sinuses and are particularly frequent in the cavernous sinus, especially in women.

12.4.4 Diagnosis and Clinical Relevance

In CT, cavernomas appear as rounded, hyperdense masses, sometimes with calcification. In MRI, the aspect is frequently inhomogeneous on T1–T2 images. In large cavernomas, the pattern is frequently characterized by a mass of several rounded cavities.

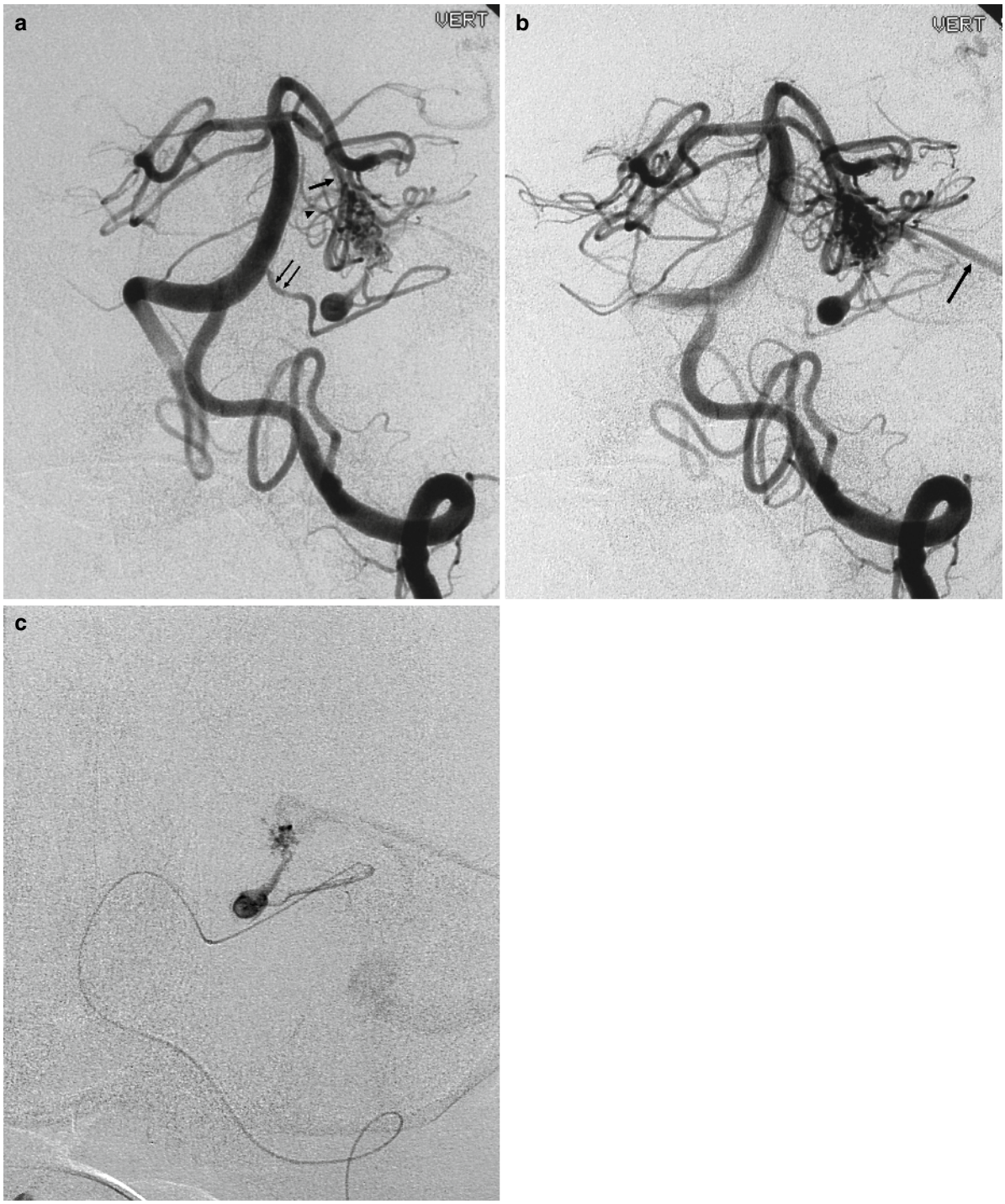

Fig. 12.14 Older patient presenting with severe SAH involving predominantly the left cerebellopontine angle. (**a**) Vertebral angiogram (oblique view) showing the AVM supplied by branches of the superior cerebellar artery (*large arrow*). A lateral pontine artery (*arrowhead*) seems also to be involved. There is a further supply from the anterior inferior cerebellar artery (AICA, *arrows*). On its course, a flow-dependent aneurysm is recognizable. (**b**) Later phase, showing the drainage in the superior petrosal sinus. (**c**) Selective study of AICA preceding the occlusion of the aneurysm and distal AICA with coils. The patient recovered. The AVM was later treated with surgery

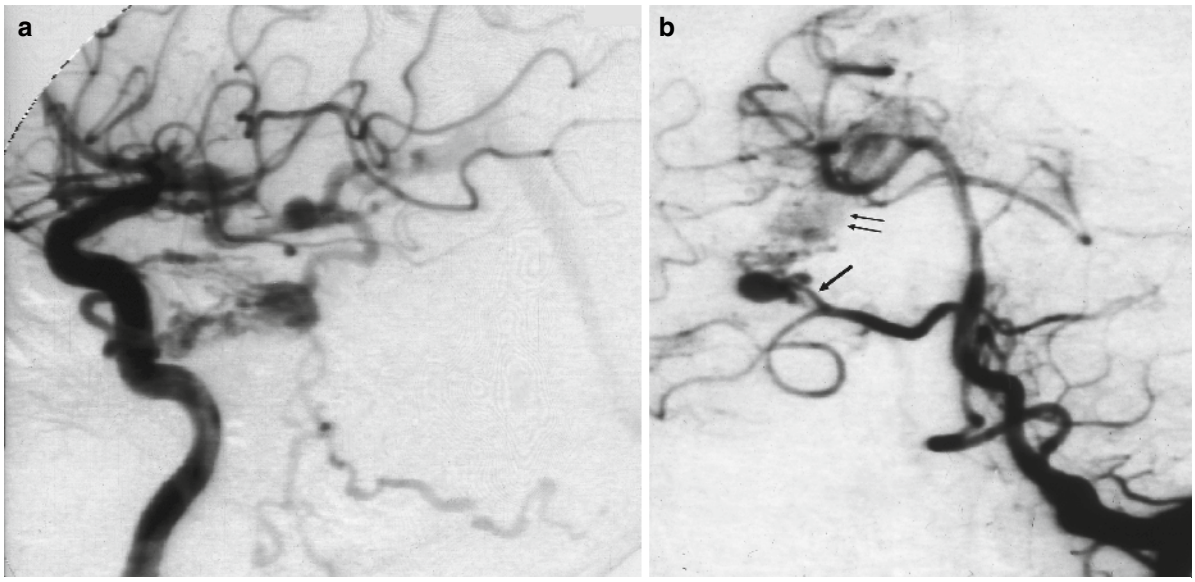

Fig. 12.15 Older patient presenting with SAH. A complete angiographic study showed a petrotentorial dural arteriovenous fistula (DAVF) on the right. (**a**) Right internal carotid angiogram, lateral view, showing the typical feature of the fistula supplied by cavernous branches of ICA. (**b**) Vertebral angiogram, AP view, disclosing, on the right, a well-developed AICA, partially supplying the DAVF (*arrows*) through its rostro-lateral branch (*arrow*). An aneurysm, probably flow dependent, is recognizable on the supplying artery

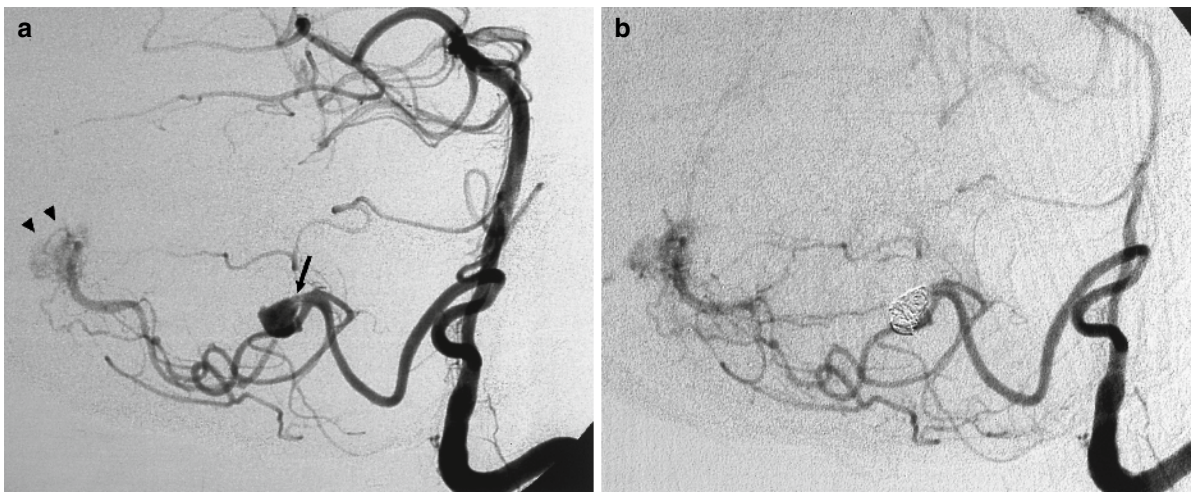

Fig. 12.16 Severe SAH in an older patient. (**a**) Small cerebellar AVM (*arrowheads*) supplied by distal branches of the PICA was visible on the vertebral angiogram. A flow-dependent aneurysm (*arrow*) is recognizable on the supratonsillar segment of the PICA. This was occluded with coils (**b**). The patient remained comatose and died

Enhancement in CT and MRI is typical (Rigamonti et al. 1987). Angiograms are commonly negative. In cases of cavernomas within the cavernous sinus, the differential diagnosis with cavernous meningioma can be very difficult (Bradac et al. 1987).

Cavernomas are frequently asymptomatic. They present clinically with seizures or hemorrhage. With regard to the association with DVA, see Chap. 12.6.

12.5 Capillary Malformations (Telangiectasias)

The Telangiectasias are similar to cavernous angiomas. Unlike the latter, there is brain parenchyma between the vascular channels. The incidence on autopsy is reported to be 0.1–0.15% (McCormick 1984; Jellinger 1986). They are frequently associated with cavernous angiomas, and some authors have suggested that these lesions represent the phenotypic spectrum within a single pathological entity (Rigamonti et al. 1991; Chaloupka and Huddle 1998).

Telangiectasias can be found everywhere in the brain parenchyma and spinal cord, with a predominance in the pons and basal ganglia. The neuroradiological diagnosis is similar to that with cavernous angiomas.

12.6 Developmental Venous Anomaly (DVA)

12.6.1 Pathology

Also called venous angioma, DVA is prevalently located in the white matter of the cerebral hemisphere, whereby several medullary veins converge on a unique collector draining further superficially in one of the sinuses or in one of the subependymal or basal veins.

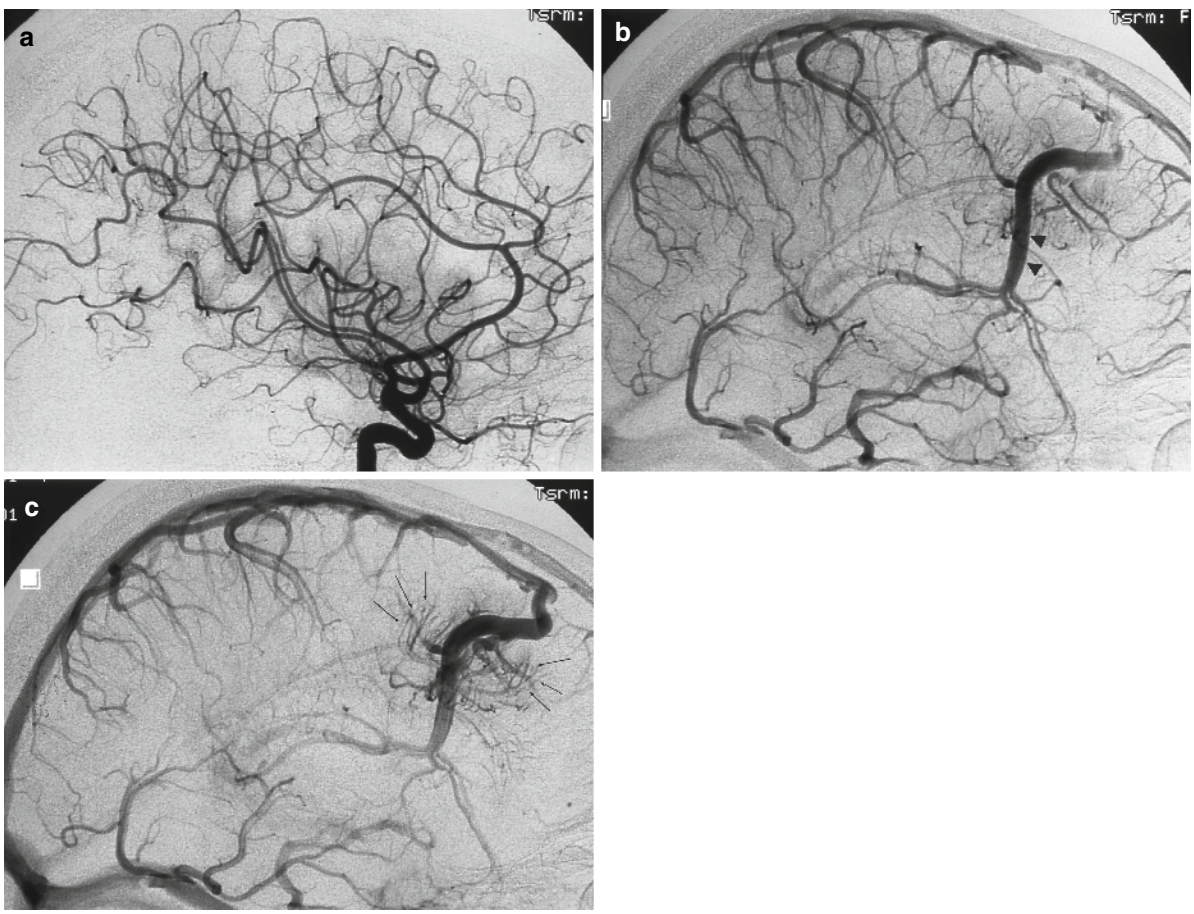

Fig. 12.17 DVA. Carotid angiogram, (**a**) normal arterial phase; (**b**, **c**) in the late venous phase a large frontal cortical vein, draining also partially the temporal region, is recognizable (*arrowheads*). To this converge all the medullary veins of the area (*arrow*). The septal vein is not visible, probably absent. Further drainage occurs in the superior sagittal sinus

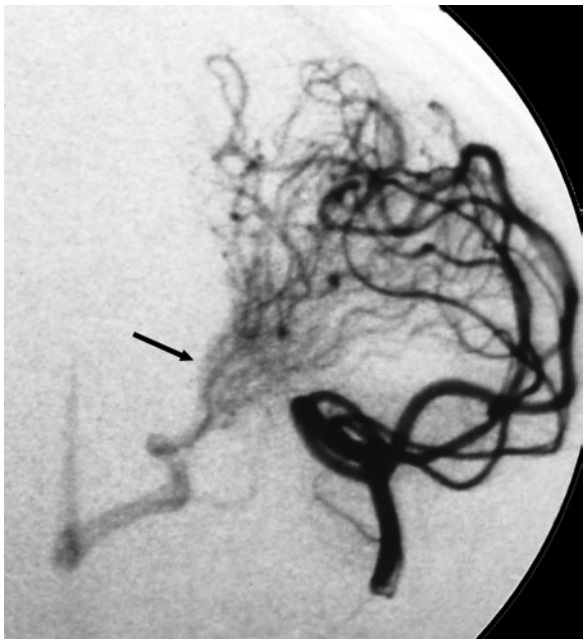

Fig. 12.18 Mixed angioma, carotid angiogram, AP view, selective study of the middle cerebral artery. There is a pathological network (*arrow*), consisting of a medullary vein injected early through connections with medullary branches of the middle cerebral artery. All the veins converge on a dilated atrial vein continuing into the Galen vein

Another typical location is the white matter of the cerebellar hemisphere, where medullary veins converge on the vein of Galen or petrosal vein.

12.6.2 Incidence

DVA has been reported as being the most common vascular malformation detected on autopsy (Sarwar and McCormick 1978; McCormick 1984), with an incidence of 2.6%. Today, it is not considered a malformation (Saito and Kobayashi 1981; Lasjaunias et al. 1986a).

12.6.3 Clinical Relevance

Most DVAs are asymptomatic. Hemorrhages can occur, and these are considered to be due to the associated cavernous angiomas (Ostertun and Solymosi 1993). Rarely, thrombosis of the main collector can lead to hemorrhagic ischemia (Ostertun and Solymosi 1993).

On an angiogram, typical DVAs are recognizable in the capillary–venous phases, where several medullary veins converge on a large collector (Fig. 12.17). The arterial phase is normal.

A few DVAs do not completely fit the typical features described above. These lesions probably represent a transition form between DVA and AVM (Awad 1993; Mullan et al. 1996a, 1996b; Bergui and Bradac 1997). On an angiogram, numerous undilated arterial feeders are connected with veins that have the features of DVA, but appear early (Fig. 12.18).

12.7 Central Nervous System Vascular Malformation: Part of Well-Defined Congenital or Hereditary Syndromes

12.7.1 Rendu–Osler Syndrome (Hereditary Hemorrhagic Telangiectasias)

Rendu-Osler syndrome is a familial neurocutaneous disease, characterized by teleangiectasias of the skin and mucosa of the oral-nasal cavities and gastrointestinal tract. Arteriovenous angiomas and fistulae are also frequently present in the lung and liver. In addition, different types of vascular malformations can involve the central nervous system. The most frequent are AVMs, which are often small and multiple (Chaloupka and Huddle 1998; Berenstein and Lasjaunias 1992). The malformation of the oral-nasal cavities is frequently responsible for severe hemorrhage (Fig. 3.18).

12.7.2 Sturge–Weber Syndrome (Encephalotrigeminal Angiomatosis)

Sturge-Weber syndrome is a familial neurocutaneous disease, characterized by a facial vascular nevus in the trigeminal distribution, mainly in the first branch, a retinal angioma, and leptomeningeal angiomatosis.

12.7.2.1 Pathology

The pathology consists of a network of thin-walled capillaries and venules lying between the pial and subarachnoid membrane. There is also typically a paucity of cortical veins; this is responsible for the stasis and progressive hypoxia of the cortex, which becomes atrophic and partially calcified.

It is assumed today that the primary cause of the syndrome is a problem in the development of the venous drainage, involving the cortical veins and distal part of the superficial medullary vein. The drainage is redirected through a collateral circulation, particularly via the deep medullary veins among the subependymal veins and choroid plexus.

12.7.2.2 Diagnosis

The dystrophic, calcified cortex can be well studied with CT and MRI, which allow enhancement of the angiomatous network as well as demonstration of the redirected venous circulation. (Smirniotopoulos and Murphy 1992; Osborn 1999; Chaloupka and Huddle 1998). On an angiogram, the absence or paucity of the cortical veins can be demonstrated as well as the redirected drainage toward the deep venous system (Berenstein and Lasjaunias 1992).

12.7.3 Wyburn–Mason Syndrome

Wyburn-Mason syndrome is an exceptionally rare neurocutaneous disease, characterized by cutaneous facial nevi in the distribution of the trigeminus and an extensive, high-flow AVM, involving visual pathways, including the retina, optic nerve, optic tract, and sometimes the diencephalon and occipital lobe (Chaloupka and Huddle 1998). Some authors have proposed the term unilateral retinocephalic vascular malformation for this syndrome (Theron et al. 1974). Unusual variants of the syndrome include bilateral intracranial vascular anomalies (Patel and Gupta 1990). CT and MRI are useful diagnostic tools, but angiography is the essential diagnostic step to decide if there is a possibility of partial endovascular treatment.

12.7.4 Klippel–Trenaunay–Weber Syndrome

This syndrome is a very rare condition, characterized by limb hemihypertrophy, cutaneous nevi, venous malformations, and/or occasional high-flow AVM of the affected limb. Vascular malformations can be present in other organs, including the brain. CT and MRI are useful in detecting the lesions; angiography is essential when endovascular treatment has been taken into consideration.

12.8 Arteriovenous Shunts Involving the Vein of Galen

The real incidence is unknown: it can be estimated to be less than 1 per 1,000,000. The first description of aneurysm of the vein of Galen was made in 1937 by Jaeger et al. Today, we know that these malformations constitute a group of lesions that have been more precisely classified only in recent years.

- *Vein of Galen aneurysmal malformations*. Nowadays, the majority of authors (Raybaud et al. 1989; Berenstein and Lasjaunias 1992; Mickle and Quisling 1994; Burrows et al. 1996; Lasjaunias 1997; Chaloupka and Huddle 1998) agree that the pathogenesis of this malformation, which can be termed a true vascular malformation, is a malfunction in embryogenesis, involving the median prosencephalic vein (PV). In accordance with the radioanatomical studies of Raybaud et al. (1989), the PV receives drainage from the deep cerebral structures and choroid plexus, and it drains further into the falcine sinus. The vein disappears in a period between the sixth and eleventh weeks, and it is replaced by the vein of Galen, arising from unification of the caudal remnant of the PV with the developing internal cerebral vein. The vein of Galen drains further into the straight sinus (SS). Failure of regression of the PV results in hypoplasia of the SS, with the venous drainage frequently diverted into a persistent falcine sinus (Raybaud et al. 1989; Mickle and Quisling 1994; Burrows et al. 1996). The cause of the abnormal arteriovenous shunts remains unknown. Raybaud et al. (1989) suggested that the malformation may be linked to an

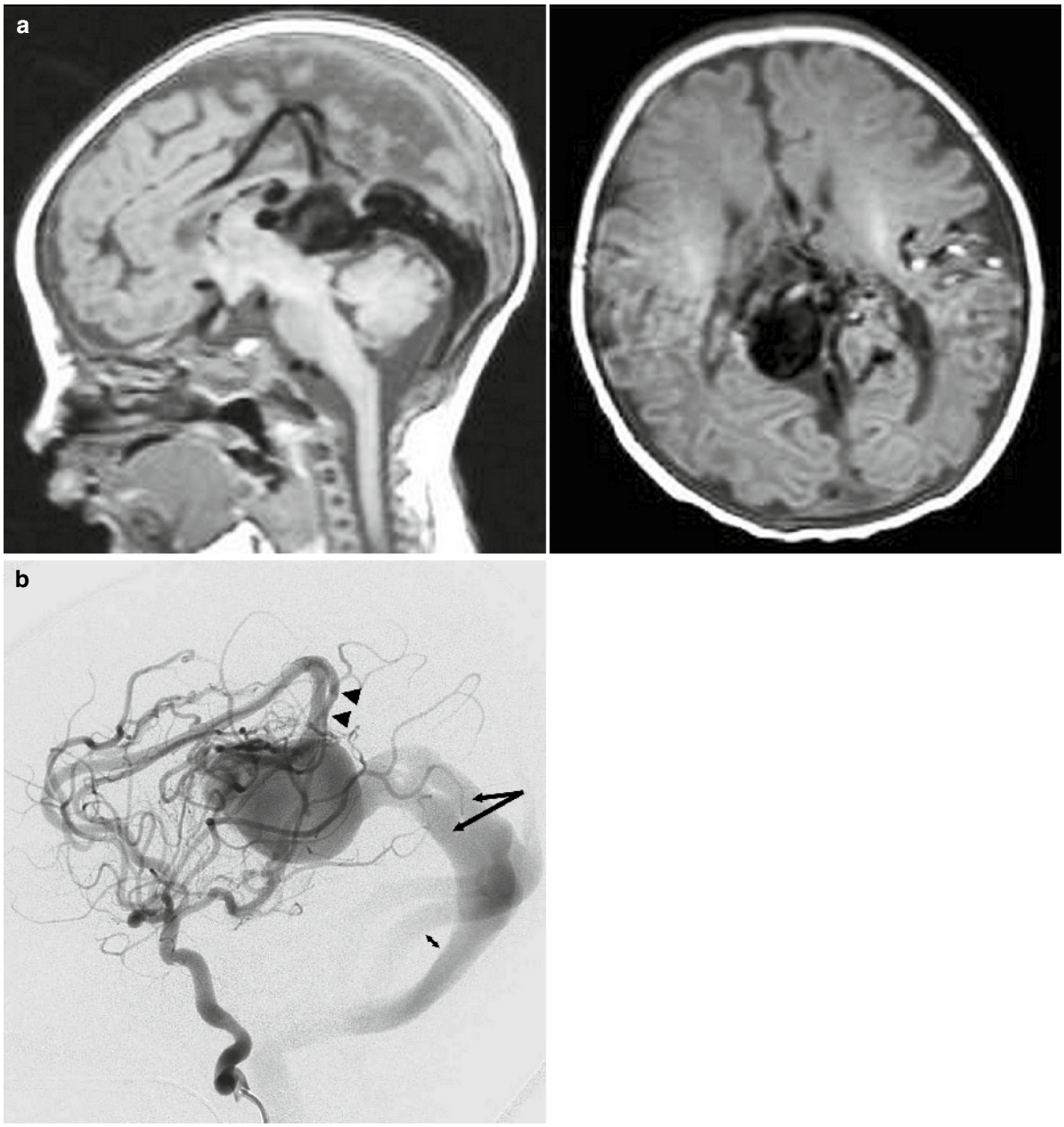

Fig. 12.19 Vein of Galen malformation in 3-month-old child, endovascularly treated owing to heart failure. (**a**) MRI T1-weighted image showing the malformation. (**b**) Right carotid angiogram, lateral view, showing the dilated prosencephalic vein draining into the dilated and fenestrated (*arrow with angle*) straight sinus. The malformation is supplied by the distal pericallosal artery (*arrowhead*) and by the posterior choroidal arteries of the posterior cerebral artery. Anterior and posterior systems converge forming the so-called limbic arch. The double arrow shows further drainage into the transverse sinuses and dilated occipital sinus (**c**) Right vertebral artery, AP and lateral views, showing the supplying arteries arising from the left posterior cerebral artery. Posterior thalamo-perforating artery (*arrow*). Medial and lateral (*arrow with angle*) choroidal arteries. Following selective catheterization, coils were placed in the choroidal arteries close to the shunt, leading to a decrease in flow with significant clinical improvement (**d**). Two years later, a control vertebral angiogram showed a partial persistence of the shunt, which was completely occluded with glue after selective catheterization (**e**). Selective catheterization of the small remaining suppllying branches. The arrow indicates the catheter tip. The nonsubtracted image shows the cast of coils and glue in the malformation. (**f**) Final control vertebral and left carotid angiogram

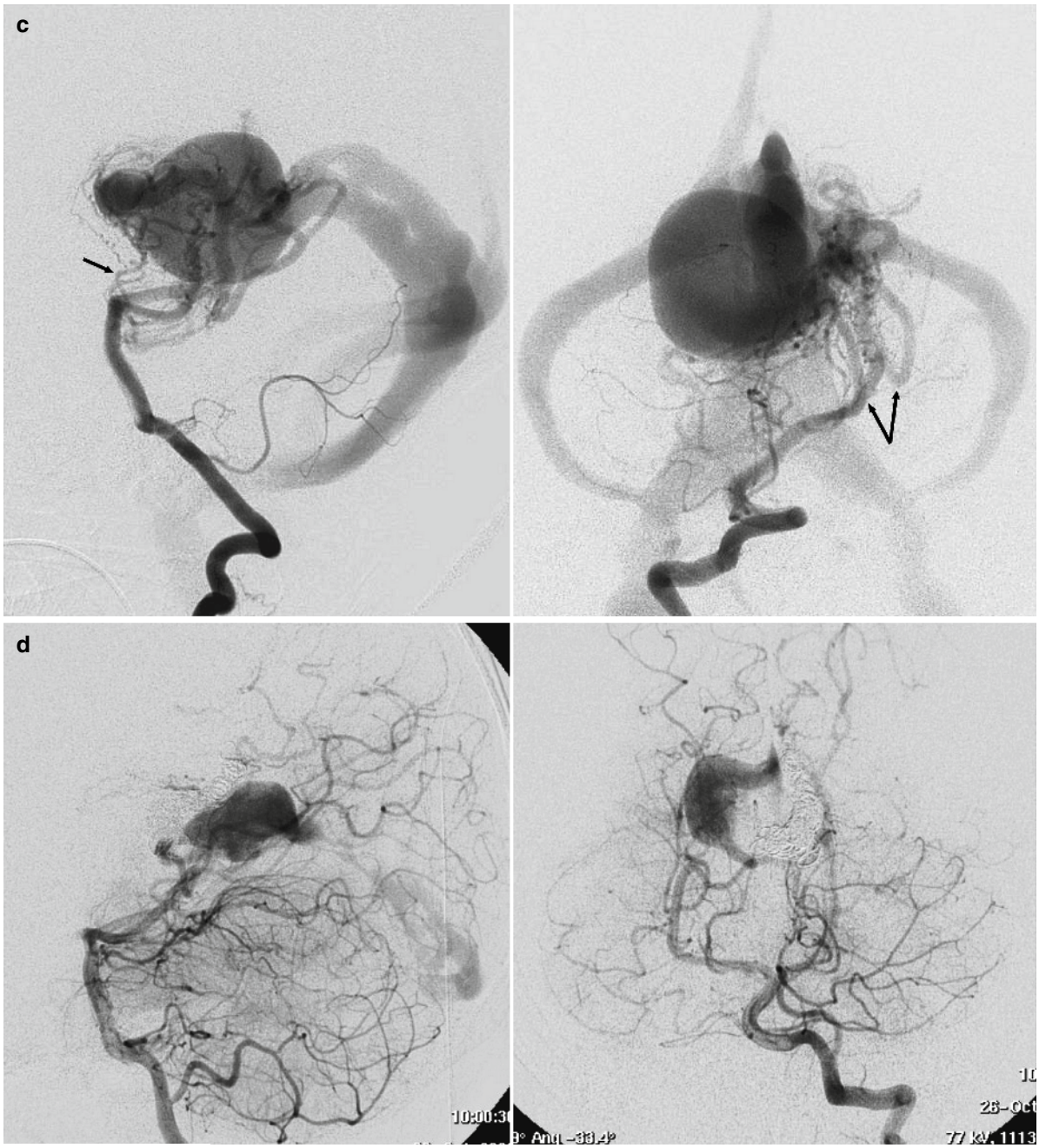

Fig. 12.19 (continued)

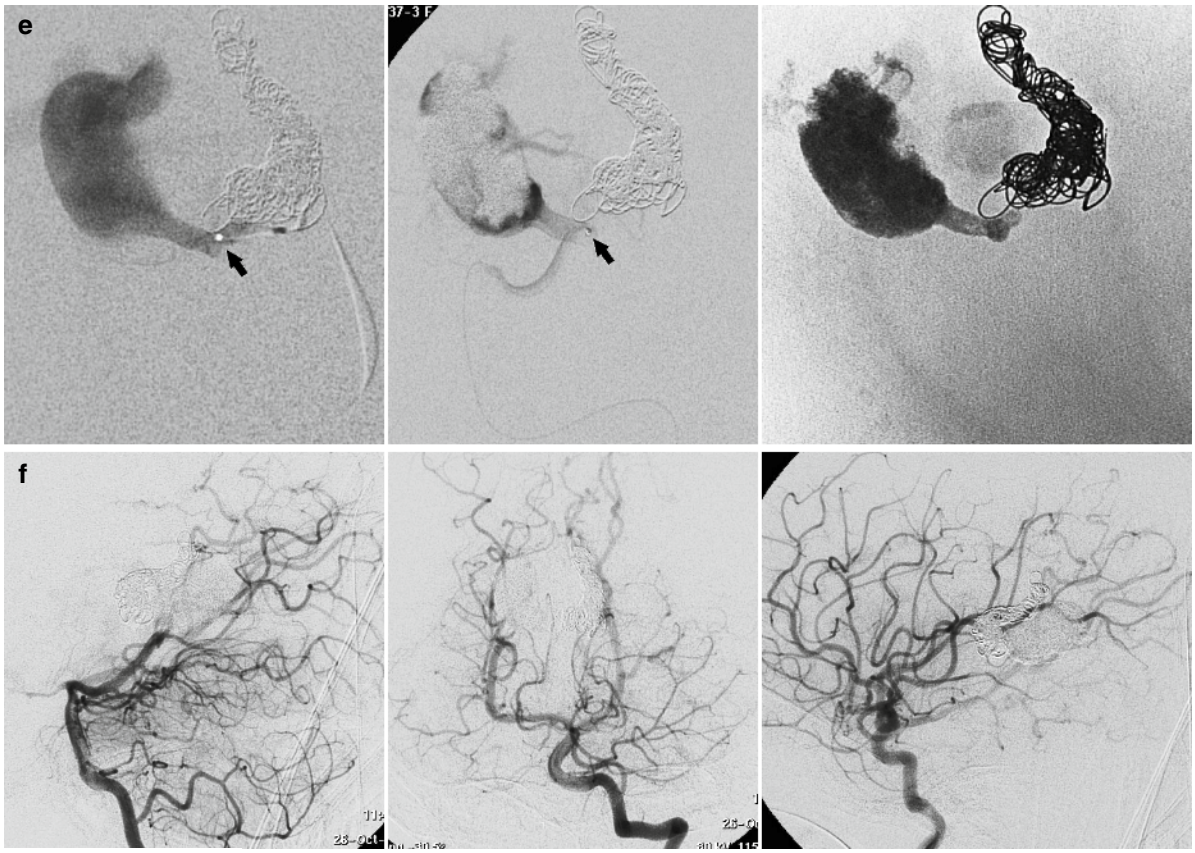

Fig. 12.19 (continued)

embryogenetic error involving the choroidal arteries, which, in the same embryonic period when the PV is prominent, are the most active arterial structures present; thus, they are the most vulnerable to maldevelopment.

- *Diagnosis and treatment*. CT and MR allow easy identification of this kind of malformation. Selective and super-selective angiography is essential for precise study. Angiography in patients with this condition presents a series of technical problems. Among them is the femoral approach and the necessity to limit the quantity of contrast medium; thus, it is prudent and rational to postpone the angiography until the patient is at least five to six months old. Angiographic study and endovascular treatment should be performed earlier if rapid clinical deterioration, particularly as a result of heart failure, occurs.
- On an angiogram (Figs. 12.19 and 12.20), two types of shunts can be recognized (Berenstein and Lasjaunias 1992; Lasjaunias 1997): the choroidal type, characterized by many feeders shunting with the PV, commonly on the anterior surface; and the mural type, in which one or two feeders are connected with the inferior, lateral part of the PV. The feeders can be uni- or bilateral. The most common arteries involved are the posterior choroidal, followed by the distal segment of the pericallosal arteries. In the embryo, the posterior branch of the pericallosal artery runs around the splenium and extends anteriorly into the tela choroidea, anastomosing with the posterior medial choroidal artery. This connection normally disappears, but it can persist in the vein of Galen malformation (Raybaud et al. 1989), forming the so-called limbic arch. The collicular and posterior thalamic arteries may also be involved as well as the anterior choroidal artery; sometimes, secondary feeders can arise from peripheral branches of the middle cerebral artery (MCA) and its perforators.
- The venous drainage occurs into a dilated PV, which appears rounded or elongated, with the greatest dimension along the sagittal axis. In at least 50% of

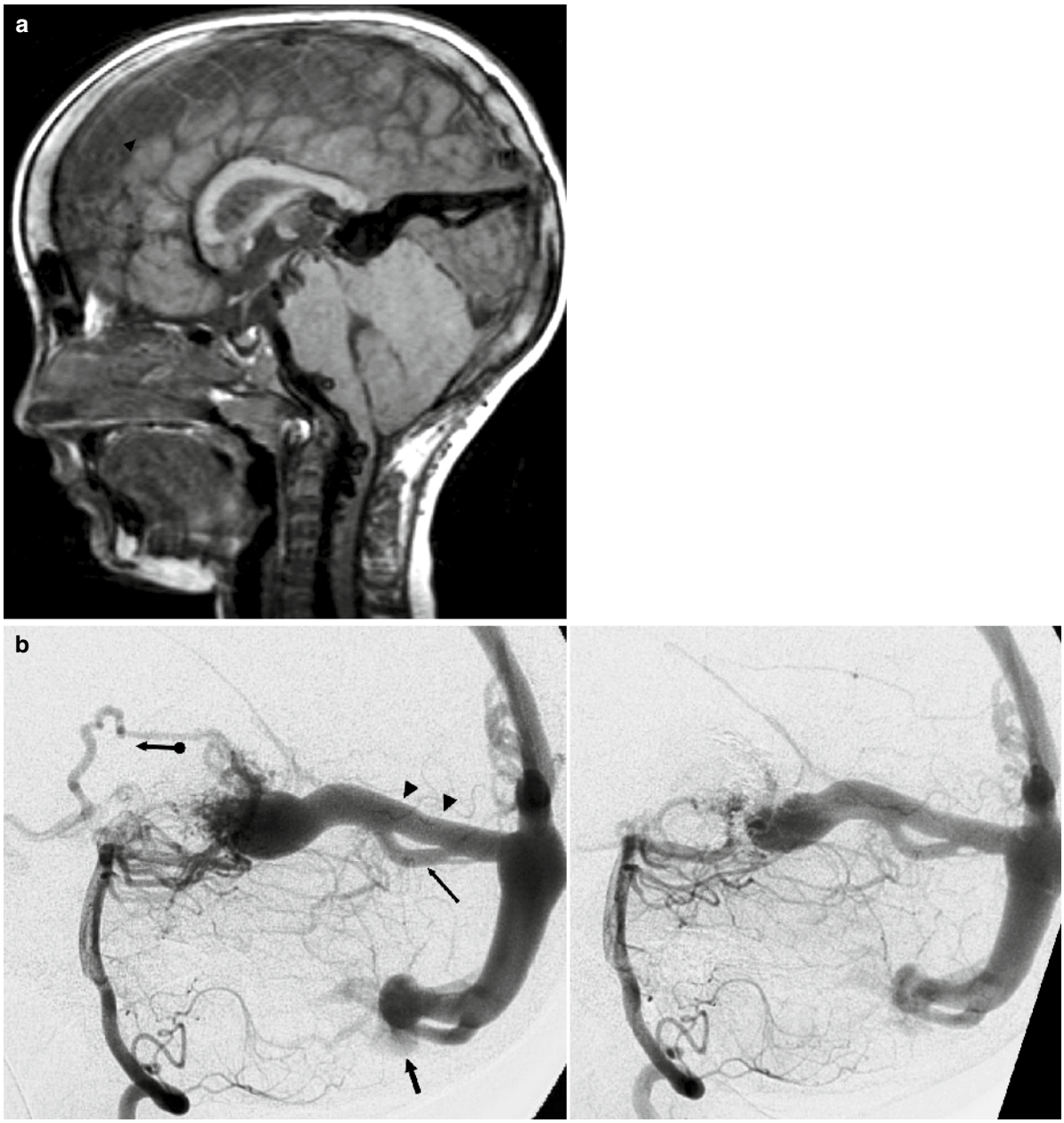

Fig. 12.20 Vein of Galen malformation in a 5-year-old patient (**a**) MRI T1-weighted image showing the malformation draining into the falcine sinus. (**b**) Vertebral angiogram, lateral view, showing, on the left, the supplying arteries, represented by the posterior thalamo-perforating arteries and posterior choroidal arteries. Large prosencephalic vein draining into the falcine sinus (*arrowhead*) and small fenestration (*smaller arrow*). Partial rerouting of the venous drainage (*arrow with dot*), anteriorly directed and continuing further, probably into the anterior pontomedullary and perimedullary veins, as visible in MRI. On the right, there is occlusion of the transverse sinus (*larger arrow*). Occlusion of the supplying arteries, with reduction of the shunt after selective catheterization and injection of glue

cases, further drainage occurs into the falcine sinus (Raybaud et al. 1989). This is an embryonic sinus channel running within the falx cerebri, directed posterosuperiorly to reach the superior sagittal sinus (SSS). Rarely, a normal straight sinus can be associated with the falcine sinus; in the majority of cases, the straight sinus is absent, hypoplastic, or malformed. Other anomalies of the dural sinuses characterized by lack of injection due to aplasia or thrombosis are frequent, involving, especially the transverse sinus (TS) and sigmoid sinus. The jugular vein can also be absent. These venous changes can promote the development of dural shunts. The presence of two falcine sinuses (falcine loop), one directed toward the SSS and the other connecting the SSS with the torcular herophili or TS, has been reported (Raybaud et al. 1989).

- *Vein of Galen dilatation.* In this group of lesions, which occur in older children, the ectatic vein is the great vein of Galen, into which drains an AVM. The dilatation is frequently associated with an obstruction of the venous drainage, involving the SS or torcular herophili. Reflux in normal cerebral veins (deep/superficial) can frequently be demonstrated on an angiogram, and it can be used in the differential diagnosis with the true vein of Galen malformation, where the normal drainage is not present (Lasjaunias 1997).

Dural Arteriovenous Fistulas

13

Isolated cases of dural arteriovenous fistula (DAVF) have been reported by some authors (Verbiest 1951; Obrador and Urquiza 1952). Progressive identification and precise description of this pathology came at the end of the 1960s, especially after selective and superselective angiographic studies (Hayes 1963; Laine et al. 1963; Newton et al. 1968; Newton and Hoyt 1970; Djindjian et al. 1968, 1973).

13.1 Incidence

DAVFs account for 10–15% of all intracranial vascular malformations. Both sexes are affected but a sexual predominance occurs in some types of DAVF. The fistulas are more frequent among middle-aged and older patients, though younger patients and children can be affected.

13.2 Pathology and Pathogenesis

DAVFs consist of a shunt between dural arteries and sinuses, either directly or mediated by cortical or other sinusal veins. DAVF is considered to be an acquired pathology (Houser et al. 1979; Chaudary et al. 1982). The specific pathogenesis, however, is still debated. Some authors believe (Houser et al. 1979; Mironov 1995) DAVFs are preceded by thrombosis of a sinus. When the lumen recanalizes, microscopic AV shunts, normally present within the wall of the sinus (Kerber and Newton 1973), may enlarge and open into the sinus. Considering, however, that sinus thrombosis is not necessarily associated with DAVF and that DAVFs are not always associated with sinus thrombosis, other authors (Chaloupka–Huddle 1998) have suggested that the primary cause is angiogenesis within the sinus wall. This leads to the formation of abnormal arteriovenous connections and finally to DAVF. Indeed, abnormal artery-vein connections have been demonstrated in histological studies of resected specimens of sinuses of patients with DAVF (Nishijima et al. 1992; Hamada et al. 1997). The cause of the microfistulas in the sinus wall is not clear. Some authors have shown with studies in animal models that venous hypertension can lead to DAVF formation more frequently in animals with induced hypertension than in those without (Terada et al. 1994; Lawton et al. 1997). Other studies (Uranishi et al. 1999; Shin et al. 2007a) have demonstrated in resected dural specimens of DAVF patients and in rat models the presence of an angiogenic growth factor that can participate in the fistular formation. More difficult to explain are DAVFs located in the dura, close to the sinus but not draining directly into it. The outflow is characterized by pial veins, which, after a more or less course, enter a near or distant sinus. In these cases, a nonspecific thrombophlebitis involving the pial veins has been suggested (Djindjian and Merland 1978).

13.3 Clinical Relevance

Many DAVFs remain asymptomatic or have a benign course. In other cases, DAVFs can have a more aggressive course, characterized by cranial nerve palsy, ischemia, hemorrhage, and cognitive disorders. In this context, it has become increasingly clear that the main factor responsible for the symptoms and evolution of DAVFs is the pattern of venous drainage (Lasjaunias et al. 1986b; Halbach et al. 1988; Awad et al. 1990; Awad 1993; Barnwell et al. 1991; Lasjaunias and Rodesch 1993; Cognard et al. 1995; Davies et al. 1996).

G.B. Bradac, *Cerebral Angiography*,
DOI: 10.1007/978-3-642-15678-6_13, © Springer-Verlag Berlin Heidelberg 2011

13.4 Location

DAVFs can occur anywhere. The most frequent are those involving the transverse–sigmoid sinuses, followed by the cavernous and superior sagittal sinus. Less common are ethmoidal (anterior cranial fossa) and tentorial DAVFs, and DAVFs located in the area of the foramen magnum involving different venous channels.

13.5 Diagnosis

DAVFs involve the preexisting vascular structure (dural branches, dural sinuses, pial veins) of the area in which they develop, and a typical repetitive pattern can be expected, corresponding to the site and type of fistula. However, it should be noted that there are many variants concerning the arteries supplying the dura and the venous drainage of the area involved. Furthermore, such variants can be altered by sinus thrombosis, and so it is not surprising that fistulas at the same site can have different angiographic patterns.

A complete angiographic study with examination of the external carotid artery (ECA), internal carotid artery (ICA), and vertebral artery (VA) is essential for the diagnosis. This provides information about all the dural branches involved and the venous drainage. The site, extension of the DAVF, and, in particular, the type of venous drainage explain the symptoms and offer information about the risk and prognosis of the fistula. Furthermore, a decision can be made about whether the fistula should be treated and, if so, whether surgical or endovascular therapy should be used; in the case of endovascular treatment, the better route—arterial or venous—has to be decided.

13.6 Classification

Castaigne et al. (1976) first distinguished DAVFs draining directly into the sinus from those in which the drainage into the sinus was mediated by a cortical vein. Taking into consideration mainly the type of venous drainage, Djindjian and Merland (1978) made the first classification. This was revised by Cognard et al. (1995) and Borden et al. (1995). Five type of DAVFs can be identified:

1. Drainage into a main sinus with an anterograde flow
2. (a) Drainage into a main sinus with reflux within the sinus but not into the pial veins; the latter drain normally into the affected sinus
   (b) Drainage into the sinus with reflux into the pial veins alone or associated with sinus reflux
3. Drainage into the sinus is mediated by the pial veins
4. Drainage into the sinus is mediated by the pial veins, which present a large ectasia
5. Drainage involves the spinal perimedullary vein.

Type 1 commonly has a benign course. In types 2 and 3, the impaired normal drainage can lead progressively to venous congestion, ischemia, and/or intracranial hypertension. In types 3 and 4, hemorrhage is frequent owing to rupture of the pial vein draining the shunt. Cranial nerve palsy can occur, particularly in DAVF of the cavernous sinus and DAVFs located close to the brainstem. Drainage involving the spinal perimedullary vein can lead to involvement of the cervical spinal cord and brainstem.

13.7 Situations Deserving More Detailed Consideration

1. DAVFs involving the transverse sinus (TS) and sigmoid sinus (SiS) are the most frequent (Halbach et al. 1987; Awad 1993). In many cases, these belong to type 1and so can be characterized by a benign course. The only symptom is bruit since the fistula is close to the petrous bone, containing the auditory apparatus. In some cases, the bruit can become very loud and intolerable for the patient, necessitating treatment. Some of these fistulas can change (Piton et al. 1984) and become type 2, with a progressively large reflux in the temporal veins, leading to venous congestion. This is particularly the case when a distal or proximal thrombosis of the sinus occurs. In other less common cases, the sinus can be occluded proximally and distally (isolated sinus). The symptoms in such patients can be very severe, characterized by cognitive disorders, epileptic seizures, and, when on the left, by aphasia (Naito et al. 2001; Bradac et al. 2002; Kiura et al. 2007). The supplying arteries can vary, but commonly branches of the ECA—occipital, ascending

pharyngeal artery (APhA), middle meningeal artery (MMA)—are involved uni- or bilaterally. Meningeal branches of the cavernous portion of the ICA and meningeal branches of the VA can also supply the fistula. Endovascular treatment with an arterial or venous approach is commonly the therapy of choice. Surgery is frequently used in cases of an isolated sinus, even if an endovascular approach has been successfully used in some cases (Figs. 13.1 and 13.2). To this group of DAVFs can be included (Fig. 13.10) also those of the torcular herophili (see also tentorial DAVF). These are very rare fistulas belonging commonly to type 2. The feeders are the MMA and occipital arteries bilaterally, the meningeal branches of the cavernous portion of the ICA, and meningeal branches from the VA uni- or bilaterally. Pial branches of the cerebellar arteries can be also be involved. The torcular herophili is frequently thrombosed, with thrombosis extending to the proximal TS uni- or bilaterally and sometimes to the distal superior sagittal sinus (SSS). The venous drainage is rerouted in the straight sinus, vein of Galen, and then in the basal vein and deep cerebral veins. Venous congestion in the cerebral hemispheres and cerebellar hemispheres is frequent. Intracranial hypertension and hemorrhage are the typical symptoms. Surgical excision has been the treatment of choice. Endovascular treatment, with selective catheterization of the feeders, followed by injection of acrylic glue or Onyx, and the venous approach when at least one TS is patent, followed by placement of coils, is in many cases a valid and successful alternative.

2. DAVFs involving the cavernous sinus (CS) are the second-most frequent fistulas (Awad 1993; Cognard et al. 1995) after those of the TS and SiS. Women are predominantly affected. The fistula can be uni- or bilateral. Also in cases of a unilateral shunt, a bilateral supply may be present. It is common for many feeders to arise from the distal internal maxillary artery (IMA), APhA, MMA, and cavernous portions of the ICA, uni- or bilaterally. More rarely, only branches of the ECA or ICA can be involved (Figs.13.3 and 13.4). The venous drainage can show different patterns. As we have described in Chap. 9.3.10, the CS consists of a plexus of several veins, which have different connections depending on their location. Since the anterior part is connected with the superior ophthalmic vein (SOV) and inferior ophthalmic vein (IOV), a fistula in this sector will create a drainage to these vessels. It should be noted that the IOV connects with the pterygoid plexus. A fistula posteriorly located will be characterized by a drainage into the inferior petrosal sinus (IPS) and superior petrosal sinus (SPS) since this posterior location communicates with these venous channels (Cheng et al. 1999; Agid et al. 2004). Such a situation can occur when the two compartments do not communicate with each other or the links are minimal. A dominant drainage can also occur when one of the routes (ophthalmic veins or IPS, Fig. 13.3) is occluded by thrombosis, which leads to a rerouting of the drainage. In other cases, the two compartments probably are largely in communication, and so both draining patterns are present. Since the CSs are connected by a large intercavernous anastomotic channel, the contralateral sinus can also be involved. More infrequently, retrograde injection of the pial veins can occur through the several connections linking the CS with the pial veins (Fig. 13.5). The possible involvement of the pial veins is as follows.

- The superficial and deep middle cerebral veins can drain into the CS and paracavernous sinus (PCS), and so they can be retrogradely filled. It should be noted that the PCS is connected with the pterygoid plexus.
- The basal vein (BV) can be retrogradely filled following involvement of the deep middle cerebral vein, which is normally a tributary of the BV. The CS is connected through a bridging vein with the ponto-mesencephalic vein. This latter communicates with the peduncular vein, which is a tributary of the BV. Furthermore, the injection of the SPS can lead to involvement of the petrosal vein, which is connected with the lateral mesencephalic vein, and then with the BV or posterior mesencephalic vein.
- Many cerebellar veins, which can be retrogradely injected, also converge at the petrosal vein.
- All these pathological venous drainages explain the clinical symptoms, which are proptosis, chemosis, nerve palsy, pain, and impairment of visual acuity; however, in some cases the symptoms become more serious because of hemorrhage or venous congestion in the temporal area, basal ganglia, brainstem, and cerebellum (Takahashi et al. 2001; Suh et al. 2005; Kim et al. 2006;

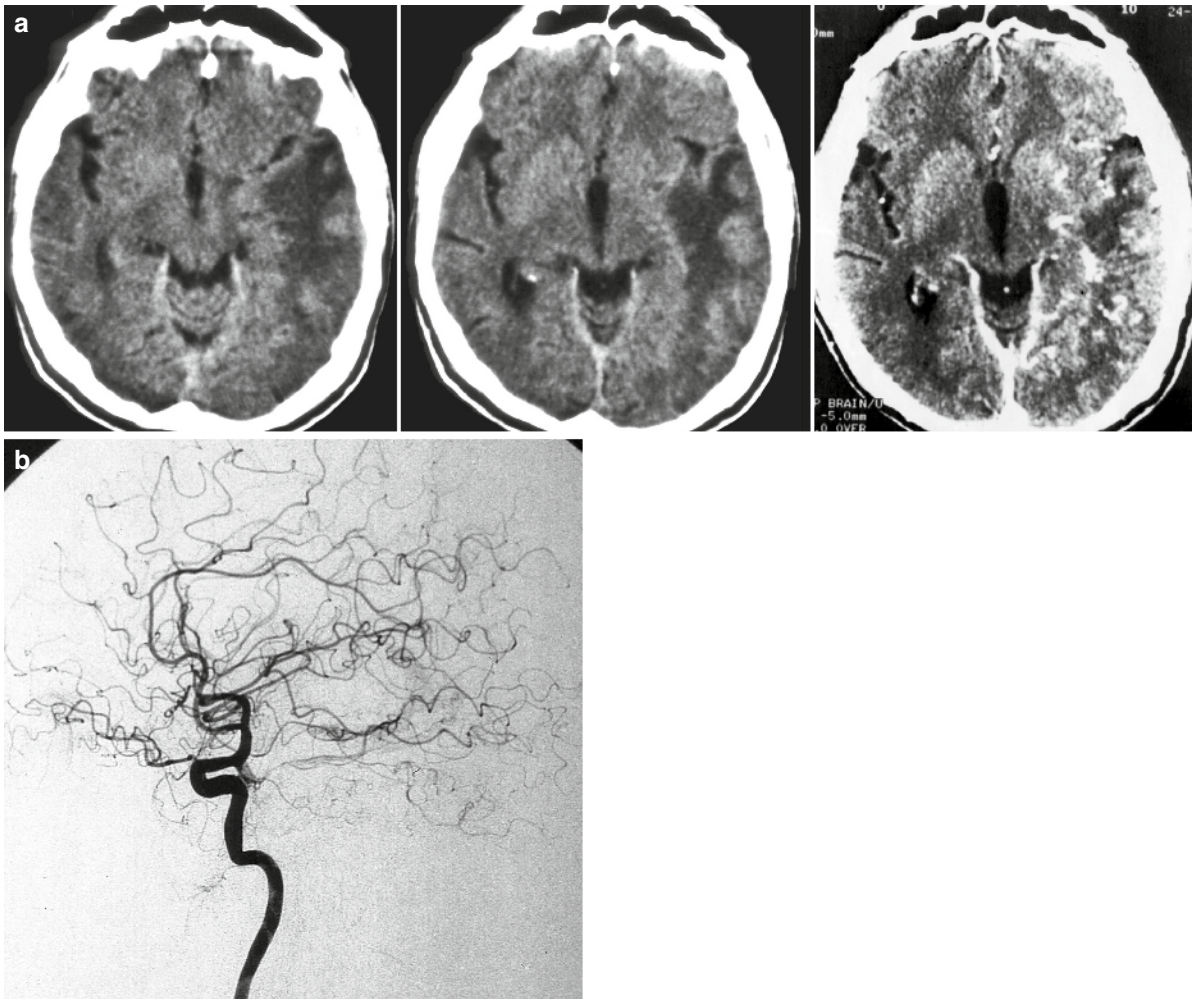

Fig. 13.1 Patient with mild aphasia and progressive cognitive disorder. CT (**a**) showed changes involving predominantly the white matter in the left temporal area, with rich irregular enhancement suggesting vascular malformation. Angiographic study showed the internal carotid artery (ICA) to be normal (**b**). On the angiogram of the external carotid artery (ECA), a dural arteriovenous fistula (DAVF) involving the left transverse sinus was demonstrated. The sinus was proximally and distally occluded, and a rich retrograde injection of the cortical temporal veins, including a large vein of Labbé, was present. The main supplying arteries (shown in **c**) were the occipital artery with its stylomastoid (*S*) and mastoid (*M*) branches, and the middle meningeal artery (*MMA*, shown in **d**). A partial supply came from the posterior meningeal artery (*arrow*) and C1 branches (*double arrows*) of the left vertebral artery (**e**). Selective distal catheterization of the MMA and stylomastoid artery (**f**) preceding the injection of acrylic glue followed by injection of polyvinyl alcohol (PVA) into the supplying branches of the vertebral artery, leading to complete occlusion of the fistula. ICA, ECA, and vertebral angiogram performed 3 months later (**g**) confirming occlusion of the DAVF. Normalization of the CT (**h**) corresponding to complete recovery of the patient

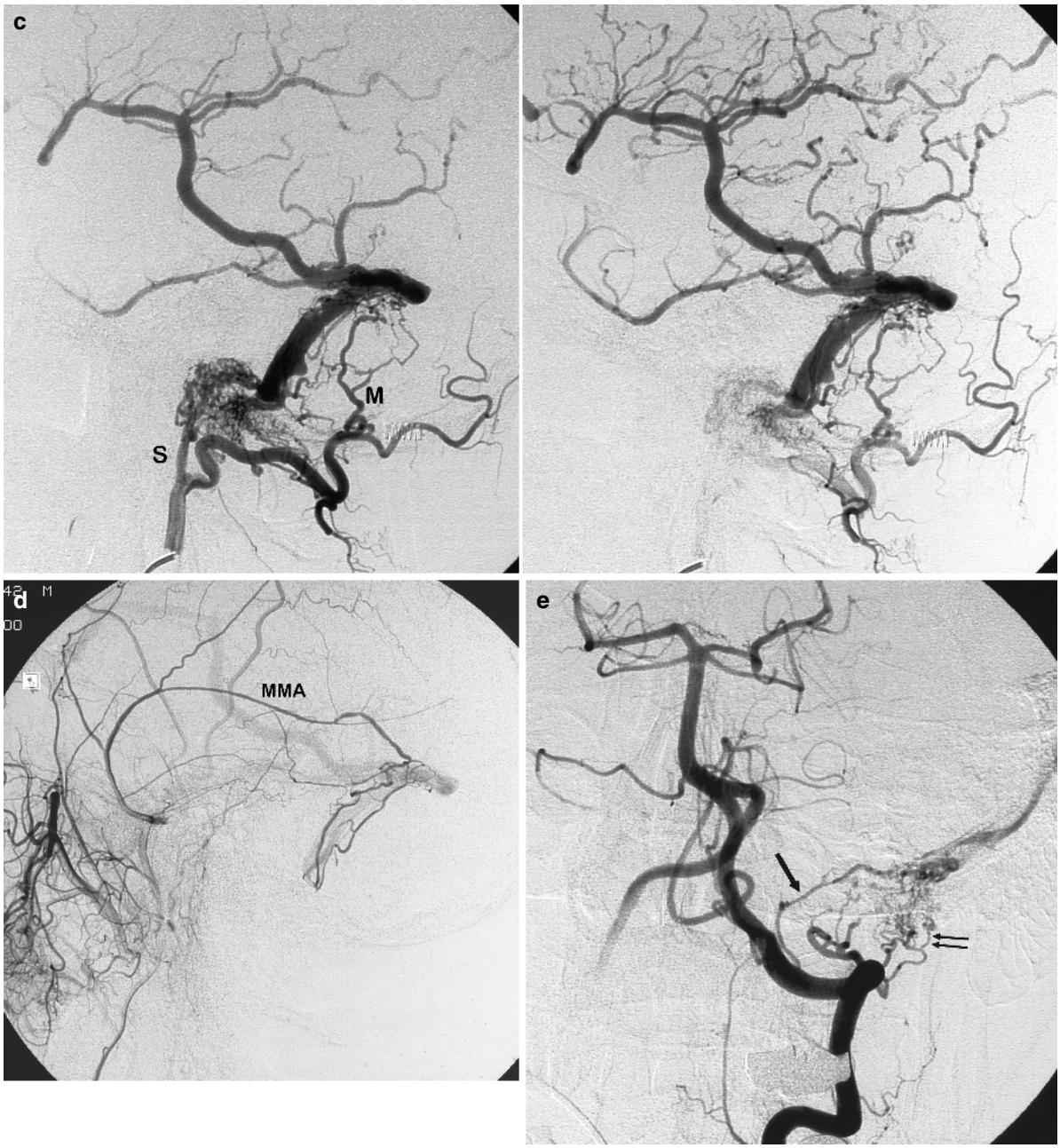

Fig. 13.1 (continued)

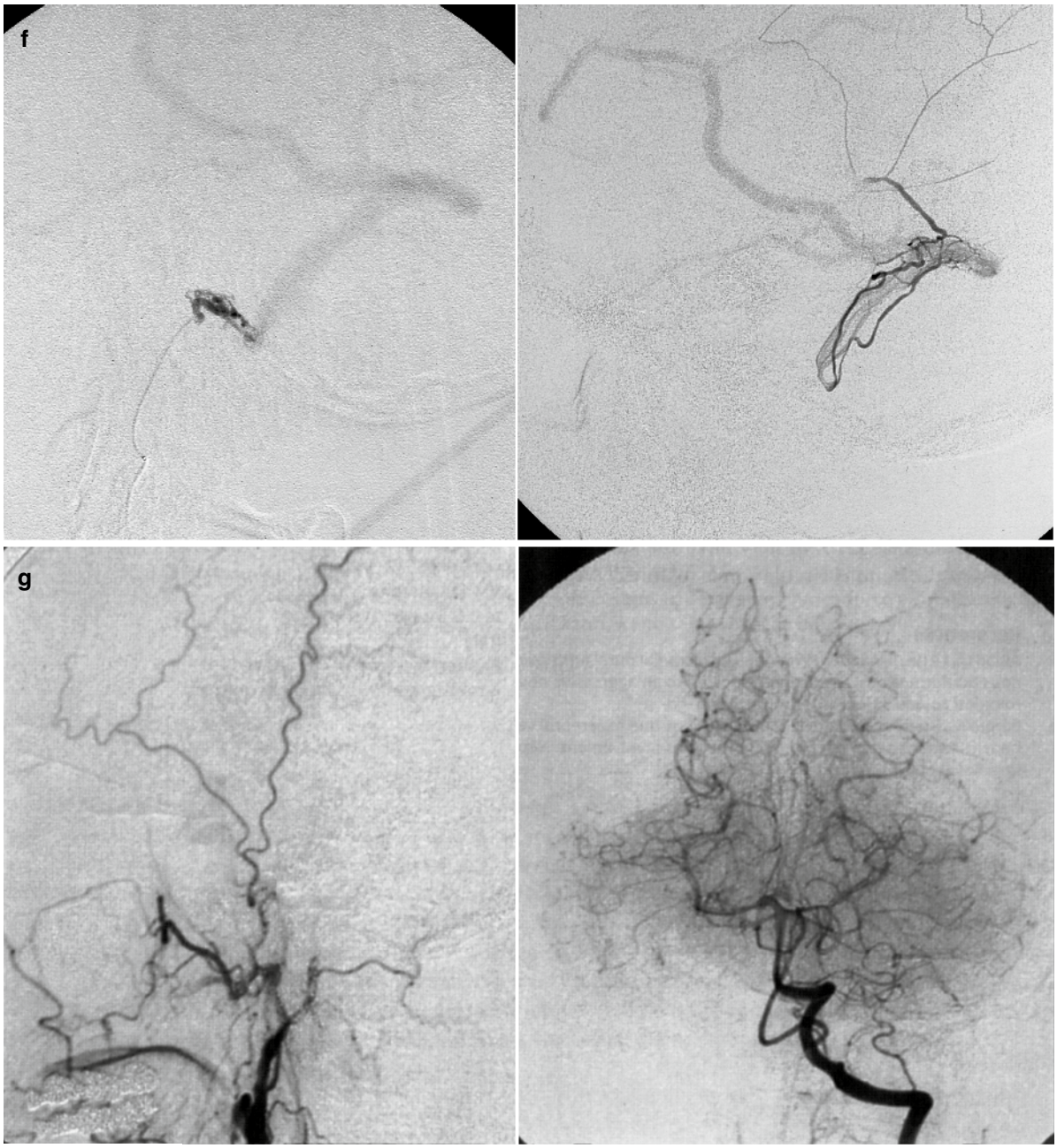

Fig. 13.1 (continued)

Fig. 13.1 (continued)

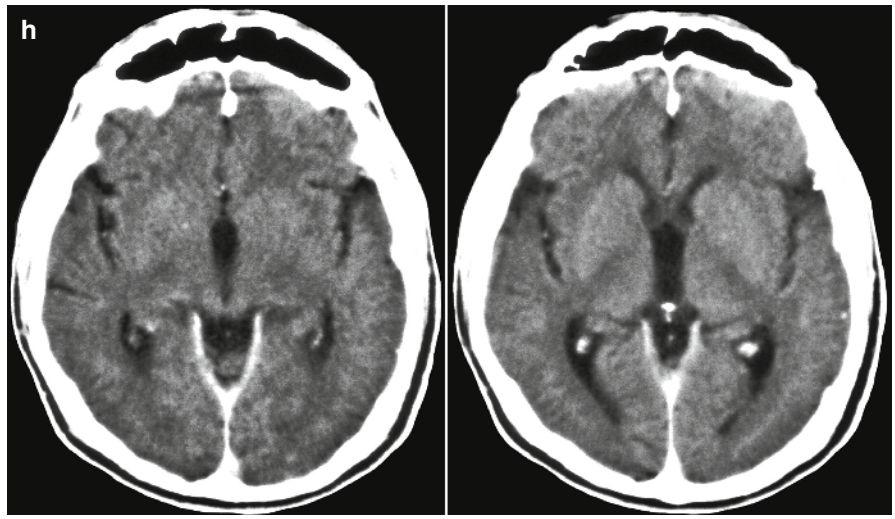

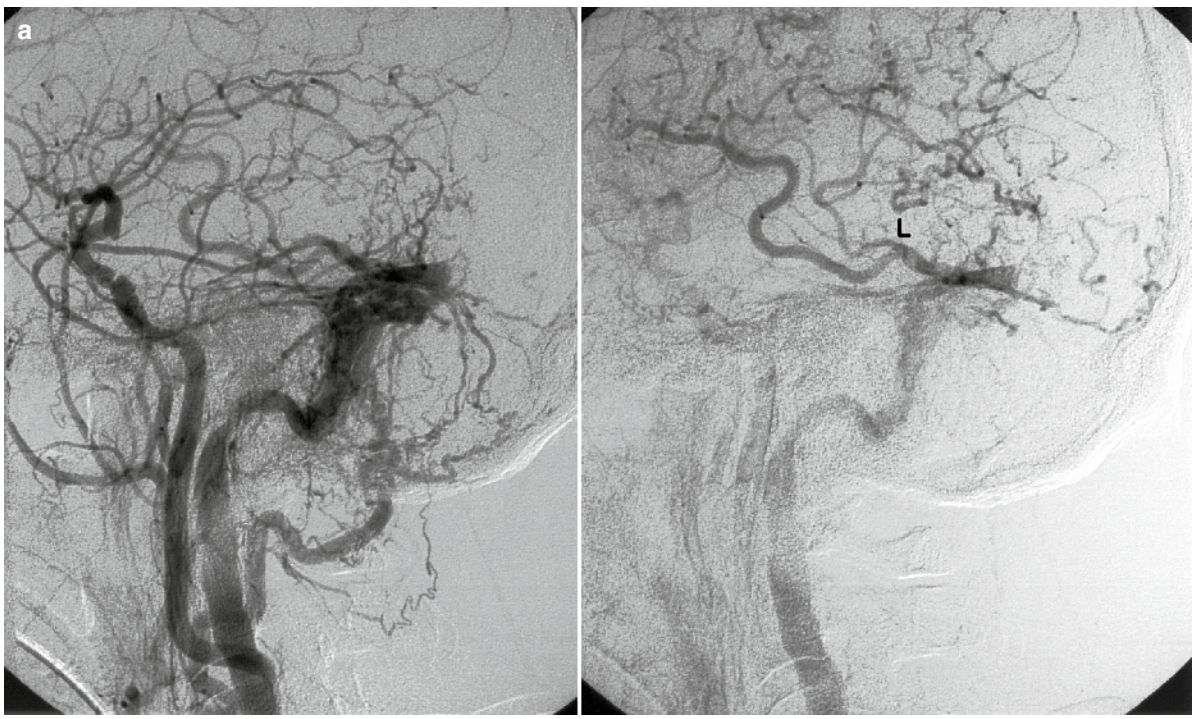

Fig. 13.2 Older patient with a known DAVF involving the transverse sinus (TS) treated with occlusion of several supplying branches of the ECA with PVA. The patient returned 6 months later suffering from the same symptoms, characterized by high bruit and headache. The carotid angiogram (**a**) showed complete recanalization of the fistula, involving the TS, which was proximally occluded. A rich retrograde injection of temporal veins, including a large vein of Labbé (*L*), was also present. On the venous phase of the ECA angiogram (**b**) retrograde injection of the cortical veins is evident. Note also the duplication of the sinus. The sigmoid sinus had already been catheterized. A microcatheter was advanced into the TS at the level of the fistula, where coils were placed (**c**). Control angiogram showing complete occlusion of the fistula (**d**)

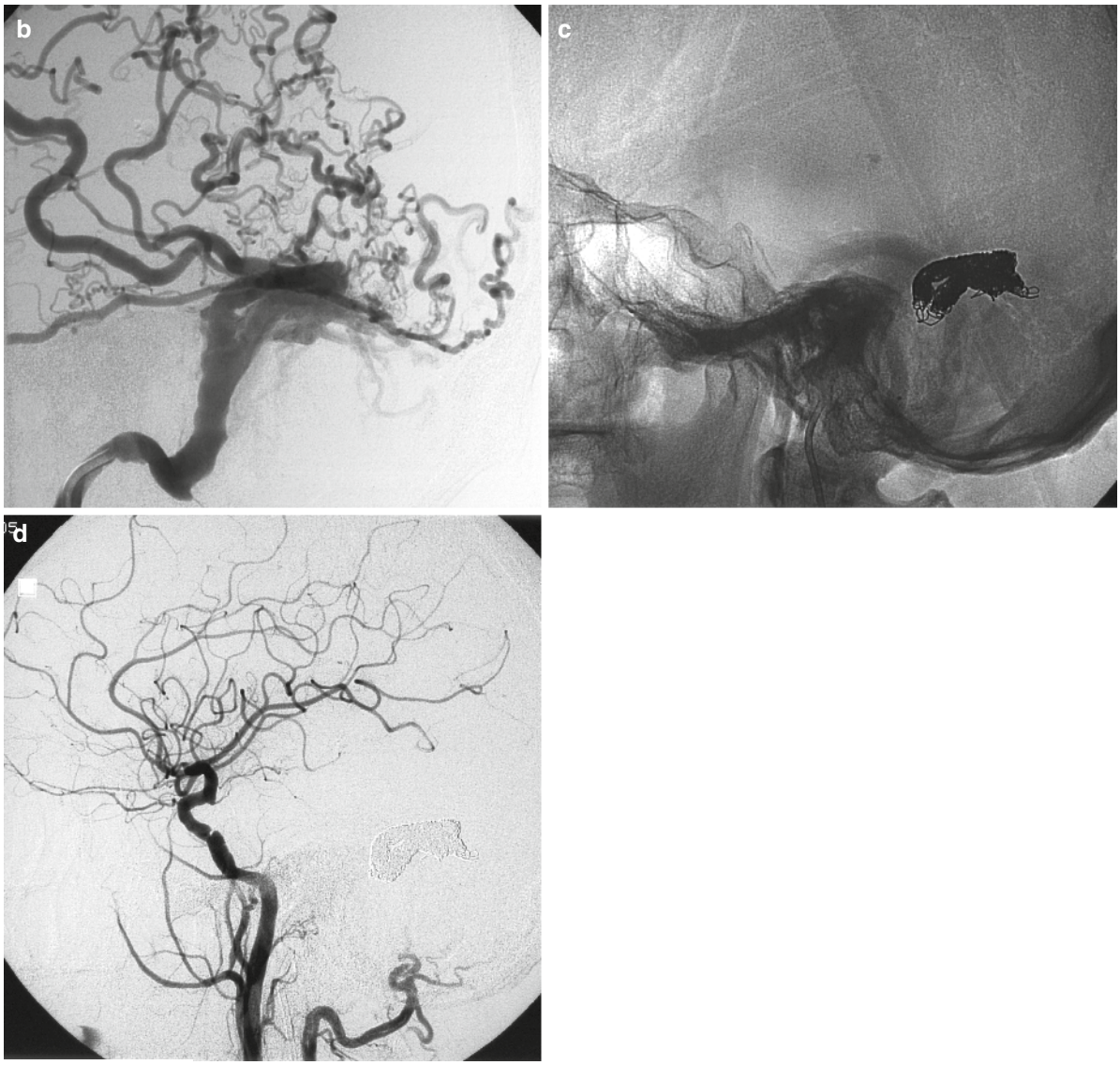

Fig. 13.2 (continued)

Kiyosue et al. 2008; Miyamoto et al. 2009). Moreover, the treatment of these fistulas is commonly endovascular: thus, with a venous approach, identification of the predominant venous drainage allows the optimal approach to be chosen in a given case (Halbach et al. 1989; Quinones et al. 1997; Cheng et al. 1999; Benndorf et al. 1999, 2001; Agid et al. 2004; Kirsch et al. 2006; Kato et al. 2007).

3. DAVFs of the SSS are more infrequent. They can be of type 1, but it is not seldom for them to be of types 2 and 3 (Figs. 13.6 and 13.7). In type 2, the venous reflux can be extensive and involve a large part of the cortical veins of the hemisphere. In type 3, the drainage in the sinus is mediated by dilated cortical veins, which enter the sinus after a fairly long, tortuous course. Branches of the ECA, mainly the

MMA, are commonly involved, frequently bilaterally. Transosseous branches of the superficial temporal artery and occipital artery can be present. The anterior meningeal artery, arising from the ophthalmic artery, and the meningeal branches of the VA may sometimes supply the shunt. Epileptic seizures, hemorrhage, and/or signs of intracranial hypertension, such as headache and cognitive disorders, can be present (Halbach et al. 1988; Riva et al. 1991). Surgical disconnection of the shunt or selective embolization with acrylic glue (Collice et al. 2000; Van Dijk et al. 2004; Rodesch et al. 2009) may be effective treatments.

4. Tentorial DAVFs are relatively rare, representing about 8% of all DAVFs. They are commonly of type 3, characterized by a high hemorrhagic risk (Picard et al. 1990; Awad et al. 1990; Awad 1993; King and Martin 1992; Cognard et al. 1995; Deasy et al. 1999; Tomak et al. 2003; Seong et al. 2006; Jiang et al. 2009). Tentorial DAVFs can be schematically

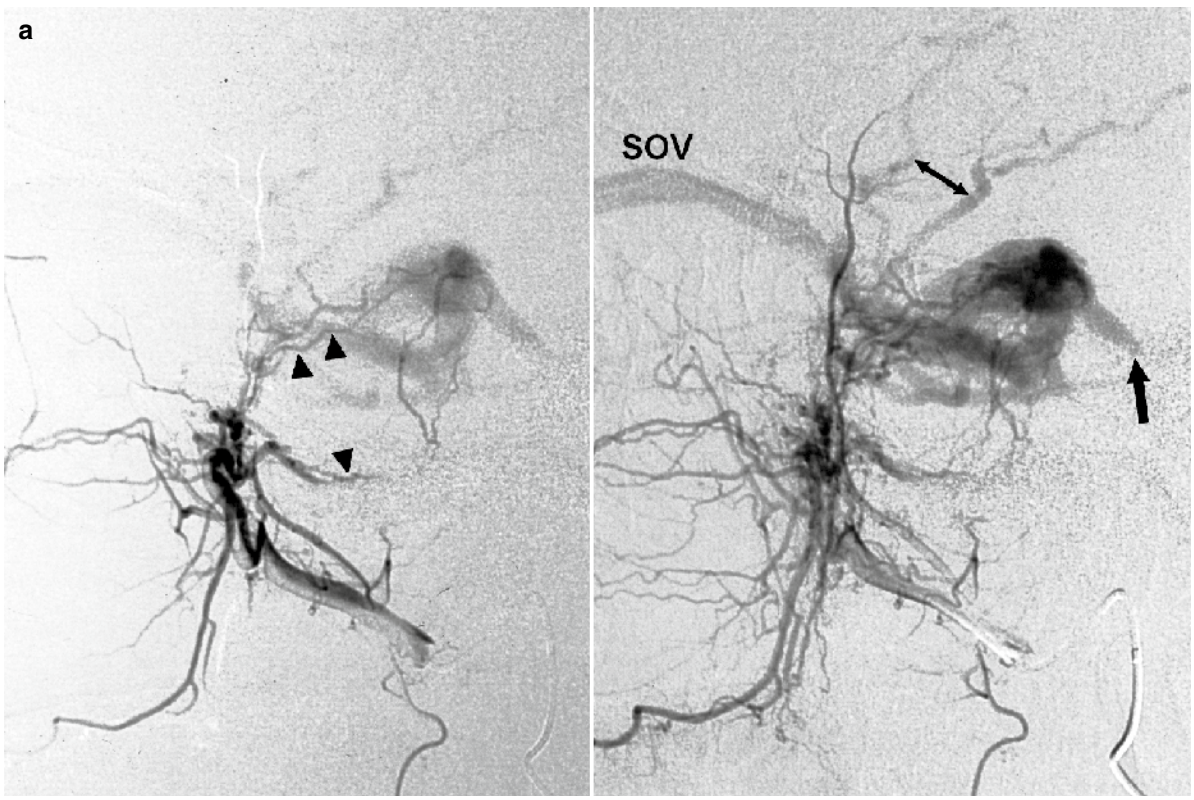

Fig. 13.3 Older woman presenting with bilateral exophthalmos, chemosis, and diplopia. The angiographic study of the bilateral ICA, ECA, and vertebral artery revealed DAVF at the level of the left cavernous sinus (*CS*) supplied by branches of the distal internal maxillary artery (*IMA*) and ascending pharyngeal artery. (**a**) Lateral angiogram of the distal left IMA showing the involvement of the foramen rotundum (*arrowheads*) and vidian arteries (*arrowhead*). Partial injection of the inferior petrosal sinus, which appears to be thrombosed (*arrow*). There is also a partial retrograde injection of the middle cerebral veins (*bidirectional arrow*). (**b**) Lateral angiogram of the ascending pharyngeal artery (APhA), showing the supply through its clival branches (*arrows*). (**c**) Lateral angiogram of the MMA involved with several branches (*arrows*). (**d**) ECA angiogram, AP view, showing involvement of the left cavernous sinus. Through intercavernous anastomoses (*arrowhead*), injection of the right cavernous sinus (*CS*) of the right superior ophthalmic vein (*SOV*) and further of the facial vein (*FV*). The left ophthalmic vein was not injected, probably thrombosed. Middle cerebral veins (*arrow*). Occlusion with PVA of the supplying arteries was performed, followed by treatment with low doses of heparin. Clinical improvement

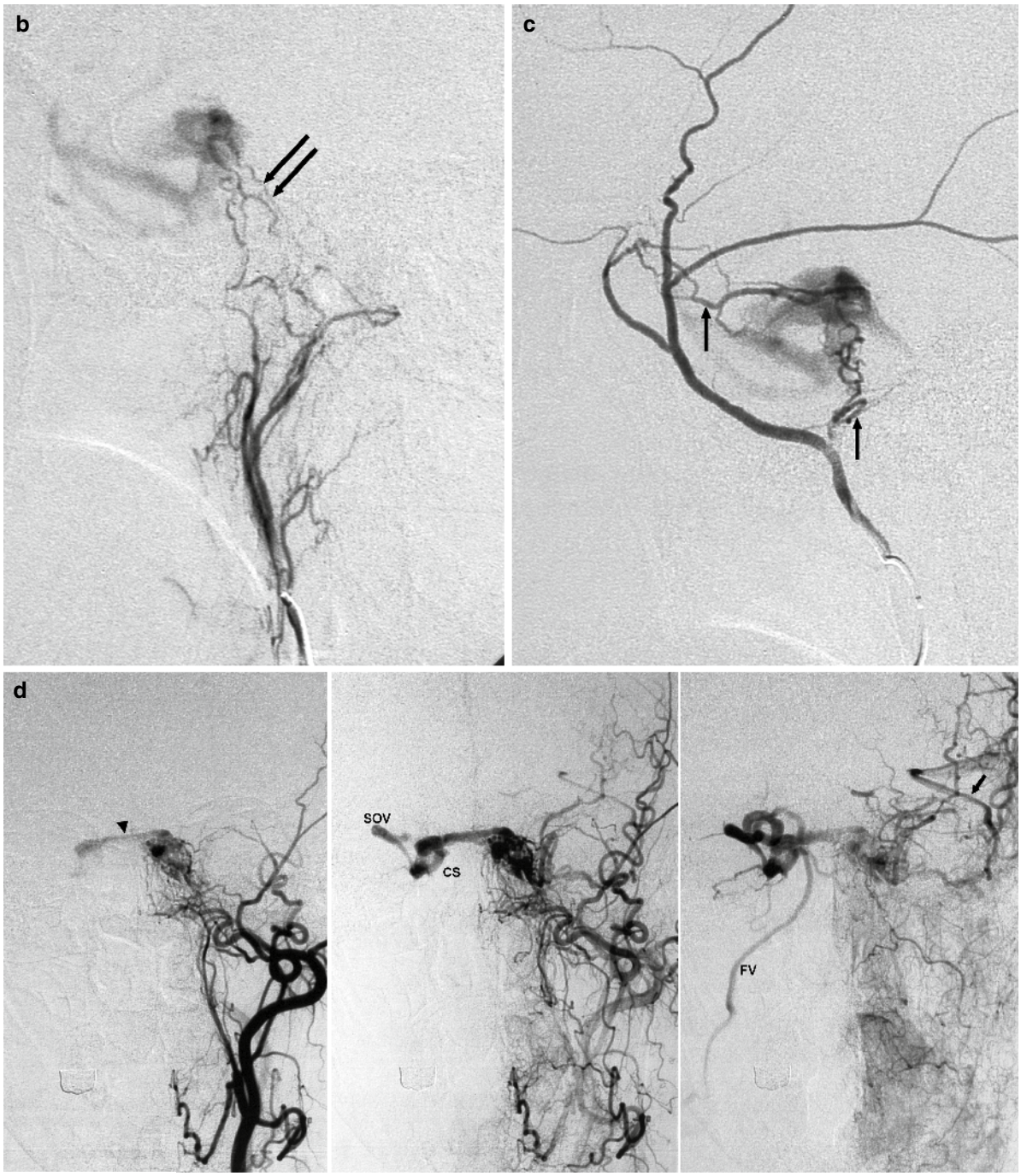

Fig. 13.3 (continued)

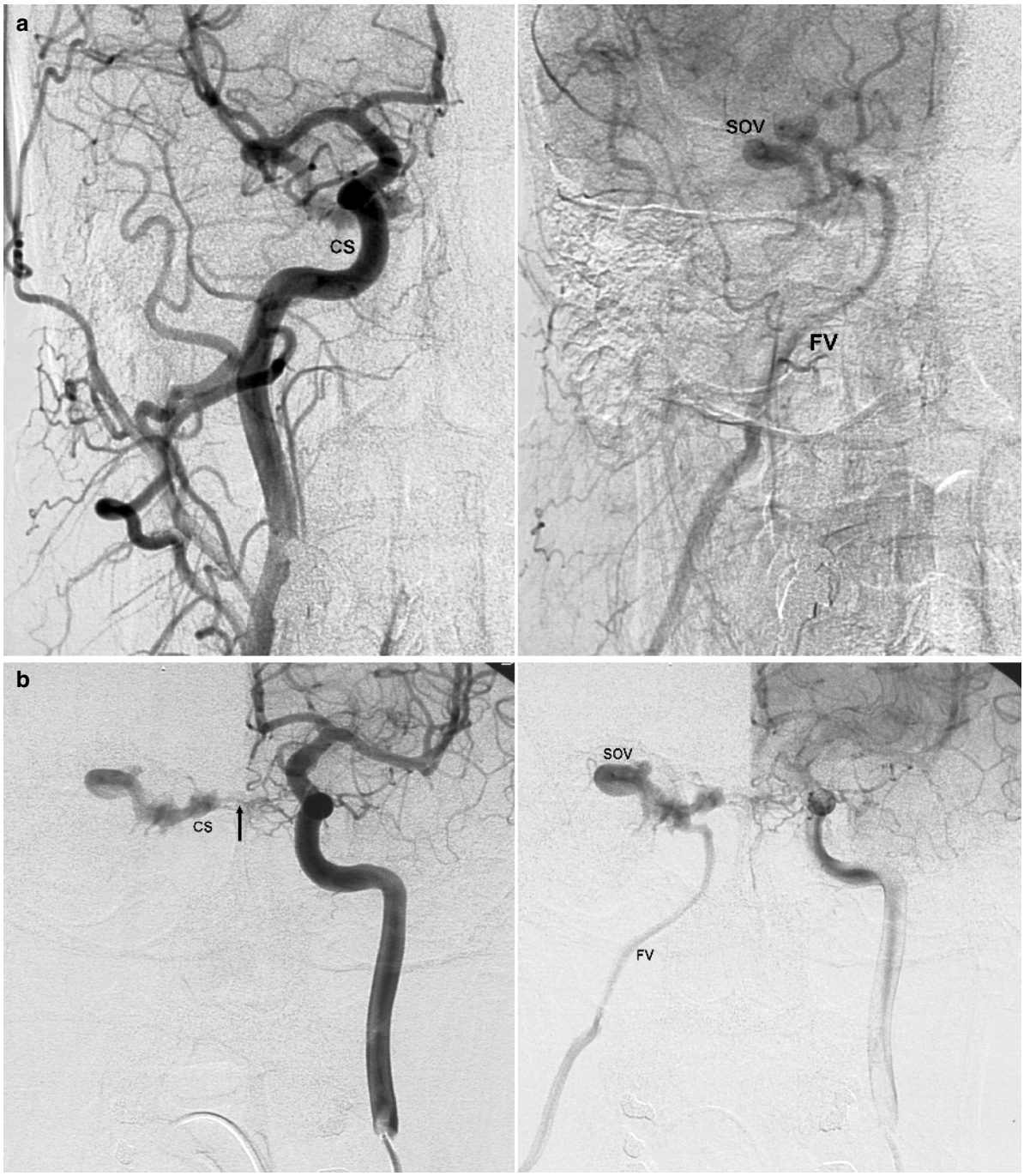

Fig. 13.4 Middle-aged man with sudden onset of exophthalmos and diplopia due to a cavernous fistula located in the right sinus, supplied mainly by cavernous branches of both ICAs. There was a minimal involvement of the ECA. The drainage occurred anteriorly in the superior ophthalmic vein and further in the facial vein. This venous route was used to occlude the fistula with coils. (**a**) Right carotid angiogram, AP view. Cavernous sinus (*CS*), superior ophthalmic vein (SOV), facial vein (FV). (**b**) Left carotid angiogram, AP view. Left cavernous branches of the ICA supplying the fistula (*arrow*). Right cavernous sinus (CS), right superior ophthalmic vein (SOV), facial vein (FV). (**c**) Injection of contrast medium into the ophthalmic vein, near the cavernous sinus, during selective catheterization with microcatheter (*arrows*). The small arrow shows the distal microcatheter during its progress. (**d**) Right and left carotid angiogram post-treatment

Fig. 13.4 (continued)

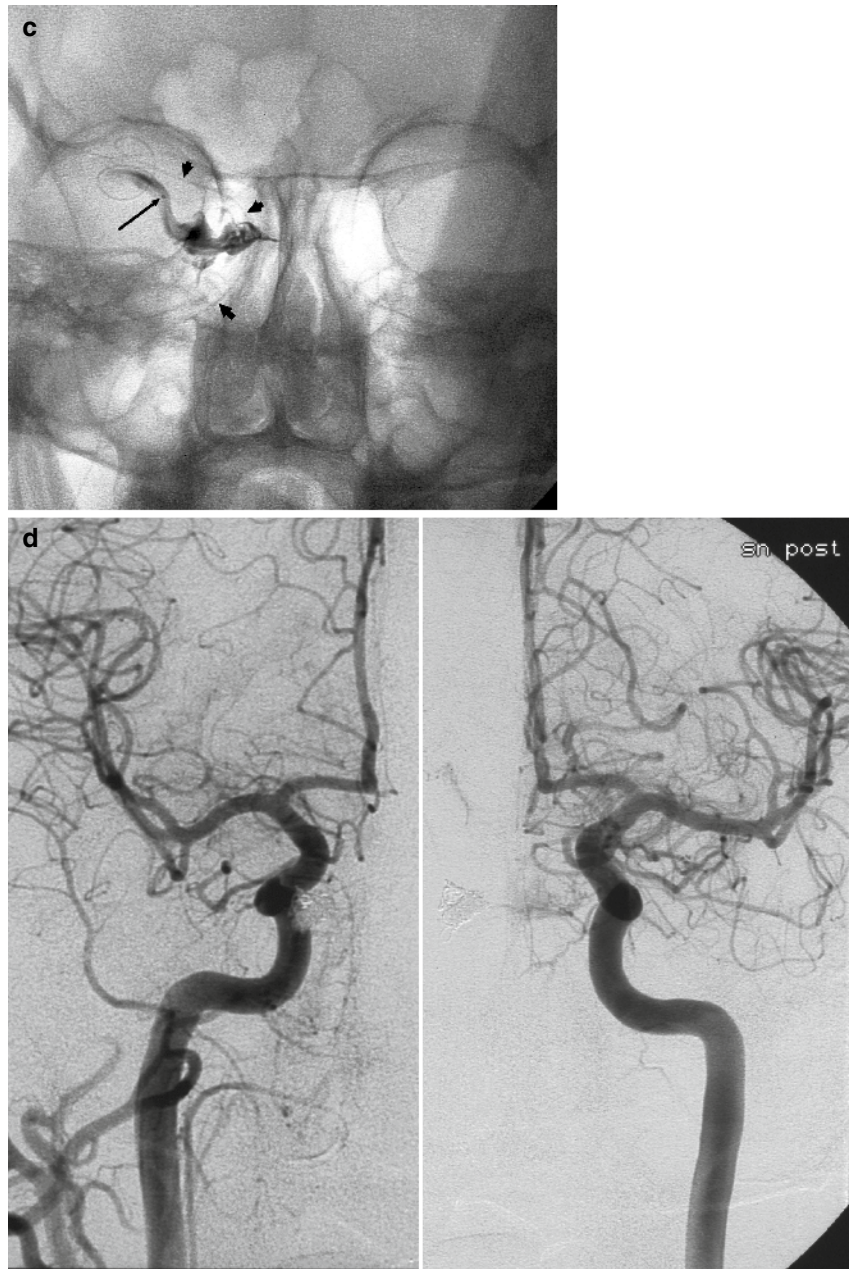

Fig. 13.5 Large DAVF involving the right cavernous sinus (CS) in an older woman with bilateral exophthalmos and diplopia. Typically, several branches of the IMA, APhA, MMA, and intracavernous branches of the ICA bilaterally are involved. The patient had already been treated with distal occlusion of branches of the ECA. Reappearance of symptoms after a short period of clinical improvement. Right carotid angiogram, AP view: (**a**), (**b**), and (**c**). There is immediate filling of the right CS. Through large intercavernous anastomoses (*double arrow*), there is rapid filling of the left CS, then of the inferior petrosal sinus (IPS) and jugular vein. The IPS does not enter the jugular bulb but the jugular vein more distally (*arrow*). There is a large anastomosis between the left CS and paracavernous sinus (*short arrow*) and retrograde filling of the deep middle cerebral vein (DMCV) and then of the basilar vein (BV) bilaterally. In the later phase (**c**), drainage through the ophthalmic vein and right dilated facial vein (FV) is evident. Right carotid angiogram, lateral view (**d**) showing drainage in the dilated superior ophthalmic vein (SOV), continuing to the facial vein (FV). Filling of the contralateral IPS. Selective catheterization (**e**) of the right cavernous sinus, advancing the microcatheter to the right jugular vein, then to the facial vein and finally to the ophthalmic vein. Almost complete occlusion of the fistula obtained by placing coils in the right CS

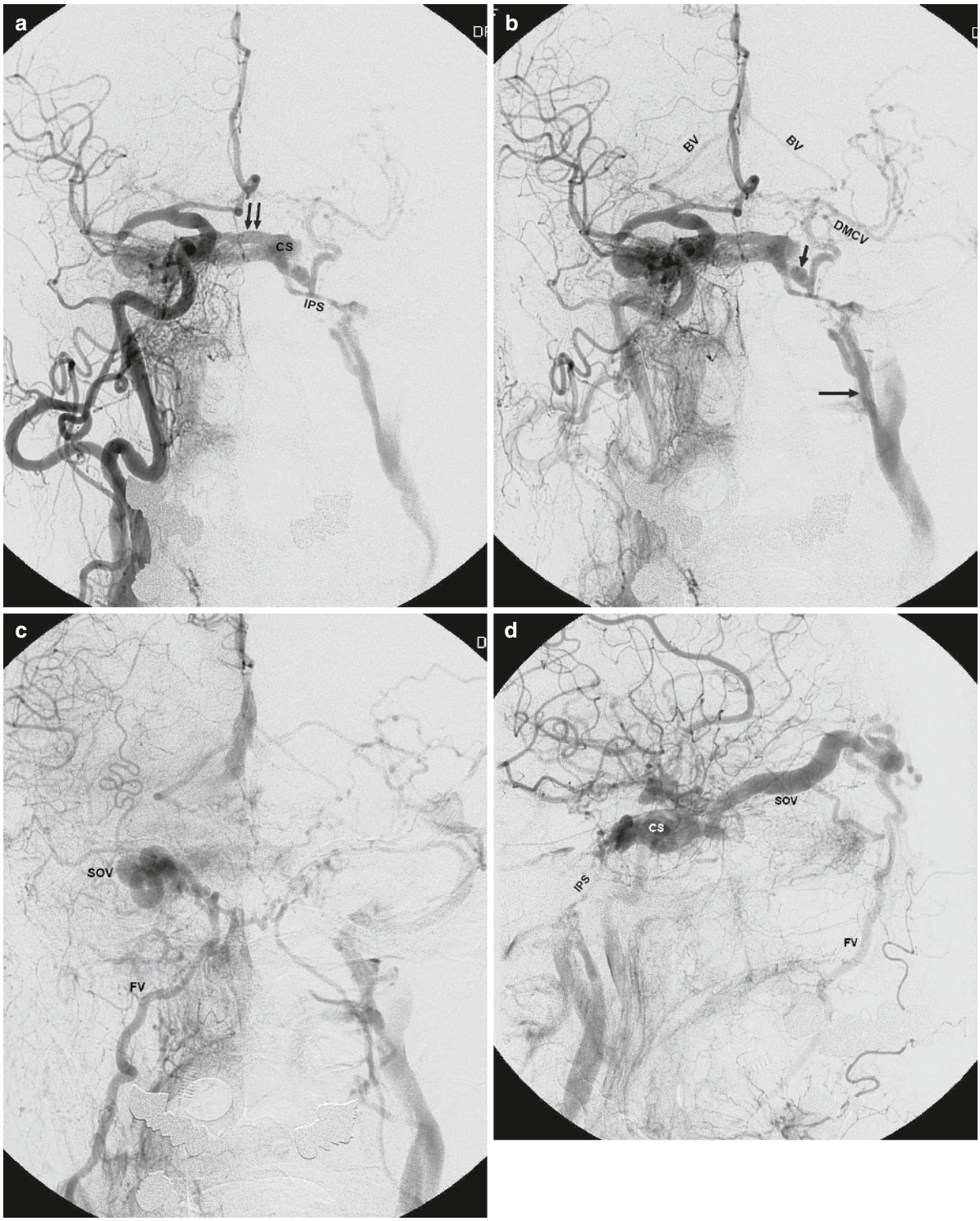
a
CS
IPS
b
BV
BV
DMCV
c
SOV
FV
d
SOV
CS
IPS
FV

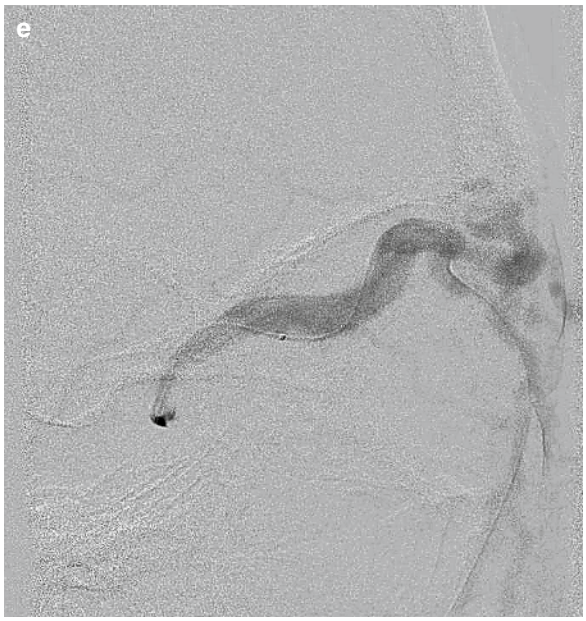

Fig. 13.5 (continued)

divided into anterior and posterior groups. The anterior, also called petrotentorial fistulas, are located in the area corresponding to the attachment of the tentorium to the superior ridge of the petrous bone. The pattern of these DAVFs is typical (Figs. 13.8 and 13.9), characterized by many arterial tributaries represented by the petrosquamosal branch of the MMA, artery of the foramen rotundum, and branches of the occipital arteries and the APhA. Cavernous branches of the ICA are also frequently present. A rich network of vessels is recognizable at the level of the superior ridge of the petrous bone. Leptomeningeal branches coming from the cerebral and superior cerebellar artery are sometimes involved. The SPS is not recognizable and probably thrombosed. Venous drainage occurs in the petrosal vein and continues through the brachial vein to the dilated mesencephalic vein, then to the posterior mesencephalic vein, and further

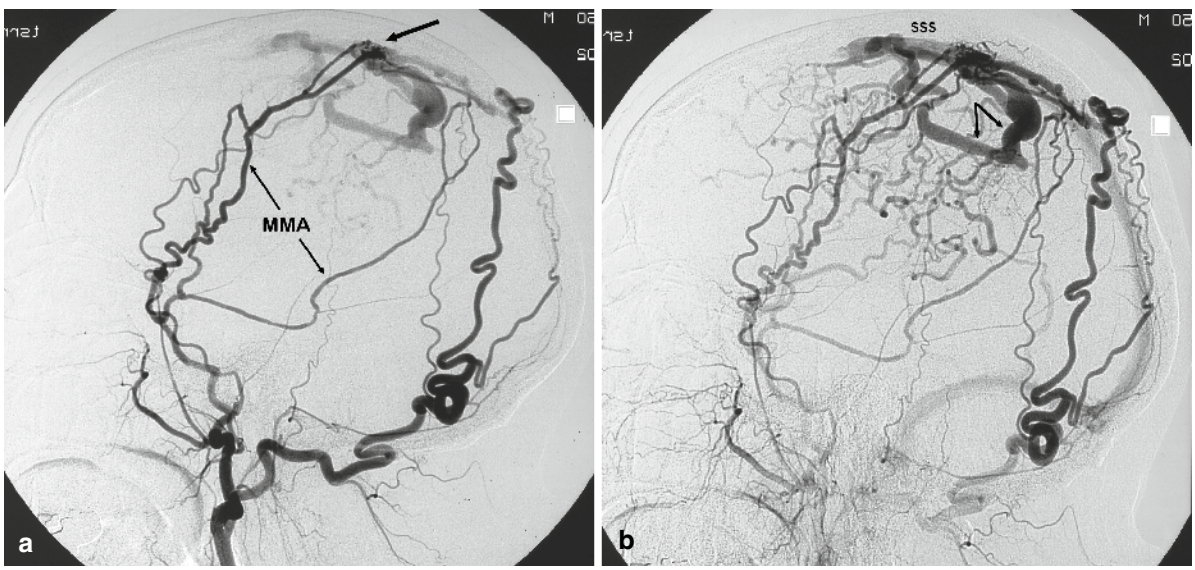

Fig. 13.6 Middle-aged patient with increased headache and suspected epileptic seizures. The angiographic study shows DAVF located in the right parietal area, close to the SSS. Right (**a**), (**b**), and (**c**) and left (**d**) ECA angiograms showing the DAVF supplied by branches of both middle meningeal arteries (MMA) and by transosseous branches of the occipital arteries. Site of the shunt (*arrow*). The drainage occurs in the enlarged cortical veins (*inclined arrows*), which after a tortuous course enter the SSS. There is retrograde injection of a large part of the cortical veins of the right hemisphere. On the right ICA angiogram (**e**), a minimal supply through the anterior meningeal artery (*arrows*) is visible. In the venous phase (**f**), congestion in the venous drainage explains the irregular and poor injection of the veins (*arrows*). The patient underwent surgical treatment

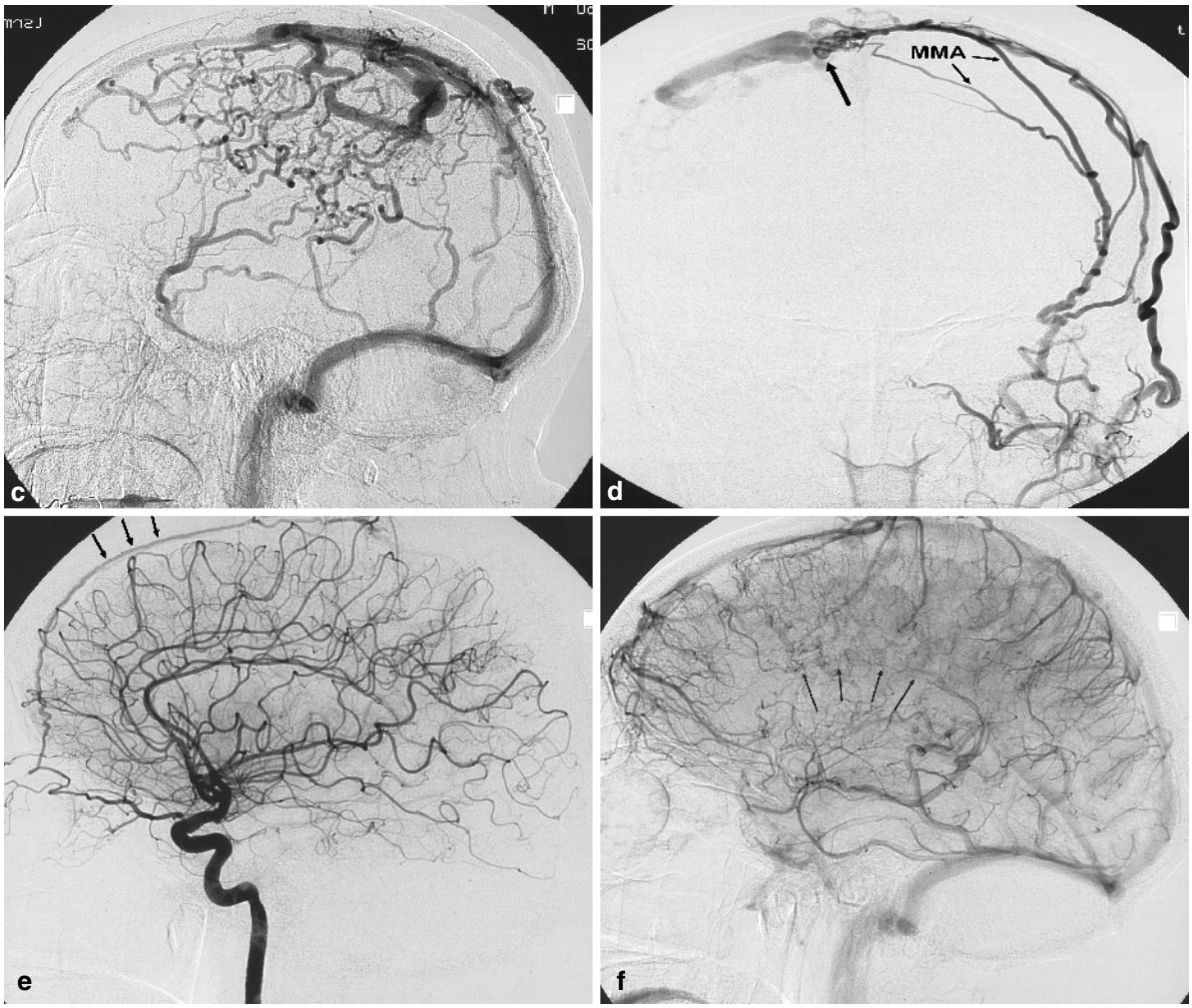

Fig. 13.6 (continued)

to the vein of Galen and straight sinus. The vein of Galen or straight sinus are sometimes thrombosed, and so the venous drainage is redirected anteriorly to the BV and internal cerebral vein. Tentorial DAVFs can be located in the posterior part of the tentorium (Figs. 13.11 and 13.12), close to the straight sinus, either near the torcular herophili or more anteriorly at the notch of the tentorium. They may also be located more laterally, near the cerebral convexity. The supplying arteries are similar to those already described, but there is greater involvement of the falx cerebelli artery and pial branches of the superior cerebellar arteries and posterior cerebral arteries, particularly when medially located. Furthermore, a meningeal branch can arise from the posterior cerebral artery (Figs. 13.11 and 13.12). The venous drainage may vary largely and frequently involve the vein of Galen. Otherwise the TS, SSS, or straight sinus are involved, directly or indirectly, via the occipital or cerebellar veins. Drainage directed caudally into the perimedullary veins may also occur (Cognard et al. 1995). The vein of Galen or straight sinus can be thrombosed, leading to a redirection of the venous drainage. Both surgical and endovascular treatment are difficult. With endovascular treatment, good results can be obtained by injecting acrylic glue or, more recently, Onyx into the feeding arteries.

5. DAVFs of the anterior fossa, also called ethmoidal, are rare, amounting to around 6% of all DAVFs

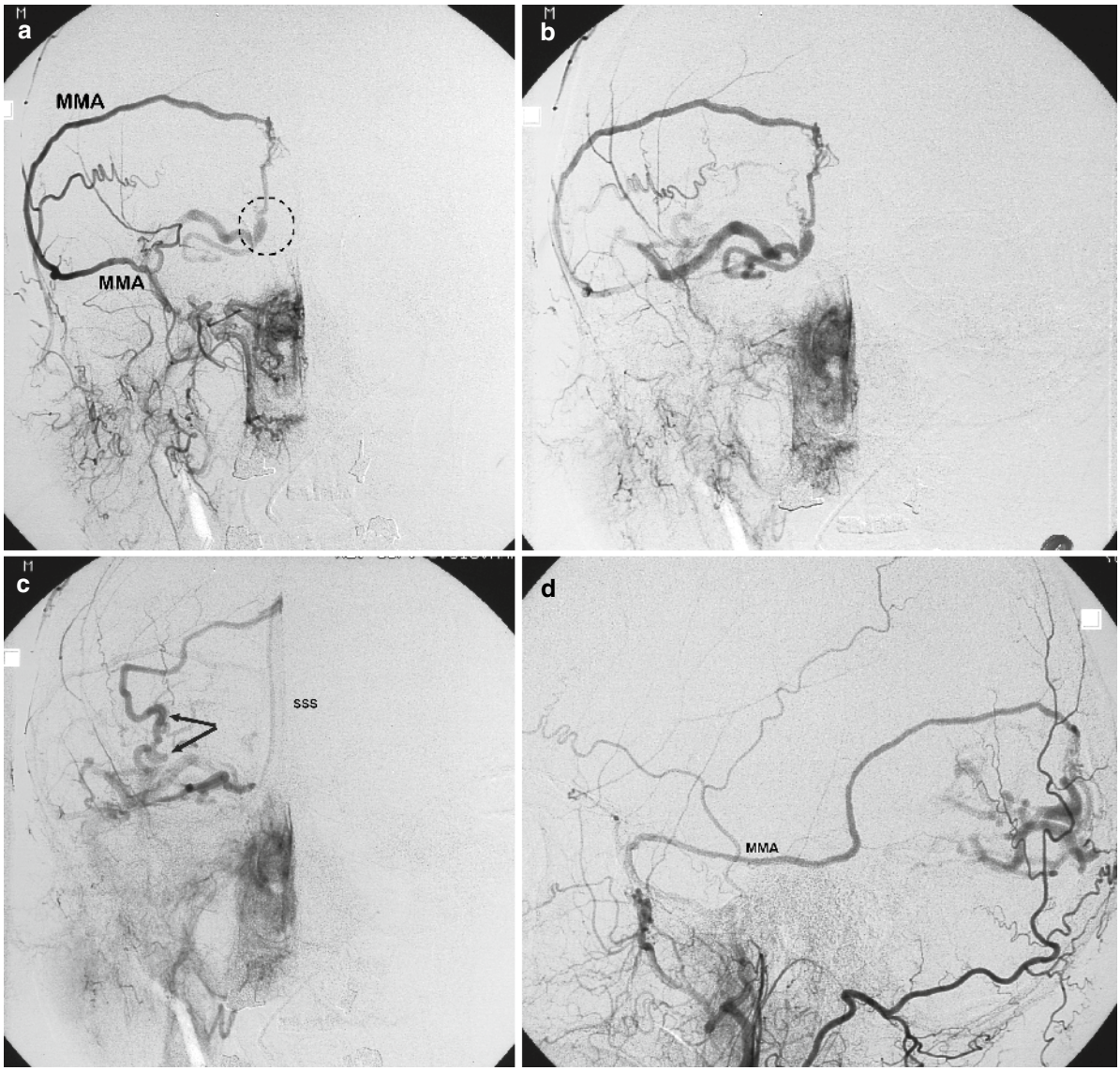

Fig. 13.7 Older patient suffering from acute headache. CT showed a suspected vascular malformation in the right occipital area. Angiography indicated a DAVF located in the right occipital area, close to the SSS. Angiogram of the right ECA, AP view (**a**), (**b**), and (**c**) showing the middle meningeal artery (*MMA*) supplying the malformation. Site of the shunt (*circle*). The venous drainage occurs through the cortical veins (*inclined arrow*), which after a tortuous course enter the superior sagittal sinus (*SSS*). Lateral angiogram of the ECA (**d**) followed by selective catheterization of the MMA (**e**), showing the site of the shunt (*arrows*) and venous drainage. There was no involvement of the ICA but a supply through the falx cerebelli artery (*FCA*), arising from the intracranial vertebral artery, was visible on the vertebral angiogram (**f**). Endovascular treatment with Onyx injected into the MMA allowed complete occlusion of the fistula. Carotid and vertebral control angiograms (**g**) and (**h**) post-treatment

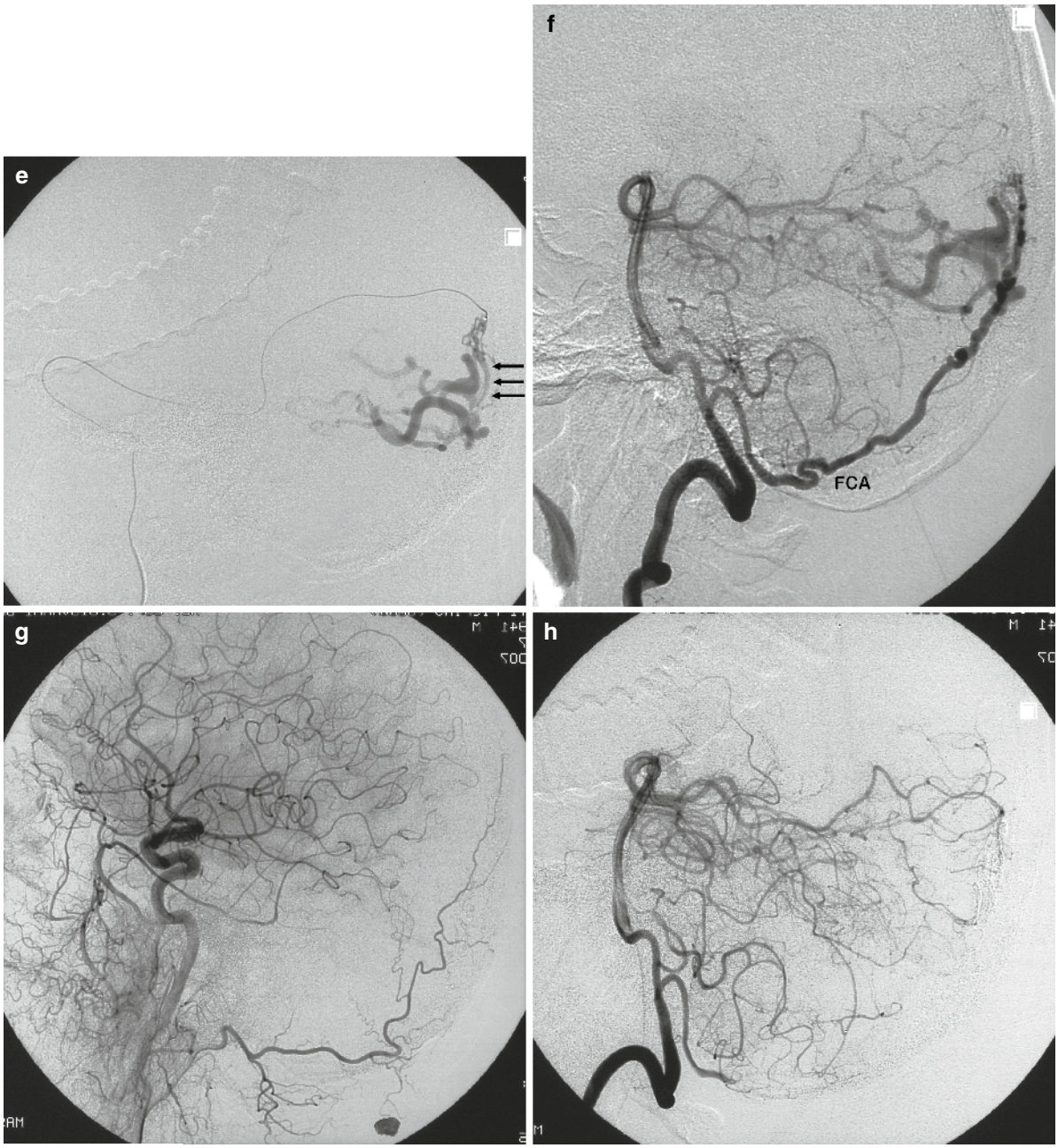

Fig. 13.7 (continued)

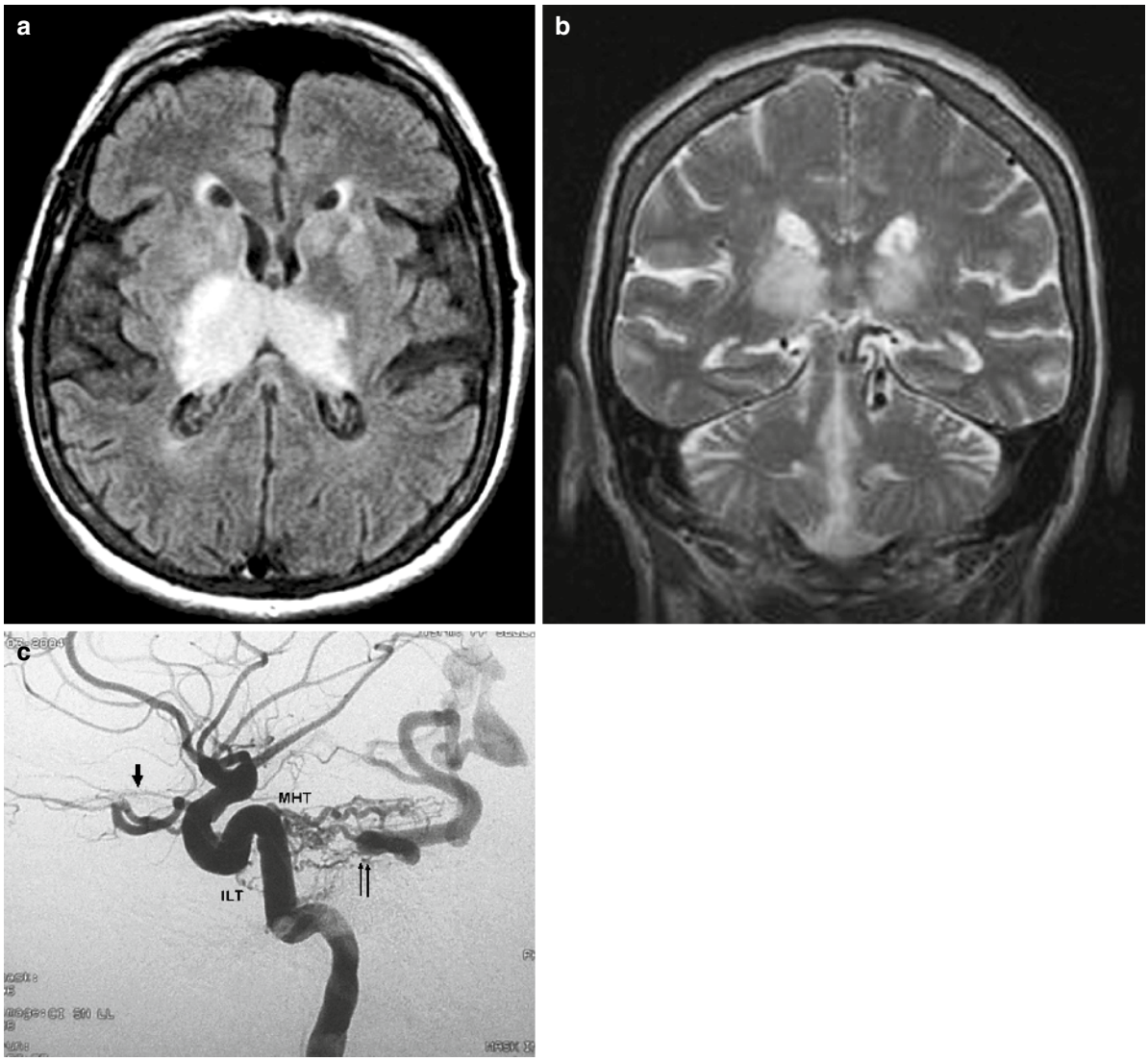

Fig. 13.8 Petrotentorial DAVF in a patient with slowly progressive cognitive disorder. MRI-fluid-attenuated inversion-recovery (FLAIR), T2-weighted (**a**) nonspecific hyperintensity involving both thalami. MRI T2-weighted, coronal image (**b**) showing anomalous vascular structure localized lateral to the midbrain, suggesting vascular malformation. Angiography of the ICA (**c**) disclosed a dural DAVF with a shunt (*arrows*) in the area where the tentorium attaches to the superior ridge of the petrous bone supplied by dilated branches of the meningohypophyseal trunk (MHT) and inferolateral trunk (*ILT*) of the ICA. A recurrent branch of the ophthalmic artery is also involved (*large arrow*). The ECA angiogram in AP and lateral views (**d**) showed the shunt (*arrows*) supplied by the mastoid branches (*M*) of the occipital artery and branches of the MMA (*arrowhead*) especially through its petrosquamous branch (*PS*). There is also involvement of the accessory meningeal artery (*arrow*). The superior petrous sinus is thrombosed. The venous drainage involves the petrosal vein, which continues through an enlarged brachial vein to the lateral mesencephalic vein (*LMV*), then to the posterior mesencephalic vein and the vein of Galen. The straight sinus (*SS*) is occluded, probably thrombosed. The drainage is rerouted anteriorly in the contralateral basilar vein (*BV*), continuing to the deep middle cerebral vein (*arrow with dot*) and superficial middle cerebral vein (*double arrow with dot*). Retrograde injection also of the internal cerebral vein. Selective angiographic study (**e**) of the MMA better showing the shunt (*arrow*) and venous drainage. The fistula was occluded with acrylic glue. MRI FLAIR T2-weighted, performed a few weeks later (**f**) showed the progressive reduction of the hyperintensity of the thalami, which was due to a venous congestion of the deep venous drainage. Gradually, there was clinical improvement of the patient

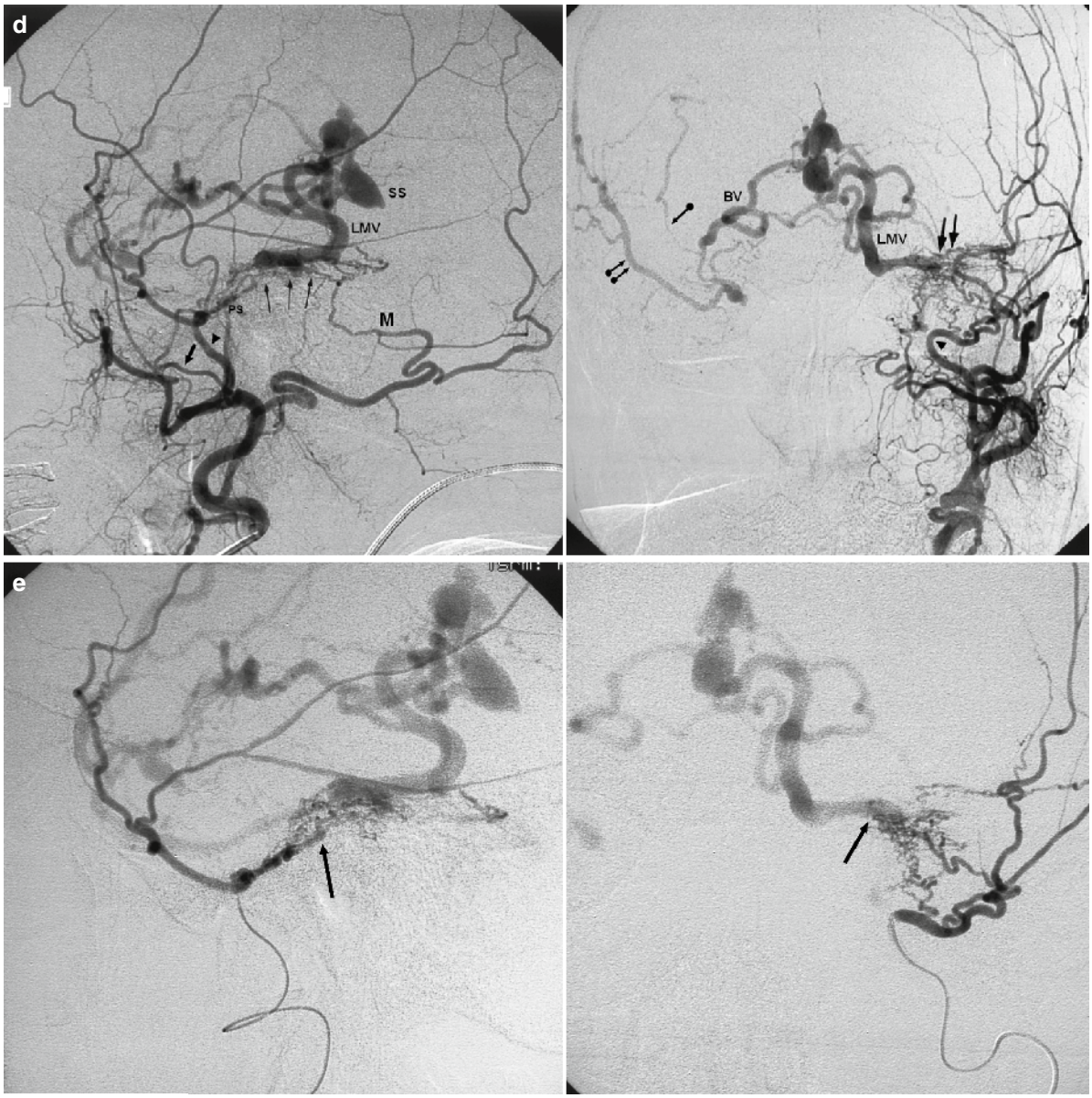

Fig. 13.8 (continued)

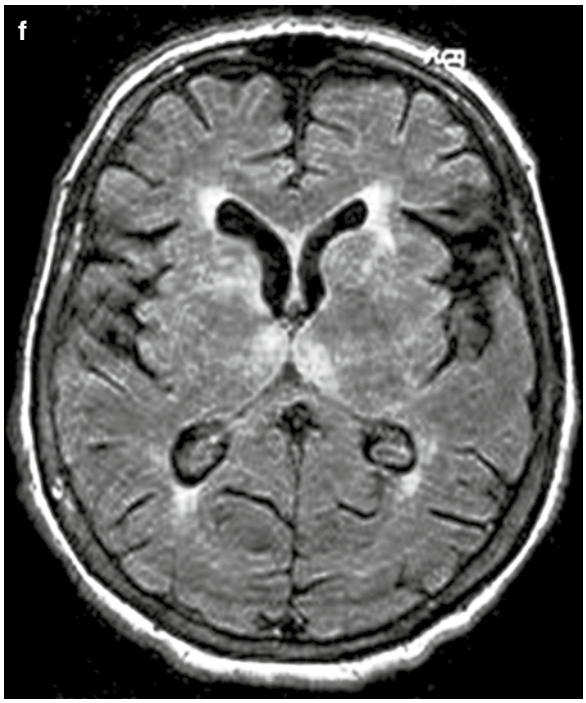

Fig. 13.8 (continued)

(Picard et al. 1987; Kobayashi et al. 1988; Cognard et al. 1995; Awad 1993). They are reportedly more frequent in males (Martin et al. 1990; Van Dijk et al. 2004). These DAVFs are of types 3 and 4 and are commonly present with hemorrhage (Ito et al. 1983; Martin et al. 1990; Awad 1993). The supplying arteries are the posterior and anterior ethmoidal arteries, which are branches of the ophthalmic arteries. The ethmoidal arteries enter the cranial fossa through the cribriform plate and normally supply the dura of the medial anterior cranial fossa. Among the anterior ethmoidal arteries, the anterior meningeal artery is often largely involved; the anterior meningeal artery normally supplies the dura of the falx and adjacent dura of the frontal convexity. Since this artery anastomoses with the corresponding falx branch of the MMA, the latter may also be involved. The ethmoidal arteries anastomose with the ethmoidal branches of the IMA, which arise from the sphenopalatine branches supplying the nasal fossa, and so this consequently becomes involved. Drainage is via the pial veins of the frontal convexity (Fig. 13.13), which are frequently dilated, forming large venous pouches, and enter the SSS. Less commonly, the venous drainage is directed posteriorly to the cavernous sinus (Martin et al. 1990). The involvement of the ophthalmic artery and the drainage in some cases to the cavernous sinus explain the impairment of visual acuity and ocular motility dysfunction. Surgical excision is the therapy of choice. Endovascular treatment, with selective catheterization of the distal ophthalmic artery followed by injection of acrylic glue or Onyx, has been successfully reported by some authors (Lv et al. 2008; Agid et al. 2009).

6. Another complex group of DAVFs is that located at or close to the foramen magnum (Barnwell et al. 1991; McDougall et al. 1997; Ernst et al. 1999; Miyachi et al. 2008; Abiko et al. 2008; Manabe et al. 2008). These DAVFs involve several uni- or bilateral feeders that arise from the APhA, occipital artery, VA, and, more rarely, from the IMA and ICA. The venous drainage can vary since this area is a crossing point for several venous channels, represented by the IPS, jugular vein, sigmoid sinus, anterior condylar vein with its connections, and marginal sinus with its connections (Figs. 9.17–9.21). MRI angiography can be very useful in identifying the precise site of these fistulas.

In a few of these fistulas, as reported by others (Rodesch et al. 1991), the shunt directly involves the pial veins surrounding the medulla, draining further caudally to the perimedullary veins of the cervical spinal cord and cranially to the ponto-mesencephalic veins (Figs. 13.14–13.16).

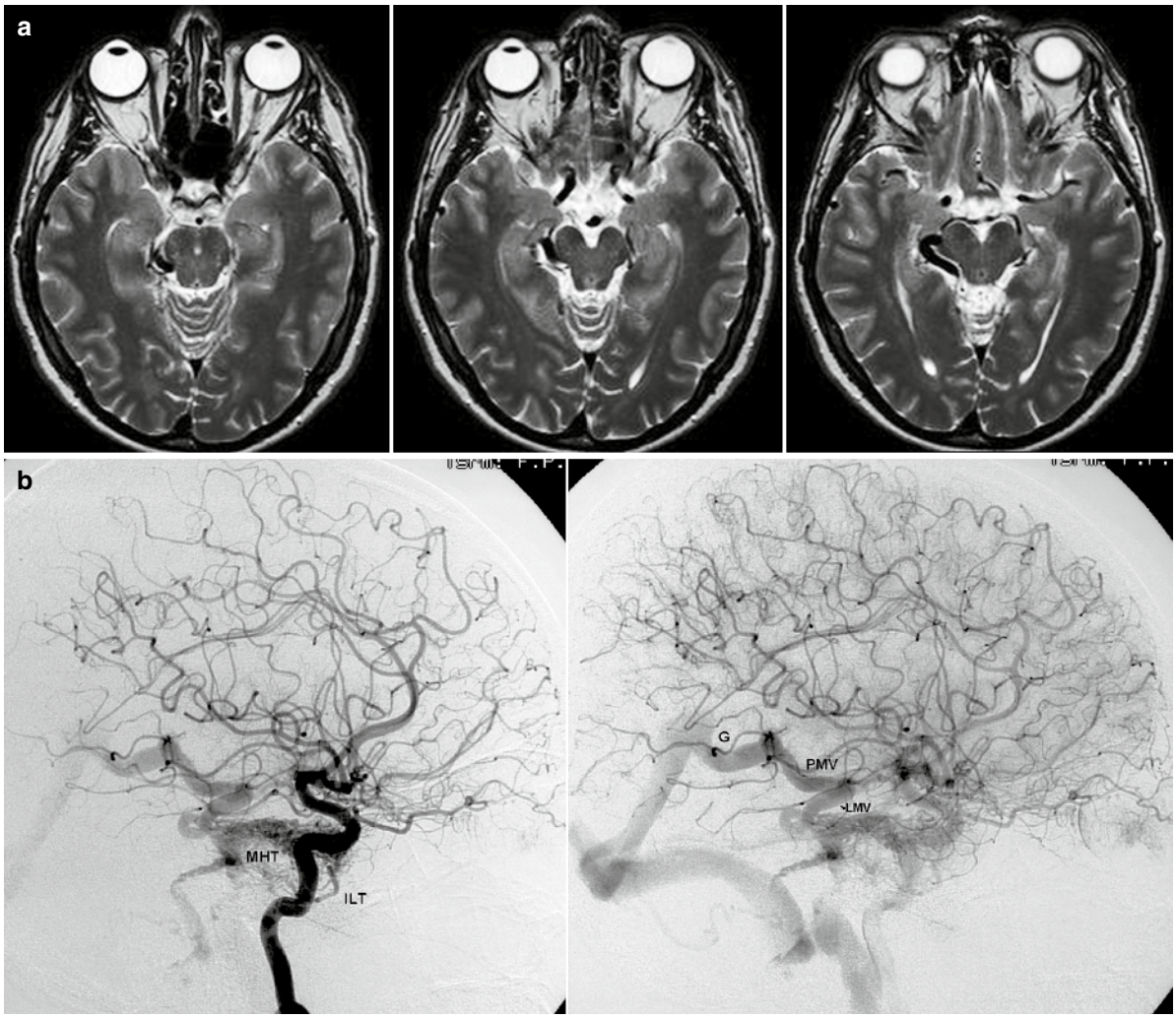

Fig. 13.9 Petrotentorial DAVF in a young patient with sudden onset of cranial nerve IV palsy. MRI (**a**) showed an abnormal vessel running laterally to the midbrain. On the ICA angiogram (**b**), there are several branches arising from the MHT and ILT converging on the petrotentorial area. The superior petrosal sinus is not evident, probably thrombosed. The drainage involves the petrosal vein continuing to the large lateral mesencephalic vein (*LMV*) and posterior mesencephalic vein (*PMV*), then to the vein of Galen (*G*) and straight sinus. A minimal drainage is directed toward the transverse sinus. Other feeders are (**c**), (**d**), and (**e**) the mastoid branch (*M*) of the occipital artery, the clival branches (*arrow*) of the neuromeningeal trunk (*NM*), and tympanic branch of the APhA. Branches of the middle meningeal artery (*small arrows*), especially the petrosquamous branch (*PS*) and branches of the accessory meningeal artery (*large arrow*), are also involved. There is perhaps a minimal component from the foramen rotundum artery. On the image (**f**), the route of the microcatheter advanced through the TS and SS into the Galenic and mesencephalic veins to the site of the shunt is shown. Injection of contrast medium during treatment characterized by placement of coils. Angiogram of the ICA and ECA post-treatment (**g**) showing occlusion of the fistula

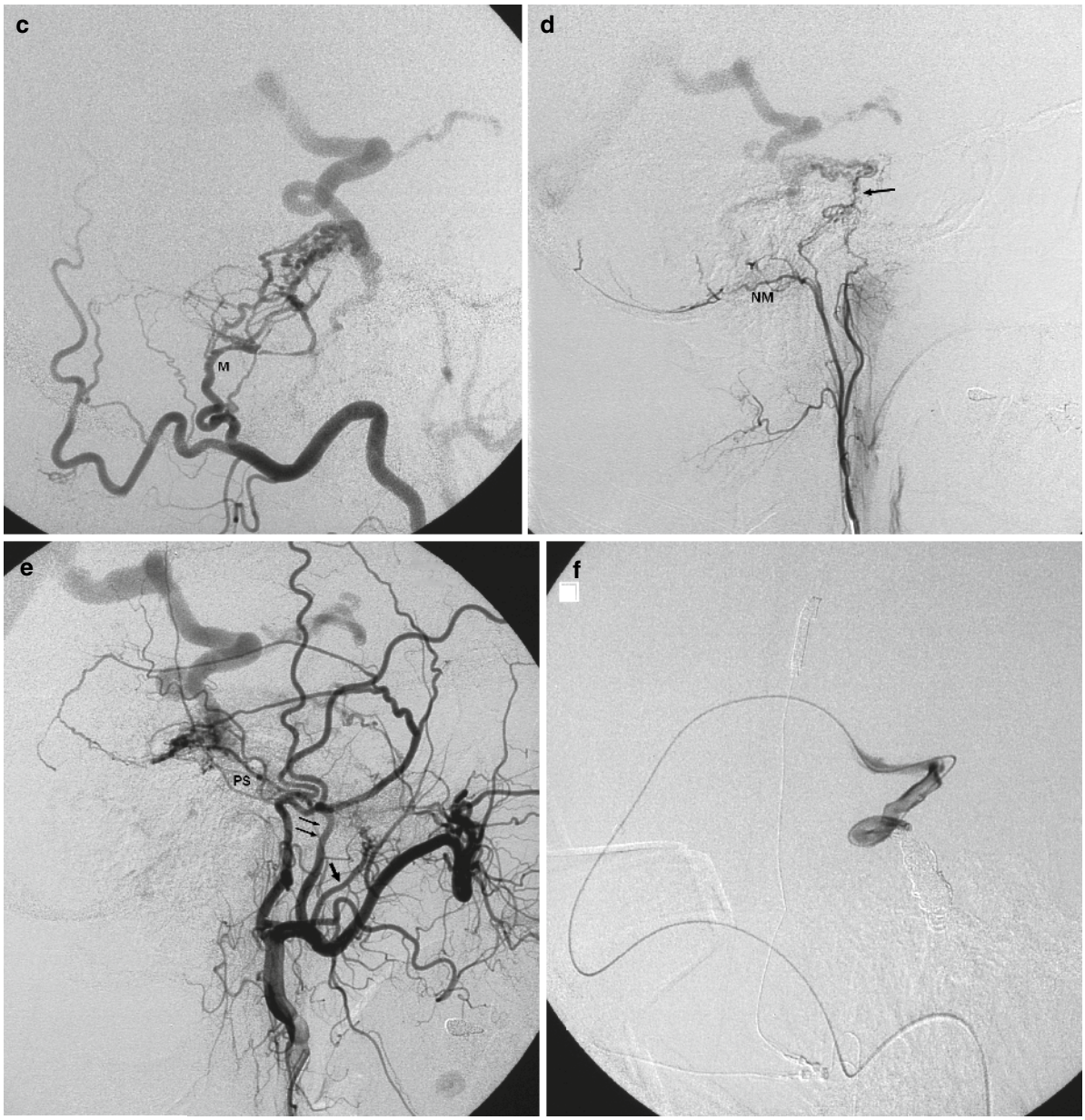

Fig. 13.9 (continued)

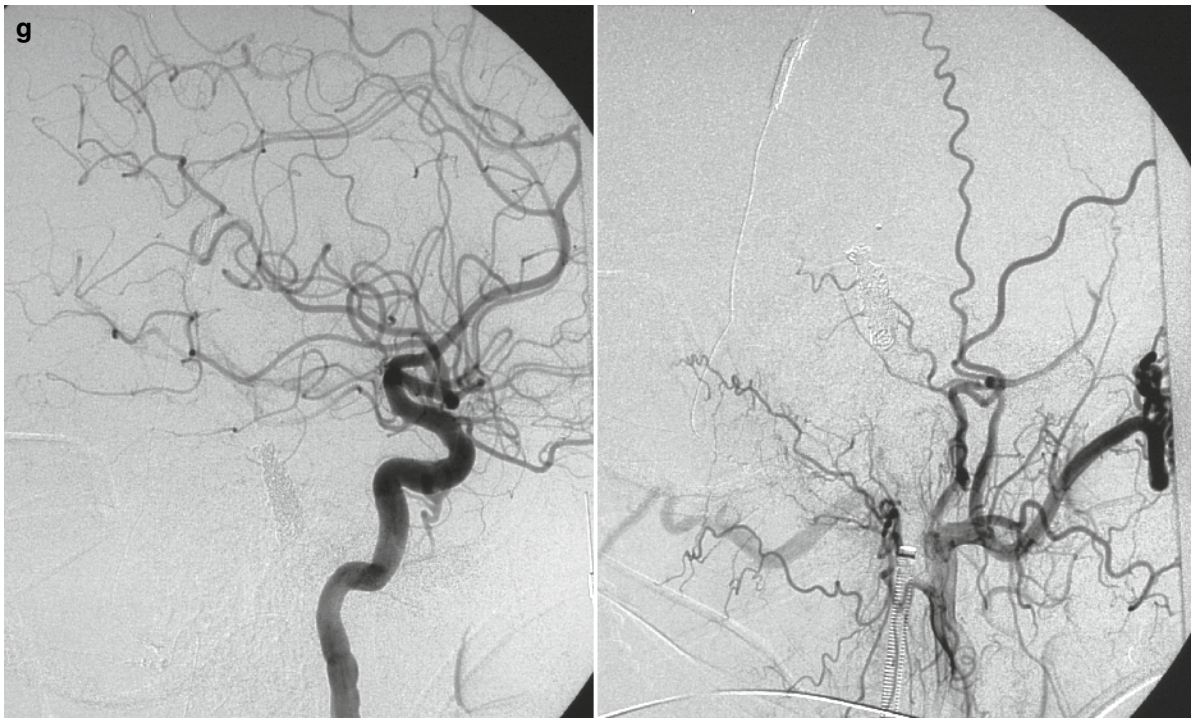

Fig. 13.9 (continued)

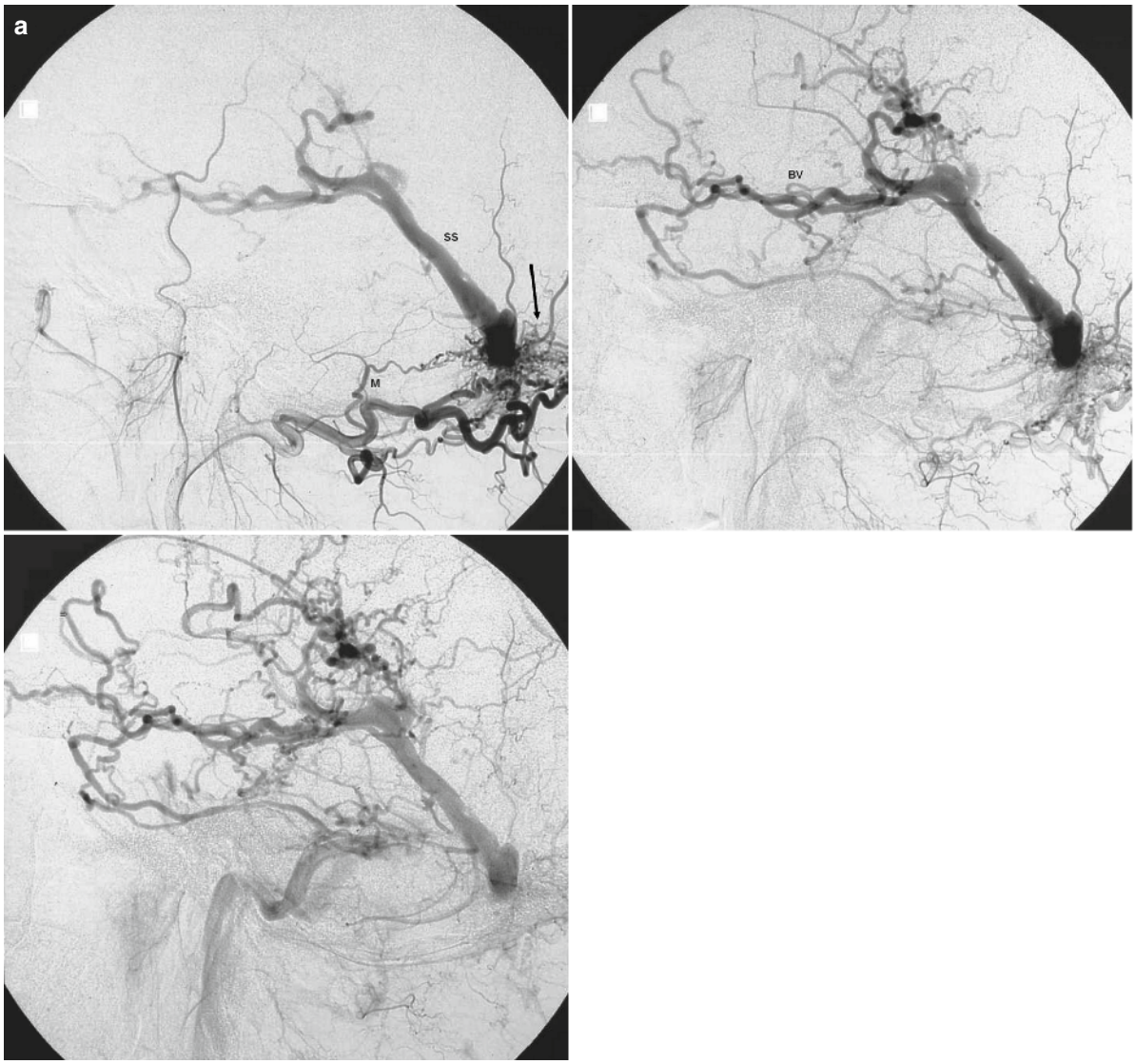

Fig. 13.10 DAVF of the torcular herophili in a patient with signs of intracranial hypertension (headache, cognitive disorder, impairment of visual acuity). Bilateral angiographic study of the ICA and ECA and of both vertebral arteries showed a DAVF at the level of the torcular herophili supplied by the occipital artery and MMA bilaterally. Neither ICA was involved. A minimal supply arose from pial branches of the cerebellar arteries, visible on the left vertebral angiogram. Occlusion of the fistula was obtained by selective injection of acrylic glue in both occipital arteries and the MMA. Complete recovery of the patient. (**a**) Lateral left occipital angiogram, showing a rich network of branches arising from the mastoid (M) and distal transosseous (*arrow*) branches of the occipital artery, converging on the torcular herophili, probably thrombosed. There is retrograde injection of the straight sinus (SS) and both basilar veins (BV), continuing to the anterior tributary and then to the temporal vein. There is also retrograde injection of the internal cerebral vein, dilated medial atrial vein, and inferior sagittal sinus. (**b**) Right occipital angiogram (AP views) showing the shunt and retrograde injection of the SS. The TS on the right is proximally thrombosed and filled distally (*arrows*) through anastomosis involving retrograde injection of the subependymal veins, then the medullary vein and further the cortical vein. The TS on the left is also thrombosed and filled distally through anastomosis involving the BV and temporal vein. (**c**) Left lateral vertebral angiogram, showing a minimal supply from the pial branches of the cerebellar arteries (*arrow*). (**d**) Left carotid angiogram (venous phase). There is a diffuse venous congestion owing to impairment of the deep venous drainage and partial thrombosis also of the distal superior sagittal sinus (SSS). (**e**) Left vertebral angiogram, AP view, venous phase. There is diffuse congestion involving the drainage of the cerebellar vein as a result of thrombosis of the proximal transverse sinus bilaterally. Normal filling of the distal transverse sinus (TS). (**f**) Left common carotid angiogram, lateral view, arterial and venous phases, showing occlusion of the fistula and normalization of the venous drainage after treatment. Similar results on the right common carotid angiogram, not shown. (**g**) Vertebral angiogram, presenting occlusion of the fistula after treatment

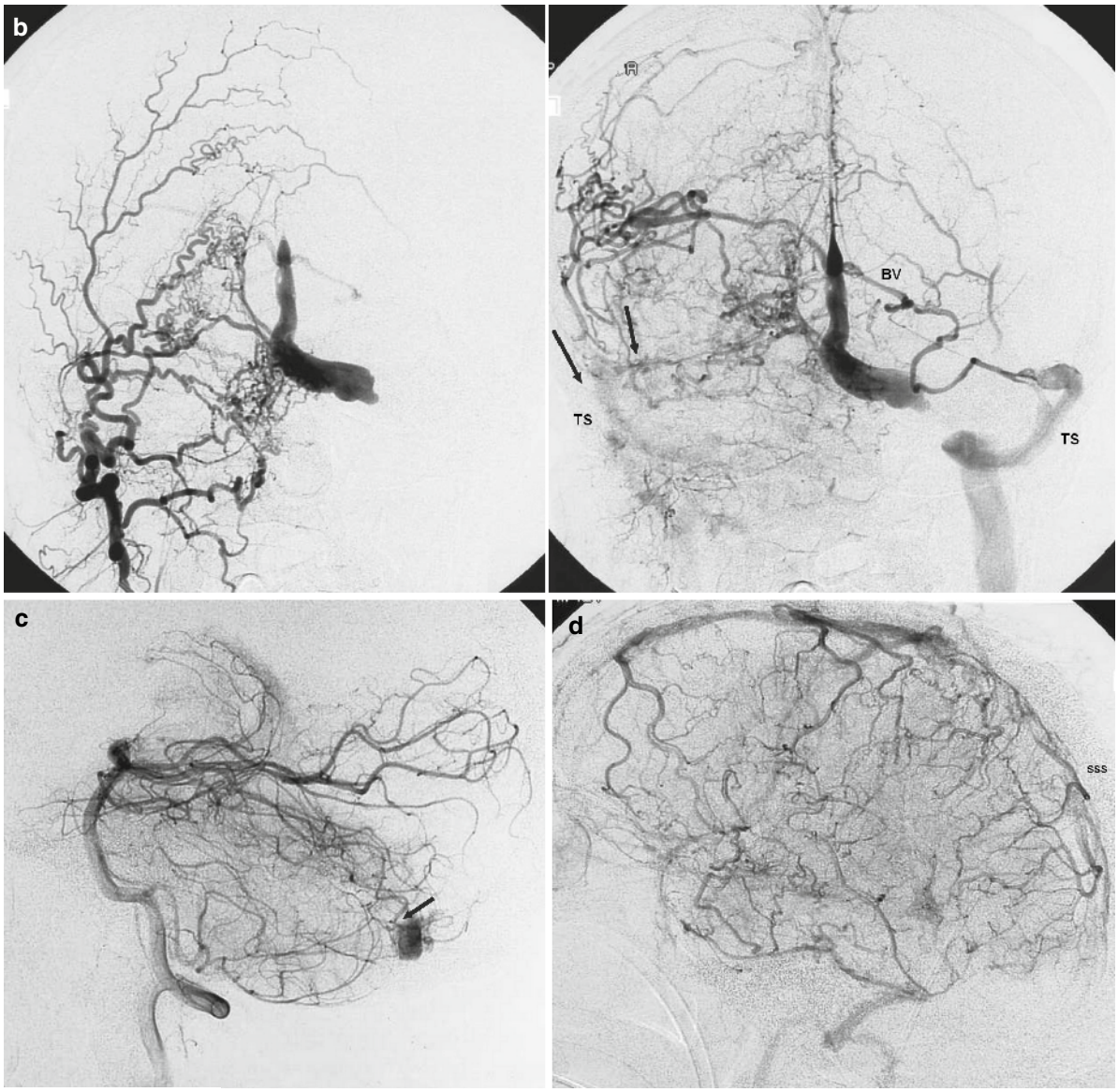

Fig. 13.10 (continued)

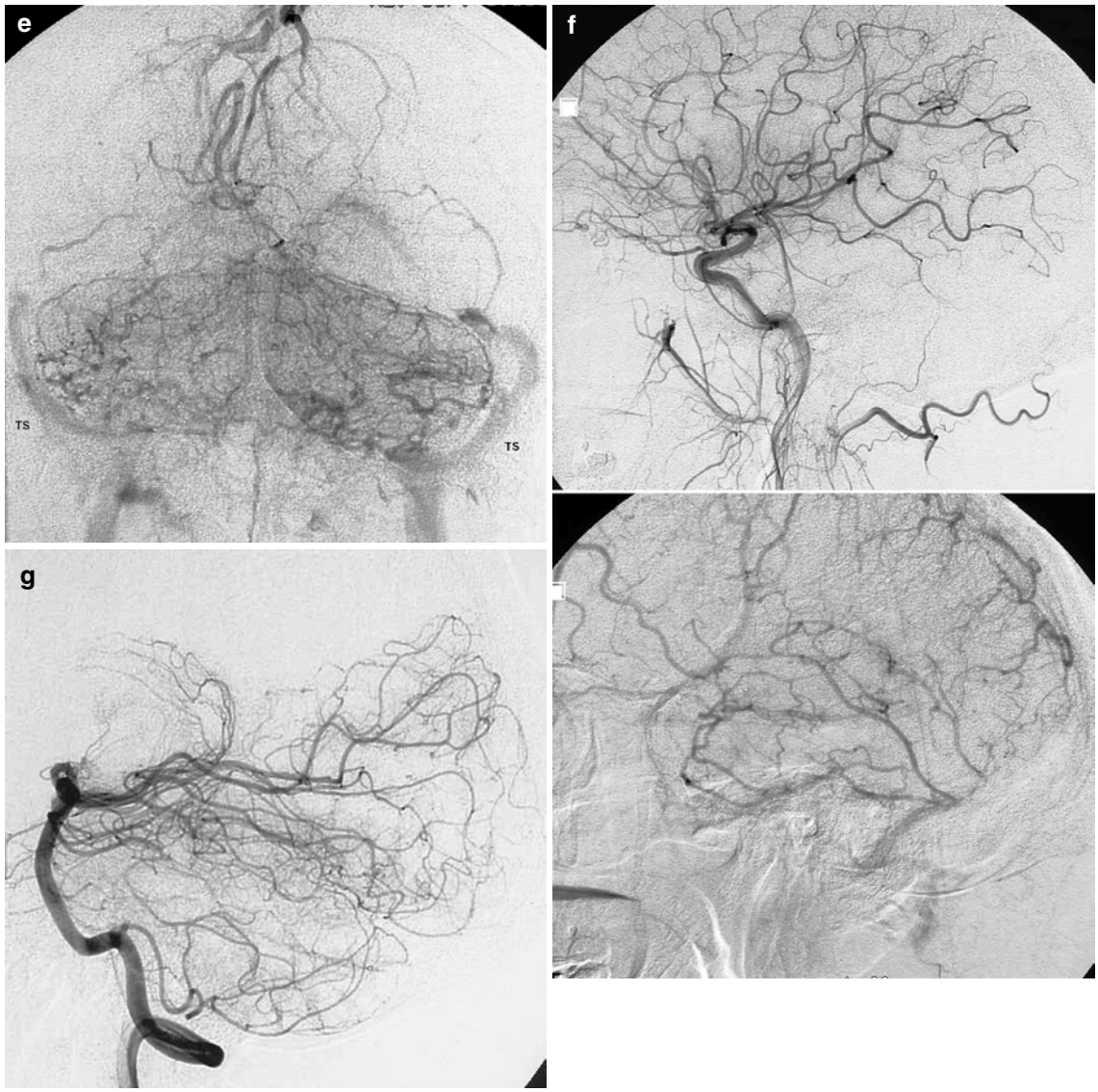

Fig. 13.10 (continued)

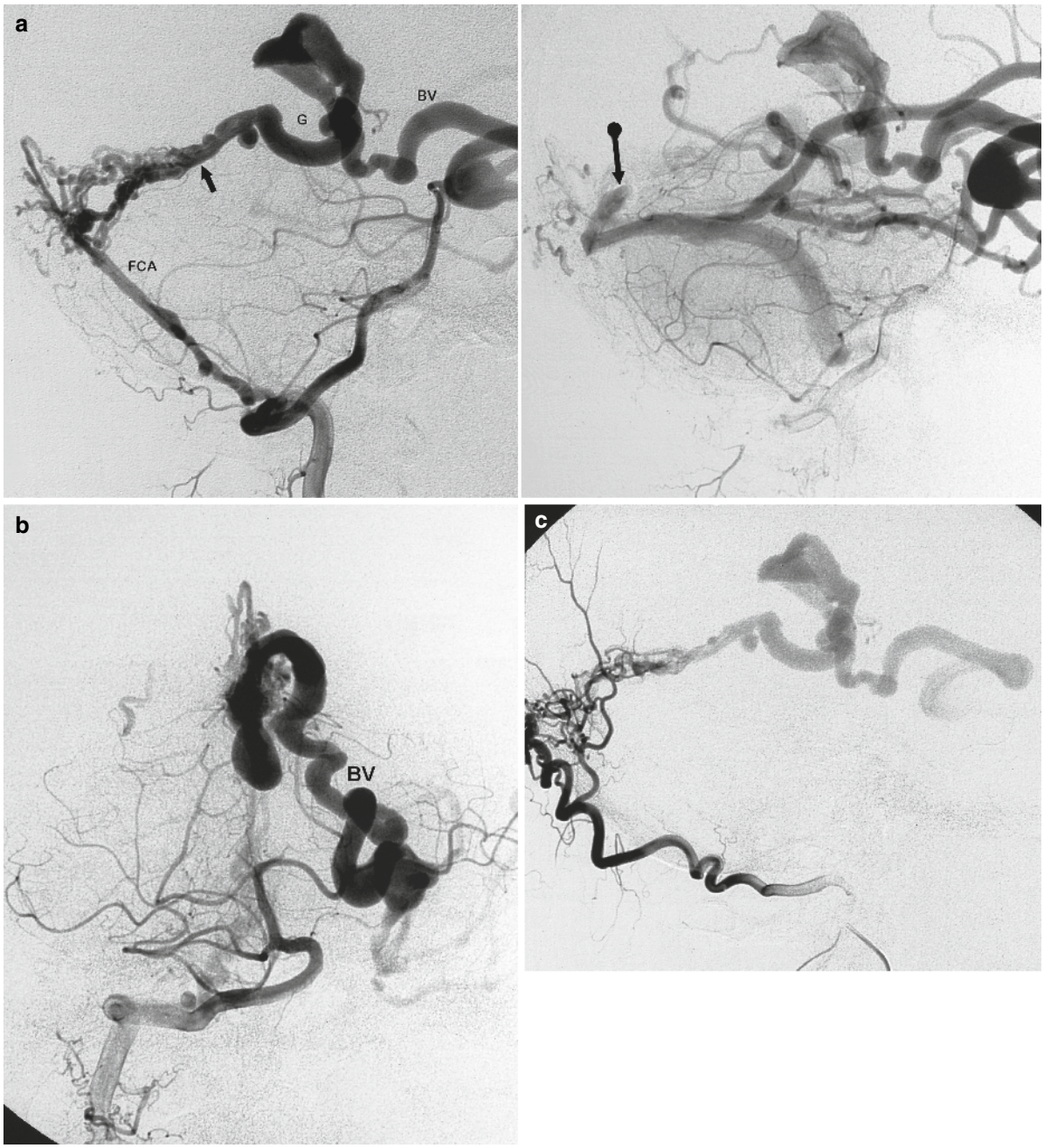

Fig. 13.11 Posterior tentorial DAVF in a patient suffering from headaches and cognitive disorder. Close to the thrombosed straight sinus, angiography disclosed a malformation supplied by the falx cerebelli artery (FCA) arising from the right VA. A small meningeal branch arose also from the left VA. Other feeders were the bilateral occipital and MMA arteries. The ICA was not involved. Lateral right vertebral angiogram (**a**), showing a dilated falx cerebelli artery (*FCA*), continuing into branches (*arrow*), running in the dura along the straight sinus, connected with the vein of Galen (*G*), which extends to the dilated tortuous basal vein (*BV*). This drains further to the temporal veins. In the later venous phase, the stump of the occluded straight sinus (*arrow with dot*) is recognizable. (**b**) Right vertebral angiogram (AP view) showing the drainage to the retrograde injected BV. Left occipital artery (**c**), selective left MMA (**d**) supplying the DAVF. ICA angiogram (**e**), venous phase, showing the diffuse venous congestion due to impairment of the deep venous drainage. Right vertebral angiogram (**f**) after endovascular treatment. Acrylic glue was injected close to the shunt after selective catheterization of the right FCA and left MMA. The shunt is not completely occluded. The supply (*arrow*) may be due either to pial branches of the SCA or to a meningeal branch (see also Fig. 13.12). A selective study was not performed. The patient improved and refused further treatment

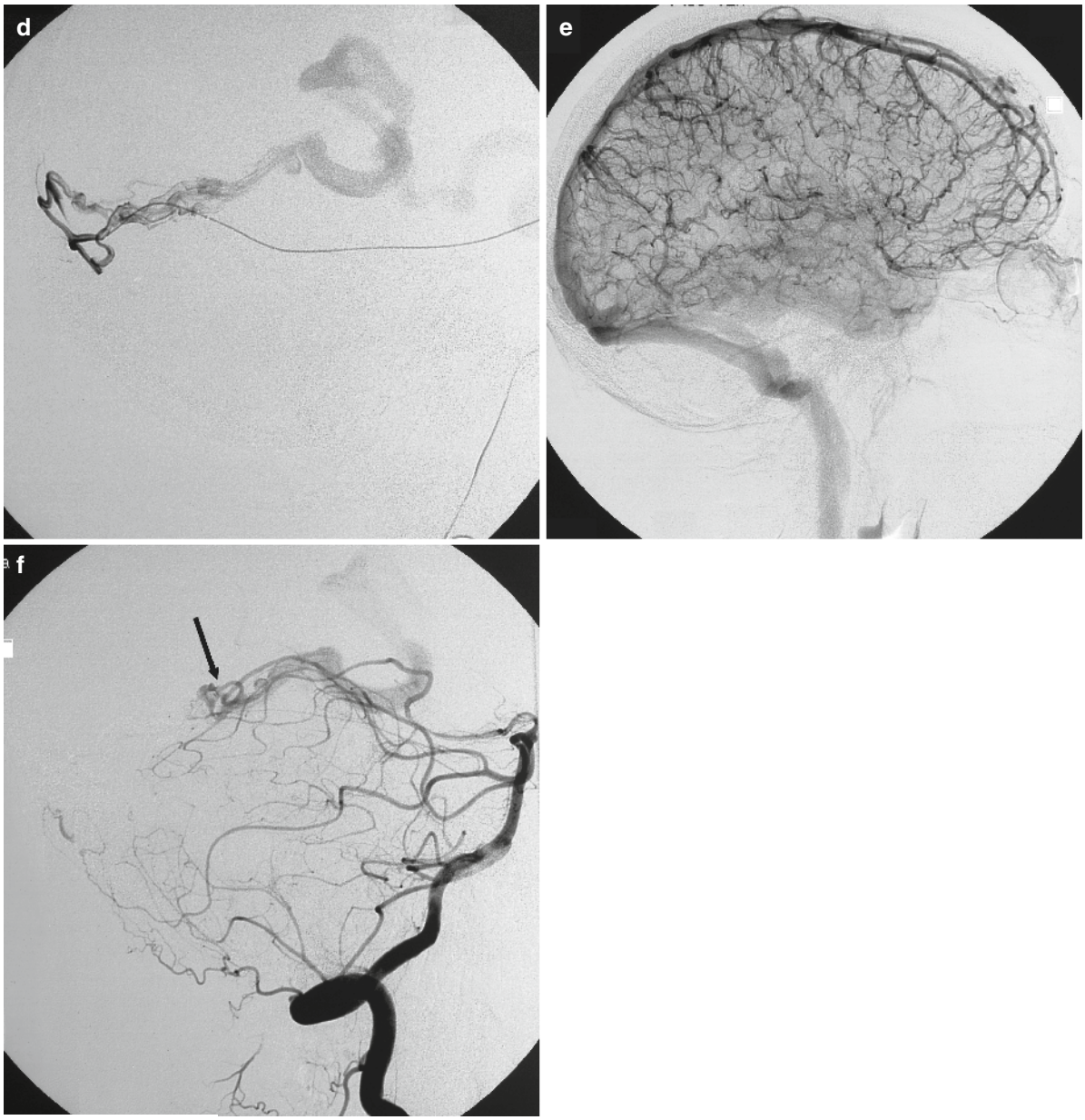

Fig. 13.11 (continued)

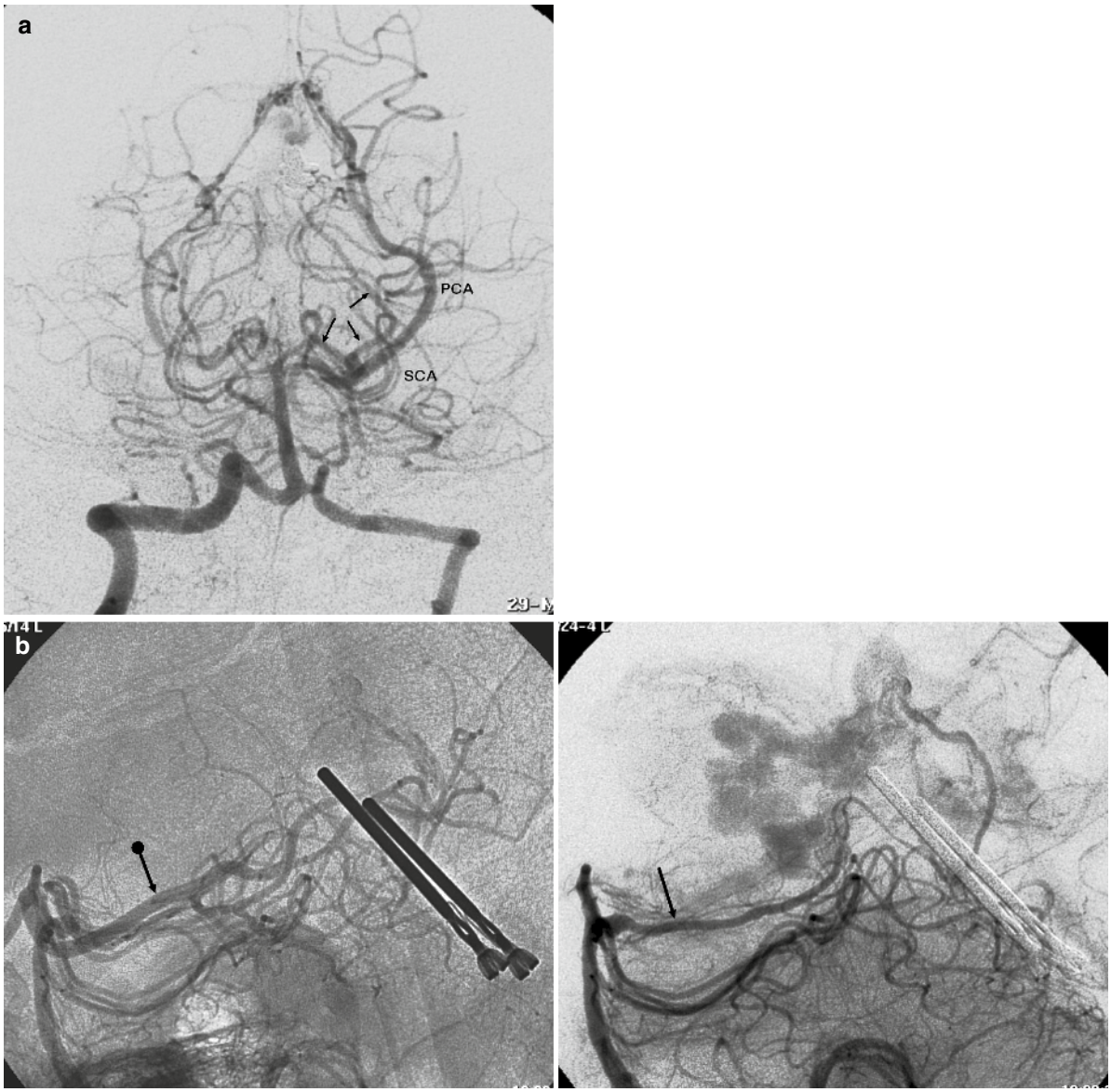

Fig. 13.12 Posterior tentorial DAVF. (**a**) Vertebral angiogram, AP view. Left posterior cerebral artery (*PCA*), superior cerebellar artery (SCA), meningeal branch (*arrows*) arising from the PCA close to its origin from the basilar artery. (**b**) Lateral vertebral angiogram. Owing to overlap with the PCA (*arrow with dot*), the meningeal branch (*arrow*) connected with the vein of Galen is better evident only later, when the contrast medium has left the PCA. Clips of previous surgery are present. (**c**) Selective catheterization of the meningeal branch, lateral and AP view, showing its supply of the DAVF. Injection of Onyx followed. The patient recovered

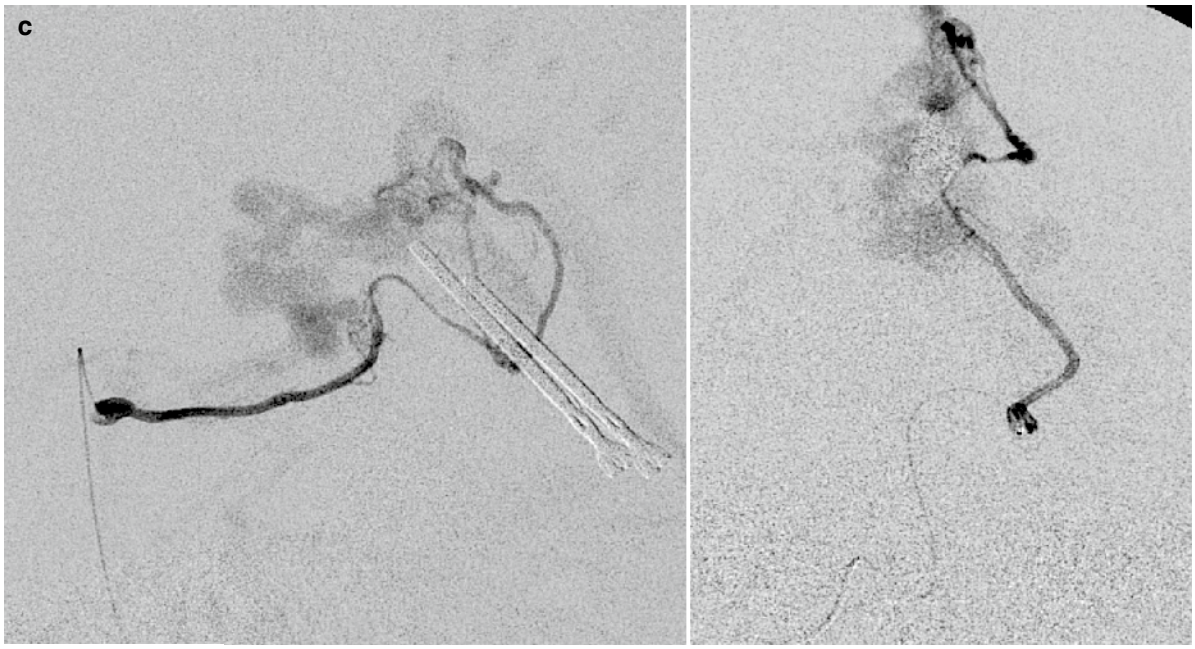

Fig. 13.12 (continued)

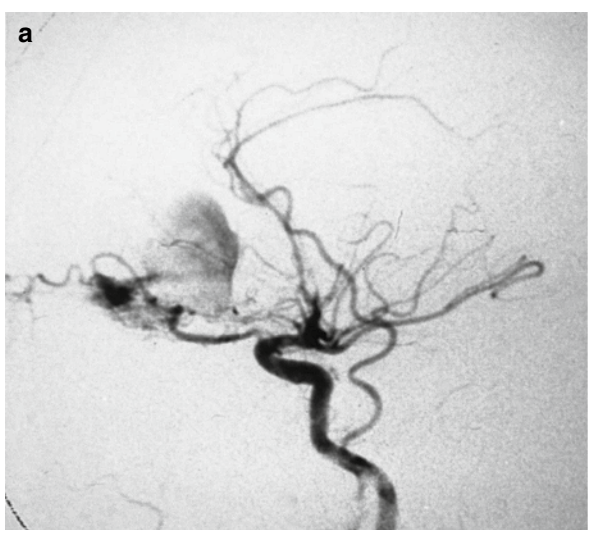

Fig. 13.13 DAVF of the anterior cranial fossa presenting with hemorrhage, supplied by anterior ethmoidal branches of the ophthalmic artery as visible on the lateral ICA angiogram (**a**). On the lateral angiogram of the internal maxillary artery (**b**), branches of the sphenopalatine artery anastomosing with ethmoidal branches of the ophthalmic artery are also involved as well as the anterior falx branch of the middle meningeal artery (*MM*). Arrows show the site of the shunt. The drainage occurred in the pial veins, forming a large pouch entering the SSS. Selective angiographic study (**c**) in the lateral and AP views of the MMA better showing its supply to the fistula

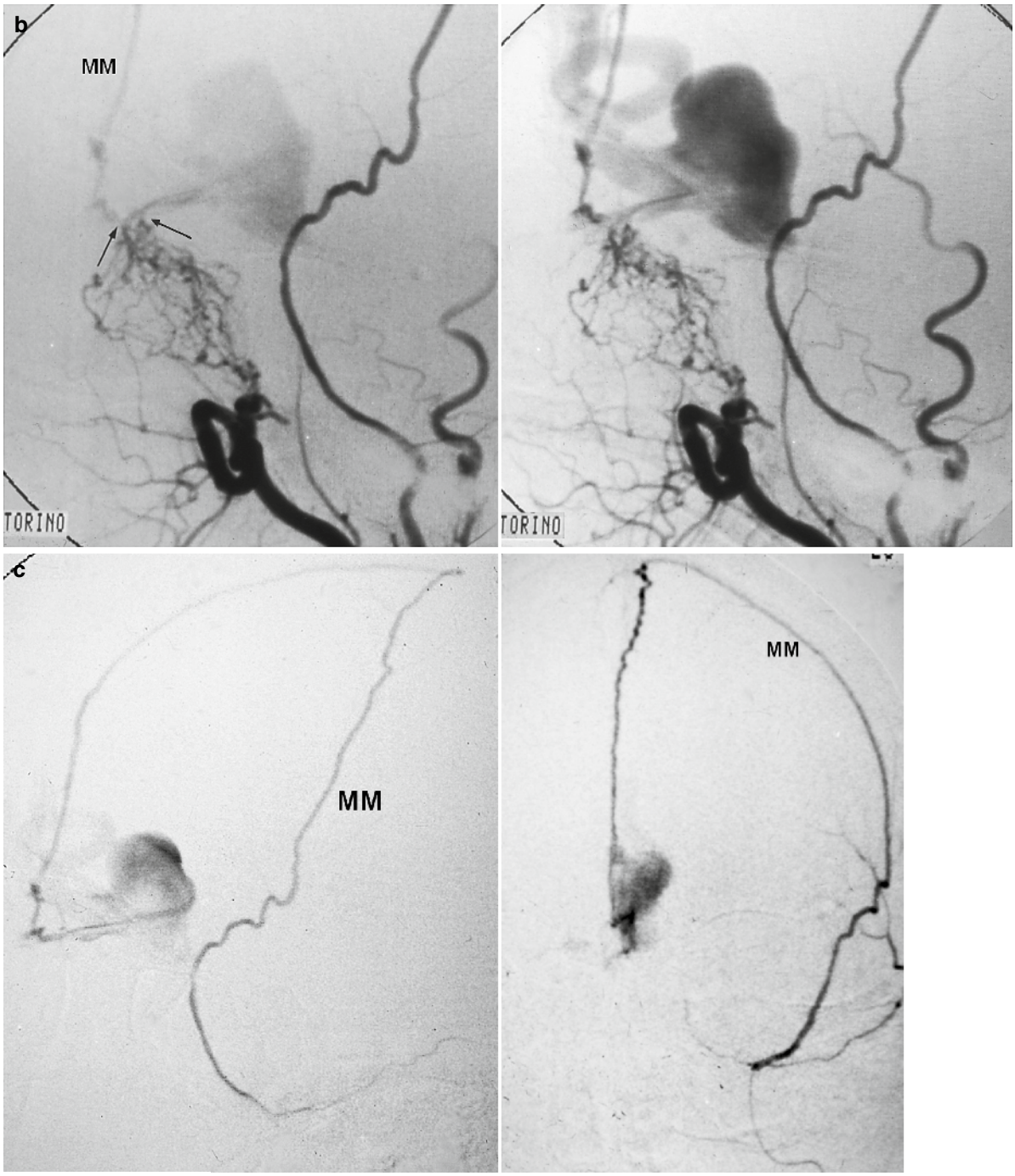

Fig. 13.13 (continued)

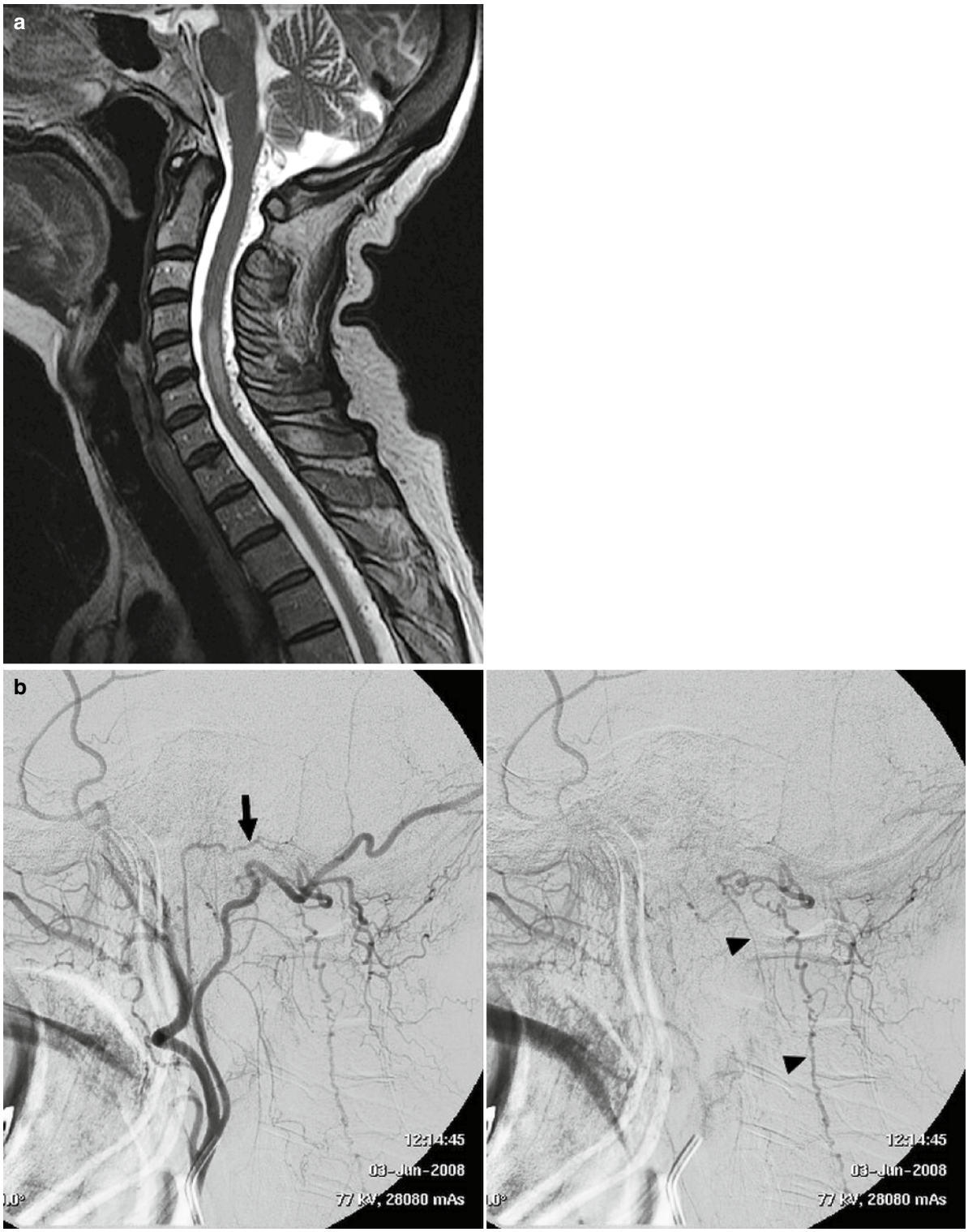

Fig. 13.14 Middle-aged patient presenting with paraparesis. (**a**) MRI T2-weighted image, showing hyperintensity lesion in the cervical spinal cord. (**b**) Lateral external carotid angiogram. There is a fistula involving the hypoglossal branch (*arrow*) of the ascending pharyngeal artery (APhA) connected with dilated medullary veins continuing caudally in the perimedullary veins of the cervical cord (*arrowheads*)

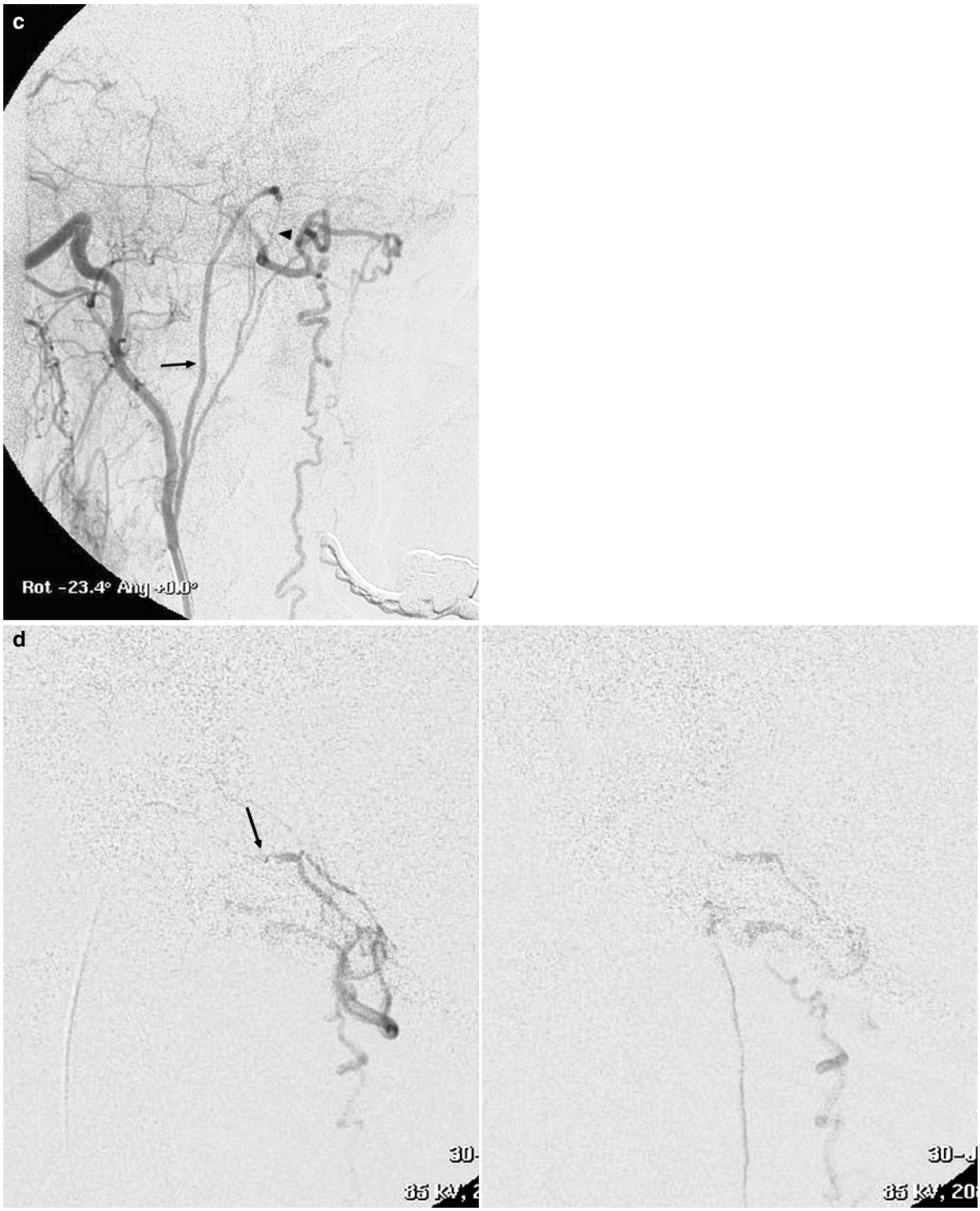

Fig. 13.14 (continued) (**c**) AP angiogram of the occipital and APhA (*arrow*) arising as a common trunk. The hypoglossal branch of the APhA supplies the fistula (*arrowhead*). (**d**) Selective study (lateral oblique view) preceding the injection of Onyx. Distal tip of the microcatheter in the hypoglossal branch at the site of the shunt (*arrow*)

Fig. 13.14 (continued) (**e**) MRI T2-weighted image showing the disappearance of the lesion with complete recovery of the patient

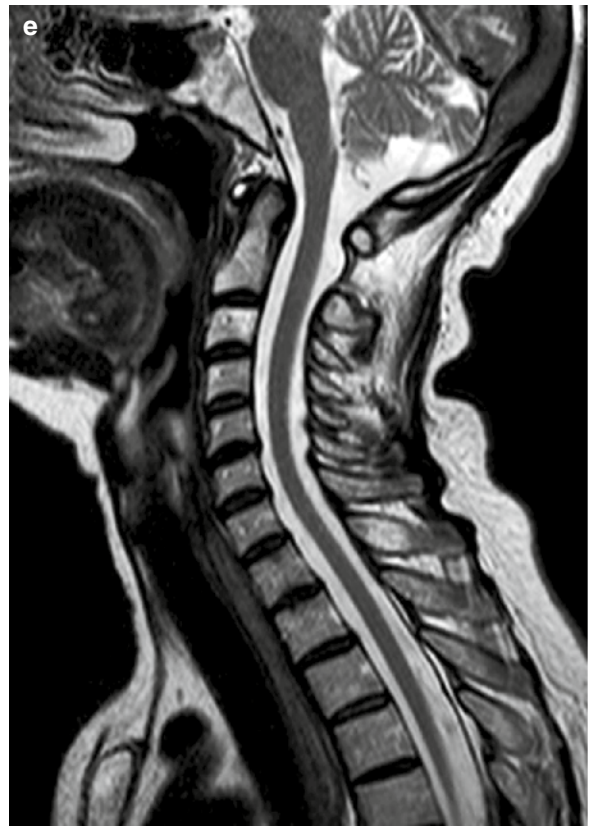

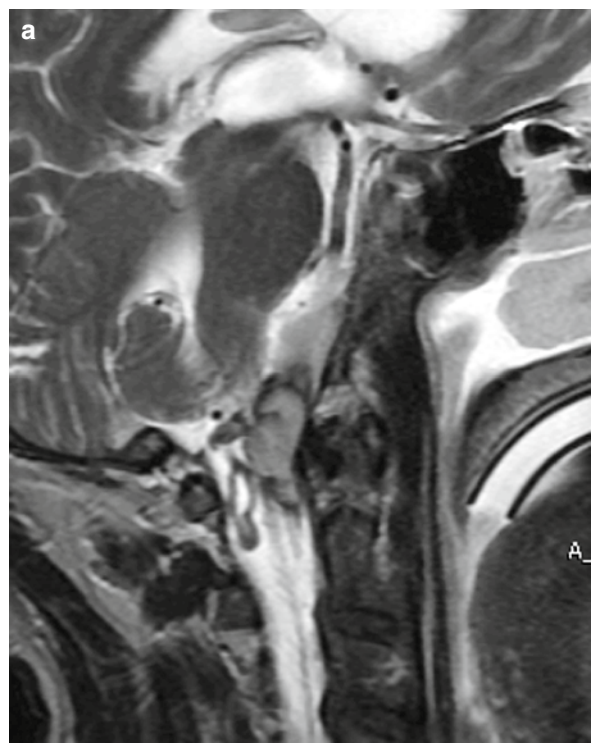

Fig. 13.15 DAVF of the foramen magnum presenting with SAH and subdural hematoma localized in front of the medulla in a young patient. (**a**) MRI T2-weighted sagittal image showing the hematoma and dilated perimedullary veins. (**b**) External carotid angiogram, lateral views, early and later phases, showing the fistula supplied by the hypoglossal branch of the APhA (*arrowhead*) and mastoid branch of the occipital artery (*arrow*). (**c**) Selective study of the APhA showing the site of the shunt and venous drainage involving dilated veins lateral to the medulla, continuing caudally to the perimedullary veins (*arrows*) of the spinal cord. The drainage is also directed intracranially, involving, among others, the pontine veins (*arrowheads*). (**d**) The same site of the shunt visible on the selective occipital artery angiogram. (**e**) Right vertebral angiogram showing a small meningeal component (*arrowhead*). In the later phases, the drainage (*inclined arrows*) in the enormous dilated pontine vein is visible. Acute endovascular treatment with almost complete occlusion of the fistula with acrylic glue followed by surgical evacuation of the hematoma was performed. The deeply comatose patient recovered

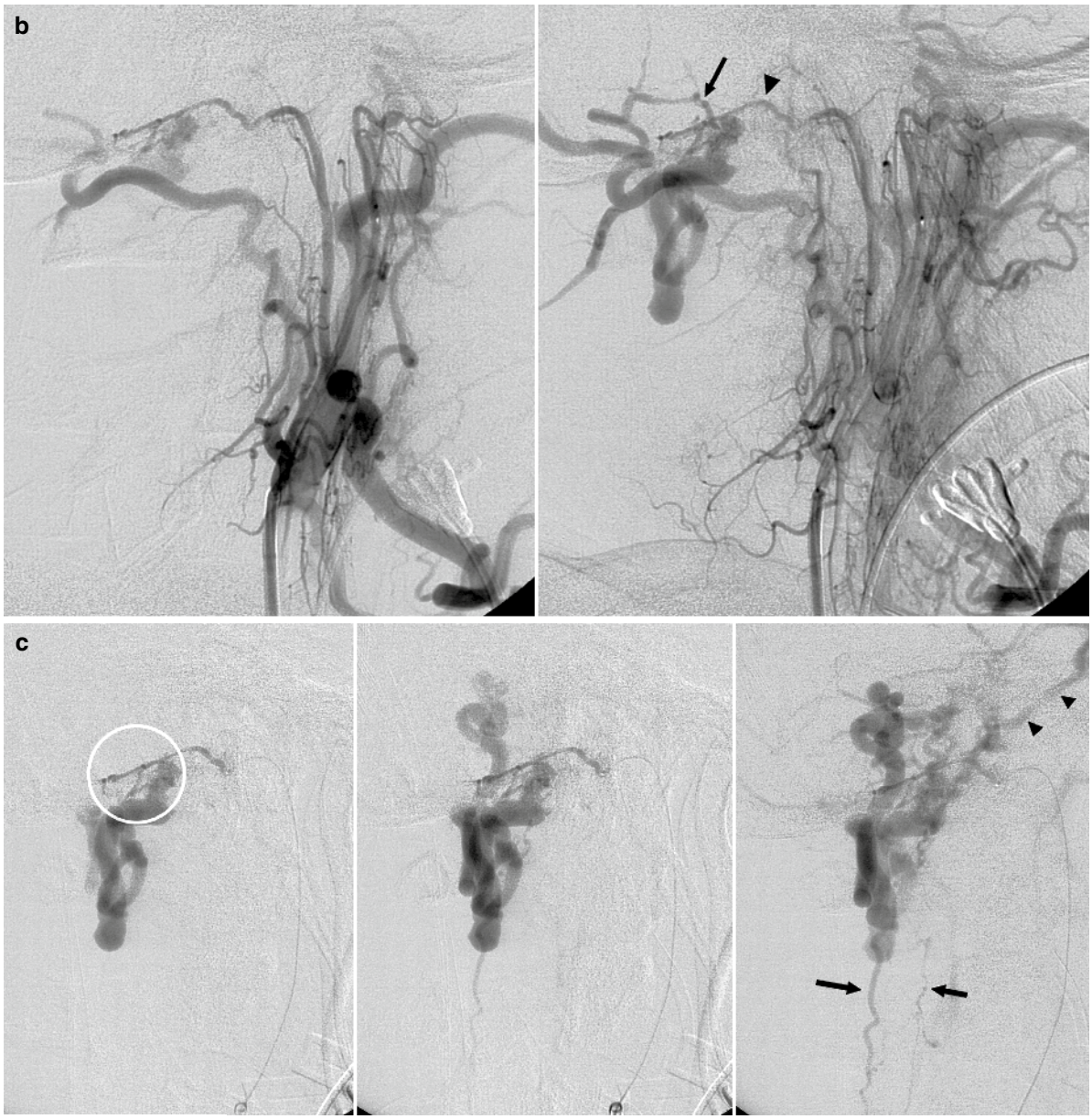

Fig. 13.15 (continued)

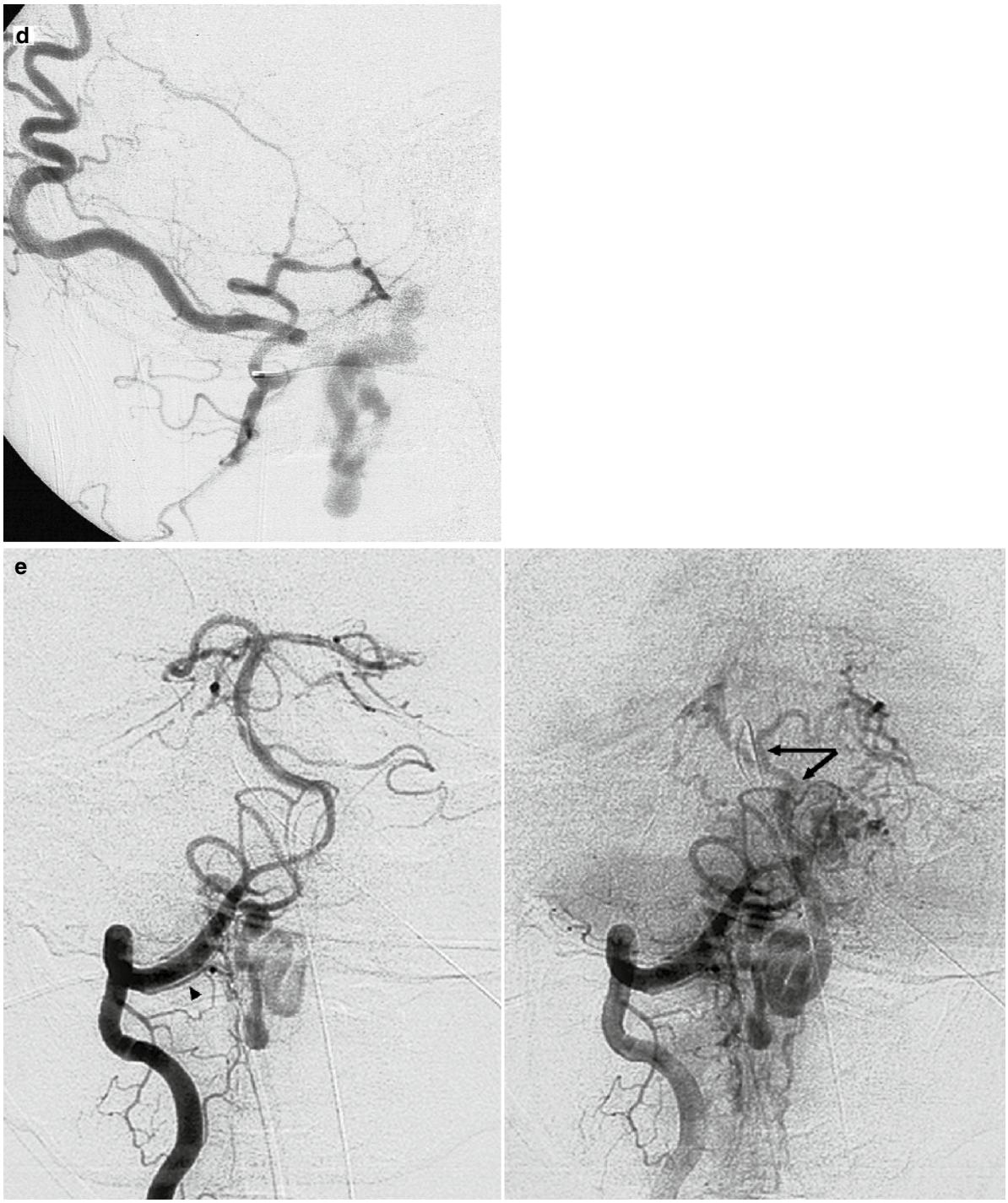

Fig. 13.15 (continued)

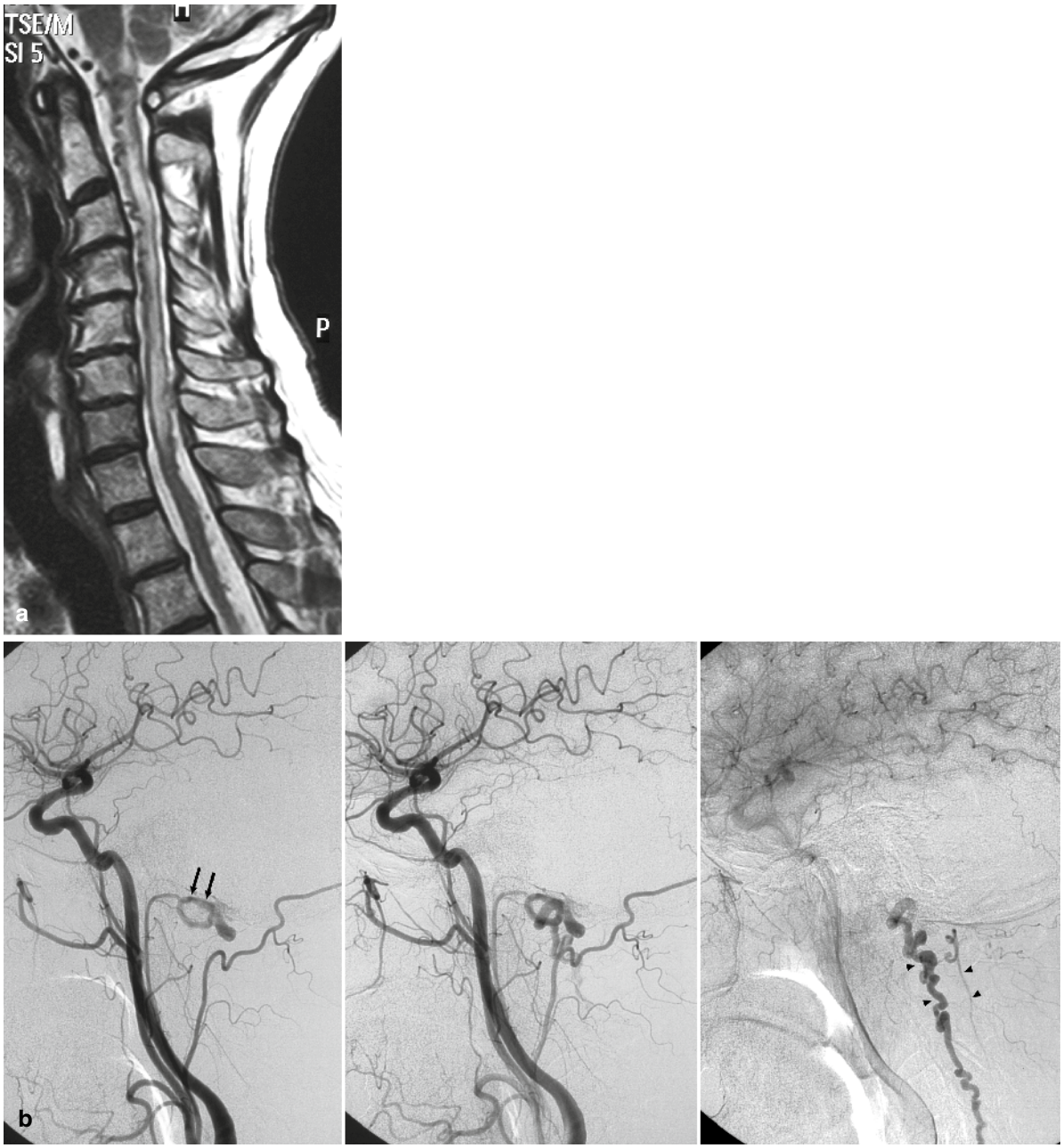

Fig. 13.16 Very old patient presenting with rapid progressive tetraplegia. (**a**) MRI T2-weighted, sagittal image. Diffuse hyperintensity involving the cervical spinal cord. Dilated vascular structures are evident, suggesting vascular malformation. (**b**) Common carotid angiogram, lateral view. DAVF supplied by the hypoglossal branch of the APhA. Site of the shunt (*double arrow*). In later phases, drainage in the dilated perimedullary veins of the cervical cord is recognizable (*arrowheads*). (**c**) Vertebral angiogram. A supply from the small meningeal branch is present (*arrow*). Perimedullary drainage (*arrowheads*). Despite rapid endovascular treatment with occlusion of the fistula with acrylic glue, the patient did not recover and died

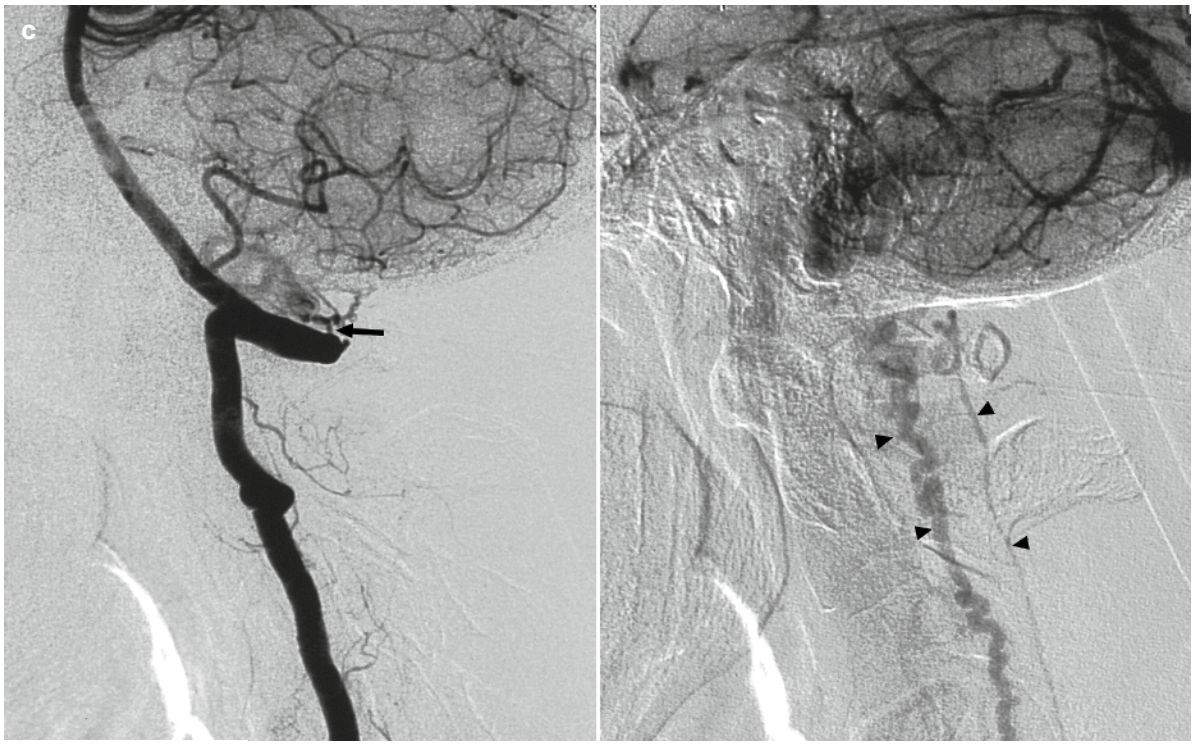

Fig. 13.16 (continued)

13.8 DAVFs in Pediatric Patients

These are rare malformations. According to (Lasjaunias 1997), they can be divided into the following two groups.

- *DAVFs in neonates and younger children.* These are characterized by huge dural lakes, which are thought to be the primary pathology (Lasjaunias 1997), commonly involving the SSS and, less commonly, the transverse–sigmoid sinuses, associated with thrombotic occlusion or hypogenesis of one jugular vein. There is slow-flow communication with other sinuses. Secondary to the sinus malformation, many DAVF shunts develop within the wall of the sinus.
- *DAVFs in older children*. They can share the same features as those in adults. In one-third of cases, however, some particular aspect is present (Garcia Monaco et al. 1991; Lasjaunias 1997). The DAVFs are multifocal and show in addition the development of new shunts, which involve the pial arteries. The sinuses to which high-flow dural shunts converge can be dilated without, however, the presence of the huge lakes visible in the previous group (Fig. 13.17).

The prognosis of both these malformations is frequently poor despite the progress in surgical and, especially, endovascular therapy.

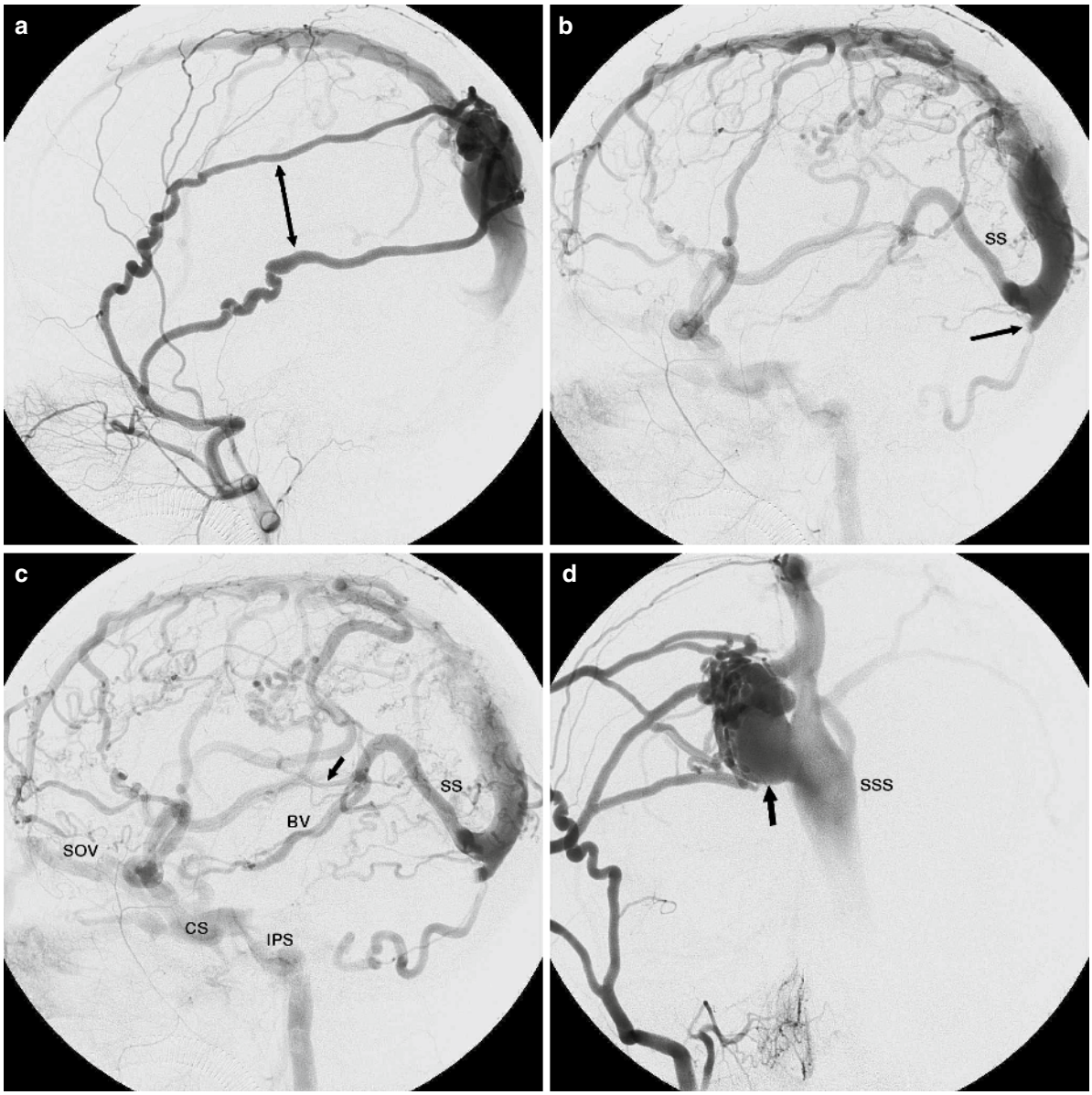

Fig. 13.17 Dural arteriovenous fistula at the level of the SSS in a child. Angiogram (**a**) of the right external carotid artery (lateral view). Dilated branches of the middle meningeal artery (MMA) (*arrow*), supplying the fistula in the middle portion of the enlarged SSS. A meningeal supply also came from the left MMA. Early (**b**) and late (**c**) venous phase. The SSS is distally occluded at the level of the torcular herophili (*arrow*). There is a venous congestion, with rerouting of the venous drainage partially in the straight sinus (*SS*) and further in the internal cerebral vein (*arrow*), especially in the basal vein (*BV*) bilaterally, continuing to its anterior tributaries. The superficial venous system drains mainly into the cavernous sinus (CS) and further to the inferior petrosal sinus (*IPS*), jugular vein, and superior ophthalmic vein (*SOV*). There is also a retrograde injection of the dilated cerebellar vein. Right external carotid angiogram, AP view (**d**) showing that the connection to the SSS occurs through a large venous pouch (*arrow*), to which converge several branches of the MMA. In the late phase (**e**), the of both transverse sinuses (*arrows*) and rerouting of the venous drainage are visible. Bilateral injection of the basal veins (*BV*)

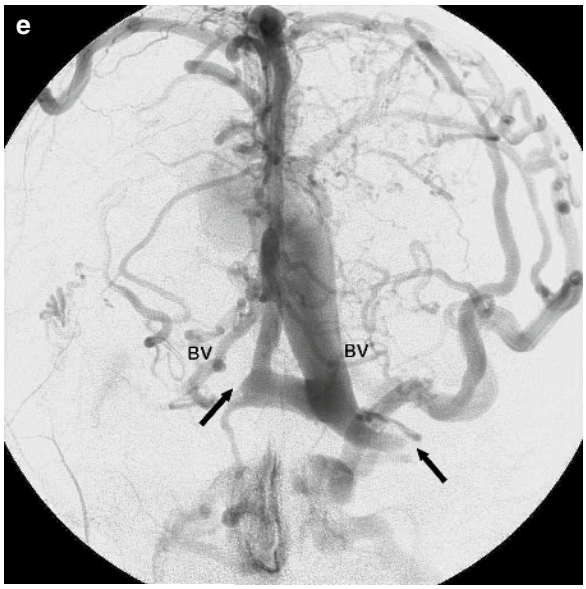

Fig. 13.17 (continued)

Arteriovenous Fistulas 14

Arteriovenous fistulas are direct abnormal communications between arteries and veins. They can occur in any location where both vessels run very close to each other.

14.1 Carotid–Cavernous Fistulas

These are the most frequent type of arteriovenous fistulas and are characterized by a direct shunt between the intracavernous segment of the internal carotid artery (ICA) and the surrounding venous plexus of the cavernous sinus. The pathogenesis is commonly a rupture of the artery and vein, after a penetrating or blunt trauma. Spontaneous fistulas can occur: these are commonly due to a rupture of an intracavernous aneurysm, frequently linked to an associated angiodysplasia: fibromuscular dysplasia (FMD, neurofibromatosis, and Ehlers-Danlos syndrome. Fistulas resulting from spontaneous dissection of the ICA have been reported (Bradac et al. 1985), and fistulas arising from laceration of the artery during transsphenoidal surgery can also occur.

14.1.1 Clinical Presentation

Carotid-cavernous fistulas are characterized by a typical cavernous sinus syndrome with ophthalmoplegia, visus involvement, pulsating exophthalmos, chemosis, and bruit. The symptoms can appear acutely or slowly, progressively days or weeks after the trauma. Ischemia or intracerebral hemorrhage may occur. Similar to dural arteriovenous fistulas involving the cavernous sinus, also in carotid-cavernous fistulas ischemic and hemorrhagic cerebral complications can occur as the result of a connection with the pial veins, especially the ponto-mesencephalic veins, through bridging veins.

14.1.2 Diagnosis and Treatment

The dilated cavernous sinus and superior ophthalmic vein can be easily recognized on CT or MRI. Angiography, however, is essential for a precise diagnosis and in planning treatment. Carotid-cavernous fistulas are high-flow fistulas with a rapid injection on the angiogram of the cavernous sinus. Depending on the location of the fistula and anatomical variant, further drainage can be prevalently directed as follows: anteriorly, in the superior inferior ophthalmic veins, in which the flow is reversed; extracranially, draining into the facial vein system; or posteriorly, into the superior inferior petrosal sinuses. Through intercavernous anastomoses, the contralateral cavernous sinus may be involved. The ponto-mesencephalic veins, basal vein, and deep and superficial middle cerebral veins also can be involved as a result of anastomoses of the cavernous sinus with these venous channels (see Chapter 9.3.10). In cases of severe lacerations of the ICA, the blood flow passes completely in the venous sector, and on the angiogram no cerebral arteries are recognizable.

The angiographic study consists of a bilateral carotid examination to exclude the possibility of bilateral lesions and to check for a collateral circulation. The external carotid artery should also be selectively examined since in some cases the branches

G.B. Bradac, *Cerebral Angiography*,
DOI: 10.1007/978-3-642-15678-6_14, © Springer-Verlag Berlin Heidelberg 2011

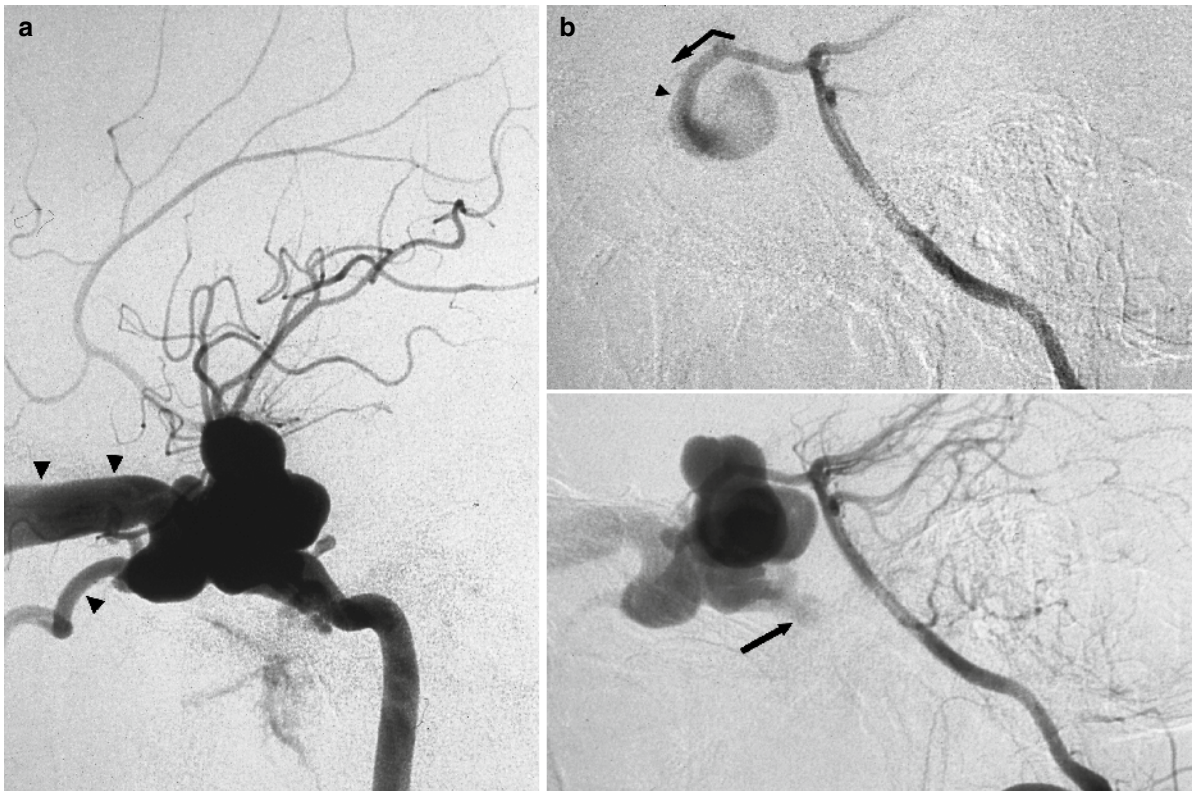

Fig. 14.1 Traumatic carotid-cavernous fistula. (**a**) Internal lateral carotid angiogram. There is an immediate injection of the dilated and deformed cavernous sinus and filling of the dilated superior (*arrowheads*) and inferior ophthalmic veins. (**b**) Lateral vertebral angiogram with compression of the involved internal carotid artery. Through the posterior communicating artery, there is injection of the internal carotid artery and fistula. Site of the shunt (*arrowhead*). In a later phase, there is a partial injection of the inferior petrosal sinus, which could be thrombosed (*arrow*)

(internal maxillary artery, ascending pharyngeal artery) can be involved. To precisely identify the site of the shunt, a vertebral angiogram with compression of the involved ICA can be very useful.

Endovascular treatment with a detachable balloon to occlude the shunt, which was proposed and developed by Serbinenko (1974) and Debrun et al. (1975), has progressively become the therapy of choice. The treatment is performed today with a balloon or coils, which has led to good clinical and anatomical results, with limited morbidity and mortality (Berenstein and Kricheff 1979; Debrun et al. 1981; Scialfa et al. 1983; Kendall 1983; Lasjaunias and Berenstein 1987; Gupta et al. 2006). An alternative route, introduced by Mullan (1979) and Manelfe and Berenstein (1980) and increasingly used today, is the endovascular venous approach through the facial or superior ophthalmic vein, or through the inferior petrosal sinus (Figs. 14.1–14.3).

14.2 Vertebral Arteriovenous Fistulas

This is a very uncommon pathology, characterized by a direct shunt between the vertebral artery and the surrounding vertebral venous plexus. The pathogenesis is traumatic due to penetrating or blunt cervicovertebral trauma (Goodman et al. 1975), and it is sometimes associated with bony fractures. Spontaneous fistulas can occur, linked to angiodysplasia, such as FMD and neurofibromatosis (Deans et al. 1982; Bahar et al. 1984;

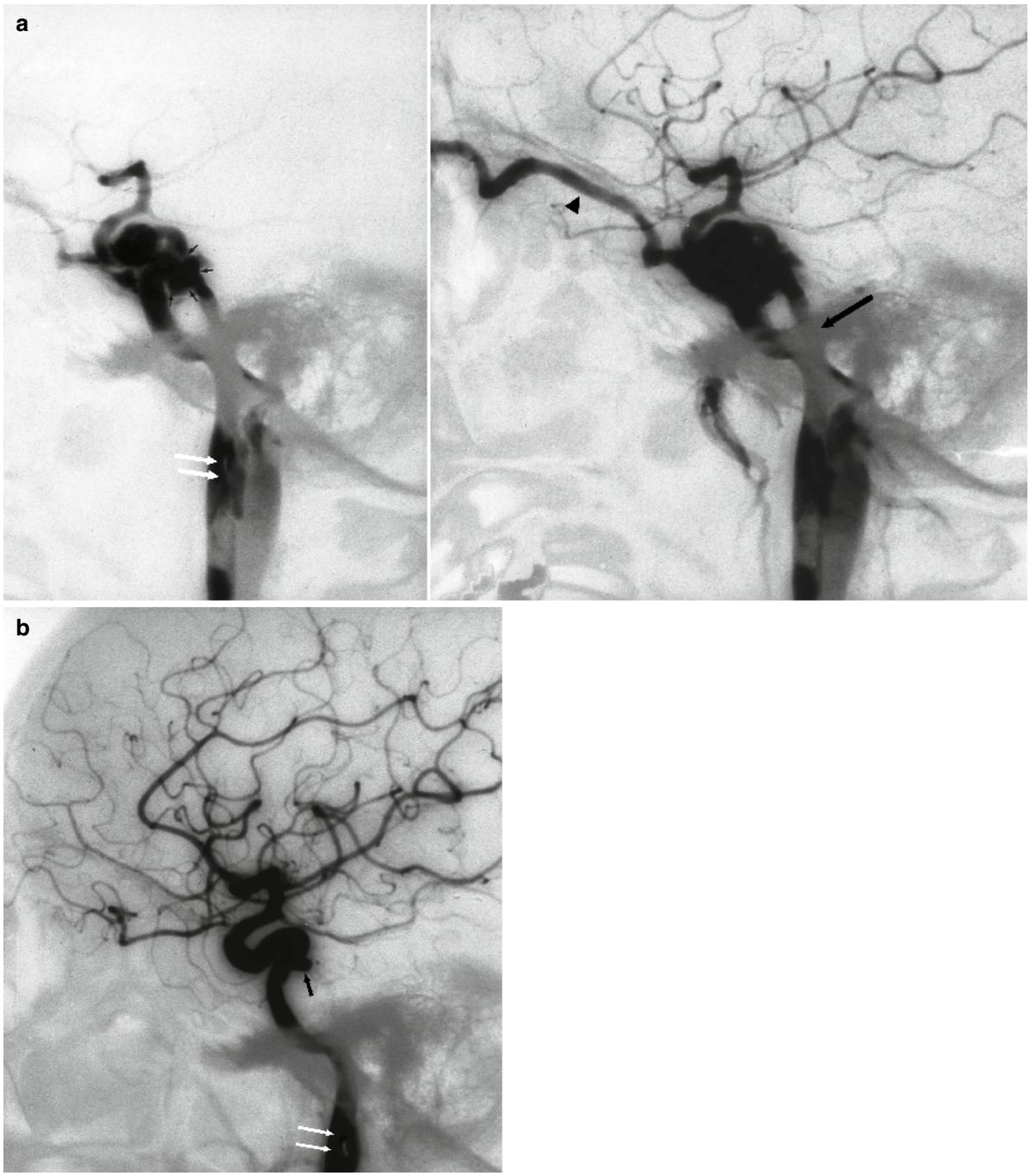

Fig. 14.2 Spontaneous carotid-cavernous fistula in a young patient, which appeared after heavy vomiting caused by alcohol intoxication. (**a**) Lateral carotid angiogram. The small arrows show the site of the shunt. There is drainage in the superior ophthalmic vein (*arrowhead*) and inferior petrosal sinus (*arrow*). There is also a minimal injection of the pterygoid plexus. The extracranial internal carotid artery is slightly enlarged, and there is an intraluminal defect (*white arrows*), suggesting dissection. It is possible that the dissection has extended intracranially, leading to formation of the fistula. The shunt was occluded with a balloon. (**b**) Control angiogram 2 months later. The balloon is now deflated. A small pseudoaneurysm (*arrow*) at the site of the fistula is recognizable. The dissection is unchanged (*white arrow*)

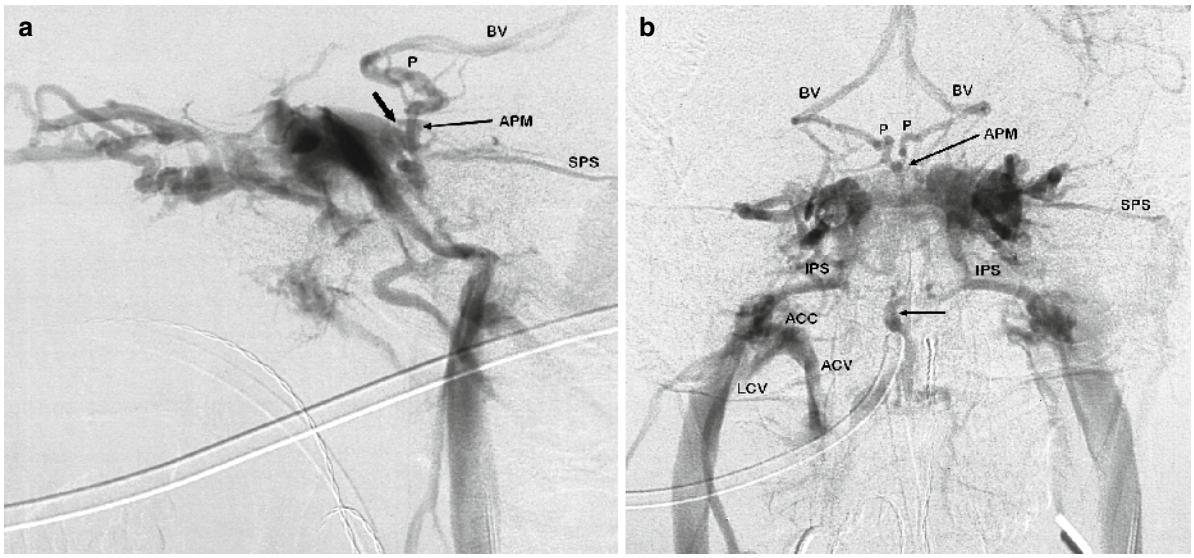

Fig. 14.3 Large traumatic carotid-cavernous fistula. Left carotid angiogram, lateral and AP view 2 seconds after injection into the internal carotid artery. Extensive anterior (ophthalmic veins) and posterior (petrosal sinuses) drainage. There is also an injection of the contralateral sinus. Bridging veins visible in the lateral view (*arrow*) connect the cavernous sinus with the anterior ponto-mesencephalic veins (*APM*), which via the peduncular veins (*P*) continue into the basal vein (*BV*) bilaterally. Inferior petrosal sinus (*IPS*), superior petrosal sinus (*SPS*), and anterior condylar confluence (*ACC*) continuing into the anterior condylar vein (*ACV*) and lateral condylar vein (*LCV*). Through injection of the clival venous plexus, filling also of the anterior epidural vertebral plexus (*arrow*)

Lasjaunias and Berenstein 1987). The fistula results from weakness of the artery and probably dissection. The fistula can occur at any level of the vertebral artery, but C1, C2, and C3 are the most frequent locations.

14.2.1 Clinical Presentation

Progressive vertebrobasilar insufficiency leading to ischemia in the brainstem and/or spinal cord can occur. The dilated venous sector can compress the nerve root. Paraspinal bruit and cervical pain are present.

14.2.2 Diagnosis and Treatment

Angiography is essential to define the lesion precisely and plan the treatment, which will basically be endovascular using the arterial-venous route (Moret et al. 1979; Kendall 1983; Miller et al. 1984; Lasjaunias and Berenstein 1987; Gupta et al. 2006) (Figs. 14.4 and 14.5).

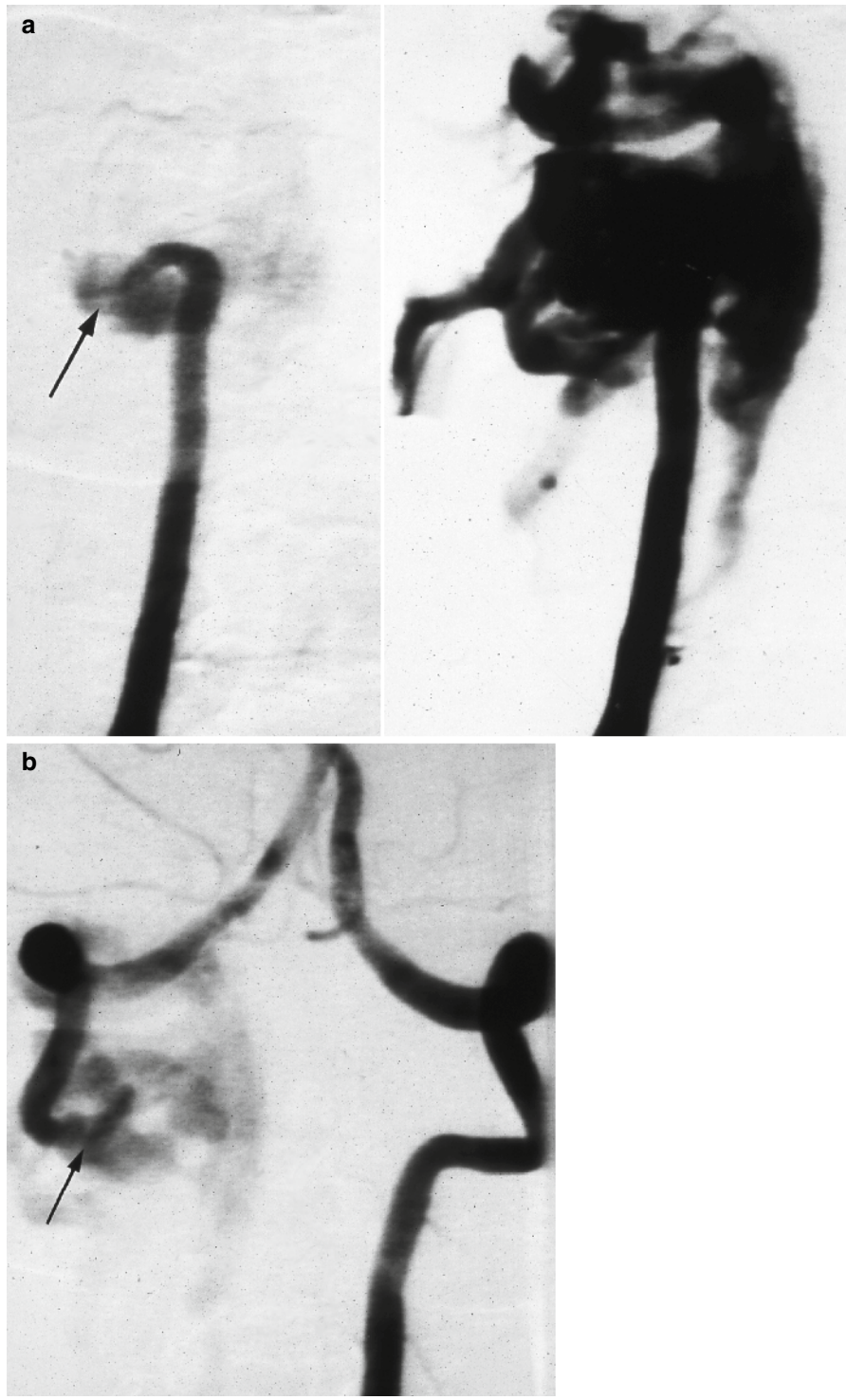

Fig. 14.4 Spontaneous vertebral arteriovenous fistula. (**a**) Right vertebral angiogram, showing the site of the shunt (*arrow*) at the C2 level. There is immediate extensive venous drainage. (**b**) Left vertebral angiogram with retrograde injection of the right vertebral artery better displaying the site of the shunt. Occlusion of the fistula and right vertebral artery with a balloon. (**c**) Control angiograms of the right and left vertebral artery

Fig. 14.4 (continued)

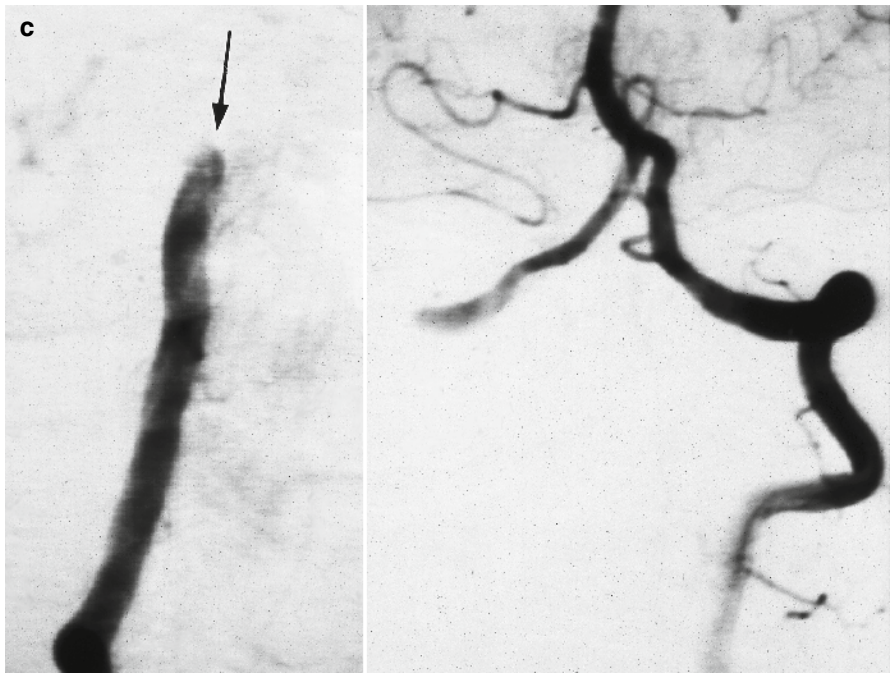

Fig. 14.5 Spontaneous fistula between the left vertebral artery and surrounding venous plexus at the level of C1. Left vertebral angiogram, AP view (**a**), lateral view (**b**). There is a shunt between the dilated vertebral artery and venous plexus, which is dilated and forming a large pouch (*arrow with line*). The venous drainage continues into the retrogradely injected and dilated lateral or posterior condylar vein (*arrowhead*) and further into the internal jugular vein (*large arrow*). There is also drainage into the deep cervical vein (*double arrows*). Right vertebral angiogram (**c**) prior to endovascular treatment. There is retrograde injection of the left vertebral artery and venous pouch site of the shunt. A microcatheter has been advanced into the left vertebral artery and placed in the venous pouch. The white arrow shows the distal marker of the microcatheter. Left vertebral angiogram (**d**) post-treatment. Occlusion of the fistula with coils

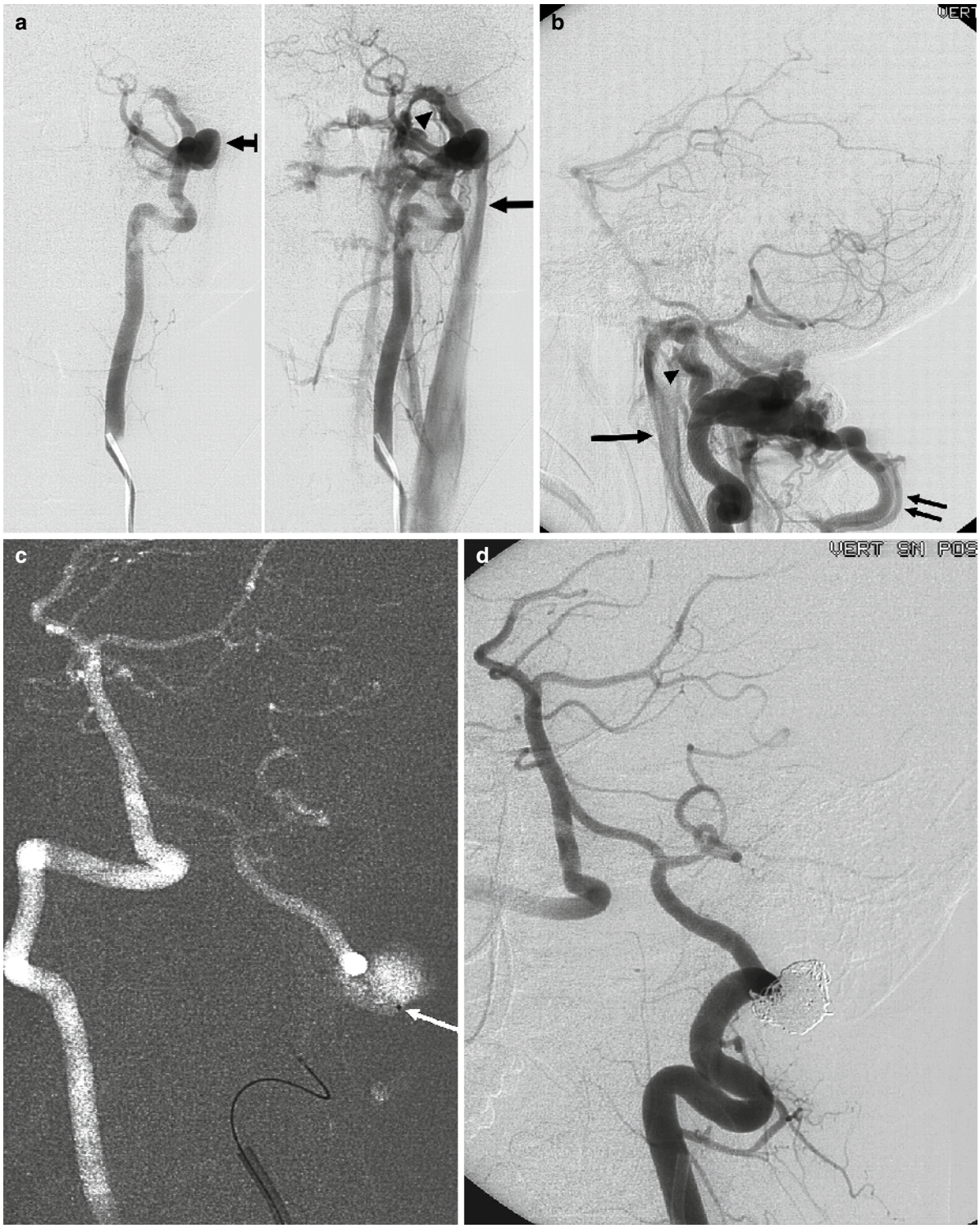
a
b
c
d
VERT SN POS

Atherosclerosis 15

Atherosclerosis is the principal pathological process affecting the extracranial and intracranial arteries responsible for ischemic stroke. Less commonly, ischemic stroke is due to other conditions, such as spontaneous dissection and other nonatherosclerotic arteriopathies as well as heart disease. All of these diseases are described in the chapters 16–19.

Atherosclerosis is a generalized condition that predominantly involves certain vascular territories: the aorta and iliac, extraintracranial, and coronary arteries. It is a typical pathology of adulthood, and the likelihood of occurrence increases with the age. There is a slight predominance among men.

15.1 Pathology

Initially, there is microinjury of the endothelial cells due to various stress factors (such as elevated cholesterol hypertension, cigarette smoking, diabetes, and homocystinuria), which promote the passage and deposit of cholesterol (especially low-density lipoproteins) in the subendothelial space. This leads to a reaction of both endothelial and smooth muscle. The metabolic products of these cells result in further damage of the endothelial, promoting the passage into the subendothelial space of monocytes, which progressively engulf lipids and become foam cells. Migration of lymphocytes, cell necrosis, and collagen production follow (Garcia et al. 1998; Witznum and Steinberg 1991; Ohara et al. 1993; Libby and Clinton 1993). All these aspects lead to the formation of the atheromatous plaque covered by a well-formed fibrous cap, which can extend progressively into the lumen of the artery, resulting in stenosis. The evolution of the plaque can vary from a stable course to a slow or rapid growth. Hemodynamically, stenosis—leading to a major reduction of flow and thereby increasing the risk of ischemia—has to be rather severe, as previously described (Brice et al. 1964; Archie and Feldtman 1981). It is, however, important to note that in a relatively high number of cases, the plaque can slowly progress up to complete occlusion, but remain asymptomatic. *This occurs when the collateral circulation is efficient and there is no distal embolization during the process.*

Erosion of endothelial cells and breakdown of the fibrous cap lead to exposure and delivery of the material inside the plaque, promoting distal embolism (Sitzer et al. 1995). Further reduction of the lumen up to occlusion can occur because of the formation of an intraluminal thrombus or an intraplaque hemorrhage. The latter can be due to the entry of blood in the plaque through erosion of the fibrous cap or rupture of the lesion in the vasa vasorum (Fisher and Ojeman 1986; Beach et al. 1993). There are no precise criteria using current diagnostic tools to predict the evolution.

15.2 Location

Atherosclerosis affects mainly the extracranial segments of arteries. Especially involved are the internal carotid artery (ICA) at the bifurcation and the common carotid and vertebral arteries at their origins. Other less frequent sites are the aortic arch and subclavian arteries. Atherosclerosis of the intracranial arteries is less frequent but not as rare as was previously supposed. According to some reports, the incidence of significant intracranial atherosclerotic stenosis in patients with transientischemic attacks (TIAs) or stroke has been

G.B. Bradac, *Cerebral Angiography*,
DOI: 10.1007/978-3-642-15678-6_15, © Springer-Verlag Berlin Heidelberg 2011

given as 4% (Thijs and Albers 2000). The incidence of these lesions is reported to be higher among blacks and Asians (Feldmann et al. 1990; Caplan et al. 1986; Caplan 1989; Wong et al. 1998; Min et al. 2000; Thijs and Albers 2000). The commonest sites visible on the angiogram are the terminal ICA and basilar and intracranial vertebral arteries. Also involved are the first segment of the middle cerebral artery (MCA; M1), the first segment of the anterior cerebral artery (ACA; A1), the pericallosal artery around the genu of the corpus callosum, and the first segments of the posterior cerebral artery (PCA; P1–P2) (Fisher et al. 1965; Fisher and Caplan 1971; Castaigne et al. 1973, 1981; Kavase et al. 1979; Hinton et al. 1979; Bradac and Oberson 1983; Caplan et al. 1986; Caplan 1989). Today, the intracranial lesions are the object of greater attention due to the possibility, in selected cases, of endovascular treatment.

15.3 Mechanisms Leading to Ischemia

The mechanisms leading to ischemia can be grouped in three categories:

- Thromboembolic occlusion or severe stenosis of arteries leads to ischemia strictly related to the supplied territory. These infarcts are also called territorial infarcts by some authors (Ringelstein et al. 1983, 1985; Weiller et al. 1991).
- The occlusion or severe stenosis can be proximal and the suffering territory is more distal and not in the vascular territory of a defined artery. Instead, the infarct is located at the borders of two different vascular territories (border-zone infarcts). A typical example is a lesion of the ICA bifurcation leading to ischemia; this is also termed hemodynamic becauses of hypoperfusion in the distal area, in which the collateral circulation is insufficient or absent. These infarcts can be cortical or involve the white matter.
- A particular form of infarct is the lacunar infarct or lacune (from Latin, *lacuna,-ae*, small cavity). The term was first used by Dechambre in 1838 and later by Durand-Fardel in 1843 to express pathological findings due to small infarcts, hemorrhages, or other causes. More precise reports were presented by Pierre Marie (1901) and Ferrand (1902), who used the term "lacune" to describe small infarcts in the basal ganglia, capsula interna, and pons that presented some typical clinical aspects. The clinical relevance, however, and the peculiar aspects of this pathology, termed lacunar syndrome, was emphasized and comprehensively discussed by Fisher (1965, 1969, 1979). CT and MRI have played an important role in the diagnosis and identification of these lesions. Today, lacunar infarcts are reported to account for about 25% of all cerebral infarcts [Bamford et al. 1987; Bogousslavsky et al. 1988b (Stroke); Boiten and Lodder 1991]. Lacunar infarcts are due to involvement of the perforators (deep and superficial), which are occluded directly by lipohyalinosis or through a thromboembolic process or atheroma, involving the large parent artery from which they arise; the perforators may be occluded indirectly in cases with hypoperfusion due to more proximal occlusion or cardiac failure.

All these mechanisms can act in isolation or be variously associated with one another. Taking this into consideration, the neuroradiological diagnosis of patients should include CT and MRI to examine the brain parenchyma, followed by a complete study of the arteries in the extraintracranial segments. The latter can be performed today with highly accurate CT and MRI angiography. Angiography should, however, be instituted every time the diagnosis is insufficiently clear or in cases where endovascular treatment is considered. Endarterectomy is performed in many centers only after a diagnosis with noninvasive methods without angiography. The validity of this approach is open to question.

15.4 Mechanism of Ischemia of the Anterior Circulation

15.4.1 *Carotid Artery*

Severe stenosis or occlusion of the ICA is not uncommonly asymptomatic provided that the development of the plaques is slow, allowing sufficient time for a collateral circulation to be established, and no distal embolization occurs. In the case of ischemia, despite frequently similar clinical syndromes, the pathogenetic process and the pattern visible on the angiographic examination can differ, as detailed in the following section.

- The extracranial ICA is patent. There is, however, occlusion of its intracranial branches, commonly due to embolic material arising from atheroma of the common carotid artery or, more frequently, from the ICA; alternatively, it can be cardiac in origin. In cases of TIA, the occlusion may be temporary owing to spontaneous thrombolysis, and it may no longer be recognizable on the angiogram.
- Considering the atheromatous plaque, an important aspect is the degree of stenosis of the lumen involved. Here, four degrees of stenosis have been distinguished: mild, when the lumen is reduced by less than 30%; moderate, with 30–70% reduction of the lumen; severe, if the reduction is greater than 70%; preocclusion state, more than 90%. The greater the stenosis, the higher is the risk of formation of a superimposed thrombus, which can be the source of the emboli. The stenosis can increase, reducing the flow with hypoperfusion and leading to ischemia in the distal vascular border territories or in the vascular territories of the perforators, since they are end arteries. An important role in the latter situation is played by the association of a severe contralateral ICA lesion and severe heart diseases (Bogousslavsky and Regli 1986; Bladin and Chambers 1993). The stenosis can be great, with considerable impairment of the blood flow, which is evident on the angiogram as a subocclusion pattern (Fig. 15.8).
- To measure the stenosis on the angiogram, a few methods have been proposed; among them, the European Carotid Surgery Trial (ECST, 1998) and North American Symptomatic Carotic Endarterectomy Trial (NASCET, 1991) are the most used (Fig. 15.1).

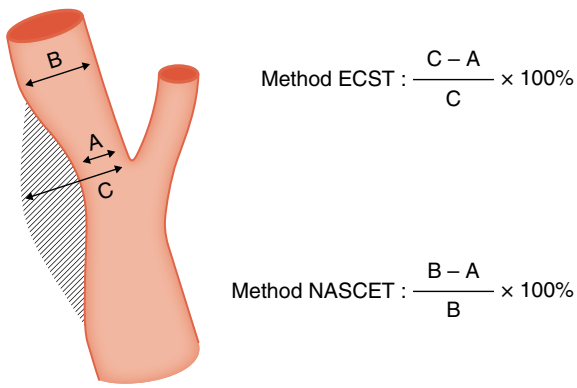

Fig. 15.1 Methods to measure ICA stenosis on the angiogram: European Carotid Surgery Trial (*ECST*) and North American Symptomatic Carotic Endarterectomy Trial (*NASCET*)

Differences in the applied criteria lead to differences in the results with these methods. There is broad agreement that a stenosis of 70% with NASCET (corresponding to a stenosis of about 80% with ECST) is a clear indication for endarterectomy, thereby reducing significantly the risk of stroke. Alternatively, endovascular treatment has increasingly been successfully performed (Wholey et al. 2000; Bonaldi 2002; Ringleb et al. 2006; Wittkugel et al. 2008; Stingele et al. 2008; Clark 2010) (Figs. 15.2 and 15.3).

- There are, however, some other aspects of the atheroma that should be considered. Ulceration, with the risk of distal embolization, can also occur in relatively small atheromas, and the progression and evolution of the atheroma may vary. Taking this into account, attention today is being progressively given to the aspects and components of the atheroma. In addition to angiography, information can be obtained using ultrasound technology, CT angiography, and contrast-enhanced MRI. In our opinion, these are important complementary methods to angiography, but they do not replace it. Data from these sources along with the age of the patient can influence the decision as to whether therapy should be medical, surgical, or endovascular (Stingele et al. 2008; Clark 2010; Rosenkranz and Gerloff 2010).
- Atheromas can also occur in the intracranial segments of the ICA, especially in the distal petrous and cavernous portion. The clinical importance of these lesions has been revaluated, and now endovascular treatment may be undertaken in selective symptomatic patients (Fig. 15.4). Finally, stenosis of both the proximal and distal ICA (tandem lesions) is also reported, with a frequency of about 10% of cases (Craig et al. 1982; Kappelle et al. 1999). This aspect should be considered when planning therapy.
- With regard to asymptomatic lesions, it should be noted that there is no general agreement about the therapy (medical or more aggressive) to be applied. The decision depends on the degree of stenosis, the presence or absence of a good collateral circulation, age, general clinical condition of the patient, and the experience of the medical team involved (Fig. 15.3).
- The ICA is occluded, and the occlusion extends from the ICA bifurcation to its intracranial segment, proximal to the ophthalmic artery. In such cases, it can be assumed that the thrombus has extended from the ICA bifurcation to its intracranial terminal segment. Another possibility is that an embolus has occluded

the intracranial ICA, followed by the retrograde formation of a thrombus extending proximally toward the ICA bifurcation. In some cases, despite the proximal occlusion, the distal part of the ICA is still patent (Seckar et al.1986). This can be demonstrated on the angiogram in later phases. In such cases, which are very rare, rapid surgical or endovascular treatment can completely restore the lumen of the artery.

- In all of the above cases, ischemia can be avoided or limited in relation to the efficiency of the collateral circulation through the ECA and circle of Willis, provided that no further embolization of the intracranial branches occurs. On the indirectly injected intracranial branches, which are visible on the angiogram obtained from the contralateral ICA, vertebrobasilar artery, or ECA, emboli can sometimes be identified.
- The occlusion is on the terminal ICA, sometimes involving partially also the A1 and M1 (the so-called T occlusion). This is a very serious clinical condition since there is a lack of a collateral circulation through the ECA and circle of Willis (Fig. 15.5). The only collateral circulation is the distal leptomeningeal anastomosis from the homolateral ACA and PCA—provided that these arteries are not involved (Fig. 15.6). The cause of terminal ICA occlusion varies. It can be due to emboli that are cardiac in origin

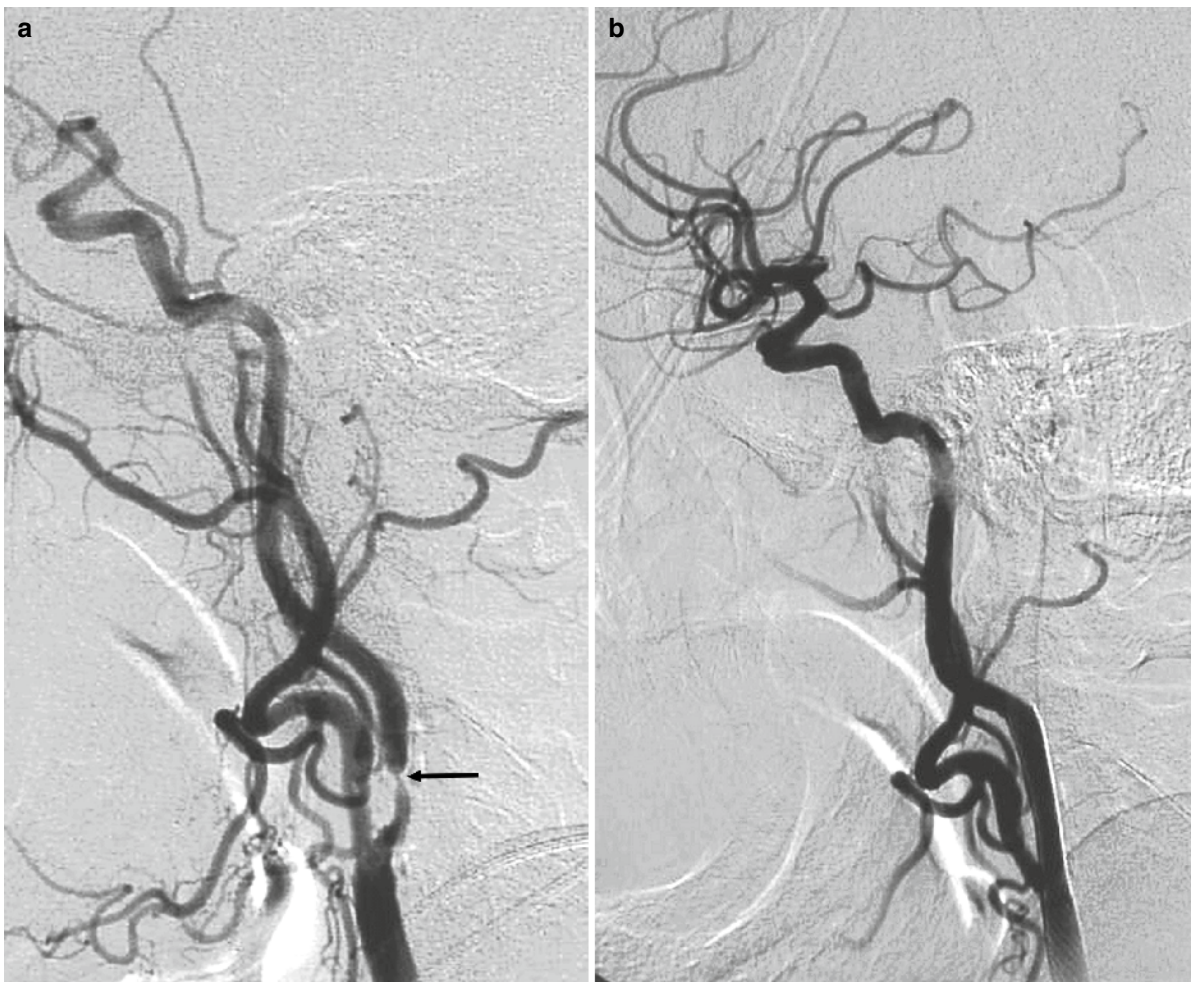

Fig. 15.2 Two examples of atherosclerotic plaque leading to severe stenosis of the ICA. (**a**) Carotid angiogram showing the stenosis (*arrow*) with slowing of the flow. (**b**) Angiogram after angioplasty and stent showing normalization of the lumen and flow. (**c**) Carotid angiogram showing the stenosis (*arrow*). (**d**) Angiogram after angioplasty and stent with normalization of the lumen and improvement in flow

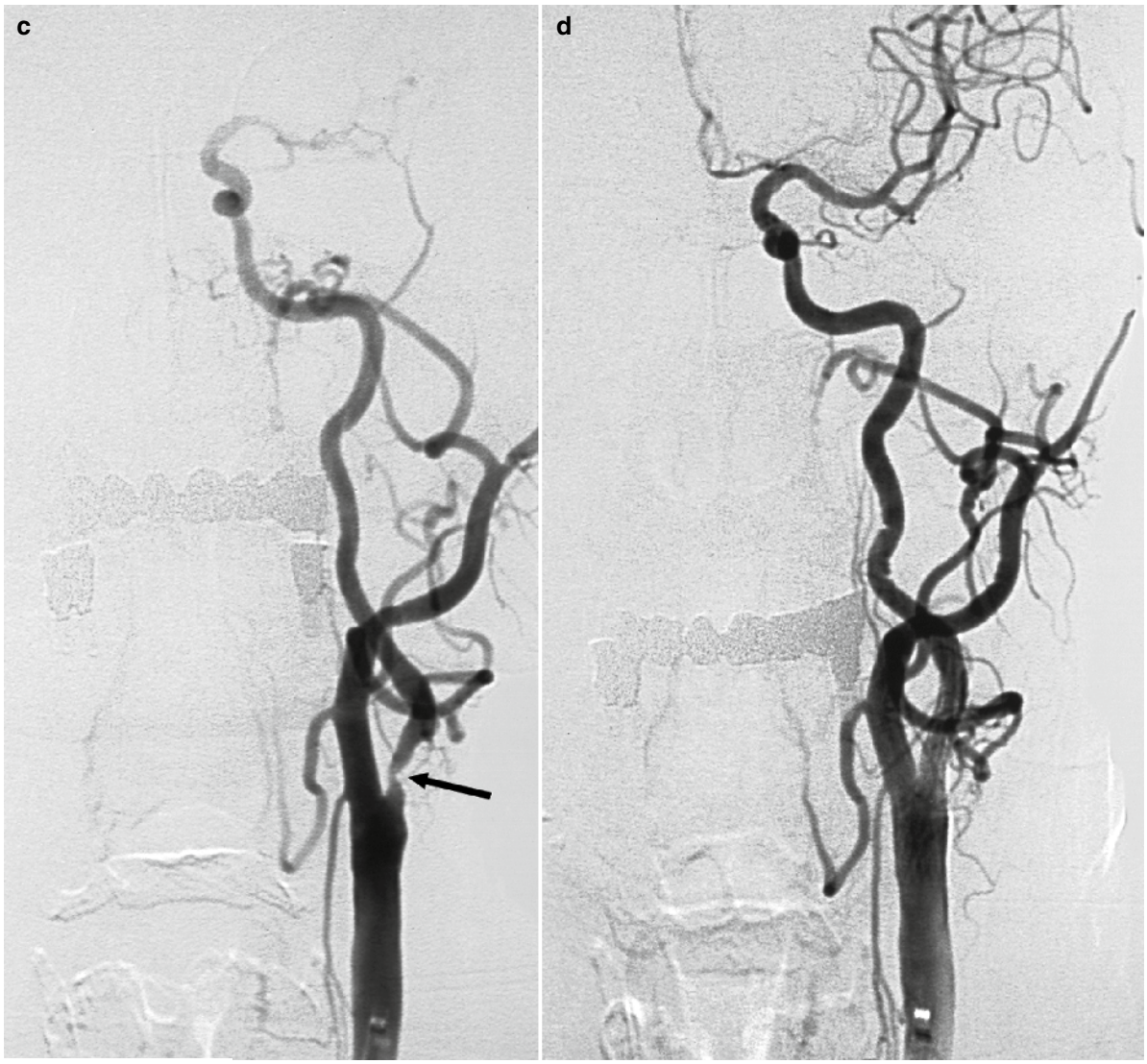

Fig. 15.2 (continued)

or from an atheromatous plaque of the proximal ICA. The latter can be very extensive and lead to severe stenosis or occlusion of the ICA at the bifurcation, with thrombosis extending to the distal ICA. Finally, an atheromatous plaque involving the distal ICA can lead progressively to thrombosis of the vessel. In selected cases, endovascular treatment with reopening of the artery has been successfully performed and produced a good clinical outcome. In some other cases, endovascular treatment makes it possible to reopen the distal ICA while the extracranial segment remains occluded. This allows restoration of the collateral circulation through the circle of Willis (Fig. 15.7). However, it should be noted that the risk of a large hemorrhagic transformation of the existing ischemia is high (Zeumer et al. 1993; Jansen et al. 1995; Ringer et al. 2001; Qureshi et al. 2001; Song et al. 2002; Flint et al. 2007; Malgorzata et al. 2008; Choi et al. 2009).

- In patients who have a known occluded ICA, ischemia can occur months or years later. In these cases, the etiopathogenesis may be hemodynamic or embolic. Indeed, emboli arising from atheromas in the stump of the ICA, in the common carotid artery or ECA, can reach the intracranial vessels via the collateral

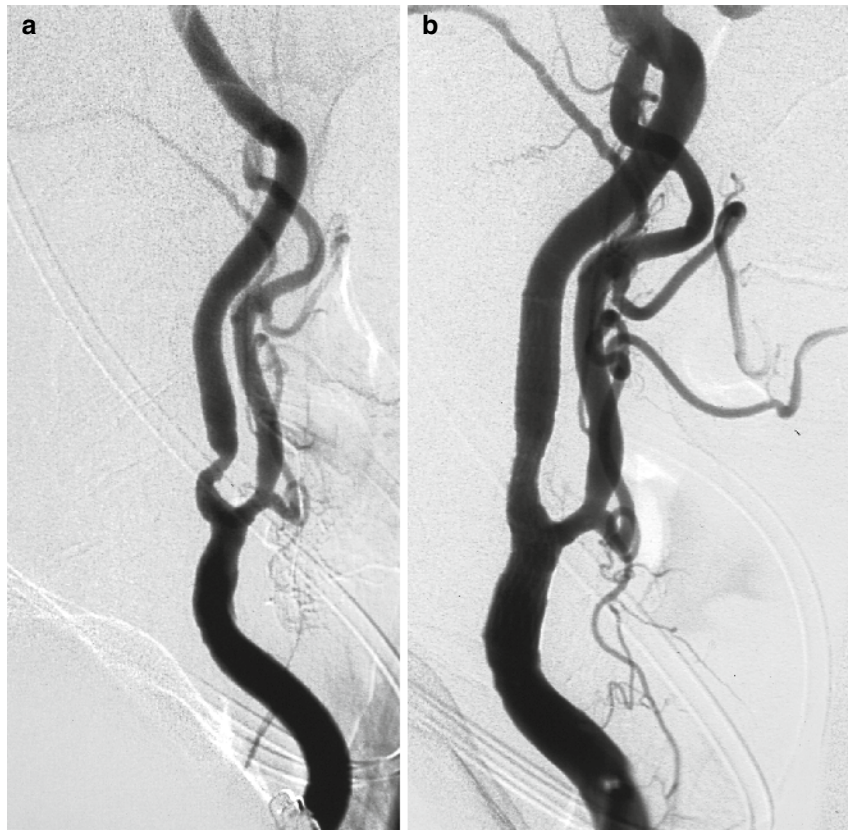

Fig. 15.3 Very old female patient with asymptomatic moderate to severe stenosis of the left ICA (**a**). The ICA was an important collateral way through the circle of Willis for the right carotid sector since the right ICA was occluded. A preventive endovascular treatment with stent and angioplasty (**b**) was performed without any clinical problems

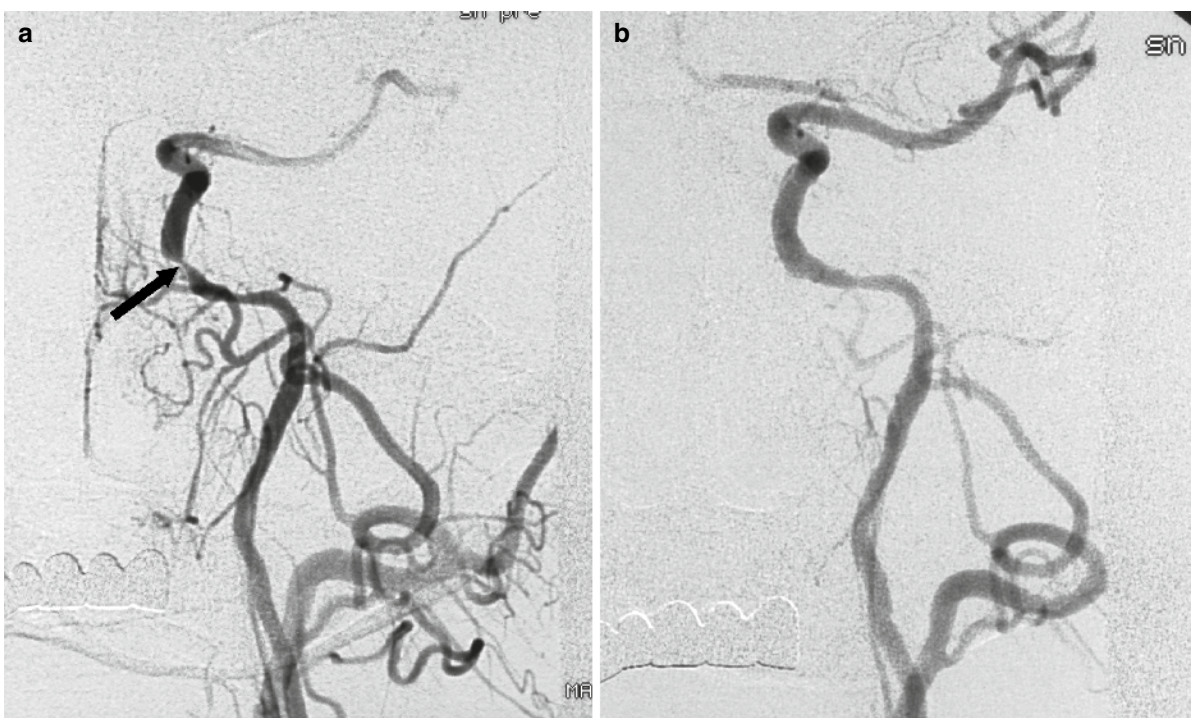

Fig. 15.4 Carotid angiogram, AP view. Severe stenosis of the proximal intracavernous segment of the ICA (**a**), with intracranial flow impairment, leading to transient ischemic attacks (TIAs) not responsible for medical therapy. Endovascular treatment with angioplasty and stent; restoration of the intracranial circulation (**b**)

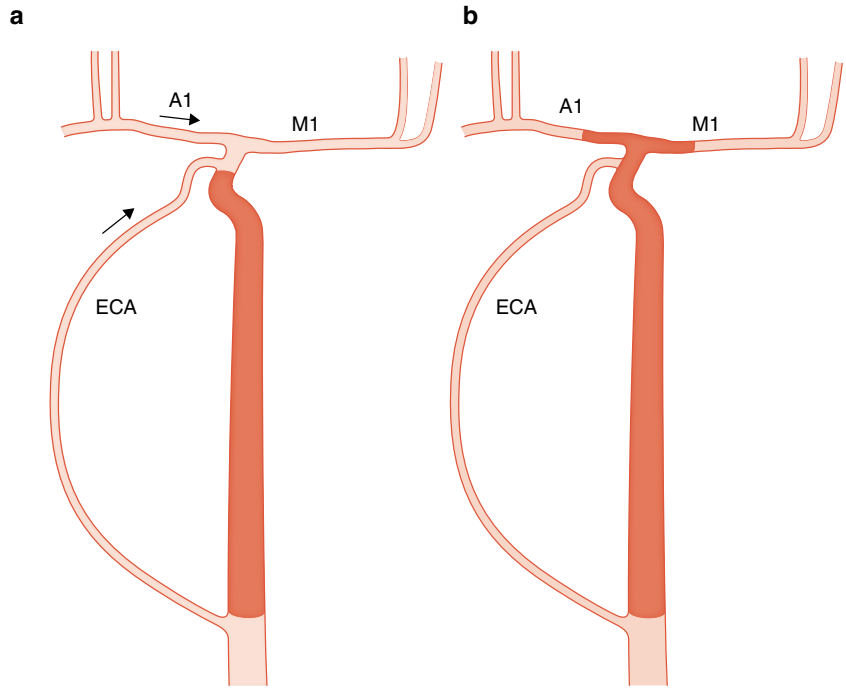

Fig. 15.5 Different findings in occlusion of the ICA proximal to the ophthalmic artery (**a**) and distal to it, with involvement of the A1 and M1 segments (**b**). In (**a**), a collateral circulation occurs through the external carotid artery (ECA)–ophthalmic artery anastomosis and through the circle of Willis provided that this is not impaired by hypo/aplasia of the A1. In (**b**), the above described collateral ways are involved in the thrombotic process. The only possible collateral circulation is leptomeningeal anastomosis with distal branches of the middle cerebral artery (MCA) and posterior cerebral artery (PCA)

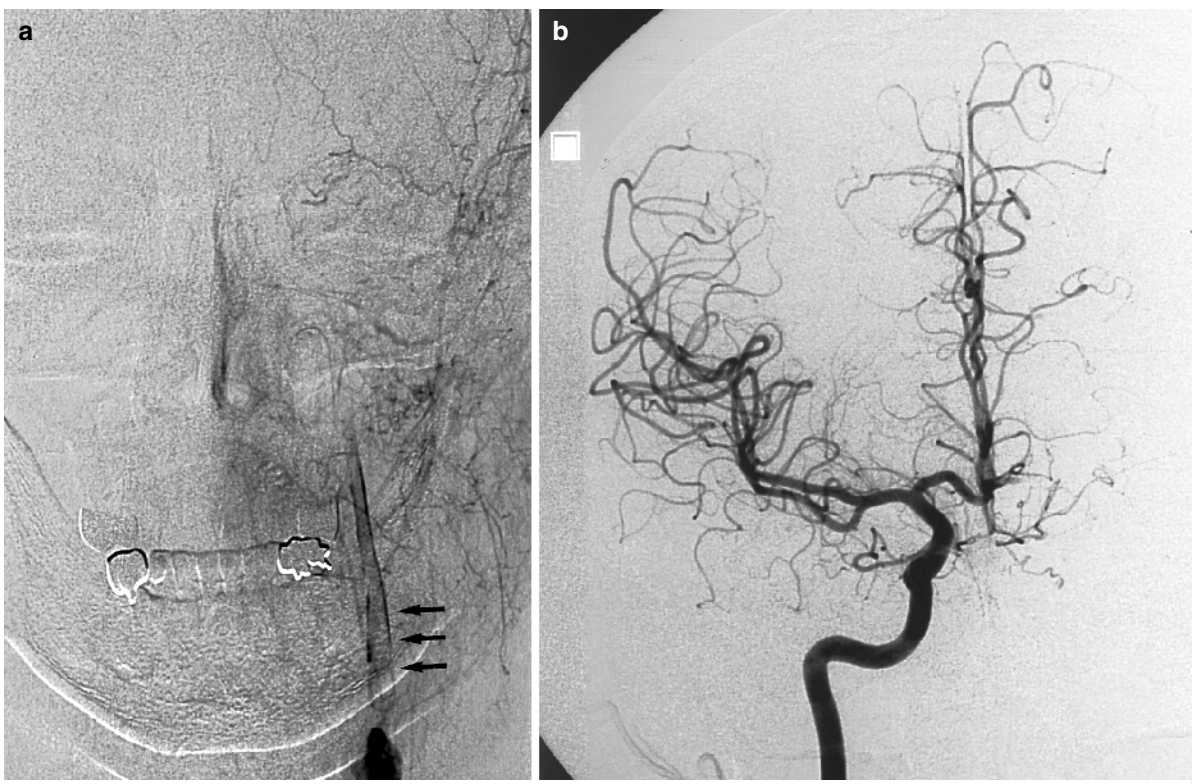

Fig. 15.6 Thromboembolic acute occlusion of the distal left ICA (T occlusion). Left carotid angiogram (**a**) showing stenosis of the ICA with the distal thrombus extending intracranially (*arrows*). There is collateral circulation neither through the ECA nor the circle of Willis. The stump of the proximally occluded ACA is recognizable in 15.6c. There is, however, a rich leptomeningeal collateral circulation (*arrow*) through distal branches of the left anterior cerebral artery (ACA), visible on the right carotid angiogram (**b**, **c**, and **d**) and through branches of the PCA visible on the vertebral angiogram (**e**). Medical therapy was chosen, and the patient recovered with minimal neurological deficit

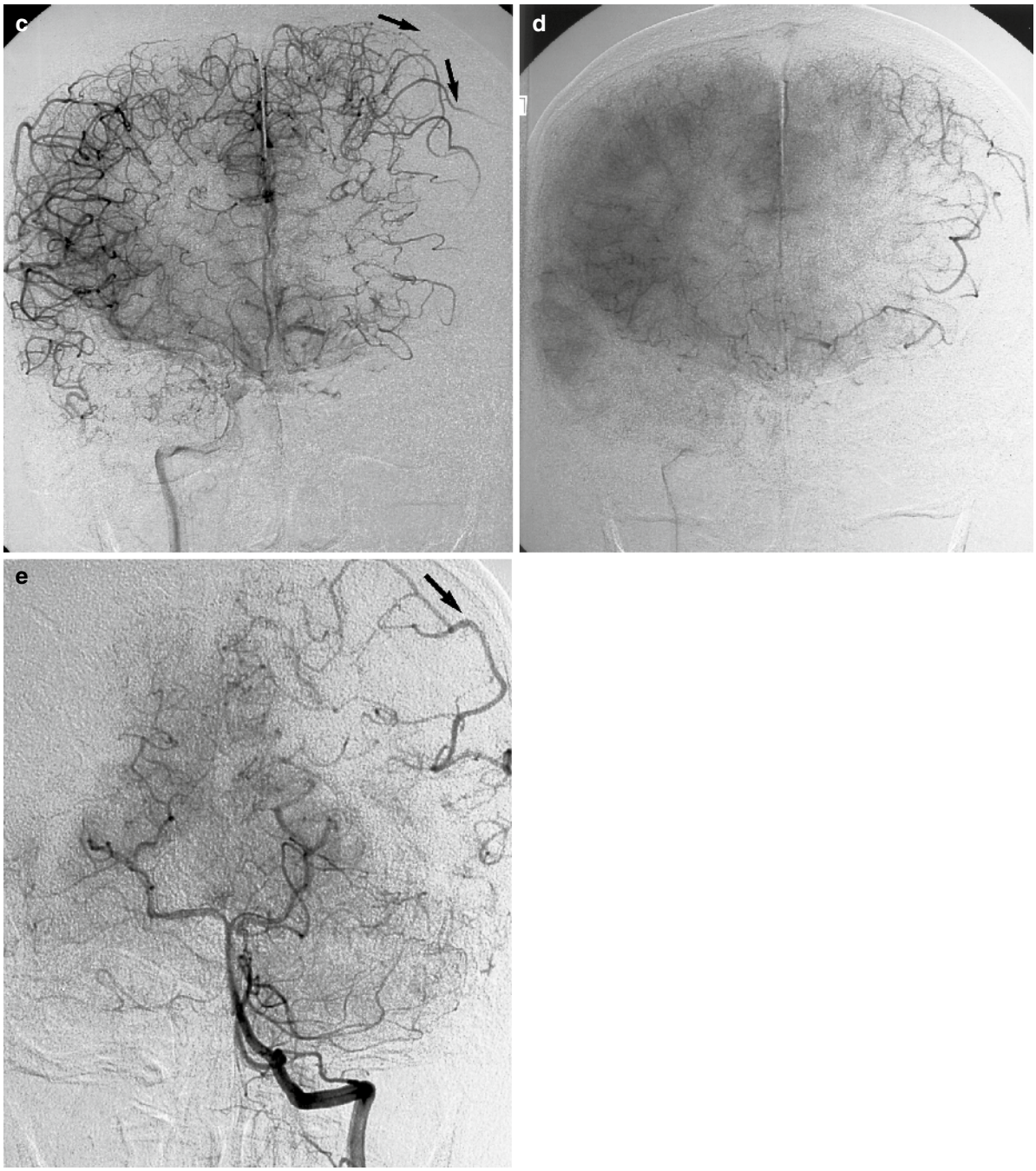

Fig. 15.6 (continued)

circulation and involve branches of the ECA, particularly those of the internal maxillary artery, which leads to a retrograde injection of the ophthalmic artery and ICA (Countee and Vijayanathan 1979; Countee et al. 1981; Bradac and Oberson 1983).

15.4.2 Middle Cerebral Artery

The MCA is the most frequently involved vessel in cerebral infarction. The pathogenesis is commonly artery-to-artery (carotid bifurcation) or cardiac embolism, which leads to occlusion of the M1 and/or more distal branches. In some cases, after successful reopening of the vessel, it appears clear that the embolus has been arrested at the level of the stenotic microatheroma.

In occlusion of the M1, the perforators are always involved to a greater or lesser degree. The degree depends on the location of the embolus (in the proximal or more distal M1), morphological aspects (short or long) of the M1, and the site of origin of the perforators (see anatomy). Perforators are end arteries, and so their occlusion, even for a relatively short time, can lead to ischemia in their territories. This is confirmed in cases where despite rapid reopening of the occluded M1 through the endovascular treatment, small ischemic lesions in the basal ganglia are frequently demonstrated in CT and MRI (Bradac et al. 2008b) (Figs. 15.9–15.11). In other cases, in CT performed after successful endovascular reopening of the M1, small hemorrhages are recognizable in the basal ganglia following the hemorrhagic transformation of the ischemia in this area.

In occlusion of the M1, the peripheral vascular territories can be more protected. This depends on the efficiency of the leptomeningeal collateral circulation, which can be impaired by distal embolization. In other cases (Figs. 18.2 and 18.3), the M1 is patent and the peripheral branches can be occluded owing to distal embolization. The therapeutic endovenous or selective intra-arterial pharmacological associated increasingly with mechanical thrombolysis using different devices has improved in many cases the prognosis of patients

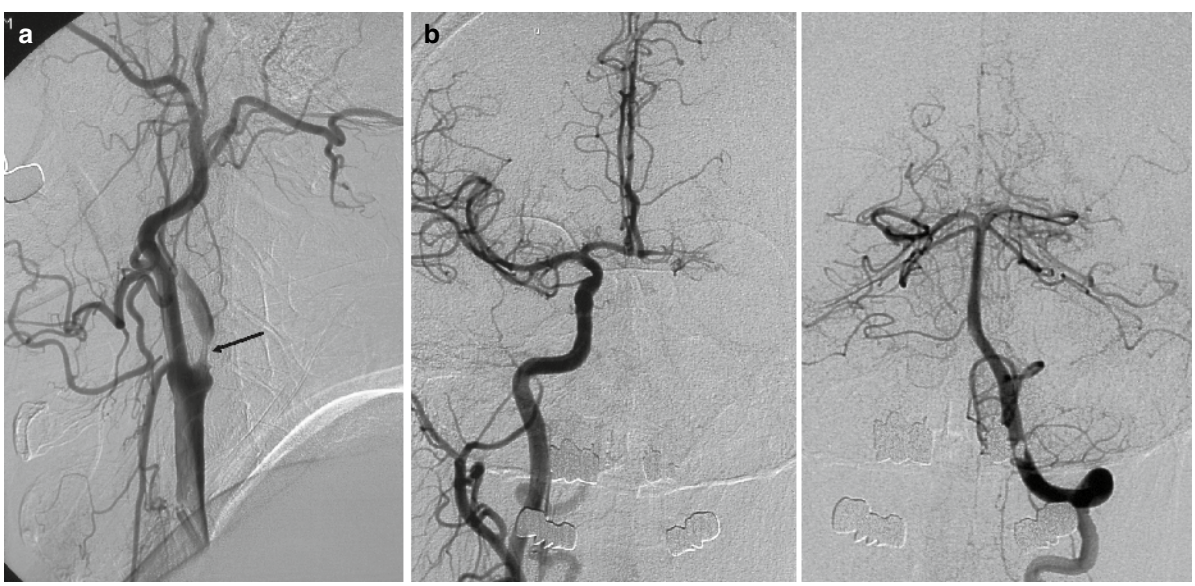

Fig. 15.7 Old patient presenting with aphasia, right hemiplegia and progressive cognitive disturbances. (**a**) Left carotid angiogram showing severe stenosis of the left ICA (*arrow*). There was no filling of the distal ICA and no collateral circulation through the ECA. (**b**) Right carotid and vertebral angiogram showing no collateral circulation through the circle of Willis, with the exception of a minimal injection of the left A1. (**c**) After stent application at the left ICA bifurcation, a microcatheter was advanced into the distal ICA, followed by mechanical thrombolysis, leading to reopening of the distal ICA and the collateral circulation through the circle of Willis (*arrow*). The proximal ICA remained occluded. (**d**) CT 24 hours post-treatment showing hemorrhagic ischemia of the basal ganglia and minimal cortical temporo-parietal ischemia. The patient recovered slowly over subsequent weeks

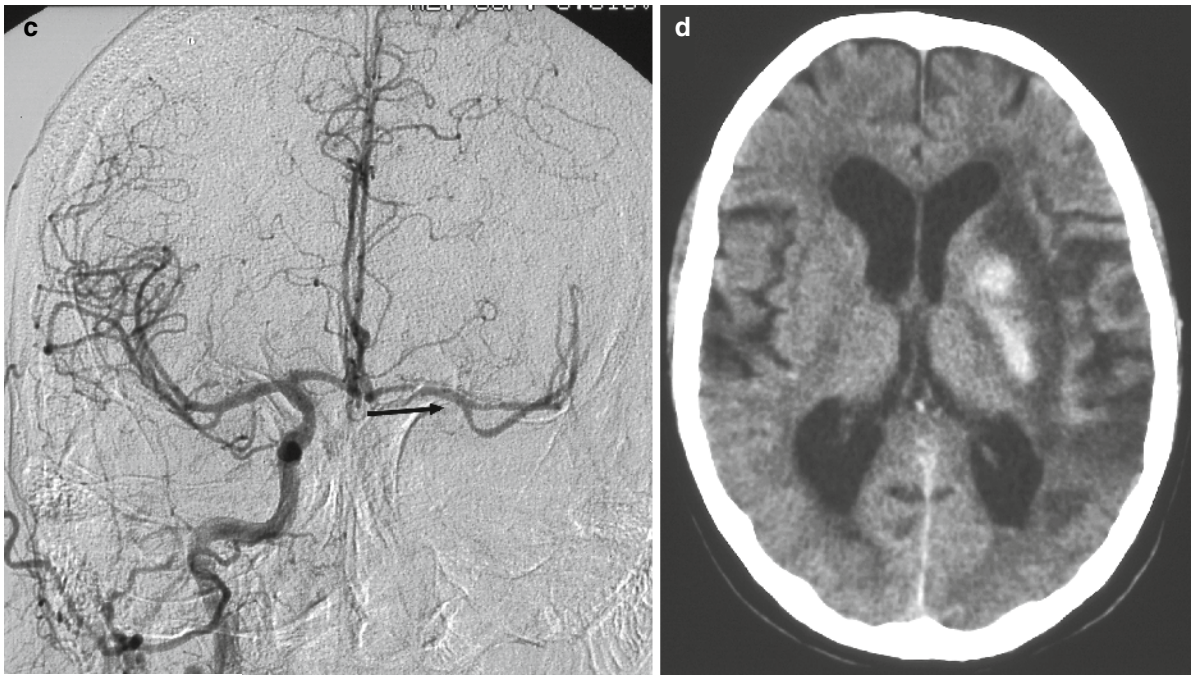

Fig. 15.7 (continued)

(Arnold et al. 2002; Qureshi et al. 2002; Noser et al. 2005; Zaidat et al. 2005; Tauntopoulou et al. 2008; Eckert 2009; Choi et al. 2009).

Microatheroma of the M1 (Caplan 1989; Bogousslavsky et al. 1991) is another less common cause of ischemia and directly involves the perforators. Distal cortical and white matter vascular territories can also be involved in these cases by either hypoperfusion or distal embolization. Stenosis of the M1, as with stenosis of other intracranial arteries—particularly of the terminal ICA and basilar artery when symptomatic and not responsible for the medical therapy—is reported to have a bad prognosis (Thijs and Albers 2000; Wasid 2003). Endovascular treatment (angioplasty, stent) has opened up new ways of therapy (Berkefeld et al. 2003; Gupta et al. 2003; Bose et al. 2007; Turk et al. 2008; Bradac et al. 2008b (The Neuroradiology Journ.); Qureshi 2008; Berkefeld and Zanella 2009) (Figs. 15.12 and 15.13) and produced promising results. The rate of complications with this treatment, however, is still relatively high. Hemorrhage due to vessel rupture, reperfusion, and new ischemic lesions can occur. The latter are commonly the result of occlusion of the perforating branches from the stent struts crossing their origin or displacement of microatheromatous material. Fortunately, and somewhat surprisingly, this is relatively seldom. Taking these considerations into account, the treatment should be performed only in selected patients in whom medical therapy has failed, especially when the stenosis is severe and not in the acute phase after stroke (Chaturvedi and Caplan 2003; Kurre et al. 2010).

15.4.3 Anterior Choroidal Artery

Infarcts in the territory of the anterior choroidal artery (AChA) are frequently associated with ischemia in other vascular territories, especially the MCA and PCA. The pathogenesis is carotid or cardiac embolism, or atheroma in the terminal ICA (Helgason 1986; Boiten and Lodder 1992; Hupperts et al. 1994; Levy et al. 1995) (Fig. 15.14). Selective embolization can also occur. Ischemia may be due to an inadvertent occlusion of the artery in surgical or endovascular treatment of aneurysm in this area (Friedman et al. 2001). As already described, the vascular territories of the AChA can be replaced by other arteries. Furthermore, there are many anastomoses with branches of the PCA,

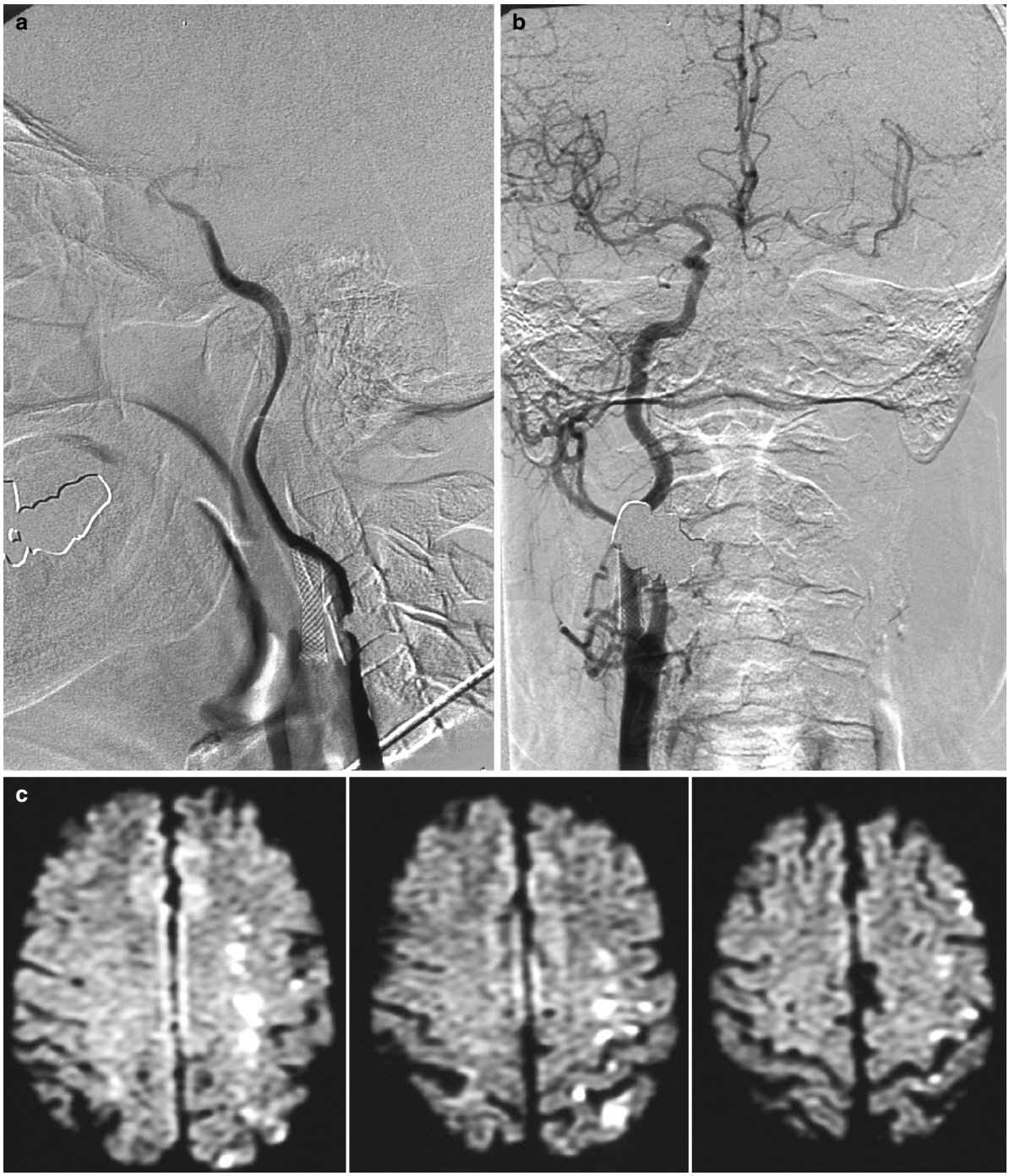

Fig. 15.8 Patient already treated with stent for stenosis of the right internal carotid artery (ICA). Acute mild neurological symptoms owing to impairment of the circulation of the left cerebral hemisphere. On the angiogram, subocclusion of the left ICA (**a**) due to a large atheroma with severe flow impairment. Collateral circulation from the right carotid artery (**b**). On MRI (**c**) (diffusion-weighted images), there were ischemic lesions in the vascular territory of the medullary arteries as a result of hypoperfusion. The small associated cortical lesions were probably embolic. Endarterectomy was successfully performed a few days later, with good clinical results

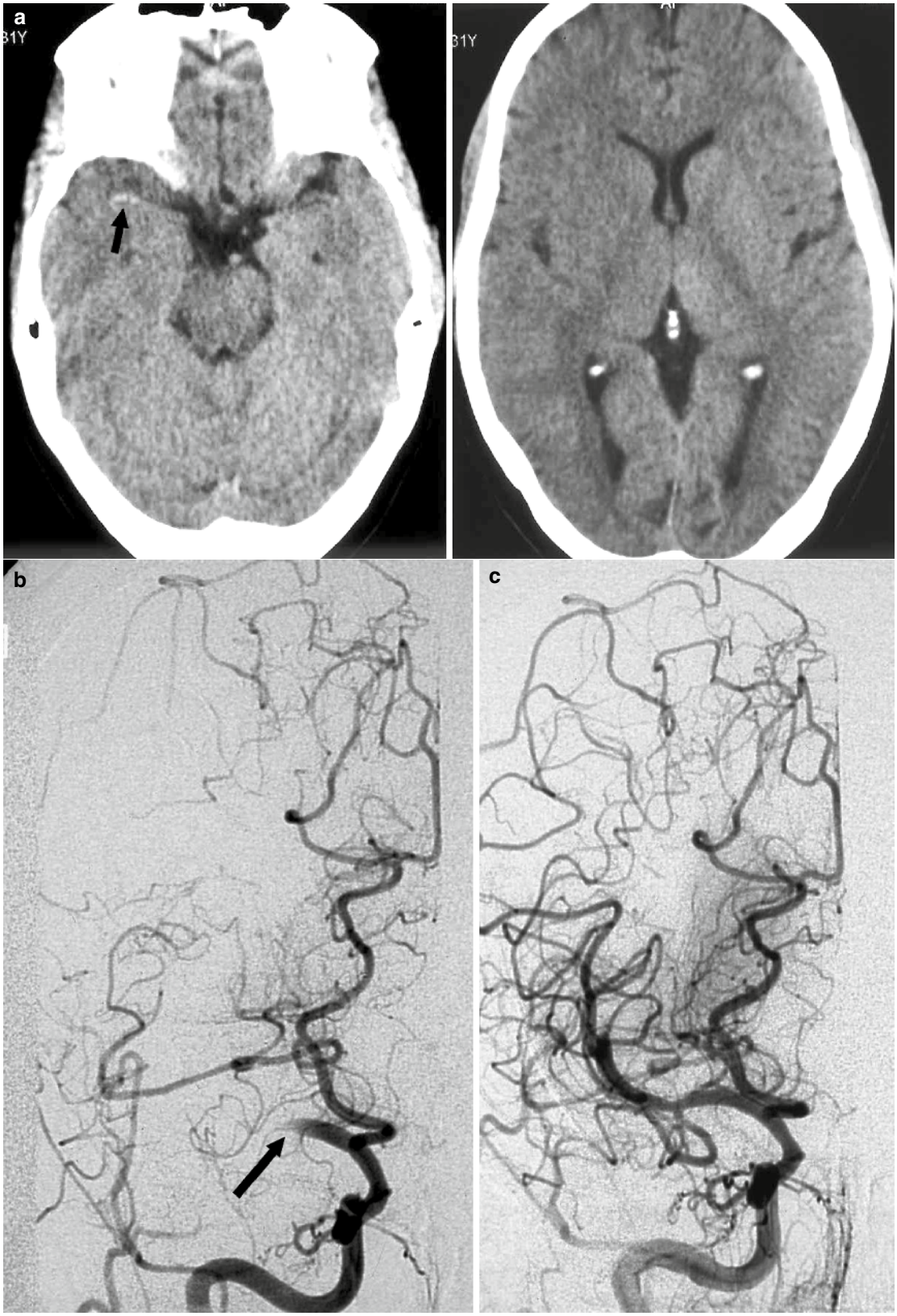
a
b
c

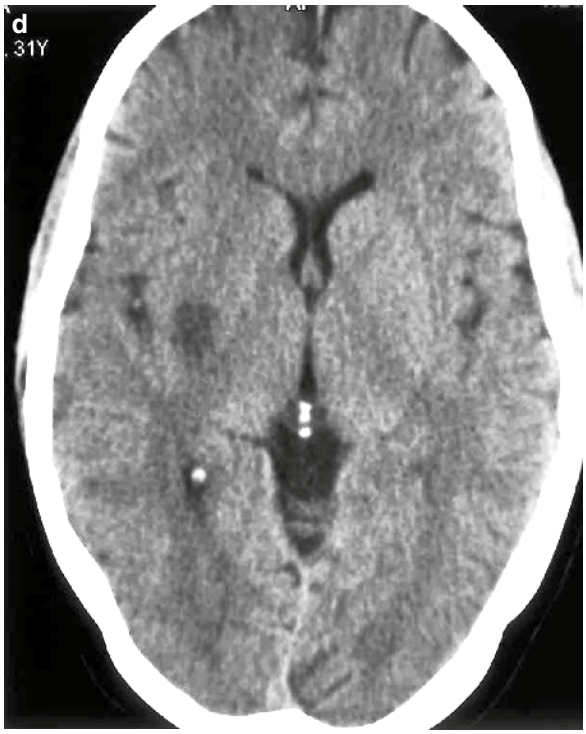

Fig. 15.9 (continued)

and this explains the irregular presence of ischemic lesions in cases of occlusion of the AChA.

15.4.4 Anterior Cerebral Artery

Infarcts in the territory of the ACA are commonly associated with ischemia in other vascular territories after carotid or cardiac embolism (Figs. 15.16 and 18.2). Embolization is not infrequently associated with variants in the anterior portion of the circle of Willis, which favors the passage in the ACA (Kazui et al. 1993).

Microatheromas located in the pericallosal segment can be another rare cause of ischemia (Fig. 15.15). Also, the inadvertent occlusion of the artery of Heubner in treating aneurysm of the ACA can lead to ischemia.

15.4.5 Lacunar Infarcts in the Anterior Circulation

These infarcts are due to involvement of the deep perforators supplying the basal ganglia and capsula interna and perforators supplying the superficial and deep white matter, which are called medullary arteries. As already described, these arteries do not anastomose to each other, and neither are connections between the deep perforators and medullary arteries present (De Reuck 1972; Mody et al 1988, 1990). Both vascular territories or only one can be involved.

A frequent pathogenesis is a special form of atherosclerosis called lipohyalinosis. This occurs particularly, but not always, in patients with hypertension and diabetes. The lesions can be very numerous and disseminated on both hemispheres; they are commonly small (less than 20 mm in diameter). No pathological changes of the arteries can be detected on the angiogram in many of these patients.

In other cases, the ischemic lesions are frequently larger and extensively involve the vascular territory of deep perforators from the ICA, AChA., ACA, and MCA. The most typical lesion is termed the striatocapsular infarct (Ghika et al. 1989; Boiten and Lodder 1992; Nicolai et al. 1996; Horowitz and Tuhrim 1997; Bradac et al. 2008b). The pathogenesis of these lesions varies. They may be due to emboli; they can be cardiac in origin or arise from atheromas of the ICA. Another mechanism frequently reported is occlusion or severe stenosis of the ICA, which leads to hypoperfusion (Boiten and Lodder 1992; Horowitz and Tuhrim 1997). More rarely, microatheroma of the terminal ICA or MCA occurs (Fisher 1965; Caplan 1989; Bogousslavsky et al. 1991), leading to hypoperfusion or direct occlusion of the perforators (Figs. 15.8, 15.12, and 15.13).

Fig. 15.9 Young cardiopatic patient with sudden onset of left hemiplegia. On CT (**a**), hyperdensity of the MCA (*arrow*) and ill-defined borders of the right basal ganglia are evident. Angiography (**b**) disclosed occlusion of the proximal segment of the M1 (*arrow*). Fetal origin of the PCA from the ICA. ACA arising from the left. Partial collateral leptomeningeal circulation from the PCA. Selective pharmacological thrombolysis was performed, with reopening of the M1 (**c**) and complete clinical recovery. On CT (**d**) performed 3 days later, a small asymptomatic ischemic lesion in the vascular territory of the perforators was visible

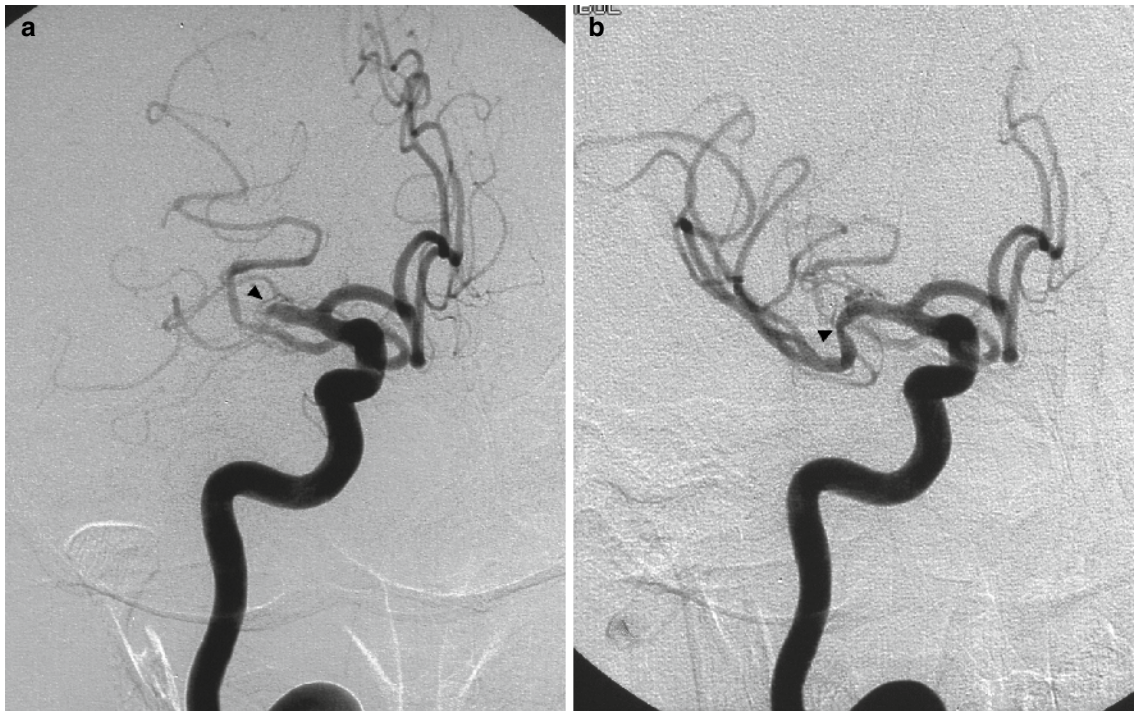

Fig. 15.10 Older woman with heart dysrhythmia presenting with sudden onset of hemiplegia with cognitive disorders. The right carotid angiogram (**a**) disclosed occlusion of the M1 segment (*arrowhead*). Endovascular treatment with reopening of the artery using a Solitaire stent was performed (**b**). The post-treatment angiogram showed the presence of microatheroma (*arrowhead*) associated with a tortuous distal M1, which probably favored the arrest of the embolus. A small infarct in the basal ganglia was visible on CT. In spite of this, the patient recovered completely

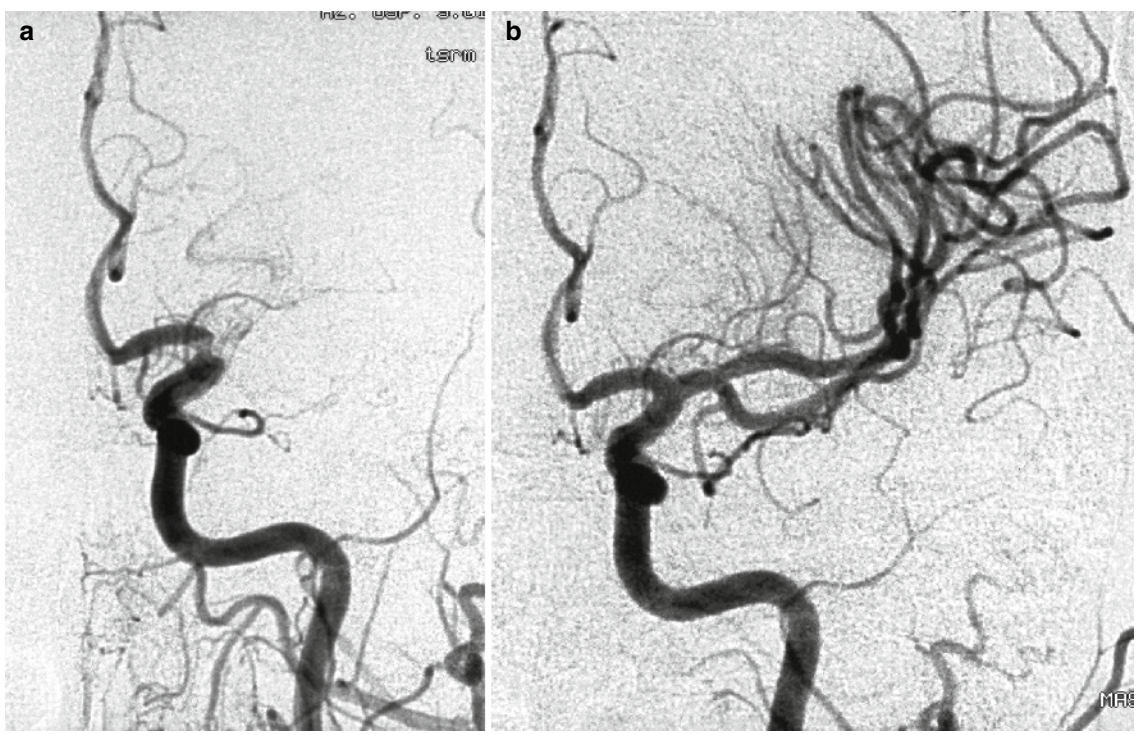

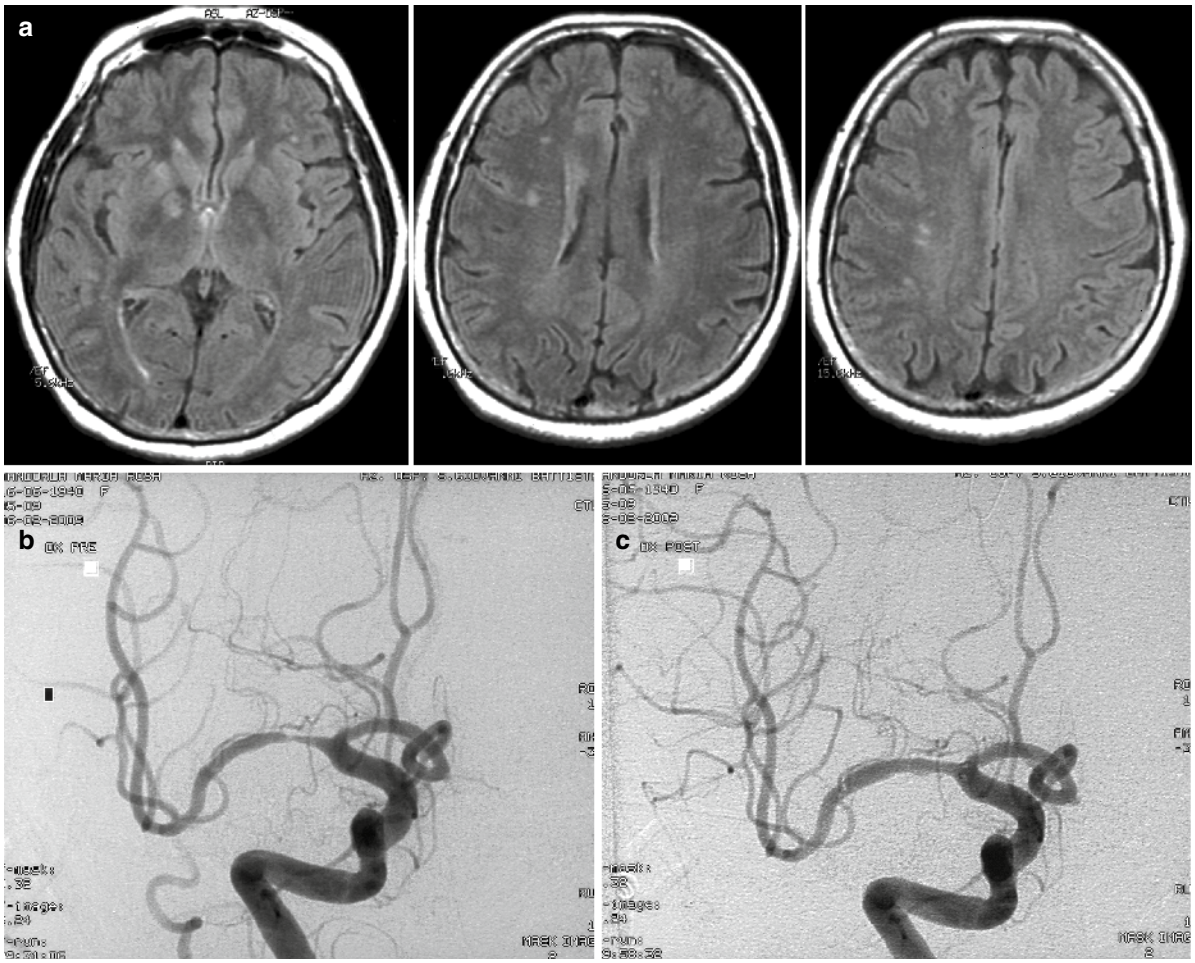

Fig. 15.12 Middle-aged patient with mild neurological deficit indicating impairment of the right ICA vascular territory. MRI (**a**) showed an ischemic lesion in the right basal ganglia and white matter. A few lesions were also present on the left. Angiogram (**b**) disclosed severe stenosis of the M1 with normal distal perforators. Endovascular treatment (angioplasty and stent) was performed (**c**). It is conceivable that the proximal perforators were occluded by the microatheroma while the distal perforator and medullary artery were involved by hypoperfusion

The pathogenetic process cannot always be assessed with certainty since several mechanisms can occur together. In this context, morphological variants should be considered, as already described (see anatomy). In particular, it should be noted that lenticulostriate arteries can arise as a common trunk (Umanski et al. 1995), which, if involved by lipohyalinosis, can also be responsible for a large lesion.

The same pathogenetic factors are responsible for infarcts in the vascular territory of the medullary arteries. In hypertensive and diabetic patients, lipohyalinosis is common. In patients with severe stenosis or occlusion of the ICA or stenosis of the MCA, hypoperfusion is reported as being the most frequent pathogenetic factor (Waterston et al. 1992; Weiller et al. 1991; Boiten and Lodder 1992; Bogousslavsky and Regli 1992; Bladin

Fig. 15.11 Young patient with acute occlusion of the M1 at its origin owing to cardiac embolism. Pharmacological selective thrombolysis with complete reopening of the MCA and full clinical recovery. Small ischemic lesions in the basal ganglia were visible on CT performed some days later

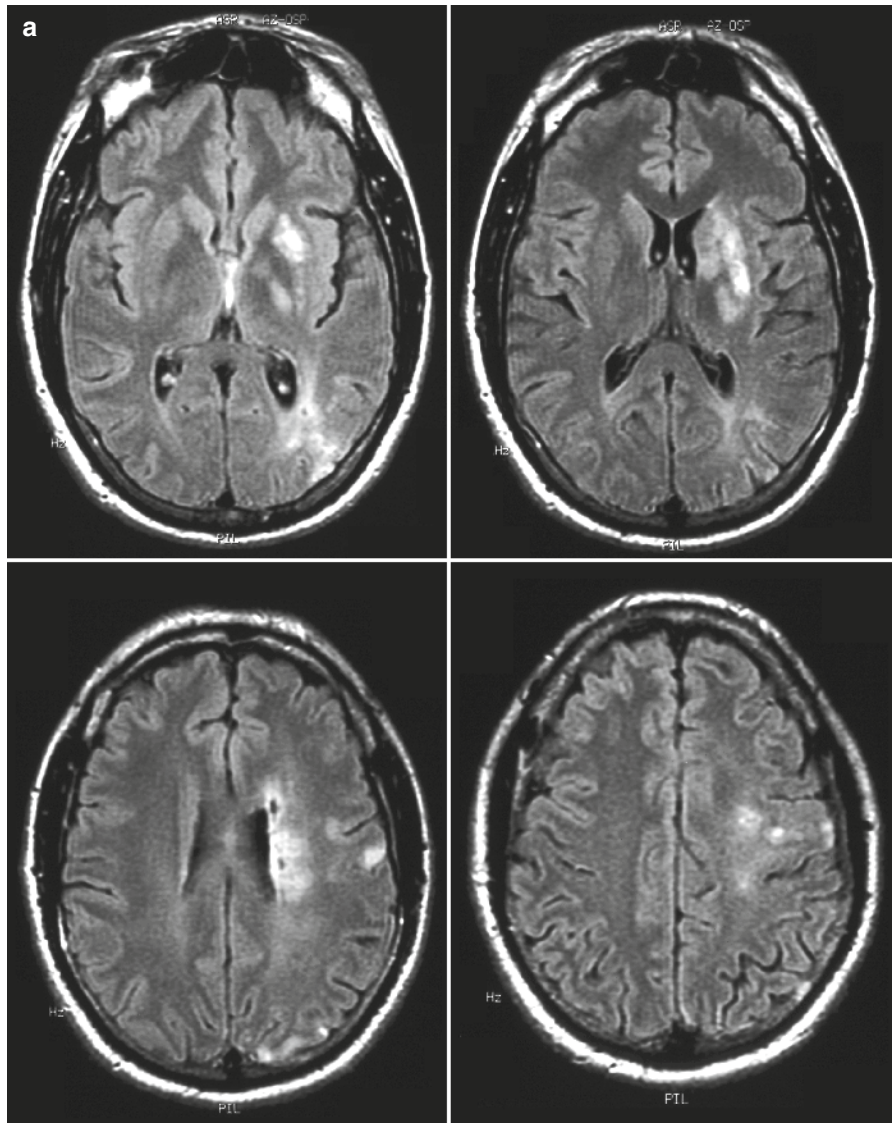

Fig. 15.13 Acute ischemia in a middle-aged patient involving the left basal ganglia, white matter, and cortex as demonstrated on MRI (**a**). Angiography (**b**) disclosed severe stenosis of the M1 (*arrow*). Some proximal perforators are occluded at their origin. Ischemia in the basal ganglia was due partially to direct occlusion of the proximal perforators at their origin and hypotension in the more distal branches. Ischemia in the white matter and in the temporo-occipital region was probably due to hypoperfusion, involving the medullary and distal cortical branches, respectively. Small ischemic cortical lesions in the frontoparietal area were embolic. Three weeks later, endovascular treatment (angioplasty plus stent) was performed (**c**). The patient recovered completely

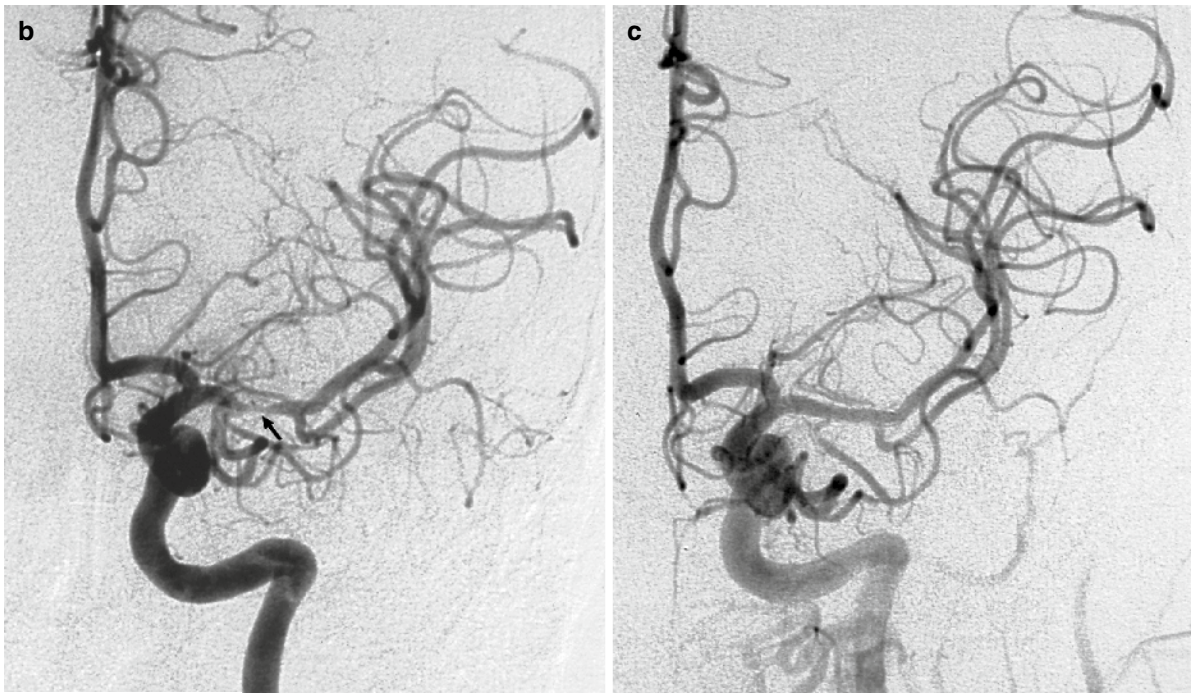

Fig. 15.13 (continued)

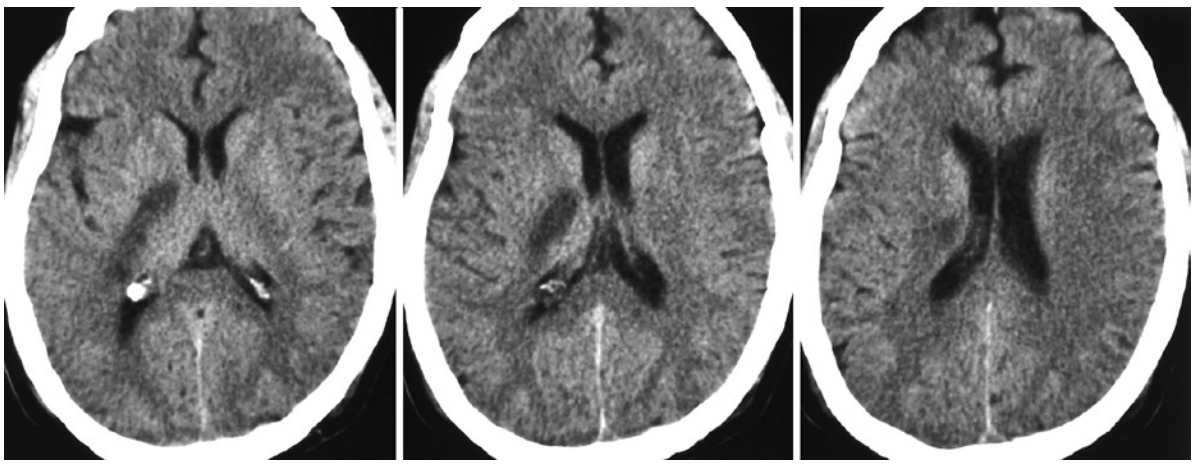

Fig. 15.14 Middle-aged patient with cardiac dysrhythmia presenting with stroke due to occlusion, probably embolic, of the anterior choroidal artery. CT showing ischemia in the corresponding vascular territory

and Chambers 1993; Horowitz and Tuhrim 1997; Reed et al. 1998; Bradac et al. 2008b).

Selective embolism of the medullary arteries may also occur. Indeed, a large infarct in the white matter without involvement of the cortex owing to embolic occlusion of the peripheral branches of the MCA has been demonstrated by angiography (Angeloni et al. 1990). In this case, because of the rich collateral circulation, there were no ischemic lesions in the cortex, while infarcts were present in the vascular territories of the medullary end arteries. It is conceivable that in some cases hemodynamic and embolic mechanism can occur together (Angeloni et al. 1990; Bradac et al. 2008b) (Figs. 15.8, 15.12, and 15.13).

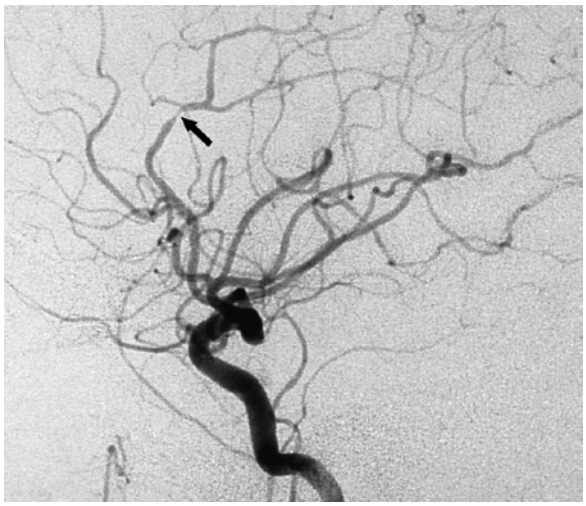

Fig. 15.15 Typical location of a microatheroma leading to stenosis of the pericallosal artery (*arrow*) in an asymptomatic patient

In this context, a rare form of infarct involving the white matter is that occurring in the area of the external capsule lateral to the basal ganglia in the border area between the deep perforators and medullary arteries that arise from the insular branches. These lesions have been termed subinsular infarcts by Pullicino et al. (1992).

15.5 Posterior Circulation

The composition of atherosclerotic plaques in the vertebrobasilar sector does not differ from that in the carotid sector (Fisher and Ojeman 1986; Amarenco et al. 1998). The most frequent sites are the origins of the vertebral artery and intracranial vertebral artery shortly after it perforates the dura (Castaigne et al.

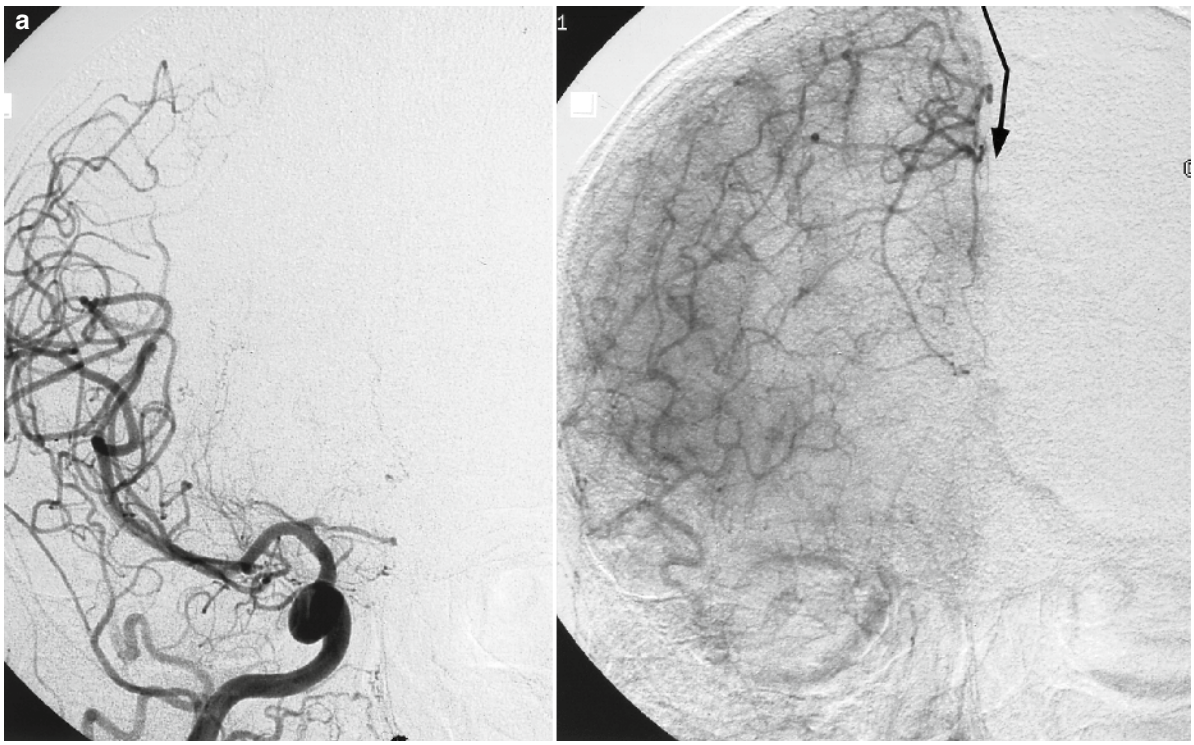

Fig. 15.16 Old female patient with stroke due to bilateral occlusion of the ACA. (**a**) Right carotid angiogram showing the occlusion at the passage of the A1-A2 segments. In the late phase, the beginning collateral circulation (*arrow*) through opening of anastomoses with distal branches of the MCA. (**b**) Left carotid angiogram showing a similar finding

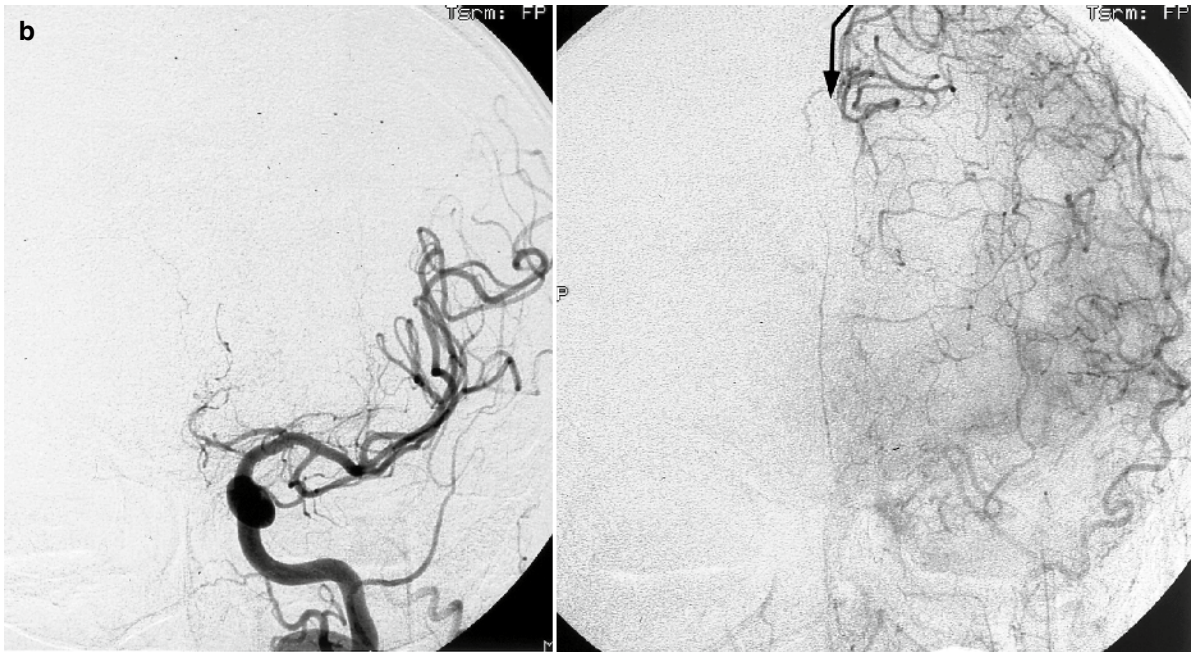

Fig. 15.16 (continued)

1973; Caplan 1996). The plaques are less commonly ulcerated than in the carotid sector, but ulceration is not rare in the subclavian arteries near the origin of the vertebral artery (VA) (Amarenco et al. 1992). The third-most frequent location of atheromatous plaque is the basilar artery, particularly in its middle segment (Castaigne et al. 1973; Pessin et al. 1987; Caplan 1996). Atheromas can be found at the P1-P2 segment (Bradac and Oberson 1983; Fisher 1986; Pessin et al. 1987).

15.5.1 Subclavian and Innominate Arteries

Atheromas of the subclavian and innominate arteries are frequent and commonly asymptomatic. The atheroma can grow, which leads to severe stenosis or occlusion of the artery. When this occurs proximal to the origin of the VA, blood flows from the normal VA intracranially and then down into the contralateral VA, further filling the distal subclavian artery. This situation, which was first described by Reivich et al. (1961) is termed the subclavian steal syndrome. This can present with TIAs involving the brainstem or pain in the ischemic arm, but frequently it remains completely asymptomatic. Symptoms occur commonly in patients with diffuse atherosclerotic lesions that also involve the carotid sector (Hennerici et al. 1988). Since it has a benign course, this syndrome only rarely needs aggressive treatment (Fig. 15.17).

15.5.2 Vertebral Artery

Severe stenosis or occlusion of one VA at its origin remains frequently asymptomatic provided that no embolization occurs and the other VA as well as the Circle of Willis sufficiently supply the vertebrobasilar sector. In contrast to thrombus of the ICA, which can extend intracranially up to the ophthalmic artery, thrombus of the extracranial VA does not extend intracranially, probably because the rich collateral circulation that arises from the other VA, the deeply ascending cervical artery, and the ECA maintains sufficient flow (Fig. 15.18).

Occlusion of the intracranial VA following artery-to-artery or cardiac embolism or progression of an intracranial atheromatous plaque is a much more serious condition since it involves the perforators of the VA that supply the anterolateral medulla. Depending on the

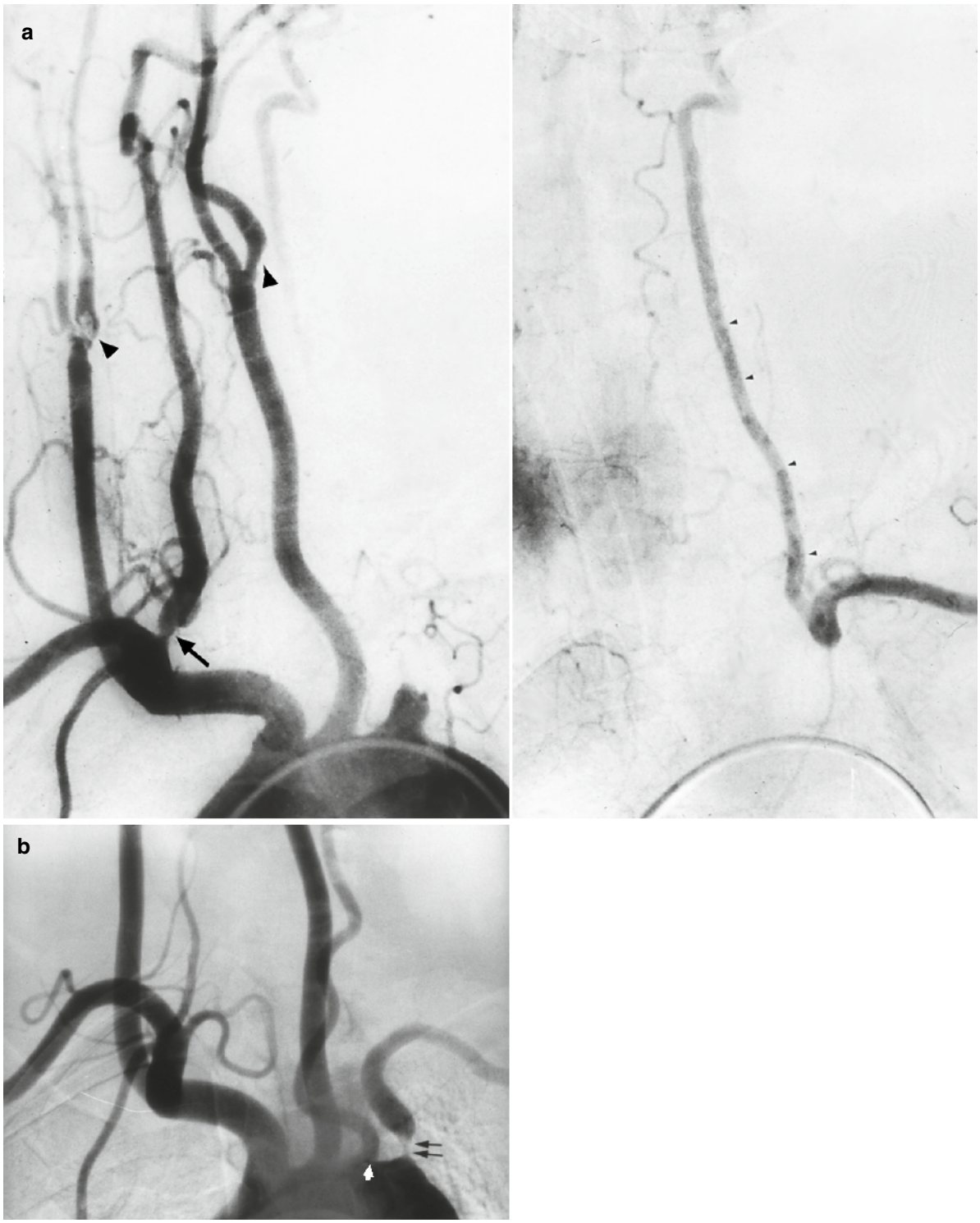

Fig. 15.17 (**a**) Subclavian steal syndrome, aortic arch angiogram. Occlusion of the proximal left subclavian artery. There is a large right vertebral artery, stenotic at its origin (*arrow*). The blood flows from the right vertebral artery intracranially and then down into the left vertebral artery (*small arrowheads*) and further into the distal subclavian artery. There are also atheromatous changes involving both carotid bifurcations (*arrowheads*). (**b**) Severe stenosis of the proximal left subclavian artery (*arrows*). The left vertebral artery (*white arrow*) is not, however, involved since it originates directly from the aortic arch

distal extension of the superimposed thrombus, the posterior inferior cerebellar artery (PICA), supplying prevalently the dorsal medulla and cerebellum, and the anterior spinal artery, supplying the anterior medulla, can be involved (Figs. 15.19 and 15.20). In the most unfavorable cases, the thrombus can extend to the basilar artery and its branches (Fig. 15.25). Frequently, however, probably owing to rapid spontaneous lysis of the embolus or thrombus in the VA, there is a limited ischemic lesion in the PICA territory of variable extent, which has a benign clinical course; the exception is rare cases in which swelling of the cerebellar hemisphere occurs. In other favorable cases, probably only selective embolic occlusion of the PICA takes place.

15.5.3 Basilar Artery

Involvement of the basilar artery (BA) is another serious condition. It can occur as an extension of the thrombus in the case of occlusion of the intracranial VA (Castaigne et al. 1973). Another very frequent cause is embolism that is cardiac in origin or results from extra- or intracranial plaque of the VA. Emboli flow into the distal part of the BA (Caplan 1980) provided that no stenotic plaque is located along the artery and arrests their course, which would lead to the formation of a superimposed thrombus.

Zeumer et al. (1982) performed the first pharmacological selective thrombolysis in the early 1980s in a patient with acute occlusion of the BA. Since then, selective endovascular treatment with pharmacological and/or mechanical thrombolysis has progressively improved, and it is today the therapy of choice; in many cases, it has improved the patient's prognosis (Eckert et al. 2002; Arnold et al. 2004; Mangiafico et al. 2005; Bergui et al. 2006; Nogueira et al. 2008; Eckert 2009; Choi et al. 2009) (Figs. 15.21–15.26).

Microatheromas of the BA can involve perforators at their origin and lead to pontine lacunar infarct (Fisher and Caplan 1971; Caplan 1989). The occlusion usually involves the paramedian branches; less commonly it involves those that are more lateral. Microatheromas can be very thin and thus escape neuroradiological diagnosis. In other cases, they are large enough to lead to stenosis of various degrees of the BA, which is recognizable on MRI angiography and CT angiography; in selected cases, microatheromas can be subjected to endovascular treatment (Fig. 15.27) (Phatouros et al. 2000; Berkefeld et al. 2003; Gupta et al. 2003; Bose et al. 2007; Bradac et al. 2008b; Qureshi et al. 2008; Berkefeld – Zanella 2009).

The same risks we have described in the treatment of M1 atheroma are present in treating similar lesions of the VA and BA. In particular, there is a risk of occlusion of the perforating branches. Careful selection is recommended (Chaturvedi and Caplan 2003; Kurre et al. 2010).

As in other parts of the brain, lacunar infarcts can also occur owing to involvement of the perforators by lipohyalinosis. They often occur in hypertensive and diabetic patients (Fisher and Caplan 1971; Caplan 1996; Bradac et al. 2008b). The prognosis of these lacunar lesions are *quoad vitam* better than those due to occlusion of the branches by microatheromas.

15.5.4 Cerebellar Arteries

The cerebellar arteries—PICA, anterior inferior cerebellar artery (AICA), and superior cerebellar artery (SCA)—are involved in different degrees in acute occlusion of the intracranial VA and/or BA. Selective occlusion can occur because of atheroma at the origin of the arteries. Artery-to-artery or cardiac embolism is another cause of ischemia (Amarenco et al. 1990; Amarenco and Caplan 1993). Finally, involvement of these arteries can occur in the surgical and endovascular treatment of vertebrobasilar aneurysm. In this context, peripheral occlusion of the cerebellar arteries in the treatment of distal aneurysm is commonly well tolerated clinically, even if CT and MRI post-treatment reveal small ischemic lesions in the cerebellum. Indeed, peripheral occlusion spares the perforators for the brainstem that arise from the first segment of the arteries. Furthermore, the peripheral portion of the artery can be largely protected through the leptomeningeal collateral circulation among the cortical distal branches of the PICA, AICA, and SCA.

15.5.5 Border-Zone Infarcts

Small infarcts can occur in the cortical border zone between the vascular territories of the cerebellar

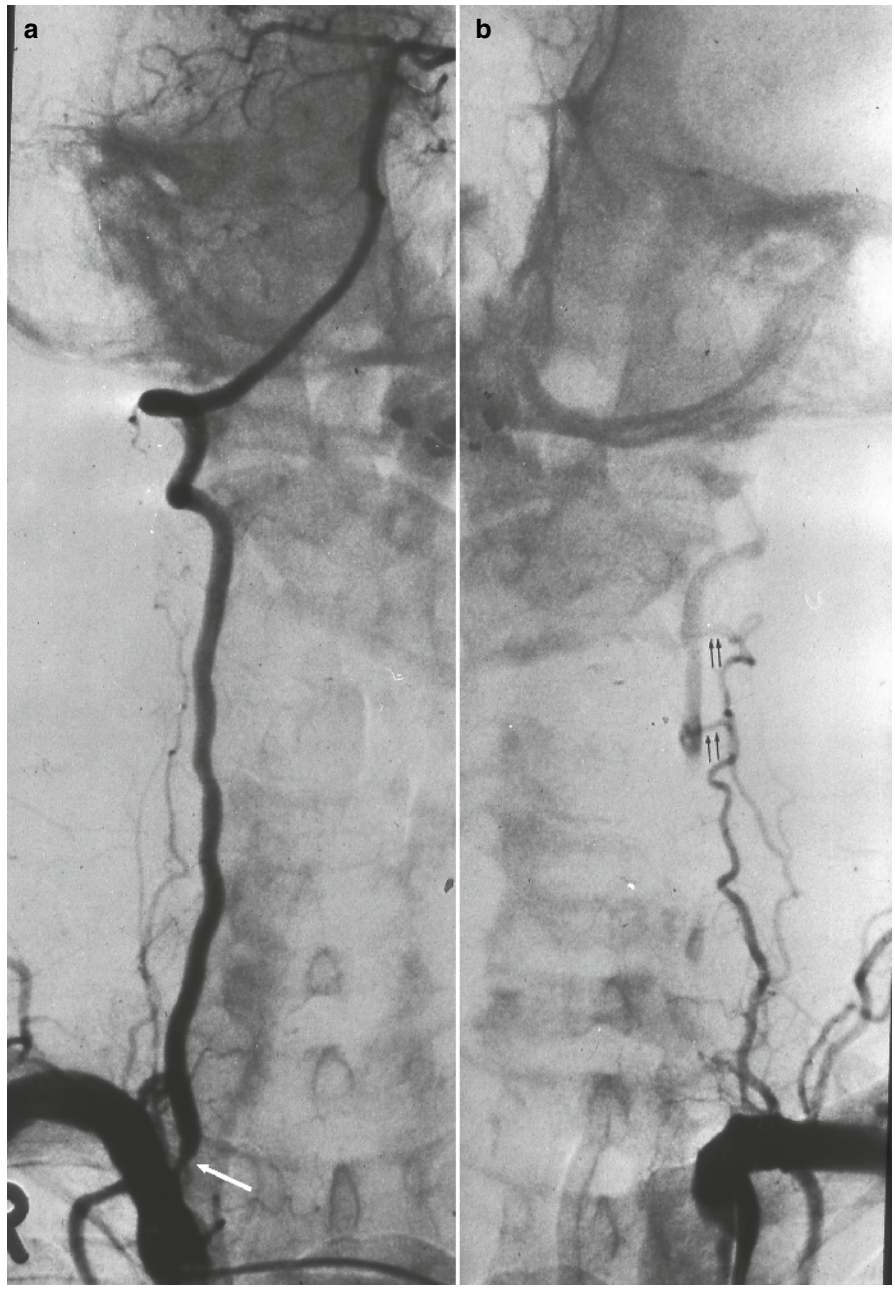

Fig. 15.18 Middle-aged patient with acute symptoms characterized by vertigo, ataxia, and nystagmus. The right vertebral angiogram (**a**) showed a moderate stenosis of the vertebral artery at its origin (*arrow*) with normal filling and flow of the intracranial vertebrobasilar sector. The posterior inferior cerebellar artery (PICA) was not recognizable, but a well-developed anterior inferior cerebellar artery (AICA) was present. The left vertebral artery (**b**) was occluded. There was a partial collateral circulation through anastomosis with the ascending cervical artery. The patient recovered, and the stenosis on the right was later treated with angioplasty and stent

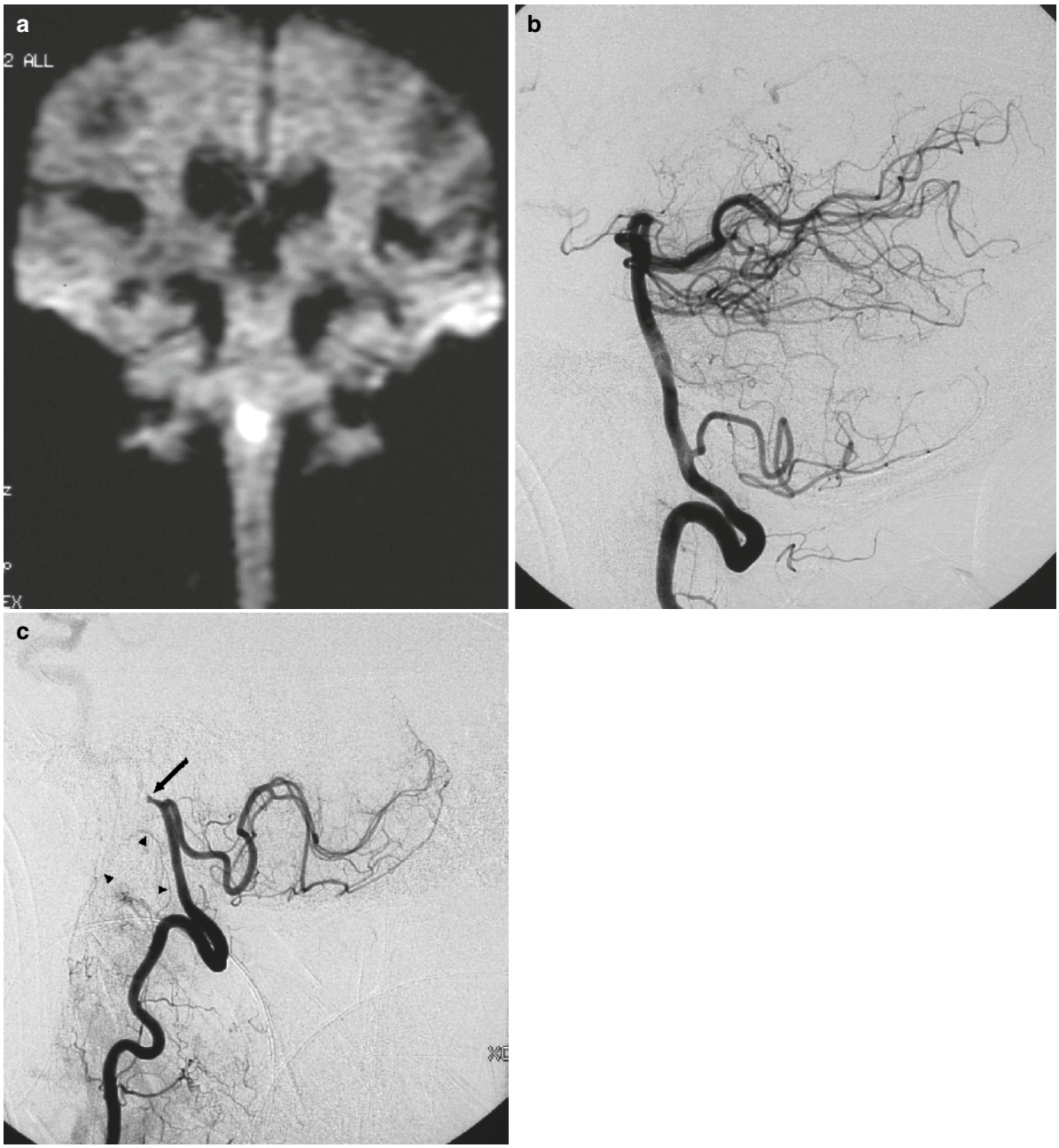

Fig. 15.19 Acute ischemia involving the anterior medulla corresponding to the vascular territory of the anterior spinal artery (ASA), demonstrated on MRI, diffusion-weighted image (**a**). Angiography showed a normal left angiogram (**b**). The right vertebral artery is occluded (**c**) distally to the PICA (*arrow*). Presence of the odontoid arch (*arrowhead*). It is conceivable that the occlusion (embolus or microatheroma) involved the ASA, which in this case probably has a unilateral origin

arteries or in the deep cerebellar white matter (Savoiardo et al. 1987; Amarenco et al. 1994). These are due to involvement of the perforator branches, which, like the medullary artery of the cerebral hemisphere, enter the cerebellar white mater and are end arteries. The cause of these lesions varies: hypoperfusion because of severe stenosis or occlusion of the large arteries (VA, BA), cardiac or artery-to-artery embolism, and intrinsic atherosclerotic disease have been suggested (Amarenco et al. 1994; Amarenco et al. 1998).

15.5.6 Posterior Cerebral Artery

Occlusion of the PCA, uni- or bilaterally, can be due to extension to the P1 segment of the thrombus following thromboembolic occlusion of the BA. The most frequent cause of isolated occlusion of the PCA is embolism from plaques of the extra- or intracranial VA or, less frequently, it can be cardiac in origin (Castaigne et al. 1973, 1981; Milandre et al. 1994; Caplan 1996; Yamamoto et al. 1999; Brandt et al. 2000; Kumral et al. 2004). Embolism to the PCA can arise from the ICA in cases of fetal origin of the PCA (see Chap. 18). Another rarer cause is a primary microatheroma that is commonly located at P1-P2 (Bradac and Oberson 1983; Fisher 1986; Pessin et al. 1987; Caplan 1996), which can be complicated by a superimposed thromboembolism (Fig. 15.28).

The ischemic lesion can differ according to the site and extent of the stenosis/occlusion; it can involve the deep or cortical territories or both [Bogousslavsky et al. 1988a (Neurology), Caplan et al. 1988b; Caplan 1996; Brandt et al. 2000]. Involvement of the posterior thalamoperforating branches (P1) leads to ischemia of the medial midbrain and medial thalamus. The ischemia may be bilateral when both P1 are involved or when the perforators arise unilaterally just from the affected P1 (Figs. 15.21, 15.29, and 11.17).

Occlusion of the thalamogeniculate artery (P2) is responsible for ischemia in the lateral thalamus (Fig. 15.30). Perforators for the lateral midbrain (P2) and branches for the posterior thalamus (posterior choroidal arteries, P1-P2) can also be involved (Fig. 15.23). These areas, however, may be more protected since they have a complementary supply from the AChA and SCA.

The distal territories have greater protection owing to the presence of leptomeningeal anastomoses among the PCA, MCA, and ACA. Ischemia can, however, occur probably because of further embolism occluding the distal branches. Among the distal vascular territories, the primary visual cortex is frequently involved, with an incidence of up to around 90% of cases (Kumral et al. 2004). Another cause of ischemia is lipohyalinosis, which is responsible for small lacunary infarcts in the midbrain and thalamus as a result of involvement of the perforators.

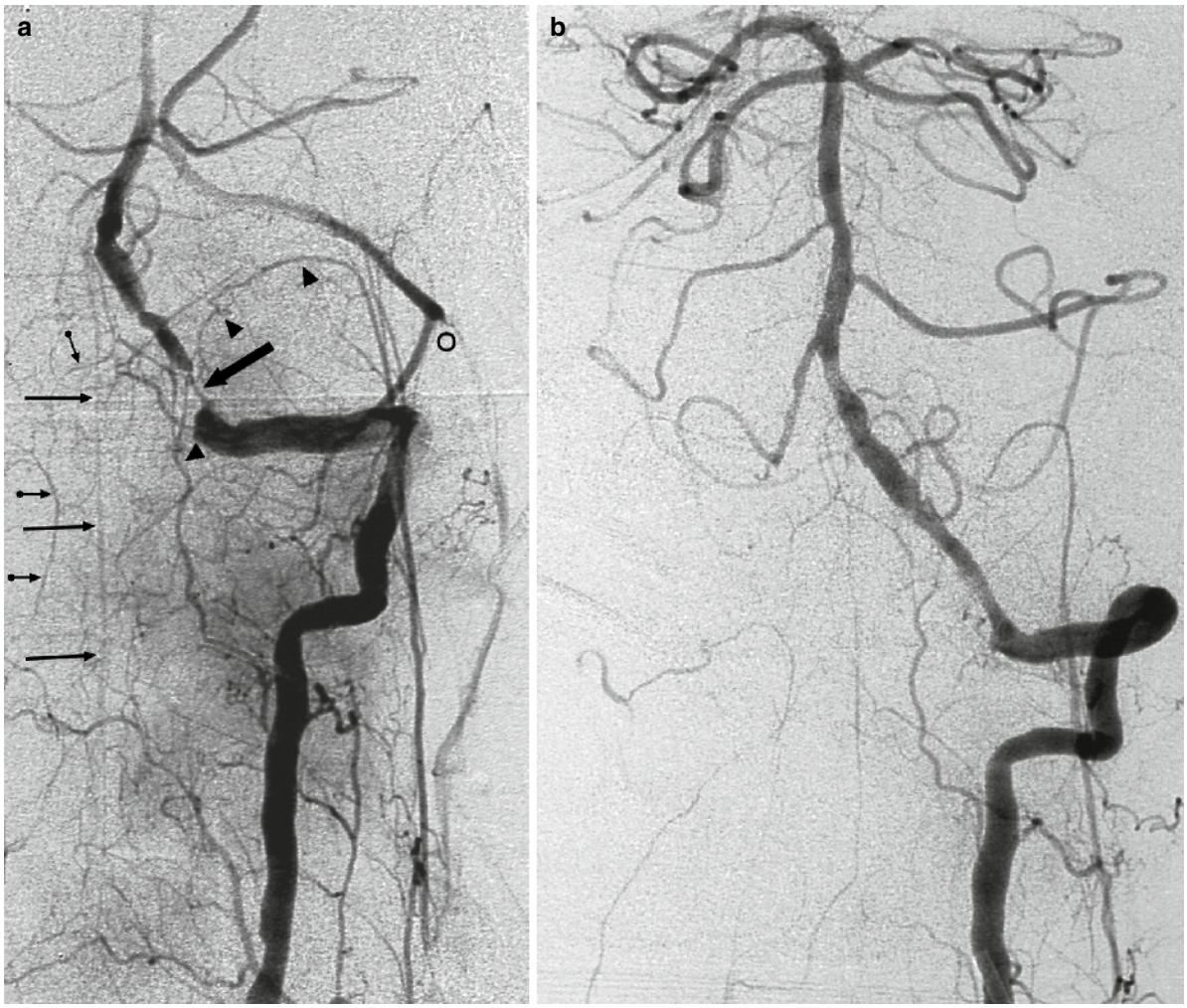

Fig. 15.20 TIAs in the vertebrobasilar sector in a patient in whom MRI disclosed an ischemic lesion in the inferior pons. (**a**) Left vertebral angiogram showed diffuse atherosclerosis and severe stenosis (*arrow*) of the vertebral artery (VA) at its entrance in the cranial cavity. The PICA is not recognizable, though the ASA is well injected (*small arrows*). There is slowing down of the distal flow. The right VA was hypoplastic. Probably due to impairment of the flow in the vertebral artery, there is injection of the occipital artery (*O*) through the opening of the C1 anastomosis. There is also injection of the odontoid arch (*arrowhead*) through a connection of the hypoglossal branch of the ascending pharyngeal artery (APhA) with the ascending meningeal branch of the VA. Furthermore, at the level of the odontoid process, the radiculomeningeal branch of the VA is connected with the contralateral branch (*arrow with dot*). Endovascular treatment (**b**) of the stenosis (angioplasty plus stent) was performed with morphologically, hemodynamically, and clinically good results. Note the injection of the left PICA. Following normalization of the flow in the vertebral artery, the occipital artery is no longer injected. The connection with the APhA is less evident

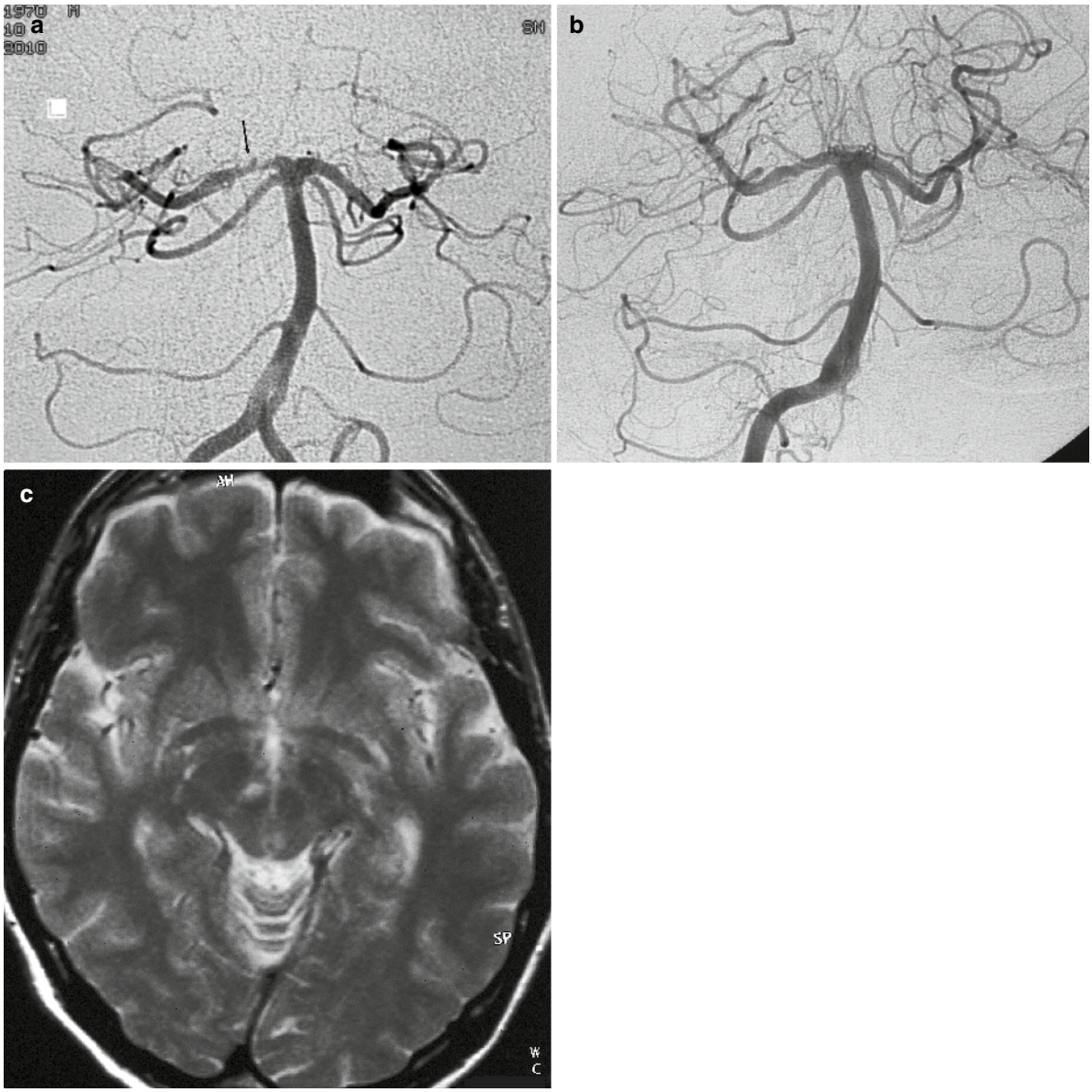

Fig. 15.21 Acute "top of the basilar" syndrome. On the angiogram normal filling of the basilar artery. There is, however, irregularity of the right P1 segment (*arrow*) and there is no injection of the posterior thalamo perforating arteries (**a**). After selective pharmacological thrombolysis normalisation of the P1 segment and reappearance of the perforators (**b**). The comatose patient recovered completely. On the routine MR (**c**) 3 days later performed in an asymptomatic patient, small ischemic lesions in the medial right midbrain was recognizable

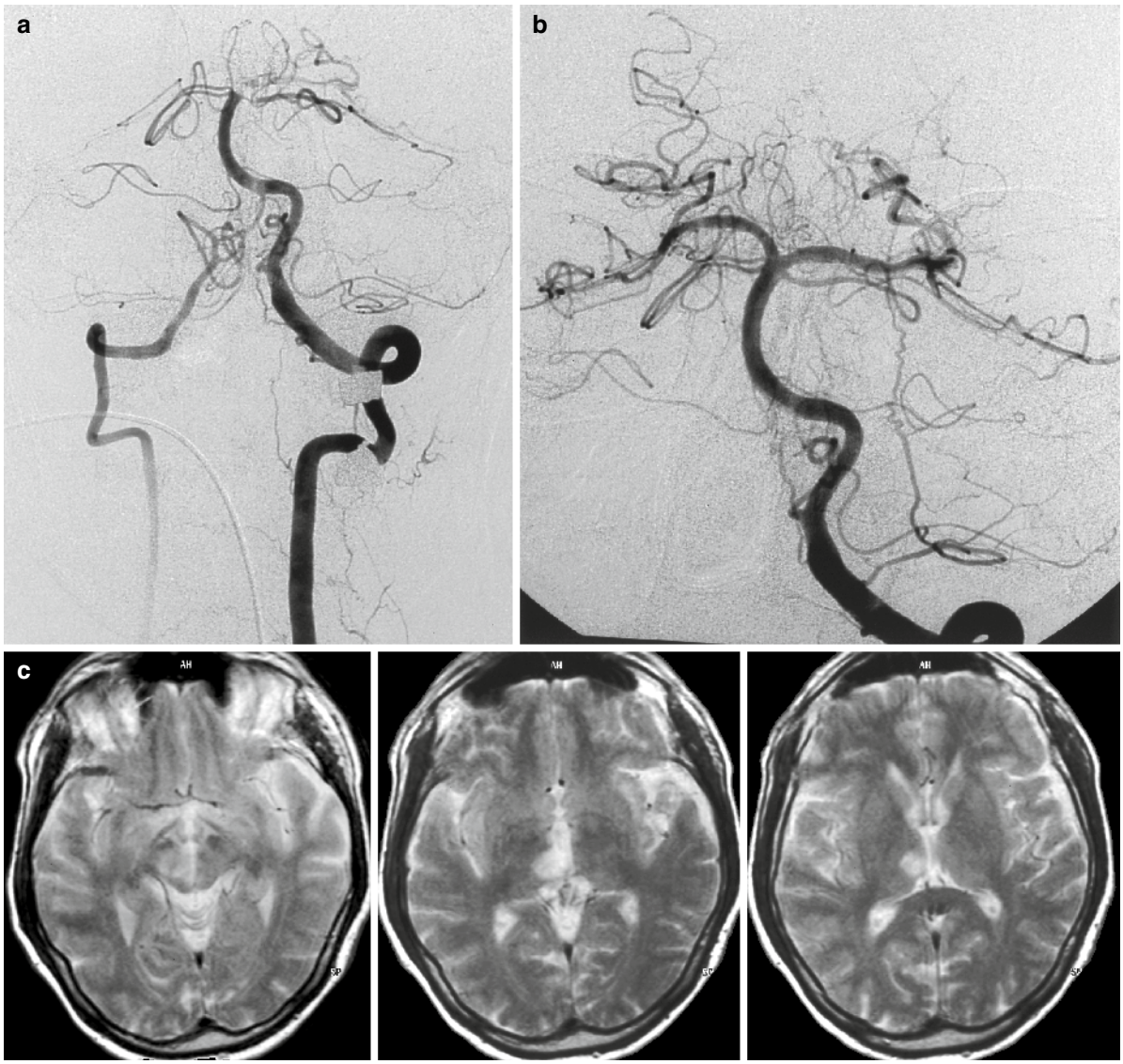

Fig. 15.22 Acute "top of the basilar" syndrome. Angiogram (**a**) of the left well-developed vertebral artery with retrograde injection of the hypoplastic right vertebral artery. Occlusion of the distal basilar artery. There is no injection of either PCA, normal right SCA, and partial embolic occlusion of the left SCA. After selective pharmacological thrombolysis (**b**), reopening of the distal basilar artery and its branches. Note the injection of the perforators coming from both P1. The comatose patient recovered slowly with a good final outcome. On the MRI (**c**), a few days later, ischemic lesions involving the medial midbrain and medial thalamus on the right were recognizable

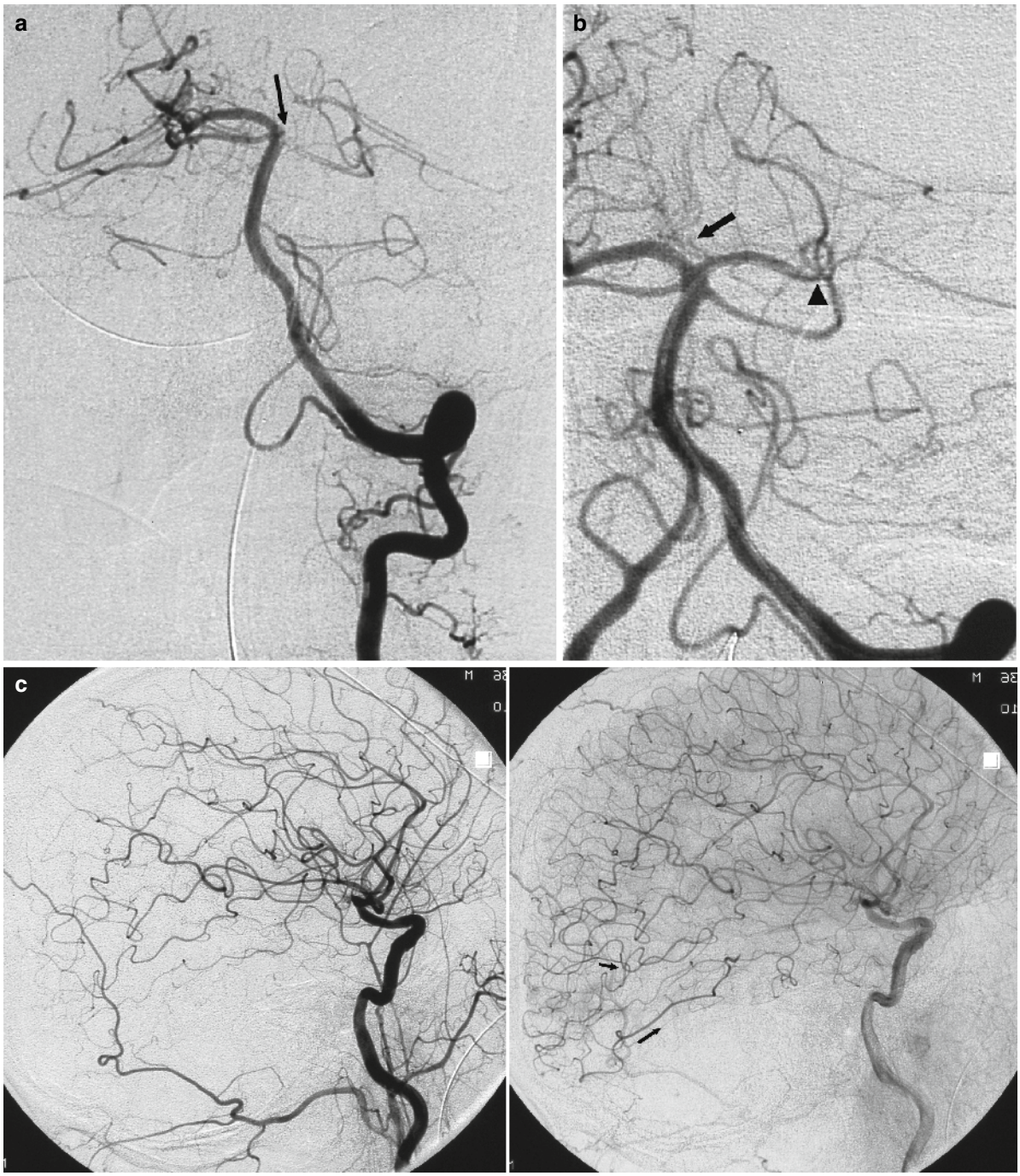

Fig. 15.23 Cardioembolic occlusion of the top of the basilar artery in an old patient presenting with symptoms indicating vertebrobasilar insufficiency followed by coma. (**a**) Left vertebral angiogram showing the occlusion (*arrow*) of the top of the basilar artery involving also the superior left cerebellar and left posterior cerebral artery. (**b**) Vertebral angiogram followed selective endovascular pharmacological fibrinolysis, showing the reopening of the basilar artery and, in particular, of the posterior thalamoperforating arteries (*arrow*). It seems that the latter arise predominantly from the left P1. There is also revascularization of the superior cerebellar artery and posterior cerebral artery which, however, remained occluded in its P2 segment (*arrowhead*). (**c**) Left carotid angiogram. In the later phases, a partial filling of the left posterior cerebral artery through opening of a leptomeningeal anastomosis with the middle cerebral artery (*arrows*) is visible. (**d**) MRI performed 24 hours later showed minimal ischemic lesion involving the medial thalamus bilaterally owing to the temporary occlusion of the posterior thalamoperforating arteries. There is also minimal ischemia in the left posterior thalamus. In spite of this lesion, the patient recovered completely and was asymptomatic within a few weeks

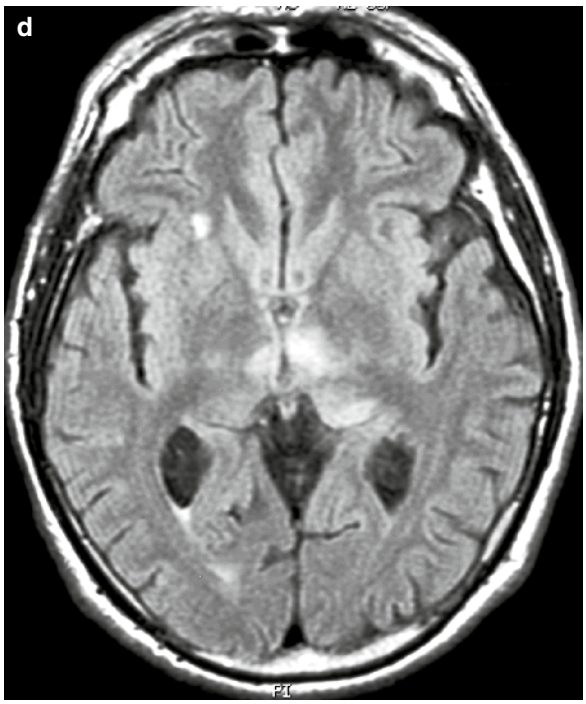

Fig. 15.23 (continued)

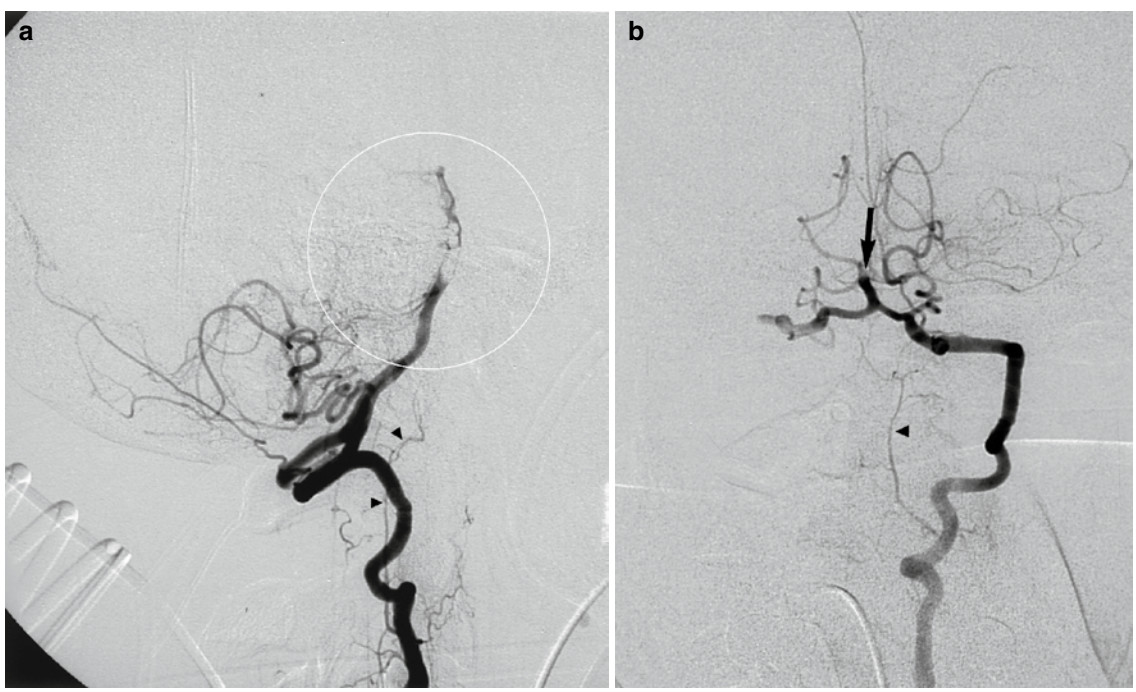

Fig. 15.24 Acute brainstem syndrome. On the vertebral angiogram (**a**, **b**), occlusion of the basilar artery in its middle segment distal to the origin of the AICA is evident. Radiculomeningeal artery (*arrowhead*). The carotid angiogram (**c**) showed a patent distal segment of the basilar artery (*arrow*) with indirect demonstration of the thrombus. There was injection of both the PCA and SCA. Detail obtained (**d**) during selective study with a microcatheter showed the thromboembolic material in the basilar artery. Selective thrombolysis (**e**) allowed complete recanalization of the basilar artery. Good clinical outcome. Small ischemic pontine lesions were demonstrated on CT some days after the treatment

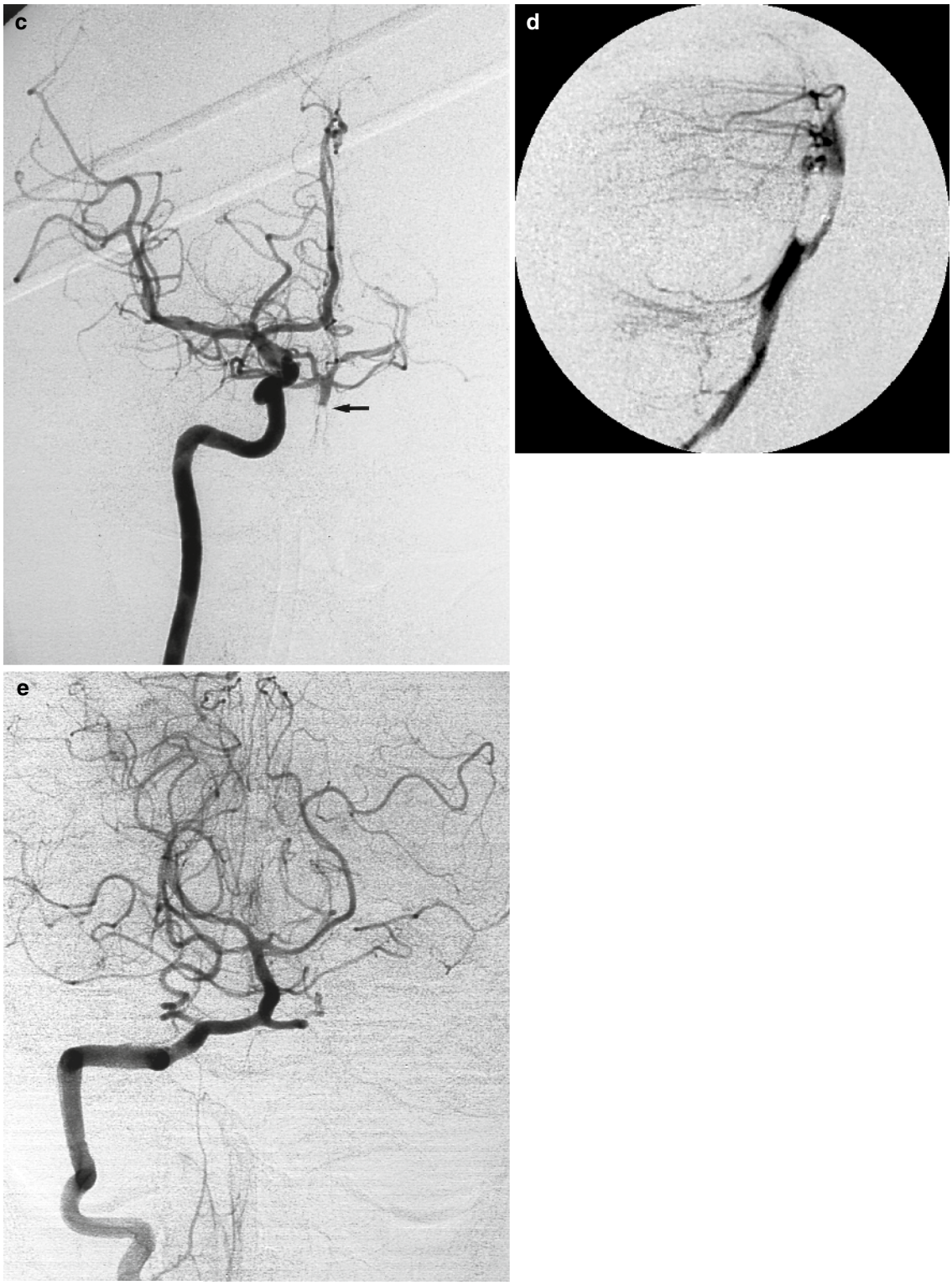

Fig. 15.24 (continued)

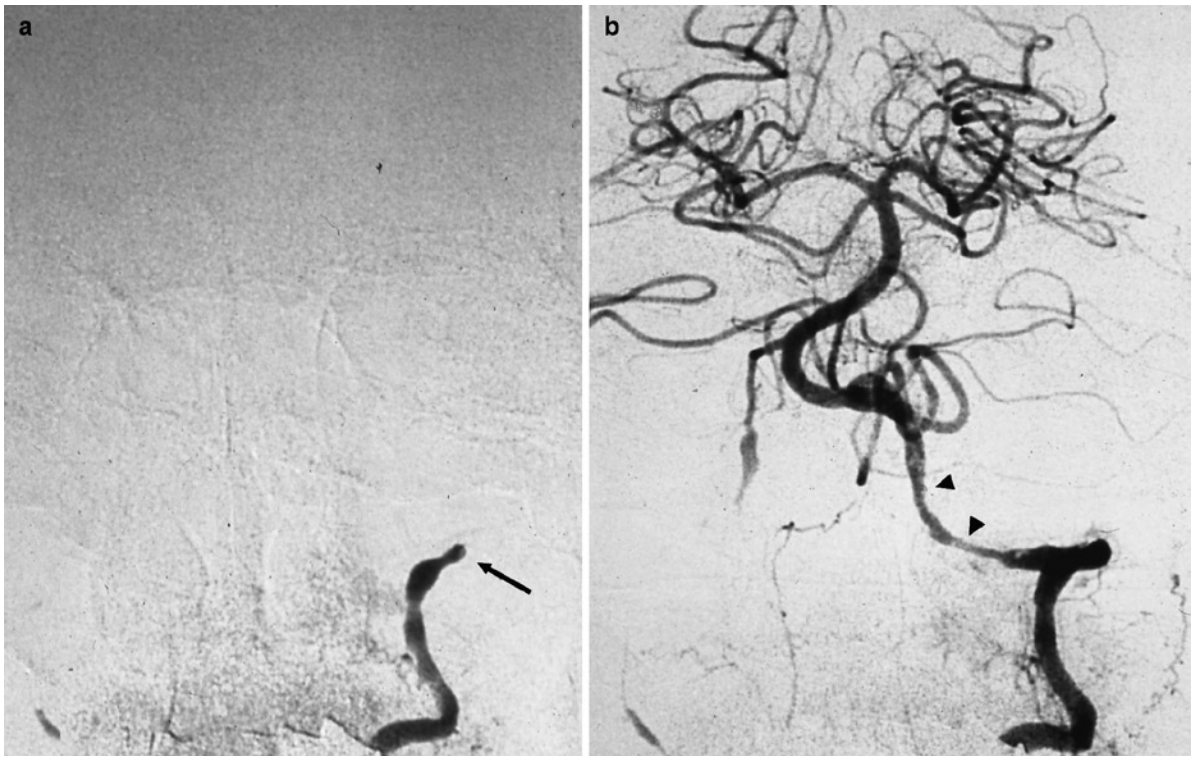

Fig. 15.25 Acute thromboembolic occlusion of the left vertebral artery at the extracrainial–intracranial passage in a patient with an old occlusion of the right vertebral artery. Left vertebral angiogram (**a**) showing the occlusion (*arrow*) with extension to the basilar artery. Angiogram (**b**) after selective thrombolysis with reopening of the vertebral and basilar arteries. The atheromatous changes in the vertebral artery (*arrowheads*), on which the thrombus probably developed, are now recognizable. Partial retrograde injection of the occluded right vertebral artery

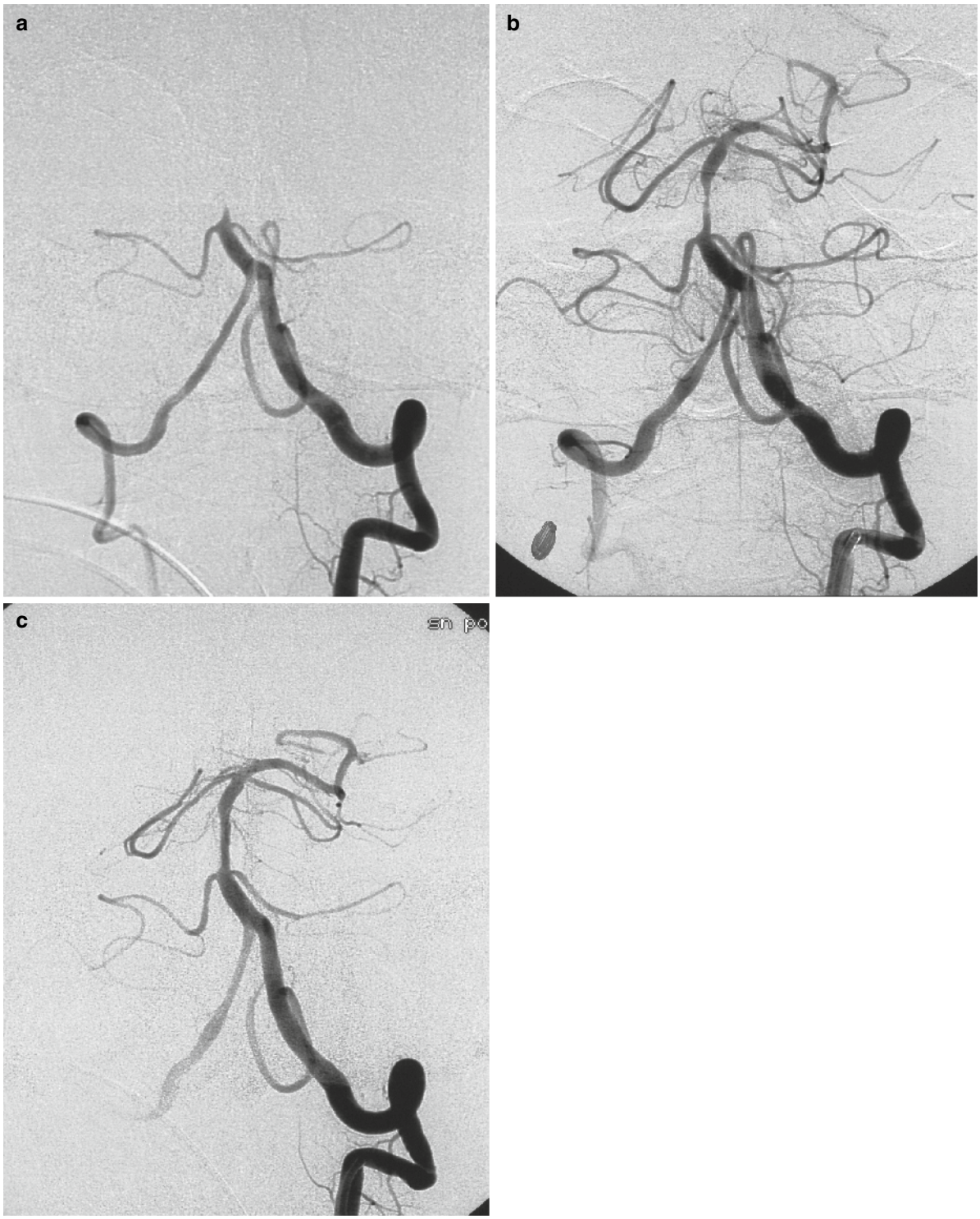

Fig. 15.26 Old patient with acute occlusion of the middle basilar artery owing to thrombosis superimposed on a long microatheroma. (**a**) Left vertebral angiogram. Occlusion of the basilar artery distal to the origin of the AICA. Retrograde injection of the hypoplastic right vertebral artery. (**b**) Reopening of the basilar artery after selective injection of recombinant tissue plasminogen activator (rtPA). A severe long stenosis is now visible. (**c**) Angiogram after angioplasty showing improvement of the stenosis

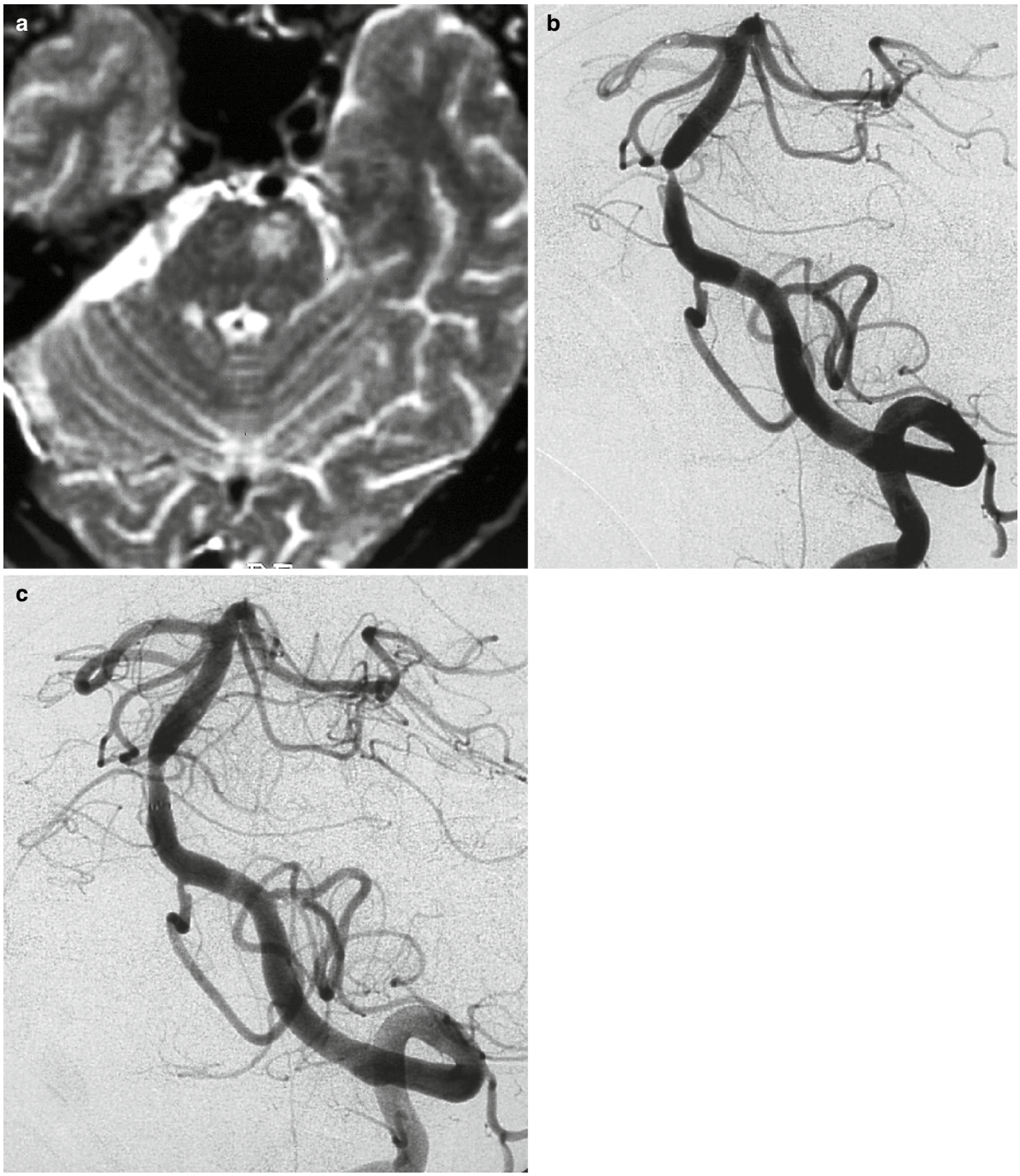

Fig. 15.27 Patient with repeated mild stroke episodes involving the brainstem, not responsible for medical therapy. MRI (**a**) disclosed a small paramedian pontine lacunar infarct. Vertebral angiogram (**b**) showed severe stenosis of the basilar artery, which was treated with angioplasty and stent (**c**)

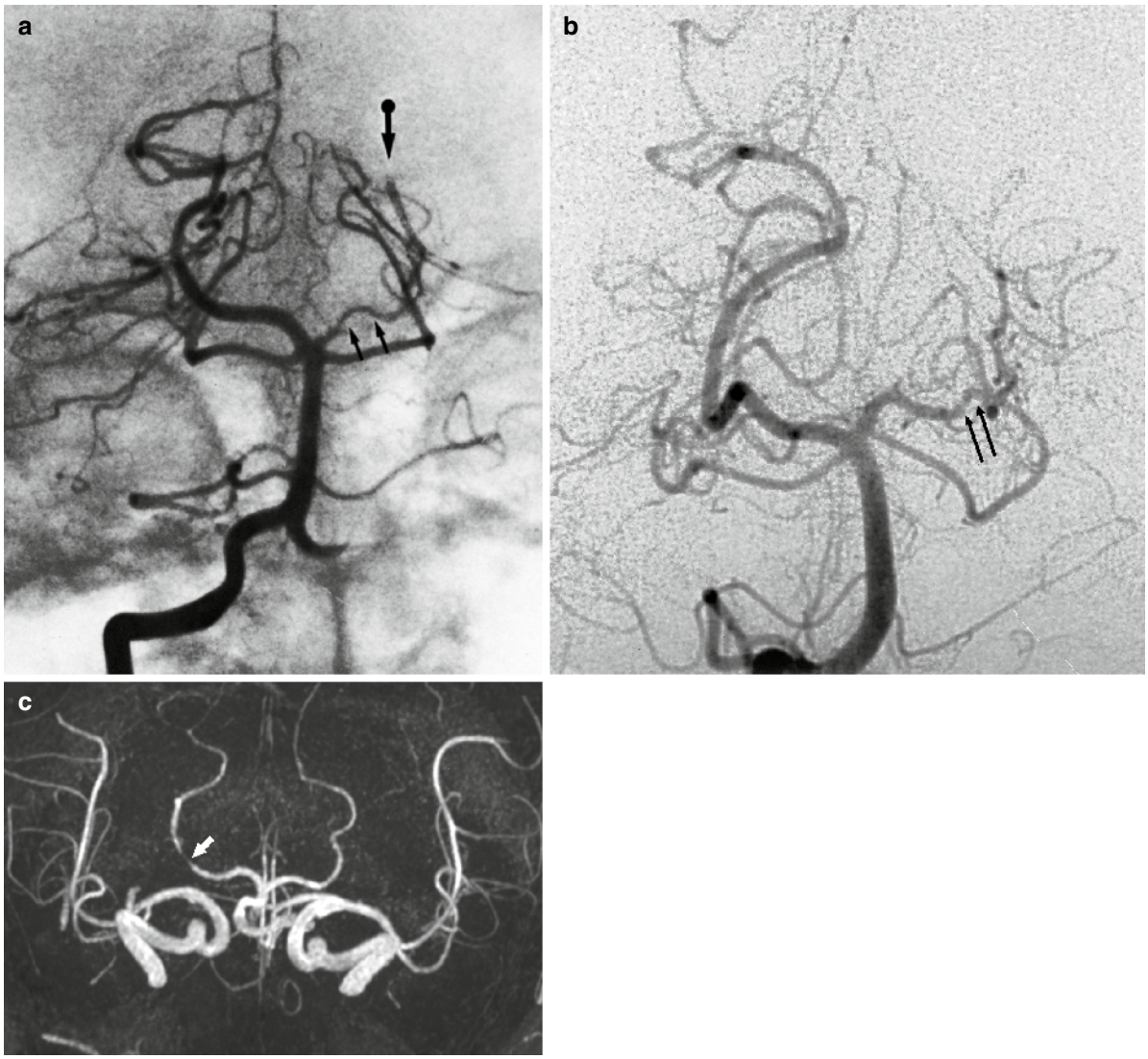

Fig. 15.28 Atheromatous changes involving the P1-P2 segment of the PCA demonstrated on the angiogram (**a**, **b**) and on MRI angiography (**c**). On the angiograms, the distal segment of PCA is probably occluded by emboli

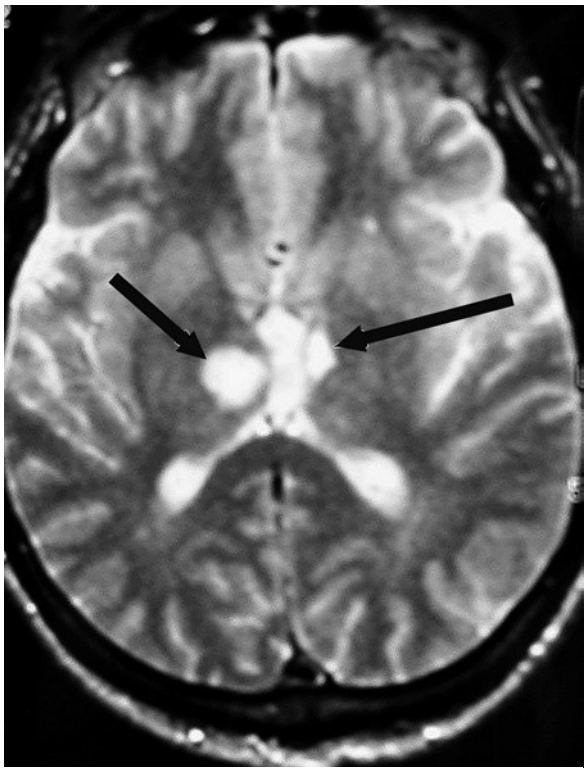

Fig. 15.29 Cardioembolic occlusion of the right PCA. On MRI, a bilateral medial thalamic infarct was present. This is the vascular territory of the posterior thalamoperforating branches arising from the P1. It is possible that in this case the perforating branches both arise from the occluded P1. On the right, the ischemic lesion also involves the vascular territories of the thalamogeniculate artery

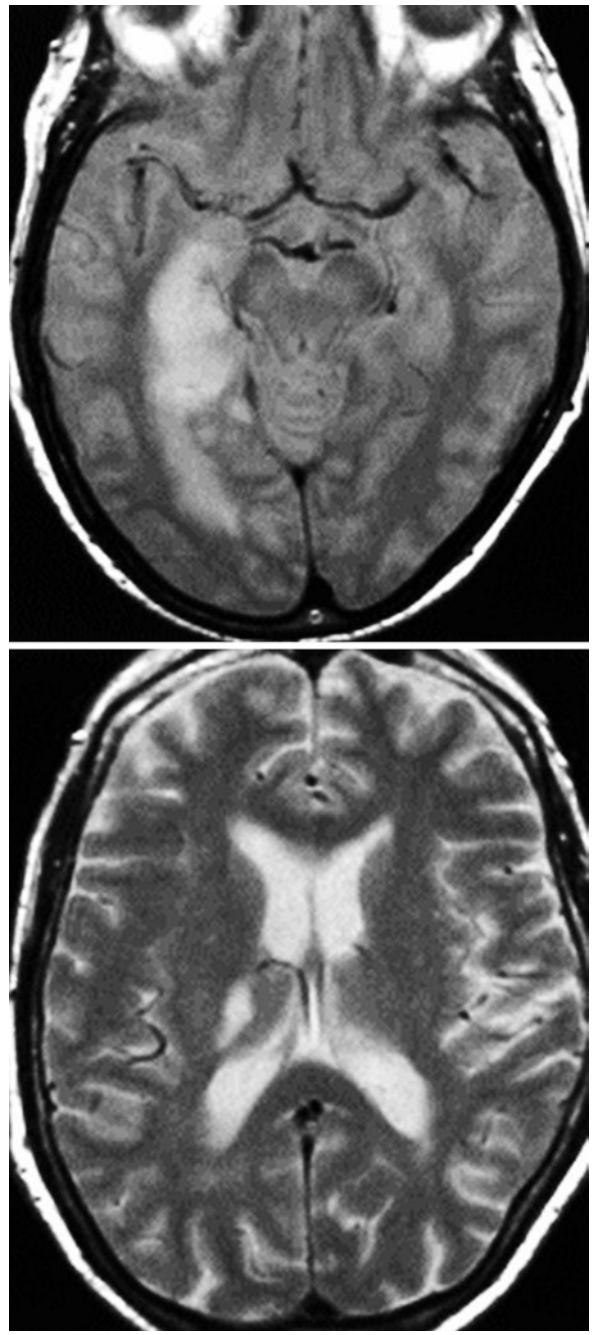

Fig. 15.30 Old patient with embolic occlusion, cardiac in origin, of the PCA in its P2 segment with ischemia in the temporomedial and partial occipital territories and in the lateral thalamus (thalamogeniculate artery). The medial midbrain and medial thalamus corresponding to the vascular territories of the perforators arising from P1 are spared

Spontaneous Dissection of Carotid and Vertebral Arteries

16

16.1 Introduction

The first case of spontaneous dissection of the internal carotid artery (ICA) was reported in 1954 by Jentzer. Since then, other cases have been described (Bostrom and Liliequist 1967; Ehrenfeld and Wylie 1976; Fisher et al. 1978; Mokri et al. 1979; Anderson et al. 1980; Friedman et al. 1980; Bradac et al. 1981), and these have helped widen our understanding of the clinical and angiographic aspects of this disease. Spontaneous dissection is today a well-recognized pathology that is responsible for stroke in many cases. Its incidence is reported to be three to four cases per 100,000 persons yearly (Schievink 2001; Menon and Norris 2008; Redekop 2008). Young and middle-aged patients are predominantly affected.

16.2 Pathology and Pathogenesis

From a pathological point of view, the lesion is characterized by a subintimal hemorrhage, leading to stenosis or occlusion of the artery. The hemorrhage can involve the outer media or the subadventitial layer, resulting in the formation of pseudoaneurysms. Dissection occurs because of a primary intimal tear, allowing the blood to pass into the arterial wall. Primary intramural hemorrhage can also occur through rupture of the vasa vasorum.

The pathogenesis of dissection can be traumatic, but in the spontaneous form, the pathogenesis is not completely clear. Structural changes of the arterial wall, associated with mechanical factors, are probably involved. Indeed, it is well known that dissection occurs frequently in patients with fibromuscular dysplasia (FMD), Ehlers-Danlos syndrome, Marfan syndrome, and lupus erythematosus (Anderson et al. 1980).

Association with cystic medial necrosis has also been demonstrated in some cases (Schievink et al. 1994a). Such cases are more frequent in patients with migraine and in women using oral contraceptives (Mokri et al. 1986; D'Anglejan-Chatillon et al. 1989). A family history has also been reported (Schievink and Mokri 1995). Trauma, even minor, and neck manipulation (Hufnagel et al. 1999; Nadgir et al. 2003) are present in the clinical history of some patients. In this context, the association of trauma, even minor, and raised blood alcohol as a cause of dissection, particularly in the vertebrobasilar sector, have been emphasized (Hiraiwa et al. 2005). Some authors (Konrad et al. 2003; Vila et al. 2003) have reported in cases of dissection a deficiency of alpha 1-antitrypsin. This is a proteinase that has a protective action on collagen and elastin—important components of the connective tissue of the arterial wall. The same deficiency has been identified in cases of FMD, which shows a high tendency for dissection (Schievink et al. 1998).

16.3 Location

Extracranial ICA: 2–3 cm distal to the bifurcation is the most frequent site of dissection. This commonly ends abruptly, with rare exceptions, where the artery enters the base of the skull. The second-most frequent location is the extracranial vertebral artery. Any part of the vertebral artery (VA) can be involved, but the lesions are most frequent in the distal segment of the artery, at C1-C2, and the atlas loop level because this segment is more subject to mechanical trauma (Chiras et al. 1985; Mokri et al. 1988; Shin et al. 2000; Schievink 2001). More than one vessel is involved in about 25% of cases (Schievink 2001).

G.B. Bradac, *Cerebral Angiography*,
DOI: 10.1007/978-3-642-15678-6_16, © Springer-Verlag Berlin Heidelberg 2011

Intracranial dissection is less frequent. Advanced age can be a factor, but there is a predominance of young patients. The vertebrobasilar sector is more frequently affected. Dissection usually involves the first intracranial segment of the VA, sometimes as an extension of extracranial dissection. Dissection of the basilar artery is less common: it can be primary or a secondary extension of dissection of the VA (Alexander et al. 1979; Shimoji et al. 1984; Berger and Wilson 1984; Friedman and Drake 1984; Caplan et al. 1988a; Pozzati et al. 1995; Shin et al. 2000; Lacour et al. 2000; Manabe et al. 2000; Kurata et al. 2001; Sugiu et al. 2005; Ramgren et al. 2005; Lee et al. 2006; Zhao et al. 2007). Both VAs can be involved. Dissection is frequently also the cause of aneurysms of cerebellar arteries, more commonly of the posterior inferior cerebellar artery (Ramgren et al. 2005; Bradac and Bergui 2004; Mitsos et al. 2008) as well as the posterior cerebral artery (Lazinski et al. 2000; Roh et al. 2008) (see also Chap. 11). Dissection in the anterior circulation is rarer; it can be an extension of dissection of the ICA toward the intracranial sector. Intracranially, primary dissection typically involves the terminal ICA and middle cerebral artery (MCA) (Ramsey and Mosquera 1948; Kunze and Schiefer 1971; Hochberg et al. 1975; Sasaki et al. 1991; Massoud et al. 1992; Bassetti et al. 1994; Nakatomi et al. 1997; Mizutani 1998; Ohkuma et al. 2003).

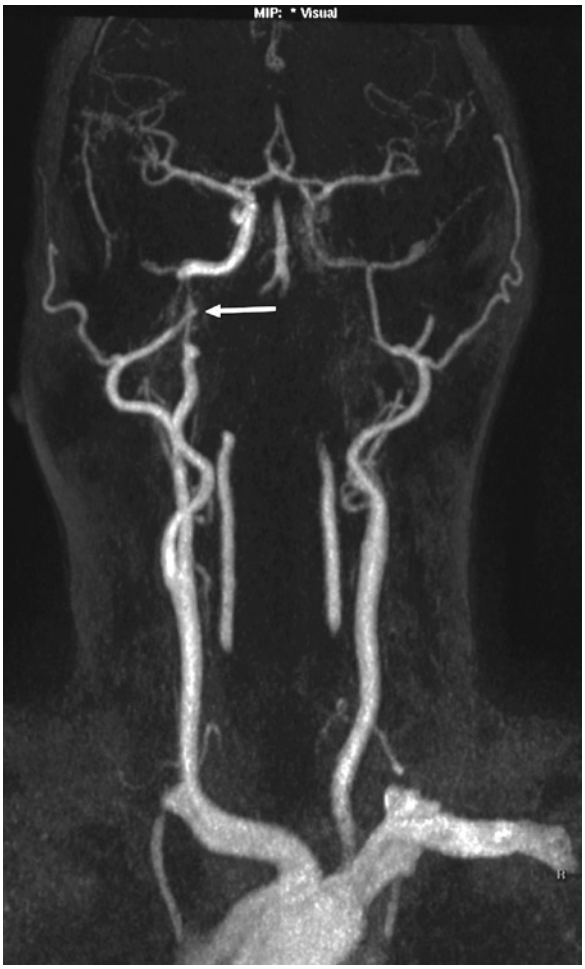

Fig. 16.1 MRI angiography showing irregular stenosis of the right internal carotid artery (ICA; *arrow*) due to spontaneous dissection. Entering the skull base, the lumen of the artery is again normal. There is occlusion of the left ICA. The vertebral arteries, not demonstrated in this slice, were normal

16.4 Morphological Diagnostic Appearance

In the extracranial sector, occlusion with a typical tapered appearance is frequent as well as an irregular stenosis, which extends for various lengths. Demonstration of a double lumen or an intimal flap can be pathognomonic, but it is rare. Pseudosaccular aneurysm can also occur (Figs. 16.1–16.6).

Intracranial dissection appears as occlusion and irregular stenosis (Figs. 16.6, 16.7b, and 16.11), pseudoaneurysm, or fusiform dilatation (Figs. 16.8 and 16.10). Not infrequently, the arterial changes are minimal. Repeated examination days or weeks later can show more conspicuous alterations (Fig. 16.9).

CT and MRI demonstrate ischemic lesions or, in cases of ruptured intracranial dissecting aneurysm, subarachnoid hemorrhage (SAH). Furthermore MRI can show hyperintensity of the involved artery or dilatation of the vessel on T1-weighted sequences. Eccentric signal void (corresponding to the residual lumen) surrounded by a semilunar hyperintensity (corresponding to the mural hematoma) can be evident. This, however, may be visible only a day or two after the acute episode, first on T1-, then on T2-weighted sequences (Zuber et al. 1994; Levy et al. 1994; Hosoya et al. 1999; Provenzale 2008; Vertinsky et al. 2008).

MRI angiography and, particularly, CT angiography can replace angiography in many cases. But the latter, owing to its precise morphological selective demonstration of the arteries, still remains the gold

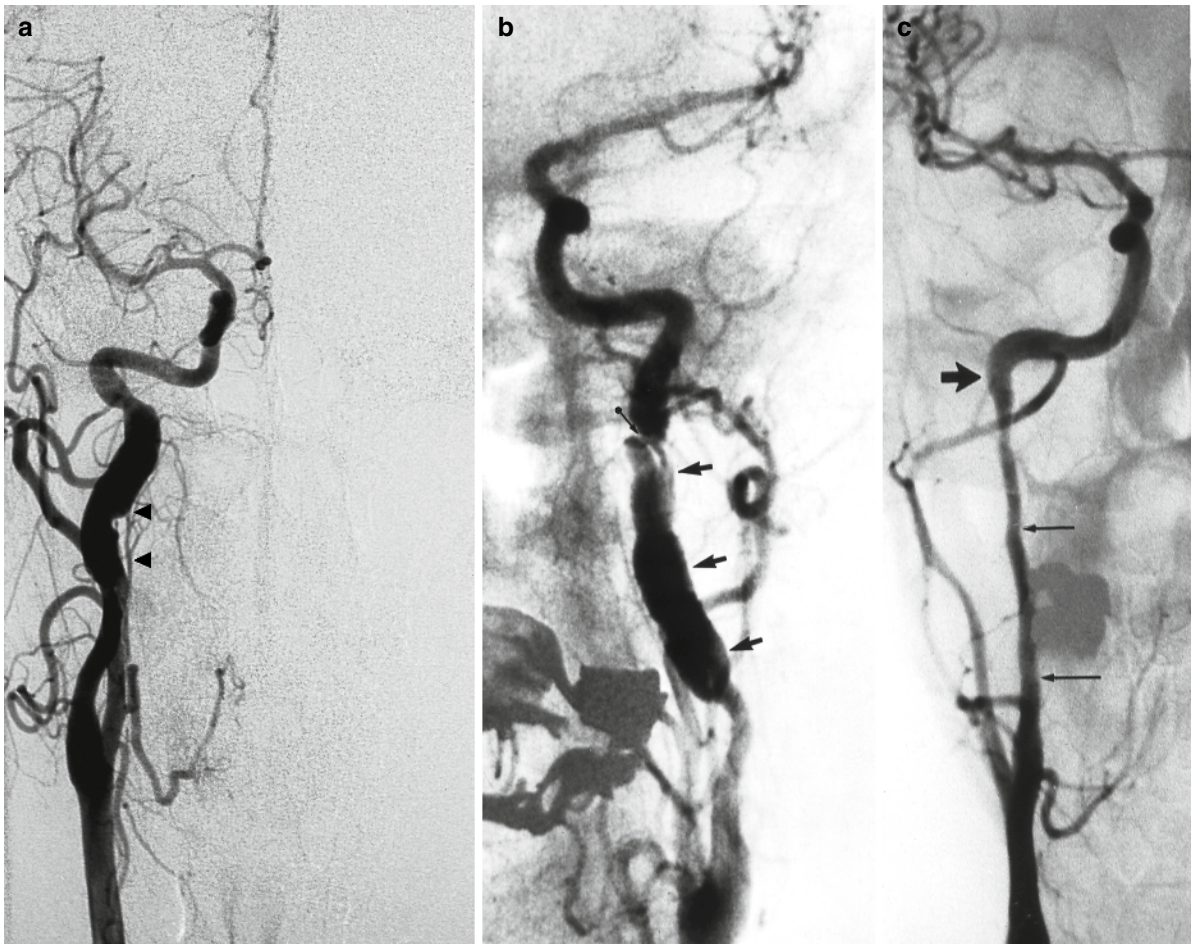

Fig. 16.2 Example of spontaneous dissection of an extracranial ICA. (**a**) Irregular fusiform dilatation arresting at the skull base. Note the ascending pharyngeal artery (APhA; *arrowheads*) running close to the ICA. (**b**) Irregular fusiform dilatation of the ICA (*arrows*). A flap is recognizable (*arrow with dot*). (**c**) Very long stenosis arresting at the base of the skull

standard and is to be used every time in young patients if the diagnosis is not clear or if treatment (surgical or endovascular) is planned.

16.5 Clinical Relevance

Dissection most commonly occurs extracranially, and it is responsible for 2% of all ischemic strokes and for about 20% of all strokes in patients under 45 years of age (Bogousslavsky et al. 1987; Schievink 2001; Redekop 2008). Some dissections may be accompanied only by cervical and facial pain (Buyle et al. 2001), which are always present, and by Horner's syndrome as a result of sympathetic fibers and palsy in the ICA dissection. All these signs can elude an imprecise neurological examination. In many cases, dissection leads to ischemia, commonly through emboli, involving the anterior or posterior circulation, depending on the artery involved (Figs. 16.1–16.6). The spinal cord can also be infrequently involved in dissection of the VA (Weidauer et al. 1999; Crum et al. 2000) (Fig. 16.7a).

An interesting aspect is palsy of the last four cranial nerves in dissection of the ICA in various combinations (Bradac et al. 1981, 1989, 2000; Maitland et al. 1983; Hommel et al. 1984; Lieschke et al. 1988; Nusbaum et al. 1988; Waespe et al. 1988; Vargas et al. 1992; Schievink et al. 1993; Mokri et al. 1996; Sturzenegger et al. 1993). This can be due to compression of pseudoaneurysms, which are not, however, always present. It has also been supposed that a slight

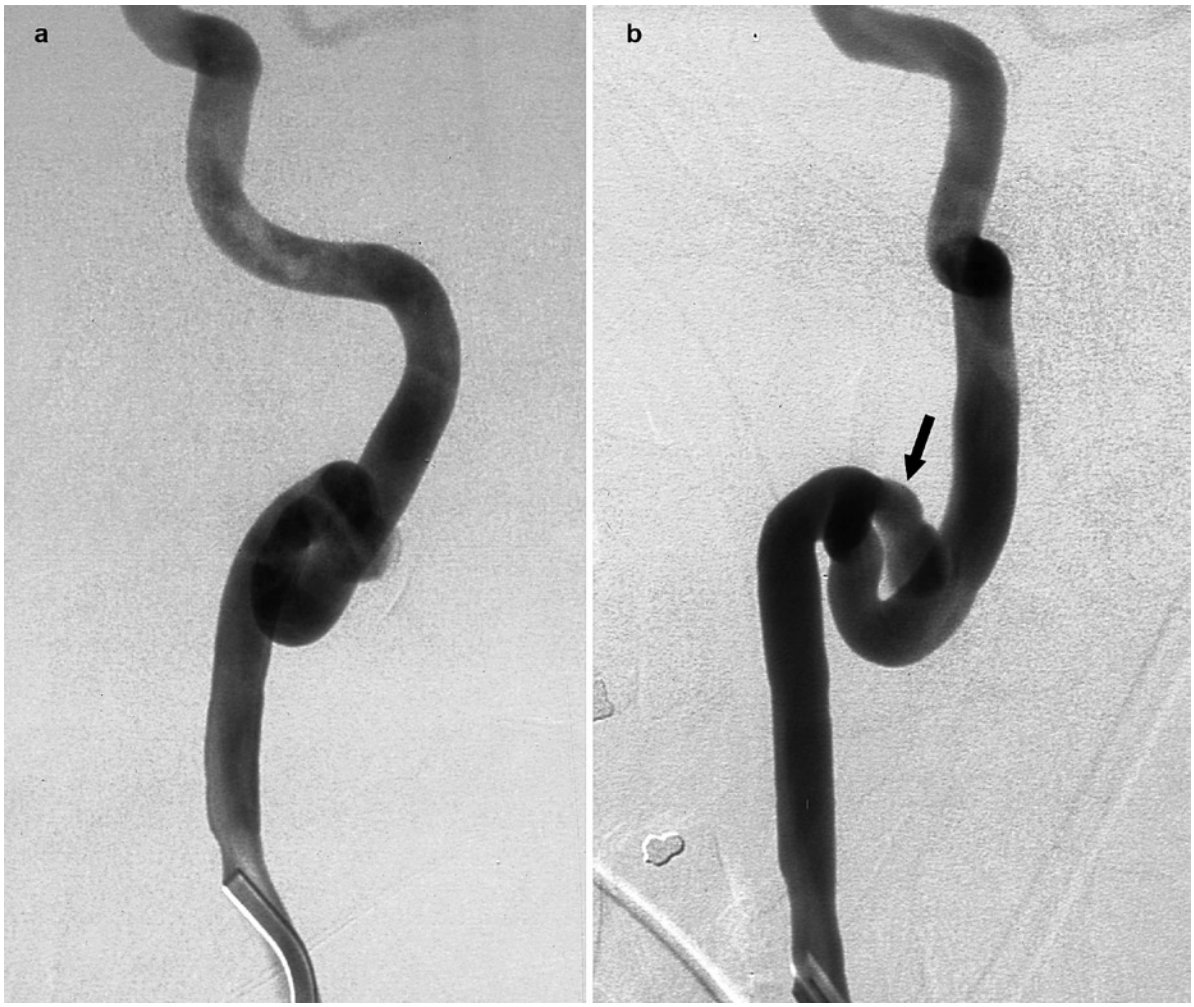

Fig. 16.3 Middle-aged patient presenting with acute cervicalgia. The complete angiographic study showed tortuosity of both ICAs. The right carotid angiogram (two oblique views) disclosed a prominent coiling associated with a probably large dissecting aneurysm (*arrow*). Conservative medical treatment was performed. Three months later, a control angiogram showed the unchanged aneurysm, which was occluded with coils

enlargement of the ICA could compress the ascending pharyngeal artery (APhA), which runs parallel and adjacent to the ICA (Bradac et al. 1990, 2000). Indeed, from previous studies, it is well established that the APhA supplies these nerves (Lasjaunias and Doyon 1978). The rare involvement of cranial nerves III, IV, and VI, supplied by branches of the inferolateral trunk (ILT), could be due to a slight extension of the dissection to the cavernous portion of the ICA. Hypoperfusion, or embolic involvement of the ILT, can also be taken into consideration (Bradac et al. 2000). Involvement of these nerves has been described in cases of ICA occlusion (Wilson et al. 1988; Kapoor et al. 1991).

Intracranial dissection involves predominantly the vertebrobasilar sector. The lesion can lead to ischemia in the cerebellum and brainstem, with varying clinical symptoms always associated with abrupt cervico-occipital pain (Yashimoto et al. 1996; Hosoya et al. 1999; Lee et al. 2006; Shin et al. 2007b) (Figs. 16.6 and 16.7b).

In many other cases, however, as increasingly reported in the literature, dissection leads to SAH (Shimoji et al. 1984; Friedman and Drake 1984; Yamamura et al. 1999; Yamamura et al. 1990; Manabe et al. 2000; Anxionnat et al. 2003; Sugiu et al. 2005; Ramgren et al. 2005) (Figs. 16.8 and 16.9). In recent histopathological studies of dissection on the intracranial vertebral artery that

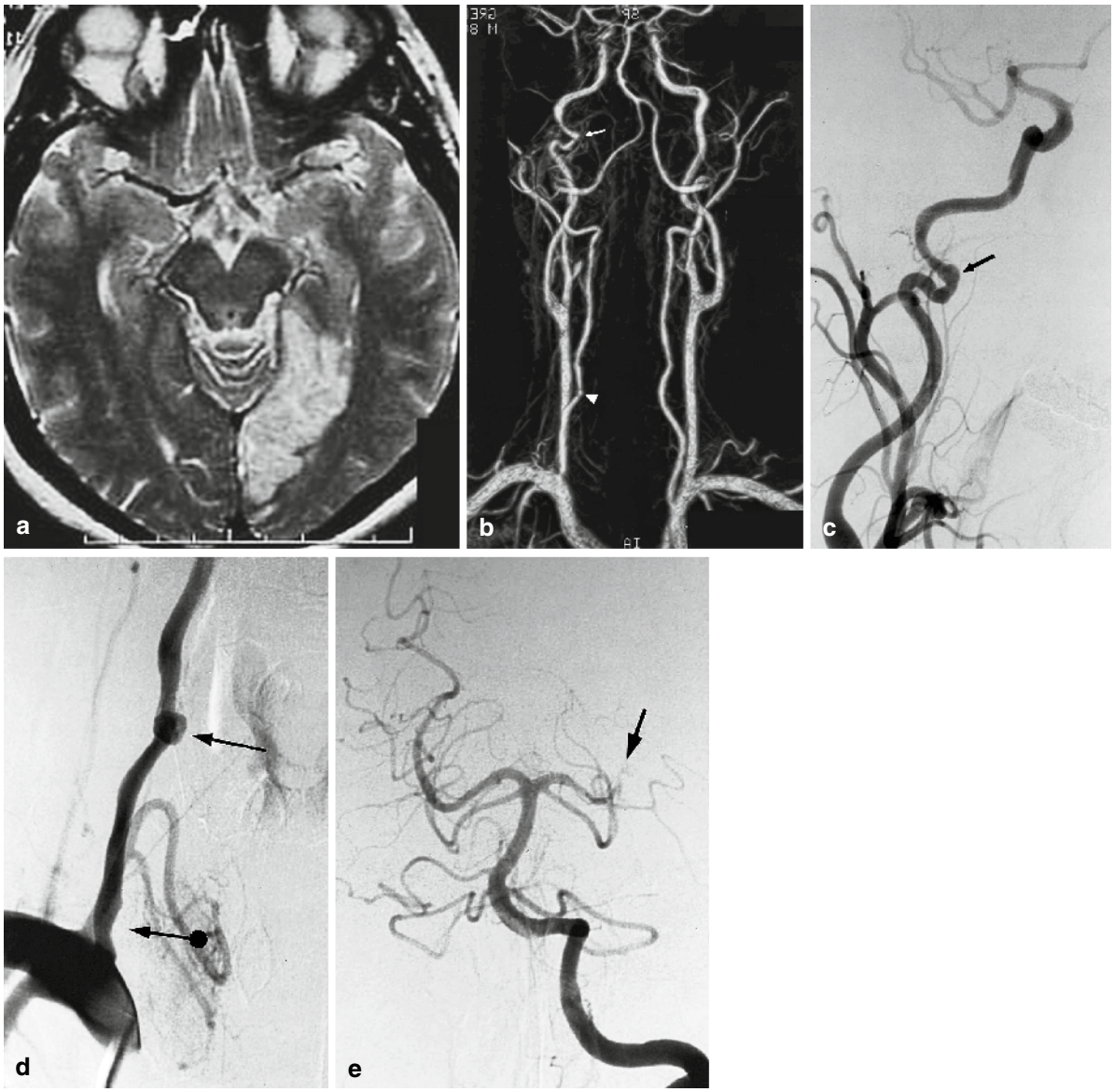

Fig. 16.4 Patient admitted with acute ischemia in the vascular territory of the left posterior cerebral artery, demonstrated on MRI. (**a**) MRI angiography, (**b**) showing irregularity of the right internal ICA (*arrow*) and a doubtful finding on the right vertebral artery (*arrowhead*). The angiogram of the right ICA (**c**) confirmed the changes to the artery, probably due to dissection (*arrow*). The right vertebral angiogram (**d**) showed mild stenosis of the vertebral artery at its origin (*arrow with dot*) and a rounded pseudoaneurysm, probably dissecting, at the level of C6 (*arrow*). This was probably the cause of the embolic occlusion (**e**) of the left posterior cerebral artery (*arrow*)

resulted in fatal SAH, autopsy revealed in addition to the ruptured dissection responsible for the acute hemorrhage, also a previous intracranial vertebral artery dissection, which was partially or completely repaired, in 43% of cases; in about half of those cases, the lesions were bilateral (Hosoya et al. 1999; Shin et al. 2000; Ro et al. 2009). For dissecting aneurysm of the cerebellar and posterior cerebral arteries, see Chap. 11.

The identification of this pathology and the progress of surgical and endovascular treatment have improved the clinical course in many patients (Yang et al. 2007) (Figs. 16.8 and 16.9).

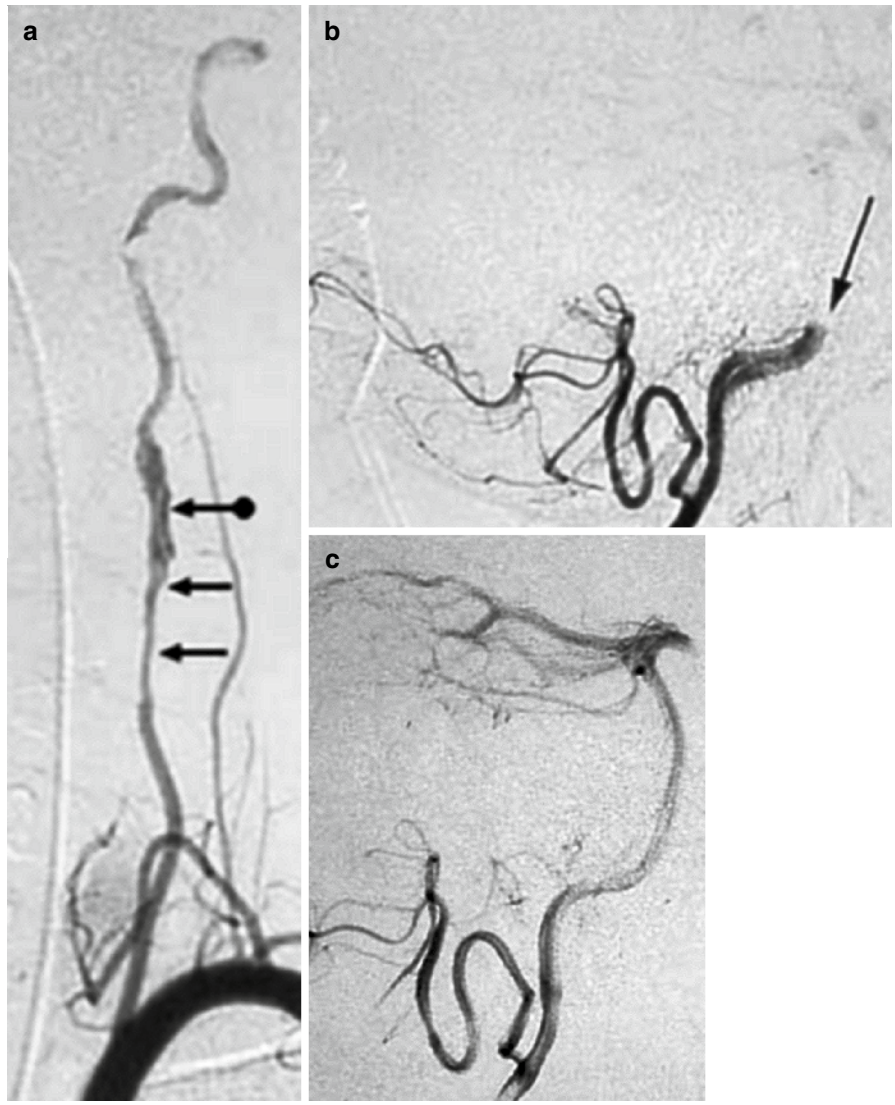

Fig. 16.5 Spontaneous dissection of the left vertebral artery in a very young patient, with embolic occlusion of the middle basilar artery. Left vertebral angiogram (**a**) showing irregularity of the artery with stenosis (*arrows*) and dilatation. A double lumen is also recognizable (*arrow with dot*). Occlusion (**b**) of the basilar artery (*arrow*). Selective catheterization with a microcatheter of the basilar artery through the right vertebral artery, followed by pharmacological fibrinolysis with reopening (**c**) of the artery. Complete recovery of the patient

Intracranial dissections in the anterior circulation are very rare (Kunze and Schiefer 1971; Hochberg et al. 1975; Sasaki et al. 1991; Massoud et al. 1992; Bassetti et al. 1994; Nakatomi et al. 1997). Ischemic stroke is frequent; SAH can occur, and it is not as uncommon as previously thought (Mizutani 1998; Ohkuma et al. 2003; Lv et al. 2009) (Fig. 16.10).

In this context, a particular type of aneurysm is that of blood blister-like aneurysms, which have been reported to be typically located on the superior wall of the supraclinoid ICA. The pathogenesis of these lesions is not completely clear. They are probably a particular form of dissection (Ishikawa et al. 1997; Okuchi et al. 1999). Some authors (Abe et al. 1998) suggest that an important role is played by atherosclerosis, whereby ulcerated plaques lead progressively to a focal defect in the artery wall and eventually to the formation of a hematoma covered by fibrous tissue. Angiograms in the acute phase can be normal or show only a small bulge on the artery wall (Okuchi et al. 1999; Biondi et al. 2009; Cronquist 2009). Over subsequent days in such cases, the lesion commonly grows and forms a saccular aneurysm. These lesions are associated with high morbidity and mortality. Regrowth after coiling is

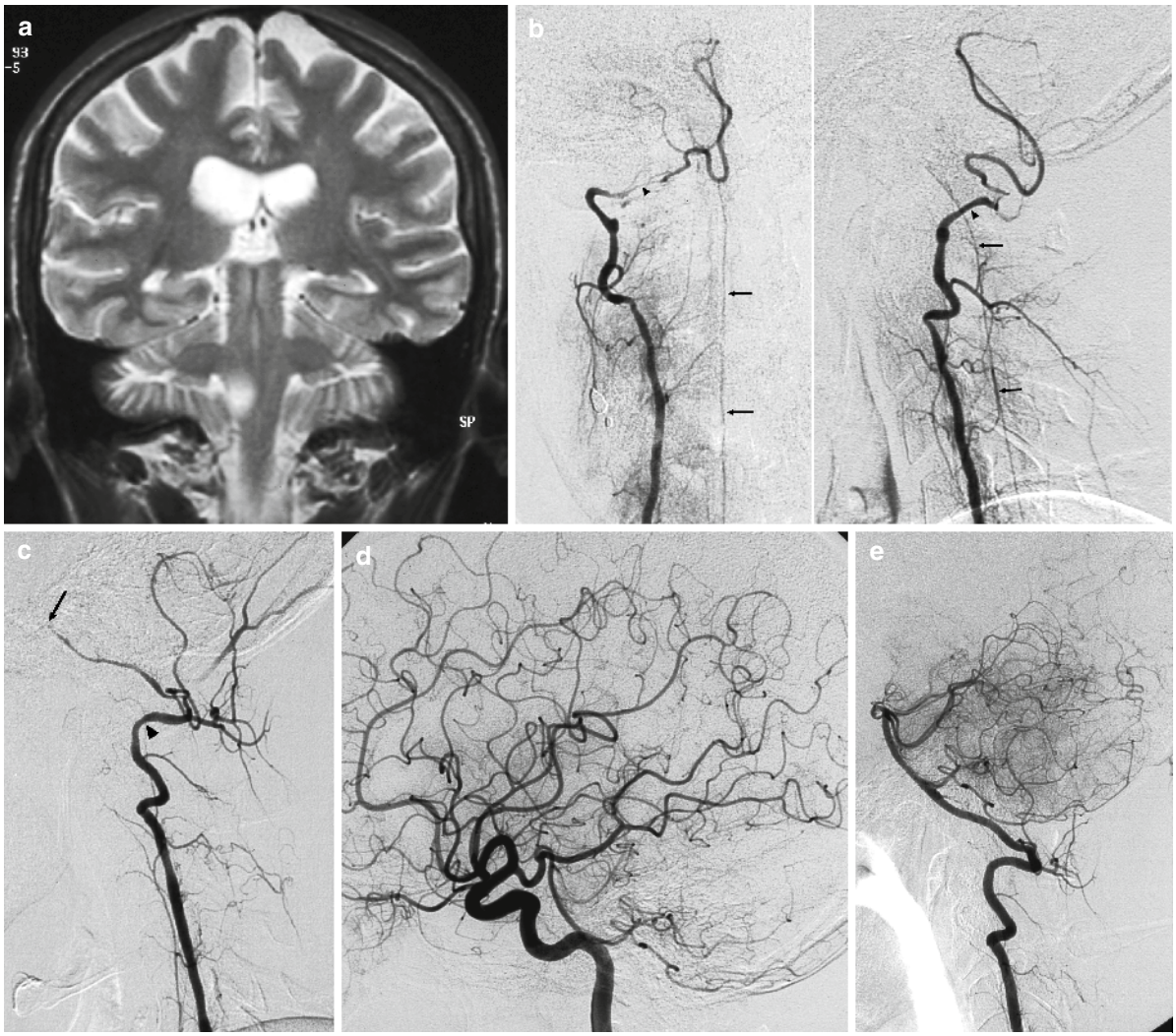

Fig. 16.6 Young patient with brainstem stroke due to dissection of both vertebral arteries (VA) with involvement also of the basilar artery (BA). (**a**) MRI, coronal view, T2-weighted image showing a small lateral bulbar ischemia. (**b**) Angiogram of the right VA (AP and lateral view) showing segmental narrowing of the VA, especially at the extracranial-intracranial passage (*arrowhead*). The VA ends in the posterior inferior cerebellar artery (PICA). There is injection of the anterior spinal artery (ASA; *arrows*) through a radiculomedullary artery. (**c**) Angiogram of the left VA, showing similar segmental narrowing of the VA (*arrowhead*) and BA, which appears occluded in its middle segment (*arrow*). (**d**) On the carotid angiogram, there is a good collateral circulation through the circle of Willis, with a retrograde injection of the BA. Medical therapy was performed. The patient improved rapidly and was symptom-free 1 month later. (**e**) Normal control vertebral angiogram

frequent. Parent artery occlusion and the use of stents are limited to the acute phase of presentation with hemorrhage (Biondi et al. 2009). Some successful surgical repair has been recently reported (Bojanowski et al. 2009). Finally, dissection of the distal branches may also infrequently occur.

16.6 Treatment

The treatment of extracranial lesions is controversial since an important aspect is normalization of the vessel lumen in many cases (Pelkonen et al. 2003). This is particularly true when stenosis is present. Recanalization

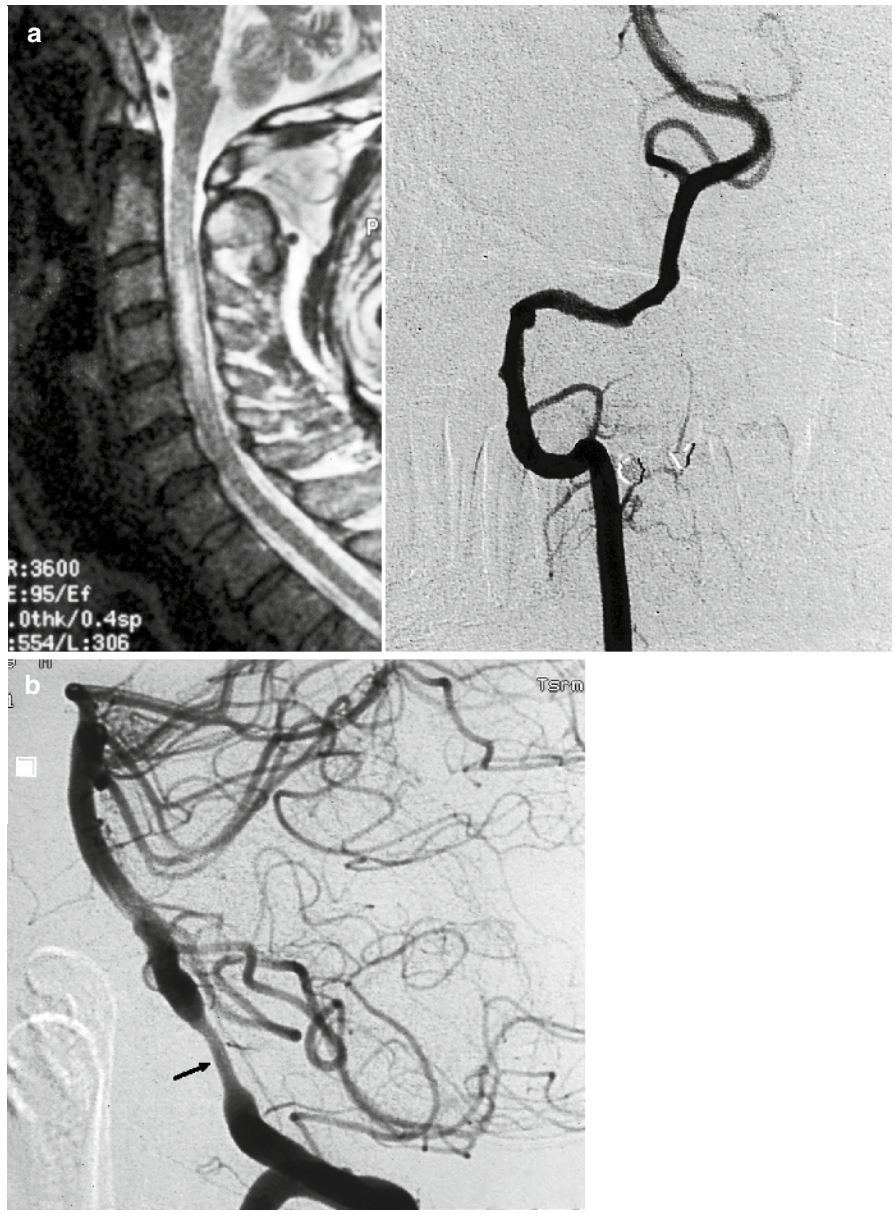

Fig. 16.7 (**a**) Spinal cord ischemia in a young patient due to dissection of the right vertebral artery. MRI T2-weighted image showing the hyperintensity lesion of the spinal cord. Right vertebral angiogram disclosing irregularity with a small pseudoaneurysmal dilatation of the distal extracranial and partially intracranial VA. The left VA was normal. The anterior spinal artery is not always visible on the vertebral angiogram. Its absence in this specific case, however, is probably due to occlusion. The patient recovered, and on the control angiogram 2 months later the VA was normal. (**b**) Dissection of the left VA in another patient presenting with transient brainstem ischemia. Irregular stenosis is recognizable in the intracranial VA. Control angiogram 2 months later showed normalization of the lumen

can also occur more rarely in cases of occlusion. When a pseudoaneurysm is present, it commonly remains unchanged or can enlarge later. In the acute phase, conservative medical therapy that avoids intracranial embolism is preferred in many centers. Endovascular therapy may be performed later if the stenosis or pseudoaneurysm remain. In selected cases, when stenosis is present but the lumen is maintained and an embolic intracranial occlusion is recognizable, selective endovascular thrombolysis can be performed (Fig. 16.5).

In cases of intracranial dissection with SAH, the lesion should be treated rapidly since the risk of rebleeding is very high. Surgical or endovascular treatment consists frequently of occlusion of the dissected segment, along with the parent artery, with balloons or coils whenever this is judged possible (Sugiu et al. 2005; Ramgren et al. 2005) (Figs. 16.8 and 16.10). The use of more appropriate stents may be possible in the future. Pseudoaneurysms can grow rapidly, and so close angiographic control is mandatory in cases when because of the poor clinical condition of the patient on admission or because of minimal vessel changes, endovascular treatment is not performed in the acute phase. This treatment

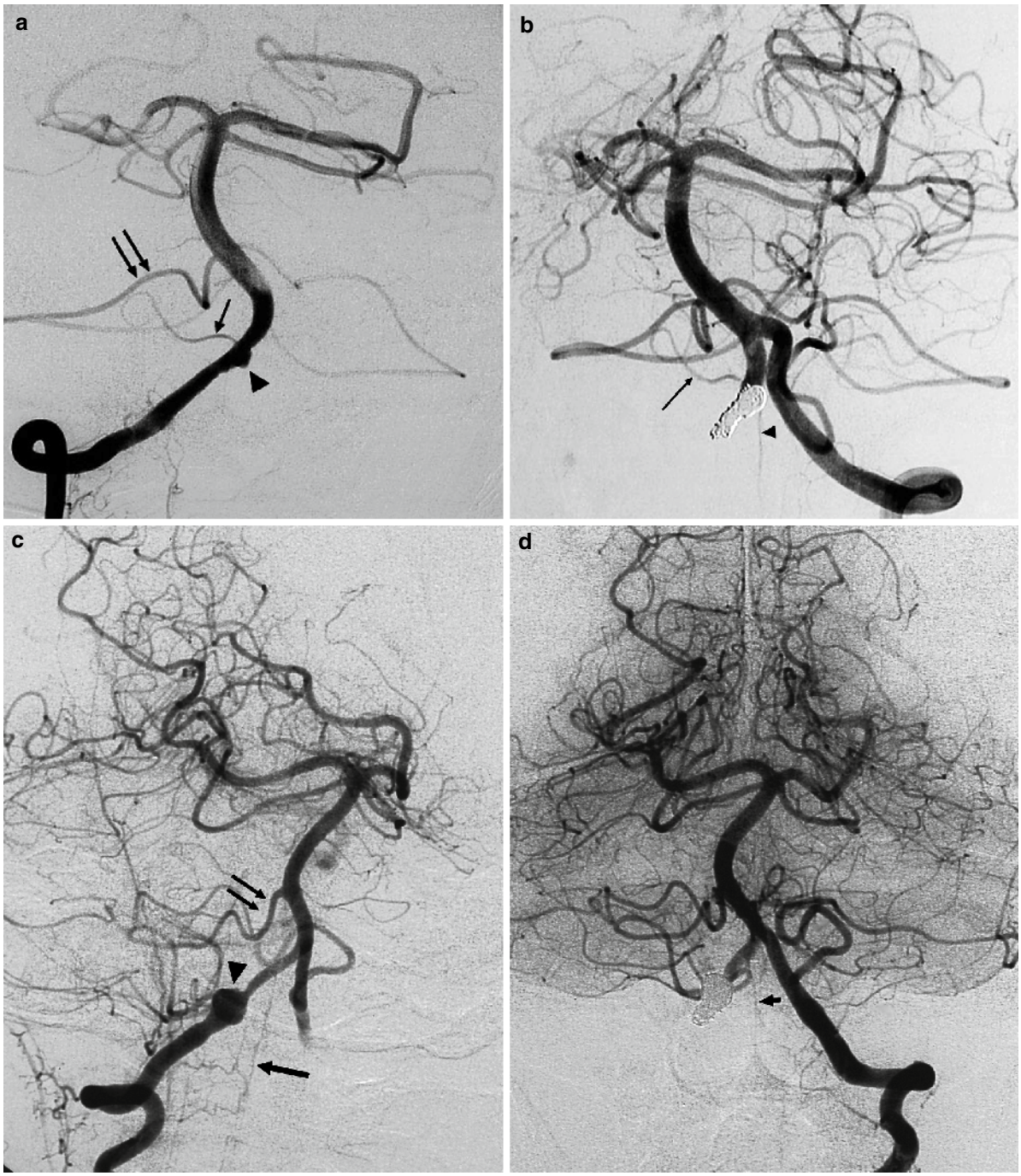

Fig. 16.8 Dissecting aneurysm of the right VA, presenting with subarachnoid hemorrhage (SAH). (**a**) Right vertebral angiogram showing irregular small fusiform aneurysm (*arrowhead*) proximal to the origin of the small PICA (*small arrow*). A large anterior inferior cerebellar artery (AICA; *arrows*) supplies the vascular territory of the PICA. (**b**) Left vertebral angiogram after occlusion of the aneurysm with coils and of the right VA. The right PICA was preserved (*arrow*) as well as the anterior spinal artery (*arrowhead*), arising typically distal to the PICA. The patient recovered well. Another example of a dissecting aneurysm of the right vertebral artery, presenting with SAH. (**c**) Right vertebral angiogram, oblique view. Round dilatation (*arrowhead*) of the VA. There is a large AICA (*double arrow*) supplying completely the vascular territory of the PICA. Anterior spinal artery (*arrow*). Well-developed PICA on the left. (**d**) Left vertebral angiogram after occlusion of the aneurysm and right VA. Anterior spinal artery (*arrow*)

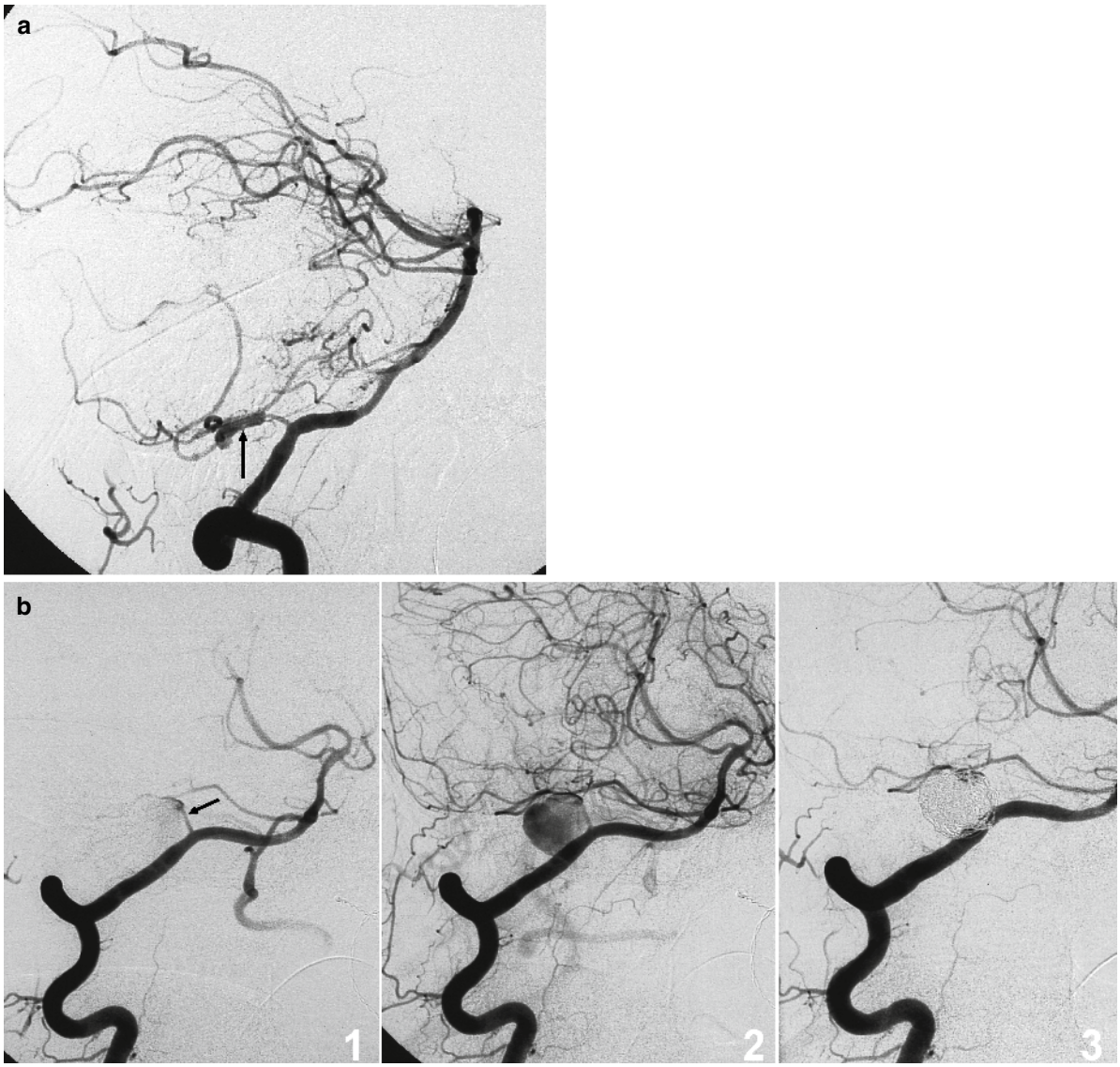

Fig. 16.9 Severe SAH in a relatively young patient. (**a**) Right vertebral angiogram showing fusiform dilatation, suggesting dissecting aneurysm (*arrow*) of the lateral bulbar segment of the PICA. The comatose patient recovered slowly. (**b**) The second angiogram 3 weeks later showed a tremendous enlargement of the aneurysm, now involving the PICA, also near its origin (*arrow*). Selective occlusion of the aneurysm with coils

can, however, be carried out as soon as the clinical condition improves or the lesion becomes more evident on the control angiogram (Fig. 16.9). In addition, stenotic lesions that involve intracranial vessels responsible for ischemia in the acute phase can sometimes change in late controls; pseudoaneurysms form, and this demands a different therapeutic approach.

16.7 Dissection and Dissecting Aneurysms in Children

In young and middle-aged adults, dissection occurs typically in the extracranial sector, while in children it is frequent also in the intracranial sector (Schievink et al. 1994b; Fullerton et al. 2001). Unlike in adults,

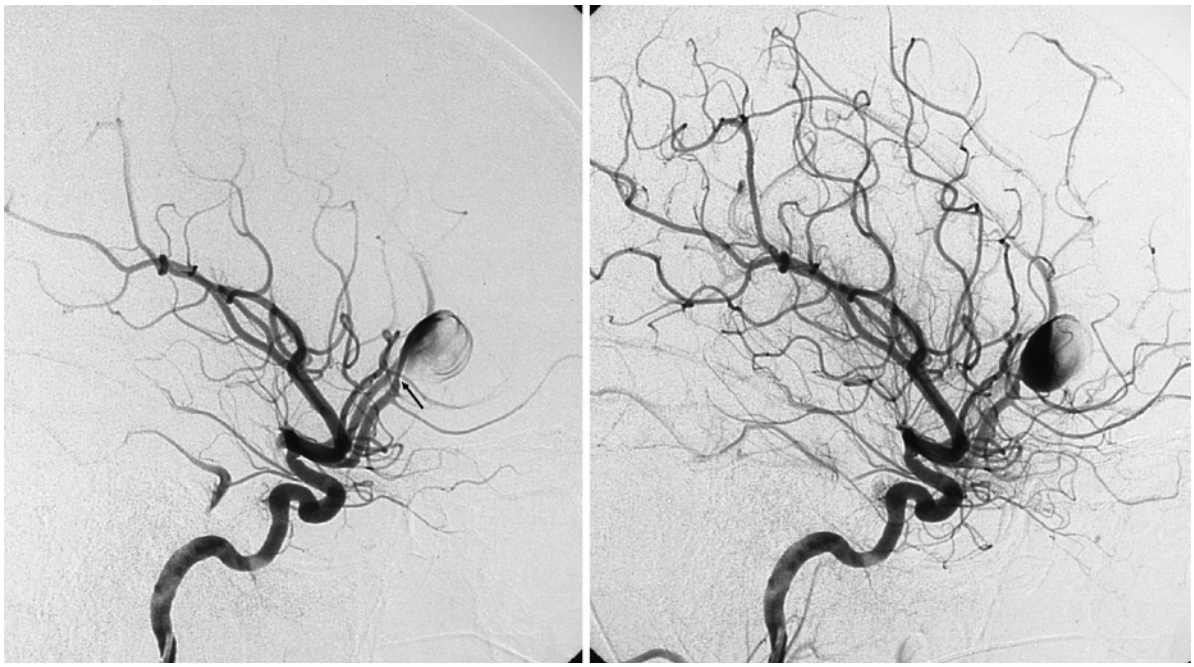

Fig. 16.10 Young patient presenting with a severe SAH hemorrhage with a parenchymatous component owing to rupture of an aneurysm, probably dissecting, of the proximal segment of the pericallosal artery. The arrow shows the small stenosis of the artery proximal to the aneurysm. In a later phase, progressive filling of the large aneurysm and distal pericallosal artery. The sac of the aneurysm was clipped, but a week later a second severe SAH occurred. A second angiographic study revealed that the aneurysm had enormously increased. It was occluded together with the pericallosal artery with coils

in whom dissecting aneurysms are prevalently in the posterior circulation, in children they are frequent also in the anterior circulation (Schievink et al. 1994b; Fullerton et al. 2001; Lasjaunias et al. 2005). Among the arteries typically involved in the anterior circulation, the most frequent are the terminal ICA and MCA; in the posterior circulation, the most commonly involved are the VA, basilar artery, and posterior cerebral artery (Hochberg et al. 1975; Nass et al. 1982; Graber et al. 1992; Schievink et al. 1994b; Laughlin et al. 1997; Fullerton et al. 2001; Lasjaunias et al. 2005; Massimi et al. 2003; Vilela and Goulão 2006; Bradac et al. 2008a).

The dissection is characterized by stenosis; occlusion leads to ischemia because of distal emboli or hypoperfusion (Fig. 16.11). Intracranially, large pseudoaneurysms can frequently have a mass effect on the surrounding parenchyma or be the cause of distal embolization. Ruptures with SAH can occur, but they are less common than in adults (Fig. 16.12).

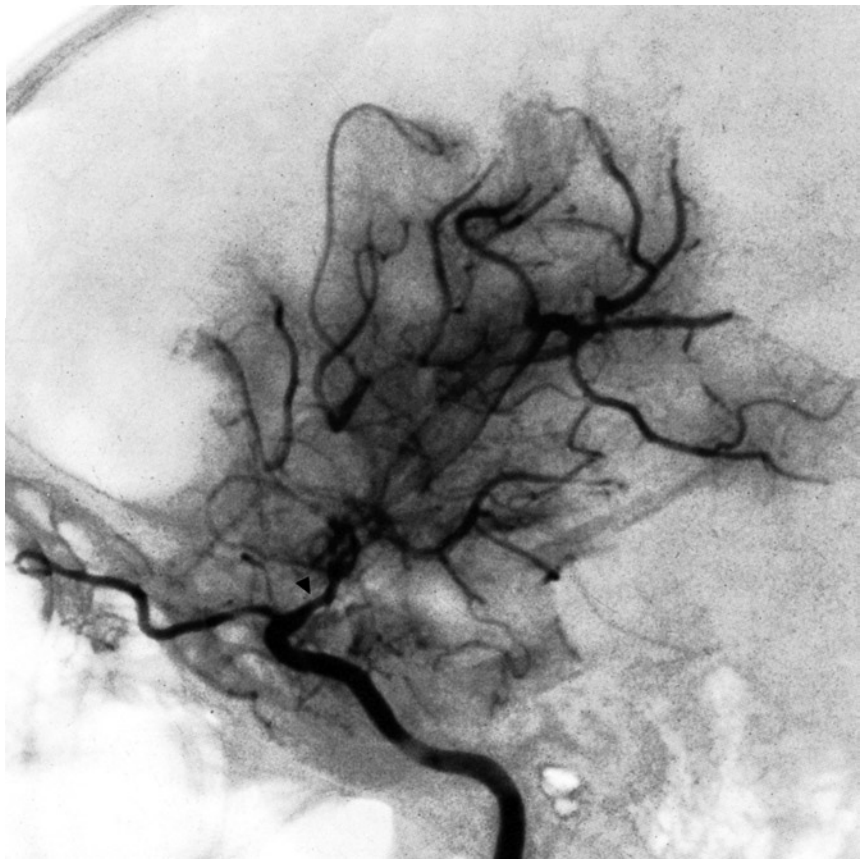

Fig. 16.11 Lateral carotid angiogram in a 5-year-old child with a sudden onset of hemiplegia and aphasia. Left lateral carotid angiogram. Narrowing of the terminal segment of the left ICA (*arrowhead*). Irregularity and occlusion of many branches of the middle cerebral artery. A spontaneous dissection with distal embolization was suspected

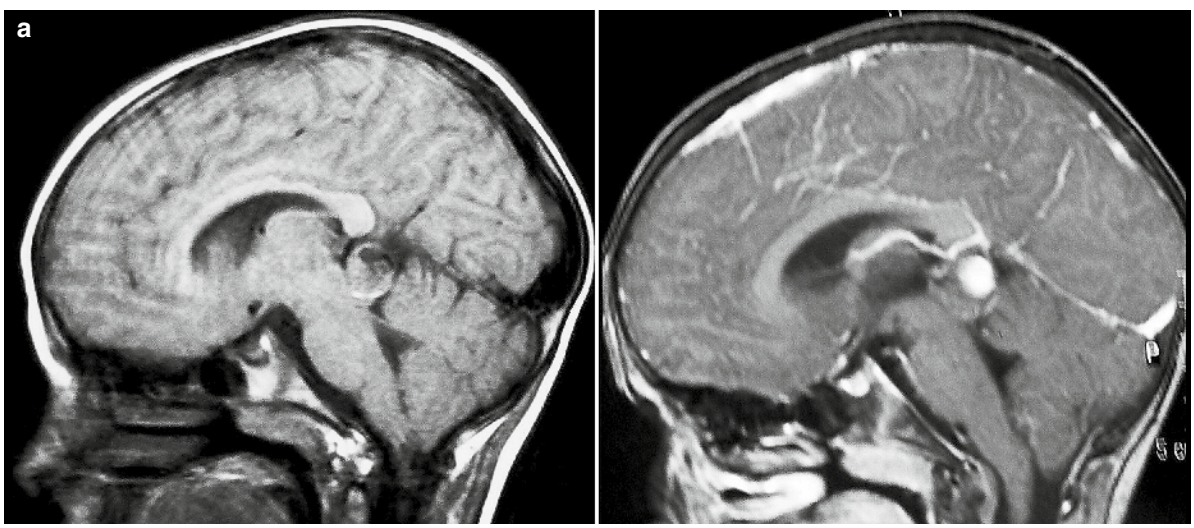

Fig. 16.12 Young boy with a short clinical history of severe headaches. (**a**) MRI T1-weighted sagittal images. A mass lesion, characterized by an inhomogeneous signal and a hyperintense peripheral rim, corresponding probably to a large aneurysm with an intramural thrombus of different ages, is visible. After contrast medium enhancement, the patent part of the aneurysm was demonstrated. There is compression of the aqueduct and midbrain. (**b**) On the vertebral angiogram, an irregularly shaped aneurysm arising from a small branch of the P3-P4 segment of the right posterior cerebral artery is visible (*1*). Focal stenotic segment proximal to the aneurysm (*arrow*). Selective catheterization of the aneurysm and its occlusion with coils (*2*). Final control angiogram (*3*). The patient recovered completely

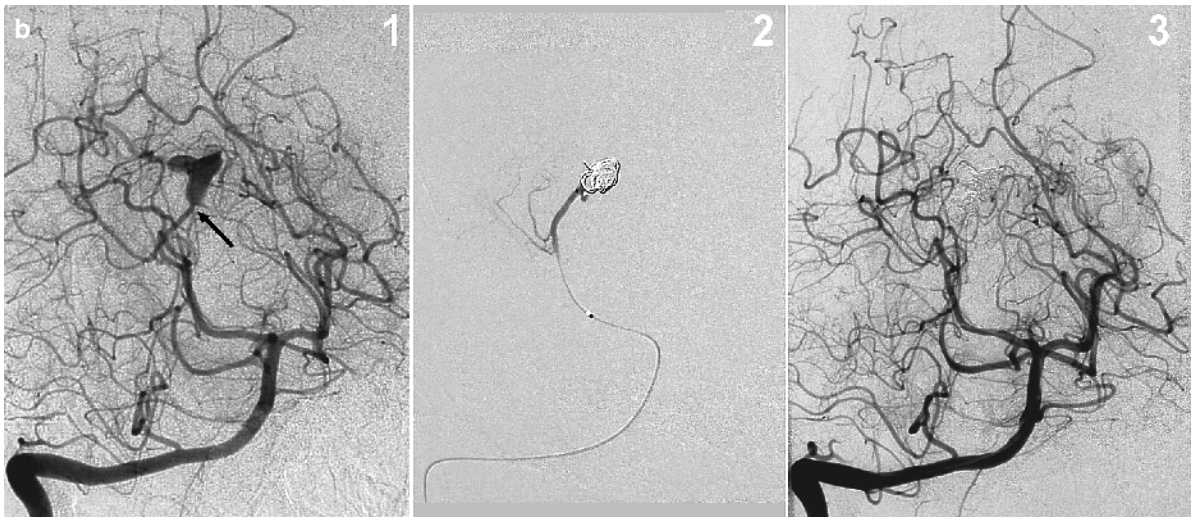

Fig. 16.12 (continued)

Other Nonatherosclerotic Vasculopathies 17

17.1 Great Variety of Diseases

Nonatherosclerotic vasculopathies comprise a great variety of diseases, as listed in Table 17.1, that result from different etiologies; they include collagenopathies, immunological, hematological, and infection mechanisms, and other rarer causes that have in common the possibility of affecting the cerebral vessels, leading to ischemia and sometimes hemorrhage. In the majority of these diseases, the angiogram shows such findings as occlusion and irregular narrowing, alternating with dilation and sometimes aneurysm. These changes are not typical of one specific disease, but are common to all, independent of their basic pathology. Furthermore, in many cases where the involved vessel is in the precapillary-capillary sector, the angiogram may be normal, so the final diagnosis is made based on clinical and laboratories findings. Some angiographic examples are presented in Figs 17.1–17.3.

Some of these pathologies are characterized by a typical angiographic pattern, which will be described in detail.

17.2 Cerebrovascular Fibromuscular Dysplasia

Fibromuscular dysplasia (FMD) is a systemic vascular disease, characterized by nonatherosclerotic changes involving the wall of small to medium-sized arteries. All vascular territories can be affected; among them, FMDs are seen in the renal arteries most frequently, and this is often responsible for hypertension in these patients. Palubinskas and Ripley (1964) and Palubinskas and Newton (1965) were the first to report the angiographic aspects of this disease in the cephalic arteries. Numerous reports followed (Palubinskas et al. 1966; Andersen 1970; Wylie et al. 1966; Houser and Baker 1968; Bradac and Heymat 1970; Stanley et al. 1974; Manelfe et al. 1974; Osborn and Anderson 1977; Bradac and Oberson 1983), clearly distinguishing FMD from atherosclerotic and other nonatherosclerotic lesions and its possible relationship with stroke.

The true incidence of FMD is unknown. In some reports, it is cited as up to 10% in angiographic studies (Chiras et al. 1985). FMD is more frequent in women, and it is rare in children (Andersen 1970).

17.2.1 Pathology and Etiopathogenesis

FMD is commonly characterized by involvement of the medial layer, with fibrous proliferation and hyperplasia of the smooth muscle cells. Less commonly, FMD involves the intima or adventitia. These changes lead to thickening and fibrosis of the layer involved. The precise etiopathogenesis has yet to be identified. A deficiency of alpha 1-antitrypsin has been reported (Schievink et al. 1998).

17.2.2 Diagnosis

The aspect of the arteries involved can be typical and is characterized on the angiogram, CT angiography, or MRI angiography by multifocal stenosis, which is sometimes severe, alternating with areas of mural dilatation, leading to the so-called string-of-beads appearance. Pseudoaneurysms and tubular stenosis can occur.

G.B. Bradac, *Cerebral Angiography*,
DOI: 10.1007/978-3-642-15678-6_17, © Springer-Verlag Berlin Heidelberg 2011

Table 17.1 Nonatherosclerotic vasculopathies

Primary angiitis of the CNS
• Granulomatous vasculitis, affecting predominantly the precapillary arterioles, occasionally large vessels (such as ICA, PCA, MCA, ACA). Small aneurysms have also been reported. Angiography frequently normal
Systemic vasculitis that can affect the CNS
• Giant cell arteritis: granulomatous vasculitis involving predominantly superficial temporal ophthalmic arteries, occasionally extracranial ICA and VA
• Takayasu arteritis: granulomatous vasculitis
• Polyarteritis nodosa: necrotizing vasculitis; large intracranial vessels can be involved; aneurysm may be present
• Wegener's granulomatosis: necrotizing vasculitis; can involve intracranial arteries with ischemia due to occlusion and hemorrhage due to rupture of arteries
• Behçet's disease: no signs of necrotizing or granulomatous vasculitis are found; frequently perivenular infiltrations are present; angiography often normal
Systemic diseases that can affect the CNS
• Systemic lupus erythematosus
• Rheumatic disease
• Sjogren's syndrome
• Behçet's disease: no signs of necrotizing or granulomatous vasculitis are found; angiography frequently normal
• Crohn's disease
• Sarcoidosis
Hematological conditions
• Sickle cell disease, Moschcowitz's disease, platelet hyperaggregability, disseminated intravascular coagulation, antiphospholipid syndrome, deficiency of factors involved in coagulation (deficiency of proteins C and S, antithrombin III, factor V Leyden), homocystinuria
Vasculopathies not linked to inflammatory processes
• Neurofibromatosis, intracranial vessel occlusion, possible intracranial aneurysm
• Ehlers-Danlos syndrome (aneurysm, frequently dissecting, of the extra- and intracranial arteries; dissecting aneurysm of the intracavernous ICA with spontaneous cavernous fistulas)
• Fibromuscular dysplasia
• Scleroderma
• Livedo reticularis (Sneddon's syndrome)
• Moyamoya disease
Infection diseases
• Bacterial, fungal, parasitic, viral (herpes zoster ophthalmicus)
Others
• Vasculopathies related to drugs, radiotherapy, intracranial tumors, trauma
• Migraine stroke

Abbreviations: ACA, anterior cerebral artery; CNS, central nervous system; ICA, internal carotid artery; MCA, middle cerebral artery; PCA, posterior cerebral artery; VA, vertebral artery

In the latter situation, in a patient with stroke, the differential diagnosis of dissection can sometimes be difficult. On control angiograms, the findings remain unchanged in FMD, while in dissection normalization frequently occurs. The vessel most often involved is the extracranial internal carotid artery (ICA) in

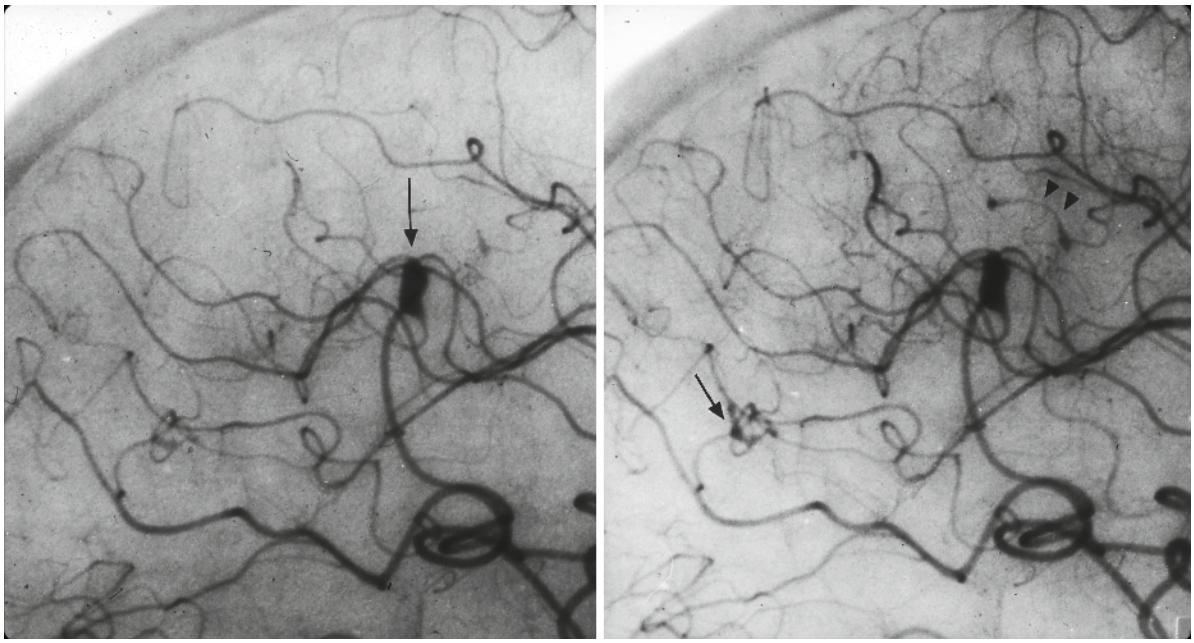

Fig. 17.1 Lateral carotid angiogram (detail with magnification) in a patient with polyarteritis nodosa, early and later phases. Aneurysmal dilatations (*arrow*) and stenotic changes (*arrowheads*) are present

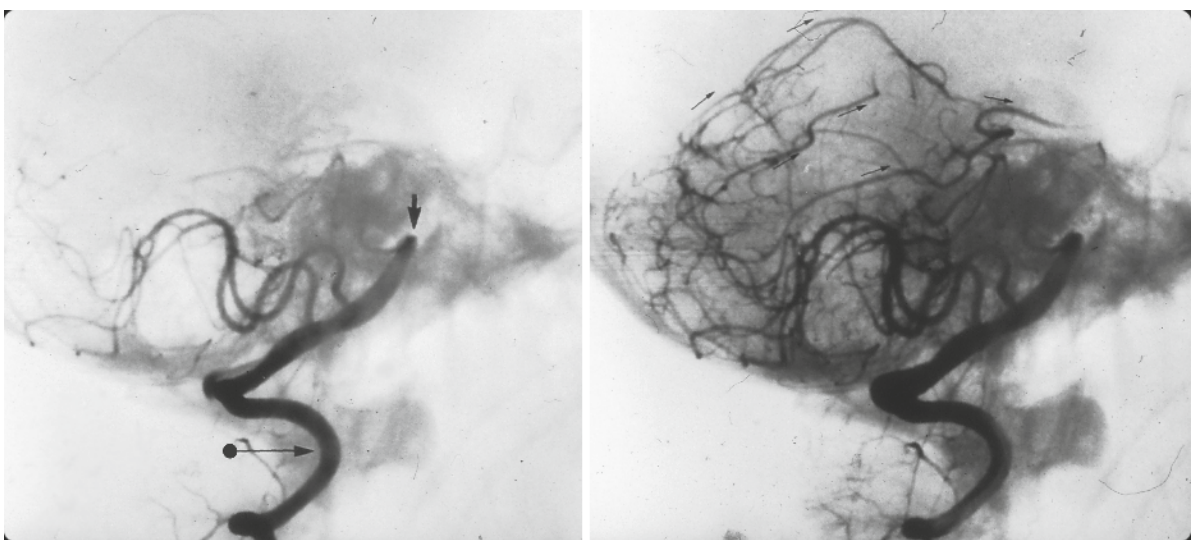

Fig. 17.2 A young boy with neurofibromatosis presenting with an acute occlusion of the basilar artery. Vertebral angiogram showing the occlusion (*arrow*). In the later phases, retrograde injection of the superior cerebellar artery (SCA) and anterior inferior cerebellar artery (AICA) through opening of the anastomosis with the posterior inferior cerebellar artery (PICA; *arrows*). There is a slight displacement of the vertebral artery at C1-C2 owing to dysplasia of the cervical spine (*arrow with dot*)

its mid-portion, frequently bilaterally (Osborn and Anderson 1977), followed by the extracranial vertebral artery (VA) in its mid-distal portion. Multiple vessels are commonly affected (Osborn and Anderson 1977; Osborn 1999). Intracranial vessels may also be affected, but this occurs less frequently (Elias 1971; Frens et al. 1974; Tomasello et al. 1976; Saygi et al. 1990) (Fig. 17.4).

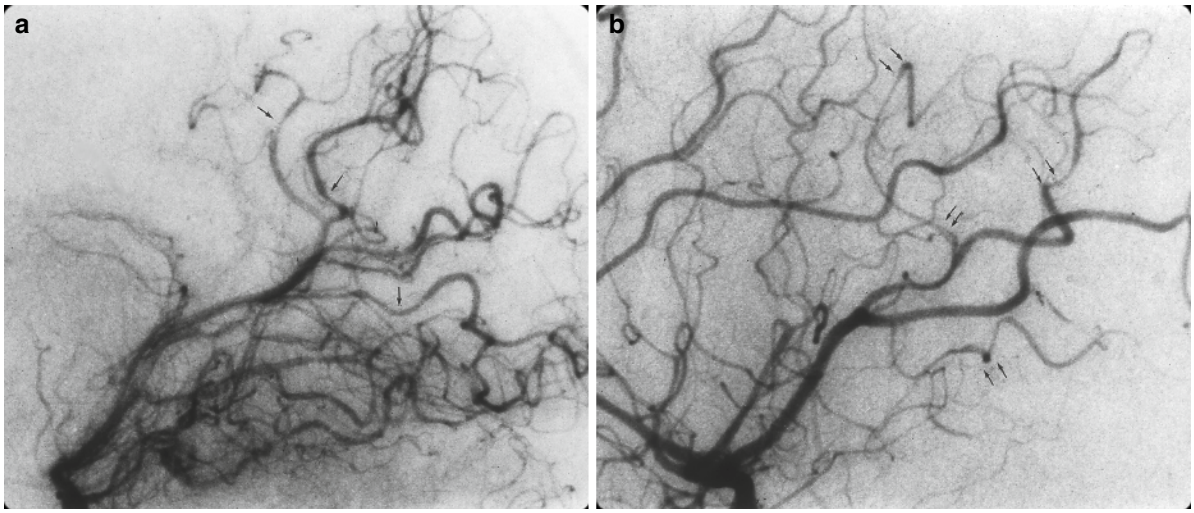

Fig. 17.3 Suspected primary angiitis in a young boy presenting with sudden onset of epileptic seizures and psychic impairment. Lateral carotid (**a**) and vertebral angiogram (**b**). Irregularity and focal narrowings of several distal branches in the anterior and posterior circulation are visible

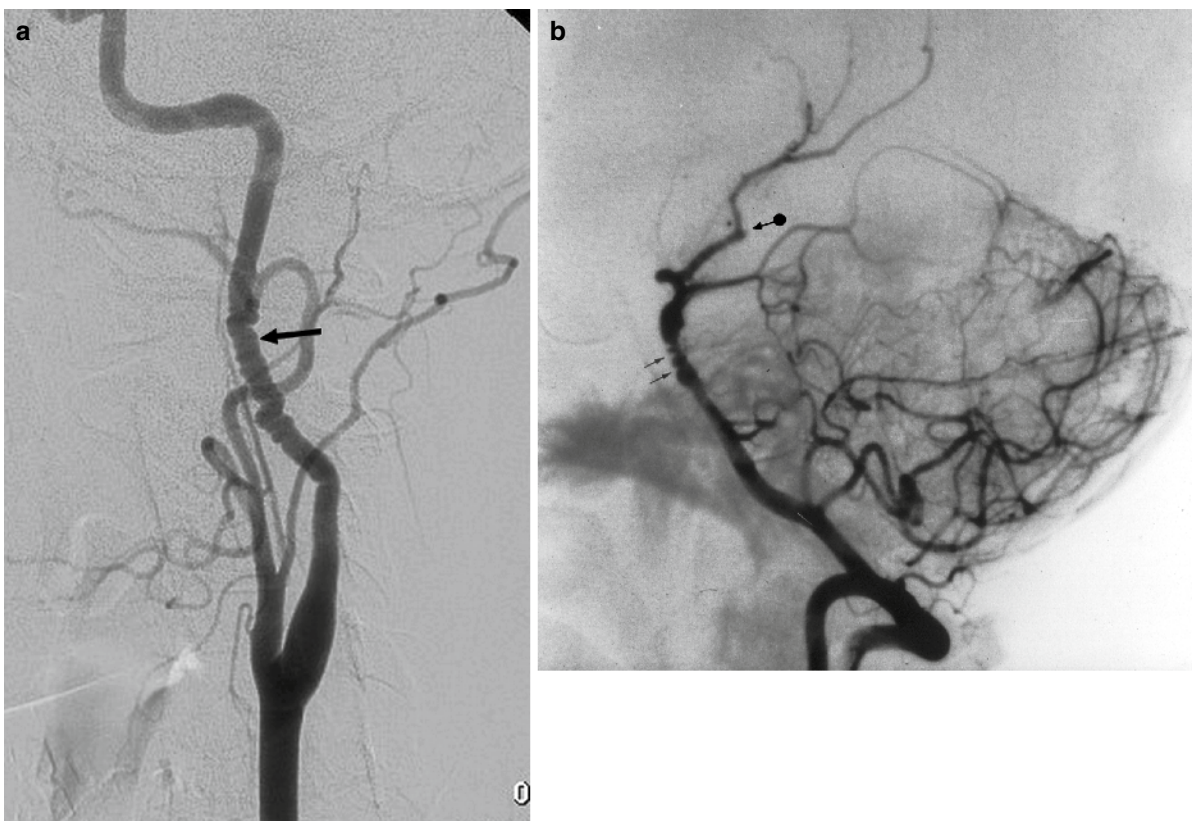

Fig. 17.4 (**a**) Typical string-of-beads appearance of the internal carotid artery (*arrow*). (**b**) String-of-beads appearance at the level of the distal basilar artery (*arrows*) associated with a similar finding involving the posterior cerebral artery (PCA) and SCA, with occlusion, probably embolic, of the distal branches (*arrow with dot*)

FMD is commonly associated with cerebral aneurysm (Handa et al. 1970b; Hirsch and Roessmann 1975; Osborn and Anderson 1977). Fistulas of the carotid-cavernous sinus and vertebral and perivertebral veins have been reported (Geraud et al. 1973; Hieshima et al. 1986).

17.2.3 Clinical Relevance

The extracranial changes of FMD can occasionally be found in patients examined for other pathologies. FMD can, however, be the cause of ischemic stroke owing to the formation of thrombus at the site of the stenosis, which is followed by intracranial embolization. The close relationship of dissection with FMD is well established. Intracranial FMD can be the cause of ischemia or be responsible for dissecting aneurysms with possible subarachnoid hemorrhage (SAH). Finally, there is a frequent association with intracranial berry aneurysm, which is responsible for the SAH in these patients. The treatment (medical, surgical, endovascular) depends on the type of lesion and stroke.

17.3 Moyamoya Disease

This is a chronic, progressive cerebrovascular disease, first described in Japanese patients by Takeuchi and Shimizu in 1957. Other Japanese reports followed (Kudo 1968; Nishimoto and Takeuchi 1968). The term moyamoya, proposed by Suzuki and Takaku (1969), means "vague puff of smoke." Despite the fact that the disease is more frequent in Japanese patients, later studies showed that it can occur also in non-Asians (Taveras 1969; Galligioni et al. 1971; Picard et al. 1974a, 1974b; Huber 1979; Bradac and Oberson 1983; Masuda et al. 1993). Children and young patients are prevalently involved, but the disease may also be seen in older patients.

17.3.1 Pathology and Etiopathogenesis

Intimal thickening due to proliferation and migration of smooth muscle cells leads to progressive occlusion of the intracranial distal ICA, with extension also to the M1 and A1. A rich network of vessels develops, involving perforators of the middle cerebral artery (MCA), anterior cerebral artery (ACA), posterior communicating artery, P1, and the anterior and posterior choroidal arteries. The significance of this network is not completely clear. Some authors (Taveras 1969; Crouzet et al. 1974; Picard et al. 1974a, 1974b) have suggested that this is a kind of collateral circulation, with anastomoses between the deep and superficial vascular territories. This interpretation is intriguing since deep perforators are commonly thought to be end arteries, with no links to one another or to the medullary arteries. However, microangiographic studies (Kodama and Suzuki 1974; Umansky et al. 1985) have shown that a few anastomoses can be present among the single perforators and between the perforators and medullary arteries. It is therefore conceivable that in slowly occurring occlusive diseases like moyamoya, anastomoses occur in these vascular territories (Fig. 17.5).

Basically, two phases of the disease can be recognized. The first phase is characterized by a progressive occlusion of the distal branches of the ICA and circle of Willis, with formation of the typical basal network involving the deep perforators. In the second phase, the occlusion of the ICA is complete, and the collateral circulation to the cortical branches occurs through dural and transosseous branches of the external carotid artery (ECA) and ophthalmic artery (Fig. 17.6).

The posterior circulation, at least in the first phases of the disease, is not affected. It is indirectly involved in the collateral circulation through its perforators and leptomeningeal anastomoses of the posterior cerebral artery toward the MCA and ACA. Later, the P1 also becomes occluded, so that only branches of the ECA are responsible for the intracranial circulation in the supratentorial sector.

The etiology of the disease is not known. Moyamoya disease can occur in different pathological conditions: vasculitis with or without an autoimmune mechanism, a postirradiation state, neurofibromatosis, hemoglobinopathies, and atherosclerosis. Genetic factors probably also play some role.

17.3.2 Diagnosis and Clinical Relevance

Angiography is the essential method for identifying the disease. Moyamoya disease has a progressive character,

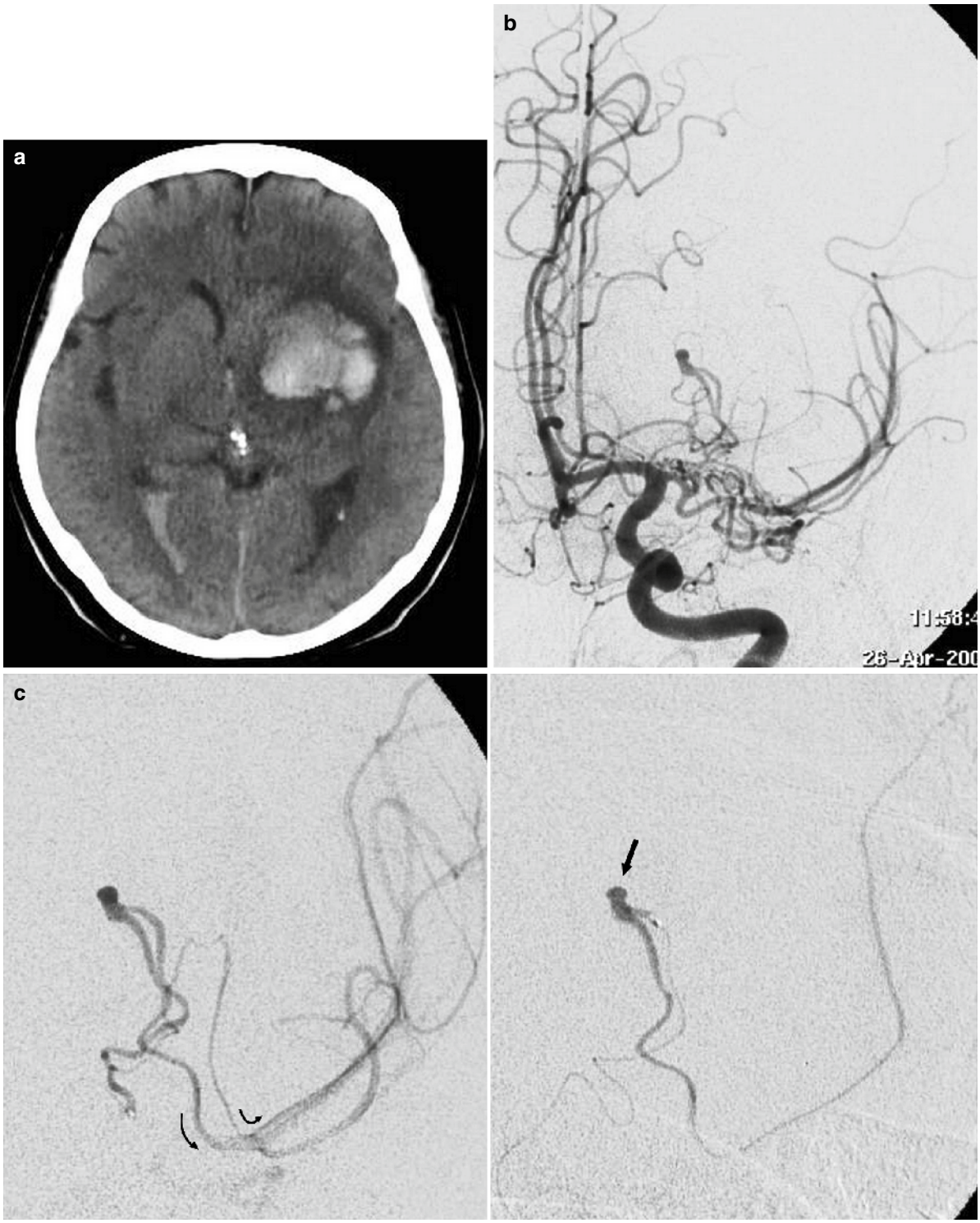

Fig. 17.5 Sixty-year-old woman presenting with sudden hemorrhage in the left basal ganglia. CT (**a**). Left carotid angiogram, AP view (**b**). Several changes are recognizable in the first segment of the middle cerebral artery (MCA). The M1 appears tortuous and very small, continuing to the normal M2 segment. There is also a well-developed network involving perforators with a pattern resembling that in moyamoya disease. As demonstrated in the selective study (**c**), at least two perforators (*curved arrows*) anastomose to each other, contributing to revascularization of the M2 segments. On one of these perforators, a small aneurysm is recognizable (*arrow*), which was responsible for the hemorrhage. This was occluded with glue. Final control angiogram (**d**)

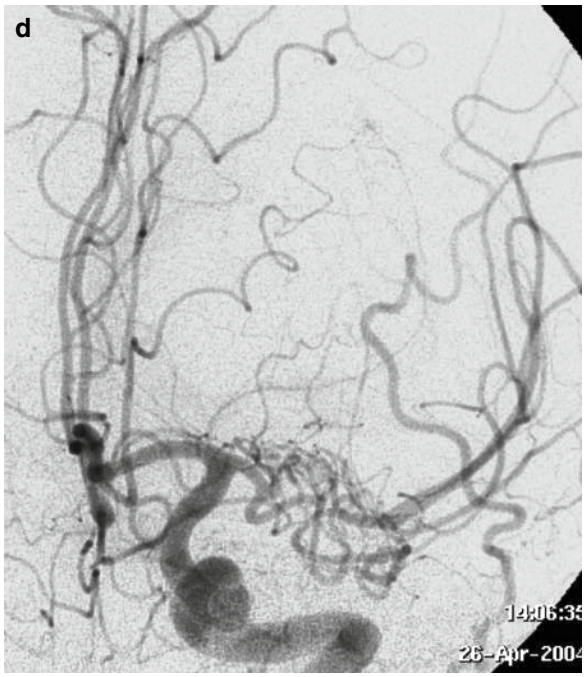

Fig. 17.5 (continued)

and it leads to ischemic stroke and hemorrhage. The latter is frequently due to small aneurysms present in the basal network.

17.4 Takayasu Arteritis

Takayasu arteritis is a granulomatous arteritis that affects the aorta and its main branches. The pathological changes are characterized by inflammatory infiltration of the artery wall by lymphocytes, plasma cells, and the presence of granulomas composed of giant cells. These pathological changes are similar to those found in giant cell arteritis, but the vessels involved are different and the affected patients are younger. On the angiogram, occlusion or stenosis of the common carotid artery and the VA at their origin is typical. Cerebral infarction and retinal ischemia occur (Fig. 17.7).

17.5 Sneddon's Syndrome

This is a syndrome with involvement of the cerebral vessels in patients with livedo reticularis. Sneddon's syndrome is a cutaneous condition that is characterized by a bluish reticulated aspect of the skin as a result of impaired superficial venous drainage. The cerebral angiogram of these patients shows occlusion of the distal branches of cerebral vessels, with a formation close to the occlusion of a typical network of capillaries and venules (Fig. 17.8). Multiple ischemia is present. Clinically, the disease is characterized by progressive strokes.

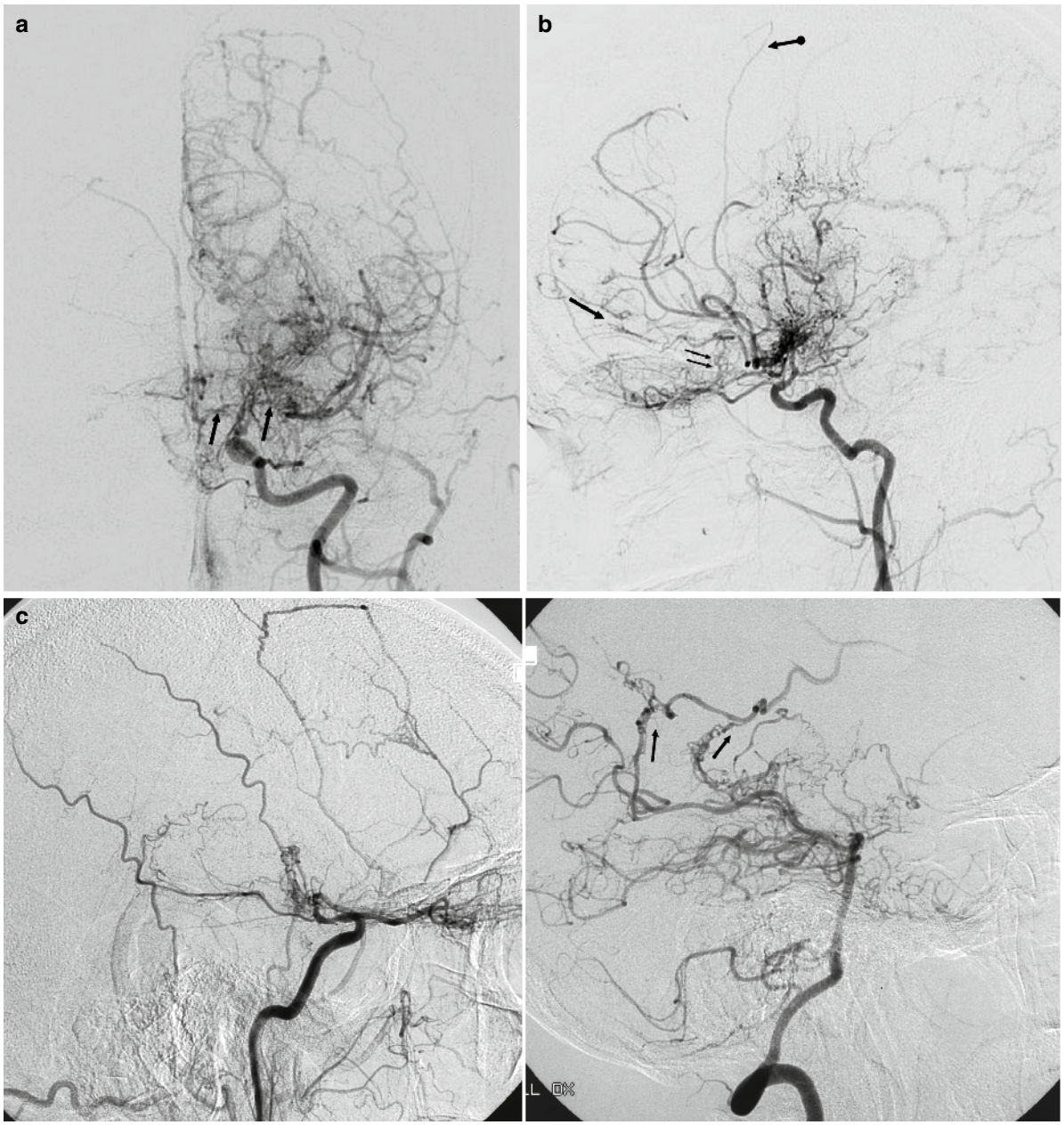

Fig. 17.6 Moyamoya disease in a young patient. (**a**) Common carotid angiogram, AP view. There is an irregular severe stenosis of the proximal M1 and A1 (*arrow*). Rich basal network involving perforators, acting probably as a collateral circulation toward the distal segments of the MCA and anterior cerebral artery (ACA). (**b**) On the lateral angiogram, there is the beginning of collateral flow toward the ACA through opening of an anastomosis from the anterior falx artery (*arrow*) and posterior ethmoidal arteries (*arrows*). There is also an initial collateral flow from the middle meningeal artery (MMA; *arrow with dot*). A partial filling of the distal pericallosal artery through anastomosis with the PCA is present. (**c**) Bilateral moyamoya disease in another patient. Lateral carotid angiogram. Complete occlusion of the ACA and MCA. Persistence of a minimal basal network. Beginning of a collateral circulation toward the anterior circulation from the left PCA visible on the left carotid angiogram and from the right PCA (*arrow*) visible on the vertebral angiogram. Partial involvement also of the MMA, recognizable on the left carotid angiogram

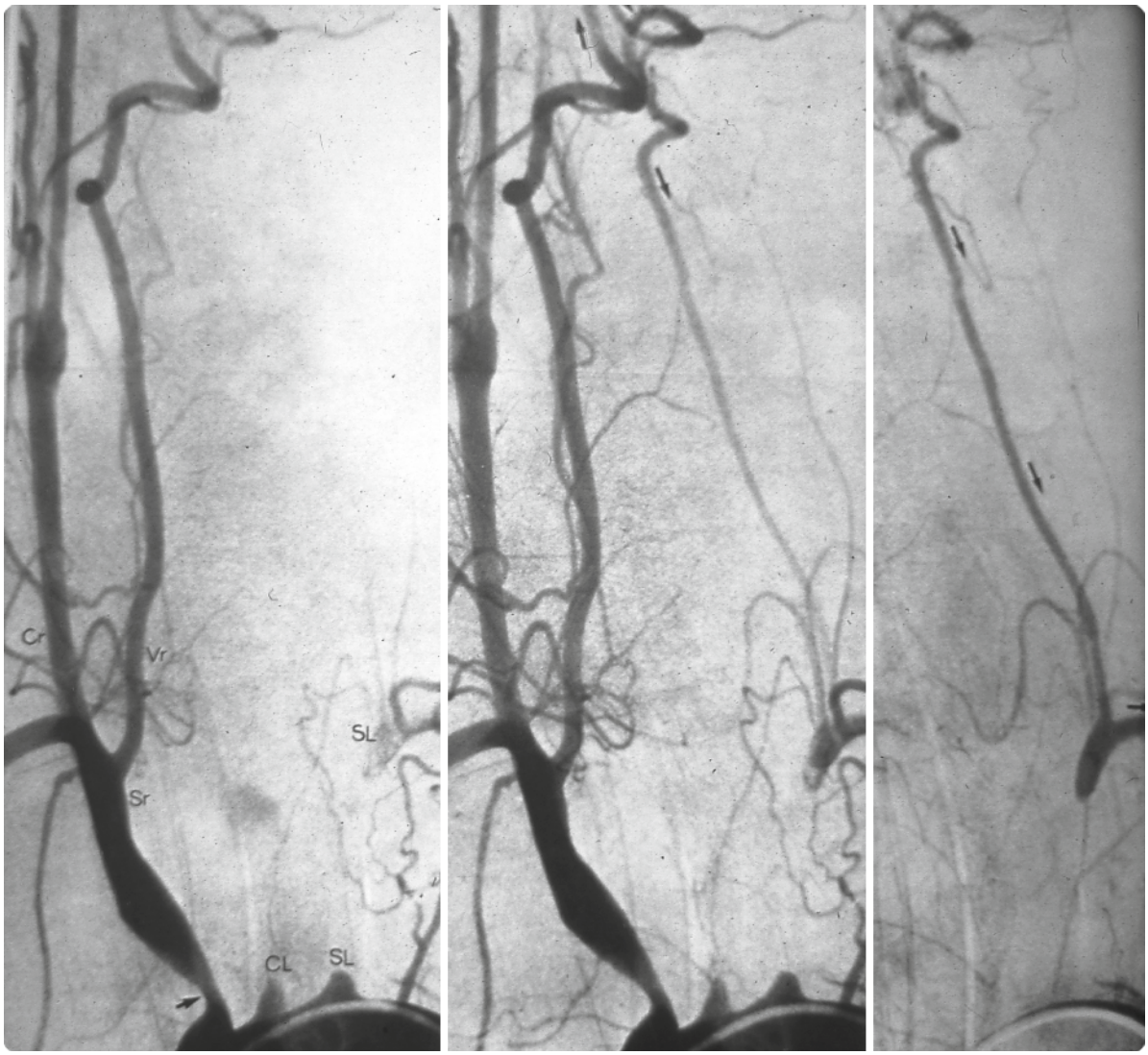

Fig. 17.7 Aortic arch angiogram in a patient with Takayasu arteritis. Occlusion of the left subclavian (*SL*) and left common carotid artery (*CL*). Severe stenosis of the brachiocephalic trunk. In the late phases, retrograde injection of the left vertebral and left subclavian artery (*arrows*) from the right vertebral-basilar artery (subclavian steal syndrome)

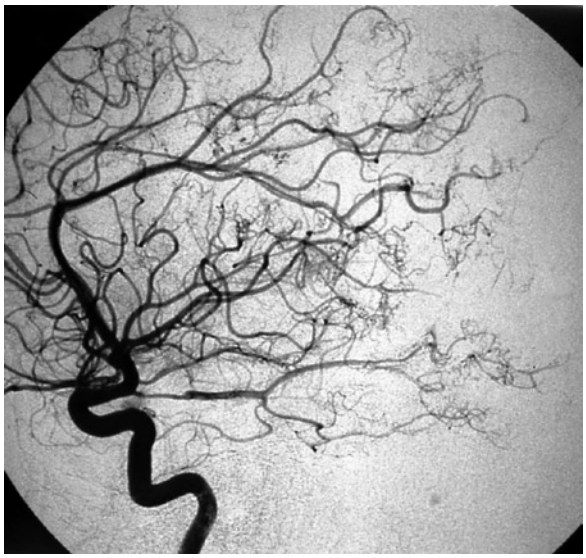

Fig. 17.8 Lateral carotid angiogram in a patient with Sneddon's syndrome. Several areas with the typical capillary network associated with vessel occlusion are evident

Cardiac Diseases

18

There are many cardiac diseases responsible for cerebral ischemia, which is frequently the result of emboli in patients with cardiac dysrhythmia, myocardial infarction, atrial septal aneurysm, cardiac valves diseases, prosthetic valves, endocarditis of various origins, and congenital heart diseases (Figs. 18.1–18.3). Recently, paradoxical embolism through a patent foramen ovale has become a frequent explanation for embolism (Lechat et al. 1988). Cardiac abnormalities responsible for embolization have been identified in systemic lupus erythematosus and in primary antiphospholipid antibody syndrome. Another rare pathology is myxoma. This is a tumor that commonly originates in the left atrium in young to middle-aged patients. The emboli consist of myxomatous tissue that leads to parenchymal tumoral localizations and vascular changes, with occlusion and aneurysmal dilation (New et al. 1970) (Fig. 18.4).

The commonest site of cardiac emboli is the anterior circulation, especially in the terminal internal cardiac artery and in the main trunk of the middle cerebral artery. The posterior circulation is less involved, with a typical location being that of the top of the basilar artery. The incidence of cardioembolism is reported to be 15–20% of all strokes. It is most frequent in young patients (Barnett 1974; Barnett et al. 1980; Bogousslavsky et al. 1988a, 1988b; Kittner et al. 1991; Broderick et al. 1992). As in other types of embolization, spontaneous rapid recanalization can occur, and so angiography performed later appears normal.

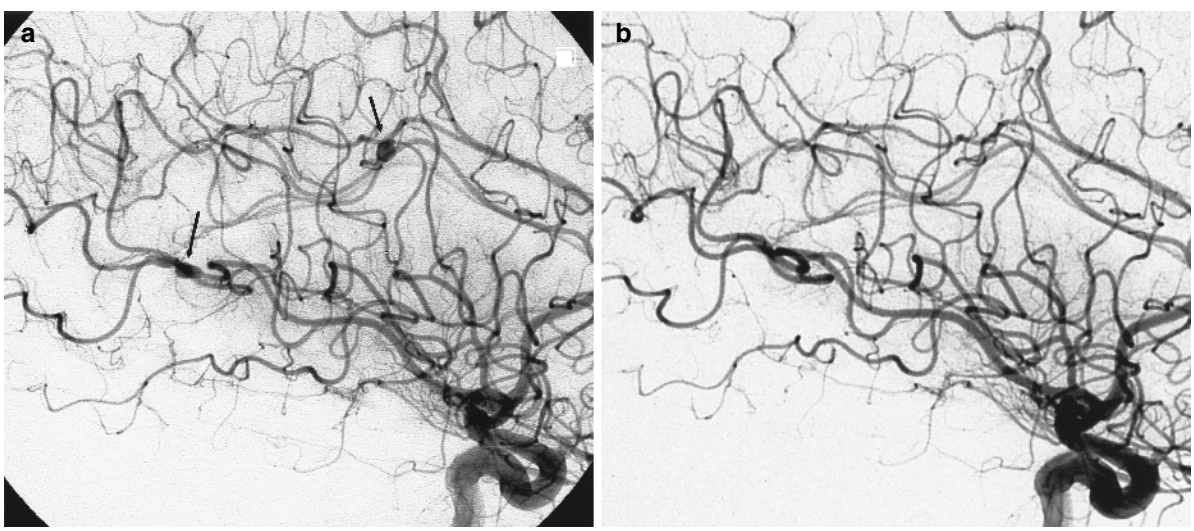

Fig. 18.1 Mycotic aneurysm in a patient with bacterial endocarditis. (**a**) Lateral carotid angiogram showing the aneurysms (*arrows*). (**b**) Control angiogram 2 months later after antibiotic therapy, showing disappearance of the aneurysm

G.B. Bradac, *Cerebral Angiography*,
DOI: 10.1007/978-3-642-15678-6_18, © Springer-Verlag Berlin Heidelberg 2011

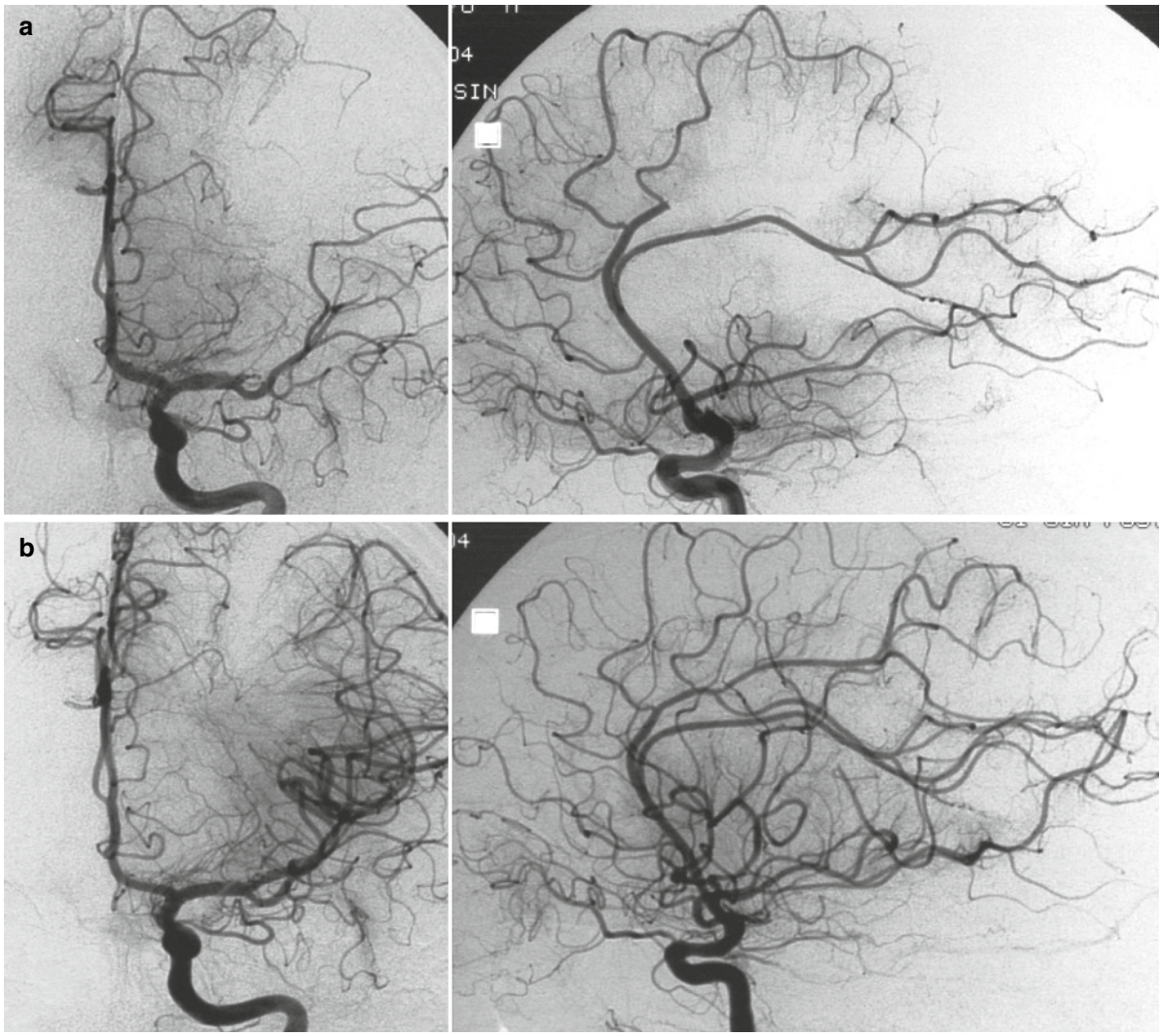

Fig. 18.2 Acute multiple occlusions involving branches of the middle cerebral artery and anterior cerebral artery in a middle-aged patient. (**a**) Carotid angiogram, AP and lateral views, showing multiple lesions. (**b**) Selective pharmacological thrombolysis, with reopening of the occlusions and good clinical results. A cardiac pathology was suspected. However, no cardiac disease was found

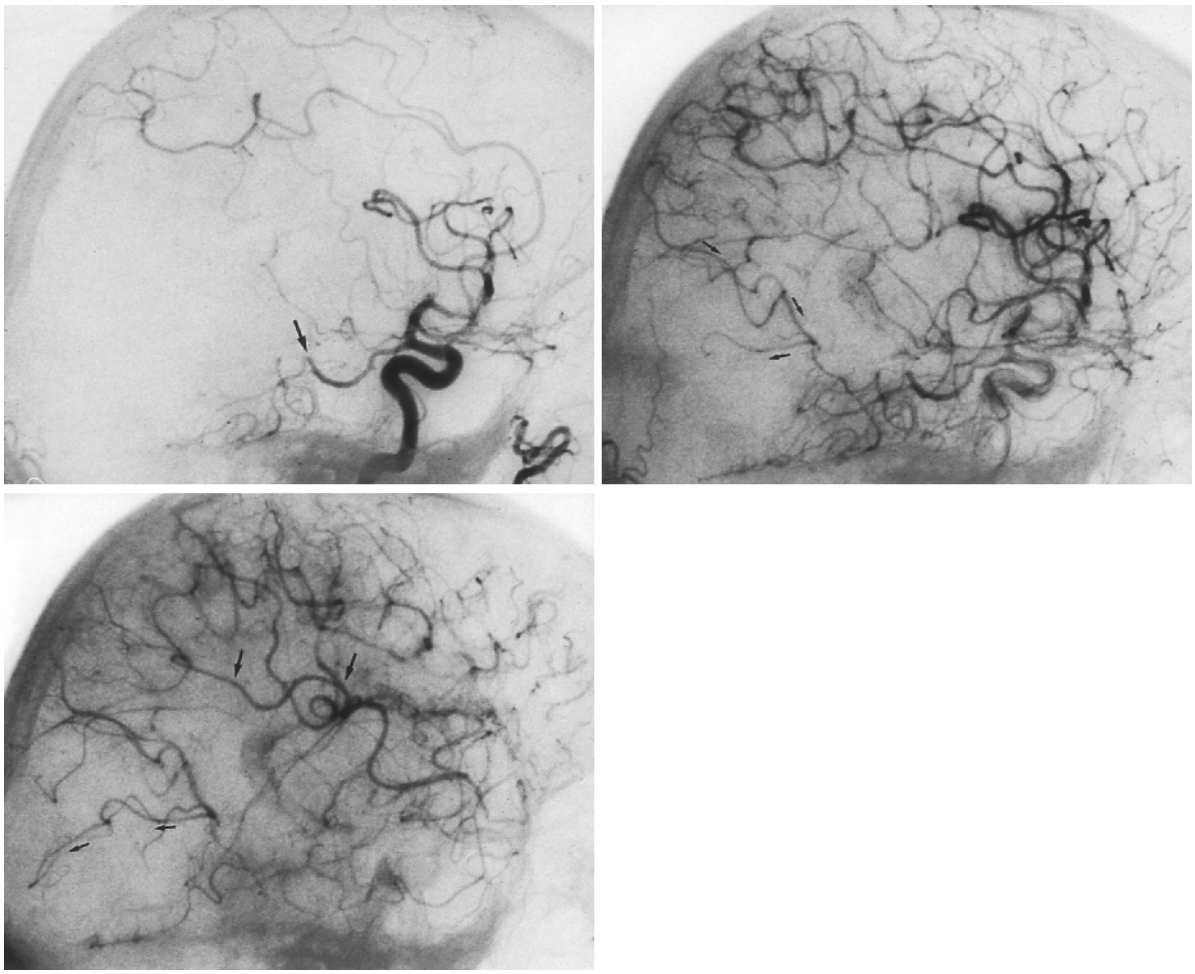

Fig. 18.3 Cardiac embolization in an old patient involving several branches of the middle cerebral artery and posterior cerebral artery (PCA; *arrow*), arising directly from the internal carotid artery. Partial retrograde injection of branches of the middle cerebral artery and distal branches of the PCA (*arrows*) through opening of pial anastomoses with the anterior cerebral artery

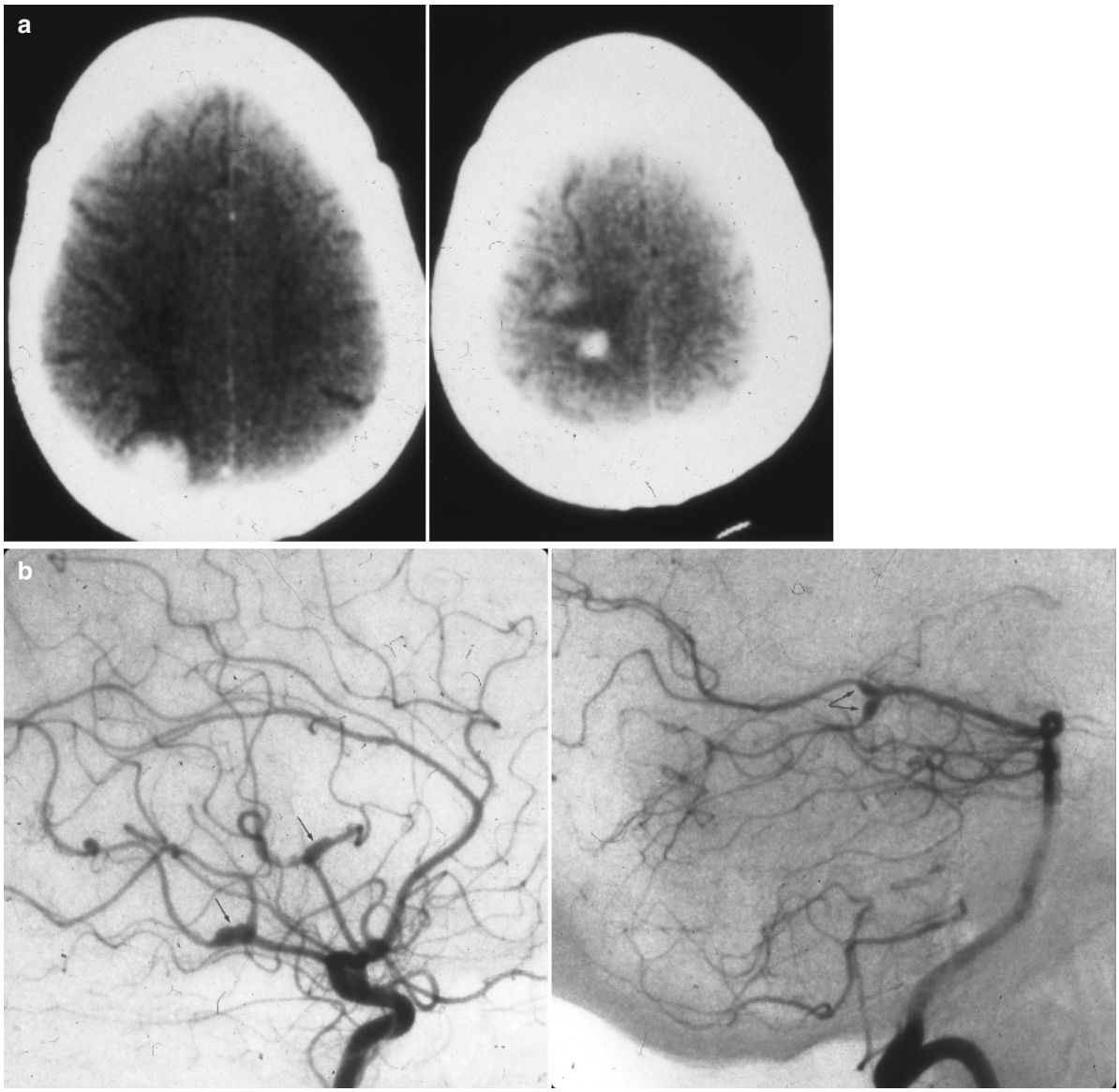

Fig. 18.4 Cerebral embolization in a patient with cardiac myxoma. (**a**) CT showing a parenchymal localization of the tumor emboli. (**b**) Carotid and vertebral angiogram disclosing aneurysmal dilatation due to tumoral infiltration of the vessel wall (*arrows*)

Arterial Occlusive Diseases in Children

19

Ischemia in children deserves some specific considerations. It is not as rare as is commonly thought (Barnes et al. 2004; Amlie-Lefond et al. 2009). Unlike in adults, it is rarely linked to factors related to atherosclerosis. Instead, it is associated with a variety of pathological processes, including cardiac diseases, spontaneous dissection, and other nonatherosclerotic arteriopathies, which are listed in the table in Chap. 17. In some cases, a precise etiology can be identified; in many others, however, it may only be suspected or remain unknown (Barnes et al. 2004; Jones et al. 2010).

Among the most frequent causes are infections, especially of the upper respiratory tract, and hematological diseases. Arteritis due to a previous Varicella-zoster infection can occur (Sebire et al. 1999; Barnes et al. 2004; Lauthier et al. 2005; Miravet et al. 2007; Jones et al. 2010). Primary cerebral angiitis has been emphasized by some authors (Elbers and Benseler 2008; Hajj-Ali and Calabrese 2009). Spontaneous dissection is another increasingly recognized cause of stroke in children (Schievink et al. 1994a; Fullerton et al. 2001; Rafay et al. 2006) (see Sect. 16.7).

The ischemia and vessel lesions in the form of stenosis or occlusion can be often diagnosed on CT and MRI as well as CT and MRI angiography. For a more detailed diagnosis, angiography remains the examination of choice. Control studies can show normalization of the vessels involved (Figs. 17.2, 17.3, and 16.11).

G.B. Bradac, *Cerebral Angiography*,
DOI: 10.1007/978-3-642-15678-6_19, © Springer-Verlag Berlin Heidelberg 2011

Cerebral Venous Thrombosis

20

Improvements in diagnostic methods, in particular angiography, MRI, and MRI angiography, have made it possible to identify this pathology in many patients. The true incidence of central venous thrombosis (CVT), however, remains unknown, even if there is no doubt that it is more frequent than had previously been thought (Krayenbuehl 1967; Ameri and Bousser 1992; Bousser et al. 1985; Einhäupl and Masuhr 1994; Bousser and Russell 1997; Linn and Brückmann 2010).

20.1 Etiopathogenesis

A frequent cause is infection, either intracranial extension of infectious diseases involving the skin-bone cavities of the craniofacial area or in cases of general bacterial septicemia or viral infection, especially due to HIV and cytomegalovirus. In young women, CVT occurs during pregnancy, in puerperium, and in patients using oral contraceptives. Other causes are pathologies of the red blood cells, such as thrombophilia, polycythemia, sickle cell disease, leukemia, and lymphoma, and in many coagulation disorders, such as protein C and S deficiency and disseminated intravascular coagulation. CVT also is frequent in patients with Behçet's disease, systemic lupus erythematosus, and in patients with severe dehydration and cardiac failure. Other causes are cranial trauma and neurosurgical intervention. Finally, intracranial tumors, especially meningiomas, can involve the adjacent sinus and cause thrombosis.

It should, however, be taken into consideration that in many cases—up to 35%—the cause remains unknown (Milandre et al. 1988; Ameri and Bousser 1992; Cantu and Barinagarrementeria 1993; Einhäupl and Masuhr 1994). As far as it concerns the sinus thrombosis in patients with dural arteriovenous fistulas, see Chap. 13.

20.2 Location

The superior sagittal sinus (SSS) is the venous channel most commonly involved, followed by the transverse sinus. Both are frequently involved together (Ameri and Bousser 1992; Cantu and Barinagarrementeria 1993; Tsai et al. 1995; Linn and Brückmann 2010). The thrombosis can be limited to the sinus, and the clinical presentation may frequently be characterized by clinical symptoms owing to intracranial hypertension, such as headache and visual disturbances. Cortical vein tributaries of the thrombosed sinus can be secondarily involved as a result of retrograde propagation of the thrombus, which commonly leads to ischemia.

Isolated cortical veins thrombosis may also occur. This had been thought to be very rare (Ameri and Bousser 1992; Einhäupl and Masuhr 1994). Recently, through improvement in MRI techniques and progressive awareness of this pathology, cases have been increasingly reported (Sagduyu et al. 2006; Boukobza et al. 2009; Albayram et al. 2009; Linn and Brückmann 2010). Moreover, the cortical veins can be an important collateral circulation, which, however, may be involved at any point of their course, leading to infarct (Bergui et al. 1999; Bradac and Bergui 2001).

Thrombosis of the deep venous system, involving the straight sinus and the vein of Galen, with retrograde extension to the internal cerebral and basal veins, is another usually severe condition that is, fortunately, less common. In these situations, transcerebral anastomoses via connections between the

G.B. Bradac, *Cerebral Angiography*,
DOI: 10.1007/978-3-642-15678-6_20, © Springer-Verlag Berlin Heidelberg 2011

superficial and deep medullary veins can act as an important collateral circulation and connect the superficial and deep venous systems (Bergui et al. 1999; Bradac and Bergui 2001).

Cavernous sinus thrombosis is another frequent localization, and it leads to a typical cavernous sinus syndrome. The lesion can extend to the inferior-superior petrosal sinus. Involvement of the intracavernous internal carotid artery, with arteritis leading to stenosis/occlusion, can occur (Segall et al. 1982). This is commonly due to infectious processes that involve the skin of the facial region, nose, paranasal sinuses, orbita, teeth, and middle ear.

20.3 Diagnosis

CT and MRI allow the detection of changes to the brain parenchyma in the form of hemorrhagic and/or nonhemorrhagic infarcts, uni- or bilateral, single or multiple, with various locations depending on the site and extension of the CVT. White matter hypodensity on CT and hyperintensity on T2 images on MRI, which indicate edema of a preceding venous infarct, is also a sign suggesting venous thrombosis. On CT, an abnormal hyperdensity can be recognized at the level of the torcular herophili, SSS, and lateral sinus. This is, however, difficult to differentiate in the majority of cases from the normally slight hyperdensity of this structure. Though it is not always present, a more reliable indicator is the so-called empty sign, which is visible after contrast injection and is due to opacification of the sinus wall contrasting with the low density of the thrombus in the lumen (Buonanno et al. 1978; Kingsley et al. 1978). In addition to CT, MRI is very useful in the diagnosis: it shows the hypointensity and isointensity of the thrombus in the involved sinus and occasionally in the cortical or deep veins, respectively, on T2-weighted turbo spin echo and T1-weighted spin-echo images in the acute phase. After three to five days, the clot becomes progressively hyperintense on both T1-T2 sequences. In this context, the high diagnostic value of the T2*-weighted gradient echo in identifying also isolated cortical vein thrombosis has been emphasized by some authors (Fellner et al. 2005; Urban and Müller-Forrell 2005; Boukobza et al. 2009; Linn and Brückmann 2010). Finally, in cases of suspected CVT, MRI angiography should be performed. However, in doubtful cases, or whenever a more specific diagnosis is required, angiography remains a practical diagnostic method. A rapid and precise diagnosis is important since anticoagulant therapy can improve the prognosis of these patients (Villringer et al. 1994) (Figs. 20.1–20.4).

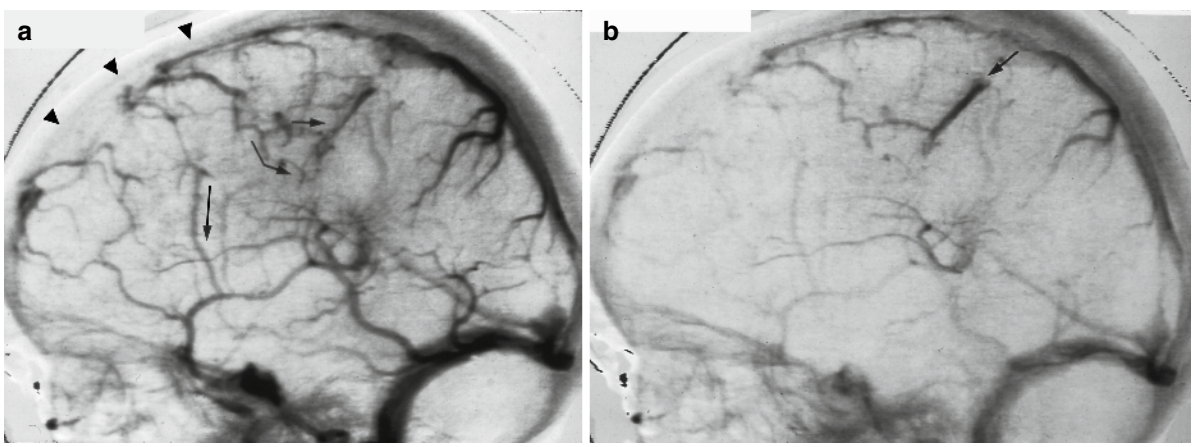

Fig. 20.1 Thrombosis of the anterior and middle segments of the superior sagittal sinus (SSS; *arrowheads*). Carotid angiogram, lateral view, venous phase (**a**). Rerouting of the venous drainage through cortical veins toward the parietal and temporal area. Some of these veins have a typical "corkscrew" appearance (*arrows*). Later phase (**b**). Distal occlusion of the cortical veins (*arrow*) probably explaining the parietal ischemia, visible on MRI (**c**)

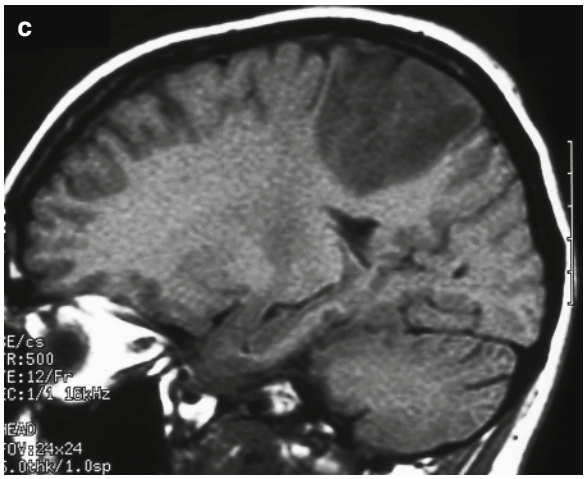

Fig. 20.1 (continued)

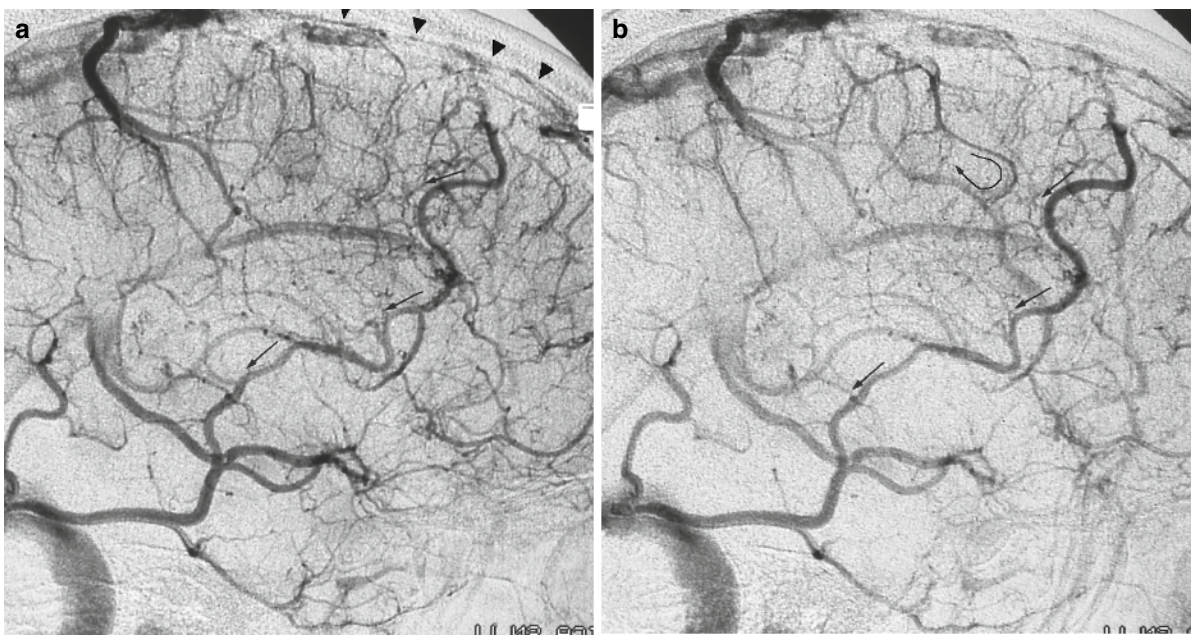

Fig. 20.2 Thrombosis of the anterior and middle segments of the SSS (*arrowheads*) involving also the distal segment of the draining cortical veins. Carotid angiogram, lateral view, venous phase (**a**). Rerouting of the venous drainage through a large vein of Trolard into the vein of Labbé (*arrows*). Later phase, (**b**) partial reorganized venous drainage in the parietal area (*curved arrow*) toward the patent segment of the SSS

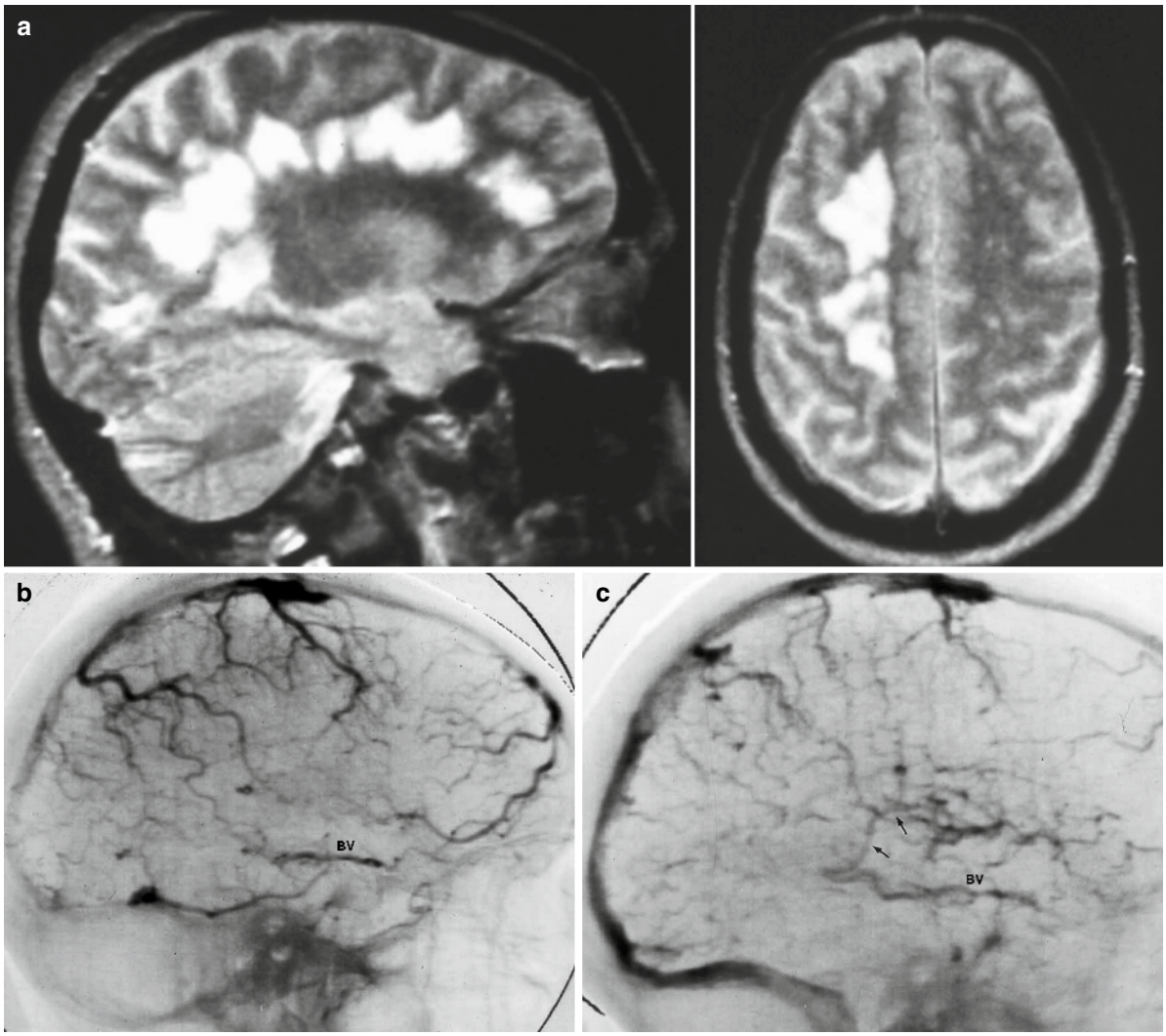

Fig. 20.3 Venous thrombosis involving the deep venous system. MRI, sagittal and axial views, T2-weighted images (**a**) showing changes corresponding to venous ischemia involving predominantly the white matter of the right hemisphere. Right (**b**) and left (**c**) carotid angiogram, venous phase. The vein of Galen and straight sinus are not injected. On the right, only the proximal part of the basal vein (*BV*) is recognizable, filled through its anterior tributaries. On the left, in addition to the basal vein reaching the proximal part of the vein of Galen, there is filling of the internal cerebral vein (*arrow*). It is conceivable that a collateral circulation involving the subependymal and medullary veins toward the cortical veins has developed, explaining the absence of ischemia in the left hemisphere

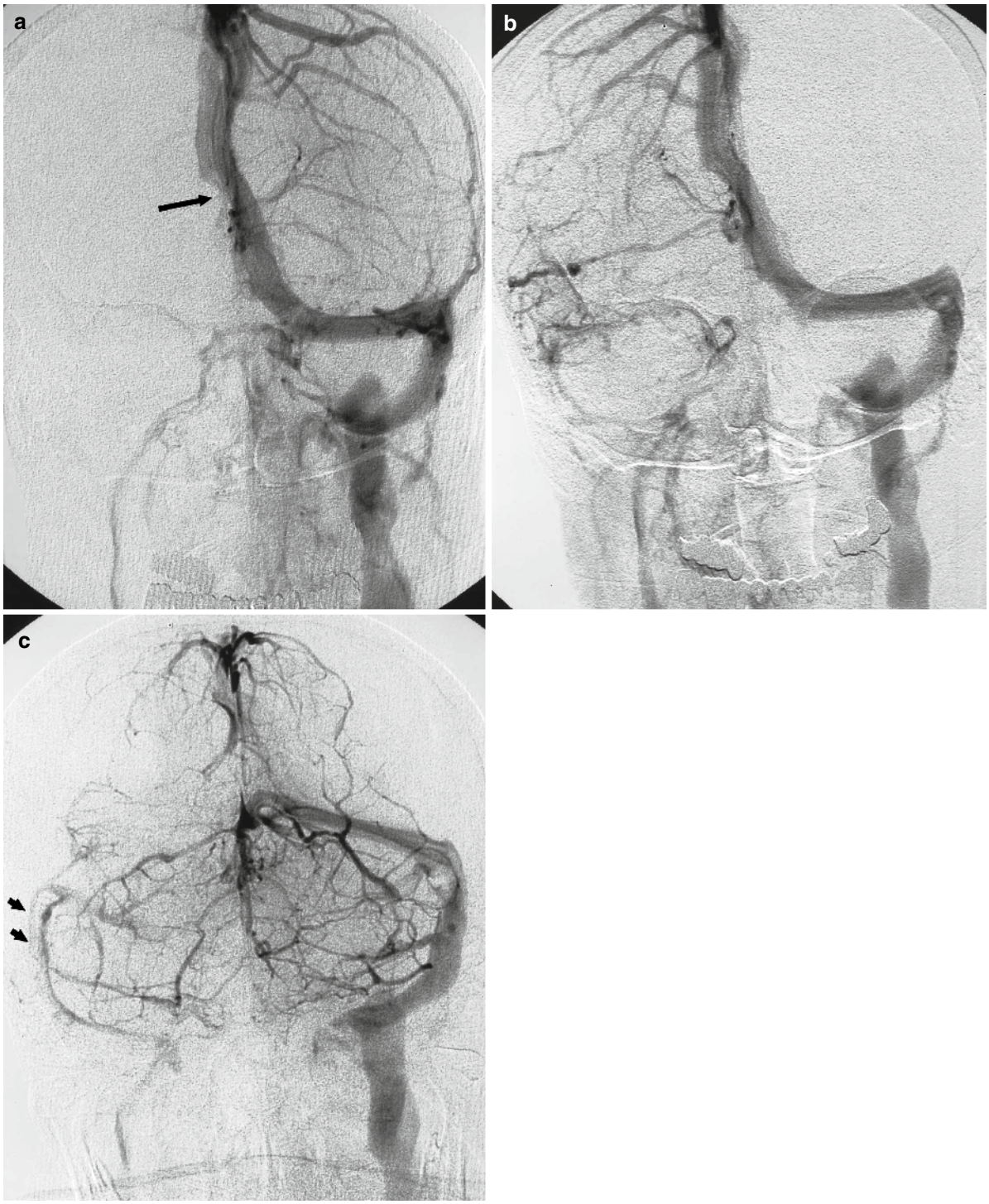

Fig. 20.4 Venous thrombosis involving the distal portion of the right segment of the duplicated SSS extending to the transverse sinus (TS). Old female patient with headache. The MRI study disclosed hyperintensity on T1-weighted images of the right TS. Angiography confirmed the suspected diagnosis of sinus thrombosis. (**a**, **b**) Left and right carotid angiogram, venous phase. There is no opacification of the distal right segment of the SSS (*arrow*) and right TS. Both internal cerebral veins are recognizable. They drain into the vein of Galen, continuing to the straight sinus and entering the left segment of the SSS, well visible on the lateral angiogram (not demonstrated). (**c**) Vertebral angiogram. The minimal laminar injection of the TS (*arrows*) allows identification of the thrombus

References

Abbie AA (1933) The clinical significance of the anterior choroidal artery. Brain 56:233

Abbie AA (1934) The morphology of the fore-brain arteries with especial reference to the evolution of the basal ganglia. J Anat 68:28

Abe M, Tabuchi K, Yokoyama H et al (1998) Blood blister like aneurysms of the internal carotid artery. J Neurosurg 89:419

Abiko M, Ikawa F, Ohbayashi N et al (2008) Endovascular treatment for dural arteriovenous fistula of the anterior condylar confluenc involving the anterior condylar vein. A report of two cases. Intervent Neuroradiol 14:313

Achrol AS, Pawlikowska L, Mc Culloch CE et al (2006) Tumor necrosis factor-alpha-238 G>A promoter polymorphism is associated with increased risk of new haemorrhage in the natural course of patients with brain arteriovenous malformations. Stroke 37:231

Agid R, Willinsky RA, How C et al (2004) Targeted compartimental embolization of cavernous sinus dural arteriovenous fistulae using transfemoral medial and lateral facial vein approaches. Neuroradiology 46:456

Agid R, TerBrugge KG, Rodesch G et al (2009) Management strategies for anterior cranial fossa (ethmoidal) dural arteriovenous fistulae with emphasis on endovascular treatment. J Neurosurg 110:79

Ahmad I, Tominaga T, Suzuki M et al (1994) Primitive trigeminal artery associated with cavernous aneurysm. Case report. Surg Neurol 41:75

Albayram S, Kara B, Ipek H et al (2009) Isolated cortical venous thrombosis associated with intracranial hypotension syndrome. Headache 49:916

Alexander CB, Burger PC, Goree JA (1979) Dissecting aneurysms of the basilar artery in two patients. Stroke 10:294

Alkadhi H, Kollias SS, Crelier GR et al (2000) Plasticity of the human motor cortex in patient with arterio – venous malformations: a functional MR imaging study. Am J Neuroradiol 21:1423

Alves JV, Andersson T, Edner G et al (2005) Subarachnoid haemorrhage from a large cerebral aneurysm visible only on repeated angiography. Interv Neuroradiol 11:59

Amarenco P, Caplan L (1993) Vertebrobasilar occlusive disease: review of selected aspects. 3. Mechanisms of cerebellar infarctions. Cerebrovasc Dis 3:66

Amarenco P, Hauw JJ, Gautier JC (1990) Arterial pathology in cerebellar infarction. Stroke 21:1299

Amarenco P, Levy C, Cohen A et al (1994) Causes and mechanisms of territorial and non territorial cerebellar infarcts in 115 consecutive cases. Stroke 25:105

Amarenco P, Caplan L, Pessin MS (1998) Vertebrobasilar occlusive disease. In: Barnett HJM, Mohr JP, Stein BM, Yatsu FM (eds) Stroke. Churchill Livingstone, New York/London, pp 551–570

Ameri A, Bousser MG (1992) Cerebral venous thrombosis. Neurol Clin 10:87

Amlie-Lefond C, Bernard TJ, Sebire G et al (2009) International pediatric study subgroup. Predictors of cerebral arteriopathy in children with arterial ischemic stroke: results of the international pediatric stroke study. Circulation 119:1417

Andersen PE (1970) Fibromuscular hyperplasia of the carotid arteries. Acta Radiologica 10:90

Anderson CA, Collins GJ Jr, Rich NM (1980) Spontaneous dissection of the internal carotid artery associated with fibromuscular dysplasia. Am Surg 4:263

Angeloni V, Bozzao L, Fantozzi LM et al (1990) Internal border-zone infarction following acute middle cerebral artery occlusion. Neurology 40:1196

Antunes JL, Correll JW (1976) Cerebral emboli from intracranial aneurysms. Surg Neurol 6:7

Anxionnat R, Ferreira de Melo Neto J, Bracard S, et al (2003) Treatment of heorrhagic intracranial dissections. Neorosurgery 53:289

Arat A, Jslak C, Saatci I (2002) Endovascular parent artery occlusion in large-giant or fusiform distal posterior cerebral artery aneurysms. Neuroradiology 44:700

Archie JP, Feldtman RW (1981) Critical stenosis of the internal carotid artery. Surgery 89:67

Arnold M, Schroth G, Nedeltchev K et al (2002) Intraarterial thrombolysis in 100 patients with acute stroke due to middle cerebral artery occlusion. Stroke 33:1828

Arnold M, Nedeltchev K, Schroth G et al (2004) Clinical and radiological predictors of recanalisation and outcome of 40 patients with acute basilar artery occlusion treated with intraarterial thrombolysis. J Neurol Neurosurg Psychiatry 75:857

Awad IA (1993) Dural arteriovenous malformations with aggressive clinical course. In: Awad IA, Barrow DL (eds) Dural arteriovenous malformations. AANS, Park Ridge

Awad IA, Little JR, Akravi WP et al (1990) Intracranial dural arteriovenous malformation: factors predisposing to an aggressive neurological course. J Neurosurg 72:839

DOI: 10.1007/978-3-642-15678-6, © Springer-Verlag Berlin Heidelberg 2011

Babin E (1971) Contribution a l'etude radioanatomique de la veine basilaire normale et des ses affluents. Diplome d' Electroradiologie, Strasbourg

Bahar F, Chiras JP et al (1984) Spontaneous vertebral arteriovenous fistula associated with fibromuscular dysplasia. Neuroradiology 26:45

Bamford J, Sandercock P, Jones L et al (1987) The natural history of lacunar infarction. The Oxfordshire Community Stroke Project. Stroke 18:5

Bandeira A, Ribeiro C, Reis J (2007) Treatment of vasospasm secondary to subarachnoid haemorrhage using intraarterial nimodipine in low dosage. Interv Neuroradiol 13:403

Barnes C, Newall F, Furmedge J et al (2004) Arterial ischemic stroke in children. J Paediatr Child Health 40:384

Barnett HJM (1974) Transient cerebral ischemia: pathogenesis, prognosis and management. Ann R Coll Physicians Surg Can 7:153

Barnett HJM, Boughner DR, Taylor WD et al (1980) Further evidence relating mitral-valve prolapse to cerebral ischemic events. N Engl J Med 302:149

Barnwell SL, Halbach VV, Dowd CF et al (1990) Dural arteriovenous fistulas the inferior petrosal sinus: angiographic finding in 6 patients. Am J Neuroradiol 11:511

Barnwell SL, Halbach VV, Dowd CF et al (1991) A variant of arteriovenous fistulas within the wall of dural sinuses. J Neurosurg 74:199

Barrow DL, Spector RH, Braun IF et al (1985) Classification and treatment of spontaneous carotid-cavernous sinus fistulas. J Neurosurg 62:248

Bassetti C, Bougouslavsky J, Eskenasy-Cottier AL et al (1994) Spontaneous intracranial dissection in the anterior circulation. Cerebrovasc Dis 4:170

Beach KW, Hatsukami T, Detmer PR et al (1993) Carotid artery intraplaque haemorrhage and stenotic velocity. Stroke 23:314

Beigelman C, Mowrey-Gerosa I, Gamsu G et al (1995) New morphologic approach to the classification of anomalies of the aortic arch. Eur Radiol 5:435

Bekov DB (1965) Some structural differences among posterolateral tributaries of the great cerebral vein. Fed Proc Transl Suppl 24:166

Beltramello A, Zampieri P, Ricciardi GK et al (2005) Combined treatment of brain AVMs: analysis of 5 years (2000–2004) in the Verona experience. Interv Neuroradiol 11(Suppl 1):63

Ben Amor M, Maion CH, Heldt N (1971) Normal and pathological radioanatomy of the superior choroid vein. Neuroradiology 3:16

Benndorf G, Campi A (2002) Aberrant inferior petrosal sinus: unusual transvernous approach to the cavernous sinus. Neuroradiology 44:158

Benndorf G, Lehman TN, Molsen HP et al (1999) Punture of the superficial sylvian vein for embolization of cavernous dural arteriovenous fistula. Interv Neuroradiol 5:167

Benndorf G, Bender A et al (2001) Treatment of cavernous sinus dural arteriovenous fistula by deep puncture of the superior ophthalmic vein. Neuroradiology 43:499

Berenstein A, Kricheff II (1979) Balloon catether of the investigating of carotid cavernous fistulas. Radiology 132:762

Berenstein A, Lasjaunias P (1992) Endovascular treatment of cerebral lesions, vol 4. Springer, Berlin/Heidelberg

Berger MS, Wilson CB (1984) Intracranial dissecting aneurysms of the posterior circulation. Report of six cases and review of the literature. J Neurosurg 61:882

Bergui M, Bradac GB (1997) Uncommon symptomatic cerebrovascular malformations. Am J Neuroradiol 18:779

Bergui M, Bradac GB, Daniele D (1999) Brain lesions due to cerebral venous thrombosis do not correlate with sinus involvement. Neuroradiology 41:419

Bergui M, Stura G, Daniele D et al (2006) Mechanical thrombolisis in ischemic stroke attributable to basilar artery occlusion as first-line treatment. Stroke 37:145

Berkefeld J, Zanella FE (2009) Intracranial stenting of atherosclerotic stenosis, current status and perspectives. Clin Neuroradiol 19:38

Berkefeld J, Du Mesnil de Rochemont R, Rohde S et al (2003) Intracranial stenting of high grade atherosclerotic stenoses. Follow up results in elective cases. Riv Neuroradiol 16:1330

Bernasconi V, Cassinari V (1957) Caratteristiche angiografiche dei meningiomi del tentorio. Radiol Med 43:1015

Biondi A, Ricciardi GK, Puybasset L et al (2004) Intraarterial nimodipine for the treatment of symptomatic cerebral vasospasm after aneurysmal subarachnoid haemorrhage: preliminary results. Am J Neuroradiol 25:1067

Biondi A, Pescillo S, Daumas-Duport B et al (2009) Blood blister-like aneurysms of the supraclinoid internal carotid artery: high risk lesions with difficult management. Interv Neuroradiol 15(Suppl 1):126

Bisaria KK (1984) Anomalies of the posterior communicating artery and their potential clinical significance. J Neurosurg 60:572

Bladin GF, Chambers BR (1993) Clinical features, pathogenesis and computed tomographic characteristic of internal watershed infarction. Stroke 24:1925

Boccardi E, Branca V, Valvassori L et al (1998) Endovascular treatment with GDCs: results in 100 patients. J Neurosurg Sci 42(Suppl 1):127–129

Bogousslavsky J, Regli F (1992) Centrum ovale infarcts: subcortical infarction in the superficial territory of the middle cerebral artery. Neurology 42:1992

Bogousslavsky J, Despland PA, Regli F (1987) Spontaneous carotid dissection with acute stroke. Arch Neurol 44:137

Bogousslavsky J, Regli F, Huske A (1988a) Thalamic infarcts: clinical syndromes aethiology and prognosis. Neurology 38:837

Bogousslavsky J, van Melle G, Regli F (1988b) The lacunar stroke registry: analysis of 1000 consecutive patients with first stroke. Stroke 19:1083

Bogousslavsky J, Regli F, Maeder PH (1991) Intracranial large artery disease and lacunar infarction. Cerebrovasc Dis 1:154

Boguosslavsky J, Regli F (1986) Borderzone infarctions distal to internal carotid artery occlusion: prognostic implications. Ann Neurol 20:346

Boiten J, Lodder J (1991) Lacunar infarcts. Pathogenesis and validity of the clinical syndromes. Stroke 22:1374

Bojanowski MW, Laroche M, Leveque M et al (2009) Surgical treatment of blister-like aneurysms. Interv Neuroradiol 15(Suppl 1):126

Boker DK, Solymosi L, Wassmann H (1985) Immediate post angiographic intraarterial treatment of cerebral vasospasm after subarachnoid haemorrhage with nimodipine, report of three cases. Neurochirurgie (Stuttgart) 28:118

Bonaldi G (2002) Angioplasty and stenting of the cervical carotid bifurcation: report of a 4 year series. Neuroradiology 44:164

Borden JA, Wu JK, Schucart WA (1995) A proposed classification for spinal and cranial dural arteriovenous fistulous malformations and implications for treatment. J Neurosurg 82:166

Bose A, Hartmann M, Henkes H et al (2007) A novel self expanding nitinol stent in medically refractary intracranial atherosclerotic stenosis: the Wingspan study. Stroke 38:1531

Bostrom K, Liliequist B (1967) Primary dissecting aneurysm of the extracranial part of the internal carotid and vertebral artery. Neurology 17:179

Boukobza M, Crassard I, Bousser MG et al (2009) MR images features of isolated cortical vein thrombosis: diagnosis and follow up. Am J Neuroradiol 30:344

Bousser MG, Russell RR (1997) Cerebral venous thrombosis. Saunders, London

Bousser MG, Chiras J, Sauron B et al (1985) Cerebral venous thrombosis. A review of 38 cases. Stroke 16:199

Bracard S, Arrue P, Banal FC et al (1999) Management of vasospasm from subarachnoid haemorrhage: attitude of French Center-French Society of Neuroradiology. J Neuroradiol (Masson) 26(Suppl 1):44

Bradac GB (1970) The pontomesencefalic veins (Radioanatomical study). Neuroradiology 1:52

Bradac GB, Bergui M (2001) Role of the different venous structures involved in cerebral venous thrombosis. Klin Neuroradiol 11:20

Bradac GB, Bergui M (2004) Endovascular treatment of the posterior inferior cerebellar artery aneurysms. Neuroradiology 46:1006

Bradac GB, Bergui M, Ferrio MF et al (1997) False-negative angiograms in subarachnoid haemorrhage due to intracranial aneurysms. Neuroradiology 39:772

Bradac GB, Heymat F (1970) Considerations concerning a case of fibromuscolar hyperplasia of the carotid arteries. Neuroradiology 1:217

Bradac GB, Oberson R (1983) Angiography and computed tomography in cerebro-arterial occlusive diseases. Springer, Berlin/Heidelberg

Bradac GB, Wackenheim A, Braun JP (1967) Contribution a l'etude des phlebogramme de l'angiographie vertebrale. Neurochirurgie (Stuttgart) 12:1

Bradac GB, Holdorff B, Simon RS (1971) Aspects of the venous drainage of the pons and mesencephalon. Neuroradiology 3:102

Bradac GB, Simon RS, Leonhardt W (1974) The ophthalmic vein in the carotid angiogram. Neuroradiology 8:39

Bradac GB, Kaernbach A, Bolk-Weiscedel D et al (1981) Spontaneous dissecting aneurysm of cervical cerebral arteries. Report of six cases and review of the literature. Neuroradiology 21:149

Bradac GB, Bender A, Curio G et al (1985) Report of two cases of spontaneous direct carotido-cavernous fistula. Diagnostic and therapeutic considerations. Neuroradiology 27:436

Bradac GB, Riva A, Schörner W et al (1987) Cavernous sinus meningiomas: an MRI study. Neuroradiology 29:578

Bradac GB, Riva A, Stura G et al (1989) Dissection spontanée de la carotide interne aves paralyse du XII. J Neuroradiol (Masson) 16:197

Bradac GB, Ferszt R, Kendall BE (1990) Cranial meningiomas diagnosis, biology, therapy. Springer, Berlin/Heidelberg

Bradac GB, Bergui M, Ferrio MF et al (2000) Cranial nerve palsy in spontaneous dissection of the internal carotid artery. Klin Neuroradiol 10:1

Bradac GB, Bergui M, Stura G (2001) Endovascular treatment of brain arteriovenous malformations. Riv Neuroradiol 14:373

Bradac GB, Bergui M, Genovese E (2002) Considerations about ischemia in intracranial dural arterovenous fistula. Klin Neuroradiol 12:40

Bradac GB, Bergui M, Stura G et al (2007) Periprocedural morbidity and mortality by endovascular treatment of cerebral aneurysms with GDG: a retrospective 12 year experience of a single center. Neurosurg Rev 30:117

Bradac GB, Peretta P, Stura G et al (2008a) Paediatric dissecting aneurysms of the posterior cerebral artery, case report and review of the literature. Interv Neuroradiol 14:325

Bradac GB, Daniele D, Bergui M et al (2008b) Lacunes and other holes: diagnosis, pathogenesis, therapy. Neuroradiol J 21:35

Brandt T, Sternke W, Thie A et al (2000) Posterior cerebral artery territory infarcts: clinical features, infarct topography, causes and outcome. Cerebrovasc Dis 10:170

Brassier G, Morandi X, Fournier D et al (1998) Origin of the perforating arteries of interpeduncular fossa in relation to the termination of the basilar artery. Interv Neuroradiol 4:109

Brice JG, Dowsett DJ, Lowe RD (1964) Haemodynamic effect of carotid artery stenosis. Br Med J 2:1363

Brismar J (1976) Persistent hypoglossal artery, diagnostic criteria. Acta Radiol Diagn 17:160

Brocheriou I, Capron F (2004) Malformations arteriovenouses intracraniennes. Aspects anatomo-pathologiques. J Neuroradiol (Masson) 31:359

Broderick JP, Phillips SJ, O'Fallon M et al (1992) Relationship of cardiac disease to stroke occurrence, recurrence and mortality. Stroke 23:1250

Brunsteins DB, Ferreri AJ (1990) Microsurgical anatomy of VII and VIII cranial nerves and related arteries in the cerebellopontine angle. Surg Radiol Anat 12:259

Bull J, Kozlowski P (1970) The angiographic pattern of the petrosal veins in the normal and pathological. Neuroradiology 1:20

Bulsara KR, Alesander MJ, Villavicencio AJ et al (2002) De novo cerebral arteriovenous malformations: case report. Neurosurgery 50:1137

Buonanno F, Moody DM, Ball MR et al (1978) Computed cranial tomographic findings in cerebral sinuses-venous occlusion. J Comput Assist Tomogr 2:281

Burrows PE, Robertson RL, Barnes PD (1996) Angiography and the evaluation of cerebrovascular disease in childhood. Neuroimaging Clin N Am 6:561

Buyle M, Engelborghs S, Kuneren J et al (2001) Headache as only symptom in multiple cervical artery dissection. Headache 41:509

Calzolari F (2002) Unusual termination of the inferior petrosal sinus. Neuroradiology 44:796

Cantu C, Barrinagarrementeria F (1993) Cerebral venous thrombosis associated with pregnancy and puerperium. Review of 67 cases. Stroke 24:1880

Caplan LR (1980) "Top of the basilar" syndrome: selected clinical aspects. Neurology (NY) 30:72

Caplan LR (1989) Intracranial branch atheromatous disease: a neglected, understudied and underused concept. Neurology (NY) 39:1246

Caplan LR (1996) Posterior circulation disease. Blackwell, Cambridge

Caplan LR, Gorelick PB, Hier DB (1986) Race, sex, and occlusive cerebrovascular disease: a review. Stroke 17:648

Caplan LR, Baquis GD, Pessin MS et al (1988a) Dissection of intracranial vertebral artery. Neurology 38:868

Caplan LR, Dewitt LD, Pessin MS et al (1988b) Lateral thalamic infarcts. Arch Neurol 45:959

Carmichel R (1950) The pathogenesis of non inflammatory cerebral aneurysms. J Path Bact 62:1

Carpenter MB, Noback CR, Moss ML (1954) The anterior choroidal artery. The origin, course, distribution and variations. Arch Neurol Psychiatry 71:714

Castaigne P, Lhermitte F, Gautier JC et al (1973) Arterial occlusions in the vertebral basilar system. Brain 96:133

Castaigne P, Bories J, Brunet P et al (1976) Les fistulas arterioveneuses meningées a drainage venoux cortical. Rev Neurol 132:169

Castaigne P, Lhermitte F, Buge A et al (1981) Paramedian thalamic and midbrain infarcts: clinical and neuropathological study. Ann Neurol 10:127

Cebral JR, Castro MA, Burgess JE et al (2005) Characterisation of cerebral aneurysms for assessing risk of rupture by using patient-specific computational haemodynamics models. Am J Neuroradiol 26:2550

Cellerini M, Mangiafico S, Ammannati F et al (2008) Ruptured dissecting posterior inferior cerebella artery aneurysms: endovascular treatment without parent vessel occlusion. Neuroradiology 50:315

Challa VR, Moody DM, Brown WR (1995) Vascular malformations of the central nervous system. J Neuropathol Exp Neurol 54:609

Chaloupka J, Putman C, Awad I (1996) Endovascular therapeutic approach to peripheral anedurysm of the superior cerebellar artery. AJNR Am J Neuroradiol 17:1338

Chaloupka JC, Huddle DC (1998) Classification of vascular malformations of the central nervous system. Neuroimaging Clin N Am 8:295

Chapot R, Stracke P, Meyn H et al (2009) Experience with Silk in 25 aneurysms. Interv Neuroradiol 15(Suppl 1):112

Chase NE, Taveras JM (1963) Temporal tumors studied by serial angiography. A review of 150 cases. Acta Radiol Diagn 1:225

Chaturvedi S, Caplan LR (2003) Angioplasty for intracranial atherosclerosis. Is the treatment worse than the disease? Neurology 61:1647

Chaudary MY, Sachdev VP, Cho CH et al (1982) Dural arteriovenous malformation of the major venous sinuses. An acquired lesion. Am J Neuroradiol 3:13

Cheng KM, Chan CM, Cheung JL et al (1999) Transvenous embolization of spontaneous carotid-cavernous fistulas by sequential occlusion of the cavernous sinus. Interv Neuroradiol 5:225

Chiras J, Marciano S, Vega Molina J et al (1985) Spontaneous dissecting aneurysms of the extracranial vertebral artery (20 cases). Neuroradiology 27:327

Choi JW, Kim JK, Choi BS et al (2009) Adjuvant revascularisation of intracranial artery occlusion with angioplasty and/or stenting. Neuroradiology 51:33

Chyatte D, Mjerzejewski C (1991) Novel restriction fragment length polymorphism associated with gene for type III collagen (COL3A1) in patients with cerebral aneurysms. Congress of Neurological Surgeons, Orlando, p 163

Chyatte D, Brophy C, Reilly J et al (1990) Morphometric analysis of reticular elastic and Type III collagen fibers in the cerebral arteries of patients with intracranial aneurysms. Stroke 21:161

Ciceri EF, Klucznik RP, Grossman RG et al (2001) Aneurysms of the posterior cerebral artery: classification and endovascular treatment. AJNR Am J Neuroradiol 22:27

Clark WM (2010) On behalf of the CREST investigators. Carotid revascularisation endarterectomy versus stenting trial. Paper presented at the International stroke conference, San Antonio 2010

Cognard C, Gobin YP, Pierot L et al (1995) Cerebral dural arteriovenous fistulas: clinical and angiographic correlations with revised classification of venous drainage. Radiology 194:671

Cohen JE, Gomori JM, Umansky F (2003) Endovascular management of spontaneous bilateral symptomatic vertebral artery dissections. Am J Neuroradiol 24:2052

Collice M, D'Aliberti G, Arena O et al (2000) Surgical treatment of the intracranial dural arteriovenous fistulae: role of the venous drainage. Neurosurgery 47:56

Colombo F, Pozza F, Chierego G et al (1994) Linear accelerator radiosurgery of cerebral arteriovenous malformations: an update. Neurosurgery 34:14

Countee RW, Vijayanathan T (1979) External carotid in internal carotid artery occlusion. Angiographic, therapeutic and prognostic considerations. Stroke 10:450

Countee RW, Vijayanathan T, Chavis P (1981) Recurrent retinal ischemia beyond cervical carotid occlusion. Clinical-angiographic correlation and therapeutic implications. J Neurosurg 55:532

Craig DR, Meguro K, Watridge C et al (1982) Intracranial internal carotid artery stenosis. Stroke 13:825

Crawford PM, West CR, Chadwick DW et al (1986) Arteriovenous malformations of the brain: the natural history in unoperated patients. J Neurol Neurosurg Psychiatry 49:1

Crompton MR (1962) The pathology of ruptured middle cerebral artery aneurysms with special reference to the differences between the sexes. Lancet 2:421

Crompton MR (1966a) Mechanisms of growth and rupture in cerebral berry aneurysms. Br Med J 1:1138

Crompton MR (1966b) The pathogenesis of cerebral aneurysms. Brain 89:797

Crompton MR (1979) Familial incidence of cerebral aneurysms. Br Med J 1:292

Cronquist M (2009) Endovascular stenting combined with modified antiplatelet regime in acute blister like aneurysms. A multi-center presentation. Interv Neuroradiol 15(Suppl 1):125

Crouzet G, Agnettaz G, Pellat J et al (1974) Les voies de supplence en cours de Moya-Moya. J Neuroradiol (Masson) 1:87

Crum B, Mokri B, Fulgham J (2000) Spinal manifestation of vertebral artery dissection. Neurology 55:304

Cushing H, Bailey P (1928) Tumours arising from the blood vessels of the brain, angiomatous malformations and haemangioblastomas. Balliere, Tindall and Cox, London

D'Anglejan-Chatillon J, Ribeiro V, Mas JL et al (1989) Migraine – a risk factor for dissection of cervical arteries. Headache 29:560

Dandy WS (1928) Arterio-venous aneurysms of the brain. Arch Surg 17:190
Davies MA, Terbrugge K, Willinsky R et al (1996) The validity of classification for the clinical presentation of intracranial dural arteriovenous fistulas. J Neurosurg 85:830
De Reuck J (1972) The cortico-subcortical arterial angio-architecture in the human brain. Acta Neurol Belg 72:323
De Vriese B (1905) Sur la signification morphologique des artères cerebrales. Arch Biol 21:357
Deans WR, Block S, Leibrock L et al (1982) Arteriovenous fistula in patients with neurofibromatosis. Radiology 144:103
Deasy NP, Gholkar AR, Cox TCS et al (1999) Tentorial dural arteriovenous fistulae: endovascular treatment with transvenous coil embolisation. Neuroradiology 41:308
Debrun G, Lacour P, Caron JP et al (1975a) Inflatable and released balloon technique. Experimental in dog-application in men. Neuroradiology 9:267
Debrun G, Lacour P, Caron JP et al (1975b) Traitment des fistules arterioveneiseuses et des aneurysms par balloon gonflable et largable. Nouv Presse Med 8:2315
Debrun G, Lacour P, Vinuela F et al (1981) Treatment of 54 traumatic carotid-cavernous fistulas. J Neurosurg 55:678
Debrun G, Aletich V, Ausman J et al (1997) Embolization of the nidus of brain AV malformations with butyl-cyanoacrylate. Neurosurgery 40:112
Dechambre A (1939) Memoire sur la curabilitè du rammollissement cerebral. Gaz Med Fr 6:305
Djindjian R, Merland JJ (1978) Superselective arteriography of the external carotid artery. Springer, Berlin/Heidelberg
Djindjian R, Cophignon J, Comoy J et al (1968) Polimorphisme neuroradiologique des fistules carotido-cavernouse. Neurochirurgie 14:881
Djindjian R, Manelfe CF, Picard L (1973) Fistules arterioveneuses carotide externe-sinus caverneux; etude angiographique à propos de 6 observations et revue de la literature. Neurochirurgie 19:91
Doyon DL, Aron Rosa DS, Ramèe A (1974) Orbital vein and cavernous sinus. In: Newton Th, Potts DG (eds) Radiology of skull and brain, Book 3. Mosby, St. Louis
Dunker RO, Harris AB (1976) Surgical anatomy of the proximal anterior cerebral artery. J Neurosurg 44:359
Durand-Fardel M (1843) Traitè du rammollissement du cerveau. Baillière J. B, Paris
Duret H (1874) Recherches anatomiques sur la circulation de l'encephale. Arch Physiol Norm Pathol 1:60;2:919
Duvernoy HM (1975) The superficial veins of the human brain. Springer, Berlin/Heidelberg
Duvernoy HM (1999) The human brain stem vessels. Springer, Berlin/Heidelberg
Echiverri HC, Rubino FA, Gupta SR et al (1989) Fusiform aneurysms of the vertebrobasilar arterial system. Stroke 20:1741
Eckert B (2009) Acute stroke therapy 1981-2009. Clin Neuroradiol 19:8
Edelsohn L, Caplan L, Rosenbaum AE (1972) Familial aneurysms and infundibular widening. Neurology 22:1056
Ehrenfeld WK, Wylie EJ (1976) Spontaneous dissection of the internal carotid artery. Arch Surg 111:1294
Einhäupl KM, Masuhr F (1994) Cerebral venous and sinus thrombosis. An update. Eur J Neurol 1:109
Elbers J, Benseler SM (2008) Central nervous system vasculitis in children. Curr Opin Rheumatol 20:47
Elias WS (1971) Intracranial fibromuscular hyperplasia. JAMA 218:254
Epstein F, Ronsohoff J, Budzilovich G (1970) The clinical significance of junctional dilatation of the posterior communicating artery. J Neurosurg 33:529
Ernst R, Bulas R, Tomsick Th et al (1999) Three cases of dural arteriovenous fistula of the anterior condylar vein within the hypoglossal canal. Am J Neuroradiol 20:2016
European Carotid Surgery Trialists' collaborative group (1998) Randomized trial of endarterectomy for recently symptomatic carotid stenosis: final results of the MRC European Carotid Surgery Trial (ECST). Lancet 351:1379
Feldmann E, Daneault N, Kwan E et al (1990) Chinese-white differences in the distribution of occlusive cerebrovascular disease. Neurology 40:1541
Fellner FA, Fellner C, Aichner FT et al (2005) Importance of T2*-weighted gradient echo MRI in diagnosis of cortical vein thrombosis. Eur J Radiol 56:235
Fiehler J, Stapf C (2008) ARUBA-beating natural history in unruptured brain AVMs by intervention. Neuroradiology 50:465
Fisher CM (1965) Lacunes: small deep cerebral infarcts. Neurology 13:30
Fisher CM (1969) The arterial lesion underlying lacunes. Acta Neuropathol (Berlin) 12:1
Fisher CM (1979) Capsular infarcts. Arch Neurol 36:65
Fisher CM (1986) The posterior cerebral artery syndrome. Can J Neurol Sci 13:232
Fisher CM, Caplan L (1971) Basilar artery branch occlusion: a cause of pontine infarction. Neurology 21:900
Fisher CM, Ojeman RG (1986) A clinico-pathologic study of carotid endarteriectomy placques. Rev Neurol (Paris) 142:153
Fisher CM, Gore I, Okabe N et al (1965) Calcification of the carotid siphon. Circulation 32:538
Fisher CM, Ojeman RG, Roberson GH (1978) Spontaneous dissection of cervico-cerebral arteries. Can J Neurosci 5:9
Flemming KD, Wieber DO, Brown RD Jr et al (2004) Perspective risk of hemorrhage in patients with vertebrobasilar non saccular intracranial aneurysms. J Neurosurg 101:82
Flint AC, Duckwiller GR, Budzik RF et al (2007) Mechanical thrombectomy of intracranial internal carotid occlusion: pooled results of the Merci and multi Merci part I trials. Stroke 38:1274
Foix C, Hillemand P (1925a) Les artères de l'axe encefalique jusq'au diencephale inclusivement. Rev Neuro 41:705
Foix C, Hillemand P (1925b) Les syndromes de la region thalamique. Presse Méd 1:113
Forbus WD (1930) On the origin of military aneurysms of the superficial cerebral arteries. Bull Johns Hopkins Hosp 47:239
Frens DB, Petajan JH, Anderson R et al (1974) Fibromuscolar dispalsia of the posterior cerebral artery: report of a case and review of the literature. Stroke 5:161
Friedlander RM, Ogilvy CS (1996) Aneurysmal subarachnoid haemorrhage in patients with bilateral A1 fenestrations associated with an Azygos anterior cerebral artery. Case report and literature review. J Neurosurg 84:681
Friedman AH, Drake CG (1984) Subarachnoid hemorrhage from intracranialdissecting aneurysm. J Neurosurg 60:325
Friedman JA, Pichelmann MA, Piepgras DG et al (2001) Ischemic complications of surgery for anterior choroidal artery aneurysms. J Neurosurg 94(4):565–572

Friedmann WA, Day AL, Quisling RG Jr et al (1980) Cervical carotid dissecting aneurysms. Neurosurgery 7:207
Fujii K, Lenkey C, Rhoton A Jr (1980) Microsurgical anatomy of the choroidal arteries: lateral and 3rd ventricles. J Neurosurg 52:165
Fullerton HJ, Johnston S, Smith ZS (2001) Arterial dissection and stroke in children. Neurology 57:1155
Gacs G, Vinuela F, Fox AL et al (1983) Peripheral aneurysms of the cerebellar arteries. J Neurosurg 58:63
Gailloud P, Fasel JH, Muster M et al (1997) Termination of the inferior petrousal sinus. An anatomical variant. Clin Anat 10:92
Gailloud P, San Millan Ruiz D, Muster M et al (2000) Angiographic anathomy of the latero-cavernous sinus. Am J Neuroradiol 21:1923
Gall G, Nepper Rasmussen J (2009) Initial experience with the Silk stent. Interv Neuroradiol 15(Suppl 1):115
Gallas S, Pasco A, Cottier JP et al (2005) A multicenter study of 705 ruptured intracranial aneurisms treated with Guglielmi Detacheable Coils. Am J Neuroradiol 26:1723
Galligioni F, Andrioli GC, Marin G et al (1971) Hypoplasia of the internal carotid artery associated with cerebral pseudoangiomatosis. Report of 4 cases. Am J Roentgenol Radium Ther Nucl Med 112:251
Galloway JR, Greitz T (1960) The medial and lateral choroid arteries; an anatomic and roentgenographic study. Acta Radiol 53:353
Garcia JH, Ho KL, Pantoni L (1998) Pathology. In: Barnett HJM, Mohr JP, Stein BM, Yatzu FM (eds) Stroke. Churchill Livingstone, New York/London, pp 139–140
Garcia Monaco R, Alvarez H, Goulau Z et al (1990) Posterior fossa arteriovenous malformations. Angioarchitecture in relation to their haemorrhagic episodes. Neuroradiology 31:471
Garcia Monaco R, Rodesch G, Alvarez H et al (1993) Pseudoaneurysm within ruptured intracranial arteriovenous malformations: diagnosis and early endovascular management. Am J Neuroradiol 14:345
Garcia Monaco R, Rodesch G, Terbrugge K et al (1991) Multifocal dural arteriovenous shunts in children. Childs Nerv Syst 7:425
Geibprasert S, Pongpech S, Armstrong D et al (2009) Multifocal Dangerous extra-intracranial anastomoses and suplly to the cranial nerves: vessels the neurointerventionalist needs to know. Am J Neuroradiol 30:1459
Geraud J, Manelfe C, Caussaud JP et al (1973) Fistule arteroveneuse spontanèe de l'artère vertebrale: role eventuelle de la displasie fibromuscolaire dans ça patologie. Rev Neurol (Paris) 128:206
Ghika J, Bougosslavsky J, Regli F (1989) Infarcts in the territory of the deep perforators from the carotid system. Neuroradiology 39:507
Gibo H, Lenkey C, Rhoton AL Jr (1981) Microsurgical anathomy of the supraclinoid portion of the internal carotid artery. J Neurosurg 55:560
Giudicelli G, Faure I, Salamon G (1970) The veins of the thalamus. Neuroradiology 1:92
Glynn LE (1940) Medial defects in the circle of Willis and their relation to aneurysm formation. J Path Bact 51:213
Goddard AJP, Annesley-Williams D, Guthrie JA et al (2001) Duplication of the vertebral artery: report of two cases and review of the literature. Neuroradiology 43:477
Goldberg HL (1974) The anterior choroidal artery. In: Newton Th, Potts DG (eds) Radiology of the skull and brain. Mosby, St Louis
Gonzalez LF, Bristol RE, Porter RW et al (2005) De novo presentation of an arteriovenous malformation. Case report. J Neurosurg 102:726
Goodman SJ, Hasso A, Kirkpatrick D (1975) Treatment of vertebro – jugular fistula by balloon occlusion. J Neurosurg 43:362
Gozzoli L, Crasto S, Leombruni S et al (1998) Magnetic resonance angiography in a case of agenesis the left carotid artery associated with transellar intercarotid anastomosis. Riv Neuroradiol 11:883
Graber D, Flurin-Chollet V, Chaix Y, et al (1992) Dissection de l artere sylviennw avec anevrysme sequellaire chez un enfant de 6 ans. Arch Fr Pediatr 49:445
Graf CJ, Perret GE, Torner JC (1983) Bleeding from cerebral arteriovenous malformations as part of their natural history. J Neurosurg 58(3):331
Greitz T, Lauren T (1968) Anterior meningeal branch of the vertebral artery. Acta Radiol 7:2
Grzyska U, Fieler J (2009) Pathophysiology and treatment of brain AVMs. Clin Neuroradiol 19:82
Guglielmi G, Vinuela F, Dion J et al (1991a) Electrothrombosis of saccular aneuryms via endovascular approach. II: preliminary clinical experience. J Neurosurg 75:8
Guglielmi G, Vinuela F, Sepetka I et al (1991b) Electrothrombosis of saccular aneurims via endovascular approach I: electrochemical basis, technique and experimental results. J Neurosurg 75:1
Gunnel M, Awad IA, Finberg K et al (1996) A gender mutation as a cause of cerebral cavernous malformation in Hispanic Americans. N Engl J Med 334:946
Gupta R, Schumacher HG, Mangla S et al (2003) Urgent endovascular revascularisation for symptomatic intracranial atherosclerotic stenosis. Neurology 61:1729
Gupta A, Purkayastha S, Krishnamoorthy T et al (2006) Endovascular treatment of direct carotid cavernous fistulae: a pictorial review. Neuroradiology 48:831
Hacker H (1968) Abflusswege der sylvischen Venengruppe. Radiologie 8:383
Hacker H (1974) Superficial supratentorial veins and dural sinuses. In: Newton Th, Potts AG (eds) Angiography, Book 3. Mosby, St Louis
Hacker H, Porrero M (1969) Darstellung und Bedeutung der vena ophthalmica im Carotids Angiogram. Fortschr Roentgen 110(5):656
Hajj-Ali RA, Calabrese LH (2009) Central nervous system vasculitis. Curr Opin Rheumatol 21:10
Halbach VV, Higashida RT, Hieshima GB et al (1987) Dural fistulas involving the transverse and sigmoid sinus: results of treatment in 28 patients. Radiology 163:443
Halbach VV, Higashida RT, Hieshima GB et al (1988) Treatment of dural arteriovenous malformations involving the superior sagittal sinus. Am J Neuroradiol 9:337
Halbach VV, Higashida RT, Hieshima GB et al (1989) Transvenous embolization of dural fistulas involving the cavernous sinus. Am J Neuroradiol 10:337
Halbach VV, Higashida RT, Hieshima GB et al (1990) Dural arteriovenous fistulas supplied by ethmoidal arteries. Neurosurgery 26:816

Hallacq P, Piotin M, Moret J (2002) Endovascular occlusion of the posterior cerebral artery for the treatment of p2 segment aneurysms: retrospective review of a 10-year series. Am J Neuroradiol 23:1128

Hamada Y, Goto K, Inoue T et al (1997) Hystopathological aspects of dural arteriovenous fistulas in the transverse-sigmoid sinus region in nine patients. Neurosurgery 40:452

Hanafee W, Rosen LM, Weidner GH et al (1965) Venography of the cavernous sinus orbital veins and basal venous plexus. Radiology 84:751

Hanafee W, Shiu P, Dayton GO (1968) Orbital venography. Am J Roentgenol 104:29

Handa J, Kamijyo Y, Handa H (1970a) Intracranial aneurysm associated with fibro-muscular hyperplasia of renal and internal carotid arteries. Br J Radiol 43(511):483

Handa J, Shimizu Y, Matsuda M et al (1970b) The accessory middle cerebral artery. Report of further two cases. Clin Radiol 21:415

Hänggi D, Turowski B, Beseoglu K et al (2008) Intra-arterial nimodipine for severe cerebral vasospasm after aneurysmal subarachnoid hemorrhage: influence on clinical course and cerebral perfusion. Am J Neuroradiol 29(6):1053

Hardy DG, Rhoton AL Jr (1978) Microsurgical relationships of the superior cerebellar artery and the trigeminal nerve. J Neurosurg 49:669

Harnsberger HR (1995) Handbook of head and neck imaging (carotid space). Mosby, St Louis

Hashimoto I (1977) Familial intracranial aneurysms and cerebral vascular anomalies. J Neurosurg 46:419

Hassler O, Salzmann GF (1967) Angiographic and histological changes in infundibular widening of the posterior communicating artery. Acta Radiol 1:321

Haughton VM, Rosenbaum EE (1974) The normal and anomalous aortic arc and brachio-cephalic arteries. In: Newton Th, Potts DG (eds) Radiology of skull and brain. Mosby, St. Louis

Haughton VM, Rosenbaum EE, Pearce J (1978) Internal carotid artery origins of the inferior cerebellar arteries. Am J Roentgenol 130:1191

Hayes GJ (1963) External carotid cavernous sinus fistulas. J Neurosurg 20:692

Hayreh SS (1962) The ophthalmic artery. III-Branches. Br J Ophthalmol 46:212

Hayreh SS, Dass R (1962a) The ophthalmic artery II - Intraorbital course. Br J Ophthalmol 46:165

Hayreh SS, Dass R (1962b) The ophthalmic artery. I - Origin, intracranial and intracanalicular course. Br J Ophthalmol 46:65

Hegedus K (1985) Ectasia of the basilar artery with special reference to possible pathogenesis. Surg Neurol 24:463

Heiskanen O (1989) Ruptured intracranial arterial aneurysm of children and adolescents. Surgical and total management results. Childs Nerv Syst 5:66

Helgason C, Caplan LR, Goodman J et al (1986) Anterior choroidal artery territory infarction: case reports and review. Arch Neurol 43:681

Henkes H, Fisher S, Weber W et al (2004) Endovascular coil occlusion of 1811 intracranial aneurisms: early angiografical and clinical results. Neurosurgery 54:268

Hennerici M, Klemm C, Rautemberg W (1988) The subclavian steal phenomenon: a common vascular disorder with rare neurologic deficits. Neurology 38:669

Herman LH, Fernando OU, Gurdjian ES (1966) The anterior choroidal artery: an anatomical study of its area of distribution. Anat Rec 154:95

Heubner O (1872) Zur topographie der Ernährungsgebiet der einzelnen Hirnarterien. Cent Med Wissen 52:816

Hieshima GB, Cahan LD, Mehringer CM et al (1986) Spontaneous arteriovenous fistulae of cerebral vessels in association with fibromuscular dysplasia. Neurosurgery 18(4):454

Hillbom M, Kaste M (1982) Alcohol intoxication: a risk factor for primary subarachnoid haemorrhage. Neurology 32:706

Hinton RG, Mohr JP, Hackerman RH et al (1979) Symptomatic middle cerebral artery stenosis. Ann Neurol 5:152

Hiraiwa K, Sato T, Sasaki T, et al (2005) Medico-legal aspects of traumatic injury of the vertebro basilar artery. Neurol Med Chir (Tokyo) 45:549

Hirsch CS, Roessmann U (1975) Arterial dysplasia with ruptured basilar artery aneurysm: report of a case. Hum Pathol 6:749

Hochberg FH, Bean C, Fisher M et al (1975) Stroke in a 15-year old girl secondary to terminal carotid dissection. Neurology 25:725

Hofmeister C, Stapf C, Hartmann A et al (2000) Demographic morphological and clinical characteristics of 1289 patients with brain arteriovenous malformations. Stroke 31:1307

Hommel M, Pollak P, Gaio JM et al (1984) Paralyses du nerf grand hypoglosse par deux aneurysms et un aneurysme dissequant de l'artère carotide interne. Rev Neurol 140:415

Horiuchi T, Tanaka Y, Hongo K, et al (2003) Characteristics of distal posteroinferior cerebellar artery aneurysms. Neurosurgery 53:589

Horowitz DR, Tuhrim S (1997) Stroke mechanisms and clinical presentation in large subcortical infarction. Neurology 49:153

Hosoya T, Adachi M, Yamaguchi K et al (1999) Clinical and neuroradiological features of intracranial vertebrobasilar artery dissection. Stroke 30:1083

Houdart E, Gobin YP, Casasco A et al (1993) A proposal angiographic classification of intracranial arteriovenous fistulae and malformations. Neuroradiology 35:381

Houser OW, Baker HL Jr (1968) Fibromuscolar displasia and other uncommon disease of the cervical carotid artery: angiographic aspects. Am J Roentgenol 104:201

Houser OW, Campbell JK, Campbell RJ et al (1979) Arteriovenous malformations affecting the transverse sinus. An acquired lesion. Mayo Clin Proc 54:651

Hoyt F, Newton Th, Margolis TM (1974) The posterior cerebral artery. In: Newton TH, Potts DG (eds) Radiology of skull and brain, vol 2, Angiography. Mosby, St. Louis

Huang YP, Wolf BS (1964) Veins of the white matter of the cerebral hemispheres (the medullary vveins): diagnostic importance in carotid angiography. Am J Roentgenol 92:739

Huang YP, Wolf BS (1965) The veins of the posterior fossa; superior or galenic draining group. Am J Roentgenol 95:808

Huang YP, Wolf BS (1967) The veins of the lateral recess of the IV ventricle and its tributaries; roentgen appearance and anatomic relationships. Am J Roentgenol 101:1

Huang YP, Wolf BS, Autin BS et al (1968) The veins of the posterior fossa, anterior or petrosal draining group. Am J Roentgenol 104:36

Huang YP, Wolf BS, Okudera T (1969) Angiographic anatomy of the inferior vermian vein of the cerebellum. Acta Radiol Diagn 9:327

Huang J, McGirt MJ, Gailloud P (2005) Intracranial aneurysms in the pediatric population: case series and literature review. Surg Neurol 63(5):424

Huber P (1979) Zerebrale Angiographie für Klinik und Praxis. Thieme, Stuttgart

Hufnagel A, Hammers A, Schönle PW et al (1999) Stroke following chiropractic manipulation of the cervical spine. J Neurol 246(8):683

Hupperts RMM, Lodder J, Hents van Raak EPM et al (1994) Infarcts with anterior choroidal artery territory Anatomical distribution, clinical syndromes, presumed pathogenesis and early outcome. Brain 117:825

Hutchings M, Weller RO (1986) Anatomical relationships of the pia mater to cerebral blood vessels in man. J Neurosurg 65:316

Ingebrigtsen T, Morgan MK, Faulder K et al (2004) Bifurcation geometry and the presence of cerebral artery aneurisms. J Neurosurg 101:108

Ishikawa T, Nakamura N, Houkin K et al (1997) Pathological consideration of a "blister-like" aneurysm at the superior wall of the internal carotid artery. Neurosurgery 40:403

Ito J, Imamura H, Kobayashi K et al (1983) Dural Arteriovenous malformations of the anterior cranial fossa. Neuroradiology 24:149

Jaeger JR, Forbes RP, Dandy WE (1937) Bilateral congenital cerebral arteriovenous communication aneurysm. Trans Am Neurol Assoc 63:173

Jansen O, von Kummer R, Forsting M et al (1995) Thrombolytic therapy in acute occlusion of the intracranial internal carotid artery bifurcation. Am J Neuroradiol 10:1977

Jefferson G (1938) On the saccular aneurisms of the internal carotid artery in the cavernous sinus. Br J Surg 102:267

Jellinger K (1986) Vascular malformations of the central nervous system: a morphological overview. Neurosurg Rev 9:177

Jentzer A (1954) Dissecting aneurysm of the left internal carotid artery. Angiology 5:232

Jiang CH, Lv X, Li Y et al (2009) Endovascular treatment of high-risk tentorial dural arteriovenous fistulas: clinical outcomes. Neuroradiology 51:103

Johanson C (1954) The central veins and deep dural sinuses of the brain. Acta Radiol Suppl 107:1

Jones BP, Ganesan V, Saunders DE et al (2010) Imaging in childhood arterial ischemic stroke. Neuroradiology 52:577

Juvela S, Hillbom M, Numminen H et al (1993) Cigarette smoke and alcohol consumption as risk factors for aneurismal subarachnoid haemorrhage. Stroke 24:639

Kalimo H, Kaste M, Haltia M (1997) Vascular disease. In: Graham DI, Lantos PI (eds) Greenfield neuropathology, vol 1. Arnold, London, pp 345–347

Kanai H, Nagai H, Wakabanashi S et al (1992) A large aneurysm of the persistent primitive hypoglossal artery. Neurosurgery 30:794

Kaneko T, Nomura M et al (2001) Serial neuroimaging of a growing thrombosed giant aneurysm of the distal anterior cerebral artery - case report. Neurol Med Chir 41:33

Kaplan HA (1959) The transcerebral venous system. An anatomical study. Arch Neurol Psychiatry 1:148

Kaplan HA (1965) The lateral perforating branches of the anterior and middle cerebral arteries. J Neurosurg 23:305

Kaplan HA, Ford DH (1966) The brain vascular system. Amsterdam, Elsevier

Kaplan HA, Browder A, Browder J (1973) Narrow and atretic transverse subdural sinuses: clinical significance. Ann Otol Rhinol Laryngol 82:351

Kapoor R, Kendall BE, Harrison MJG (1991) Permanent oculomotory palsy with occlusion of the internal carotid artery (letter). J Neurol Neurosurg Psychiatry 54:745

Kappelle LS, Eliasziw M, Fox AJ et al (1999) Importance of intracranial arteriosclerotic disease in patients with intracranial stenosis of the internal carotid artery. Stroke 30:282

Karameshev A, Schroth G, Mordasini P et al (2010) Long term outcome of symptomatic severe ostial vertebral artery stenosis. Neuroradiology 52:371

Katayama Y, Tsubokawa T, Miyazaki S et al (1991) Growth of totally thrombosed giant aneurysms within the posterior cranial fossa. Diagnostic and therapeutic considerations. Neuroradiology 33:168

Kato S, Ishihara H, Nakayama H et al (2007) Transvenous embolization of dural arteriovenous shunts of the cavernous sinus. Interv Neuroradiol 13:353

Katsuta T, Rhoton AL Jr, Matsushima T (1997) The jugular foramen: microsurgical anatomy and operative approaches. Neurosurgery 41:149

Kazui S, Saweda T, Naritomi H et al (1993) Angiographic evaluation of brain infarction limited to the anterior cerebral artery territory. Stroke 24:549

Kendall B (1983) Results of treatment of arterovenous fistulae with the Debrun technique. Am J Neuroradiol 4:405

Kerber CW, Newton TH (1973) The macro- and microvascularization of the dura mater. Neuroradiology 6:175

Kim DJ, Kim DI, Shu SH et al (2006) Results of transvenous embolization of cavernous dural arteriovenous fistula: a single centre experience with emphasis on complications and management. Am J Neuroradiol 27:2078

King WA, Martin NA (1992) Intracerebral haemorrhage due to dural arteriovenous malformations and fistulae. Neurosurg Clin N Am 3:577

Kingsley DPE, Kendall BE, Moseley IF (1978) Superior sagittal sinus thrombosis, an evaluation of the changes demonstrated on computed tomography. J Neurol Neurosurg Psychiatry 41:1065

Kirsch M, Henkes H, Liebig T et al (2006) Endovascular management of dural carotid-cavernous sinus fistulas in 141 patients. Neuroradiology 48:486

Kittner SJ, Sharkness CM, Price TR et al (1991) Infarcts with a cardiac source of embolism in the NINCDS Stroke Data Bank: historical features. Neurology 40:281

Kiura Y, Ohba S, Shibukawa M et al (2007) Transfemoral transvenous embolization of dural arteriovenous fistulas involving the isolated transverse-sigmoid sinus. Interv Neuroradiol 13(Suppl 1):109

Kiyosue H, Tanoue S, Sagara Y et al (2008) The anterior medullary-anterior pontomesencephalic venous system and its bridging veins communicating to the dural sinuses: normal anatomy and drainage routes from dural arteriovenous fistulas. Neuroradiology 50:1013

Kobayashi H, Hasayashi M, Noguchi Y et al (1988) Dural arteriovenous malformations in the anterior cranial fossa. Surg Neurol 30:396

Kobayashi S, Koike G, Orz Y et al (1995) Juxta-dural ring aneurysms of the internal carotid artery. J Clin Neurosci 2:345

Kodama N, Suzuki J (1974) Cerbrovacular Moya-Moya disease. IIIrd report-the study of the aging of the perforating branches and the possibility of collateral pathway. Neurol Med Chir 14:55
Komotar RJ, Zacharia BE, Valhora R et al (2007) Advances in vasospasm treatment and prevention. J Neurol Sci 261:134
Konrad C, Nabavi DG, Junker R et al (2003) Spontaneous internal carotid artery dissection and alpha-1-antitrypsin deficiency. Acta Neurol Scand 107:233
Krayenbuhl H (1967) Cerebral venous and sinus thrombosis. Clin Neurosurg 14:1
Krayenbühl HA, Yaşargyl MG, Flamm ES et al (1972) Microsurgical treatment of intracranial saccular aneurysms. J Neurosurg 37:678
Krings T, Alvarez H, Reinacher P et al (2007) Growth and rupture mechanisms of partially thrombosed aneurysms. Interv Neuroradiol 13:117
Kudo T (1968) Spontaneous occlusion of the circle of Willis: a disease apparently confined to Japanese. Neurology 18:485
Kumral E, Bayulchem G, Atac C et al (2004) Spectrum of superficial posterior cerebral artery infarcts. Clinical and outcome correlates. Eur J Neurol 11:237
Kunze ST, Schiefer W (1971) Angiographic demonstration of a dissecting aneurysm of the middle cerebral artery. Neuroradiology 2:201
Kurata A, Ohmomo T, Miyasaka Y et al (2001) Coil embolization of the treatment of ruptured dissecting vertebral aneurysms. Am J Neuroradiol 22:11
Kurosu A, Fuji T, Ono G (2000) Distal superior cerebellar aneurisms. Br J Neurosurg 14:244
Kurre W, Berkefeld J (2008) Material and technique for coiling of cerebral aneurisms: how much scientifical evidence do we have. Neuroradiology 50:909
Kurre W, Chapot R, Mesnil de Rochemont R et al (2010) Intracranial stenting in atherosclerotic disease-recent results and challenges to face. Neuroradiology 52:633
Lacour JC, Ducrocq X, Auxionnat R et al (2000) Isolated dissection of the basilar artery. Rev Neurol 156:654
Laine E, Galibert P, Lopez C et al (1963) Aneurysmes arterioveineux intraduraux (developpèes dans l'epeisseur de la dure mère) de la fosse posterieure. Neurochirurgie 9:147
Lasjaunias P (1997) Vascular disease in neonates, infants and children. Springer, Berlin/Heidelberg
Lasjaunias P, Berenstein A (1987) Surgical neuroangiography, vol 1-2. Springer, Berlin/Heidelberg
Lasjaunias P, Berenstein A (1990) Surgical neuroangiography, vol 3. Springer, Berlin/Heidelberg
Lasjaunias P, Doyon D (1978) The ascending pharyngeal arteries and the blood supply of the lower cranial nerves. J Neuroradiol 5:287
Lasjaunias P, Rodesch G (1993) Lesion types, hemodynamics and clinical spectrum. In: Awad IA, Barrow DL (eds) Dural arteriovenous malformations. AANS, Park Ridge
Lasjaunias P, Moret J, Manelfe C et al (1977) Arterial anomalies at the base of the skull. Neuroradiology 13:267
Lasjaunias P, Moret J, Theron J (1978a) The so called anterior meningeal artery of the cervical vertebral artery. Neuroradiology 17:51
Lasjaunias P, Theron J, Moret J (1978b) The occipital artery. Neuroradiology 15:31
Lasjaunias P, Burrows P, Planet C (1986a) Developmental venous anomalies (DVA). The so called venous angioma. Neurosurg Rev 9:233
Lasjaunias P, Chiu M, Terbrugge K et al (1986b) Neurological manifestations of intracranial dural arteriovenous malformations. J Neurosurg 64:724
Lasjaunias P, Wuppalapati S, Alvarez H et al (2005) Intracranial aneurysms in children aged under 15 years: review of 59 consecutive children with 75 aneurysms. Childs Nerv Syst 21:437
Laughlin S, ter Brugge KG, Willinsky RA et al (1997) Endovascular management of pediatric intracranial aneurysms. Interv Neuroradiol 3:205
Lauthier S, Armstrong D, Domi T et al (2005) Post-varicella arteriopathy of childhood: natural history of vascular stenosis. Neurology 64:660
Lawton MT, Jacobowitz R, Spetzler RF (1997) Redefined role of angiogenesis in the pathogenesis of dural arteriovenous malformations. J Neurosurg 87:267
Lazinski D, Willinsky RA, Terbrugge K et al (2000) Dissecting aneurysms of the posterior cerebral artery: angioarchitecture and a review of the literature. Neuroradiology 42:128
Lazorthes G, Salamon G (1971) The arteries of the thalamus: an anatomical and radiological study. J Neurosurg 34:23
Lazorthes G, Gouaze A, Salamon G (1976) Vascularisation et circulation de l'encephale. Masson, Paris
Lazzaro NA, Wright B, Castillo M et al (2010) Artery of Percheron infarction: imaging patterns and clinical spectrum. Am J Neuroradiol 31(7):1283–1289; published 18/3/2010
Lechat P, Mas JL, Lescault G et al (1988) Prevalence of patent foramen ovale in patients with stroke. N Engl J Med 318:1148
Lee JS, Yong SW, Bang OY et al (2006) Comparison of spontaneous intracranial vertebral artery dissection with large artery disease. Arch Neurol 63:1738
Leonardi M, Simonetti L, Andreoli A (2001) Endovascular treatment of a distal aneurysm of the superior cerebellar artery by intra-aneurysmal injection of glue. Interv Neuroradiol 7:343
Levy C, Laissy JP, Raveau V et al (1994) Carotid and vertebal artery dissections: three dimensional time of flight MR angiography and MR imaging versus conventional angiography. Radiology 190:97
Levy R, Diuyckaerts C, Hauw JJ (1995) Massive infarcts involving the territory of the anterior choroidal artery and cardioembolism. Stroke 26:609
Lewis SB, Chang DJ, Peace DA, et al (2002) Distalposterior inferior cerebellar aneurysms: clinical feature and management. J Neurosurg 97:756
Li TL, Fang B, He XY et al (2005) Complication analysis of 469 brain AV malformations treated with N-butyl-cyanoacrylate. Interv Neuroradiol 11:141
Li Y, Lv X, Liu A et al (2007) Endovascular treatment strategies for posterior cerebral artery aneurysms. Interv Neuroradiol 13(Suppl 2):208
Libby P, Clinton SW (1993) The role of macrophages in atherogenesis. Curr Opin Lipidol 4:355
Lie TA (1968) Congenital anomalies of the carotid arteries. Excerpta Medical Foundation, Amsterdam
Liebig Th, Henkes H (2008) Re- and deconstruction: staged treatment of large fusiform aneurysm of the vertebrobasilar junction by stent deployment and subsequent coil occlusion of one vertebral artery. Clin Neuroradiol 18:255

Lieschke GJ, Davis S, Tress BM et al (1988) Spontaneous intracranial carotid artery dissection presenting as hypoglossal nerve palsy. Stroke 19:1151

Lindergärd B, Hillbom M, Brody S (1987) High dose estrogen-progestogen oral contraceptives: a risk factor for aneurismal subarachnoid haemorrhage? Acta Neurol Scand 76:37

Linn J, Brückmann H (2010) Cerebral venous and dural sinus thrombosis. Clin Radiol 20:25

Linskey ME, Sekhar LN, Hirsch WJ et al (1990) Aneurysms of the intracavernous carotid artery: clinical presentation, radiographic features and pathogenesis. Neurosurgery 26:71

Little JR, St LP, Weinstein M et al (1981) Giant fusiform aneurysms of the cerebral arteries. Stroke 12:183

Liu JP, Kricheff II (1974) The anterior cerebral artery complex. In: Newton Th, Potts DG (eds) Radiology of the skull and brain, vol II. Mosby, St. Louis

Liu HM, Shih HG, Huang YC et al (2001) Posterior cranial fossa arteriovenous fistula with presenting as carotico cavernous fistula. Neuroradiology 43:405

Liu HM, Wang YH, Chen YF et al (2003) Endovascular treatment of brainstem arteriovenous malformations. Safety and efficacy. Interv Neuroradiol 45:644

Lo WWM, Solti-Bohmen LG, McElveen JT Jr (1985) Aberrant carotid artery: radiological diagnosis with emphasis on high resolution computed tomography. Radiographics 5:985

Locksley HB (1966a) Natural history of subarachnoid hemorrhage, intracranial aneurysms and arteriovenous malformations. J Neurosurg 25:321

Locksley HB (1966b) Report on cooperative study of intracranial aneurysms and subarachnoid haemorrhage. Section V. J Neurosurg 25:219

Lombardi G, Passerini SA (1967) The orbital veins. Am J Ophthalmol 64:440

Lubicz B, Collignon L, Lefranc F et al (2008) Circumferential and fusiform intracranial aneurysms: reconstructive endovascular treatment with self-expandable stents. Neuroradiology 50:499

Lubicz B, Leclerc X, Gauvrit IY et al (2003) Endovascular treatment of peripheral cerebellar artery aneurysms. AJNR Am J Neuroradiol 24:1209

Lv M, Lv X, Li Y, et al (2009) Dissecting Aneurysm at the proximal anterior cerebral artery treated by parent artery occlusion. Interv Neuroradiology 15:123

Lv X, Li Y, Wu Z (2008) Endovascular treatment of anterior cerebral fossa dural arteriovenous fistula. Neuroradiology 50:433

Maitland CG, Black JL, Smith WA (1983) Abducens nerve palsy due to spontaneous dissection of internal carotid artery. Arch Neurol 40:448

Malgorzata M, Jakubowska MM, Michels P et al (2008) Endovascular treatment in proximal and intracranial carotid occlusion 9 hours after symptom onset. Neuroradiology 50:599

Manabe H, Hatayama T, Hasegawa S et al (2000) Coil embolisation for ruptured vertebral artery dissection distal to the origin of the posterior inferior cerebellar artery. Neuroradiology 42:384

Manabe S, Satoh K, Matsubara S et al (2008) Characteristics, diagnosis and treatment of hypoglossal canal dural arteriovenous fistula: report of nine cases. Neuroradiology 50:715

Manelfe C, Berenstein A (1980) Treatment of carotid cavernous fistulas by venous approach. J Neuroradaiol 7:13

Manelfe C, Clausse J, Fredy D et al (1974) Dysplasie fibromuscolaire des artères cervicocephaliques. A propos de 70 cas. J Neuroradiol (Masson, Paris) 1:149

Mangiafico S, Cellerini M, Nencini P et al (2005) Intravenous glycoprotein IIb/IIIa inhibitor (Tirofibam) followed by intraarterial urokinase and mechanical thrombolysis in stroke. Am J Neuroradiol 26:2515

Mani RL, Newton TH, Glickmann MG (1968) The superior cerebellar artery: an anatomical roentgenographic correlation. Radiology 91:1102

Maraire JN, Awad IA (1995) Intracranial cavernous malformations: lesion behaviour and management strategies. Neurosurgery 37:591

Margolis MT, Newton TH, Hoyt WT (1974) The posterior cerebral artery. In: Newton Th, Potts DG (eds) Radiology of the skull and brain. Mosby, St. Louis

Marie P (1901) Des foyers lacunaire de dèsintegration et de differents autres ètats cavitaire du cerveau. Rev Méd 21:281

Marinković S, Milisavljevic M, Marinković Z (1990) Branches of the anterior communicating artery. Acta Neurochir Wien 106:78

Marks MP, Lane B, Steinberg GK et al (1992) Intranidal aneurysms in cerebral arteriovenous malformations: evaluation and endovascular treatment. Radiology 183:355

Martin NA, King WA, Wilson CB et al (1990) Management of dural arteriovenous malformations of the anterior cranial fossa. J Neurosurg 72:692

Massimi L, Moret J, Tamburini G (2003) Dissecting giant vertebro-basilar aneurysm. Childs Nerv Syst 19:204

Massoud TF, Anslow P, Molyneux AJ (1992) Subarachnoid haemorrhage following spontaneous intracranial carotid artery dissection. Neuroradiology 34:33

Mast H, Young WL, Koennecke HC et al (1997) Risk of spontaneous haemorrhage after diagnosis of cerebral arteriovenous malformation. Lancet 350:1065

Masuda J, Ogata J, Yutani C (1993) Smooth muscle cell proliferation and localization of macrophages and T-cell in the occlusive intracranial major arteries in Moya-moya disease. Stroke 24:1960

Matsushima T, Rhoton AL Jr, de Oliveira E et al (1983) Microsurgical anatomy of the veins of the posterior fossa. J Neurosurg 59:63

Mawad ME, Hilal SK, Michelson WJ et al (1984) Occlusive disease with cerebral arteriovenous malformations. Radiology 153:401

Mc Cormick WF (1966) The pathology of vascular arteriovenous malformations. J Neurosurg 24:807

Mc Cormick WF (1984) Pathology of vascular malformations of the brain. In: Wilson CB, Stein BM (eds) Intracranial arterovenous malformations. Williams-Wilkins, Baltimore, pp 44–63

Mc Cormick WF, Schochet SS Jr (1976) Atlas of cerebral disease. Saunders, Philadelphia

McDougall CG, Halbach VV, Christopher F et al (1997) Dural arteriovenous fistulas of the marginal sinus. Am J Neuroradiol 18:1565

McLennan JE, Rosenbaum AE, Haughton VM (1974) Internal carotid origin of the middle meningeal artery. The ophthalmic middle meningeal and stapedial –middle meningeal arteries. Neuroradiology 7:265

Mellado JM, Merino X, Ramos A et al (2001) Agenesis of the internal carotid artery with a trans sellar anastomosis: CT and MRI findings in late onset congenital hypopituitarism. Neuroradiology 43:237
Menon RK, Norris JW (2008) Cervical arterial dissection. Current concepts. Ann NY Acad Sci 1142:200
Meyer FB, Lombardi D, Scheithauer B et al (1990) Extraaxial cavernous haemangiomas involving the dural sinuses. J Neurosurg 73:187
Meyer FB, Sundt ThM, Fode NC et al (1989) Cerebral Aneurysms in childhood and adolescence. J Neurosurg 70:420
Michotey P, Grisoli F, Raybaud Ch et al (1974) Etude anatomique et radiologique de l'artère cèrèbrale moyenne. Procèdè de rerpèrage. Ann Radiol 17:721
Mickle JP, Quisling RG (1994) Vein of Galen fistulas. Neurosurg Clin N Am 5:529
Milandre L, Gueriot C, Giraud N et al (1988) Les thromboses veineuses cèrèbrales de l'adulte. Ann de Medecine Interne 139:544
Milandre L, Brosset C, Botti G et al (1994) Etude de 82 infarctus du territoire des artères cerebrales posterieures. Rev Neurol 150:133
Milenkovic Z (1985) Anastomosis between internal carotid artery and anterior cerebral artery with other anomalies of the circle of Willis in a fetall brain. J Neurosurg 55:701
Miller RE, Hieshima GB, Giannotta SL et al (1984) Acute traumatic vertebral arteriovenous fistula: balloon occlusion with use of a contralateral approach. Neurosurgery 14:225
Miller DL, Doppman JL, Chang R (1993) Anatomy of the junction of the inferior petrosal sinus and the internal jugular vein. Am J Neuroradiol 14:1075
Min WK, Park KK, Kim JS et al (2000) Atherosclerotic middle cerebral artery territory infarction. Topographic diversity with common occurrence of concomitant small cortical and subcortical infarcts. Stroke 31:2055
Miravet E, Dauchaivijitz N, Basu H et al (2007) Clinical and radiological features of childhood cerebral infarction following varicella-zoster virus infection. Dev Med Child Neurol 49:417
Mironov A (1995) Classification of spontaneous dural arteriovenous fistulas with regard to their pathogenesis. Acta Radiol 36:582
Mitsos AP, Corkhill RA, Lalloo S et al (2008) Idiopathic aneurysms of distal cerebellar arteries: endovascular treatment after rupture. Neuroradiology 50:261
Mitsuhashi Y, Nishio A, Kawahara S et al (2007) Morphologic evaluation of the caudal end of the inferior petrosal sinus using 3D rotational venography. Am J Neuroradiol 28:1179
Miyachi S, Ohshima T, Isumi T et al (2008) Dural arteriovenous fistula at the anterior confluence. Interv Neuroradiol 14:303
Miyamoto N, Naito I, Takatama S et al (2009) Clinical and angiographic characteristics of cavernous sinus dural arteriovenous fistola manifesting as venous infarction and/or intracranial haemorrhage. Neuroradiology 51:53
Mizutani T (1998) Subarachnoid haemorrhage associated with angiographic "stenotic" or "occlusive" lesions in the carotid circulation. Surg Neurol 49:495
Mokri B, Sundt TM Jr, Houser OW et al (1979) Spontaneous internal carotid dissection, hemicrania and Horner's syndrome. Arch Neurol 36:677
Mokri B, Sundt TM Jr, Hauser OW et al (1986) Spontaneous dissection of the cervical internal carotid artery. Ann Neurol 19:126
Mokri B, Houser OW, Sandok BA et al (1988) Spontaneous dissection of the vertebral arteries. Neurology 38:880
Mokri B, Siebert PL, Schievink WI et al (1996) Cranial nerve palsy in spontaneous dissection of the extracranial internal carotid artery. Neurology 46:356
Molineux AJ, Kerr SC, Yu LM et al (2002) International subarachnoid aneurism trial (ISAT) of neurosurgical clipping versus endovascular coiling in 2143 patients with ruptured intracranial aneurisms; a randomized comparison of effect on survival dependency seizures rebleeding subgroup and aneurism occlusion. Lancet 366:809
Moon WJ, Porto L, Laufermann H et al (2002) Agenesis of internal carotid artery associated with congenital anterior hypopituitarism. Neuroradiology 44:138
Moret J, Lasjaunias P, Theron J et al (1977) The middle meningeal artery; its contribution to the vascularization of the orbita. J Neuroradiol (Masson) 4:225
Moret J, Lasjaunias P, Doyon D (1979) Occipital approach for treatment of arteriovenous malformations of the vertebral artery by balloon occlusion. Neuroradiology 17:269
Moret J, Lasjaunias P, Theron J (1980) Vascular compartments and territory of timpano-giugular tumors. J Belg Radiol 63:321
Moret J, Cognard C, Weill A et al (1997) The "remodelling technique" in the treatment of wide neck intracranial aneurisms. Interv Neuroradiol 3:21
Morris P (1997) Practical neuroangiography. Williams-Wilkins, Baltimore/Philadelphia
Moyer DJ, Flamm ES (1992) Anomalous arrangement of the origins of the anterior choroidal and posterior communicating arteries. J Neurosurg 76:1017
Mukonoweshuro W, Laitt RD, Hughes DG (2003) Endovascular treatment of PICA aneurysms. Neuroradiology 45:188
Mullan S (1979) Treatment of carotid-cavernous fistulas by cavernous sinus occlusion. J Neurosurg 50:131
Mullan S, Mojtahedii S, Johnson DL et al (1996a) Cerebral venous malformations-arteriovenous malformations transition forms. J Neurosurg 85:9
Mullan S, Mojtahedii S, Johnson DL et al (1996b) Embryological basis of some aspects of cerebral vascular fistulas and malformations. J Neurosurg 85:1
Müller DP, Sato Y, Yu WTC (1991) Accessory middle cerebral artery as a source of collateral blood flow. Am J Neuroradiol 12:1223
Muller-Forell W, Valavanis A (1996) Bestimmung des Blutungsrisiko bei zerebralen arteriovenösen Malformationen (AVM). Klin Neuroradiol 6:71
Mulliken JB, Glowacki J (1982) Hemangiomas and vascular malformations in infants and children. A classification based on endothelial characteristics. Plast Reconstr Surg 69:348
Murayama Y, Nien YI, Duckwiller G et al (2003a) Guglielmi detachable coils embolization of cerebral aneurysms: 11 years experience. J Neurosurg 98:959
Murayama Y, Song TK, Uda K et al (2003b) Combined endovascular treatment for both intracranial aneurysm and symptomatic vasospasm. Am J Neuroradiol 24:133
Nadgir RN, Loevner LA, Ahmed T et al (2003) Simultaneous bilateral internal carotid and vertebral artery dissection

following chiropractic manipulation: case report and review of the literature. Neuroradiology 45:311
Nagahiro S, Takada A, Goto S et al (1995) Thrombosed growing giant aneurysms of the vertebral artery: growth mechanisms and management. J Neurosurg 82:796
Nagaraja S, Lee KJ, Coley SC et al (2006) Stereotactic radiosurgery for brain arterio – venous malformations: quantitative MR assessment of nidal response at 1 year and angiographic factors predicting early obliteration. Neuroradiology 48:821
Naidich Th, Kricheff II, George AE et al (1976) The normal anterior inferior cerebellar artery. Radiology 119:355
Naito I, Iwai T et al (2001) Percutaneous transvenous embolization through the occluded sinus for transverse-sigmoid dural arteriovenous fistulas with sinus occlusion. Neuroradiology 43:672
Nakatomi H, Nagata K, Kawamoto S et al (1997) Ruptured dissecting aneurysm as a cause of intracranial haemorrhage of verified etiology. Stroke 28:1278
Nakstad P, Nornes H, Hauge HN et al (1988) Cerebral panangiography in spontaneous subarachnoid haemorrhage from intracranial aneurysms. Acta Radiol 29:633
Nass R, Hays A, Chutorian A (1982) Intracranial dissecting aneurysms in childhood. Stroke 13:204
Nelson MD, Kendall BE (1987) Intracranial catecholamine secreting paragangliomas. Neuroradiology 29:277
Neumeier-Probst E (2009) Dural arteriovenous fistulas. Clin Neuroradiol 19:91
New PFS, Price DL, Carter B (1970) Cerebral angiography in cardiac mixoma; correlation of angiographic and histopathological findings. Radiology 96:335
Newton TH, Cronquist S (1969) Involvement of the dural arteries in intracranial arteriovenous malformations. Radiology 1071:1093
Newton TH, Hoyt WF (1970) Dural arteriovenous shunts in the region of the cavernous sinus. Neuroradiology 1:71
Newton TH, Weidner W, Greitz T (1968) Dural arteriovenous malformations in posterior fossa. Radiology 90:27
Nishijima M, Takaku A, Endo S et al (1992) Etiological evaluation of dural arteriovenous malformations of the lateral and sigmoid sinus based on histopathological examination. J Neurosurg 76:600
Nishimoto A, Takeuchi S (1968) Abnormal cerebrovascular network related to the internal carotid arteries. J Neurosurg 29:255
Nogueira RG, Schwamm LH, Buonanno FS et al (2008) low pressure balloon angioplasty with adjuvant farmacological therapy in patients with acute ischemic stroke caused by intracranial arterial occlusion. Neuroradiology 50:331
Norrgard Ö, Angquist KA, Fodstad H et al (1987) Intracranial aneurysms and heredity. Neurosurgery 20:236
North American Symptomatic Carotid Endarterectomy Trial (NASCET) Collaborators (1991) Beneficial effect of carotid endarterectomy in symptomatic patients with high gradde stenosis. N Engl J Med 325:445
Noser EA, Shaltoni HM, Hall ChE et al (2005) Aggressive mechanical clot disruption. A safe adjunct to thrombolytic therapy in acute stroke? Stroke 36:292
Nusbaum AO, Som PM, Dubois P et al (1845) Isolated vagal nerve palsy associated with a dissection of the extracranial internal carotid artery. Am J Neuroradiol 1988:19
Nutik ST, Dilenge D (1976) Carotid – anterior cerebral artery anastomoses. J Neurosurg 44:378
Obrador A, Urquiza P (1952) Angioma arteriovenoso de la tienda del cerebelo. Rev Esp Oto Neuro Oftal 10:387
Ohara Y, Petersen TE, Harrison DG (1993) Hypercolesterolemia increases endothelial superoxide anion production. J Clin Invest 91:2546
Ohkuma H, Suzuki S, Shimamura N et al (2003) Dissecting aneurysms of middle cerebral artery: neuroradiological and clinical features. Neuroradiology 45:143
Ohshiro S, Inoue T, Hamoda Y et al (1993) Branches of the persistent primitive trigeminal artery. An autopsy case. Neurosurgery 32:144
Okuchi K, Nagata K, Fujioka M et al (1999) Rapid growth of the interal carotid anterior wall aneurym. Riv Neuroradiol 12(Suppl 2):9
Ondra SL, Traupp H, George ED et al (1990) The natural history of symptomatic arteriovenous malformations of the brain: a 24 year follow-up assessment. J Neurosurg 73:387
Ono M, Ono M, Rhoton AL Jr et al (1984) Microsurgical anatomy of the region of the tentorial incisura. J Neurosurg 60:365
Osborn DA (1959) So called juvenile angiofibroma of nasofarinx. J Laryngol Otol 73:295
Osborn AG (1999) Diagnostic cerebral angiography. Lippincott Williams & Wilkins, Philadelphia
Osborn AG, Andersson RE (1977) Angiographic spectrum of cervical and intracranial fibromuscolar displasia. Stroke 8:617
Ostergaard JR, Oxlund A (1987) Collagen type III deficiency in patients with rupture of intracranial saccular aneurysms. J Neurosurg 67:690
Ostergaard JR, Voldby B (1983) Intracranial arterial aneurysms in children and adolescence. J Neurosurg 58:832
Ostertun B, Solymosi L (1993) Magnetic resonance angiography of cerebral developmental venous anomalies. Its role in differential diagnosis. Neuroradiology 35:97
Otomo E (1965) The anterior choroidal artery. Arch Neurol 13:656
Otten P, Pizzolato GP, Rilliet B et al (1989) A propos de 131 cas d'angiomes caavernoux (cavernoma) du SNC, repérés par l'analyes retrospective de 24535. Neurochirurgie 35:82
Padget DH (1944) The circle of Willis, its embryology and anatomy. Comstock, Ithaca, NY
Padget DH (1956) The cranial venous system in men in reference to developmental, adult configuration, and relation to the arteries. Am J Anat 98:307
Padget DH (1948) The development of the cranial arteries in the human embryo. Contrib Embryol 32:205
Padget DH (1957) The development of the cranial venous system in man from the viewpoint of comparative anatomy. Contr Embriol Carnegie Inst 36:79
Palubinskas AJ, Newton TH (1965) Fibromuscular hyperplasia of the internal carotid arteries. Radiol Clin Biol 34:365
Palubinskas AJ, Ripley AR (1964) Fibromuscolar hyperplasia in extra-renal arteries. Radiology 82:451
Palubinskas AJ, Perloff P, Newton TH (1966) Fibromuscolar hyperplasia: an arterial dysplasia of increasing clinical importance. Am J Roentgenol 98:907
Panagiotopoulos V, Gizewski E, Asgari S et al (2009) Embolization of intracranial arterio-venous malformations with ethylene – vinyl alcohol copolymer (ONYX). Am J Neuroradiol 30:99

Pasqualin A, Mazza C et al (1986) Intracranial aneurysms and subarachnoid haemorrhage in children and adolescence. Childs Nerv Syst 2:185

Patel U, Gupta SC (1990) Wyburn-Mason syndrome. A case report and review of the literature. Neuroradiology 31:544

Pedroza A, Dujovny M, Artero JC et al (1987) Microanatomy of the posterior communicating artery. Neurosurgery 20:228

Pelkonen O, Tikkakoski T, Leinonen S et al (2003) Extracranial internal carotid and vertebral artery dissection: angiographic spectrum, course and prognosis. Neuroradiology 45:71

Percheron G (1976a) Les artère du thalamus humain II. Artères et territoires thalamiques paramedians de l'artère basilaire communiquante. Rev Neurol 132:309

Percheron G (1976b) Les artères du thalamus humain. I. Artères et territoires thalamiques polaires de l'artères communiquante posterieure. Rev Neurol 132:297

Perini S, Talamini G, Pasqualin A et al (1995) Arteriovenous malformations of the brain. Risk of first bleeding, rebleeding and related risk factors in 168 untreated patients. Neuroradiology 37(Suppl 1):120

Perlmutter D, Rhoton AL Jr (1976) Microsurgical anatomy of the anterior cerebral-anterior communicating-recurrent artery complex. J Neurosurg 45:259

Perlmutter D, Rhoton AL Jr (1978) Microsurgical anatomy of the distal anterior cerebral artery. J Neurosurg 49:204

Perret G, Nischioka H (1966) Report on the cooperative study of intracranial aneurysms and subarachnoid haemorrhage. Section VI. Arteriovenous malformations. J Neurosurg 25:467

Perrini P, Cardia A, Fraser K et al (2007) A micro-surgical study of the anatomy and course of the ophthalmic artery and its possibly dangerous anastomoses. J Neurosurg 106:142

Pessin MS, Kwan ES, Dewm LD et al (1987) Posterior cerebral artery stenosis. Ann Neurol 21:85

Pessin MS, Chimowitz MI, Levine SR et al (1989) Stroke in patients with fusiform vertebrobasilar aneurysm. Neurology 39:16

Phatouros CC, Lefler JE, Higashida RT (2000) Primary stenting for high-grade basilar artery stenosis. Am J Neuroradiol 21:1744

Pia HW, Fontana H (1977) Aneurrysms of the posterior cerebral artery. Acta Neurochirurgica 38:13

Picard L, Floquet J, Andrè JM et al (1974a) Syndrome Moya-Moya. Etude anatomopatologique. J Neuroradiol (Masson) 1:113

Picard L, Levesque M, Crouzet G et al (1974b) The Moya Moya syndrome. J Neuroradiol (Masson) 1:47

Picard L, Bracard S, Moret J et al (1987) Spontaneous dural arteriovenous fistula. Sem Interv Radiol 4:219

Picard L, Bracard S, Islak C et al (1990) Dural fistulae of the tentorium cerebelli. J Neuroradiol (Masson) 17:161

Picard L, Roy D et al (1993) Aneurysm associated with a fenestrated basilar artery: report of two cases treated by endovascular detachable balloon embolization. Am J Neuroradiol 14:591

Picard L, Bracard S, Anxionnat R et al (2005) Brain AVM embolization. Retrospective study concerning 728 patients, followed between 1984–2004. Interv Neuroradiol 11:45

Pickard JD, Walker V, Vile J et al (1987) Oral nimodipine reduces prostaglandin and thromboxane production by arteries chronically exposed to a periarterial haematoma and the antifibrinolytic agent tranexamic acid. J Neurol Neursurg Psychiatry 50:727

Pierot L, Chiras J, Meder JF et al (1992) Dural arteriovenous fistulas of the posterior fossa draining into subarachnoid veins. Am J Neuroradiol 13:315

Pierot L, Cognard C, Spelle L (2004) Malformations arterioveneuses cérébrales: evolution du risque hémorragique et de sa morbiditè. J Neuroradiol (Masson) 31:369

Pitanguy I, Caldeira AML, Calixto CA et al (1984) Clinical evaluation and surgical treatment of hemangiomata. Head Neck Surg 7:47

Piton J, Guilleux H, Guibert-Trainier F et al (1984) Fistules du sinus lateral. J Neuroradiol (Masson) 11:143

Pollock BE, Flickinger JC, Lunsford LD et al (1996) Factors that predict the bleeding risk of cerebral arteriovenous malformations. Stroke 27:1

Pope FM (1989) Type III collagen mutations and cerebral aneurysms. Stroke 20:1432

Pope FM, Nicholls AC, Narisi P et al (1984) Some patients with cerebral aneurysms are deficient in type III collagen. Lancet 1:973

Powell J (1991) Model of arterial aneurysms: for the investigation of pathogenesis and pharmacotherapy: a review. Atherosclerosis 87:93

Pozzati E, Acciarri N, Tognetti F, et al (1996) Groth, subsequent bleeding and de novo appearance of cerebral cavernous angiomas. Neurosurgery 38:662

Pozzati E, Andreoli A, Padovani R (1995) Dissecting aneurysms of the basilar artery. Neurosurgery 36:254

Proust F, Tousseint P et al (2001) Pediatric cerebral aneurysms. J Neurosurg 94:733

Provenzale JM (2009) MRI and MRA for evaluation of dissection of craniocerebral arteries. Lessons from the medical literature. Emerg Radiol 16(3):185

Pullicino P, Miller LL, Munschauer EE et al (1992) Linear subinsular MR hyperintensity. Ann Neurol 32:267

Quinones D, Duckwiller G, Gobin PY et al (1997) Embolisation of dural cavernous fistulas via superior ophtalmic vein approach. Am J Neuroradiol 18:921

Qureschi AI, Hussein HM, El-Gengaihy A et al (2008) Concurrent comparison of outcomes of primary angioplasty and of stent placement in high-risk patients with symptomatic intracranial stenosis. Neurosurgery 62:1053

Qureshi AI, Ali Z, Suri MF et al (2001) Intra-arterial third-generation recombinant tissue plasminogen activator (reteplase) for acute ischemic stroke. Neurosurgery 49:41

Qureshi AI, Siddiqui AM, Suri MF et al (2002) Aggressive mechanical clot disruption and low-dose intraarterial third-generation thrombolytic agent for ischemic stroke: a prospective study. Neurosurgery 51:1319

Rafay MF, Armstrong D, De Veber J et al (2006) Cranio-cervical arterial dissection in children: clinical and radiographic presentation and outcome. J Child Neurol 21:8

Ramgren B, Cronquist M, Rommer B et al (2005) Vertebrobasilar dissection with subarachnoid haemorrhage: a retrospective study of 29 patients. Neuroradiology 47:97

Ramsey TL, Mosquera VT (1948) Dissecting aneurysm of the middle cerebral artery. Ohio State Med J 44:168

Raybaud CA, Strother CM, Hald JK (1989) Aneurysms of the vein of Galen: embryonic considerations and anatomical features relating to the pathogenesis of the malformation. Neuroradiology 31:109

Raymond J, Iancu D, Weill A et al (2005) Embolization as one modality in a combined strategy for the management of cerebral AV malformation. Interv Neuroradiol 11:57

Raymond J, Guillemin F, Proust F et al (2008) Unruptured intracranial aneurysms. A critical review of the International Study of Unruptured Intracranial Aneurysms (ISUIA) and of appropriate methods to address the clinical problem. Interv Neuroradiol 14:85

Redekop GJ (2008) Extracranial carotid and vertebral artery dissection: a review. Can J Neurol Sci 35:146

Redekop G, Terbrugge K, Montanera W et al (1998) Arterial aneurysms associated with cerebral arteriovenous malformations: classification, incidence and risk of haemorrhage. J Neurosurg 89:539

Reivich M, Holling E, Roberts B et al (1961) Reversal of blood flow through the vertebral artery and its effects on cerebral circulation. N Engl J Med 265:88

Reynolds AF Jr, Stovring J, Turner PT (1980) Persistent otic artery. Surg Neurol 13:115

Rhoton AL Jr (2002) Aneurysms. Neurosurgery 51(Suppl 1):121

Rhoton AL Jr, Fujiki K, Frad B (1979) Microsurgical anatomy of the anterior choroidal artery. Surg Neurol 12:171

Rigamonti D, Brown GB (1994) The natural history of familial cavernous malformations. Results of an ongoing study. J Neurosurg 80:422

Rigamonti D, Drayer BP, Johnson PC et al (1987) The MR imaging appearance of cavernous malformations (angiomas). J Neurosurg 67:518

Rigamonti D, Johnson PC, Spetzler RF et al (1991) Cavernous malformation and capillary telangectasias. A spectrum within a single pathological entity. Neurosurgery 28:60

Rinaldi I, Harris WO, Kopp JE et al (1976) Intracranial fibromuscolar dysplasia: report of 2 cases; one with autopsy verification. Stroke 7:511

Ring BA (1974) The middle cerebral artery. In: Newton TH, Potts DG (eds) Radiology of skull and brain. Mosby, St. Louis

Ring BA, Waddington MM (1967) Acending frontal branch of the middle cerebral artery. Acta Radiol Diagn 6:209

Ringelstein EB, Zeumer H, Angelow D (1983) The pathogenesis of strokes from internal carotid artery occlusion: diagnostic and therapeutic implications. Stroke 14:867

Ringelstein EB, Zeumer H, Schneider R (1985) Der Beitrag der zerebralen Computertomographie zur Differentialdiagnose und Differntialtherapie des ischemischen Grosshirninfarktes. Fortschr Neurol Psychiatry 53:315

Ringer AJ, Qureschi AI, Fessler RD et al (2001) Angioplasty of intracranial occlusion resistant to thrombolysis in acute ischemic stroke. Neurosurgery 6:1282

Ringleb PA, Allenberg J, Bruckmann H et al (2006) 30 day results from the space trial of stent protected angioplasty versus carotid endarterectomy in symptomatic patients: a randomized non-inferiority trial. Lancet 368:1239

Rinkel GJE, Wijdicks EFM, Vermeulen M, et al (1991) Nonaneurysmal perimesencephalic subarachnoid hemorrhage: CT and MR patterns that differ from aneurismal rupture. AJNR Am J Neuroradiol 12:829

Rinne J, Hernesniemi J, Puranen M et al (1994) Multiple intracranial aneurysms in a defined population: prospective angiographic and clinical study. Neurosurgery 35:803

Riva A, Bradac GB, Riccio A, et al (1991) Demenza in un paziente con fistula durale. Rivista di Neuroradiologia 4:369

Ro A, Kageyama N, Abe N et al (2009) Intracranial vertebral artery dissection resulting in fatal subarachnoid haemorrhage: clinical and histopathological investigations from a medicolegal perspective. J Neurosurg 110:948

Robinson JR Jr, Awad IA, Little JR (1991) Natural history of the cavernous angioma. J Neurosurg 75:709

Roche JL, Choux M et al (1988) Intracranial arterial aneurysms in children. A cooperative study. A propos of 43 cases. Neurochirurgie 34:243

Rodesch G, Lasjaunias P, Terbrugge K (1988) Lesions vasculaires arteroveineuses intracraniennes de l'enfant. Place des techniques endovsasculaires. A propos de 44 cases. Neurochirurgie 34:293

Rodesch G, Comoy J, Hurth M et al (1991) Jugular foramen arteriovenous shunt with subarachnoid haemorrhage. Skull Base Surg 1:132

Rodesch G, Malherbe V, Alvarez H et al (1995) Non galenic cerebral arteriovenous malformations in neonates and infants. Childs Nerv Syst 11:231

Rodesch G, Guedin P, Gaillard S et al (2009) Terapeutic management of intracranial dural arteriovenous shunts with leptomeningeal venous drainage: report of 53 consecutive patients with emphasis on transarterial embolization with acrylic glue. Interv Neuroradiol 5(Suppl 1):106

Rodriguez-Arias C, Martinez R, Rey G et al (2000) Recurrence in different location of a cerebral arteriovenous malformation in a child after radiosurgery. Childs Nerv Syst 16:363

Roh HG, Kim SS, Han H et al (2008) Endovascular treatment of posterior cerebral artery aneurysms using detachable coils. Neuroradiology 50:237

Rosa M, Viale GL (1970) Diagnostic value of vertebral phlebogram. Neuroradiology 1:147

Rosenkranz M, Gerloff Ch (2010) Diagnostic workup in carotid stenosis. A neurologist's perspective. Neuroradiology 52:619

Rosenthal F (1824) De intimis cerebri venis seu de venae magnae Galeni ramis. Nova Acta Phisiocomedica Academiae Caesareae Leopoldino-Carolinae Naturae Curiosorum 12:302

Rosner SS, Rhoton AL Jr, Ono M et al (1984) Microsurgical anatomy of the anterior perforating arteries. J Neurosurg 61:468

Roy D, Milot G, Raymond J (2001) Endovascular treatment of unruptured aneurysms. Stroke 32:1998

Rüfenacht DA (2005) Aneurysms: the role of the perianeurysmal environment. Interv Neuroradiol 11(Suppl 2):50

Russell DS, Rubinstein LJ, Lumsden CF (1959) Tumours and hamartomas of blood vessels. In: Russel DS, Rubinstein LJ (eds) Pathology of tumours of the nervous system. Arnold, London, pp 72–92

Saeki N, Rhoton AL Jr (1977) Microsurgical anatomy of the upper basilar artery and the posterior circle of Willis. J Neurosurg 46:53

Sagduyu A, Sirin H, Mulayim S et al (2006) Cerebral cortical and deep venous thrombosis without sinus thrombosis: clinical MRI correlates. Acta Neurol Scand 114:254

Sakata S, Fujii K, Matsushima T, et al (1993) Aneurysms of the posterior cerebral artery :report of eleven cases-surgical approaches and procedures. Neurosurgery 32:163

Saito Y, Kobayashi N (1981) Cerebral venous angiomas. Clinical evaluation and possible etiology. Radiology 139:87

Salamon G, Huang YP (1976) Radiologic anatomy of the brain. Springer, Berlin/Heidelberg

San Millan Ruiz D, Gailloud P, De Miquel Miquel MA (1999) The latero-cavernous sinus: an anatomical study. Anat Rec 254:7

San Millan Ruiz D, Gailloud P, Rüfenacht DA et al (2002) The craniocervical venous system in relation to the cerebral venous drainage. Am J Neuroradiol 23:1500

Sarwar M, Mc Cormick WF (1978) Intracerebral venous angioma: case report and review. Arch Neurol 35:323

Sasaki O, Koike T, Tanaka R et al (1991) Subarachnoid haemorrhage from a dissecting aneurysm of the middle cerebral artery. J Neurosurg 74:504

Savoiardo M, Bracchi M, Passerini A et al (1987) The vascular territory in the cerebellum and brainstem. CT and MR study. Am J Neuroradiol 8:199

Saygi S, Bolay H, Tekkok IH et al (1990) Fibromuscolar dysplasia of the basilar artery: a case with brainstem stroke. Angiology 41:658

Schievink WI (2001) Spontaneous dissection of the carotid and vertebral arteries. N Engl J Med 344:898

Schievink WI, Mokri B (1995) Familial aortocervical cephalic arterial dissection and congenital bicuspid aortic valve. Stroke 26:1935

Schievink WI, Mokri B, Ganity JA et al (1993) Ocular motor nerve palsy in spontaneous dissections of the cervical internal carotid artery. Neurology 43:1938

Schievink WI, Björnsson J, Piepgras DG (1994a) Coexistence of fibromuscolar dysplasia and cystic medial necrosis in a patient with Marfan's syndrome and bilateral carotid artery dissection. Stroke 25:2492

Schievink WI, Mokri B, Pipgras D (1994b) Spontaneous dissections of cervico-cephalic arteries in childhood and adolescence. Neurology 44:1607

Schievink WI, Meyer FB, Parisi JE et al (1998) Fibromuscolar dysplasia of the internal carotid artery associated with alpha-1-antitripsin deficiency. Neurosurgery 43:229

Schlesinger B (1939) The venous drainage of the brain with special reference to the galenic system. Brain 62:274

Schmit BP, Burrows PE, Kuban K et al (1996) Acquired cerebral arteriovenous malformation in a child with Moya-Moya disease. Case report. J Neurosurg 84:677

Schubiger O, Valavanis A, Wichmann W (1987) Growth mechanism of giant intracranial aneurysm; demonstration by CT and MR imaging. Neuroradiology 29:266

Schwartz MJ, Baronofsky ID (1960) Ruptured intracranial aneurysm associated with coartation of the aorta: a report of a patient treated by hypothermia and surgical repair of the coartation. Am J Cardiol 6:982

Scialfa G, Bank W, Megret M et al (1976) The posterior fossa arteries: the morphology and variations of the anterior inferior cerebellar artery. The arteriographic localization of the fourth ventricle. In: Salamon G (ed) Advances in cerebral angiography. Springer, Berlin/Heidelberg

Scialfa G, Valsecchi F, Scotti G (1983) Treatment of vascular lesions with balloon catheter. Am J Neuroradiol 4:395

Scotti G (1975) Anterior inferior cerebellar artery originating from the /cavernous portion of the internal carotid artery. Radiology 116:93

Sebire G, Meyer L, Chabrier S (1999) Varicella as a risk factor for cerebral infarction in childhood: a case-control study. Ann Neurol 45:679

Segall HD, Ahmodi J, McComb JC et al (1982) Computed tomographic observations pertinent to intracranial venous thrombotic and occlusive disease in childhood. Radiology 143:441

Sekhar LN, Heros RC, Lotz PR et al (1980) Atheromatous pseudoocclusion of the internal carotid artery. J Neurosurg 52:782

Seong SO, David C, Choi IS (2006) Bilateral petrous ridge dural arteriovenous malformations treated by a combination of endovascular embolization and surgical excision. A case report. Interv Neuroradiol 12:269

Sepehrnia A, Tatagiba M, Brandis A et al (1990) Cavernous angioma of the cavernous sinus. Case report. Neurosurgery 27:151

Serbinenko FA (1974) Balloon catheterization and occlusion of major cerebral vessels. J Neurosurg 41:125

Shimoji T, Bando K, Nakajima K et al (1984) Dissecting aneurysm of the vertebral artery: report of seven cases and angiographic findings. J Neurosurg 61:1038

Shin JH, Suh DCh, Choi CG et al (2000) Vertebral artery dissection: spectrum of imaging findings with emphasis on angiography and correlation with clinical presentation. Radiographics 20:1687

Shin Y, Nakase H, Nakamura M et al (2007a) Expression of angiogenetic growth factor in the rat DAVF model. Neurol Res 29:727

Shin YS, Kim AS, Kim SY (2007b) Stenting for vertebrobasilar dissection: a possible treatment option for non haemorrhagic vertebrobasilar dissection. Neuroradiology 49:149

Shiu PC, Hanafee WN, Wilson GH, et al (1968) Cavernous sinus venography. Am J Roentg 104:57

Sitzer M, Müller W, Siebler M et al (1995) Plaque ulceration and lumen thrombus are the main sources of cerebral microemboli in high-grade internal carotid stenosis. Stroke 26:1231

Smirniotopoulos JG, Murphy FM (1992) The phakomatoses. AJNR Am J Neuroradiol 13:725

Song JK, Cacayorui ED, Campbell MS et al (2002) Intracranial balloon angioplasty of acute terminal internal carotid artery occlusion. Am J Neuroradiol 23:1308

Song JK, Miimi Y, Kuresmiths MJ et al (2007) Posta natal growth and development of cerebral arteriovenous malformation on serial magnetic resonance imaging in a child with haemangiomatosis. J Neurosurg 106(Suppl 5):384

Sorteberg A, Farhoudi D (2006) The influence of aneurysm configuration on intra-aneurysmal pressure and flow. Interv Neuroradiol 12:203

Spetzler RF, Martin NA (1986) A proposed grading system for arterio – venous malformations. J Neurosurg 65:4–76

Stanley JC, Fry WJ, Seeger JF, et al (1974) Extracranial internal carotid and vertebral artery fibrodysplasia. Arch Surg 109:215

Stapf C, Labovitz DL, Sciacca RR et al (2002) Incidence of adult brain arteriovenous malformation haemorrhage in a prospective population-based stroke survey. Cerebrovasc Dis 13:43

Stapf C, Mast H, Sciacca R et al (2006) Predictors of haemorrhage in patients with untreated brain arteriovenous malformations. Neurology 66:1350

Stehbens WE (1959) Medial defects of cerebral arteries of man. J Path Bact 78:179

Stehbens WE (1972) Pathology of cerebral blood vessels. Mosby, St Louis

Stehbens WE (1989) Aethiology of intracranial berry aneurysms. J Neurosurg 70:823
Stehbens WE (1990) Pathology and pathogenesis of intracranial berry aneurysms. Neurol Res 12:29
Stevens J, Leach JL, Abruzzo T et al (2009) De novo cerebral arteriovenous malformations: case report and literature review. Am J Neuroradiol 30:111
Stewart RM, Samson D, Diehl J et al (1980) Unruptured cerebral aneurysms presenting as recurrent transient neurologic deficit. Neurology 30:47
Stingele R, Berger J, Alfke K et al (2008) Clinical and angiographic risk factors for stroke and death within 30 days after carotid endarteriectomy and stent protected angioplasty: a subanalysis of the SPACE study. Lancet Neurol 7:216
Sturzenhegger M (1995) Spontaneous internal carotid artery dissection: early diagnosis and management in 44 patients. J Neurol 242:231
Sugiu K, Tokunaga K, Watanabe K et al (2005) Emergent endovascular treatment of ruptured vertebral artery dissecting aneurysms. Neuroradiology 47:158
Suh DC, Lee JC, Kim SJ et al (2005) New concept in cavernous sinus dural arteriovenous fistula: correlation with presenting symptom and venous drainage pattern. Stroke 36:1134
Suzuki J, Takaku A (1969) Cerebrovascular "Moya-moya disease": a disease showing abnormal net-like vessels in base of brain. Arch Neurol 20:288
Szikora I, Paal G, Ugron A et al (2008) Impact of aneurismal geometry on aneurysmal flow: a computerized flow simulation study. Neuroradiology 50:411
Tacconi L, Johnston FG, Symon L (1995) Accessory middle cerebral artery. J Neurosurg 83:916
Takahashi M, Wilson G, Hanafee W (1968) The anterior inferior cerebellar artery. Its radiographic anatomy and significance in the diagnosis of extraaxial tumors of posterior fossa. Radiology 90:281
Takahashi M, Tamakawa Y et al (1973) Fenestration of the basilar artery. Report of three cases and review of the literature. Radiology 109:79
Takahashi M, Arii H, Tamakawa Y (1980) Anomalous arterial supply of temporal and occipital lobes by anterior Choroidal artery. Angiographic study. Am J Neuroradiol 1:537
Takahashi S, Hoshino F, Vemura K et al (1989) Accessory middle cerebral artery: is it a variant form of the recurrent artery of Heubner? Am J Neuroradiol 10:563
Takahashi S, Suga T, Kawata Y et al (1990) Anterior choroidal artery: angiographic analysis of variations and anomalies. Am J Neuroradiol 11:719
Takahashi S, Kato K, Tomura N et al (2001) Dural arteriovenous fistula of the cavernous sinus with cortical venous reflux of the posterior fossa via a bridging vein. Radiat Med 19:219
Takeuchi K, Shimizu K (1957) Hypoplasia of the bilateral internal carotid arteries. No To Shinkei 9:37
Tanaka M, Kikuchi Y, Ouchi T (2006) Neuroradiological analysis of 23 cases of basilar artery fenestration based on 2280 cases of MR angiographies. Interv Neuroradiol 12(1):39
Taptas JN (1982) The so called cavernous sinus: a review of the controversy and its implications for neurosurgeons. Neurosurgery 11:712
Tatu L, Moulin T, Bougosslavsky J et al (2001) Arterial vascular territory of human brain. In: Bougosslawsky J, Caplan L (eds) Stroke syndromes. Cambridge University Press, Cambridge
Tauntopoulou A, Ahl B, Weissenborn K et al (2008) Intra arterial thrombolysis using rtPA in patients with acute stroke due to vessel occlusion of anterior and –or posterior cerebral circulation. Neuroradiology 50:75
Taveras JM (1969) Multiple progressive intracranial arterial occlusion: a syndrome of children and youg adults. AJR 106:235
Tekkök IH, Ventureyra ECV (1996) De novo familial cavernous malformation presenting with hemorrhage 12.5 years after the initial hemorrhagic Ictus: natural history of an infantile form. Pediatr Neurosurg 25:151
Terada T, Higashida RT, Halbach VV et al (1994) Development of acquired arteriovenous fistulas in rats due to venous hypertension. J Neurosurg 80:884
Theron J, Newton TH (1976) Anterior choroidal artery. 1 anatomic and radiographic study. J Neuroradiol 3:5
Theron J, Newton TH, Hoyt WF (1974) Unilateral retinocephalic vascular malformations. Neuroradiology 7:185
Thijs VN, Albers GW (2000) Symptomatic intracranial atherosclerosis, outcome of patients who fails antithrombotic therapy. Neurology 55:490
Tomak PR, Cloft HJ, Kaga A et al (2003) Evloution of the management of tentorial dural arteriovenous malformations. Neurosurgery 52:750
Tomasello F, Cioff FA, Albanese V (1976) Fibromuscolar dysplasia of the basilar artery. Neurochirurgie 19:29
Tornow K, Piscol K (1971) The evaluation of the superior ophtalmic vein on the carotid angiogram. Neuroradiology 2:30
Tournade A (1972) Les veines superficielles du bulbe et du pont chez l'homme. Thesis, Strasbourg
Trolard P (1868) Anatomie du système veneux de l'encephale et du crane. These de la facultè de medecine de Paris, Paris
Tsai FY, Wang AM, Matovich VB et al (1995) MR staging of acute dural sinus thrombosis: correlation with venous pressure measurements and implications for treatment and prognosis. Am J Neuroradiol 16:1021
Turjman F, Massoud TF, Vinuela F et al (1994) Aneurysms related to cerebral arteriovenous malformations: superselective angiographic assessment in 58 patient. Am J Neuroradiol 15:1601
Turjman F, Massoud TF, Vinuela F et al (1995) Correlation of the angioarchitectural features of cerebral arteriovenous malformations with clinical presentation of haemorrhage. Neurosurgery 37:856
Turk AS, Levy EI, Albuquerque FC et al (2008) Influence of patient age and stenosis location on Wingspan in-stent restenosis. Am J Neuroradiol 29:23
Turnbull I (1962) Agenesis of the internal carotid artery. Neurology 12:588
Umansky F, Nathan H (1982) The lateral wall of the cavernous sinus. J Neurosurg 56:228
Umansky F, Gomes FB, Dujovny M et al (1985) The perforating branches of the middle cerebral artery: a microanatomical study. J Neurosurg 62:261
Umansky F, Dujovny M, Ausman J et al (1988) Anomalies and variations of the middle cerebral artery; a microanatomical study. Neurosurgery 22:1023
Uranishi R, Nakase H, Sakaki T (1999) Expression of angiogenic growth factors in dural arteriovenous fistulas. J Neurosurg 91:781

Urbach H, Zentner J, Solymosi L (1998) Neuroradiology. Jan; 40(1):6–10
Urban PP, Müller-Forrell W (2005) Clinical and neuroradiological spectrum of isolated cortical vein thrombosis. J Neurol 252:1476
Valavanis A (1996) The role of angiography in the evaluation of cerebral vascular malformations. Neuroimaging Clin N Am 6:679
Valavanis A, Yaşargil MG (1998) The endovascular treatment of brain arterovenous malformations. Adv Tech Stand Neurosurg 24:131
Valavanis A, Pangalu A, Tanaka M (2004) Endovascular treatment of cerebral arteriovenous malformations with emphasis on the curative role of embolization. Swiss Arch Neurol Psychiatr 7:341
Valdueza JM, Von Munster T, Hoffman O et al (2000) Postural dependency of the cerebral venous outflow. Lancet 355:200
Van Dijk JMC, Terbrugge KG, Willinsky RA et al (2004) Selective disconnection of cortical venous reflux as treatment for cranial dural arteriovenous fistulas. J Neurosurg 101:31
Van Roij WJ, Sluzewski M (2009) Endovascular treatment of large and giant aneurysms. Am J Neuroradiol 30:12
Vargas ME, Desrouleaux JR, Kupersmith MJ (1992) Ophthalmoplegia as a presenting manifestation of internal carotid artery dissection. J Clin Neuroophthalmol 12:268
Ventureyra ECG, Higgins MJ (1994) Traumatic intracranial aneurysms in childhood adolescence. Case report and review of the literature. Childs Nerv Syst 10:361
Verbiest MH (1951) Intradural arteriovenous aneurysm. Revue Neurologique 85:189
Vertinsky AT, Schwartz NE, Fischbein NJ et al (2008) Comparison of multidetector CT angiography and MR imaging of cervical artery dissection. Am J Neuroradiol 29:1753
Vignaud J, Clay C, Aubin M et al (1972) Orbital arteriography. Radiol Clin North Am 10:39
Vila N, Millan M, Ferrer X et al (2003) Levels of alpha-1-antitripsin in plasma and risk of spontaneous cervical artery dissections. Stroke 34:168
Vilela P, Goulão A (2006) Pediatric dissecting posterior cerebral aneurysms: report of two cases and review of the literature. Neuroradiology 48:541
Villringer A, Mehraein S, Einhaupl KM (1994) Treatment of sinus venous thrombosis. Beyond the recommendation of anticoagulation. J Neuroradiol 21:72
Vinuela F, Fox AJ, Debrun GM et al (1984) Spontaneous carotid-cavernous fistulas: clinical, radiological and therapeutic considerations. J Neurosurg 60:976
Vinuela F, Nombela L, Roach MR et al (1985) Stenotic and occlusive disease of the venous drainage system of deep brain AVMs. J Neurosurg 63:180
Vinuela F, Drake CG, Fox AJ et al (1987) Giant intracranial varices secondary to high flow arteriovenous fistulae. J Neurosurg 66:198
Vinuela F, Duckwiller GR, Johan R et al (2005) Therapeutic management of cerebral arterio – venous malformations. Present role of interventional Neuroradiology. Interv Neuroradiol 11:13
Virchow R: Die Krankhaften Geschwulste. Dreissig Vorlesungen gehalten während des Wintersemester 1862–1863 an der Universitat zu Berlin
Vitek JJ, Reaves P (1973) Toracic bifurcation of the common carotid artery. Neuroradiology 5:133
Wackenheim A, Braun JP (1970) Angiography of the mesencephalon. Normal and pathologic findings. Springer, Berlin/Heidelberg
Wackenheim A, Braun JP (1978) The veins of the posterior fossa. Springer, Berlin/Heidelberg
Waespe W, Niesper J, Imhoff HG et al (1988) Lower cranial nerve palsies due to internal carotid artery dissection. Stroke 19:4561
Warfarin-Aspirin Symptomatic Intracranial Disease (WASID) Trial investigators (2003) Design, progress and challenges of double-blind trial of warfarin versus aspirin for symptomatic intracranial arterial stenosis. Neuroepidemiology 22:106
Waterston JA, Brown MM, Butler P et al (1990) Small deep cerebral infarcts associated with occlusive internal carotid artery disease. Arch Neurol 47:953
Weidauer S, Claus D, Gartenschläger M (1999) Spinal sulcal artery syndrome due to spontaneous bilateral vertebral dissection. J Neurol Neurosurg Psychiatry 67:550
Weiller C, Ringelstein EB, Reiche W et al (1991) Clinical and haemodynamic aspects of low-flow infarcts. Stroke 22:1117
Weinstein M, Stein R, Pollock J et al (1974) Meningeal branch of the posterior cerebral artery. Neuroradiology 7:129
Weir B (1987) Aneurysms affecting nervous system. Williams-Wilkins, Baltimore
Westberg G (1966) Arteries of the basal ganglia. Acta Radiol Diagn 5:581
Wholey MH, Wholey M, Mathias K et al (2000) Global experience in cervical carotid artery stent placement. Catheter Cardiovasc Interv 50:160
Wiebers DO, Whisnant JP, Huston J 3rd et al (International Study of Unruptured Intracranial Aneurysms Investigators) (2003) Unruptured intracranial aneurysms: natural history, clinical outcome and risk of surgical and endovascular treatment. Lancet 362:103
Willinsky R, Lasjaunias P, Terbrugge K et al (1988) Brain arteriovenous malformations. An analysis of the angioarchitecture in relationship to haemorrhage. J Neuroradiol (Masson) 15:225
Willinsky R, Lasjaunias P, Terbrugge K et al (1990) Multiple cerebral arteriovenous malformations. Review of our experience from 203 patients with cerebrovascular lesions. Neuroradiology 32:207
Willis Th (1684) Cerebri anatomiae nervorumque descritpio et usus. Willis Th (1964) (trans: Prodage S). J. Fletcher, London
Wilson WB, Laevengood JM, Ringel SP (1989) Transient ocular motor paresis associated with acute internal carotid artery occlusion. Ann Neurol 25:286
Wintermark M, Ko NU, Smith WS et al (2006) Vasospasm after subarachnoid haemorrhage: utility of perfusion CT and CT angiography on diagnosis and management. Am J Neuroradiol 27:26
Wittkugel O, Gbadamosi J, Rosenkranz M et al (2008) Long-term outcome after angioplasty of symptomatic internal carotid artery stenosis with and without stent. Neuroradiology 50:243
Witznum JL, Steinberg D (1991) Role of oxidized low density lipoprotein in atherogenesis. J Clin Invest 88:1785
Wolf BS, Huang YP (1963) The insula and deep middle cerebral venous drainage system: normal anatomy and angiography. Am J Roentgenol 90:472

Wolf BS, Huang YP (1964) The subependymal veins of the lateral ventricle. Am J Roentgenol 91:406
Wolf BS, Huang YP, Newman CM (1963) The lateral anastomotic mesencephalic vein and other variations in drainage of the basal cerebral vein. Am J Roentgenol 89:411
Wollschlaeger PB, Wollschlaeger G (1965) Eine infratentorielle meningeale Arterie. Radiologe 5:451
Wollschlaeger G, Wollschlaeger PB (1974) The circle of Willis. In: Newton TH, Potts DG (eds) Radiology of skull and brain, vol 2, Angiography. Mosby, St. Louis
Wong KS, Huang YN, Gao S et al (1998) Intracranial stenosis in Chinese patients with acute stroke. Neurology 50:812
Wylie EG, Binkley FM, Palubinkas AJ (1966) Extracranial fibromuscolar hyperplasia. Am J Surg 112:149
Yamamoto Y, Georgiades A, Chang HM et al (1999) Posterior cerebral artery territory infarcts in the New England Medical Center (NEMC). Posterior circulation registry. Arch Neurol 56:824
Yamamura A, Watanabe Y, Saeki N (1990) Dissecting aneurysms of the intracranial vertebral artery. J Neurosurg 72:183
Yamamura I, Tani E, Yokota M et al (1999) Endovascular treatment of ruptured dissecting aneurysms aimed at occlusion of the dissected site by using Guglielmi detachaeble coils. J Neurosurg 90:853
Yang X, Mu S, Lu M et al (2007) Endovascular treatment of huge dissecting aneurysms involving the basilar artery. Experience and lessons from two cases. Interv Neuroradiol 13:369
Yaşargyl MG (1984a) Microneurosurgery I: microsurgical surgical anatomy of the basal cisterns and vessels of the brain. Thieme, New York
Yaşargyl MG (1984b) Microneurosurgery II: clinical considerations, surgery of the intracranial aneurysms and results. Thieme, New York
Yaşargyl MG (1987) Microsurgery. AVM of the brain. History, embryology, pathological considerations, haemodynamics, diagnostic studies, microsurgical anatomy. Thieme Medical Publisher, New York
Yaşargyl MG (1999) A legacy of microsurgery: memoirs, lessons and axioms. Neurosurgery 45:1025
Yazbak PA, Mc Comb JC et al (1995) Paediatric traumatic intracranial aneurysm. Pediatr Neurosurg 223:15
Zager EL, Shaver EG, Hurst RV et al (2002) Distal anterio inferior cerebellar artery aneurisms: report of 4 cases. J Neurosurg 97:692
Zaidat OO, Suarez JI, Sunshine JL et al (2005) Thrombolytic therapy of acute ischemic stroke: correlation of angiographic recanalisation with clinical outcome. Am J Neuroradiol 26:880
Zak F, Lawson W (1982) Paraganglionic chemoreceptor system: physiology pathology and clinical medicine. Springer, New York
Zambranski JM, Wascher TM, Spetzler RF et al (1994) The natural history of familial cavernous malformations. Results of an ongoing study. J Neurosurg 80:422
Zeal AA, Rhoton AJ Jr (1978) Microsugical anatomy of the posterior cerebral artery. J Neurosurg 48:534
Zeumer H, Hacke W, Kolmann HL et al (1982) Lokale Fibrinolyse Therapie bei Basilaris Thrombose. Dtsch Med Woch 107:728
Zeumer H, Freitag HJ, Zanella F et al (1993) Local intraarterial fibrinolitic therapy in patients with stroke: urokinase versus recombinant tissue plasminogen activator (rTPA). Neuroradiology 2:159
Zhao WY, Krings T, Alvarez H et al (2007) Management of spontaneous haemorrhagic intracranial vertebrobasilar dissection: a review of 21 consecutive cases. Acta Neurochir (Wien) 149:585
Zuber M, Meary E, Meder JF et al (1994) Magnetic resonance imaging and dynamic CT scan in cervical artery dissections. Stroke 25:576
Zülch KJ (1957) Brain tumors: their biology and pathology. Springer, Berlin/New York

Index

G.B. Bradac, *Cerebral Angiography*,
DOI: 10.1007/978-3-642-15678-6, © Springer-Verlag Berlin Heidelberg 2011